iarigai
print and media research
www.iarigai.org

Advances in Printing and Media Technology

Vol. XXXIV

Edited by Nils Enlund and Mladen Lovreček

Acta Graphica Publishers
Zagreb MMVII

Advances in Printing and Media Technology

Proceedings of the 34th International Research Conference of iarigai

Grenoble, France
September 2007

Published by Acta Graphica Publishers, Zagreb, Croatia for
the International Association of Research Organizations for
the Information, Media and Graphic Arts Industries

Co-edited by

Nils Enlund, Stockholm, Sweden
Mladen Lovreček, Zagreb, Croatia

The facts published in this book are obtained from sources believed to be reliable. However, publishers can accept no legal liability for the contents of papers, nor for any information contained therein, nor for conclusions drawn by any party from it.

No part of this publication may be reproduced, stored in a retrieval system or transmitted in any form or by any means eletronic, mechanical, photocopying, recording or otherwise without the prior written premission of the publisher.

CIP zapis dostupan u računalnom katalogu
Nacionalne i sveučilišne knjižnice u Zagrebu pod brojem 654118

CIP record available in the computer catalog of the
National and University Library in Zagreb under number 654118

ISBN 978-953-7292-04-1

Cover design: Acta Graphica

Printed in Croatia by Sveučilišna tiskara, Zagreb - December 2007

Contents

Introduction

Preface: Printing and media technology research in 2007 3
Nils Enlund

Polymer nanocomposites reinforced with polysaccharide nanocrystals 5
Alain Dufresne

1. Printing processes and materials

Mechanisms of non-image area accumulation in heatset web offset 15
Soile Passoja, Ulla Mattila, Asko Sneck

Tack, ink transfer and ink distribution on paper 23
Martin Dubé, François Drolet, Jean-Francis Bloch, Claude Daneault, Patrice J. Mangin

Aquapiling: Coated substrate-related influences on reverse piling from a one-side single colour image in multicolour offset printing 31
Patrick A. C. Gane, Cathy J. Ridgway, Peter Burri, Manfred Arnold, Karl-Heinz Kagerer, Barry Madden, Matti Ristolainen, Jarkko Purontaus

Predicting print-through in coldest newsprint 49
Christine Antoine

Aspects of water-induced mottle when printing on coated paper in sheet-fed lithographic offset 59
Christer Lie, Petter Kolseth

Modelling the anilox-plate micro contact 69
David Bould, Simon Hamblyn, John Cherry, Tim Claypole

Analysis of interferometric data to obtain accurate geometric characterisation of engraved cells 77
D. Deganello, T. C. Claypole, D. T. Gethin

Effects of elevated temperature on flexographic printing 85
Robert Olsson, Li Yang, Jan van Stam, Magnus Lestelius

Time-dependent rheology effects on print quality using water-based ink compositions 93
Scott Williams, Stephanie Pieruccini

Study of the rheological behaviour of conventional, hybrid and UV offset inks 101
Marie Kaplanová, Katarína Remenárová, Bohumil Jašúrek, Jan Vališ

Wavelet automatic classification system of substrates in flexography 109
Amparo Sánchez-Alandí, Susana Otero, Vicente de Gracia

A lumped parameter model for thermal conductivity of paper coatings 115
Philip Gerstner, Jouni Paltakari, Patrick A.C. Gane

Digital paper and print surface topography 123
Vernhes Pierre, Blayo Anne, Pineaux Bernard, Bloch Jean-Francis

2. Color and quality

Achieving color agreement: evaluating the options 131
Robert Chung, Fred Hsu, Wuhui Liu

Comparing corresponding colors 141
Lidija Mandić, Darko Agić, Maja Strgar Kurečić

Spectral color reproduction versus color reproduction 147
Jérémie Gerhardt, Jon Y. Hardeberg

An evaluation of colour differences and tolerances in soft proofing 153
Janne Laine

The development of a six colour separation algorithm 163
Eifion Jewell, Tim Claypole, Barry Palmer

Correcting method of optical dot gain to full color halftone image printed on white paper 181
Michitaka Nonaka, Susumu Kitazawa

Deriving optimal spectra for standard offset primaries 189
Philipp Urban, Andreas Kraushaar

Implementing process color printing by colorimetry 197
Robert Chung

Influence of paper and printing process on the visual perception and colorimetric characteristics of newsprint 205
Tim C. Claypole, Eifion H. Jewell, Nigel Wells, Paul Casey

Improved proofing method for postage stamps 213
Erzsébet Novotny

Effect of drops interactions on ink-jet print quality 221
Christophe Mercier, Magalie Peralba, Martin Dubé, Jean-Francis Bloch, Patrice J. Mangin

New ink absorption method to predict inkjet print quality 231
Taina Lamminmäki, Pasi Puukko

3. Special printing and printed functionality

The problem of a quantitative evaluation of adhesive strength in printing on polymer films 243
Evgeny Bablyuk, Vadim Bakanov, Konstantin Farenbrukh

Colour differences on offset printed PET and PVC shrink sleeve labels 251
Gorazd Golob, Diana Gregor Svetec, Dejana Đorđević, Boštjan Žorž

Quality control for printed interference colours - investigation for a basic measuring geometry 257
Heike Hupp, Edgar Dörsam

Photoacoustic study of varnished solids printed by different techniques 267
Markéta Držková, Jiří Hejduk, Klára Grolichová

A micro-scale study of optical dot gain in color halftone 271
Daniel Nyström, Björn Kruse, Li Yang1

Flip flop and spatial (3D) graphics in lenticular technique 277
Ivana Žiljak, Jana Žiljak Vujić, Klaudio Pap

Carbon black loaded paper: an intelligent substrate for electronic sensors design 285
Rodolphe Koehly, Denis Curtil, Theodorus G. M. van de Ven, Marcelo M. Wanderley

Printing of functional layers using flexography 293
Ulrike Herzau-Gerhardt, Henning Nagel

Rotogravure and pad printing of microstructures for electronic applications like oFETs 297
Gunter Hübner, Werner Till

Printing process for Lithium-ion electrodes elaboration 307
Franck Medlege, Anne Blayo, Hélène Rouault, Naceur Belgacem

An experimental study to identify key factors affecting the performance of RFID tag antennas 313
Yung-Cheng Hsieh, Hui-wen Cheng

4. Strategic issues in the media industry

Positioning in the printing industry - differentiation in terms of price, lead time, print quality and flexibility 327
Thomas Mejtoft, Magnus Viström

Importance of short production runs, variable data printing and web interfaces - a comparison of digital and conventional printing houses 337
Magnus Viström, Thomas Mejtoft

Consumer expectations as drivers of media change 345
Cecilia Teljas, Alex Jonsson, Nils Enlund

Tabloid versus broadsheet: is format change the magic bullet for newspapers? The results of a comparative eye-tracking study of a German daily 355
Hans-Jürgen Bucher

Designing community-based print products 365
Katri Grenman, Minna Forsell, Marjoriikka Ylisiurua, Hanne Roschier, Mikael Malanin

User centric approach for designing cross media applications in personal photography 375
Sami Vihavainen, Risto Sarvas, Jaana Näsänen, Katri Grenman

Potential applications for hybrid media, the benefits and the roles in the operations model 387
Elina Rusko, Liisa Hakola

New business models for printed functionality 395
Ulf Lindqvist, Liisa Hakola, Hannu Linna, Pertti Moilanen, Timo Siivonen

Energy efficiency improvement for graphic/media SME´s - How it can be managed? 401
Anastasios Politis, Michael Dattner

Customer oriented and sustainable printed paper 413
Helena Wessman, Anna Leinonen, Eero Hiltunen, Minna Forsell, Catharina Hohenthal-Joutsimo

Screening environmental life cycle assessment of printed, internet-based and tablet e-paper newspaper 419
Åsa Moberg, Martin Johansson, Göran Finnveden, Alex Jonsson

Index of authors 431

Introduction

Printing and media technology research in 2007

Nils Enlund

Co-editor, Chairman of the Program Committee
E-mail: nilse@kth.se

One might easily imagine that the ancient and thoroughly established technology of printing would be completely understood today. Not so. Ever since the introduction of woodblock printing in China, around 1800 years ago, and Bi Sheng's revolutionary invention of movable type 960 years ago, the technical challenges of quality mass production of text and images has required continued research and process development.

This volume contains the scientific and technical research contributions presented at the 34th International Research Conference of iarigai, the International Association of Research Organizations for the Information, Media and Graphic Arts Industries, held in Grenoble, France, on September 9 - 12, 2007. The papers, selected by international experts through a double-blind review process, present scientific recent work aiming at the advancement of printing and media technology and at a better understanding of the processes and changing conditions of the media producing industry.

One especially interesting challenge for printers is the development of new materials, both substrates for printing and new types of substances to be placed on the substrates by a process of printing. The invited introductory paper describes the potential of nanotechnology, especially in the use of polysaccharide nanocrystals, for creating new types of pigments and thin films.

The materials theme is further explored in the first section of this volume with papers addressing the problems of print surface topology, thermal conductivity of substrates, rheological behaviour of inks, as well as other current topics. The section also contains papers on materials behaviour in different printing processes.

The second section of the book discusses color reproduction and print quality. The included papers report findings on color comparison, evaluation and agreement, on new methods for color separation and printing, and on quality issues in both conventional and non-impact printing.

In the papers in the third section, the authors tackle the challenges of special purpose printing and printed functionality. The themes vary from printed electronics to the problems of printing on plastics, from security printing to the uses of paper loaded with carbon black.

The final section of this volume focuses on the ongoing changes in the media industry and on the need for new business strategies. The papers address the emergence of new media formats and genres, the changing consumer behaviour, new industry developments, and the increasingly important environmental and sustainability aspects of industrial media activities.

All these, and many more, scientific studies included in this book provide a valuable overview of current international research in the broad and diverse field of media and printing technology. I am convinced that the findings of the participating scientists will give practitioners new insights and ideas, and researchers deeper knowledge and inspiration for further work.

Polymer nanocomposites reinforced with polysaccharide nanocrystals

Alain Dufresne

Ecole Française de Papeterie et des Industries Graphiques
Institut National Polytechnique de Grenoble (EFPG-INPG), BP65
F-38402 Saint-Martin d'Hères Cedex, France
E-mail: Alain.Dufresne@efpg.inpg.fr

1. Introduction

Nanoscience and nanotechnology correspond to science and technology that extend from about 100 nm down to atomic orders of magnitude around 0.2 nm, and to the physical phenomena and material properties observed when operating in this size range. Conceptually, nanocomposites refer to multiphase materials where at least one of the constituent phases has one dimension less than 100 nm. This field has attracted the attention, scrutiny and imagination of both scientist and industrial communities in recent years. Behind the push for nanocomposites, a large window of opportunity has opened to overcome the limitations of traditional micrometer-scale composites. Research in this scope is literally exploding because of the intellectual appeal of building blocks on the nanometer scale and because the technical innovations permit to design and create new materials and structures with unprecedented flexibility, improvements in their physical properties and significant industrial impact.

A possible source of inspiration is the nature and its wonderful nanocomposite structures. Among biologically inspired nanocomposites, polysaccharides are probably among the most promising sources for the production of nanoparticles. These abundant biorenewable raw materials are increasingly used in non-food applications. They can also be used for the preparation of crystalline nanoparticles with different geometrical characteristics providing a wide range of potential nanoparticules properties. Huge quantities of these nanoparticules are potentially available, often as waste products from agriculture. Moreover, polysaccharide surfaces provide potential for significant surface modification using well-established carbohydrate chemistry. The latter allows tailoring the surface functionality of the nanoparticles. In this field, scientific and technological challenges to take up are tremendous.

2. Polysaccharide nanocrystals

Stable aqueous suspensions of polysaccharide nanocrystals can be prepared by acid hydrolysis of the biomass. Throughout the chapter different descriptors of the resulting colloidal suspended particles will be used, including whiskers, monocrystals and nanocrystals. The designation "whiskers" is used to designate elongated rod-like nanoparticles. These crystallites have also often been referred in literature as microfibrils, microcrystals or microcrystallites, despite their nanoscale dimensions. Most of the studies reported in the literature refer to cellulose. A recent review reported the properties and application in nanocomposite field of cellulosic whiskers [1].

The procedure for the preparation of such colloidal aqueous suspensions is described in detail in the literature for cellulose and chitin [2, 3]. The biomass is generally first submitted to a bleaching treatment with NaOH in order to purify cellulose or chitin by removing other constituents. The bleached material is then disintegrated in water, and the resulting suspension is submitted to a hydrolysis treatment with acid. The amorphous regions of cellulose or chitin act as structural defects and are responsible of the transverse cleavage of the microfibrils into short monocrystals under acid hydrolysis. Under controlled conditions, this transformation consists of the disruption of amorphous regions surrounding and embedded within cellulose or chitin microfibrils while leaving the microcrystalline segments intact. It is ascribed to the faster hydrolysis kinetics of amorphous domains compared to crystalline ones. The resulting suspension is subsequently diluted with water and washed by successive centrifugations. Dialysis against distilled water is then performed to remove free acid in the dispersion. Complete dispersion of the whiskers is obtained by a sonication step. The dispersions are stored in the refrigerator after filtration to remove residual aggregates and addition of several drops of chloroform. Determination of the whisker content can be done by weighing aliquots of the solution before and after drying.

This general procedure has to be adapted depending on the nature of the substrate. The constitutive nanocrystals occur as elongated rod-like particles or whiskers. The precise physical dimensions of the crystallites depend on several factors, including the source of the cellulose or chitin, the exact hydrolysis conditions and ionic strength. The typical geometrical characteristics for crystallites derived from different species and reported in the literature are collected in Table I. The length is generally of the order of few hundreds nanometers and the width is of the order of few nanometers. The aspect ratio of these whiskers is defined as the ratio of the length to the width.

Table I: Geometrical characteristics of polysaccharide nanocrystals from various sources: length (L) and diameter (D) of rod-like particles obtained from cellulose or chitin

Nature	Source	L (nm)	D (nm)	Ref.
Cellulose	Algal (*Valonia*)	> 1000	10-20	[4]
	Bacterial	100-several 1000	5-10 × 30-50	[5]
	Cladophora	-	20 × 20	[6]
	Cotton	100-300	5-10	[7]
	Cottonseed linter	170-490	40-60	[8]
	MCC	150-300	3-7	[9]
	Sisal	100-500	3-5	[10]
	Sugar beet pulp	210	5	[11]
	Tunicin	100-several 1000	10-20	[12]
	Wheat straw	150-300	5	[13]
	Wood	100-300	3-5	[14]
Chitin	Crab shell	80-600	8-50	[15]
	Riftia tubes	500-10000	18	[16]
	Shrimp	50-300	5-70	[17]
	Squid pen	150-800	10	[18]

Aqueous suspensions of starch nanocrystals can be prepared according to the well known "lintnerization" procedure described in the literature [19]. Degradation of native starch granules by acid hydrolysis depend on many parameters. It includes the botanical origin of starch, namely crystalline type, granule morphology (shape, size, surface state) and relative proportion of amylose and amylopectin. It also depends on the acid hydrolysis conditions, namely acid type, acid concentration, starch concentration, temperature, hydrolysis duration and stirring.

The main drawbacks for the use of such hydrolysis residues in composite applications are the duration (40 days of treatment) and the yield (0.5 wt%) of the hydrochloric acid hydrolysis step [19]. Response surface methodology was used [20] to investigate the effect of five selected factors on the selective sulfuric acid hydrolysis of waxy maize starch granules in order to optimize the preparation of aqueous suspensions of starch nanocrystals. These predictors were temperature, acid concentration, starch concentration, hydrolysis duration and stirring speed. The preparation of aqueous suspensions of starch nanocrystals was achieved after 5 days of 3.16 M H_2SO_4 hydrolysis at 40°C, 100 rpm and with a starch concentration of 14.69 wt% with a yield of 15.7 wt%. Waxy maize starch nanocrystals consist of 5 - 7 nm thick platelet-like particles with a length ranging from 20 to 40 nm and a width in the range 15 - 30 nm. The detailed investigation on the structure of these platelet-like nanoparticles was reported [21]. Such nanocrystals are generally observed in the form of aggregates having an average size around 4.4 µm, as measured by laser granulometry [22].

The stability of resulting suspensions depends on the dimensions of the dispersed particles, their size polydispersity and surface charge. The use of sulfuric acid for polysaccharide nanocrystals preparation leads to more stable aqueous suspension than that prepared using hydrochloric acid [22]. Indeed, the H_2S0_4-prepared nanoparticles present a negatively charged surface while the HCl-prepared nanoparticles are not charged.

3. Processing of polysaccharide nanocrystals reinforced polymer nanocomposites

Because of the high stability of aqueous polysaccharide nanocrystals dispersions, water is the preferred processing medium. High level of dispersion of the filler within the host matrix in the resulting composite film is expected when processing nanocomposites in aqueous medium. Therefore, this restricts the choice of the matrix to hydrosoluble polymers. The use of aqueous dispersed polymers, i.e. latexes, is a first alternative, which allows

the use of hydrophobic polymers as matrix and ensure a good dispersion level of the filler indispensable for homogenous composites processing. The possibility of dispersing polysaccharide nanocrystals in non-aqueous media is a second alternative and it opens other possibilities for nanocomposites processing.

In the first announcement of the preparation of polysaccharide nanocrystals reinforced polymer nanocomposites a latex obtained by the copolymerization of styrene and butyl acrylate (poly(S-co-BuA)) with a Tg around 0°C and tunicin whiskers were used [12]. Composite materials are generally obtained by casting and evaporation. The dispersion of polysaccharide nanocrystals in non polar media can be obtained by chemically modifying their surface.

4. Thermal properties

In most studies, no modification of glass transition temperature (Tg) values are reported when increasing the amount of whiskers, regardless the nature of the polymeric matrix. This result appears to be surprising because of the high specific area of these nanoparticles that is around 170 m^2g^{-1} for instance for tunicin whiskers [23].

In glycerol plasticized starch based composites, peculiar effects of tunicin whiskers on the Tg of the starch-rich fraction were reported depending on moisture conditions [24]. For low loading level (up to 3.2 wt%), a classical plasticization effect of water was reported. However, an antiplasticization phenomenon was observed for higher whiskers content (6.2 wt% and up). These observations were discussed according to the possible interactions between hydroxyl groups on the cellulosic surface and starch, the selective partitioning of glycerol and water in the bulk starch matrix or at whiskers surface, and the restriction of amorphous starch chains mobility in the vicinity of the starch crystallite coated filler surface. For glycerol plasticized starch reinforced with cellulose crystallites prepared from cottonseed linter [8], an increase of Tg with filler content was reported and attributed to cellulose/starch interactions. For tunicin whiskers/sorbitol plasticized starch [25], Tgs were found to increase slightly up to about 15 wt% whiskers and to decrease for higher whiskers loading. Crystallization of amylopectin chains upon whiskers addition and migration of sorbitol molecules to the amorphous domains were proposed to explain the observed modifications.

For waxy maize starch nanocrystals reinforced natural rubber, a decrease of the onset glass transition temperature with the increase of the nanoparticles content was reported [26]. Using a glycerol plasticized starch matrix, it was reported a temperature increase of the main relaxation process associated with the glass-rubber transition of amylopectin-rich domains with the increasing of the starch nanocrystals content [27]. The reduction in the molecular mobility of matrix amylopectin chains for filled materials was explained by the establishment of hydrogen bonding forces between both components. A similar observation was reported for polyvinyl acetate (PVA) reinforced with sisal cellulose whiskers [10] and carboxymethyl cellulose (CMC) reinforced with cotton cellulose whiskers [28]. For waxy maize starch nanocrystals reinforced glycerol plasticized starch the increase of Tg led to a considerable slowing down of the retrogradation of the matrix [27]. This is a very interesting result since retrogradation and crystallization of thermoplastic starch during aging is one of the main drawbacks of this material and lead to an undesired change in thermomechanical properties.

Melting temperature (Tm) values were reported to be nearly independent on the filler content in plasticized starch [24, 25] and in POE-based materials [29 - 31] filled with tunicin whiskers. The same observation was reported for polycaprolactone reinforced with *Riftia* tubes chitin whiskers [16] and cellulose acetate butyrate (CAB) reinforced with native bacterial cellulose whiskers [5]. However, for the latter system, Tm values were found to increase when the amount of trimethylsilylated whiskers increased. It was ascribed to the stronger filler-matrix interaction in the case of chemically modified whiskers.

A significant increase in crystallinity of sorbitol plasticized starch [25] was reported when increasing cellulose whiskers content. This phenomenon was ascribed to an anchoring effect of the cellulosic filler, probably acting as a nucleating agent. For POE based composites the degree of crystallinity of the matrix was found to be roughly constant up to 10 wt% tunicin whiskers [29 - 31] and to decrease for higher loading level [29]. Incorporation of shrimp shells chitin whiskers did not have any effect on the crystallinity of PVA [17] and chitosan [32].

It seems that the nucleating effect of cellulosic nanocrystals is mainly governed by surface chemical considerations. Indeed, when untreated or surfactant-coated, whiskers were also reported to be very good nucleating agents for isotactic polypropylene (iPP). The unmodified whiskers have the largest nucleating effect [33]. On the contrary, whiskers grafted with maleated polypropylene did not modify the crystallization of iPP. It was shown from both

X-ray diffraction and differential scanning calorimetry (DSC) analysis that the crystallization behavior of films containing unmodified and surfactant-modified whiskers displayed two crystalline forms (α and β), whereas the neat matrix and the nanocomposite reinforced with nanocrystals grafted with maleated polypropylene only crystallized in the α form. It was suspected that the more hydrophilic the whisker surface, the more it appeared to favor the appearance of the β phase. It was observed that native bacterial fillers impede the crystallization of the CAB matrix whereas silylated ones help to nucleate the crystallization [5]. A decrease of the degree of crystallinity of polycaprolactone was reported when adding *Riftia* tubes chitin whiskers [16]. It was suggested that during crystallization, the rod-like nanoparticles are most probably first ejected and then occluded in intercrystalline domains, hindering the crystallization of the polymer. In iPP reinforced with tunicin whiskers, a mechanical coupling between the polypropylene crystallites and filler/filler interactions was reported [33].

For tunicin whiskers filled semi-crystalline matrices such as poly(β-hydroxyoctanoate) (PHO) [34] and glycerol plasticized starch [24] a transcrystallization phenomenon was reported. It consists on a preferential crystallization of the amorphous polymeric matrix chains during cooling at the surface of nanoparticles. For glycerol plasticized starch based systems, the formation of the transcrystalline zone around the whiskers was assumed to be due to the accumulation of plasticizer in the cellulose/amylopectin interfacial zones improving the ability of amylopectin chains to crystallize. These specific crystallization conditions were evidenced at high moisture content and high whiskers content by DSC and wide angle X-ray scattering (WAXS). It was displayed through a shoulder on the low temperature side of the melting endotherm and the observation of a new peak in the X-ray diffraction pattern. This transcrystalline zone could originate from a glycerol-starch V structure. In addition, the inherent restricted mobility of amylopectin chains was put forward to explain the lower water uptake of cellulose/starch composites for increasing filler content.

In silk fibroin reinforced with tunicin whiskers composites a conformational change of fibroin chains from a random coil to an ordered structure was reported [35]. This change was ascribed to the highly ordered surface of cellulosic whiskers. For waxy maize starch nanocrystals reinforced glycerol plasticized starch an increase of the degree of crystallinity of the thermoplastic starch matrix was reported [27]. It was suggested that crystallization of the matrix occurred at the interface between the filler and the matrix owing to the similar chemical structure of both components.

5. Mechanical properties

Nanoscale dimensions and impressive mechanical properties make polysaccharide nanocrystals, particularly when occurring as high aspect ratio rod-like nanoparticles, ideal candidate to improve the mechanical properties of the host material. These properties are profitably exploited by Mother Nature. In the ten recent years, a great interest was focused on investigating the use of polysaccharide nanocrystals, especially cellulose whiskers, as a reinforcing phase in a polymeric matrix, evaluating the mechanical properties of the resulting composites and elucidating the origin of the mechanical reinforcing effect.

The first demonstration of the reinforcing effect of cellulose whiskers was reported for poly(S-co-BuA) reinforced with tunicin whiskers [12]. The authors measured a spectacular improvement in the storage modulus after adding the filler even at low content into the host polymer. This increase was especially significant above the glass-rubber transition temperature of the thermoplastic matrix because of its poor mechanical properties in this temperature range. For instance, the rubbery modulus of the composite reinforce with 6 wt% tunicin whiskers was more than two order of magnitude higher than the one of the unfilled matrix. Moreover, the introduction of 3 wt% or more cellulosic whiskers provides an outstanding thermal stability of the matrix modulus up to the temperature at which cellulose starts to degrade (500K).

They tried to understand the unusual reinforcing effect from the high modulus of cellulose whiskers [12], that was reported to be of the order of 150 GPa [36]. In this perspective they used a classical model for randomly dispersed short fiber reinforced composites that is the model of Halpin-Kardos [37]. In this mean-field approach, fibers are supposed to be dispersed in a continuous matrix and no interaction between fillers is taken into account. The description of equations used in this approach can be found elsewhere [13]. It was found that the predicted rubbery modulus fails to describe the experimental data. The cellulose whiskers seemed to act as fibers much longer than expected from geometrical observation.

The outstanding properties observed for these systems were ascribed to a mechanical percolation phenomenon [12]. A good agreement between experimental and predicted data was reported when using the series-parallel

model of Takayanagi modified to include a percolation approach. It was suspected that all the stiffness of the material was due to infinite aggregates of cellulose whiskers. Above the percolation threshold the cellulosic nanoparticles can connect and form a tri-dimensional continuous pathway through the nanocomposite film. For rod-like particles such as tunicin whiskers with an aspect ratio of 67, the percolation threshold is close to 1 vol% [38]. The formation of this cellulose network was supposed to result from strong interactions between whiskers, like hydrogen bonds [39]. This phenomenon is similar to the high mechanical properties observed for a paper sheet, which result from the hydrogen-bonding forces that hold the percolating network of fibers. This mechanical percolation effect allows explaining both the high reinforcing effect and the thermal stabilization of the composite modulus for evaporated films.

Any factor that affects the formation of the percolating whiskers network or interferes with it changes the mechanical performances of the composite [40]. Three main parameters were reported to affect the mechanical properties of such materials, as the morphology and dimensions of the nanoparticles, the processing method, and the microstructure of the matrix and matrix/filler interactions.

6. Morphology and dimensions of the nanoparticles

Cellulose and chitin nanocrystals occur as rod-like nanoparticles in opposite to starch nanocrystals, which consist of nanometer scale platelet-like particles. For rod-like particles, the geometrical aspect ratio is of course an important factor since it determines the percolation threshold value. This factor is linked to the source of cellulose or chitin and whiskers preparation conditions. Fillers with high aspect ratio give the best reinforcing effect. For instance, the rubbery storage tensile modulus was systematically lower for wheat straw whiskers/poly(S-co-BuA) composites than for tunicin whiskers based materials [40]. The following relation was found between the percolation threshold (v_{Rc}) and aspect ratio of rod-like particles:

$$v_{Rc} = \frac{0.7}{L/d} \qquad (1)$$

Also, the flexibility and tangling possibility of the nanofibers plays an important role [11]. These authors reported the mechanical properties of poly(S-co-BuA) reinforced with cellulose rod-like nanoparticles extracted from sugar beet and submitted to different hydrolysis conditions. Unhydrolyzed cellulose microfibrils were prepared by submitting sugar beet pulp to a chemical treatment consisting of an alkali extraction with a sodium hydroxide solution to solubilize most of the pectins and hemicelluloses [41]. The resulting insoluble residue was bleached with a sodium chlorite solution, suspended in distilled water and homogenized by successive passes through a Manton-Gaulin laboratory homogenizer. Individualized flexible cellulose microfibrils, almost 5 nm in width and practically infinite in length, result from this treatment. These microfibrils were submitted to a hydrolysis treatment using different sulfuric acid concentrations. As the acid concentration increased, it was observed that the length of the microfibrils decreased because of the increased probability of removal of the amorphous material with the concentration of acid. For the strongly hydrolyzed material, most of the amorphous domains were hydrolyzed and rigid whiskers were obtained. Linear mechanical measurements performed on poly(S-co-BuA) reinforced with these microfibrils did not show significant differences by varying the strength of the hydrolysis step and then the length and flexibility of the nanoparticles. However, for nonlinear mechanical tensile tests it was observed that as the hydrolysis strength increased both the modulus and the strength of the composite decreased, whereas the elongation at break increased. This result showed the strong influence of entanglements on the mechanical behavior of the nanocomposites.

7. Processing method

The processing method governs the possible formation of a continuous nanocrystals network and then the final properties of the nanocomposite material. Slow processes such as casting/evaporation were reported to give the highest mechanical performance materials compared to freeze-drying/molding and freeze-drying/extruding/molding techniques. It was ascribed to the probable orientation of these rod-like nanoparticles during film processing due to shear stresses induced by freeze-drying/molding or extrusion techniques.

It was shown that whiskers dimensions affect their ability to align within a shear field. Neutron and X-ray scattering data were used to monitor shear alignment of softwood-derived nanocrystals isolated from the same source, but with different sizes [42]. It was shown that as the aspect ratio falls below 20, shear alignment of

whiskers, and the ability to maintain this alignment drops significantly. In addition, this difference was suggested to be due to the predominance of the whiskers/whiskers interactions and their contribution to the overall reinforcing effect in the evaporated films in relation to homogeneous fillers dispersion into matrix. During slow water evaporation, because of Brownian motions in the suspension or solution (whose viscosity remains low, up to the end of the process when the latex particle or polymer concentration becomes very high), the rearrangement of the nanoparticles is possible. They have time enough to interact and connect to form a percolating network which is the basis of their reinforcing effect. The resulting structure is completely relaxed and direct contacts between nanocrystals or microfibrils are then created. Conversely, during the freeze-drying/hot-pressing process, the nanoparticle arrangement in the suspension is first frozen, and then, during the hot-pressing stage, because of the polymer melt viscosity, the particle rearrangements are strongly limited. Thus, in this case, contacts are made through a certain amount of polymer matrix. However, although the freeze-drying/hot-pressing process limits the possibility of creation of hydrogen bonds it is expected that for high polysaccharide nanoparticles content some bonds may evenly be created.

When using a polymeric matrix in latex form, the particle sizes seems to play a predominant role [43]. Larger latex particle size results in higher mechanical properties. Indeed, the polymeric particles act as impenetrable domains to polysaccharide nanoparticles during the film formation due to their high viscosity. Increasing latex particle size leads to an increase of the excluded volume and these geometrical constraints seem to affect the whiskers network formation.

8. Microstructure of the matrix and matrix/filler interactions

The microstructure of the matrix and the resulting competition between matrix/filler and filler/filler interactions also affect the mechanical behavior of the polysaccharide nanocrystals reinforced nanocomposites. Classical composite science tends to privilege the former as a fundamental condition for optimal performance. In polysaccharide nanocrystals based composite materials the opposite trend is generally observed when the materials are processed via casting/evaporation method. Increasing the affinity between the polysaccharide filler and the host matrix, decreasing the mechanical performances is observed. This unusual behavior is ascribed to the originality of the reinforcing phenomenon of polysaccharide nanocrystals resulting from the formation of a percolating network due to hydrogen bonding forces.

Tensile tests performed on silk fibroin/microcrystalline cellulose composites showed a linear trend, additive dependence on the mixing ratio for the Young's modulus, whereas the tensile strength and elongation at break showed a maximum around 70 - 80 cellulose content, reaching five times those of fibroin-alone or cellulose-alone films [35]. Strong interactions between cellulose crystallites prepared from cottonseed linters and between the filler and the glycerol plasticized starch matrix were reported to play a key role in reinforcing properties [8]. In non-percolating systems, for instance for materials processed from freeze-dried cellulose nanocrystals, strong matrix/filler interactions enhance the reinforcing effect of the filler. This observation was reported using poly(ethylene-co-vinyl acetate) (EVA) matrices with different vinyl acetate contents and then different polarities [44].

A higher reinforcing effect for unmodified cellulose whiskers than for trimethylsilylated whiskers was reported [5]. Apart the fact that 18% of the weight of the silylated crystals was due to the silyl groups, they attributed this difference to restricted filler/filler interactions. Similar results and loss of mechanical properties were reported for natural rubber based nanocomposites reinforced with both unmodified and surface chemically modified chitin whiskers [45] and starch nanocrystals [46].

The transcrystallization phenomenon reported for semicrystalline PHO on cellulose whiskers resulted in a remarkable decrease of the mechanical properties (especially above the melting temperature of the matrix) when compared to fully amorphous PHO [34]. In these systems, the filler/matrix interactions and distance away from the surface at which the molecular mobility of the amorphous PHO phase is restricted were quantified using a physical model predicting the mechanical loss angle [23]. The determination of the ratio between experimental and predicted magnitude of the main relaxation process allows to remove the filler reinforcement effect keeping only the interfacial effect, and used it to calculate the thickness of the interphase. It was shown that when using semicrystalline PHO as matrix, the molecular mobility of amorphous PHO chains was only slightly affected by the presence of tunicin whiskers, owing to a possible transcrystallization phenomenon leading to the coating of the nanoparticles with the crystalline PHO phase. The thickness of the transcrystalline layer, around 2.7 nm, was found to be independent of the cellulose whiskers content. In

contrast when using an amorphous PHO as matrix, the flexibility of polymeric chains in the surface layer is lowered by the conformational restrictions imposed by cellulose surface. This results in a broader interphase and in a broadening of the main relaxation process of the matrix.

Similar transcrystallization was reported for plasticized starch reinforced with cellulose whiskers [47]. This strong loss of performance demonstrates the event of outstanding importance of the filler/filler interactions to ensure the mechanical stiffness and thermal stability of these composites. When using unhydrolyzed cellulose microfibrils extracted from potato pulp rather that cellulose nanocrystals to reinforce glycerol plasticized thermoplastic starch, a completely different mechanical behavior was reported [48, 49], resulting in a significant reinforcing effect of unhydrolyzed microfibrils. It was suspected that tangling effect contributed to this high reinforcing effect [47]. However, for POE-based nanocomposites the formation of the percolating cellulose network is not altered by the crystallization of the matrix and filler/POE interactions [29-31, 50-52].

9. Conclusions

Polysaccharide nanocrystals are building blocks biosynthesized to provide structural properties to living organisms. They can be isolated from the biomass through acid hydrolysis with concentrated mineral acids under strictly controlled conditions of time and temperature. Acid action results in an overall decrease of amorphous material by removing polysaccharide material closely bonded to the crystallite surface and breaks down portions of glucose chains in most accessible, non crystalline regions. A leveling-off degree of polymerization is achieved corresponding to the residual highly crystalline regions of the original material, i.e. cellulose or chitin fiber, or starch granule. Dilution of the acid and dispersion of the individual crystalline nanoparticles complete the process and yield an aqueous suspension of polysaccharide nanoparticles. These nanoparticles occur as rod-like nanocrystals that can display chiral nematic properties depending on the mineral acid chosen for the hydrolysis in the case of cellulose- or chitin-based materials, or platelet-like nanoparticles when using starch granules as the raw material.

Polysaccharide nanocrystals are inherently low cost materials which are available from a variety of natural sources and in a wide variety of aspect ratios. They take advantage of both renewable materials, such as abundance, renewability and self-assembling into well-defined architectures, and nanosized particles, including mechanical properties e.g. strength, modulus and dimensional stability, decreased permeability to gases and water, thermal stability and heat distorsion temperature, surface appearance and optical clarity in comparison to conventionally filled polymers. They are an attractive nanomaterial for multitude of potential applications in a diverse range of fields. Indeed, nanotechnology has applications across most economic sectors and allows the development of new enabling science with broad commercial potential. Possible and suggested areas of application include optically variable films and ink iridescent pigments for security papers. Polysaccharide nanocrystals reinforced polymer nanocomposites display outstanding mechanical properties and can be used to process high-modulus thin films. The growing literature studying polysaccharide, mainly cellulose, nanocrystals is a clear indication of this evolution. Practical applications of such fillers and transition into industrial technology require a favorable ratio between the expected performances of the composite material and its cost. To exploit their potential, research and development investments must be made in the science and engineering that will fully determine the properties and characteristics of polysaccharides at the nanoscale, develop the technologies to manipulate self-assembly and multifunctionnality, and develop these new technologies to the point where industry can produce advanced and cost-competitive polysaccharide nanoscale products. There are still significant scientific and technological challenges to take up.

References

[1] Azizi Samir, M. A. S., Alloin, F., Dufresne, A. Biomacromolecules, 6(2), 612 - 626 (2005)

[2] Wise, L. E.; Murphy, M., D'Addiecco, A. A. Pap. Trade J., 122(2), 35 - 43 (1946)

[3] Marchessault, R. H.; Morehead, F. F.; Walter, N. M. Nature, 184(9), 632 - 633 (1959)

[4] Revol, J. F. Carbohydr. Polym., 2(2), 123 - 134 (1982)

[5] Grunert, M.; Winter, W. T. J. Polym. Environ., 10(1-2), 27 - 30 (2002)

[6] Kim, U. J.; Kuga, S.; Wada, M.; Okano, T.; Kondo, T. Biomacromolecules, 1(3), 488 - 492 (2000)

[7] Ebeling, T.; Paillet, M.; Borsali, R.; Diat, O.; Dufresne, A.; Cavaillé, J. Y.; Chanzy, H. Langmuir, 15(19), 6123 - 6126 (1999)

[8] Lu, Y.; Weng, L.; Cao, X. Macromol. Biosci. 5(11), 1101 - 1107 (2005)

[9] Kvien, I.; Bjørn, S. T.; Oksman, K. Biomacromolecules, 6(6), 3160 - 3165 (2005)
[10] Garcia de Rodriguez, N. L.; Thielemans, W.; Dufresne, A. Cellulose, 13(3), 261 - 270 (2006)
[11] Azizi Samir, M. A. S.; Alloin, F.; Paillet, M.; Dufresne, A. Macromolecules, 37(11), 4313 - 4316 (2004)
[12] Favier, V.; Canova, G. R.; Cavaillé, J. Y.; Chanzy, H.; Dufresne, A.; Gauthier, C. Polym. Adv. Technol., 6(5), 351 - 355 (1995)
[13] Helbert, W.; Cavaillé, J. Y.; Dufresne, A. Polym. Compos., 17(4), 604 - 611 (1996)
[14] Beck-Candanedo, S.; Roman, M.; Gray, D. G. Biomacromolecules, 6(2), 1048 - 1054 (2005)
[15] Gopalan Nair, K.; Dufresne, A. Biomacromolecules, 4(3), 657 - 665 (2003)
[16] Morin, A.; Dufresne, A. Macromolecules, 35(6), 2190 - 2199 (2002)
[17] Sriupayo, J.; Supaphol, P.; Blackwell, J.; Rujiravanit, R. Polymer, 46(15), 5637 - 5644 (2005)
[18] Paillet, M.; Dufresne, A. Macromolecules, 34(19), 6527 - 6530 (2001)
[19] Battista O. A., in Microcrystal Polymer Science, McGraw-Hill Book Company, New York (1975), p. 138
[20] Angellier, H.; Choisnard, L.; Molina-Boisseau, S., Ozil, P.; Dufresne, A. Biomacromolecules, 5(4), 1545 - 1551 (2004)
[21] Putaux, J. L.; Molina-Boisseau, S.; Momaur, T.; Dufresne A. Biomacromolecules, 4(5), 1198 - 1202 (2003)
[22] Angellier, H.; Putaux, J. L.; Molina-Boisseau, S.; Dupeyre, D.; Dufresne, A. Macromol. Symp., 221, 95 - 104 (2005)
[23] Dufresne, A. Compos. Interfaces, 7(1), 53 - 67 (2000)
[24] Anglès, M. N.; Dufresne, A. Macromolecules, 33(22), 8344 - 8353 (2000)
[25] Mathew, A. P.; Dufresne, A. Biomacromolecules, 3(3), 609 - 617 (2002)
[26] Angellier, H.; Molina-Boisseau, S.; Lebrun, L.; Dufresne, A. Macromolecules, 38(9), 3783 - 3792 (2005)
[27] Angellier, H.; Molina-Boisseau, S.; Dole, P.; Dufresne, A. Biomacromolecules, 7, 2, 531 - 539 (2006)
[28] Choi, Y. J.; Simonsen, J. J. Nanosci. Nanotechnol., 6(3), 633 - 639 (2006)
[29] Azizi Samir, M. A. S.; Alloin, F.; Sanchez, J. Y.; Dufresne, A. Polymer, 45(12), 4033 - 4041 (2004)
[30] Azizi Samir, M. A. S.; Alloin, F.; Sanchez, J. Y.; El Kissi, N.; Dufresne, A. Macromolecules, 37(4), 1386 - 1393 (2004)
[31] Azizi Samir, M.A.S.; Alloin, F.; Gorecki, W.; Sanchez, J.Y.; Dufresne, A. J. Phys. Chem. B, 108(30), 10845 - 10852 (2004)
[32] Sriupayo, J.; Supaphol, P.; Blackwell, J.; Rujiravanit, R. Carbohydr. Polym., 62(2), 130 - 136 (2005)
[33] Ljungberg, N.; Cavaillé, J. Y.; Heux, L. Polymer, 47(18), 6285 - 6292 (2006)
[34] Dufresne, A.; Kellerhals, M. B.; Witholt, B. Macromolecules, 32(22), 7396 - 7401 (1999)
[35] Noishiki, Y.; Nishiyama, Y.; Wada, M.; Kuga, S.; Magoshi, J. J. Appl. Polym. Sci., 86(13), 3425 - 3429 (2002)
[36] Sakurada, I.; Nukushina, Y.; Ito, T. J. Polym. Sci., 57(165), 651 - 660 (1962)
[37] Halpin, J. C.; Kardos, J. L. J. Appl. Phys., 43(5), 2235 - 2241 (1972)
[38] Favier, V.; Dendievel, R.; Canova, G. R.; Cavaillé, J. Y.; Gilormini, P. Acta mater., 45(4), 1557 - 1565 (1997)
[39] Favier, V.; Canova, G. R.; Shrivastava, S. C.; Cavaillé, J. Y. Polym. Eng. Sci., 37(10), 1732 - 1739 (1997)
[40] Dufresne, A. J. Nanosci. Nanotechnol., 6(2), 322 - 330 (2006)
[41] Dufresne, A.; Cavaillé, J. Y.; Vignon, M. R. J. Appl. Polym. Sci., 64(6), 1185 - 1194 (1997)
[42] Orts, W. J.; Godbout, L.; Marchessault, R. H.; Revol, J. F. Macromolecules, 31(17), 5717 - 5725 (1998)
[43] Dubief, D.; Samain, E.; Dufresne, A. Macromolecules, 32(18), 5765 - 5771 (1999)
[44] Ljungberg, N.; Bonini, C.; Bortolussi, F.; Boisson, C.; Heux, L.; Cavaillé, J. Y. Biomacromolecules, 6(5), 2732 - 2739 (2005)
[45] Gopalan Nair, K.; Dufresne, A.; Gandini, A.; Belgacem, M. N. Biomacromolecules, 4(6), 1835 - 1842 (2003)
[46] Angellier, H.; Molina-Boisseau, S.; Dufresne, A. Macromolecules, 38, 22, 9161 - 9170 (2005)
[47] Anglès, M. N.; Dufresne, A. Macromolecules, 34(9), 2921 - 2931 (2001)
[48] Dufresne, A.; Vignon, M. R. Macromolecules, 31(8), 2693 - 2696 (1998)
[49] Dufresne, A.; Cavaillé, J. Y. J. Polym. Sci. Part B, 36(12), 2211 - 2224 (1998)
[50] Azizi Samir, M. A. S.; Montero Mateos, A.; Alloin, F.; Sanchez, J. Y.; Dufresne, A. Electrochim. Acta, 49(26), 4667 - 4677 (2004)
[51] Azizi Samir, M. A. S.; Alloin, F.; Sanchez, J. Y.; Dufresne, A. Macromolecules, 37(13), 4839 - 4844 (2004)
[52] Azizi Samir, M. A. S.; Chazeau, L.; Alloin, F.; Cavaillé, J. Y.; Dufresne, A.; Sanchez, J. Y. Electrochim. Acta, 50(19), 3897 - 3903 (2005)

1

Printing processes and materials

Mechanisms of non-image area accumulation in heatset web offset

Soile Passoja, Ulla Mattila, Asko Sneck

Oy Keskuslaboratorio - Centrallaboratorium Ab
P.O. Box 70, FIN-02151 Espoo, Finland
E-mail: Soile.Passoja@kcl.fi, Asko.Sneck@kcl.fi

Abstract

Newly developed on-line microscopic imaging system provides new information about non-image area accumulation in the ink transfer unit. Ink/fountain solution compatibility together with the printing plate define the accumulation sensitivity. The blanket properties affect ink film splitting and the location of the accumulation. The paper grade influences the formation of accumulation on the blanket: coated grades form sharper accumulation edges between halftone dots and non-image areas than uncoated grade.

Keywords

Accumulation, build-up mechanism, heatset offset

1. Introduction

Traditionally, non-image area accumulation on blanket in offset printing is considered as an unavoidable process property, which lowers print quality. The accumulation looks like ink and it is visible to the naked eye after several thousands of copies. This accumulation can cause uneven dot gain leading to ghosting or decrease dot sizes, causing finally vanishing dots. It poses both press runnability and productivity problems. At worst, even 10% of the efficient printing time goes to removing these accumulations from the printing blanket thus lowering the productivity. So it is understandable that a lot of effort is put to solve these complicated problems.

In this work we demonstrate the power of the newly developed on-line microscopic imaging technique to monitor the status of the printing blanket. The microscopic imaging has been used before to study the location and state of fountain solution in ink film in laboratory scale offset roller trains [Rosenberg, 1986; Iwaki, 1990]. The development of the imaging techniques has enabled us to monitor ink transfer during printing directly from the blanket. These microscopic images give additional information on the blanket status e.g. show how dot size changes as the printing proceeds. On-line information of the press status provides tools to enhance productivity, runnability and print quality in offset printing. Moreover, timely information of the status of the blanket would ease the daily life of a printer.

2. Methods and experimental set-up

An on-line microscopic imaging system was used to monitor the accumulation build-up on blanket. A schematic illustration of the microscopic system is presented in Figure 1. The system consisted of a colour CCD-camera with a high resolution zoom lens. The field of view was about 1.3 mm x 1.7 mm. Imaging system captured on-line still images. A high speed and intensive gas-discharge illumination system was used for "freezing" the magnified image of the rolling blanket (web speed 6.2 m/s). With a 100 ns flash duration the image moved only 0.6 µm during image capturing, which made it possible to get images with a micrometer scale resolution. The camera system had trigger input from the blanket cylinder rotation to get images from the desired and constant position of the layout during print run. The microscopic imaging was done from the 15% magenta halftone area.

Small samples were cut from the blanket after printing to examine the accumulation in more detail. The location of accumulation on the blanket was examined using Hitachi S-3400N scanning electron microscope (SEM) and Thermo Scientific's Noran System Six energy dispersive x-ray spectrometer (EDX). The blanket samples were examined under SEM with secondary electron image and back scattered image mode revealing topography variations and elemental contrast variation of the accumulation. Elemental distribution over the accumulation was studied with X-ray maps.

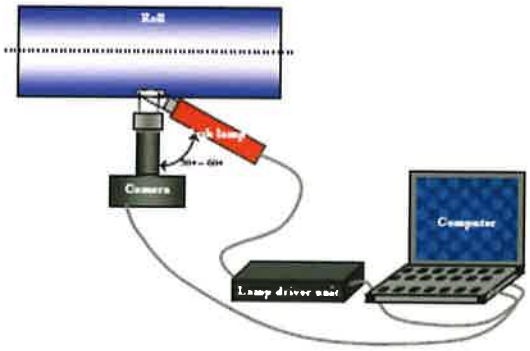

Figure 1: Schematic presentation of the microscopic imaging system

Accumulations of all types typically occur during longer print runs. Therefore 4-colour full-scale printing trials were run using appropriate test layouts to clarify the effect of materials on accumulation tendency and to find out the possible mechanisms behind the accumulation build-up. The on-line imaging was performed on the 4th printing unit of KCL's Albert Frankenthal A 101 S HSWO press at speed of 6.2 m/s. The trial was done with ink order KCYM following magenta ink transfer. Commercial inks and non-alcoholic fountain solution were used. Printings were run with traditional UV-exposure HSWO plate.

Both commercial coated (MWC, LWC) and uncoated (SC) paper grades were printed. The properties of the printed papers are gathered to Table I. The papers were printed to constant density: target density for magenta with coated grades was 1.3D and with uncoated grades 1.1D (Gretag Macbeth D196).

Table I: Properties of the printed papers

Paper sample	**MWC**	**LWC**	**SC**
Grammage, g/m^2	80	65	60
PPS-10 roughness, µm	0.92	1.05	1.15
Oil absorption, ml/m^2 a)	2.5	2.4	3.2

a) Transferred amount of mineral oil during 10 ms with KCL nozzle applicator

Two totally different compressible printing blankets were used: B1 conventional, rough surface blanket and B2 newly developed, smooth and tacky surface blanket. Besides the roughness level also the surface chemistry and the compressibility of the chosen blankets differed. Compressibility differences of similar thickness blankets were resulted as nip pressure values at the press. The nip pressure was measured with pressure sensitive foil as density values. Both blankets had lower compressibility than the normally used blankets, resulting in higher nip loads. The blanket properties are gathered to Table II.

Table II: Properties of the tested blankets used in the printing trials

Blanket sample	**B1, rough**	**B2, smooth**
Thickness, mm	1.96	1.96
Roughness, 80-1280 µm scale 1)	1.19	0.45
Surface energy, mJ/m^2 2)	18.7	31.2
Contact angle, θ, (FS 0.5 s) 2)	56.9	45.6
Contact angle, θ, (DIM 0.5 s) 2)	77.8	58.3
Nip pressure at the press, D 3)	0.69	1.34

1) Laser profilometer, NanoFocus µScan
2) Fibro DAT 1100
3) Fuji Pressure sensitive foil

On-line microscopic imaging was done separately from the blanket and from the plate cylinder. On blanket cylinder imaging was done after ink transfer and on plate cylinder before ink transfer. The experimental set-up is described in Figure 2.

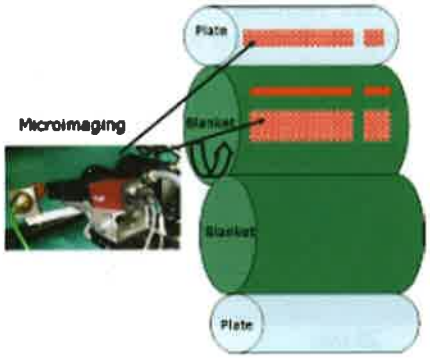

Figure 2: Experimental set-up of the microscopic imaging on the 4th printing unit

The microscopic dot sizes from the printed samples were measured with Soft Imaging Systems Analysis 3.2 image analysis program.

3. Results

The microscopic imaging system was used to monitor the status of the halftone area on blanket when printing with different materials, blankets and paper grades. The system was positioned after ink transfer. The effect of blanket properties on ink film splitting and the formation of accumulation were monitored with the rough B1 and the smooth B2 blanket. The used blankets were totally different, thus the general conclusions of the role of the blanket properties on the formation of accumulation are not conceivable. The printings were done with coated LWC paper.

After blanket wash, ink was found only in the halftone dots with the rough B1 blanket. As the printing continued, ink-like material was accumulated to the non-image area around the halftone dots in relation to machine direction. Furthermore, the dot areas were covered with ink indicating that the ink splitting occurred from the ink layer leaving some ink in the dot areas (see Figure 3 upper image series). The rough surface seems to have more intensive adhesion to ink than the internal cohesion of the ink, thus forcing the ink film split occurring from the ink layer.

As printing with the smooth blanket B2, the dot areas were covered with ink immediately after blanket wash. After a while the accumulation started to cover the whole non-image area of the blanket leaving the dot areas clean from ink (see Figure 3 lower image series). This indicates ink film splitting more near from the ink-blanket interface, thus revealing weaker adhesion forces at the interface than the cohesion forces of the ink film.

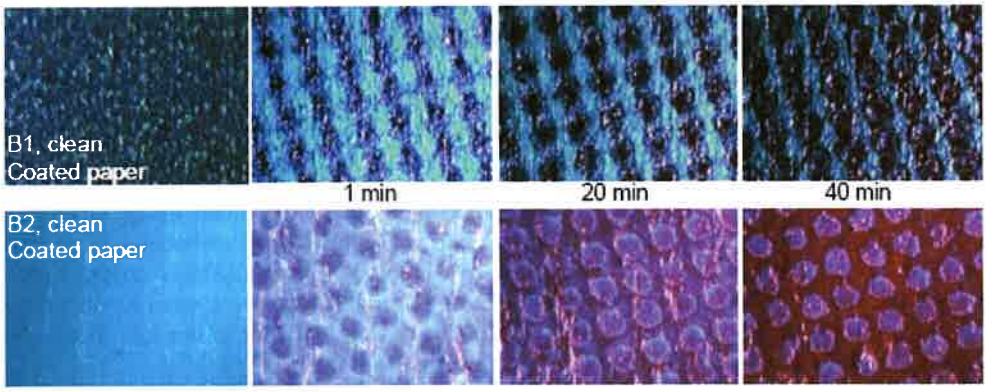

Figure 3: Blanket surface state during printing (15% magenta halftone area, ink transfer unit). Printed with coated paper. Upper image series: rough B1 blanket, lower image series: smooth B2 blanket

The effect of paper grade on accumulation build-up was examined by printing both coated (MWC) and uncoated (SC) papers with the smooth B2 blanket. The accumulation build-up on blanket was similar with both paper grades: the non-image area of the blanket was covered with accumulation. During press run-down the ink and fountain solution feeds were switched off and the blankets were run clean from ink (i.e. all available material was transferred to paper). The main difference in accumulation formation was noted in the dot areas: the dots were clean with the coated paper (upper image series in Figure 4) as the dots were having fibrous material after printing the uncoated paper (lower series in Figure 4).

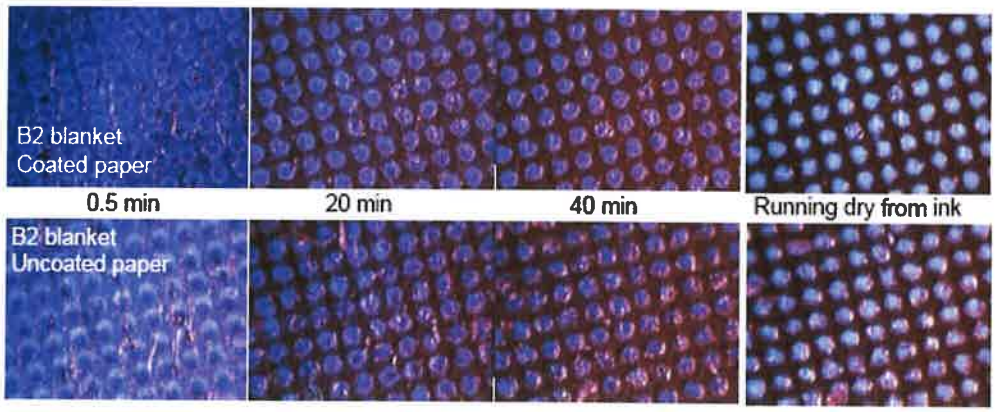

Figure 4: State of the smooth B2 blanket surface during printing (15% magenta halftone area, ink transfer unit). Upper image series: coated paper, lower image series: uncoated paper

Since the accumulation build-up on smooth B2 blanket seemed so distinct from the traditional one (rough B1 blanket), it was decided to be studied more thoroughly. After printing small samples were cut from the smooth B2 blanket to examine the accumulation in more detail. SEM images were taken from the samples.

The SEM images illustrated the accumulation crater formation on blanket where non-image areas appeared as hills and the halftone dot areas remained in valleys (see Figure 5). The results indicate that with coated paper the accumulation is collected sharply around the dots and at the end (when running dry of ink) the halftone dots are clean from accumulated material. On the contrary, with uncoated paper the accumulated material seemed to be both in the dot and around it without a sharp edge formation. Moreover, the accumulation remained in the halftone dots in running dry leaving relatively large accumulated particles both inside and around the dots (see Figure 4 and Figure 5).

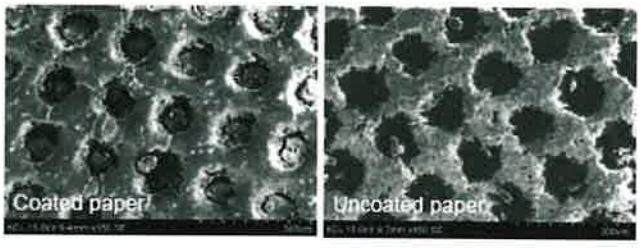

Figure 5: SEM topography images from the accumulation build-up on smooth B2 blanket. On the left: coated paper, on the right: uncoated paper

The location and type of accumulation on the blanket samples were examined using SEM/EDX and IR techniques. The coloured accumulated material consist mainly aluminium and carbonate. Clay and carbonate are elements that are both in the ink and in the paper, so it is impossible to say their origin. These elements had spread into the dot areas and their surroundings. Thus, the non-image areas were having more material than the dot areas. Fluorine was detected as Teflon, which origin is the wax in the ink. Teflon was clearly gathered as a circle around the dot or on its edges in the accumulated material.

The role of printing plate in accumulation build-up was monitored with the imaging of the plate cylinder before ink transfer to blanket. The results from the print start-up are compiled in Figure 7.

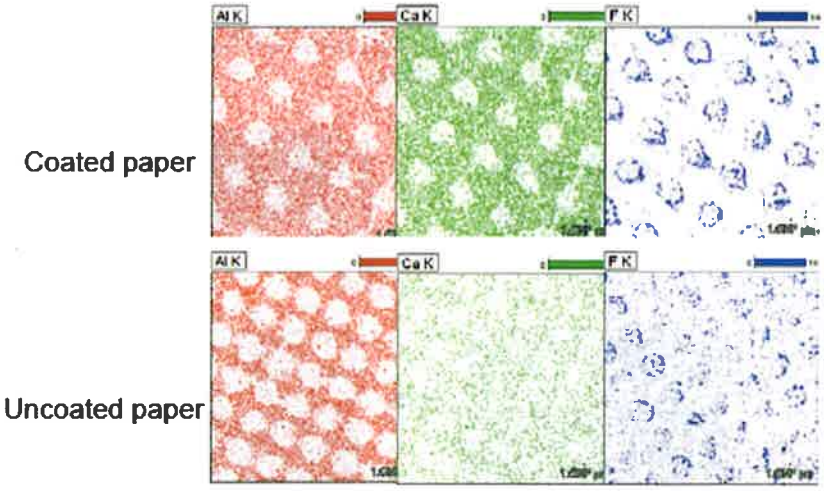

Figure 6: Example of elemental distribution in accumulated material on smooth B2 blanket (SEM/EDX method)

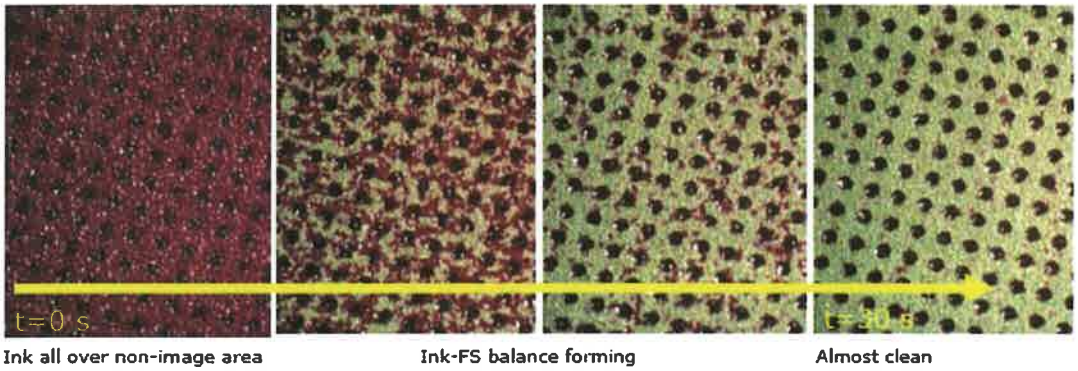

Figure 7: Microscopic imaging from plate cylinder before ink transfer to blanket. First 30 sec at start-up: inked plate, ink-FS balance forming, 15% halftone area and non-image area

The image series in Figure 7 shows the beginning of the print run, where the ink feed is switched on. At first the plate is totally covered with ink. As the fountain solution feed is turned on the ink-fountain solution balance is formed. After about 30 seconds the image and non-image area are separated on the plate. However, during print run small ink spots on both large non-image areas and around the halftone dots are detected. At the next cylinder rotation these spots have disappeared, indicating ink transfer either to blanket cylinder or to rollers in the inking unit. The former case is more likely, since the blanket cylinder is the first contact after the images have been captured and due to the fact that the ink easily transfers to the blanket. According to this monitoring it seems that the origin of the accumulation is on the printing plate.

4. Discussions

Accumulation mechanism

When starting this work, two possible mechanisms of non-image area accumulation were considered and two hypotheses were created. In *Mechanism 1,* the accumulation build-up starts on blanket (Figure 8). In this case, the ink is located only on image areas on plate and the accumulation starts from the edges of image areas (around the halftone dots and on leaving edges of the full-tone areas) on blanket.

According to the on-line imaging, the blanket surface properties seemed to have a major role in accumulation build-up: on rough blanket surface the accumulation is gathered around the dots as a circle leaving some ink into the dot areas. Conversely, on smooth blanket the accumulation is covering the whole non-image area. Furthermore, the accumulation was noted also at the leaving edges of the full tone areas (see Figure 9).

Basically, the assumed accumulation *Mechanism 1* was noted on both blankets depending on blanket surface properties: around the halftone dots and at the leaving edges of the full tone areas. However, in this notion the ink was expected to be only on the image areas of the plate.

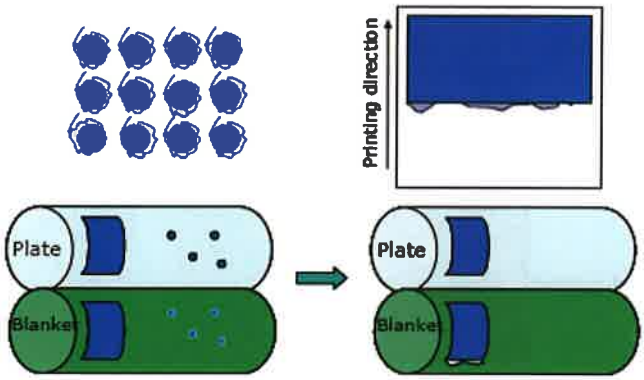

Figure 8: Assumed accumulation Mechanism 1, non-image area accumulation starts on blanket

Figure 9: Accumulation on blanket. On the left, rough B1 blanket: accumulation around the dots and in the dot area. In the middle, smooth B2 blanket: non-image area totally covered with accumulation. On the right: Ink accumulation at full-tone area leaving edge (smooth, B2 blanket). Scale bar 500μm is shown in the right image

In another considered accumulation mechanism, Mechanism 2, the accumulation build-up starts on plate (Figure 10). In this case, the accumulation starts either by reverse emulsification or by pinhole mechanism. The former term means that ink transfers to fountain solution in the form of small droplets, which start to collect on blanket, whereas the latter term refers to small fountain solution deficient areas on plate where ink can adhere. In both cases the ink is efficiently transferred to blanket, where it starts to accumulate.

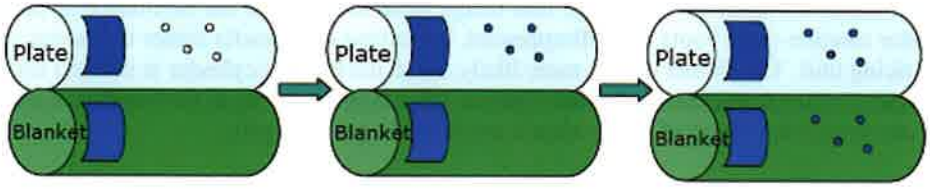

Figure 10: Assumed accumulation Mechanism 2, non-image area accumulation starts on plate

The images in Figure 11 suggest that there were ink spots on both large non-image areas and around the halftone dots. At the next cylinder rotation these spots had disappeared, indicating ink transfer to blanket cylinder. To summarize, the *Mechanism 2* type of accumulation origin was present during printing. This proves the importance of the fountain solution wetting ability and furthermore, its compatibility with the printing plate.

As comparing the accumulation formation of the coated and uncoated paper it can be seen that the accumulation with the coated grade has formed very distinct difference between the dot areas and its surroundings (i.e. accumulation), see Figure . The dot remained more in a sharp edged valley with the coated grade (MWC) than with the uncoated (SC) grade. This sharp edge might inhibit the ink transfer either from

the blanket to paper, lowering the contact area between the valley and paper surface, or prevent the contact between the plate and blanket cylinder, thus retarding efficient ink transfer there. Could the sharpness of the edge of accumulation and the location of the accumulation only around the dots be the reason for the more severe print quality problems with coated grades, such as vanishing dots?

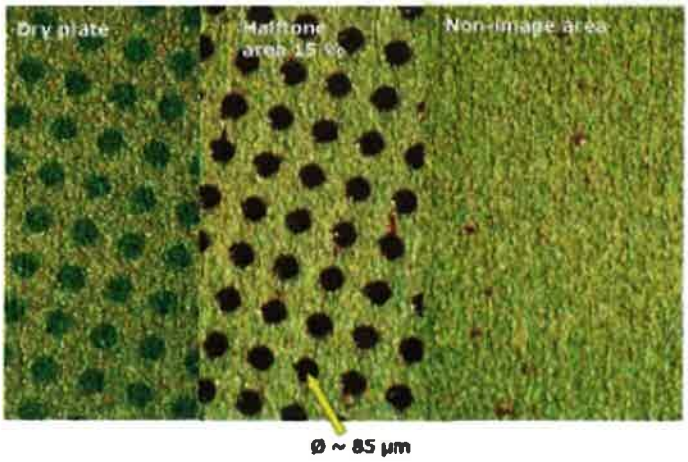

Figure 11: Microscopic imaging from plate cylinder before ink transfer to blanket: dry plate, halftone area and non-image area

With uncoated grade the edge between the dot and the accumulation was ragged and had fibrous material on it (see Figure on the right). This fibrous material cause changes in the dot edges retarding sharp edge formation. Furthermore, these ragged edges are slightly changing their position during printing thus allowing sufficient ink transfer from the ragged edges and dot areas. These ragged edge dots can also be seen in the printed uncoated paper samples, see Figure 12.

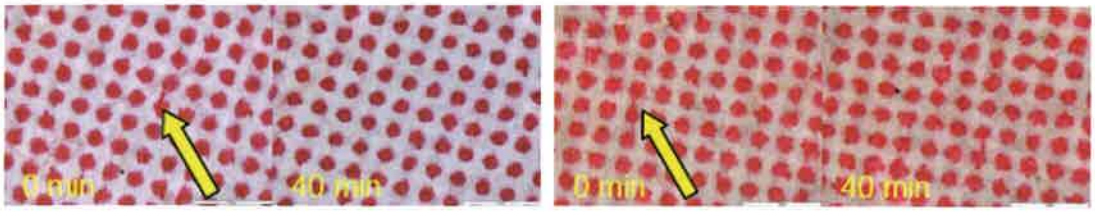

Figure 12: Microscopic images of the printed samples, printed with smooth B2 blanket. On the right: coated paper, on the left: uncoated paper

Unfortunately in this case, the printed samples had only minor differences in the dot sizes (less than 5% with microscopy method), most likely due to the high nip pressure with the blanket. Despite that, the results indicate that the changes in dot size were the biggest with coated grades. This is a finding that should be looked into more detail in future studies.

5. Conclusions

The non-image area accumulation is an unavoidable offset process property. The accumulation problems like vanishing dots and ghosting are known to be most severe offset printing problems. In this work the mechanism behind accumulation were observed with newly developed on-line imaging system. The study showed that the origin of the accumulation could be on the printing plate: between the halftone dots and on the non-image areas small ink droplets could be detected. These droplets were transferred further to the blanket where they started to accumulate during printing. The blanket properties had an effect on where the accumulation was located (either around dots or on whole non-image area). In addition, the accumulation problems were most severe with coated grades, most likely due to the sharp edge between the dot and accumulated material.

Acknowledgements

The authors wish to thank the excellent Contact Group from the paper industry: Jarkko Purontaus and Tessa Tuohikumpu (UPM-Kymmene), Jouni Marttila and Joonas Järvinen (M-real), Heikki Pietilä and Petter Kolseth (Stora Enso), Dan Forsberg (Myllykoski). The authors also wish to thank MacDermid Printing Solutions for providing the tested blankets.

References

[1] Iwaki, T., Sato, K., Nimoda, T., (1990), *Ink-Water Emulsified State in Offset Printing, TAGA proc. pp. 251 - 267*

[2] Rosenberg, A., (1986), *Feuchtmittelaufnahme von Skalendruckfarben Cyan, Magenta und Gelb für den Offsetdruck, Fogra-Forschungsbericht 5.208: München*

Tack, ink transfer and ink distribution on paper

Martin Dubé[1], François Drolet[2], Jean-Francis Bloch[3], Claude Daneault[1], Patrice J. Mangin[1]

[1] Centre Intégré and Pâtes et Papiers, Université du Québec à Trois-Rivières
3351 boul Des Forges, C.P. 500 Trois-Rivières, Québec, Canada G9A 5H7
E-mail: Martin.Dube@cipp.ca, Claude.Daneault@cipp.ca, Patrice.Mangin@cipp.ca

[2] Pulp and Paper Research Institute of Canada
570 boul. St-Jean, Pointe-Claire, Québec, Canada H9R 3J9
E-mail: fdrolet@paprican.ca

[3] EFPG
461 Rue de la papeterie, BP 65, F-38402 Saint-Martin d'Hères, France
E-mail: jean-francis.bloch@efpg.inpg.fr

Abstract

We discuss the hydrodynamic flow of a half-tone dot pressed onto model porous substrates in a range of parameters representative of printing processes. We first simulate the transfer of a fluid dot onto a two-dimensional network of pores and find that, at constant porosity, fluid transfer increases with decreasing pore size and decreases with porosity at fixed pore radius. We show that the porosity and pore size can be combined as a single variable, the specific capillary pressure, to explain the ink transfer curves. We then discuss how the tack in relation to the porous structure. We show that Stefan's law, often criticised in the literature, *correctly* predicts how tack changes with the thickness of the ink layer. Finally, we show how ink distribution is affected by horizontal pores in the network.

Keywords

Ink transfer, network, tack, porosity

1. Introduction

The transfer of a fluid from a cylinder to a porous substrate is at the heart of the printing process. The amount of fluid transferred is usually described by empirical relations such as the Walker-Fetsko equation [Fetsko, 1955; De Grâce, 1984; De Grâce, 1985], which decomposes the process into three separate phases: contact, immobilization and splitting. In general, these relations provide limited insight into the relative influence of the different parameters affecting ink transfer such as printing pressure, press speed, ink viscosity, and substrate properties. In addition, when considering the transfer of a single half-tone dot, the volume of ink that is transferred is very small and the discrete nature of the porous medium becomes important [Senden, 2000]. In such cases, transfer cannot be described in terms of macroscopic quantities such as the Darcy permeability.

One of the key quantities describing the ink is its "tack", related to the force that the fluid exerts on the substrate. It is clearly dependent on the viscosity of the ink itself, but also on operating parameters (such as press velocity) and on the paper itself through its porosity, compressibility, etc... As for ink transfer, much of the understanding about tack rests on phenomenological descriptions (Stefan's law), although precise measurements have led to further comprehension of the phenomenon [Kelha, 1974; Zang, 1991; Xiang, 1999; Gane, 2000; Guijari, 2006].

The main purpose of this communication is to discuss how the pore structure of the paper affects ink transfer and ink tack, as well as ink distribution. Specifically, we consider a drop of Newtonian liquid pressed onto a fixed porous medium and solve the corresponding Navier-Stokes equations in a range of parameters relevant to the printing process. Despite its simplifications, we believe that the model can provide valuable insights into the influence of pore morphology and press parameters on ink transfer and ink tack. We introduce in more detail our model in Section 2 and discuss ink transfer into a collection of vertical pores in Section 3. We find that, at constant porosity, the amount of fluid transferred to the substrate is largest when the pores are

small. We also show how the transfer depends on press velocity and surface forces. In Section 4, we show that Stefan's law correctly predicts how tack changes with ink volume in a printing press and show the effect of the porous structure. Finally, we discuss in Section 5 ink distribution in more complex porous structures, characterised by the presence of horizontal pores.

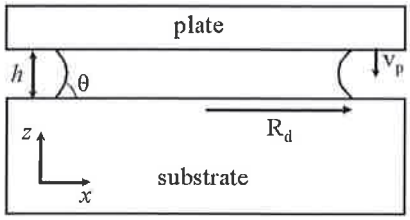

Figure 1: Model setup: a thin fluid drop is pressed between a substrate and a flat plate that moves at a prescribed velocity $v_p(t)$. The liquid-air interface meets the substrate at a contact angle θ

2. Model description of printing nip

We consider the transfer of a single halftone dot, of initial radius $R_d(0)$, from a printing cylinder onto a porous substrate. The press has velocity v_0. However, since both the cylinder and the paper have the same tangential velocity v_0, with the dot size much smaller than the radius of the printing cylinder, we neglect the horizontal component of motion [Kelha, 1994; Bohan, 2000] and consider a flat plate subject to uniform *vertical* acceleration, with velocity

$$v_p(t) = a(t - t_0) \tag{2.1}$$

as illustrated in Figure 1. The plate initially moves downward, reaches its lowest point at time t_0 and is then pulled upward. In a conventional printing unit with a rotating image cylinder, the acceleration is given by $a = v_0^2/R_c$, where R_c is the radius of the cylinder. For a cylinder with radius $R_c = 25$ cm and tangential velocity $v_0 = 1$ m/s, the acceleration $a = 4$ m/s^2. The time evolution for the plate height

$$h(t) = h_{min} + \frac{1}{2}a(t - t_0)^2 \tag{2.2}$$

introduces h_{min}, the lowest point reached by the plate, at time t_0. The value of h_{min} is not completely equivalent but related to the nip engagement and can be adjusted to yield pressures typical of a variety of printing processes [Lie, 2006]. We consider that $t = 0$ is the time at which the dot touches the substrate. The value $h(0)$ then corresponds to the initial thickness of the dot.

At this point, we do not consider any deformation of the plate or of the substrate and we treat the ink as an incompressible Newtonian fluid. The velocity field of the fluid, $\mathbf{v}(\mathbf{x},t)$ is then governed by the Navier-Stokes equations [Landau, 1998]:

$$\rho\left(\frac{\partial \mathbf{v}}{\partial t} + \mathbf{v}(\nabla \mathbf{v})\right) = -\nabla p + \eta \nabla^2 \mathbf{v} \tag{2.3}$$

where ρ is the density of the fluid, η its viscosity and p is pressure. The incompressibility condition $\nabla \cdot v = 0$, must also be imposed. Eq. (2.3) must be solved not only in the region separating the plate from the substrate but also within the pore volume invaded by the ink.

The wetting property of the fluid is described by the contact angle θ at which the liquid/air interface meets a solid surface, given by the Young-Dupré equation:

$$\sigma_{sa} - \sigma_{sl} = \sigma\cos\theta \tag{2.4}$$

where σ_{sl} and σ_{sa} are the surface tensions of the solid with the fluid and air respectively and σ is the tension of the liquid/air interface. The contact angle is also related to the capillary pressure difference p_c across that surface, through the radius of curvature of the interface. For a fluid in a cylindrical capillary of radius R_0, $p_c = 2\sigma\cos\theta / R_0$, and small pores generate larger capillary forces than large pores.

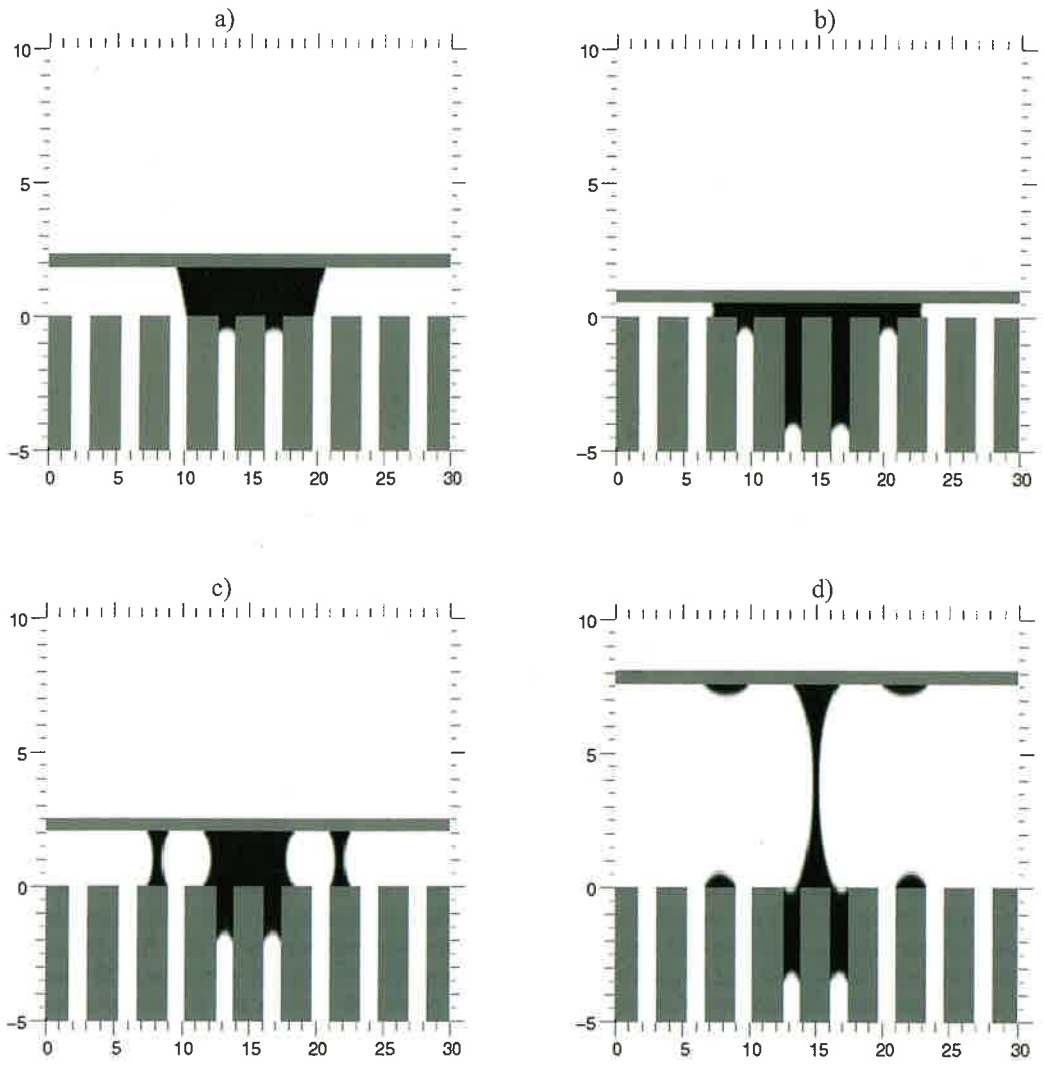

Figure 2: Numerical simulations of a half-tone dot, of radius $R_d(0)$ = 10 μm and initial thickness $h(0)$ = 2 μm pressed onto an array of vertical capillaries. The following parameter values were used: acceleration of the plate a = 1 m/s^2, surface tension of the liquid σ = 20 nN/m, fluid viscosity η = 0.2 Pa^s. The equilibrium contact angle was set to θ = 60° on both the plate and substrate. The vertical pores have size R_0 = 0.5 μm, separated by a distance of 1 μm. The figure shows the evolution (from inset a) to d)) of the fluid configuration during the transfer process. The separation between the plate and substrate corresponding to each configuration is: a) h = 2 μm during the pressing stage, b) $h = h_{min}$ = 0.5 μm, c) h = 2.0 μm during the pulling stage and d) h = 7.5 μm just before breakup of the main filament

The model proposed to solve this problem has been described previously [Dube, 2006]. We introduce a field $c(\mathbf{x}, t)$ which takes value $c = 1$ in the liquid and $c = 0$ in the air. This field has a thermodynamic origin and there exists an interface, with a finite width ζ between fluid and air regions. This interface also gives rise to a surface tension σ at the liquid/air and liquid/solid interfaces. The dynamics of the contact angle and filament breaking thus occur naturally from the dynamics and thermodynamics of the fluids. Numerically, we solve simultaneously the dynamics of the field $c(\mathbf{x}, t)$, together with the velocity field $v(\mathbf{x}, t)$ as given by the Navier-Stokes equations.

3. Ink transfer

We first discuss ink transfer for a pore structure consisting of a network of vertical capillaries. Already, this simple system shows how ink flow is influenced by the discrete nature of the substrate. For computational simplicity, the simulations are performed in a two-dimensional system, but the conclusions are readily applicable to three-dimensional cases.

An example of the network is shown on Figure 2. Each capillary has radius R_0 with L_s the distance between pores. The pore density (numbers of pores per unit area (or per unit length in two dimensions)) n of this network is thus $n = 1/(L_s + 2R_0)$ and the porosity $\phi = 2R_0/(L_s + 2R_0) = 2R_0n$. Figure 2 shows four snapshots obtained at different times during a typical simulation. In that particular example, a liquid drop of initial thickness $h(0) = 2$ μm and radius $R_d = 10$ μm was pressed into a network with porosity $\phi = 0.33$ and $R_0 = 0.5$ μm. In the initial stages of the fluid transfer process, the drop of liquid is pressed onto the porous structure, forcing liquid into the pores (Figure 2a and Figure 2b). Then, as the plate is pulled back (after the time t_0), some of the fluid is removed from the pores and filaments form between the substrate and plate (Figure 2c). Eventually, these filaments break, leaving a fraction of the fluid transferred to the substrate (Figure 2d).

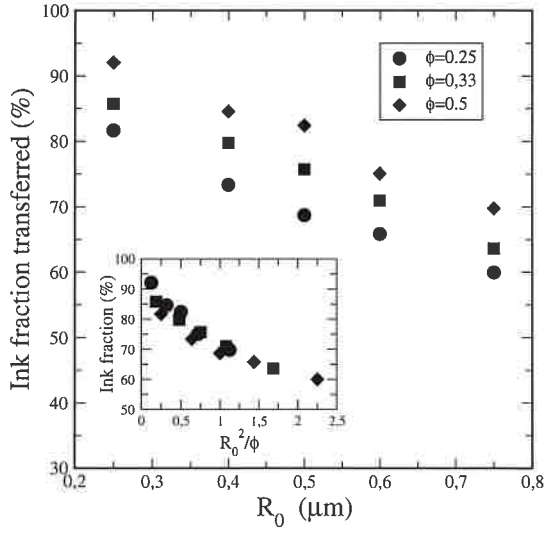

Figure 3: Fluid transfer as a function of pore size at fixed porosity $\phi = 0.25$, $\phi = 033$ and $\phi = 0.5$. The dot has initial radius $R_d = 10$ μm and thickness $h(0) = 2$ μm. The acceleration $a = 1$ m/s^2 and the minimal distance of approach $h_{min} = 0.5$ μm. The surface tension $\sigma = 20$ mN/m and viscosity $\eta = 0.2$ Pa^{-s}. The contact angle is the same on the plate and substrate ($\theta = 60°$). The inset shows transfer as a function of the specific capillary pressure. The collapse of the curves onto a single curve indicates that this is the appropriate variable to describe simultaneously the effect of pore size and porosity in the present case

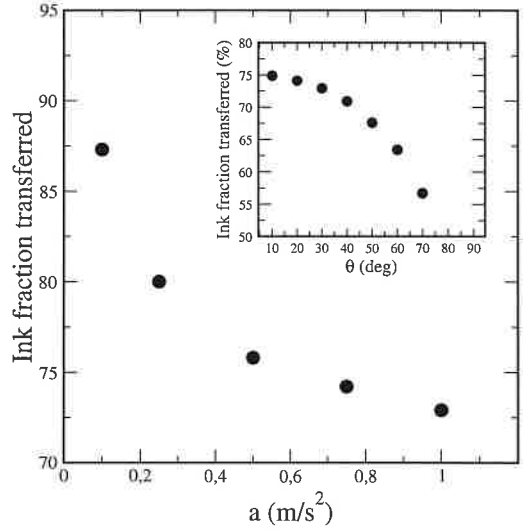

Figure 4: Fluid transfer as a function a press velocity and wetting properties of the substrate. The dot has initial radius $R_d = 15.5$ μm and thickness $h(0) = 5$ μm and the network is composed of pore of radius $R_0 = 0.5$ μm, with porosity $\phi = 0.4$. The minimal distance of approach $h_{min} = 2$ μm, with surface tension $\sigma = 20$ mN/m and viscosity $\eta = 0.4$ Pa-s. The contact angle on the plate is set to $\theta = 30°$. In the inset, the contact angle of a drop in contact with part of the substrate is changed. Transfer is more effective on more wettable substrates (low value of the contact angle)

Figure 3 shows the percentage of fluid transferred as a function of pore size at a fixed porosity ϕ. It is clear that there is more transfer for smaller pores than for larger ones. This is due to capillary forces; although large pores can take up more ink, small pores are more efficient at retaining it. The figure also shows that for a fixed value of pore size R_0, fluid transfer increases with porosity. This is in part simply because there are more pores to absorb the ink at larger porosities. We now show that those two effects (capillary and pore density) can be combined in a single variable. We recall that the capillary pressure $p_c = 2\sigma\cos\theta/R_0$. The quantity $p_c n = 2\phi\sigma\cos\theta/R_0^2$ then represents the capillary pressure per relevant unit area and introduces the combination of pore size and porosity as ϕ/R_0^2. A plot of the ink transfer curve as a function of this new variable shows a collapse of the data onto a single curve, showing that the capillary pressure per unit area is the main factor controlling ink transfer in the present case.

The effect of press velocity v_0 and wetting properties of the substrate can be observed on Figure 4. The main figure shows ink transfer as a function of plate acceleration. We recall that press velocity v_0 is related to vertical acceleration a and press radius R_c through $a = v_0^2/R_c$. For a press of radius $R_c = 25$ cm, the range of acceleration shown in Figure 4 corresponds to a range in press velocity $0.16 \text{ m/s} < v0 < 0.5 \text{ m/s}$. It is clear that there is more transfer at lower velocities, both because there is more time available for the ink to penetrate into the substrate and because the pulling forces are smaller as the plate recedes from that substrate. The inset of Figure 4 shows that the wetting properties of the substrate have a large effect on ink transfer. In particular, transfer decreases rapidly with increasing contact angle above 40° or so.

4. Ink tack

4.1 Stefan's law

The concept of ink tack is often linked to Stefan's law, which describes the force F(t) that is exerted by a liquid column placed between two moving plates, when capillary effects are neglected. For a circular column, that force is given by [Landau, 1998]:

$$F(t) = \frac{3\pi}{2}\frac{\eta v_p(t)}{h^3(t)}R_d^4(t) \tag{4.1}$$

where η is the viscosity of the fluid, $v_p(t)$ is the velocity of the plate at time t, h(t) their separation and $R_d(t)$ the radius of the column. This result is valid within the so-called lubrication approximation, which implies a thin dot ($h/R_d \ll 1$) and a flow that is predominantly parallel to the plate. Those conditions are reasonably satisfied in a printing press.

However, it is often argued that Stefan's law does not apply to printing because it predicts that the tack of ink should decrease as the ink film thickness increases, contrarily to what is seen in most experiments [MacPhee, 1997a; MacPhee 1997b]. In general, however, that argument is incorrect, as we now show by calculating the value of the tack explicitly. First, we note that ink volume is conserved at all times, which implies that $R_d^2(t)h(t) = R_d^2(0)h(0)$ and allows us to rewrite Eq. (4.1) as

$$F(t) = \frac{3}{2\pi}\frac{\eta v_p(t)}{h^5(t)}\Omega^2 \tag{4.2}$$

where $\Omega = \pi R_d^2(t)h(t)$ is the volume of the dot. Already this argument shows that tack will increase with ink volume. However, further discussion requires a more precise definition of tack. We define tack as the maximum force exerted by the fluid on the plate. After some straightforward algebra using Eq. (2.1), Eq. (2.2) and Eq. (4.2), together with volume conservation, we find,

$$F_{max} = \frac{\pi}{\sqrt{2}}\left(\frac{9}{10}\right)^5 \eta\sqrt{a}R_d^4(0)h^2(0)h_{min}^{-9/2} \tag{4.3}$$

Tack is now expressed as a function of plate acceleration (related to press velocity), viscosity, initial volume of the dot and nip engagement. It is clear that tack increases linearly with viscosity and press velocity. Tack

also increases strongly with dot radius. However, the dependence of tack on dot thickness h(0) and nip engagement h_{min} depends on the type of experiment that is performed:

i) When the dot is pressed onto and then pulled from the substrate, as in a printing process, h(0) and h_{min} are independent, with $h_{min} < h(0)$. eq. (4.3) then predicts that whereas tack decreases as the minimum distance between the plate and substrate is made larger ($F_{max} \sim h_{min}^{-9/2}$), it *increases* with the initial thickness of the halftone dot ($F_{max} \sim h^2(0)$).

ii) The situation is different if the dot simply rests on the substrate and the plate is pulled upward. This is similar to the setup used by Stefan in his original experiment. In that case, the minimum separation h_{min} is equal to its initial value h(0) which also corresponds to the initial dot thickness. Equation (4.3) now predicts $F_{max} \sim h^2(0)\, h_{min}^{-9/2} = h^{-5/2}(0)$ implying that tack *decreases* with the initial thickness of the ink layer.

These results explain why tack is found to increase with film thickness when measured between two rollers [Zang, 1991] (which squeeze the fluid before pulling on it) while the opposite trend is observed when measured with a parallel plane tackmeter (which only involves pulling of the fluid layer between two plates) [Kelha, 1974]. Nevertheless, it is clear that Stefan's law, as presented above, does not quantitatively apply to the printing process, since it neglects the effect of the porous structure.

4.2 Tack for a network of capillaries

The inset of Fig. 5 shows how the pressure acting on the substrate changes in time for a collection of vertical capillaries (similar to the one shown in Fig. 2) of various sizes. The pressure is positive in the pressing phase (plate moving towards the substrate), indicating that the plate is pushing on the substrate, and it is negative in the receding phase (plate moving away from the substrate), which corresponds to a pull on the substrate. The figure shows that there is a clear asymmetry in the pressure, the negative peak being larger than the positive peak, and we thus define tack as the peak in pressure during the receding phase of plate motion. The three curves in the inset also indicate that tack is larger for smaller pores, due to the increased capillary pressure which opposes the motion of the plate.

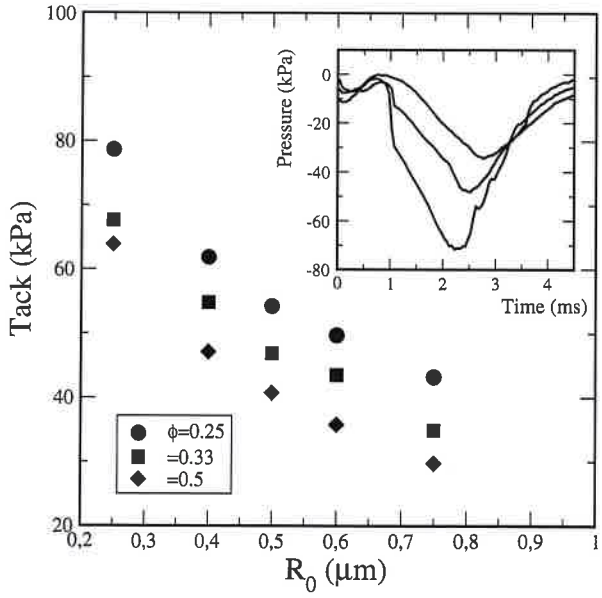

Figure 5:
Tack as a function of pore size at fixed porosity for an ensemble of vertical pores and the parameters described in Fig. 5. The tack is defined as the maximum in force during the receding phase of plate motion and increases with decreasing pore size. The inset shows the evolution of the force as a function of time for the case $R_0 = 0.25$ µm (largest value of the tack), 0.5 µm and 0.75 µm (smallest tack)

This is also confirmed in the main figure which shows tack for various porosities and pore sizes. At fixed porosity, tack clearly increases with decreasing pore size. For a fixed pore size, however, tack decreases with increasing porosity, since there are less solid surfaces on which to exert the pull.

5. Ink distribution

Finally, we discuss qualitatively the effect that pores of various sizes and position may have on fluid transfer. Here, we also include horizontal pores in the network. Those pores can have a large influence on fluid

transfer. At an intersection between vertical and horizontal pores, the liquid front is stopped until the pressure is large enough to force it into the crossed pores [Senden, 2000]. Typically, if a pore has radius R_0, a pressure of the order σ/R_0 is necessary to push the fluid out of it. However, if some liquid has been transferred to a horizontal pore, it then remains trapped in that pore, since tack is essentially a vertical force.

The numerical simulations show that the *local* quantity of fluid transferred depends to a large extent on the local pore structure. Smaller pores can lead to a large overall transfer and tend to keep the fluid close to the surface of the porous medium. Figure 6 shows the distribution of fluid transferred within a porous structure containing both large and small vertical pores, together with horizontal pores. The four different cases correspond to four different values of the parameter h_{min} in Eq. (2.2), describing the minimal distance between the plate and the surface. Smaller values of h_{min} lead to larger values of pressure. These figures show the fluid configuration at $h = 1.0$ μm, as the plate is being pulled. It is clear that there is less transfer to horizontal pores as the pressure is reduced. However, it is interesting to note that it is those horizontal capillaries adjacent to large vertical pores that remain filled most easily. This is because the pressure for breakthrough decreases as the pore size increases.

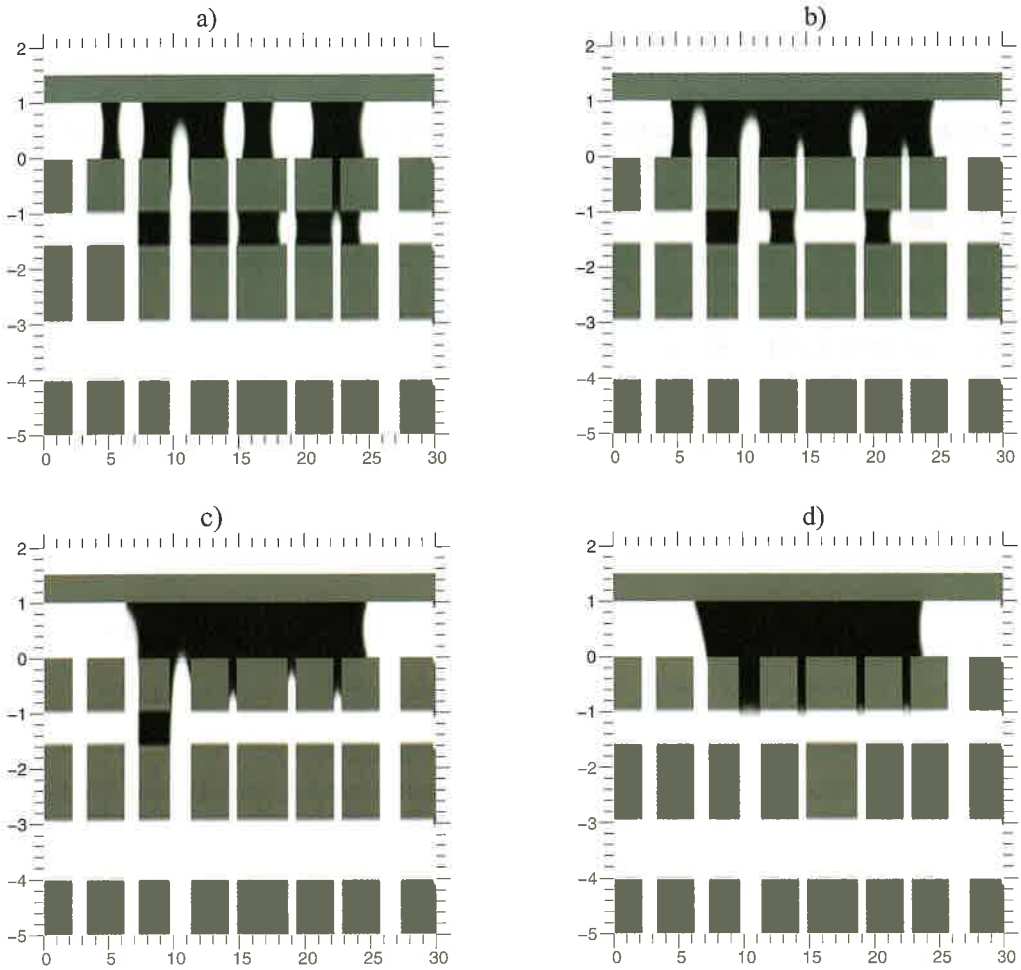

Figure 6: Fluid configuration as a function of the pressure on the plate.
The values of h_{min} = 0.25 μm, 0.50 μm, 0.75 μm and 1.00 μm correspond to the inset a), b), c) and d) respectively

6. Conclusion

The results presented above illustrate the role of pores in ink transfer phenomena. We have shown that both the size of the pores and their density are important variables [Schoelkopf, (2000); Preston, (2002)], and that, in the cases considered, they can be combined into a single variable, the specific capillary pressure. We also find that small pores influence ink tack. For two networks of similar porosities, ink tack will be larger for the network with the smaller pores. At equal pore size however, networks with a lower porosity will lead to larger

tack. We have also shown that one has to be careful about how tack experiments are performed and that Stefan's law does indeed predict correctly how tack varies with ink film thickness.

Acknowledgements

We thank J. Aspler from Paprican and P. Lepoutre for useful comments and advices, as well as the National Sciences and Engineering Research Council of Canada for funding.

References

[1] Fetsko J. M., Walker W. C. (1955). Measurements of Ink Transfer in Printing Coated Paper, Am. Ink Maker 33 (11), 38

[2] De Grâce J. H., Mangin P. J. (1984). A mechanistic approach to ink transfer. Part I: Effect of substrate properties and press conditions. Advances in Printing Science and Technology, W. H. Banks Ed., Pentech Press (London) 17, 312

[3] De Grâce J. H., Mangin P. J. (1985). A mechanistic approach to ink transfer. Part II: The splitting behaviour of inks in printing nip, Advances in Printing Science and Technology, W. H. Banks Ed., Pentech Press (London), 19, 146

[4] Senden T. J., Knackstedt M. B., and Lyne M. B. (2000). Droplet penetration into porous networks, role of pore morphology, Nordic Pulp Paper J.15, 554 - 563

[5] Kelha V., Manninen M., Oittinen P., Tiesmaki J (1974). Tack force measurement and picking, Tappi J. 2 (4), 86

[6] Zang Y., Aspler J. S., Boluk M. Y., De Grâce J. H., (1991). Direct measurement of tensile stress (tack) in thin ink film, J. Rheology 35(3), 345

[7] Xiang Y., Bousfield D. W., Hassler J., Coleman P., Osgood A. (1999). Measurement of Local Variation of Ink Tack Dynamics, J. Pulp Paper Sci. 25, 326

[8] Gane P. A. C., Schoelkopf J., Matthews G. P. (2000) Coating imbibition rate studies of offset inks. 2000 Tappi International Printing and Graphic Arts Conference, Savannah GA, Tappi Press

[9] Gujjari C., Batchelor W., Sudarno A., Banham P. (2006). Estimation of ink tack in offset printing and its relationship to linting in offset printing. 2006 Tappi International Printing and Graphic Arts Conference, Cincinnati

[10] Bohan M. J. F., Claypole T. C., Gethin T. D., Megat Ahmed MMH. (2000). A model for ink impression in printing contacts, J. Pulp Paper Sci. 26, 414

[11] Lie C. (2006). The influence of backpressure on ink drying and dot gain in sheet fed offset printing. Advances in Printing Science and Technology, N. Enlund and M. Lovrecek Ed., Acta Graphica (Zagreb) 32, 245

[12] Landau L. D., Lifshitz E. M. (1998). *Fluid Mechanics*. Butterworth-Heineman (Oxford UK)

[13] Dubé M., Drolet F., Daneault C., Mangin P. J. (2006). Hydrodynamics of ink transfer. Tappi International Printing and Graphic Arts Conference, Cincinnati (2006)

[14] MacPhee J. (1997a). A unified view of the film splitting process, part I. J. Am. Ink Maker 75 (1), 42

[15] MacPhee J. (1997b). A unified view of the film splitting process, part II. J. Am. Ink Maker 75 (2), 51

[16] Schoelkopf J., Gane P. A. C, Ridgway C. J., and Matthews G. P. (2000). Influence of inertia on liquid structure absorption into paper coating structures, Nordic Pulp Pap. Res. J. 15 (5), 480

[17] Preston J. S., Elton N. J., Legrix A., Nutbeem C., Husband J. C. (2002). The role of pore density in the setting of offset printing ink on coated paper. Tappi J. 1 (3), 3

Aquapiling: Coated substrate-related influences on reverse piling from a one-side single colour image in multicolour offset printing

Patrick A. C. Gane[1], Cathy J. Ridgway, Peter Burri, Manfred Arnold, Karl-Heinz Kagerer[2], Barry Madden, Matti Ristolainen, Jarkko Purontaus[3]

[1] Laboratory of Paper and Printing Technology, Helsinki University of Technology
P.O. Box 6300, FI-02015 TKK, Finland
E-mail: patrick.gane@omya.com

[2] Research and Technology Services, Omya AG, CH-4665 Oftringen, Switzerland
E-mail: forename.surname@omya.com

[3] UPM Research Center, UPM-Kymmene Corporation, FI-53200 Lappeenranta, Finland
E-mail: forename.surname@upm-kymmene.com

Abstract

A series of 11 coated papers, ranging from single coated LWC to multicoated woodfree grades, was tested extensively on a heatset web offset press under chosen conditions shown to create problems of heavy build-up on the blanket occurring at the non-image area of a later unit on stochastic mid tone areas where no image existed on the reverse side - termed reverse piling. The nature of the deposit, and the fact that it corresponded to the one side image area only, led to hypothesise an interaction between the printed image on the coated paper and the fountain solution gaining access at each subsequent unit from both the reverse side and the black image side where no further colour was applied. Raising the temperature on the press by reducing fountain solution cooling made the phenomenon significantly worse when using an alcohol-free fountain solution. It is shown by using methods of permeability, porosimetry, ink tack development and coating structure network modelling, that the problem is linked to the combination of two main properties: low absorption potential by the basepaper matched by a lack of permeability of the coating when and only when a predominance of nanopores (< 0.1 μm) is present - a feature needed in modern press rooms for fast setting and the required speed of turn around of the printed product. The phenomenon of reverse piling in this case of fountain solution interaction is described using the novel term, "aquapiling".

Keywords

Aquapiling, base paper absorption, coating permeability, ink-fountain interactions, reverse piling

1. Introduction

Blanket piling in the offset press is often related to the ink tack behaviour on paper, especially in relation to the relative adhesion between the blanket and the paper surface. In the case of coated papers, the tack increase as a function of time has frequently been implicated [Concannon and Wilson, 1992, Gane et al., 1994] as a cause of blanket piling. In parallel, the effect of fountain solution as the cause for water interference mottling and/or tail edge picking is often associated with an inability of a coated paper to remove fountain solution laid down on a previous unit before further ink is applied.

In the cases discussed here, the piling tendency of a series of 11 commercial papers was studied on a heatset web offset press, using an ink and fountain solution combination, which, together with the standard press settings, led in some cases to an extreme blanket build-up on a subsequent printing unit, usually the last colour unit, of the first laid-down colour. The effect was exacerbated when using high tack ink and an alcohol-free fountain solution, especially at high temperature, effected by reduced fountain solution cooling. The reverse piling effect was predominant in areas where the paper was only printed on one side by a single colour (stochastic mid tone black). The build-up was not seen as progressive along the unit train, but appeared suddenly at the last printing unit indicating that a threshold had been reached beyond which the adhesion of the ink to the coating surface failed and transfer occurred onto the printing blanket. Furthermore, the nature of the distribution of the deposit indicated a delocalisation of the ink once separated from the paper surface, i.e. a planar shearing of the ink laterally over the blanket, as shown in the photograph in Figure 1.

No simple correlation could be found between the coating pigment formulation and the reverse piling tendency. This, even though the papers in question ranged from predominantly clay-containing light weight coatings on wood containing basepapers, through higher calcium carbonate-containing coatings on alkaline wood containing and woodfree light and medium weight coatings, respectively, to carbonate dominating heavy weight multicoated alkaline woodfree grades. The commercial papers used came from both North America and from Europe.

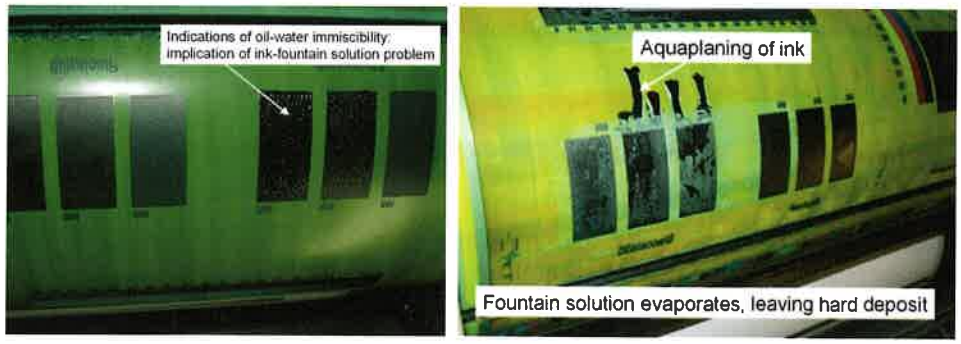

Figure 1: The photographs show the reverse piling of the first laid black ink on the last unit (yellow) of the heatset press: indications of delocalisation of ink deposits and shearing by the proposed aquaplaning ("aquapiling") mechanism

The threshold nature of the problem, i.e. its sudden appearance in the last printing unit, and the positioning of the adhesion failure to the paper coating surface, led to the hypothesis that a surfeit of fountain solution on or near the paper surface acting either to lift the ink from the surface by the action of film continuity next to the blanket [Gane et al., 2000a], where the force to separate a thin film between two plane surfaces increases dramatically as a function of the separation and speed, or by the hydraulic pressure from under the ink as excess fountain solution is expelled at the surface under the pressure of the printing nip, a proposal made previously by Ridgway et al. [Ridgway et al., 2002] in the case of a newly developed light weight coated newsprint product. To test this hypothesis the interaction of liquid and substrate is studied together with the pore structure of the coatings.

A broad range of analyses has been applied, including the absorption of liquid by wicking into the xy planar direction of the paper (machine direction), air and liquid permeability of the coated sheet in the transplanar z direction, ink-on-paper tack development using the ISIT device [Gane et al., 1994], mercury intrusion porosimetry and subsequent modelling of the coating layer permeability using a network model Pore-Cor[1].

1.1 Paper samples and ranked performance

A summary of the 11 paper samples and their component analysis for this study is shown in Table I. The ranking was made visually on the press in respect to the level of blanket build-up, together with tape-pull samples and photographs made after 35.000 - 40.000 copies. The printing plate used was half conventional screening and half stochastic. The greatest build-up occurred in the stochastic mid tone regions (20%, 35% and 50%).

All pilot printing, four trials in all, were made at the Future Printing Center (FPC) in Raisio, Finland on a Heidelberg Web 8 with a cutting length of 630 mm and web width of 500 mm. Printing was done with both typical European printing conditions and typical N. American printing conditions with this equipment. The test conditions are summarised in Table II.

The print layout (Figure 2) included both conventional and stochastic screening sections, the stochastic screening being used to represent the effect of finer dots in respect to their increased dot perimeter length, equivalent to 70 lines per inch. The web was divided into two conventional and two stochastic sectors in the machine direction. All the pictures and colour bars were printed with both screening methods. The conventional screening was elliptical 60 lines per cm screening and the stochastic was Staccato 35, in which the average dot size was 35 µm. The Staccato screening was done with the Creo method. With this kind of layout it was possible to see the differences in piling tendency between the screening systems.

Table I: Paper samples

Sample	Grade and pigment content	Origin EU Europe NA North America	Visual rank low = good	Basis weight / gm^{-2}	Thickness / µm	Ash content / %
A	**LWC** more clay than carbonate	EU	4	65	53	37.8
B	**LWC** more carbonate than clay	EU	4	60	52	34.4
C	**LWC** more clay than other minerals	EU	1	60	54	30.2
D	**LWC** more clay than carbonate and other minerals	EU	1	65	54	31.6
E	**LWC** only clay	NA	3	60	52	27.6
F	**MWC** only clay	NA	3	60	83	31.8
G	**LWC single coated** more carbonate than clay	EU	5	65	51	39.4
H	**wood-free double coated** more carbonate than clay	NA	2	70	59	27.3
I	**MWC single coated** more carbonate than clay	EU	2	80	66	36.2
J	**wood-free double coated** more carbonate than clay	EU	2.5	70	67	41.9
K	**wood-free double coated** more carbonate than clay	EU	1.5	90	69	42.2

Table II: Test conditions

Inks	Commercial North American type inks Commercial European type inks
Ink sequence	1st unit: black 2nd unit: cyan 3rd unit: magenta 4th unit: yellow 5th unit: only pressure with fountain solution
Fountain solution	IPA free, N. American type fount, pH 3.9 IPA 6%, European type fount, pH 5.2
Fount temp	10°C (50 F) for cool conditions 17°C (63 F) for warm conditions (practice often > 25°C)
Web speed	5.6 ms^{-1} (32.000 rph)
Blankets	Reeves Vulcan Alto Plus
Printing Plates	Kodak Gold (Didp Gold - positive plates)
Air temperature	22°C (72 F)
Humidity	48 RH-%

Figure 2: Print form layout for the printing trials

The print runnability of the papers with respect to reverse piling was evaluated in the stochastic mid tone region of the first down ink (black) with a non-image area on the opposite face throughout, stochastic screening being shown to be the configuration having the most problems with the press running under N. American conditions. The papers were ranked in order such that the poorest performance paper is placed as 5 and the best performance paper as 1.

2. Methods and results

2.1 Impact of press parameters

The comparison of North American (NA) with European (EU) press conditions showed the European conditions of lower tack ink and isopropanol (IPA) containing fountain solution to be the less demanding in respect to the reverse piling tendency. However, clearly certain adjustments to the NA system could also be applied to reduce the problem.

One major question that is frequently posed when comparing the two running conditions is: what is the impact of fountain solution pH (NA 3.2, EU 5.9) when carbonate-containing coated papers are used? This is addressed in the following analysis of fountain solution after prolonged running.

2.1.1 Fountain solution analysis

Elemental analysis was made from the fountain solution samples taken each trial point after every 10.000 impressions. Aluminium, calcium and silicon were considered to be of the most interest following the hypothesis of pigment dissolution and especially calcium carbonate leaching. However, it could be shown that the different paper grades did not have an influence in how much calcium is found in the fountain solution, despite the widely varying amounts of carbonate present in the coating formulations. Moreover, approximately the same amount of dissolved calcium was found in the fountain solution of the EU and NA printing conditions virtually independently of the fountain pH. Only about 1-2 mgdm-3 more calcium was found in the NA fountain solution system and this amount is considered not to be significant, Figure 3.

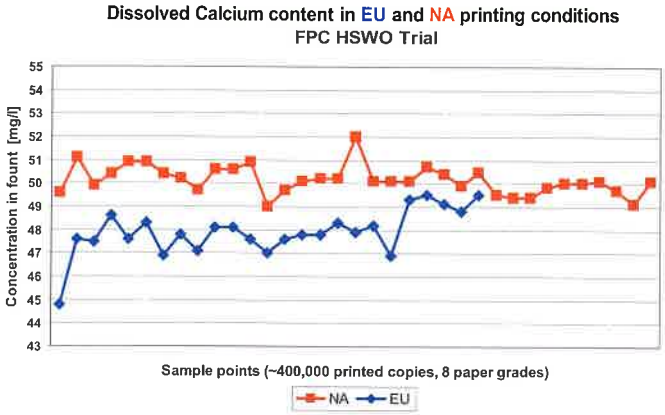

Figure 3: Measured dissolved calcium in the fountain solution supply tank after every 10.000 printed copies for each paper grade comparing North American and European fountain solution types. Clearly both systems reach a similar dynamic equilibrium concentration despite their difference in pH, far away from the static equilibrium saturation level of 475 mg Ca^{2+} dm^{-3}

2.2 Paper-ink and paper-liquid interactions

2.2.1 Ink-surface interaction testing

The first interaction analysis of the 11 papers was made using the Ink Surface Interaction Tester ($ISIT^2$) [Gane et al., 1994]. Ink-on-paper tack is measured by a special attachment which consists of a solenoid, a coil spring, a load cell and a contact disc. The separation process using the ISIT, Figure 4, relies on the adhesion of the ink surface to a rubber-like blanket material, resembling that of an offset blanket, which is brought into contact with the ink at a given time after printing. This is achieved by a tack wheel which has the blanket material attached to its surface. The tack wheel is rolled into contact with the ink layer, held stationary and then removed under a controlled force regime (constant rate of change of acceleration). The maximum force required to remove the tack wheel is recorded

as the tack force. The sequence is automatically repeated for a predefined number of cycles chosen to span the regions of the tack force under study. The build-up of the tensile force required to achieve each individual separation is recorded with time and can be analysed through specifically designed software. The maximum level of tensile force at each test point is plotted as measured tack force development with time.

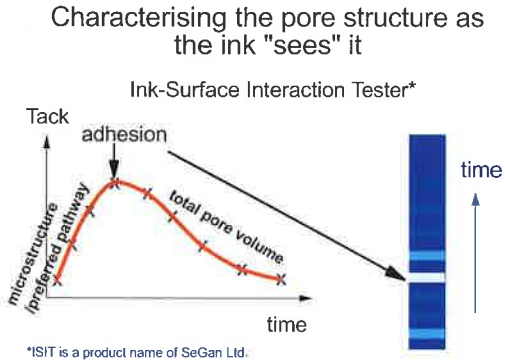

Figure 4: Ink-Surface Interaction Tester: the apparatus and the measurement of ink tack cycle and ink-coating adhesion at maximum tack

The curve can be interpreted in three parts: the tack rise, the maximum tack force and the tack decay. The tack rise time, t_{max}, is a measure predominantly of the capillary action of the finest pores in the coating, the maximum tack force is a measure of the cohesion in the ink competing against the "affinity" that the ink has for the coating surface. If the tack rise time is short and/or removal of ink occurs at this maximum tack force, i.e. the adhesion of the ink to the coating is poor, it can lead to potential piling problems. Too high a maximum leads to rupture at the weakest point in the paper. The tack decay is a measure of the total pore volume characteristic of the coating "as seen by the ink". It typically shows the level of coating consolidation that has taken place, for example in calendering or during drying, together with the diffusional properties of ink oils into the polymer network of synthetic binders, such as latex. Often, too fast a fall leads to poor ink curing and a tendency to rub off, and too slow a fall indicates potential for set-off. Furthermore, if the sample shows post-tack adhesion failure, due to too fast a fall, then dry print adhesion is clearly suspect. A further value used to compare samples is derived from this tack fall, the tack decay constant, $\tau_{1/2}$, which is defined as the half height decay time away from the maximum tack, Figure 5.

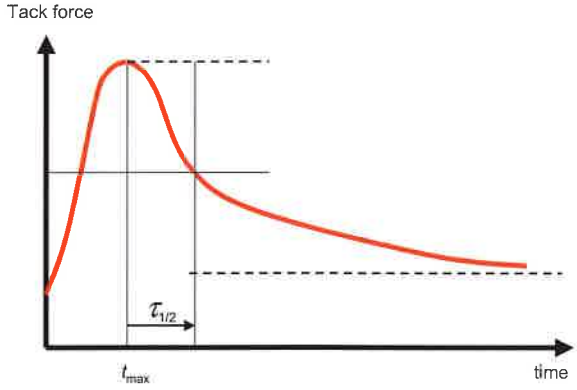

Figure 5: Tack rise time, t_{max}, and tack decay constant, $\tau_{1/2}$

The maximum tack force, T_{max}, time to maximum, t_{max}, and the tack decay constant, $\tau_{1/2}$, for all the samples are examined, Figure 6 and Figure 7 respectively. The more fine (nano)pores there are present, the faster the tack rise will be and, depending on residual available volume, the tack decay constant may or may not be dependent. When more large pores are present and fewer fine pores then the larger will be the tack decay constant.

There do not seem to be any clear trends between T_{max} or $\tau_{1/2}$ in relation to the piling-related runnability of the papers. The case of paper E is unique in the series, in that it is behaving as an uncoated paper in respect to ink

tack, i.e. not absorbing ink vehicle to promote complete tackification, except that it does have a smoother surface, higher tack maximum, than would be expected from an uncoated paper. This paper is likely to be coated with a coarse pigment formulation and/or coating coverage is very limited.

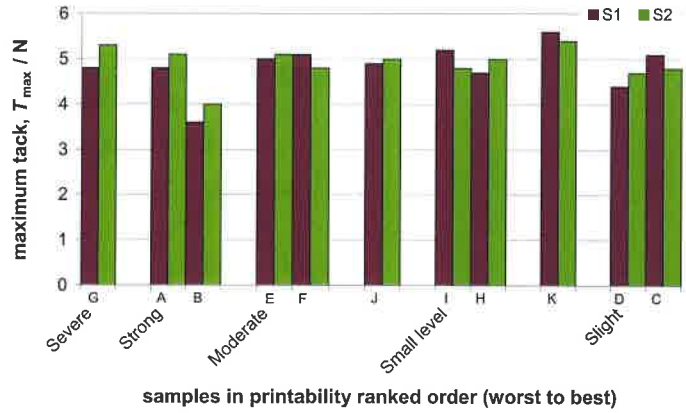

Figure 6: Maximum tack values, T_{max}, on the two sides of the paper samples S1 and S2

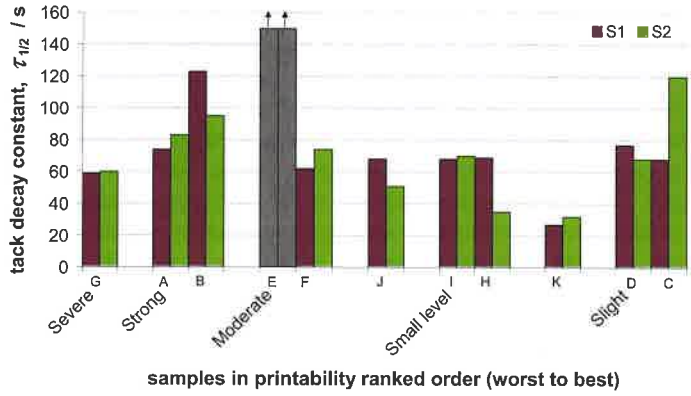

Figure 7: Tack decay constant, $\tau_{1/2}$, on the two sides of the paper samples S1 and S2. Sample E shows non-drying of the ink

In Figure 8, the time to the maximum tack point is plotted against the tack decay constant for measurements on both sides of the papers. Once again paper E is behaving anomalously and more like an uncoated sheet.

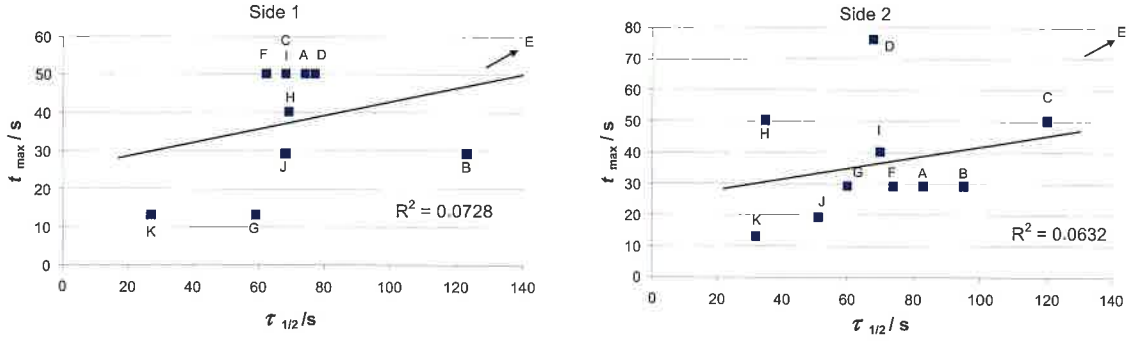

Figure 8: Time to maximum tack, t_{max}, plotted against tack decay constant, $\tau_{1/2}$, for each side of the paper samples

A number of papers do show strong deviations from side to side. Fitting trend lines to the plots of time to the maximum tack point, t_{max}, against tack decay constant, $\tau_{1/2}$, measured on each side of the samples, not surprisingly shows that there is no correlation between the two parameters across the wide range of paper

types ($R^2 < 0.1$), though correlation may be present for small variations in each paper construction subset, which suggests that they can be decoupled when considering this series of papers.

A slow tack rise and a relatively fast fall are typical for well controlled ink tack behaviour on a glossy paper. Paper K fulfils these requirements (Figure 8) and indeed lies in the upper rankings based on performance. However, this is clearly not the single controlling criterion for good runnability, i.e. the coating-ink interaction is not the key factor alone. Having stated that these two parameters are not dependent on one another and can be decoupled it is necessary to look at them independently and to determine their influence on the other print materials, including fountain solution, and properties of the press.

2.2.2 Porosimetry

Since the results for ink surface interaction alone do not provide correlation with the reverse piling phenomenon, the pore size distribution was investigated to learn more about the pore volume capacity and likely pore size distribution effects, i.e. the differences between the amount of fine and coarser pore sizes.

For these measurements a strip of the sample is wound into a spiral and held in position with nylon thread to such an outer diameter that it can be placed in the sample holder (penetrometer) without touching the wall. This is to minimise the effects from sample surface contact with itself and with the penetrometer wall during mercury intrusion, which are typical of strongly two-dimensionally biased samples. This procedure prevents the formation of pockets between the sample and the penetrometer that might fail to become intruded at low pressure, and is described in more detail in Ridgway et al. [Ridgway and Gane, 2003].

Mercury intrusion measurements were made using a Micromeritics Autopore IV mercury porosimeter. The maximum applied pressure of mercury was 414 MPa, equivalent to a Laplace throat diameter of 0.004 μm (~ nm). The equilibration time at each of the increasing applied pressures of mercury was set to 60 seconds. It is vital that the mercury intrusion measurements be corrected for the compression of mercury, expansion of the penetrometer and compressibility of the solid phase of the sample. This was performed conveniently using the software Pore-Comp[3] [Gane et al., 1996].

There are often (irreproducible) differences for a given sample at equivalent Laplace diameters greater than 10 μm, which are generally attributable to the occlusion effect due to the irregularity of surface fibres, as described in a previous publication [Ridgway and Gane, 2003]. The data have therefore been truncated at 10 μm. This means that the total porosity cannot be evaluated, rather the relative porosity in those pores with an equivalent Laplace diameter < 10 μm is derivable by direct comparison of the truncated curves. Figure 9 shows the mercury intrusion curves for the 11 paper samples supplied for testing after correction [Gane et al., 1996]. The mercury intrusion data show there is a strong bi-modal distribution for all the papers, representing the basepaper and coating interface pores, and the coating structure independently.

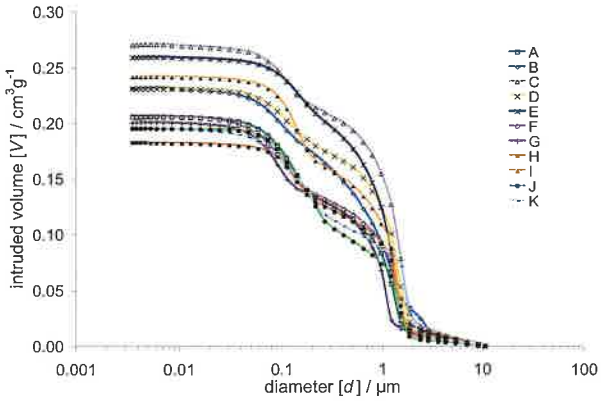

Figure 9: Mercury intrusion curves of the 11 paper samples truncated at 10 μm

The intruded volumes into the samples over the diameter range 0.004 - 10 μm are summarised in Table III.

Table III:
Total intruded volume into the 11 paper samples

Sample	Total intruded volume / cm^3g^{-1}
A	0.21
B	0.23
C	0.27
D	0.23
E	0.26
F	0.21
G	0.20
H	0.21
I	0.24
J	0.20
K	0.20

The mercury intrusion data are indicative of the packing structure and the general fine pore structure of the sheet. By taking the first derivative of the cumulative intrusion curve the pore size distributions based on equivalent Laplace diameter, inevitably including pore-shielding, are revealed. This is shown in Figure 10.

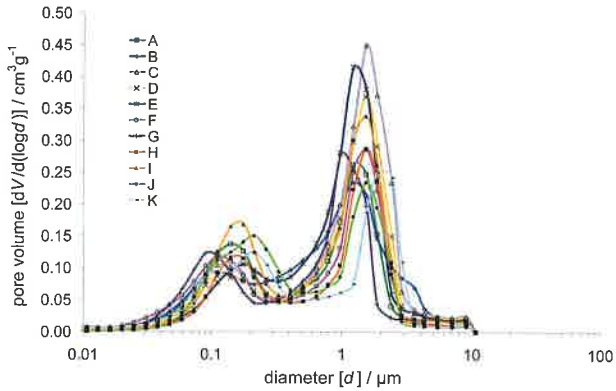

Figure 10: Pore volume distribution of the 11 paper samples

The fine pores represent the capillarity and combined with the coarse pores represent the permeability and the basepaper structure. Figure 9 shows the fine pore size distributions in more detail.

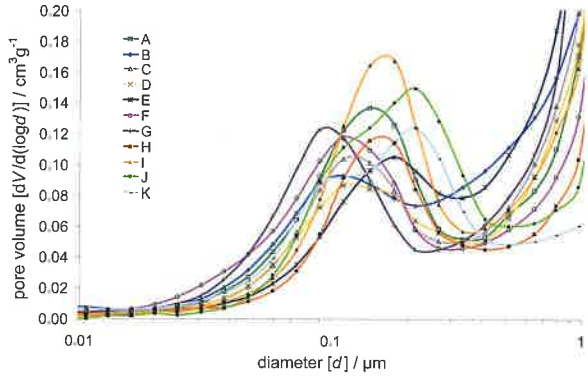

Figure 11: Fine pore volume distribution of the 11 paper samples

Here in Figure 11 we find the evidence that paper E, unique amongst the set, trends strongly toward a coarse pigment formulation having relatively large coating pores spread in distribution toward the basepaper interface pore region, and thus behaving more like a matt coating structure having a smoothing effect on a surface that otherwise is behaving as an uncoated paper. The multicoated papers J and K show nicely the precoat versus topcoat distributions, inasmuch that the breadth of the secondary peak is increased toward larger pores, i.e. for these two samples the secondary peak is itself bi-modal [Ridgway and Gane, 2003]. Papers F and G have the highest pore volume attributable to the nanopores < 0.1 µm.

The samples with more fine pores lead to a higher capillarity (faster ISIT tack rise) and hence a faster tack rise, t_{max}, and possibly tack decay, $\tau_{1/2}$, constant, and this can be seen, for example, with samples F and G. However, if a coating layer is predominantly made up of ultrafine pores, the ability of liquid to flow through the structure (permeability) will be reduced. Since the interaction related to reverse piling appears not to be solely dependent on capillarity differences, we now investigate the permeability of the structures in relation to that capillarity.

2.2.3 Permeability in z direction of the coated papers

A liquid permeability method is used, which has been described in detail in Ridgway et al. [Ridgway et al., 2003]. A stack of paper samples (approximately 125 sheets cut to 1.5 x 1.5 cm^2) is placed into a mould[4] under a slight overpressure, applied by a suitable light weight to ensure the sheets are lying flat, and resin[5] is poured around it. The quickly rising viscosity of the chosen curing resin results in a penetration of approximately 1 mm locally at the outer boundaries of the sample. This penetration depth is clearly visible because of the opacity change at the edge of the sample and can, therefore, be calibrated. The open area of the porous sample, i.e. that free from resin, is evaluated so that the permeable cross-sectional area can be established. The sample discs are placed in a dish containing the probe liquid in order to saturate the void network of the sample before placing in the apparatus. Hexadecane is used in the experiments, having density ρ = 773 kgm^{-3} and viscosity η = 0.0034 $kgm^{-1}s^{-1}$, which is known to fill the entire saturation-available void volume of a pigmented porous structure [Gane et al., 2000b], when measured gravimetrically, and largely avoids any interaction with latex or fibres. The sample disc is then placed in a specially constructed pressure cell. The use of the resin to embed the samples allows for rigid clamping and sealing of the sample into the pressure cell chamber. Gas over-pressure is supplied from a nitrogen bottle. The pressure cell is fixed over a microbalance and a PC samples the balance data using specially-developed software[6]. A drop captor device is needed in the base of the cell to guide the permeated liquid drops to the outlet. An important point of practical technique is that the whole chamber below the position of the sample has to be pre-wetted with the liquid so that each drop leaving the sample causes a drop to fall into the sampling dish. Once these precautions are taken the continuity of flow is ensured.

The continuous flow can be expressed in terms of the Darcy permeability constant, k, as

$$\frac{dV(t)}{dt} = \frac{-kA\Delta P}{\eta l} \qquad (1)$$

where dV(t)/dt is defined as the flux or volume flow rate across an area, A, ΔP is the applied pressure difference across the sample, η is the viscosity of the liquid and l is the length of the sample, in this case calculated as the number of sheets multiplied by the sheet caliper.

The permeability is dominated by the coating layer(s) when the coating coverage is complete, and dominated by the gaps in the coating and the basepaper when the coverage is poor, Figure 12.

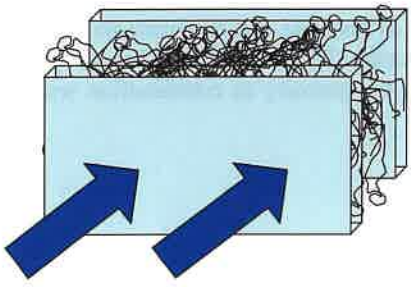

Transplanar permeability (coating dominated)

Figure 12:
Determining the effects of coating and basepaper on the transplanar permeability

These experimentally measured liquid permeability values are compared to the Bendtsen air permeability values of these papers [often mistakenly interpreted as "porosity", i.e. it is the flow through the paper and not a quantitative value of the pore space within the paper]. Figure 13 shows these values plotted together with the measured liquid permeability values. The two measurements give similar trends although there is a big

scatter with one particular outlier, paper B. Deviation between the two methods signifies a dominant role of the coating coverage - air finds it very difficult to get through a coating and compresses strongly, whereas liquid does not compress. This illustrates that the air permeability is best used for uncoated or only lightly coated papers and less so for heavy weight coated grades.

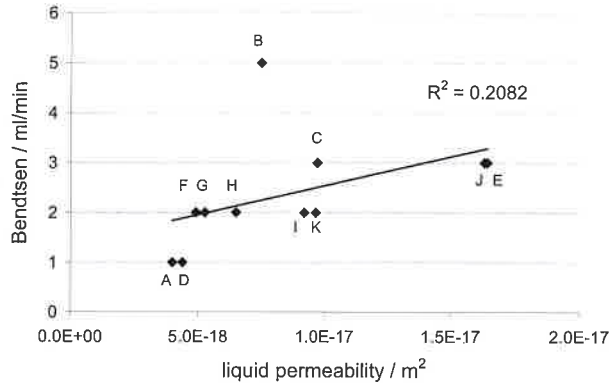

Figure 13: Liquid permeation results in comparison to the more usual air permeability test

There are frequently geographical differences in respect to basepaper permeability, for example, NA basepapers are seen to be generally more permeable than EU basepapers. When coated, the papers still tend to reflect this property, despite the use of higher levels of clay on NA papers, due to the fact that access to the basepaper in the case of LWC coatings is still a given, resulting from the limitations in coverage, exacerbated in that NA papers also generally have less coating.

Given that the permeability values strongly depend on coverage, the effects of permeability linked primarily to coating structure can only be deduced from these direct permeation measurements in the case of heavily coated papers. Due to this limitation a further step is now taken in which the measured pore structure of the coating is used to model the permeability of the coatings alone.

2.2.4 Modelling the coating pore structure

A network computer model, which simulates the void-space structure of porous material, is used to model the structures of the coatings alone to determine the permeability values directly associated with the coating. The model has been employed previously to illustrate structures of a wide range of porous materials including sandstones [Matthews et al., 1996], medicinal tablets [Ridgway et al., 1997], soil [Peat et al., 2000] and paper coatings [Ridgway et al., 2001, Schoelkopf et al., 2000]. It uses a unit cell with 1.000 cubic pores in a 10 x 10 x 10 array, connected by up to 3.000 throats, i.e. one connected to each cube face, that are either cylindrical or double conical [Ridgway et al., 2001] according to the prevailing geometry of the sample material. The structures are optimised such that the simulated intrusion curves match as closely as possible the experimental mercury intrusion curves, and the experimental porosity is accurately reproduced. The model provides not only a structure that eliminates the effects of pore shielding, by considering the porosity in combination with the given Laplace pressures, but also delivers a representative connectivity.

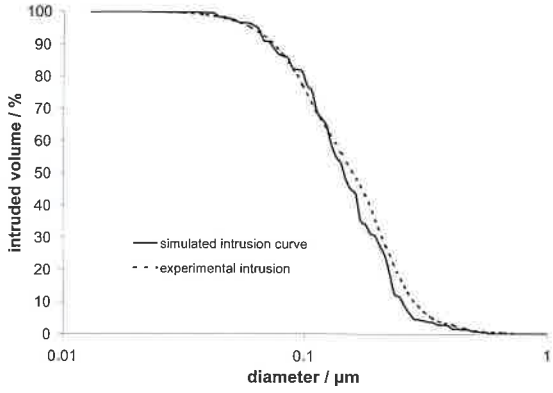

Figure 14: Simulated and experimental mercury intrusion curves for the coating fraction in sample J

The simulated intrusion curves match closely the experimental mercury intrusion curves, as exemplified in Figure 14, and the experimental porosity is accurately reproduced. The porosities of the coatings were calculated by taking the approximation of the weight proportion of the total pore volume of the sample as related to the ash content, and can be seen in Figure 15. The unit cell for sample J is shown as an example in Figure 16.

In this case of paper J, as just one example, it is clear to see that the connectivity and throat sizes in Figure 16 are limited, and so one can suspect that the permeability of the coating layer will be lower than suggested by the direct measurement, indicating the effects of reduced coverage.

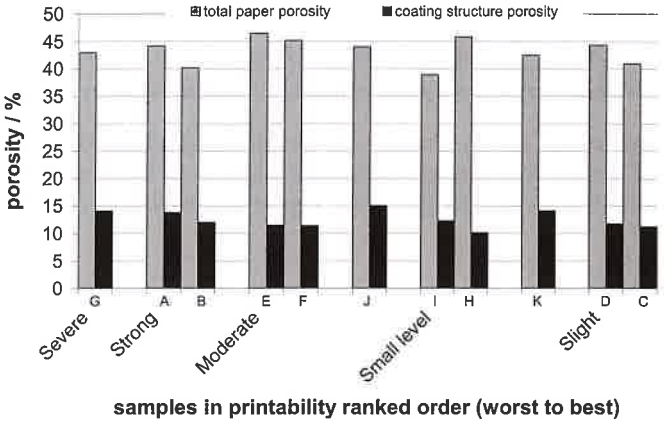

Figure 15: Porosity values of the total paper and of the coating structure alone - samples ranked from bad to good in respect of reverse piling

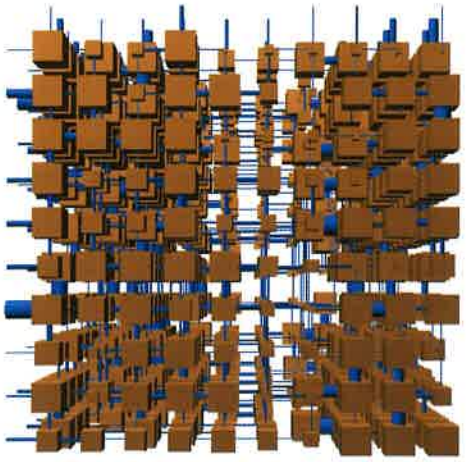

Figure 16: Simulated network structure using cylindrical throats for the coating structure of sample J, unit cell size = 17.96 μ

2.2.4.1 Simulated permeability

The continuous flow, or permeability, can be expressed as described previously in terms of the Darcy permeability constant, k, using Darcy's Law, [Darcy, 1856] [1].

The laminar flow resulting in a parabolic velocity distribution within a liquid volume V, in time t, for a horizontal circular tube of length l, radius r, containing a fluid of viscosity η, flowing under a differential pressure ΔP, is expressed via the Poiseuille equation as:

$$\frac{dV}{dt} = \frac{\pi r^4 \Delta P}{8\eta l} \qquad (2)$$

where the term r^4/l corresponds to the volumetric flow capacity Ξ. In using the Poiseuille equation, it should be recognised that it is only a first approximation to the resistive flow of a feature within the network.

Now it is assumed that Poiseuille flow occurs across the whole cell:

$$\left(\frac{dV}{dt}\right)_{cell} = -\frac{\pi}{8\eta}\,\Omega_{cell}\left(\Xi_{arcs}\right)\Delta P_{cell} \tag{3}$$

where Ω_{cell} is an averaging operator over the whole unit cell, as described in the work of [Matthews et al., 1993] operating on the flow capacities of the arcs (Ξ_{arcs}) in which an arc represents a pore-throat-pore pathway between nodes sited at the centre of each pore. Each arc in the flow network is the flow channel between adjacent nodes, positioned at the centre of each pore. It generates a term which is related to the effective Poiseuillean capacity of the cell for flow in the –z direction (from the top to the bottom face), and in the ±x and ±y direction. Flow, however, is not allowed in the +z direction, thereby applying an implicit positive pressure gradient with respect to z. A network analysis approach to this problem supplies a term $\Omega_{cell}(\Xi_{arcs})$ as the maximal flow capacity through the network of pores and throats. It is calculated by means of the 'Dinic' network analysis algorithm [Matthews et al., 1993]. There is an overall conservation of flow, so that the entire volume of fluid entering the top of the unit cell emerges at the bottom, with no build-up through the network. The value obtained, as the maximal flow, is an average of the capacity values over only those channels found to carry flow.

The combination of the Poiseuille equation, (3), with the Darcy equation, (1), results in an expression for the absolute permeability independent of the pressure gradient imposed on the sample:

$$k = \frac{\pi}{8}\,\Omega_{cell}\left(\Xi_{arcs}\right)\frac{l_{cell}}{A_{cell}} \tag{4}$$

The simulated permeabilities, representing the coating alone, are compared with the experimentally measured permeabilities, which represent the paper sample as a whole, i.e. coating and basepaper, in Figure 17.

Samples A, C, E and K stand out as points having big differences between the coating permeability and the permeability of the composite (Figure 17). Sample K is a multicoated product, whereas samples A and C are light weight products. It may be concluded that the differences shown by A and C, in respect to coating permeability, reflect their differences in coating formulation - the clay rich sample C having the lower coating permeability, as would be expected. Sample A on the other hand shows a much higher simulated coating permeability in relation to the measured permeability including basepaper. In this case the permeability of the paper is clearly limited by the basepaper. It can thus be deduced that these samples show relatively poor coating coverage (not surprisingly since they are LWC papers) since their measured permeability is related more to the basepapers than to the coatings. The deviation for sample K, on the other hand, reflects the strong influence of the thicker combined coating layers. Paper E has a highly permeable light weight coating in combination with a relatively permeable basepaper.

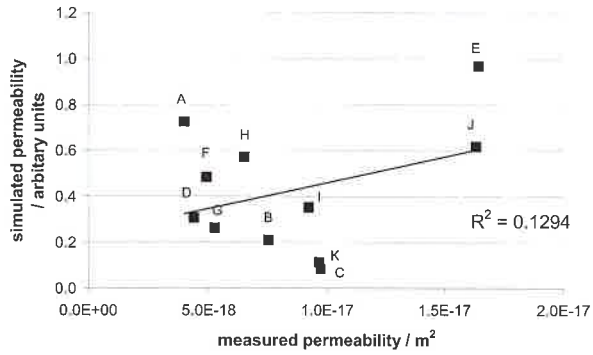

Figure 17: Simulated permeability of coating alone and experimental permeabilities of the coating and basepaper composite

The permeability is controlled by the larger pores in the structure as long as they are connected throughout the structure. The permeability, therefore, should be greater the lower the fine pore volume and the greater the

larger pore volume. The volume of fine pores less than 0.1 μm was calculated from the porosimetry measurement, Figure 18. The proportion of < 0.1 μm pores is responsible for the high capillary action pores which "hold on" to liquids and don't let them pass into the basepaper.

Paper C, as discussed above, has a particularly low coating permeability and, as we see, a rather low level of ultrafine pores, Figure 18, though the composite structure with the basepaper included has a higher measured permeability, stressing the strong role of the basepaper in this case. Combining these factors seems to have resulted in the best runnability performance, certainly amongst the light weight papers, though it must be recognised according to the ISIT curve that the reduced volume of ultrafine pores does lead to a slower initial tack response as expected. On the other hand, the isolation of the basepaper by multicoated layers, when present, such as for papers H, J and K, or when heavy coat weight is used, as for paper I, means that the interactions are likely to be overwhelmingly coating dominated, and when sufficient volume is present in such coatings the role of the basepaper is less important.

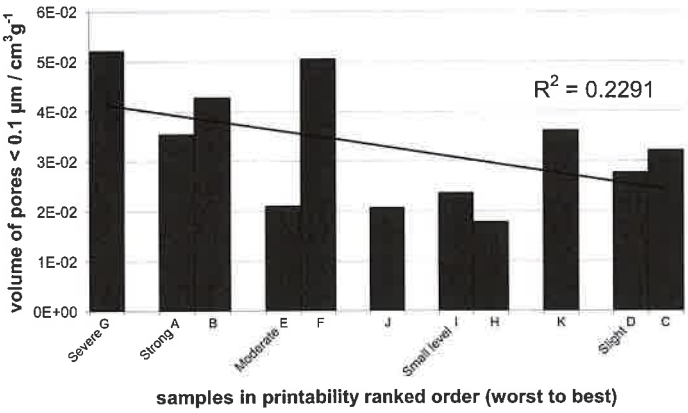

Figure 18: Fine pore volume < 0.1 μm trends weakly with piling tendency: R^2 value increases slightly to 0.34 with the exclusion of paper E

The additional information we have gained from the comparative permeability analysis now gives us an indication of the parameters requiring detailed investigation, i.e. amount of ultrafine pores, coating permeability and composite permeability in relation to the absorption power of the basepaper. Hence, the role of basepaper now receives focus so that the composite effect can be more completely elaborated.

2.2.5 Absorption by Wicking (length direction)

The accessible porous volume of paper can be measured by absorbing liquid, such as, hexadecane, which, as described in the permeability section, is known to fill the entire saturation-available void volume of a pigmented porous structure [Gane et al., 2000b]. By using this alkane, interaction with latex and with fibres, which occurs as a component of many coatings and paper stock respectively, is largely avoided. A number of paper tests that are based on oil absorption make the same assumption [TAPPI Press, 1998].

The method adopts the geometry of wicking of liquid into the xy (machine or cross-machine) directions, i.e. length-wise into the paper. These samples were measured for consistency in the machine direction. The sample is hung, dipping into a dish of liquid in a wicking configuration with its planar surface held vertically. The weight loss from the dish is continually recorded in a draught-free environment. This method is descibed in detail in Schoelkopf et al. [Schoelkopf et al., 2000]. The absorption curves during liquid uptake can be expressed as a linear relationship between the linear flux V(t)/A and $\sqrt{t}$, the gradient of which is

$$\frac{d(V(t)/A)}{d\sqrt{t}} = \frac{d((m(t)/\rho)/A)}{d\sqrt{t}} \qquad [5]$$

where m(t) is the mass uptake at time t, as defined by a volume V(t) of fluid of density ρ. The data are normalised to the cross-sectional area of the sample, A (an unknown parameter if water were being used due to reaction with fibres), such that the data become V(t)/A, the volume absorbed per unit cross-sectional area

example of the absorption rate gradient for a paper sample is shown in Figure 19, which shows the mass loss from the liquid source, the negative slope relates to the liquid being lost from the reservoir, i.e. that being absorbed by the paper. This property is not only dependent on capillarity but also on sheet permeability. The gradient of the data gives an absorption rate of the fluid uptake.

This measurement is dominated by the basepaper (in volume terms), Figure 20, and so gives a measure of absorption rate and capacity of basepaper underlying the coating.

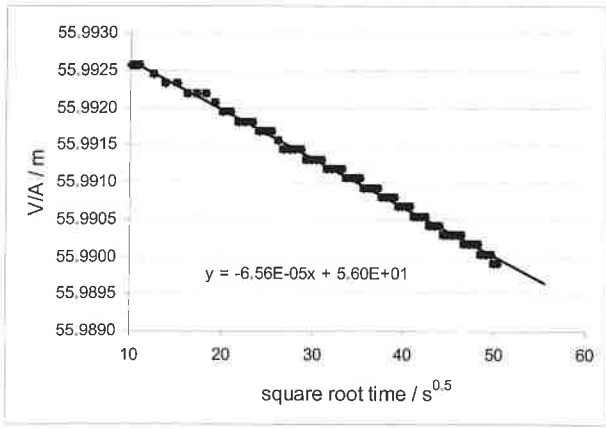

Figure 19: An example of the absorption rate gradient during wicking

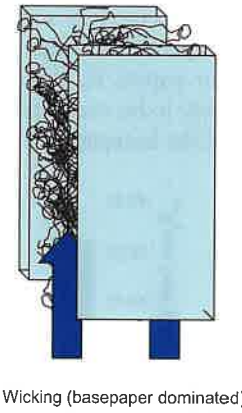

Figure 20: Determining the effects of basepaper absorption by wicking

Figure 21 shows the absorption rates of the hexadecane uptake into the papers calculated as the linear gradient of the volume uptake per unit cross-sectional area plotted against the square root of time. The absorption rates are plotted against the ranking order of the samples.

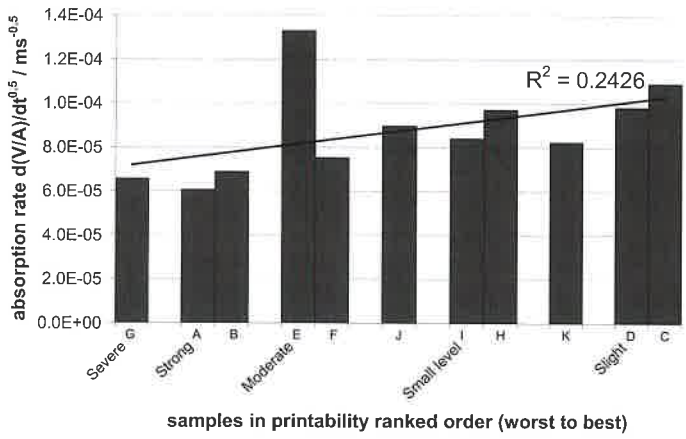

Figure 21: Absorption rate of hexadecane into the paper samples correlates weakly (apart from paper E) with improved piling resistance

Once again we see the anomalous behaviour of paper E. If this paper is removed from the series then we see a strong correlation with basepaper absorbency, and in general we can say that for most coatings, the basepaper plays a very important role.

As seen, with the exception of paper E, there is clearly a trend showing that a higher absorption rate leads to a better runnability of the paper, i.e. the absorption in the xy wicking plane, dominated by the basepaper absorption properties is an important optimisable parameter. Paper E is suspected to have an unsized basepaper, and so the unusually high basepaper wicking in the xy direction would be expected, and shows us that the role of the coating needs further description.

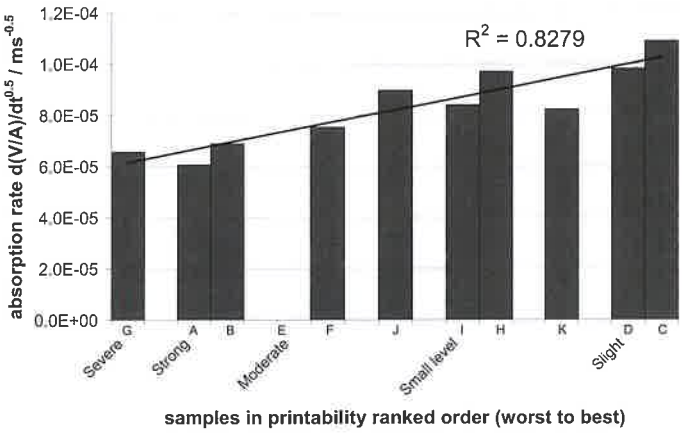

Figure 22: Absorption rate of hexadecane into the paper samples (predominantly basepaper absorbency) correlates strongly with improved piling resistance when paper E is excluded

The absorption rates are proportional to xy permeability over longer periods, provided the capillarity can drive absorption, i.e. the faster the absorption is over long time the less the role of capillarity in retaining liquid. This contrasts to the z permeability described earlier, which is a measurement of coating and basepaper together, whereas the absorption measurement here is basepaper dominated in volume terms.

3. Discussion: combining the factors - correlating with press parameter performance

We see now from Figures 18 and 21 that a good runnability against reverse piling needs a high coating permeability in the case where the coating contains a significant volume of ultrafine pores (as in most modern high bright papers), together with a high basepaper absorption rate. This combination will act to avoid a saturated surface of the paper while the ink is experiencing high tack forces. Alternatively, the coating may be non-permeable and non-absorbent: not a realistic option amongst modern high brightness papers unless uneconomic amounts of binder are incorporated.

The results show that the biggest problems on the press set-up shown to generate the reverse piling problem occur when the basepaper has low absorption and the coating is non-permeable but with high capillarity, i.e. fast ink setting but not letting liquid such as fountain solution pass through to the basepaper and preventing rapid equilibration of pressure in the printing nip. The basepaper absorption properties are therefore fundamentally important - it should be absorbent. Depending on the basepaper, the coating should be either non-permeable and low in ultrafine pores if the basepaper is highly absorbent or be permeable when ultrafine pores are present to allow the basepaper volume to be accessed - meaning not having only fine pores, particularly on non-absorbent bases, but a proportion of larger coating pores to allow permeability for liquids to reach the basepaper. This combination is vitally important in the case of light weight papers, where the pore volume in the coating is limited.

Fountain solutions formulated without IPA are frequently less viscous. Furthermore, if the temperature of the fountain solution is higher, so its viscosity will be reduced even more. The basepaper is insulating, so it stays cooler through the press. The coating, however, warms rapidly [Gane et al., 2006] and this moves the behaviour into a regime of highly absorbing coating and slow wicking basepaper. Thus, combining a low viscosity fountain solution on a hot press is likely to flood the coating structure. This analysis once again also links in well with the negative effect if the basepaper fails to absorb, as the flow of fountain solution around the laid down ink in the last nip increases. Additionally, both the emulsifying capacity of the ink will decrease generally as a function of reduced fountain viscosity and the sterically dispersed ink pigment may also suffer thermal destabilisation as temperature rises, each effect, either separately or combined, leading once again to the support of the hypothesis of an unstable ink-fountain solution relationship underlying the phenomenon.

The effect of a flooded paper surface, or flooded body of the paper entering a pressure zone, will be to form a thin film effect next to the blanket. It is known that a thin liquid film between two parallel surfaces generates an enormously high force resisting separation, [Poivet et al., 2003]. If this thin film forms in the region of the mid tone print, supplied by copious volumes of fountain solution applied at the previous non-image stations

both front and back, after the ink has become strongly tackified by capillary action of the coating, the separation forces generated are suspected to lead to ink-coating adhesion failure, particularly when the coating resists pressure equilibration through to the basepaper.

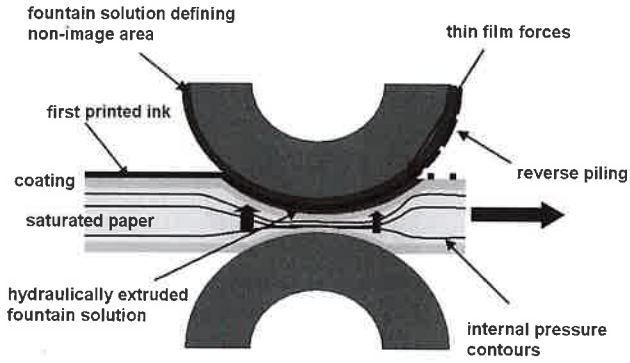

Figure 23: Mechanism of aquapiling in the printing nip. The diagram illustrates the action in the area of a one-side printed dot as the paper moves from left to right in a subsequent printing nip

The phenomenon, best described as hydraulic coupling of the blanket and ink via a layer of fountain solution forced above, and/or under the print, is described using the novel term, "aquapiling", and illustrated graphically in Figure 23.

To get at the relative importance of the combined effects, i.e. coating capillarity and permeability, and basepaper absorption potential, each with their relatively low R^2 correlation factors due to outlier points in each response separately, Figure 18 and Figure 21, respectively, a function was generated using the parameters of wicking rate in the dipping experiment, raised to the power a, multiplied by the volume of pores < 0.1 μm, raised to the power b, where a and b are adjusted to make the product approximately constant. By plotting the log of each of the parameters against each other it can be shown that the gradient is negative and that a/b is 1.07, showing that both effects are very important and can either support each other or have a cancelling property, Figure 24, but that the coating plays the slightly dominant role when viewing the complete series of papers. It also supports the obvious case of heavy weight coated papers in that the relevance of the coating is of course even greater, but for lightweight papers with porous and permeable coatings, maintaining the basepaper absorbency is the key parameter that can be used to prevent reverse piling.

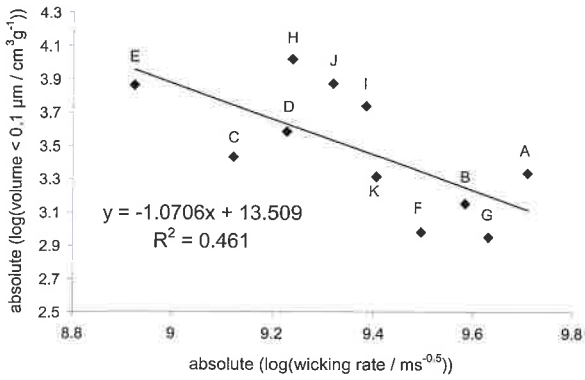

Figure 24: The relationship between wicking rate in the dipping experiment, raised to the power a, and the volume of pores < 0.1 μm, raised to the power b

We can now explain the anomalies in the previous weak correlations by incorporating coating permeability when we combine the two anti-correlating properties permeability with and without capillarity, together with basepaper absorbency, under the expression

$$\text{reversepiling} \propto \frac{[\text{coating permeability NAND capillarity}]}{[\text{basepaper absorbency}]\ [\text{coating capillarity AND permeability}]} \qquad (6)$$

where "AND" and "NAND" are Boolean operators referring to "combined with" and "not combined with", respectively.

If the coating is too permeable and its capillarity low combined with a basepaper that is wicking strongly then the fountain solution flows too easily around the sheet and can re-surface from deeper in the base paper under pressure. This is best illustrated by paper E which has high basepaper absorption potential and a high coating permeability with a low level of fine pores, i.e. low capillarity. The case E, not being a particularly good paper, therefore, resolves itself in the ranking despite the basepaper wicking by realising that the coating is of particularly low capillarity. If the basepaper has extremely high wicking, and the coating has low capillarity, the absorption in practice is brought under control by reducing the coating permeability. This is a practical solution as illustrated by paper C. The interesting role of permeability of the coating is crucial as to whether it is present together with capillarity = good in moderation, or without capillarity = bad.

The same argument vice versa applies for the anomalous case in the permeability/capillarity ranking. The permeability is the rate at which fluid reaches the basepaper, E and J being the exceptions being high showing very little coating effect on reducing permeability.

4. Conclusions

The substrate effects relating to reverse piling in the case of a one-side single colour printed image on a multicolour offset press have been analysed. No direct trend between the effect of either paper weight or coating pigment formulation alone could be drawn. The results of a range of tests, including wicking of liquid into the paper in the planar machine direction, dominated by the basepaper absorption properties, cross planar air and liquid permeability, dominated by the coating structure and coverage, ink tack behaviour using the ISIT ink-on-paper tack method, mercury intrusion porosimetry and modelling of the coating layer using a network simulator (Pore-Cor) to determine its permeability separate from that of the basepaper, have been used to support a theory concerning the interaction of the repeated application of excess surface fountain solution and the first laid-down ink. It is shown that the problem is linked to the combination of two main properties: low absorption potential by the basepaper matched by a lack of permeability of the coating in the case and only in the case when capillary forces in the coating are high, as determined by a high proportion of ultrafine pores (< 0.1 μm) which is typical of modern high brightness coated papers. The case is illustrated particularly where a highly absorbing basepaper can either assist when the coating layer is particularly impermeable, or be damaging when the coating is very permeable without high capillarity. Additionally, the negative effect of increasing the temperature of the fountain solution, i.e. reducing its viscosity, by reducing the cooling, further supported the hypothesis, in that the more thermally conducting coating layer is suspected to have run at a higher temperature than that of the more insulating basepaper, rendering a reduction in the relative absorption properties of the basepaper in comparison to the effectively increased coating permeability as the fountain solution met the cooler basepaper.

The destabilising effect of reduced emulsion capacity in some ink-fountain solution combinations and the allied potential for thermal destabilisation of sterically dispersed ink pigment in the presence of warm fountain solution are considered to be combinatory factors to the aquapiling phenomenon described, which, when combined with the substrate parameters identified in this work, lead to the problem of reverse piling.

References

[1] Concannon, P. W. and Wilson, L. A., (1992), "A Method for Measuring Tack Build of Offset Printing Ink on Coated Paper", TAGA Conference Proceedings, Vancouver

[2] Darcy, H., (1856), "Les Fontaines Publiques de la Ville de Dijon", Appendix - Note D, 559 - 603

[3] Gane, P. A. C., Kettle, J. P., Matthews, G. P. and Ridgway, C. J., (1996), "Void Space Structure of Com-pressible Polymer Spheres and Consolidated Calcium Carbonate Paper-Coating Formulations", Industrial and Engineering Chemistry Research, 35(5), 1753 - 1764

[4] Gane, P. A. C., Ridgway, C. J., Schoelkopf, J., and Bousfield, D. W., (2006), "Heat transfer through calcium carbonate-based coating structures: Observation and model for a thermal fusing process", Tappi International Printing and Graphic Arts Conference, Cincinnati, Tappi Press, Atlanta

[5] Gane, P. A. C., Schoelkopf, J., and Matthews, G. P., (2000a), "Coating imbibition rate studies of offset inks: a novel determination of ink-on-paper viscosity and solids concentration using the ink tack force-time integral.", International Printing and Graphic Arts, Savannah, Tappi Press, Atlanta

[6] Gane, P. A. C., Schoelkopf, J., Spielmann, D. C., Matthews, G. P. and Ridgway, C. J., (2000b), "Fluid Transport into Porous Coating Structures: Some Novel Findings", Tappi Journal, 83(5), 77 - 78

[7] Gane, P. A. C., Seyler, E. and Swan, A., (1994), "Some novel aspects of ink/paper Interaction in offset printing", International Printing and Graphic Arts Conference, Halifax, Nova Scotia, Tappi Press, Atlanta

[8] Matthews, G. P., Moss, A. K., Spearing, M. C. and Voland, F., (1993), "Network Calculation of Mercury Intrusion and Absolute Permeability in Sandstone and Other Porous Media", Powder Technology, (76), 95 - 107

[9] Matthews, G. P., Ridgway, C. J. and Small, J.S., (1996), "Modelling of Simulated Clay Precipitation Within Reservoir Sandstones", Marine and Petroleum Geology, 13(5), 581 - 589

[10] Peat, D. M. W., Matthews, G. P., Worsfold, P. J. and Jarvis, S. C., (2000), "Simulation of Water Retention and Hydraulic Conductivity in Soil Using a Three-Dimensional Network", European Journal of Soil Science, (March 2000), 65 - 79

[11] Poivet, S., Nallet, F., Gay, C. and Fabre, P., (2003), "Cavitation-Induced Force Transition in Confined Viscous Liquids Under Traction", Europhysics Letters, 62, 244 - 250

[12] Ridgway, C. J. and Gane, P. A. C., (2003), "Bulk Density Measurement and Coating Porosity Calculation for Coated Paper Samples", Nordic Pulp and Paper Research Journal, 18(1), 24 - 31

[13] Ridgway, C. J., Kalela, E. and Gane, P. A. C., (2002), "Ink-Coating Adhesion: Factors Affecting Deposits on the CIC in 'Satellite' Type CSWO Presses When Using VAC Papers", Journal of Graphic Technology, 1.1, 49 - 58

[14] Ridgway, C. J., Ridgway, K. and Matthews, G. P., (1997), "Modelling of the Void Space of Tablets Compacted Over a Range of Pressures", Journal of Pharmacy and Pharmacology, 49, 377 - 383

[15] Ridgway, C. J., Schoelkopf, J. and Gane, P. A. C., (2003), "A New Method for Measuring the Liquid Permeability of Coated and Uncoated Papers and Boards", Nordic Pulp and Paper Research Journal, 18(4), 377 - 381

[16] Ridgway, C. J., Schoelkopf, J., Matthews, G. P., Gane, P. A. C. and James, P. W., (2001), "The Effects of Void Geometry and Contact Angle on the Absorption of Liquids into Porous Calcium Carbonate Structures", Journal of Colloid and Interface Science, 239(2), 417 - 431

[17] Schoelkopf, J., Ridgway, C. J., Gane, P. A. C., Matthews, G. P. and Spielmann, D. C., (2000), "Measurement and Network Modeling of Liquid Permeation into Compacted Mineral Blocks", Journal of Colloid and Interface Science, 227(1), 119 - 131

[18] TAPPI Press, "1998-1999 Tappi Test Methods", Tappi Press, Atlanta, (1998)

Notes

[1] Pore-Cor is a software package of the Environmental and Fluid Modelling Group, University of Plymouth, PL4 8AA, UK.
[2] SeGan Ltd. Perrose, Lostwithiel, Cornwall PL22 0JJ, U.K.
[3] Pore-Comp is a software program developed by the Environmental and Fluids Modelling Group University of Plymouth, PL4 8AA, U.K.
[4] The PTFE-moulds used to form the cylindrical embedments were from Prüfmaschinen AG Giessenstr. 15 CH-8953 Dietikon, Switzerland and have an inner diameter of 30 mm.
[5] The resin used to embed the paper samples was Technovit 4000: a product name from Heraeus Kulzer GmbH, Philipp-Reis-Strasse 8/13, D-61273 Wehrheim/Ts, Germany
[6] Software can be obtained on request from Dr. C. J. Ridgway Omya Development AG, CH-4665 Oftringen, Switzerland

Predicting print-through in coldset newsprint

Christine Antoine

LGP2
EFPG, 461 rue de la papeterie, F-38400 Saint Martin d'Hères, France
E-mail: cantoine@abkmachinery.com

Abstract

This paper describes how the print-through of newsprint printed by the coldset offset technique can be predicted from the sheet properties which were identified from images obtained by a flat bed scanner. In this work, several scanning methods were used. It was found that variables from the transmitted light images allowed good predictive models of subjective print-through to be obtained when samples with high print-through are considered while variables from images acquired with reflective light are better to predict the score of low print-through samples. Mixing the scanning methods improved the models and could explain up to 99% of the variance. The main image variables included in the models were the mean grey level, the number of dark/light spots of area 0.03 - 0.04 mm^2, the wire marking strength, the variations in the wavelength range 0,1 - 5 mm and some grey level distribution features. Moreover, images acquired before and after laboratory printing of the same paper area were aligned and compared. An important conclusion of this work is that depending on the severity of print-through, it is either the details seen in reflective light scanned images or the details seen on transmitted light scanned images that are the more visually disturbing on scanned images of the reverse side of prints.

Keywords

Models, newsprint, non-uniformity, print-through, wire marking

1. Introduction

The printability level of any printing paper grade is a continuous major concern for the papermaker. Many physical and optical properties of paper are therefore measured at the paper mill to predict print quality prior to the paper being sent to the press rooms. For example, opacity is used as an estimator of print-through. However, this is known to be only informative and not always representative of how print-through will be perceived after printing [Pauler 84, Pauler 86]. A further step is to make laboratory printing and measure average print-through. However, this measurement is also known to not always correlate with subjective print-through [Nordman 71, Heintze 97, Eadie 98]. One reason is that local variations influence the human perception of print-through [Nordman 71, Danby 93, Heintze 97, Eadie 98, Pianta 98].

In a previous study, different characteristics measured on scanned images of the reverse side of four batches of newsprints A, B, C and D printed in coldset web offset were used to model perceptual print-through evaluated by an experienced panel of judges [Antoine 07]. These characteristics were mainly: the average grey level, the dark spots number, the wire marking strength and variations mainly in the range 0,5 - 5mm. This previous study showed that scanning of the paper surface is good at reproducing how the human eye perceived the reverse side of print. This new work has focused on the prediction of print-through from variables measured this time on scanned images from unprinted samples. To do so, we have on one hand measured the same variables on unprinted samples from the batches C and D as on the reverse side of prints and used these variables to model perceptual print-through. In a second stage, we compared aligned images from both sides of paper strips acquired before and/or after printing.

2. Methodology

2.1 Subjective print-through modelling

A series of six newspaper samples coming from a mill study of fillers (batch D) as well as another batch of eight unprinted newspaper samples coming from a benchmarking study dedicated to print-through (batch C) were scanned at a resolution of 600 dpi using transmitted light and reflective light. The original batch C comprised 11 samples [Antoine 07]. However, unprinted sheets were not available for three samples.

For the scanning with reflective light, the white backing provided with the scanner was used for both batches of samples. A black backing (black art paper) was also used for the batch C. For each scanning method, 15 images of 512 x 512 pixels were analyzed in terms of grey level distribution and basic statistics, power spectrum distribution, dark spots distribution, strength of wire marks [Antoine 07]. The frequency analysis was done by Fourier transformation (FFT) and orthogonal wavelet transformation (OWT) using the Daubechies 4 function. The frequency cut-off limits are necessarily power of 2 in OWT (1-2-4-8-16, etc.); this is not the case when a FFT is done; However, for comparison purposes, identical cutting was used for the two transformations. The size of the images analysed was 512 pixels by 512 pixels at a resolution of 42 µm/pixel, i.e. the image side was 21504 µm; so the successive limits of the wavelength ranges were 84 - 168 - 336 - 672 - 1344 - 2688 - 5376 - 10752 µm. The software Matlab version 6.5 was used to develop these calculations programs.

All these variables were analysed in terms of analysis of variance (ANOVA) and correlations with perceptual print-through. Further, they were used to model perceptual print-through by projection on latent structure (PLS), [Diserud 06a, Diserud 06b, Antoine 07]. The software Unscrambler version 8.0 was used for this task.

2.2 Correlation between aligned images

Two series of samples were used in this study. The first paper samples from the D batch (samples coded D4, D5 and D6) were printed on one side with a Prüfbau laboratory press. Printing was done at three different ink levels (0.8, 1.7 and 3.4 g/m^2) according to SCAN-P 79:02. The ink was black coldest ink (NOB80101 from Akzo Nobel (Now Flint Group)). Two strips per ink level and per sample were printed.

Two strips per side from a sample coded E which had a tendency for high print-through and two-sidedness were printed following above procedure at four different ink levels (0.8, 1.7, 3.4 and 6.8 g/m^2) both with ink and its oil vehicle alone. In fact, this sample was from the same paper machine as the worst samples of batch C. The ink level of 6.8 g/m^2 is not practically reached during commercial printing; it was however chosen to study print-through when the internal pores of the sheet start to be saturated by the vehicle oil.

The samples were scanned before and after printing at a resolution of 600 dpi using an Epson Perfection 3200 scanner. Both sides were scanned in transmittance mode before printing and both sides were also scanned before and after printing in reflective mode using the white backing provided with the scanner. An area of 2048 by 800 pixels at a resolution of 600 dpi was acquired for each strip.

The sample E was also scanned before printing in reflective mode with a black art paper as background. The paper topography was included as a studied parameter for this sample. The topographical maps were acquired with a Lehman laser profilometer.

Prior to scanning, some marks were made with a pen along the strip borders to allow further alignment of the topographic maps with the flatbed scanned images. The marks were seen as valleys/hills on the topographic maps and they were seen as colored marks on the other images.

To study locally the relation between the different images obtained for a given paper strip, all the images from a given strip were aligned. The semi-automatic 'Registration' procedure available on Image Pro 4.5 image analysis software was used. Eight particular points such as DIP speckles were chosen and marked by a mouse click on both printed and unprinted sample images. The images were corrected for translation and rotation. The points were chosen with as much precision as possible to obtain an alignment with a maximum accuracy. Images were flipped prior to registration when necessary.

The aligned images were compared two by two as described in Figure 1. Correlations R between pairwise images were calculated at the original resolution of 600 dpi and at 150 dpi after an image resizing to compensate for the potential misregistration. 2D-histograms with and without normalization with respect to reflectance as proposed by Hansson and Johansson [Hansson 99] were also built for the analysis of the D batch to study in more details the relationship between the different intensity distributions.

The surface roughness of the sample E was quantified according to the procedure developed by Chinga [Chinga 04] with ImageJ software.

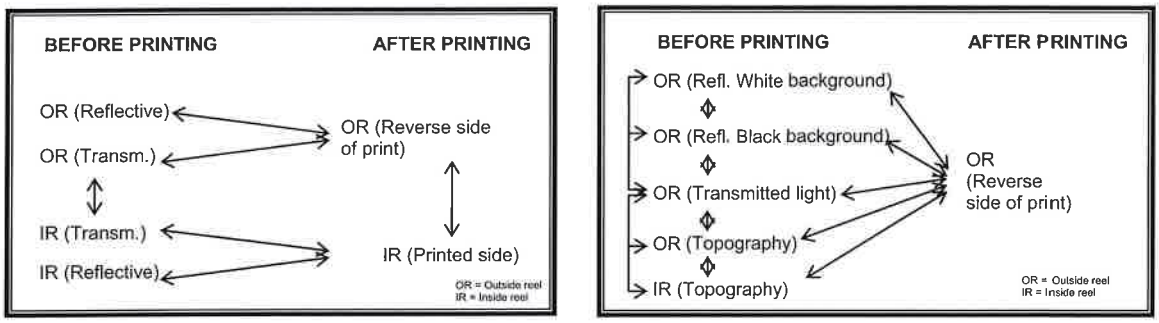

Figure 1: Schematic representation of the images that were compared pairwise for each strip of batch D (left), and for each strip of sample E (right)

2.3 Coding

In the text, the reverse side of the print images are named *rev*; the images obtained by scanning in transmitted light will be named *trans*; the images of unprinted paper scanned in reflective mode with a white(/black) background will be named *unp-w(/unp-b)*. The images from the printed side will be named *print*. The topographic maps from the side that was not printed will be called *topo-r* and the topographic maps from the side to be printed will be called *topo-p*.

3. Results and discussion

3.1 Subjective print-through modelling

Most of the variables measured on the images to quantify the grey level distribution, the dark spots, the wire marks strength, the energy distribution in the frequency domain and in the frequency/spatial domain passed the analysis of variance (ANOVA) with 95% of confidence. Similarly to the analysis of the images obtained from the reverse side of prints [Antoine 07], parameters related to high wavelength above 2688 µm were those which did not always pass the ANOVA.

The most important variables found to model subjective print-through by means of *rev* images were particularly considered [Antoine 07]. For each scanning method (*trans*, *unp-b*, *unp-w*), these variables measured on unprinted samples were correlated with the subjective ranking, Table I. The side corresponding to the reverse side of the print was also the one considered on the unprinted samples.

Table I: Coefficients of correlation, R (%) between variables measured on scanned images before and subjective ranking; batch C (8 samples) and batch D (6 samples)

Variable	Batch C, R (%)			Batch D, R (%)	
	trans	unp-w	unp-b	trans	unp-w
Mean GL	-79	**20**	**46**	**-56**	57
Var GL	-53	*49*	**-10**	*68*	*57*
Sparea17	-32	*24*	*12*	*32*	-30
TEW	-53	**-38**	**-38**	*31*	-53
NhighP	-68	**-47**	**-40**	**-16**	-70
mEOWMD1344-2688	**-22**	**-16**	-24	-53	**0**
mEOWMD2688-5376	-44	**-29**	**-21**	-43	**-13**
mEOWMD5376-10752	-44	**-6**	**14**	*-65*	**41**
fftPMD1344-2688	**-20**	**-17**	-38	**-41**	-96
fftPMD2688-5376	-35	**-28**	**-24**	**-48**	-66
fftPMD5376-10752	-43	**-29**	**-7**	-33	**-16**

The R-values in bold are the highest for a given batch and given variable amongst those obtained for the different scanning methods. The R-values in grey italic are values with a sign opposite to the expected trend (i.e; no logical explanation from physical phenomena).
Legend: GL = grey level; Var = variance; Sparea17 = number of dark spots detected in the sheet with a size of 17 to 25 pixels (0.03 to 0.044 mm^2); TEW = Total energy of the wire mark peaks detected in the Fourier domain; NhighP = normalized highest wire mark peak amplitude detected in the Fourier domain; mEOW = mean orthogonal wavelet coefficients energy in the concerned wavelength range; fftP = Power of the fast Fourier coefficients in the concerned wavelength range; MD = machine direction; CD = cross direction; 2688-5376 = wavelength range from 2688 µm to 5376µm

The subjective ranking correlated better with the variables measured on the unprinted samples scanned using transmitted light than with the same variables measured in reflective mode with a white background for the batch C including samples suffering from high print-through (Table I, left columns best results in bold). This was not repeated for the batch D including samples with low print-through which gave globally the same importance to the two scanning methods (Table I, right columns, best results in bold). Therefore, no special trend could be found at this stage of the study on which scanning method is better to use to optimize the correlation level.

Table II: Summary of the PLS modelling performed on the two batches of samples C and D with variables measured on the reverse side of printed/to be printed samples acquired by different scanning modes

Batch	Printed or unprinted sample	Scanning method	OWT variables included			FFT variables included		
			R_1 (%)	R_2 (%) cros valid.	Variables	R_1 (%)	R_2 (%) Cros valid.	Variables
C	Unprinted	Transmitted light ('trans')	99	92	• Mean GL • Histogram peak width including 50% pixels • 17 to 25 pixel large spots* • WM highest peak power • OWT energy, range 1344-2688µm, MD • OWT energy, range 84-168µm, MD or CD	100	97	• Mean GL • Histogram peak width including 50% pixels • 17 to 25 pixel large spots* • WM highest peak power • FT power, range 1344-2688µm, MD • FT power, range 84-168µm, MD or CD • FT power, range 168-336µm, MD
C	Unprinted	Reflective light White background ('unp-w')	45	-64		44	-66	
C	Unprinted	Reflective light Black background ('unp-b')	52	-32		57	-18	
C	Printed	Reflective light White background ('rev')	99	98		99	96	
C	Unprinted	Mixed	100	99	• Mean GL_{trans} • OWT energy, range 1344-2688µm, MD_{trans} • OWT energy, range 84-168µm, CD_{trans} • 17 to 25 pixel large spots being the sum of dark spot from' unp-w' images and light spots from 'trans' images for 'mixed' model	100	99	• Mean GL_{trans} • Histogram peak width including 50% $pixels_{trans}$ • FT power, range 1344-2688µm, MD_{trans} • FT energy, range 84-168µm, CD_{trans}
D	Unprinted	Transmitted light ('trans')	99	86	• Mean GL • WM highest peak power • WM peaks total energy • OWT energy, range 5376-10752µm, MD	98	77	• Mean GL • WM highest peak power • WM peaks total energy • FT power, range 5376-10752µm, MD
D	Unprinted	Reflective light White background ('unp-w')	98	74	• Mean GL • 17 to 25 pixel large spots • WM highest peak power • OWT energy, range 1344-2688µm, MD	100	97	• Mean GL • 17 to 25 pixel large spots • WM highest peak power • FT power, range 672-1344µm &1344-2688µm, MD
D	Printed	Reflective light White background ('rev')	100	99	• Mean GL • 10% darkest pixels thresh. • 17 to 25 pixel large spots • WM peaks total energy • OWT energy, range 2688-5376µm & 5376-10752µm, MD	100	99	• Mean GL • 10% darkest pixels threshold • 17 to 25 pixel large spots • WM peaks total energy • FT power, range 1344-2688µm & 5376-10752µm, MD
D	Unprinted	Mixed	100	95	• Mean GL_{trans} • Mean GL_{unp-b} • 17 to 25 pixel large $spots_{unp-w}$ • OWT energy, range 2688-5376µm &5376-10752µm, MD_{trans}	99	96	• Mean GL_{trans} • 17 to 25 pixel large $spots_{unp-w}$ • WM highest $peak\ power_{unp-w}$ • FT power, range 5376-10752µm,MD_{trans}

**: dark spots for images acquired with reflective light; light spots for images acquired with transmitted light*
Legend GL: Grey level; WM: Wire marks; OWT: Orthogonal wavelet transform; FT: Fourier transform; MD: Machine direction; CD: Cross direction

For both batches, the mean grey level of the unprinted samples scanned in transmitted light and in reflective light with a white background did not correlate with each other (R = -0.093 for batch C and R = -0.002 for batch D). However, they correlated equally well with the subjective ranking for batch D ($R \approx 0{,}55$) and in 0.8 against 0.2 proportion respectively for batch C. This difference can be explained because the mean grey level of the images scanned with transmitted light mainly reflects the opacity of the paper samples while the mean grey level of the unprinted samples scanned with reflected light is representative of the brightness of the samples. As seen previously [Antoine 07], these two paper characteristics influence the print-through judge perception. It can be seen here that this happens in different proportions for these two batches depending on the print-through level (high for batch C and low for samples containing extra fillers in batch D).

Perceptual print-through was model by PLS using the variables measured on the unprinted samples and reported in Table II. In a first step we optimized models for each scanning method and after that we optimized a model which mixed the variables from the different scanning methods. The results are summarized in Table II. Two correlation R values are shown in this Table. The first one, R_1 is the square root of the response variance (subjective print-through) explained by the model. The closer to 1 it is, the better the chosen variables are at modelling the response for the considered samples. The second one, R_2 is obtained after a cross validation routine where the model is tested to predict unknown samples by repeatedly removing one sample from the batch, [Diserud 06a]. The closer to 1 it is, the better the model is at predicting unknown samples.

From the three scanning methods, the one using transmitted light is the best to use alone to model subjective print-through for the batch C comprising samples with high print-through tendency. Concerning the batch D made of low print-through samples, the reflective mode was better to use.

By mixing the variables from the different scanning methods, predicting models as good as those built from the variables measured on the reverse side of the prints could be obtained as exemplified in Figure 2. This is true either using orthogonal wavelet variables or Fourier variables to represent print-through variations; they are as good at predicting unknown samples (see R_2 values, Table II).

3.2 Correlation between aligned images

The dimensional stability of the samples D4 - D6 was good and accuracy within ±3 pixels in the two main directions could be reached on the whole studied area which was 800 x 2048 pixels, corresponding to 28.9 cm^2. The same accuracy could not be reached for the sample E due to some local dimensional changes along the paper strip after printing. Therefore, the studied areas were chosen to be smaller: 800 x 800 pixels corresponding to 11.3 cm^2. To compensate for this, two such areas were aligned per strip. The accuracy was within ±4 pixels in the two main directions for each area.

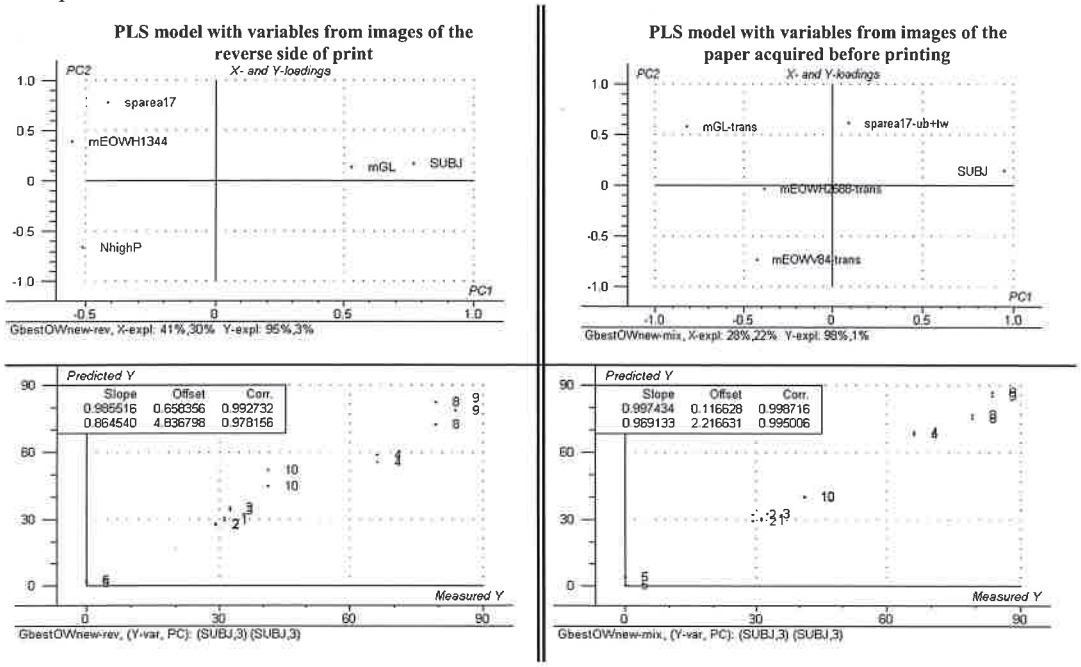

Figure 2: Model of the subjective evaluation of print-through by means of PLS, batch of sample C. left: The model is based on variables measured on the reverse side of prints; Right: The model is based on variables measured on the same side of unprinted samples scanned with transmitted and reflective light

As it was not possible to get a perfect alignment between the images, the final correlation coefficient between pairwise images was chosen as the highest one among all those calculated by successive translations of images between each other within +/- 3 pixels for batch D and +/- 4 pixels for sample E.

An ANOVA was performed on the results to verify the effect of the sample and/or ink level on the correlation between the pairwise images. The main conclusions were:

Batch D

- The *rev* images correlate more with the *unp-w* images ($0.35 < R < 0.7$) than with the *trans* images ($0.25 < -R < 0.58$). However, the correlation between *rev* and *trans* images increased with ink level while the correlation between *rev* and *unp-w* decrease with ink level. This decreased comes at a higher ink level for the sample D5 containing extra fillers.
- The correlation between the *trans* images of both sides is rather good ($0.77 < R < 0.98$), especially for the resized images at 150dpi ($0.94 < R < 0.98$). The difference between the two sides is explained by the surface details which are not equally seen by the detector when the sheet is turned. For example, a DIP spot lying at the paper surface will be clearly seen when this side is against the scanner glass, while it will not or only slightly be visible on the image when this side is against the light source.
- Concerning this *trans-trans* correlation, the best results are found for sample D4 which is significantly different at 95% of confidence level from the two other samples in this regard. This can be explained by the fact that this sample has the poorest formation. The histogram of grey level is more spread and skewed toward the high values for this sample, i.e. there are more light areas (low local basis weight) in this sample. Consequently, the surface details in *trans* images are less important for this sample than the high formation variations which are equally strongly independent of which side is in contact with the glass of the scanner.
- The correlation between the *rev* images and the *print* images is nil or very low ($-0.28 < R < 0.02$). The correlation is nil at low ink level and slightly improves with ink level.
- The correlation between the *print* and *unp-w* images from same side (R_{mean} = 44% at 150 dpi) is higher than the correlation between the *print* and *trans* images from same side (R_{mean} = 20% at 150 dpi). Sample and ink level did not significantly affect these results.
- The dark spots seen on *rev* images are both linked to the same dark spots seen on the *unp-w* or *trans* images of the same side together with the light spots of the *trans* images, Figure 3. Some extra dark spots can be seen on the *trans* images corresponding to dark spot from the opposite side or lying in the paper thickness.
- The 2D-histograms were in agreement with the above results but did not bring any extra information.

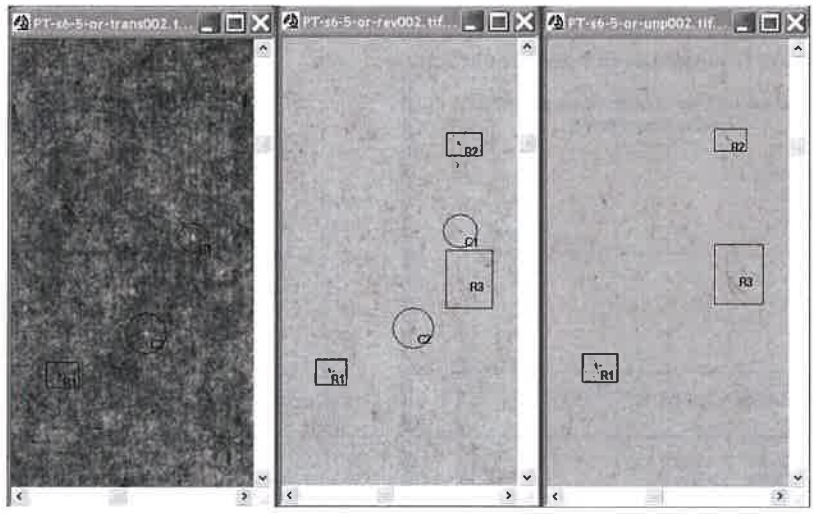

Figure 3: Left: trans image; at centre: rev image; right: unp-w image. Example of dark spots seen on rev image, also seen on the unprinted sample as dark spots on unp-w/trans images (R1, R2, R3) or as light spots (local low basis weight) on trans image (C1, C2)

Sample E

- The correlation between *trans* and *rev* images was much more important for sample E ($34.2 < -R < 70.6$) than for the samples D4 - D6 and inversely with *unp-w* and *rev* images.
- The correlation between *trans* and *rev* images increases for the three first ink levels studied but decreases for the highest level (6.8 g/m^2). The filling of most pores by the vehicle oil at this level can explain this fact (see below).

- The *unp-b* images lead to a better correlation with *rev* images than *unp-w* images but with a lower correlation than the *trans* images: the black background enhanced the local basis weight difference but the contrast was not as good as the one obtained using transmitted light.
- The correlation between *rev* and *unp-w* or *unp-b* images decreases with increasing the amount of ink deposited on the paper. The higher the ink amount, the less the surface details from the reverse side are visible.
- The *topo-r* correlated in average at 33% at 600 dpi and at 43% at 150 dpi with the *rev* images. The *topo-p* correlated in average at 23% at 600 dpi and at 39% at 150 dpi with the *rev* images. The difference is not high between the two sides, especially at 150 dpi where the correlation reaches up to 60%. These topographic maps also correlate at around 50% with the *trans* images at 150 dpi. This can be visually verified as it is possible to recognize on the *topo* images the floc shapes, Figure 4. A floc corresponds to a hill and a counter-floc to a valley.
- From the analysis of paper strips printed only with vehicle oil, it can be seen that the vehicle oil used to print some of the strips acts on the reverse side aspect in two ways: first, its dark color acts as a dark background and secondly, its penetration into the paper structure according to the pore size distribution reduces the scattering distribution both in flocs and counter-flocs decreasing the basis weight variations effect. The background effect is first more important than the pore filling phenomena at low ink level so the correlation between the *trans* images and *rev* images increase with amount of oil deposited, Figure 5 (Left). However, over a certain amount of oil, the paper starts to saturate and the induced drop in light scattering tends to remove the flocs and counter-flocs details through the whole paper thickness and to lower the contrast between the flocs and counter-flocs as seen on the *rev* images. As the ink vehicle is not so dark as the black pigments, its effect of dark background is lower which makes the correlation between the *trans* and *rev* images for all ink levels lower for the paper printed with oil than with ink.
- The two sidedness of sample E is characterized by a higher number of valleys and peaks and by a higher average depth of the valleys of the bottom side (BS), Table III. In parallel, when the paper is printed on the BS (rougher) side, the mean grey level of the reverse side is darker at all ink levels, Figure 5 (Right). This is due to a higher average ink penetration characterized by deeper surface pores which are filled by pigments while compressed in the printing press nip.
- The surface structure difference of the two sides did not bring any other significant difference between sides concerning the studied correlations at the resolution considered (150 dpi), i.e. At this resolution, print-through variations were not affected by the roughness of the paper.
- These two latter points can be summarized as follows: the average print-through increased with the roughness of the side to be printed.

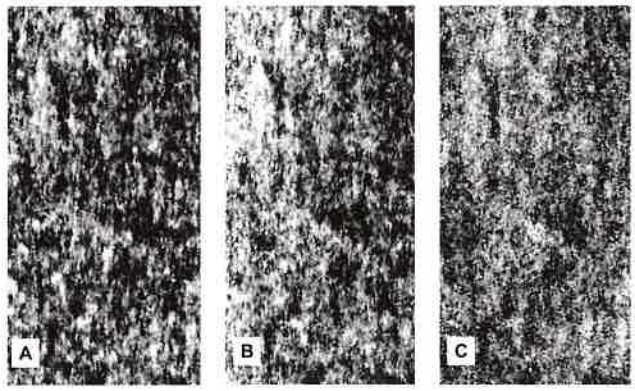

Figure 4: Example of topographic maps from each side (A and B) and trans image (C) of a same paper strip area. The original images were median filtered (5 x 5 kernel) and best fit equalized to enhance the contrast. The floc details seen on the trans images (here inverted) can be recognized in the topo images

Table III: Topographics characteristics of the surface of the sample E. All variables included passed the ANOVA at 99% confidence

Side	Rq	% Valleys	% Peaks	Mean valley depth(*)	Mean Peak height(*)
TS	5.42	17.71	18.11	8.23	8.62
BS	5.65	18.71	19.27	8.72	8.42

**: Define as mean valley(peak) depth(height) from the center line and including only valleys(peaks) deeper(higher) than 5 µm*

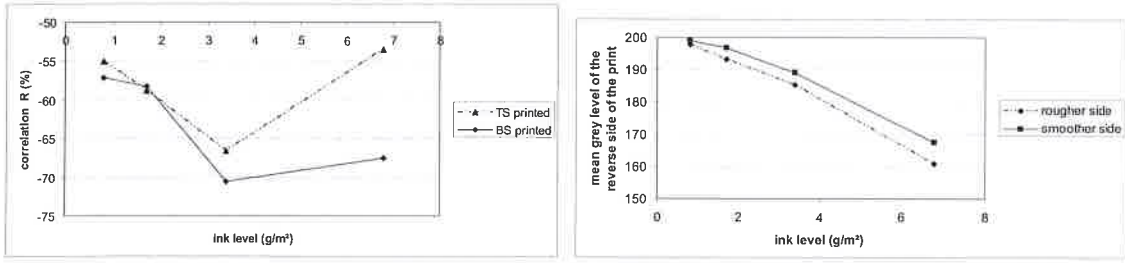

Figure 5: Left: Correlations at different ink levels between the images from the reverse side of paper strips printed with the vehicle oil and the images from the same side acquired before printing in transmittance mode; Right: Average grey level of the reverse side of prints, sample E

4. Conclusions

The average grey level, the number of dark spots of area 0.03 - 0.04 mm^2, the wire marking strength and variations in the wavelength range 0,1 - 5 mm as well as other parameters were previously calculated on scanned images from the reverse side of CSWO printed newspaper. These parameters were found to be good for modelling the visual perception of print-through [Antoine 07]. In this new study, these variables were calculated on scanned images from the corresponding unprinted newspaper samples. Different scanning parameters were applied (reflected light with a black or white background or transmitted light).

The choice of scanning mode to choose to optimise the model depended on the severity of print-through. Indeed, depending on the sample feature, more emphasis was given to the formation or to the surface details: for paper suffering from high print-through the formation details as seen on transmitted light scanned images was more visible on the reverse side of prints than the surface details as seen on images acquired in reflective illumination. For a series of papers with lower print-through tendency, the surface details correlated more with the reverse side of prints than the formation details.

This shows the complexity of predicting print-through by a general model, however, this is possible. To get a robust model, it is important to get a large range of samples covering the full scale of print-through tendency and print-through variation features (wire-marking strength, ink strike-through, formation frequency distribution). This was not available during this study. Both reflectance mode and transmittance mode must be used to acquire images from which features critical to print-through can be calculated. Such a model could be developed and use as a daily routine to estimate print-through at paper mill before printing by mill customers.

The black ink pigments act as a black background which enhances formation and surface detail features visible on the reverse side of prints. Because of its dark color, the ink vehicle oil also acts as a dark background but to a lower extent. However, it is known to simultaneously decrease light scattering by filling the pores. Over a certain amount of oil on paper (between 3.4 and 6.8 g/m^2 for 42 g/m^2 sheets in our study), the drop in light scattering in flocs and counter flocs affects more the visibility of details seen on the reverse side of prints than the oil and pigment color does: this makes the correlation between the details seen through unprinted paper and details seen on the reverse side of printed paper to decrease.

One of the studied papers was characterized by a surface roughness two-sidedness: one of the sides was rougher notably because of the presence of deep valleys. In parallel, at all studied ink levels, the reverse side of the print was darker when the rougher side is printed. This can be explained by a higher mean ink pigment penetration in the paper due to deeper surface pores reached by the ink pigments while compressed in the printing press nip. The rougher the side, the higher the ink demand; therefore, one can expect that this phenomenon is increased in commercial printing where the target is a constant print density instead of a constant ink level. Print-through variations at wavelengths over 168 µm were not affected by the roughness of the paper.

The light spots seen on transmitted images and corresponding to local low basis weight areas lead to dark spots on the reverse side of prints. These local low basis weight areas should be minimized during paper making to minimize print-through variations and better print-through subjective perception. The most probable reasons for those are air in pulp, unsuitable wet end chemistry, wrongly adjusted vacuum, or condensation in the wet end section.

Acknowledgments

The author wish to thank PFI AS and NSR who allowed her to complete this work, use their paper samples, equipment and software licence. Particularly thanks to Philip Reme and Gary Chinga from PFI, Klaus Møller and Morten Eilertsen, from NSR. NSR is also thanked for financing the printing. Kenneth Aasarød from PFI AS is acknowledged for printing sample E. Also thanks are due to Mats Person from Flint Group, Trelleborg, who kindly provided the vehicle oil sample. The author is also grateful to Øyvind Gregersen from NTNU, Trondheim and John Kettle from KCL, Espoo for reviewing this document.

References

[1] Antoine, C. (2007), Objective assessment of print-through non-uniformity by means of image analysis, TAGA Journal of Graphic Technology 3(4): 159 - 176

[2] Chinga, G. (2004), Detailed characterization of paper surface structure for gloss assessment, JPPS 30(8): 222 - 227

[3] Danby R. (1993), The impact of forming fabric structures on print quality, 79th CPPA annual meeting: A33 - A38

[4] Diserud, O. H., Antoine, C., Berli, E. (2006a), Objective Print Quality Assessment of Complex Images. Part 2: A Model for Perceptual Print Quality in Complex Black and White Images, Advances in Printing Sc. & Techn. 32: 132 - 143

[5] Diserud, O. H., Antoine, C., Berli, E. (2006b), Modelling Perceptual Print Quality in Complex Color Images, TAGA Journal of Graphic Technology 3(2): 67 - 79

[6] Eadie, D. T., Durand, R., Ford, P., Stassi, A., Popil, R. E., McCarthy, J. J. (1998), Ink and paper effects on show through in white knock out directory printing, International Printing & Graphic Arts Conference 98: 193 - 198

[7] Hansson, P. and Johansson, P-Å. (1999), A new method for the simultaneous measurement of surface topography and ink distribution on prints, Nordic Pulp and Paper Research Journal 14(4): 315 - 319

[8] Heintze, H. U. (1997), The Impact of Formation on Print-through Measurement, 1997 Process and Product Quality Conference and Trade Fair: 83 - 86

[9] Nordman, L., Makkonen, T. (1971), Studies of print-through by means of unevenness measurements, Proceedings of the 10th international Conference of printing research institutes, Krems, Austria, 1969, Ed. W. H. Banks, Advances in printing sciences and technologies 6: 271 - 282

[10] Pauler, N. and Bristow, J. A. (1984), Opacity is not Always a Direct Guide to Print-Through, Advances in Printing Science and Technology, W. H. Banks edition, Pentech press, London 17: 333 - 346

[11] Pauler, N. and Bristow, J. A. (1986), Opacity is not Always a Direct Guide to Print-Through - Effect of Special Pigments, Advances in Printing Science and Technology, W.H. Banks edition, Pentech press, London 18: 432 - 438

[12] Pianta, F. (1998), Contribution à l'amélioration de l'opacité et de la transvision des papiers minces destinés à l'impression écriture, PhD thesis, INPG, Grenoble, France

Aspects of water-induced mottle when printing on coated paper in sheet-fed lithographic offset

Christer Lie[1], *Petter Kolseth*[2]

[1] KTH School of Computer Science and Communication
Osquars Backe 2, SE-10044, Stockholm, Sweden
E-mail: lie@kth.se

[2] Stora Enso AB, Falun Research Centre, SE-791 80, Falun, Sweden
E-mail: petter.i.kolseth@storaenso.com

Abstract

Uneven print density, print mottle or mottle, can cause severe print quality problems and is a frequent problem for printers. Print mottle can occur in sheet-fed offset due to several reasons related to both the paper and its coating and the printing press. The aim of the project was therefore to improve our knowledge of the influence on mottle related to the fountain solution which dampens the paper surface, water induced mottle.

Pilot coated papers were produced and printed in a full-scale 4-colour sheet-fed offset printing press. During printing a specially designed test form was used. This must be used together with a blanket which has cut-out areas corresponding to the areas on the test form. In this way it is possible to create a number of different printing situations on the same printed paper sheet.

The results from the print trials show that fountain solution from the previous printing unit can cause a decreased print density and dot gain. Water induced print mottle is caused by the fountain solution from the previous printing unit. Back-trap from the following print units will have a smoothing effect and will decrease the mottle. The results are based on a hypothesis test at the 5% level.

Water induced mottle can be related to both the printing process and the paper. The structure of the paper coating, uneven porosity distribution, has a high influence on water induced mottle while the effect of the surface chemistry is low. The paper with high SB latex content showed the most uneven porosity distribution.

Keywords

Mottle, offset, print quality, water-induced

1. Background

Coated paper is widely used for offset printing as the higher demand for high quality four-colour print has led to a shift from uncoated to coated paper grades. For high quality four-colour printed products, books, brochures and commercial advertising offset is the dominating print method.

In offset printing a well-known problem is water-induced mottle. The effect is related to the interaction with fountain solution when the ink is transferred to the paper. "Mottling is influenced significantly by the characteristics of the paper with regard to homogeneity of its structure and its coating" [Kipphan, 2001, p. 225].

The water can come either from the previous printing unit or via emulsion in the ink. Definition "mottle due to water from the previous printing unit" is denoted as water induced mottle.

This report focuses on water-induced print mottle in full-scale printing, the effects of the conditions in the printing press and the paper coating composition. The full-scale printings were carried out by IMT, Stockholm and KCL, Espoo.

2. Objective

The tonal reproduction in conventional offset printing is based on 4-colour printing where the thickness of the ink film on the paper is kept constant and the hue is adjusted by the area of the screen. An uneven ink transfer onto the paper will thus cause an unwanted tonal variation in the printed area, referred to as mottle or print mottle.

The main objectives of this report are to clarify the influence on mottle in sheet–fed offset of fountain solution, the printing process and the paper coating.

3. Introduction

In offset printing sometimes uneven print density, referred to as print mottle or mottle, can occur. Mottle can be caused (in several ways) by: uneven paper formation, uneven composition of the coating in the Z direction [Engström, Rigdahl, 1992], poor mechanical interaction between the printing units in multi colour presses, referred to as back-trap mottle, and interaction between ink, fountain solution and the paper [Purfeest, 1991].

The principle of the lithographic process used in conventional sheet-fed offset printing is based on using water to reject the ink from the non-printing areas of the printing plate. The fountain solution used is applied onto the printing plate by the dampening unit. The fountain solution basically consists of tap water with additives, detergents and/or isopropanol, IPA, in order to reduce the surface tension leading to an increased wetting of the plate. Other additives are also added such as buffer agents for pH [Ström, 1988].

In the printing process the water feed is dependent on the water absorption of the print carrier and the ratio of the total printing area to the total non-printing area. The amount of ink and water applied must be adjusted accordingly for each print run and this is often referred to as the ink/water balance. A high water feed reduces the risk of ink being deposited in the non-printing areas but on the other hand will increase the risk of ink rejection in multi colour printing when following inks are printed [Kipphan, 2001].

From a full-scale print-trial, [Lafaye et al. 1987] report mottling on some papers when the second colour is printed. The effect was connected to fountain solution deposits on the surface with the printing of the first colour that prevented the transfer of the second ink. The effect was increased with print speed and the maximum mottling was caused at 8.000 copies/h as compared with 5.000 copies/h.

From a print trial with a Vandercook laboratory press with four paper grades with varying Latex, Purfeerst et al reports fountain solution interference, which correlates to the type of Latex in the paper coating [Purfeerst, 1991].

4. Methods

The project was based on full-scale print trials of coated paper grades. A series of well-defined pilot coatings was produced in order to achieve different chemistry and porous structure. The surface energy and porous structure of the coatings were varied in a systematic way in order to be able to separate these two parameters.

Based on laboratory print trials 18 different pilot coated papers were produced in order to be evaluated in full-scale print trials.

Printing

The print trials were carried out in two 4-colour sheet-fed offset presses of the same type, Roland Favorit RVF OB 4-colour sheet-fed printing press with alcoholic dampening units of film type giving a continuous feed of fountain solution to the printing plate. The press configuration was of 5-cylinder type, with two plate cylinders and corresponding blanket cylinders for one impression cylinder. All printings were performed with cyan ink in the number two, cyan, printing unit.

Prepared blankets

The blankets used were prepared with cut-out areas in patterns that made it possible to evaluate the effect of the pre-damping and back-trap on mottle on the same printed papers according to KCL test method. For the cut-out alternatives used see Table I. All evaluations were made on areas printed in the second print unit. By doing so it was possible to print areas with and without applied fountain solution from the first printing unit and with or without back-trap from the following print units.

Image analysis

Mottle was evaluated by image analysis of the printed areas and calculation of the coefficient of variance for the reflectance in the wavelength band 1 - 8 mm, according to STFI standard. The result was calculated as a mean value from analysis of two printed areas [Johansson, 1993].

Table I: Cut out areas in the blanket on print unit and the corresponding printing effect

Effect	Cut-out in print unit no.			
	1	2	3	4
1. No pre-dampening	x	–	–	–
2. No back-trap	–	–	x	x
3. No pre-dampening and no back-trap	x	–	x	x
4. Reference, pre-dampening and back-trap	–	–	–	–

Water content in paper
In order to correlate the percentage settings of water feed transferred to the papers a calibration method was required.

The amount of fountain solution transferred to the paper was measured by analysing Li ions added to the fountain solution in the paper by atomic absorption spectrophotometer (Perkin-Elmer).

Statistical analysis
In order to calculate differences between different print series the "Pooled t-Test" was used. The purpose of the test is to perform a hypothesis test to compare two population means, $\mu 1$ and $\mu 2$.

Assumptions for the test; simple random samples, independent samples, normal populations or large samples and equal population standard deviations.

The null hypothesis is H_0: $\mu 1 = \mu 2$, and the alternative hypothesis is H_a: $\mu 1 > \mu 2$ (right tailed). The probability needed to reject a true hypothesis is called the significance, α, of the hypothesis test. The significance level α must be decided in advance. The computed value of the statistic is denoted as t [Weiss, 2004].

In this investigation it was decided to use $\alpha = 5$.

5. Materials and print trials

Paper
A series of well-defined pilot coatings was produced with varying formulation in order to achieve different surface energy levels and porous structures. The formulations were based on commercially available pigments and binders. After evaluation of test prints made in the Prüfbau laboratory printing press with respect to surface energy 14 different formulations were chosen for producing paper for print trials in full scale. The different paper grades were produced in a pilot coater with two basic papers: one wood free, surface weight 60 g/m^2 and one wood-free pre-coated to 70 g/m^2 with format 50 x 70 cm.

The basic papers were coated with 14 different coatings on the surface treated base paper, sample SC1-14, and with 4 different coatings on the pre-coated base paper, sample DC1-4. The coating composition for the four pre-coated papers can be seen in Table II. Coating levels = 8 - 12 g/m^2.

Ink
Two commercially available inks were used, one normal setting, NS 1, and one quick setting, QS 2. Only cyan inks were used.

Table II: Coating composition for the four pre-coated papers, coating level 12 g/m^2

Sample	Pigment	Binder
DC1	Clay	10 parts hard SB-latex
DC2	Clay	20 parts hard SB-latex
DC3	Clay	15 parts PVAc-latex
DC4	Clay	6 parts hard SB-latex, 8 parts starch

Fountain solution
Two commercially available fountain solutions were used, one with 10% IPA (isopropyl alcohol) added, 1 IPA and one tenside based, 2 tenside.

Print trial 1, Stockholm
Print runs were performed at two levels for the fountain solution feed, normal and high.

Print density and dot gain in 40% - and 80% dot area was measured in a control wedge with a Gretag D186 densitometer with polarization filter. Each reported was based on 3 - 5 measurements.

Printing conditions and materials
Printing press: Roland Favorit RVF OB 4-colour, only cyan unit printing
Ink: 1 NS and 2QS
Fountain solution: 1 IPA and 2 tenside
Printing speed, imp./h: 6.000
CCI system for automatic ink control to D = 1.65 density units
Dampening settings: normal, 50% and high 90%
Impression: 0.17 mm
Paper: SC 1 - 14
Print trial 1 was carried out in six sub-trials, with two inks, 1 NS and 2 QS, two fountain solutions, 1 IPA and 2 tenside and two water-feed levels, normal and high.

Print trial 2, Espoo
Printing conditions and materials
Printing press: Roland Favorit RVF OB 4-colour, only cyan unit printing
Fountain solution:1 IPA
Ink: 1 NS
Printing speed, imp./h: 5.000
Density control: manual adjustments and density measurement with handheld densitometer, Dampening settings: normal, 40% and high 80%
Impression: 0.10 mm and 0.20 mm
Paper: sub-trial 1 - 4: SC 1 - 14 and sub-trial 5 - 8 only one paper with high mottle in sub-trial 1 - 4

Print trial 2 was carried out in eight sub-trials, with four inks, KCLref, 1 NS and 2 QS, two fountain solutions, 1 IPA and 2 tenside and two water-feed levels, normal and high.

The different combinations of inks and fountain solutions were carried out in eight sub-trials altogether, the same six as in print trial 1 and two additional sub-trials with KCL reference ink and reference fountain solution.

Print trial 3, Espoo
Printing conditions and materials
Printing press: Roland Favorit RVF OB 4-colour, only cyan unit printing
Ink: 1 NS and 2 QS
Fountain solution: 1 with IPA and 2 tenside
Printing speed, imp./h: 7.000, 4.000 in one sub-trial
Density control: manual adjustments
Dampening settings: low, normal, 50% and high 90%
Impression: 0.10 mm, 0.20 in one sub-trial
Paper: DC 1 - 4.
In total 15 different combinations of ink, fountain solution, printing speed and indentations were carried out. Printing parameters; water feed, back-pressure/indentation printing speed.

6. Results

Print trial 1, Stockholm
Visual evaluation of the printed samples showed insignificant levels of mottling. Evaluation by image analysis was therefore not considered as meaningful. Only densitometry measurements such as density and dot gain were considered. In this print trial all the 14 single coated paper grades, SC 1-14 were printed using six combinations of ink, fountain solution and level fountain solution feed.

Measurements of density in solid tone areas and dot gain in 30% areas were performed. The results were calculated as mean values and corresponding standard deviation were calculated for the six sub print trials. The mean values from all paper grades are given in Table III.

Table III: Mean density in 100% area and dot gain in 30% area for all combinations of paper, ink, fountain solution and fountain solution feed, in total 84 combinations

	Density, 100% area, Density units	Dot gain 30% area, %-units
1. With pre-dampening	1.51±0.05	29.98± 2.19
2. Without pre-dampening	1.55±0.05	31.73±2.87

Results from Table III show that there is higher mean density level for the areas that were printed without pre-dampening compared with the mean value for the pre-dampened areas. These areas also show a higher mean dot gain value.

In order to check whether the difference is statistically significant a hypothesis test was performed. The null hypothesis H_0 was that there are no differences, neither in density nor in dot gain, between the mean value for areas not pre-dampened and areas pre-dampened. The results are given in Table IV.

Table IV: Result from hypothesis test, non-pooled t-Test, 84 samples in each series. Are the lower mean values for density and dot gain in table 3 significant?

	Calculated t-value	$t_{0.01}$	Reject/accept H_0
Density	4.443	2.364	Reject
Dot gain	5.185	2.364	Reject

Since the both null hypothesises were rejected the decreased levels for density and dot gain are statistically significant at the 1% level.

The mean density values and dot gain values for the six sub-trials were calculated in order to see the influence of the type of ink, fountain solution and fountain solution feed. For the results see Table V.

Table V: Difference in density and dot gain between areas without pre-dampening and areas with pre-dampening

Sub-trial	Δ Density, Density units	Δ Dot gain 30%, %-units
1. 2 QS, 1 IPA, normal water feed	0.01±0.02	-0.60±1.08
2. 2 QS, 1 IPA, high water feed	0.01±0.02	0.43±1.16
3. 1 NS, 1 IPA, normal water feed	0.06±0.03	0.64±0.84
4. 1 NS, 1 IPA, high water feed	0.04±0.01	0.07±2.13
5. 2 QS, 2 tenside, normal water feed	0.05±0.02	4.14±1.61
6. 2 QS, 2 tenside, normal water feed	0.04±0.02	5±2.39

Positive results for Δ Density and Δ Dot indicates indicate that gain indicates lower values in pre dampened areas compared with areas not pre-dampened. No significance test was done owing to the low sample size of 14.

Print trial 2, Espoo

In print trial 2 the 14 single coated paper grades, SC 1 - 14 were printed with eight combinations of ink, fountain solution and level fountain solution feed. In this print trial evaluation of mottle was made on areas printed in print unit two and also on a solid tone area that was printed in all four print units.

Mottle measured in all four print units.

Mottle measured in solid tone areas printed in print units 1 - 4 showed that the mottle increase for each unit varied for the different paper samples but all showed the same increase of mottle for each successive print unit.

Mottle measured in print unit 2.

The influence on mottle was dependent on both the paper coating and the printing situation. The highest mottle values were found when printing on pre-dampened areas and with no back-trap.

Even though mottle occurred in this print trial the levels found were not high. It was therefore decided to make four new coatings on a pre-coated paper in order the increase the susceptibility to mottling.

Print trial 3, Espoo

A total of 60 different combinations of ink, fountain solution, printing speed and back-pressure were printed with and without pre-dampening and with and without back-pressure in 20%, 70% and 100% print areas for four coated paper grades. Mottle was measured in 70% and 100% areas for all printing combinations.

The mean value was calculated for each paper, DC1 - DC4 for the different printing situations A1 - A4 according to figure 1. For the results see Table VI.

Table VI: Results from mottle measurements in areas with and without pre-dampening (water) and with and without back-trap for all combinations of paper, ink and fountain solutions calculated as mean value for the four paper used

Printing situation	Mean mottle value in 70% area, c.f. 1 - 8 mm, %	Mean mottle value in 100% area, c.f. 1 - 8 mm, %
A1. Water and no back-trap	3.78±2.37	4.92±2.89
A2. No water and no back-trap	2.85±1.87	3.93±3.00
A3. No water and back-trap	2.21±0.85	2.70±1.60
A4. Water and back-trap	2.70±1.19	3.77±1.02

In order to see the effect of pre-dampening on mottle the differences between all pre-damped areas and areas not pre-damped were calculated and then the mean value was calculated. A positive result indicates that the mottle is increased due to the pre-dampening. For the result see Table VII.

Since the differences are small compared with the standard deviation the significance must be verified. A hypothesis test was therefore performed. The null hypothesis H_0 was that there are no differences between the two mean mottle values; the results are given in Table VII.

Table VII: Results from mottle difference for areas with and without pre-dampening (water) for all combinations of paper, ink and fountain solutions. Results from hypothesis test

Pre-damped - not pre-damped	Difference between areas	Mean mottle difference, c.v, 1 - 8 mm, %	Reject/accept H_0 Reject if $t > t_\alpha = 1.66$
No back-trap, 70% area	A1, 70 - A2, 70	0.93±1.73	t = 2.38 Reject at 5% level
No back-trap, 100% area	A1, 100 - A2, 100	0.99±2.18	t = 1.84 Reject at 5% level
Back-trap, 70% area	A4,70 - A3,70	0.49±0.68	t = 2.64 Reject at 5% level
Back-trap, 100% area	A4,100 - A3,100	1.01±1.07	t = 2.78 Reject at 5% level

Since the null hypothesis was rejected the increased mottle, water induced mottle, is statistically significant at the 5% level for both 70% and 100% areas with and without back-trap. In order to see the effect of the back-trap on mottle the differences between all areas without back-trap and areas with back-trap were calculated and then calculated as a mean value. If the result is positive the mottle is decreased due to the back-trap. For the result Table VIII.

To verify the result also in this case a hypothesis test was done. The null hypothesis H_0 was that there are no differences between the two mean mottle values; the results are given in Table VIII.

Table VIII: Results from mottle in areas with and without back-trap for all combinations of paper, ink and fountain solutions. Results from hypothesis test

Without back trap - with back-trap	Difference between areas	Mean mottle difference, c.v, 1 - 8 mm	Reject/accept H_0 Reject if $t > t_\alpha = 1.66$
Pre-damped, 70% area	A1, 70-A4, 70	1.08±1.99	t = 3.21 Reject on 5% level
Pre-damped, 100% area	A1,100-A4,100	1.15±2.26	t = 3.01 Reject on 5% level
Not pre-damped, 70% area	A2,70-A3,70	0.64±1.18	t = 2.52 Reject on 5% level
Not pre-damped, 100% area	A2,100-A3,100	1.18±1.90	t = 2.73 Reject on 5% level

Since the null hypothesis was rejected the decreased mottle from back-trap, back-trap smoothing, is statistically significant at 5% level for both 70% and 100% areas with and without pre-damping.

The mottle for the four papers DC 1 - 4 in the four printing conditions A1 - A4 with low and high water feed can be seen in figures 2 and 3. The effect on mottle caused by the levels of indentation, back-pressure, printing speed, the general water-feed in all printing units, higher water-feed in only one printing unit, type of fountain solution and type of ink are shown in figures 1 to 8.

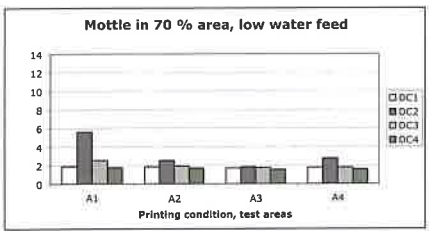

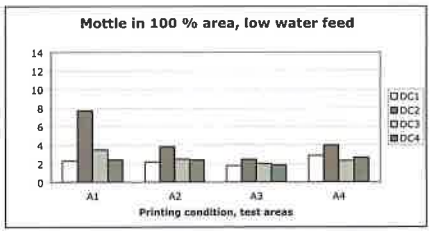

Figure 1a - 1b: The effect on mottle of the level of water feed, low level

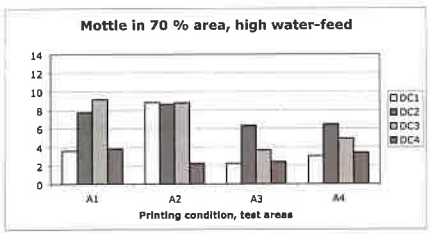

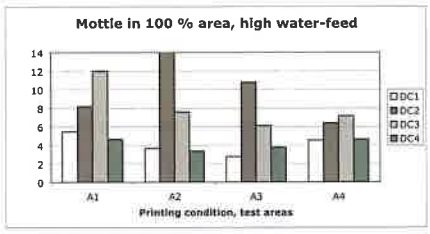

Figure 2a - 2b: The effect on mottle of the level of water feed, high level

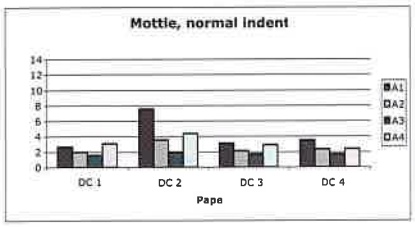

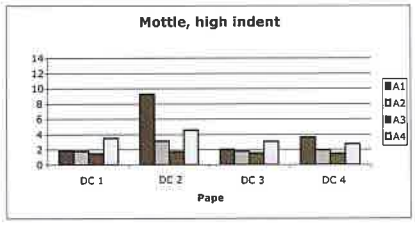

Figure 3a - 3b: The effect on mottle of the level of indentation, back-pressure. 0.10 mm and 0.20 mm

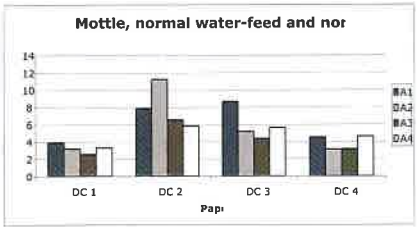

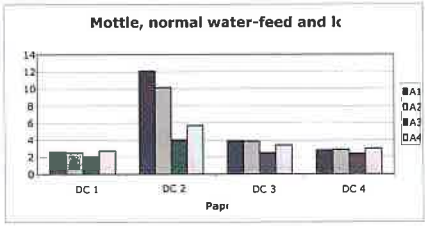

Figure 4a - 4b: The effect on mottle of the press speed, 7.000 copies/h and 4.000 copies/h

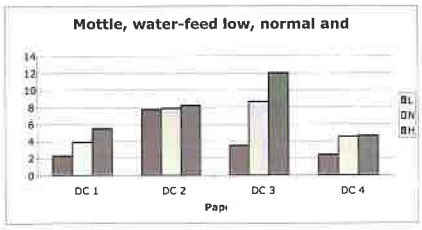

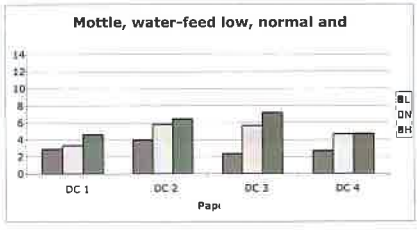

Figure 5a - 5b: The effect on mottle of the water feed, Low, Normal and High for a) without back-trap and b) with back-trap

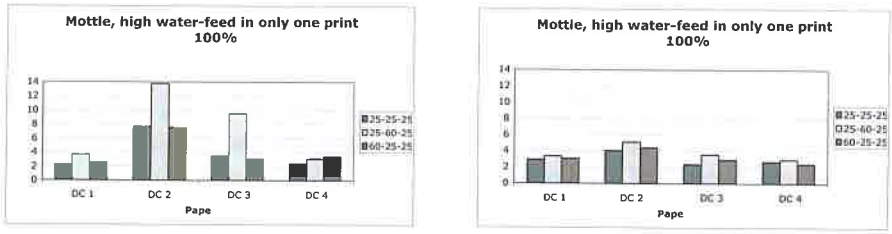

Figure 6a - 6b: The effect on mottle of the water feed in just one printing unit a) without back-trap and b) with back-trap

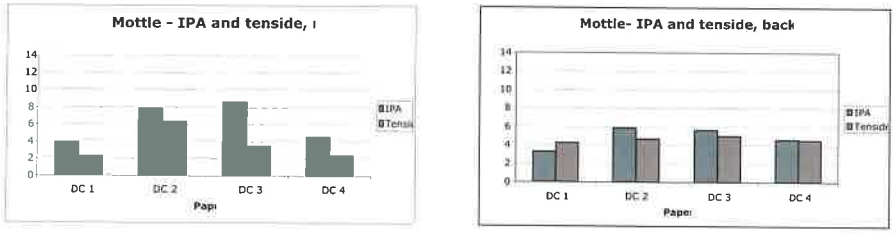

Figure 7a - 7b: The effect on mottle of type of fountain solution, IPA and tenside a) without back-trap and b) with back-trap

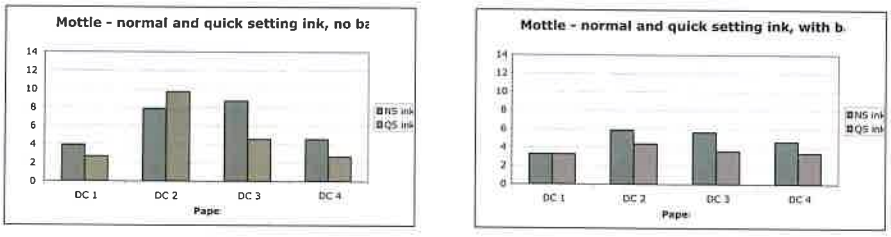

Figure 8a - 8b: The effect on mottle of the ink, normal and quick setting a) without back-trap and b) with back-trap

7. Conclusions

The highest mottle values were found in pre-damped areas with no back-trap. The levels were higher in 100% areas than in 70% areas. The levels increased when the water-feed was increased. The four paper types showed different mottle values, back-trap having a positive effect and lowering the mottle.

For the trial with an increased level of back-pressure and indentation from 0.10 mm to 0.20 mm there was no effect on mottle. This can be explained by the fact that that the papers are calendered and the paper surface is smooth enough with 0.10 mm indentation.

Lowering the speed from 7.000 to 4.000 signature/h reduced mottle clearly. One explanation is that the ink-transfer splitting force increases with the printing speed, leading to uneven ink-film split.

For all paper grades and in all printing units the mottle increased with increased general water feed. Increasing the water feed in one printing unit has a noticeable effect on mottle printed in this unit only. One explanation for this is that more fountain solution is emulsified in the ink and causes uneven ink transfer. It is shown at 95% significance level that there is a water induced mottling effect caused by fountain from the previous printing unit. It is also shown at 95% significance level that even if there is no visible print mottle the print density and dot gain is decreased. The results from the print trials show that mottle is greatly affected by the composition and structure of the coating, by the water feed ink and also by the setting of the ink. The type of fountain solution had no effect on print mottle.

Back-trap decreased the mottle. Water induced mottle is dependent on the volume of the fountain solution feed.

One conclusion is that water induced mottle can be avoided by using the correct press settings and by not using coated paper grades with high surface density.

Acknowledgements

This report is based on results from the NordPap project carried out by, STFI, YKI, KCL, VTT and IMT. The final report is NordPap DP 3/2, Växelverkan vätska-fast fas i bestrykningsskikt, SCAN-Forsk –rapport 680, 1997.

The authors wish to thank Susanna Nieminen and Viola Kunnola at KCL for their full collaboration and assistance in performing the print trials.

References

[1] Aspler, J. S., (1993), *Interactions of ink and water with the paper surface in printing, Nordic Pulp and Paper Research Journal no. 1/93*

[2] Johansson, P-Å., (1993), *Print mottle evaluation by band-pass image analysis. IARIGAI's 22nd International Research Conference, Munich, Sept 1993. Advances in Printing Science and Technology 22 (W. H. Banks Ed.), Pentech Press, pp. 403 - 413.*

[3] Kipphan, H., (2001), *Handbook of print media, Springer - Verlag*

[4] Kipphan, H., (2001), *Handbook of print media, p. 225, Springer - Verlag*

[5] Lafaye, J. F. et al., (1987), *The effect of coating with surfactant on quality and offset printability, August 1987, Tappi Journal*

[6] Purfeerst, R. D. et al., 1991, *Tail edge picking, back-trap mottle and fountain solution interference of model latex coatings on a six color press predicted by laboratory tests, TAPPI Proceedings, 1991 Coating Conference*

[7] Ström, G., (1988) *Wetting studies related to offset printing, Ph. D. Thesis, Royal Institute of Technology, Stockholm*

[8] Weiss, N. A., (2004), *Introductory Statistics, seventh edition, Pearson, Addison-Wesley*

Modelling the anilox-plate micro contact

David Bould, Simon Hamblyn, John Cherry, Tim Claypole

Welsh Centre for Printing and Coating, University of Wales Swansea
Singleton Park, Swansea SA2 8PP, UK
E-mail: d.c.bould@swansea.ac.uk

Abstract

Deformation of the flexographic printing plate against the anilox roll is an important factor in determining the withdrawal of ink from the anilox to the printing plate. A numerical model has been developed to consider how the halftone dots on the flexographic plate deform into the anilox cells. The location of the anilox cells, relative to the halftone dot on the flexographic printing plate was varied, to determine how the deformation profile of the plate varied, depending on the location of the anilox cells.

The results have shown that the greatest deformation of the dot into the cell occurs when the centre of the anilox cell is directly above the edge of the top surface of the dot. Deformation of the plate was found to be greater where the cell was situated along the axis of the line ruling of the dots on the plate than where the cells were directly above the dot edge, but at 45° to the line ruling. Increasing engagement between the anilox roll and the plate increased deflection into the cells.

Keywords

Anilox, finite element analysis, flexography, plate

1. Introduction

The release of ink from the anilox roll to the printing plate is a key factor in the flexographic process. Controlling the ink transfer from the anilox roll to the printing plate is a key factor in controlling the quality of the final printed image. During a single print cycle, the raised image regions of the plate deform against the anilox roll and ink is withdrawn from the cells of the anilox roll onto the plate. The image regions of the plate relax once separated from the anilox, but undergo further deformation as they contact the substrate. Numerical models to study the nip contacts between hard and soft rollers have previously been studied to determine the pressure distribution for both dry contact and elastohydrodynamic applications [Hannah (1951), Hooke and O'Donoghue (1972) and Hooke (1999)]. Mirle and Zettlemoyer (1988) used numerical models to study the relaxation of photopolymer plates. The theoretical model did not consider any sub-ambient pressures at the nip exit, which are likely to be a key consideration when examining the ink released from the anilox cells onto a plate. In addition, the model was limited to a solid plate contacting against a solid impression cylinder and did not consider the effects of tonal variation, or deformation against a pitted surface, such as an anilox roll. Numerical techniques have also been used to consider the effect of ink levels on rollers in printing and coating applications [MacPhee et al. (1992)]. By replicating starved and flooded nip junctions, it was shown that the quantity of ink present had a large impact on the quality of the image produced. Although the investigation was not directly related to the mechanisms by which ink transfer occurs during the flexographic process, the investigation does highlight the importance of maintaining a stable supply of ink to the plate in order to achieve consistent printed image.

Previous investigations into the flexographic printing plate [Bould et al. (2001, 2004) and Bould (2001)] have shown that as the plate deforms against the impression cylinder, the halftone dots deform, leading to an overall growth of the plate dot area. The deformation was found to be due to two separate mechanisms; expansion of the dot surface and barrelling of the dot shoulders.

Currently very little is understood about how the ink is drawn from the laser engraved cells onto the photopolymer material. Cherry et al. (2006) have shown that the percentage of ink released from the cells on the anilox roll to the plate varied considerably. For each cluster of cells that was in contact with a halftone dot, the volume of ink released varied, with some cells releasing a high proportion of the ink, whilst other cells released very little (Figure 1). It was hypothesised that this variation in ink release was due to how the dots on the plate were aligned with the anilox cells. When releasing ink to a solid region on the printing plate, around 40% of the ink was released. When the anilox cells were in contact with a halftone dot on the plate, the ink

release was shown to be significantly higher (around 76%). As a result of the investigation, it was concluded that further work needs to be carried out to investigate the variation in ink release between anilox cells.

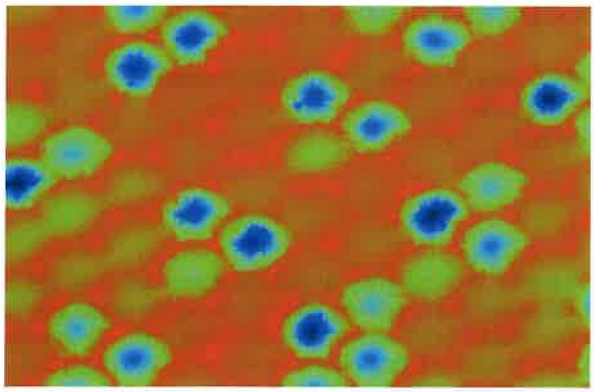

Figure 1: Irregular ink release from anilox to plate

As a result of the review of the literature, it has been shown that the interaction between the printing plate and the anilox roll is not understood. The purpose of this paper is therefore to investigate the interaction between the anilox and the plate with particular regard to how the plate deforms into the cells of the anilox roll. Finite element models were generated to explore how the halftone dots on the plate deform into the cells. The models were generated parametrically, in order that the position of the cells, relative to the dot, could be varied, to simulate variation in alignment between the cells and the halftone dots, hypothesised by Cherry et al. (2006).

2. Model development

The models used in the investigation were based on the deformation of a single dot on a plate into a cluster of cells on the anilox roll. Non-linear finite element analysis was employed since the dot geometry changes as the load is applied and contact evolves. Thus iteration is required to determine the new contact position. An incremental implicit scheme was applied to simulate the progressive engagement and to facilitate capture of the consequent deformation of the dot. Finite element meshes may comprise a structured configuration in which elements are placed in a regular lattice (say rectangular). Alternately, the meshes can be irregular (or unstructured), providing a facility to concentrate elements locally to assure solution accuracy. In this case an unstructured mesh was used to enable specific regions to be analysed using a high mesh density, leaving non-critical areas with a lower mesh density. As well as improving accuracy, it also leads to computing efficiency.

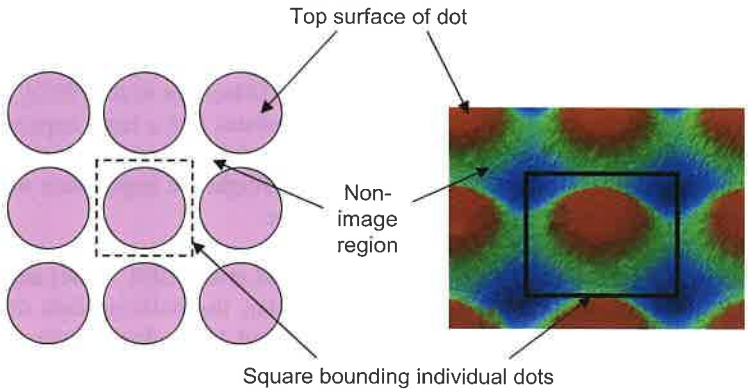

Figure 2: Determination of bounding edges of dot model

The geometry of the halftone dots on the plate was based on topographic measurements of flexographic printing plates using white light interferometry. The dots were assumed to be completely round and the top surface of the dots was assumed to be completely flat. The bounding area of the dot was considered to be a square (Figure 2). The symmetrical nature of the round halftone dots was exploited in order to optimise computational efficiency.

Therefore only a quarter of each dot was modelled. Boundary conditions were applied to the axes of symmetry and also the outer edges of the dot, such that the model was constrained perpendicularly, but was able to deform along the length model edge. A medium density mounting tape was also included as part of the model, as deformation of the top of the halftone dots on the plate is affected by the mounting tape.

Data for the modelling of the anilox cells was taken from white light interferometry measurements of anilox rolls. As the cells were assumed to be rigid, and unlikely to deform during the contact with the flexographic printing plate, the cells were modelled as a shell, with a thickness equivalent to a single element. The cells were assumed to be hemispherical and the land area between the cells was assumed to be flat with no roughness. A flat land area was used as the radius of the anilox roll is large in comparison with the size of the features being examined by the model. In order to improve computational efficiency, the bottom of each of the anilox cells was modelled as being flat, rather than continuing the hemispherical geometry to the full cell depth. This had no influence on the results, as the overall depth of the cells was greater than the engagement considered between the anilox and the flexographic plate, so the plate would not deform as far as the bottom of the cells. The mesh generated for the dot and cells is shown in Figure 3 and the parameters of the anilox and plate are summarised in Table I.

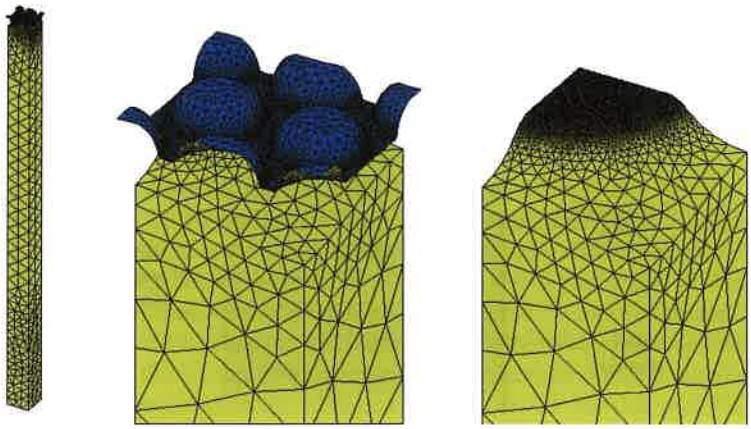

Figure 3: Mesh of quarter dot model and enlarged view of contact region

Table I: Summary of model parameters

Line ruling on plate (l/cm)	59.1
Plate coverage (%)	30
Plate thickness (mm)	1.14
Mounting tape thickness (mm)	0.38
Anilox screen ruling (l/cm)	196.8

Engagement was simulated by displacing the anilox cells onto the dot on the flexographic plate. The engagement was applied normal to the dot surface instead of a rolling engagement. For the purposes of the numerical study, the models assumed dry contact with no ink, reducing the problem to a single phase analysis. A dry contact analysis also enabled the deformation of the printing plate to be quantified. The coefficient of friction between the dot and the shell was set at 0.001 so that there was negligible friction in the contact to simulate the lubricating effect of the ink in the printing process, when printing onto a non absorbent substrate. This value was determined during a previous investigation [Bould et al (2004)] by a simple numerical investigation to examine the effect of the coefficient of friction on the stresses generated within the material of a flexographic printing plate. It was found that there was little change in stress, as the coefficient of friction fell below 0.01. Therefore, the value of 0.001 was chosen as it was well below this value and so would not affect any deformation of the dots on the plate.

Material properties were required for the flexographic plate material, the mounting tape material and the anilox roll. The properties for the plate material and the mounting tape were determined experimentally using a Hounsfield materials tester. A description of the techniques used to acquire the required properties may be found in [Bould (2001)]. As the anilox roll was considered to be rigid, the properties of steel were used. The results for the two materials are listed in Table II.

Table II: Material properties used for numerical models

	Young's Modulus (Nmm^{-2})	Poisson's Ratio	Shear Modulus (Nmm^{-2})	Density ($kgmm^{-3}$)
Flexographic Printing Plate	3.611	0.43	1.263	1.033E-6
Flexographic Mounting Tape	0.4611	0.45	0.1590	5.48E-7

Analysis of the deformation profiles of the flexographic dot was considered by varying the position of the anilox cells, relative to the edge of the dot, at the interface between the dot surface and the dot shoulder. A schematic, showing the positioning of the centre of an anilox cell, relative to the flexographic dot for each location considered is shown in Figure 4 and the engagements used for each cell location is summarised in Table III. The case where an anilox cell was positioned directly above the edge of the dot (X_1), along the axis of symmetry, was considered for both a 50 µm and a 75 µm engagement. This was to understand the effect of engagement on how the dot deforms into the anilox cell. Cases where the anilox cell was moved along the axis of symmetry (X_2, X_3 and X_4) and where the cell was located above the edge of the cell, but at 45° to the line ruling (X_5) were considered for a 50µm engagement only.

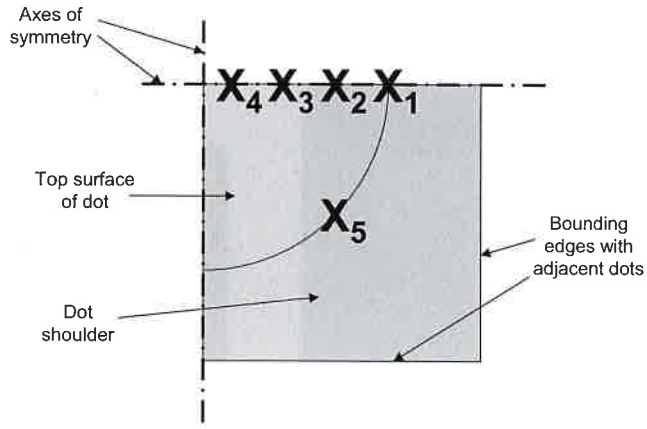

Figure 4: Schematic in plan view of location of anilox cell centre for cases studied

Table III: Summary of engagements studied for each anilox cell location

Case number	Cell Location	Engagement	
		50 µm	75 µm
1	X_1	✓	
2	X_2	✓	
3	X_3	✓	
4	X_4	✓	
5	X_5	✓	
6	X_1		✓

3. Results

Graphs showing the deformation profiles and stress profiles along the axis of symmetry for Cases 1 - 4 are shown in Figures 5 - 8. Each graph shows the undeformed dot profile, the deformed dot profile and the stress generated at each point along the axis (plotted on the secondary axis). Also included for reference purposes only is the profile of the cells of the anilox. Analysis of Figure 5 shows that the deformation of the dot is greater where only one side of the anilox cell is supporting the dot. The dot shoulder is then able to deform into the cell to a greater extent than for the middle of the dot, where it is completely supported by the land areas of the anilox roll. The points of highest stress on the dot are situated where the flexographic plate contacts against the interface between the land area and the recessed cells. Of the two peaks of high stress which occur, the greater peak occurs on the side of the cell with the greater deformation of the dot into the cell. As the anilox cell moves away from the edge of the dot to location X_2 (Figure 6), the deformation of the dot reduces, from a maximum deflection into the cell of 6.0 µm at X_1 to a deflection of 5.4 µm at X_2. As the deformation of the dot has reduced, the maximum stress generated within the flexographic dot has also

reduced, from 0.74 Nmm^{-2} to 0.53 Nmm^{-2}. The shoulder of the deformed dot is also contacting with the wall of the anilox cell, generating a third peak on the stress profile, with a maximum of 0.19 Nmm^{-2}.

Figure 7 shows the profile for Case 3, at cell location X_3. For this case, the land area of the anilox cell is contacting the flexographic dot on both sides. This has greatly reduced the deformation of the top surface of the dot, as there is no longer a free surface of the dot which is able to deflect into the cell. While the deformation has reduced, the stress profile has increased, reaching a maximum of 0.79 Nmm^{-2}. As the anilox cell moves to location X_3 (Figure 8), the dot shoulder is once again free to deflect into an anilox cell. The deflection of the dot into the cell reaches a maximum of 3.6 µm. This occurs close to the centre of the dot (near the axis of symmetry), where the dot is supported by the land areas of the anilox cell. However, in the unsupported region, the dot is only prevented from deflecting further, by the profile of the shoulder, which is falling away from the anilox at a greater rate than it is able to deform into the cell. The stress profile shows the maximum stress (0.77 Nmm^{-2}) occurs on the side of the unsupported dot, with the free surface. For all the previous cases, the peak of maximum stress has occurred on the same side as the maximum deformation of the dot into the cell. The supports the hypothesis that the free surface of the dot shoulder would have deformed further into the cell, if the dot shoulder had not decreased at the rate that was used in all of the cases considered in this investigation.

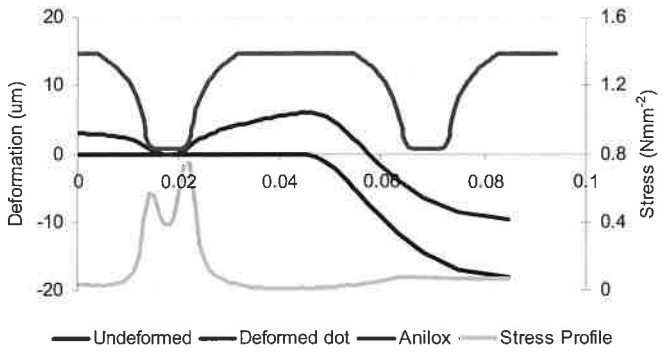

Figure 5: Deformation and Stress profiles for Case 1

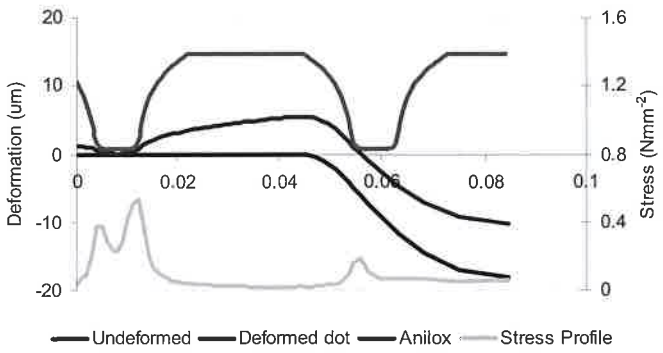

Figure 6: Deformation and Stress profiles for Case 2

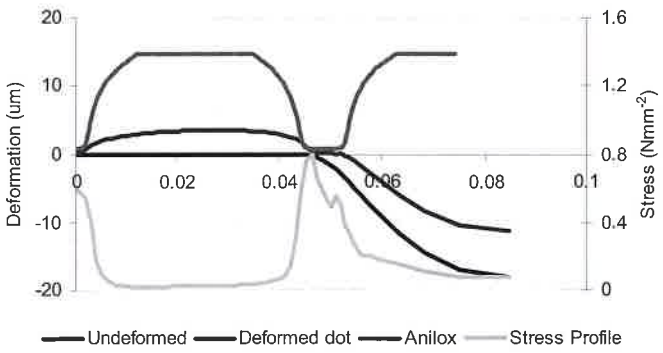

Figure 7: Deformation and Stress profiles for Case 3

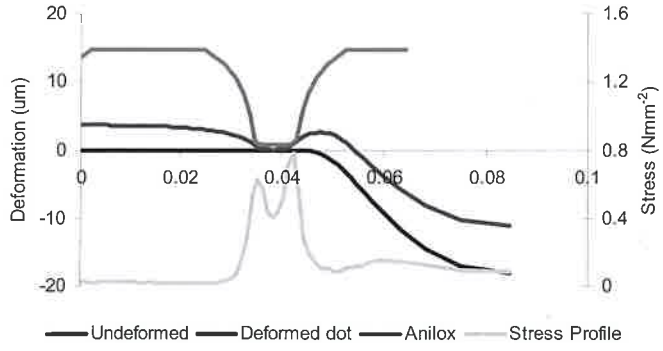

Figure 8:
Deformation and
Stress profiles for Case 4

A comparison between Case 1 and Case 5 is shown in Figure 9. Similar deformation profiles are exhibited, both along the axis of symmetry and at 45° to the axis of symmetry, although the deformation is slightly greater for the case along the axis of symmetry (6.0 μm for Case 1, 5.3 μm for Case 5). The lower deformation for Case 5 was attributed to the profile of the dot shoulder at 45° to the line ruling. Although the angle of the shoulder was the same for both regions of the dot shoulder, the profile at 45° to the axis of symmetry recessed to a greater depth. This was shown in the white light interferometry image in Figure 2, where the deepest regions at 45° to the axis of symmetry are represented by the blue regions of the image, and the lowest regions along the axis of symmetry are represented by the green regions of the image. The difference in the shoulder profile is also highlighted by the lower stress profile for Case 5, where the maximum stress is only 35% of the highest stress value for Case 1.

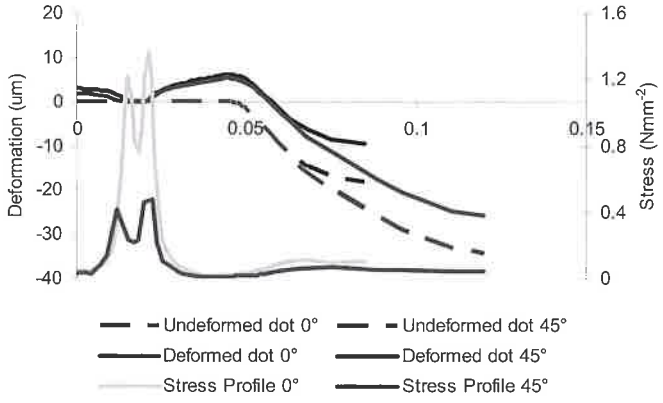

Figure 9:
Deformation and Stress
profiles for Case 1 and Case 5

The effect of anilox to plate engagement is shown in Figure 10, which compares Case 1 and Case 6. As the engagement is increased from 50 μm to 75 μm, greater deformation of the dot into the cells occurs, particularly for the unsupported free surface of the dot shoulder. The maximum deflection into the cell is 8.4 μm for Case 6, compared with 6.0 μm for Case 1. Increasing the engagement also increases the stress profile, with the maximum stress increasing from 0.74 Nmm^{-2} to 1.40 Nmm^{-2}.

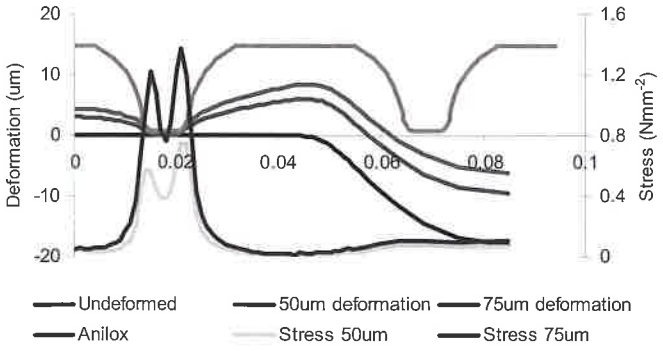

Figure 10:
Deformation and Stress
profiles for Case 1 and Case 6

This result highlights the importance of controlling the engagement between the plate cylinder and the anilox roll when setting up a flexographic press, as small variations in engagement can have a large influence on the deflection of the dots into the cells.

4. Discussion

The following section discusses the implications of the results from the investigation into the micro-contact between the anilox and the dot on a flexographic printing plate. Controlling the transfer of ink received by the plate during the flexographic printing process is fundamental to achieving consistent print quality. It is therefore essential to understand the issues that affect the ink transfer from the anilox cells to the raised regions of the printing plate.

This investigation has focused solely on a dry contact between the anilox and the plate. In reality, ink is present in the cells, which will alter the results of the deflection of the plate into the cells. This will be most significant where the anilox cell is completely covered by the flexographic dot. In these regions, the deformation of the dot into the cell will be greatly reduced, as ink will inhibit the deformation. The mechanism by which ink is withdrawn from an anilox cell, where the cell is completely encompassed by the flexographic plate, is still not understood. However, the results from this investigation have shown that the plate material has a tendency to push into the cells. When the cells are full of ink, this will generate a pressure within the ink. As the plate and the anilox separate, the pressure within the ink will reduce and a sub-ambient pressure will then be created and ink will be drawn from the cells. For cells which are only supported on one side by the plate and therefore leaving a free surface of the dot, the ink has a greatly reduced effect on the deformation of the dot. This is because as the dot deforms into the cell, ink can escape from the cell and be forced down the shoulder of the dot. This has implications for halftone printing, as any ink on the shoulder of the dot will result in greater ink being transferred from the dot to the substrate, due to the deformation of the dot shoulder against the substrate through the plate to substrate printing nip [Bould et al. (2004)]. This will contribute to a growth in the overall size of the printed dot and result in a darker image than required. A summary of how the dot will deform against an inked anilox roll is presented schematically in Figure 11.

The investigation has shown that the stresses generated on the printing plate are varied, depending on how the dots on the plate are aligned against the anilox cells. The regions of greatest pressure have been shown to be where the plate contacts against the cell / land area interface of the anilox roll. As the exact alignment of the dots and the anilox cannot be controlled during the printing process [Cherry et al. (2006)], the plate will be subjected simultaneously to varying levels of stress. However, it is not within the scope of this investigation to explore further any impact on the observation on the final print quality.

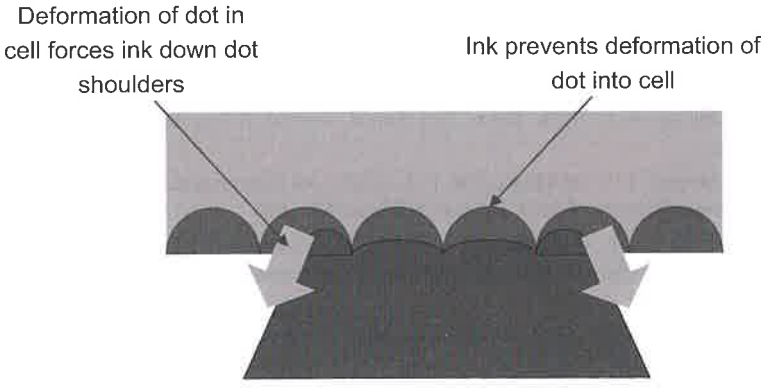

Figure 11: Schematic of role of ink on deformation of flexographic dot into anilox cells

The engagement between the anilox roll and the dot on the plate was shown to have a large effect on both the deformation of the dot into the cell and the resultant stress profile. During the printing process, this engagement is not typically controlled and is reliant on the press operator to maintain a consistent engagement between the anilox and plate, each time the press is set up. This investigation has shown that any error in setting this engagement will have a large effect on the final printed image.

This investigation has focused solely on a single dot geometry, and a single anilox geometry. There is scope to extend the investigation to analyse the effect of parameters such as plate line ruling, plate coverage, dot shoulder angle, anilox line ruling and anilox cell volume. Analysis of these parameters will enable the study of phenomena such as dot dipping, where a significant proportion of the dot enters the cell, causing the evacuation of more ink that required. This is particularly noticeable when printing small dot sizes in combination with low line ruling anilox rolls. It is also necessary to develop the investigation to consider the ink as part of the system. This will require a new model to be developed, which couples the deformation of the dot, with the fluidic properties of the ink.

5. Conclusions

A search of the literature has shown that the interaction between the printing plate and the anilox roll is not understood. By developing a parametric numerical model, this investigation has analysed the deformation of the halftone dot on the plate into the cells on the anilox roll. Whilst the investigation has been restricted to a single geometry of dot and a single anilox line ruling, the work has generic implications for the deformation of any dot structure. The numerical models only considered the deformation under dry contact conditions with planar loading, which is the first stage only towards developing full understanding of the effects of the anilox roll on the printing plate. However, this research has led to the increased predictability of the process, developing flexography from a craft to the use of a more scientific approach.

From this study, the following conclusions have been drawn:

- The location of the anilox cells relative to the dots on a flexographic printing plate has a large effect on the overall deformation of the dots into the cells and the subsequent ink release to the plate. This investigation has shown that the effects observed in Figure 1 are due, in part, to the random alignment between the anilox cells and the halftone dots on the plate.
- The greatest deformation of the dot into the cell occurred where the anilox cell was not completely in contact with the flexographic dot, resulting in a free surface of the dot, which was able to deform further into the cell. When an anilox cell was completely covered by the dot surface, deformation of the dot into the cell was greatly reduced.
- Little difference was observed between when the cell was located over the edge of the dot surface along the axis of symmetry and when the cell was located over the edge of the dot surface at 45° to the axis of symmetry. However, the stress profile of the flexographic dot was significantly lower for the profile at 45° to the axis of symmetry. This was attributed to the profile of the dot shoulder, which recessed to a greater depth than the profile along the axis of symmetry, even though the shoulder angle was kept constant.
- Engagement between the anilox to plate has a large effect on the deflection of dots into the cells, which will result in large differences in the ink released from the cells onto the plate.

References

[1] Bould D. C., 2001, 'Quality improvements in flexographic printing' PhD Thesis, University of Wales Swansea

[2] Bould D. C., Claypole T. C. and Bohan M. F. J., 2004, 'An investigation into plate deformation in flexographic printing' Proc. Instn. Mech. Eng. Part B, Journal of Engineering Manufacture, vol 218, pp 1499 - 1511

[3] Bould D. C., Claypole T. C. and Bohan M. F. J., 2005, 'An Experimental investigation into flexographic printing plates' TAGA Journal, vol 1 pp183 - 196

[4] Cherry J. A., Claypole T. C. and Gethin D. T., 2006, 'Measurement of Ink Release from the Anilox Roll', Proceedings of the 58th annual technical conference of the Technical Association of the Graphic Arts (TAGA), pp 395 - 408

[5] Hannah, M., 1951, 'Contact stress and deformation in a thin elastic layer' Q. J. Mechanics Appl. Math., vol 4, pp 94 - 105

[6] Hooke, C. J. and O'Donoghue, J. P., 1972, 'Elastohydrodynamic lubrication of soft solids' Proc. Instn Mech. Engrs, Part C: J. Mechanical Engineering Science, vol 14, pp 34 - 48

[7] Hooke, C. J., 1999, 'The behaviour of low applitude surface roughness under line contacts' Proc. Instn Mech. Engrs, Part J: J. Engineering Tribology, vol 213, pp 383 - 396

[8] MacPhee, J., Shieh, J. and Hamrock, B.J ., 1992, 'The application of elastohydrodynamic lubrication theory to the prediction of conditions existing in lithographic printing press roller nips' Adv. Printing Sci. Technol., vol 21, pp 242 - 276

[9] Mirle, S. K. and Zettlemoyer, A. C., 1988, 'Viscoelasticity of photopolymer plates and ink hydrodynamics in modelling flexographic printing' Mathematical Computer Modelling, vol 11, pp 1162 - 1165

Analysis of interferometric data to obtain accurate geometric characterisation of engraved cells

D. Deganello, T. C. Claypole, D. T. Gethin

Welsh Centre for Printing and Coating
School of Engineering, University of Swansea, SA2 8PP, Swansea, UK
E-mail: D.Deganello@swansea.ac.uk

Abstract

Engraved cells have a crucial role in the gravure and flexographic printing processes. This paper presents the development of an automatic analysis technique for a complete and accurate geometrical characterisation of the engraved cells over three-dimensional interferometric profiles. This technique allows the automatic individual identification and demarcation of engraved cells on the cylinder profile. Successive analysis allows an automatic accurate measure of geometric parameters of relevance such as engraved volume, depth, width, length, stylus angle, cell offset. Applications and preliminary verification of the technique are presented.

Keywords

Anilox, cell geometry, gravure

1. Introduction

Engraved cells have a crucial role in the gravure and flexographic printing processes acting as primary ink carriers and as the image carrier in the gravure process. Accurate geometric characterisation of the engraved cells is essential for the analysis of the effect of the cell shapes and size on the ink release process.

White light interferometry can produce high resolution descriptions of the topography of the engraved cells. Despite its sophistication, operation of the equipment and the interpretation of the data can lead to systematic errors, which can be as high as 15%. Refinement of the standard operating procedures has significantly reduced the errors [M. F. J. Bohan et al., 2001]. However, the need for the operators to make subjective judgments even with the single cell analysis technique [J. Cherry et al., 2005] still introduces errors and inter-operator inconsistency. This paper discusses the development of an automatic analysis technique for a complete and accurate geometrical characterisation of the engraved cells.

2. Measuring methodology

Key point for the development of the automatic process was the ability to identify and delimit the engraved cells over the scanned profile; this was reached with the development of a *watershed algorithm*.

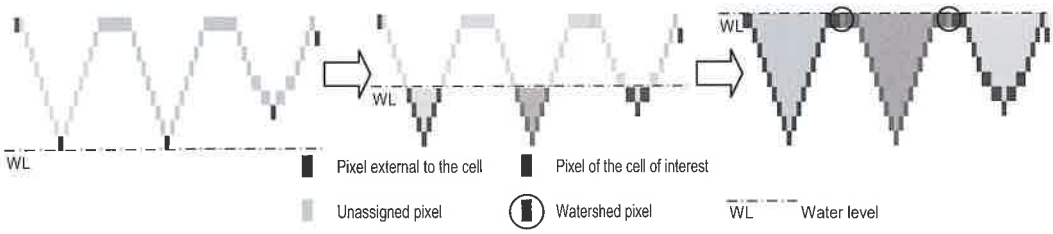

Figure 1: Watershed algorithm execution

The intuitive concept underlining this method comes from geography [Roerdink et al., 2001]: it is that of a landscape being flooded from beneath with a flow of water. Holes are pierced in local minima on the landscape. Basins will fill up with water flowing through these holes; the water level will rise uniformly with

respect to the overall water level. At points where water coming from different basins would meet, damns are built. As a result, the area will be portioned into regions separated by damns or *watersheds*. A graphical representation of the execution of a watershed algorithm is presented in Figure 1.

On a flat area, the water, coming from the two sides, would meet in the middle; following this algorithm, a ring was determined surrounding the engraved cell shown Figure 2. The scanned profile was horizontally aligned on the base of the ring. Any inter-cell channels are identified with a statistical analysis of the ring and excluded from the alignment.

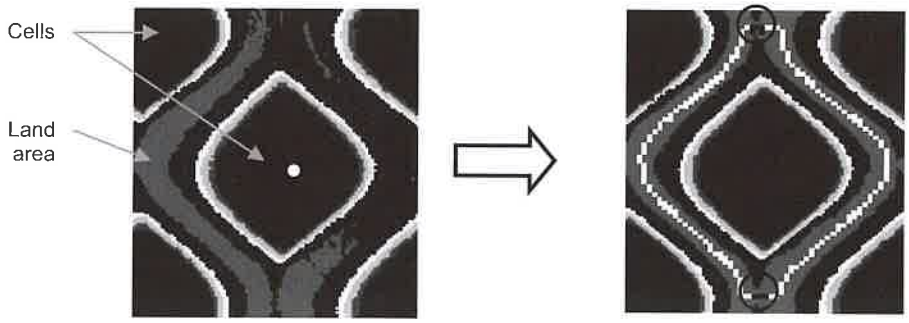

Figure 2: The engraved cell is aligned over white ring. Encircled red points on channel, not used for alignment

For the identification of cell edges, a modified watershed algorithm was developed. Giving priority to the liquid external to the cell with respect to the one inside the analysed cell, the watershed point will be exactly on the edge of the cell, Figure 3.

Figure 3:
The white line defined by
the software delimits the edge of the cells

Due to the presence of the surface roughness, this method is subject to a high variability with possible large errors, Figure 4. Integrating the watershed algorithm with a gradient analysis of the top surface is a possible solution to the problem, allowing the definition of a more reliable and referable cell edge, figure 5.

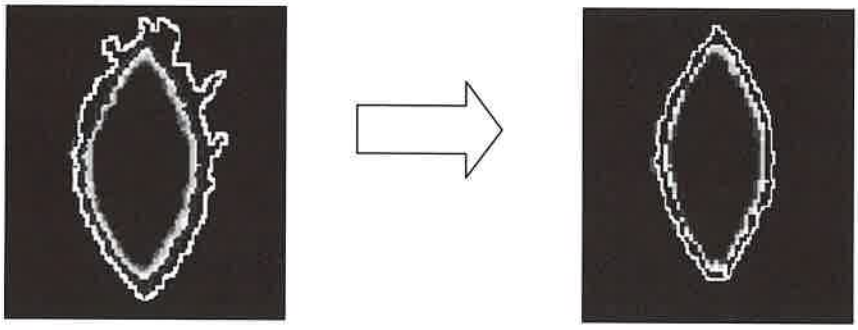

Figure 4: Limits of watershed algorithm in the definition of the border

Figure 5: Same cell but here the watershed algorithm is integrated with gradient analysis

Once the cell and its edges has been identified and delimited, the geometric parameters, which characterise the engraved cells, can be easily measured. These includes the cell cell width, length, depth, the compression ratio, the top open area, the land area roughness, the volume.

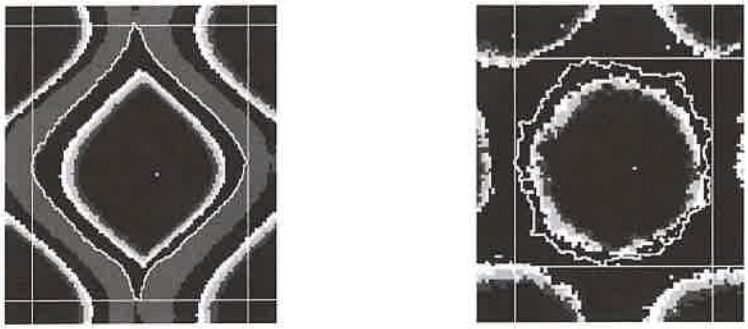

Figure 6: Picture of a mecnanical engraved gravure cell and a laser anilox cell highlighting dimensions, position of deepest point, area within the border

In addition other parameters, previously omitted due to the complexity of measurement process, can be obtained such us:

a. **Stylus angle:** not only the value of the stylus angle can be measured but also its variation with the cell depth. This is useful for the analysis of engraving tool wear or of residual ink deposit, Figure 7.

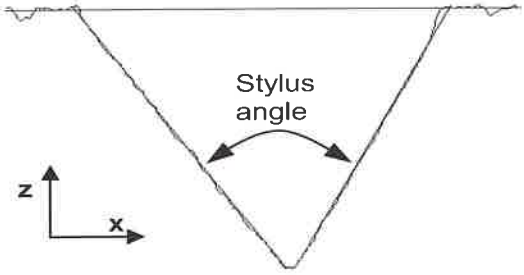

Figure 7:
Cross section profile of the cell, sylus angle

b. **Offset** between the bottom of the cell and its median axis;

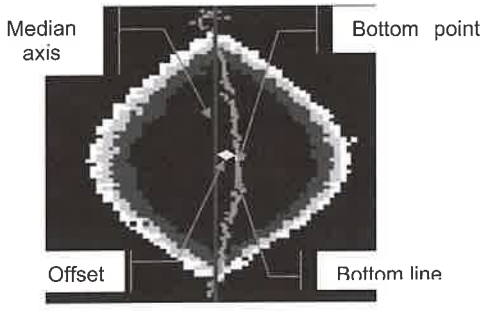

Figure 8:
Offset between the bottom of the cell and its median axis

c. **Cell edge angles**: the actual angle of the top edge of the cell is different from the compression ratio (i.e. width over length). Cell edges give the opportunity to analyse any possible asymmetry in the cell shape.

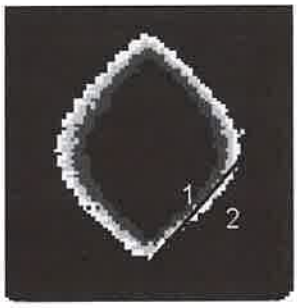

Figure 9: Compression ratio (1), Cell edge angle (2)

Figure 10: Highlighted shape of an asymmetric cell

d. **Width of cell extremes:** These are the two points of input and output of the engraving tool. Their different width can be useful for an examination of the wear of the tool.

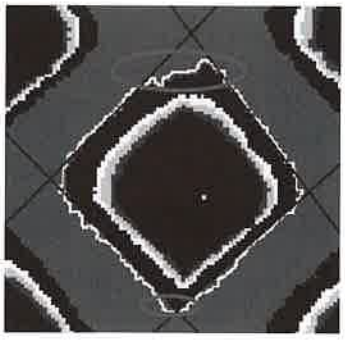

Figure 11: The two extremes of the cell length show a different width

In the case of **laser engraved cells**, additional geometric parameters are obtainable as follows:

a) Inclination of the cell walls
b) Perimeter of the border
c) Circularity of the cell top area
d) Depth to opening ratio

Figure 12: Cross section profile of a laser engraced anilox cell with highleted measured cell wall inclination

The software is also able to identify the presence of **inter-cell channels** measuring their thickness.

3. Validation

In order to verify the validity of the cell edge definition algorithm used by the software, results of the technique were compared with results obtained with a microscope. Engraved patches of a gravure cylinder were measured with a microscope and with white light interferometry. The values of width, length and top open area measured by the software on the interferometric profile were compared with the ones obtained with the optical measurement.

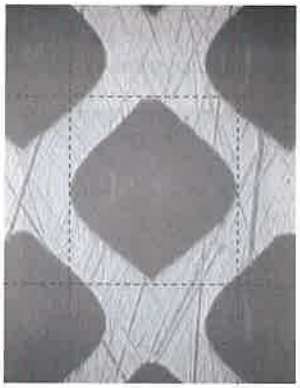

Figure 13: 2D Optical microscope picture highlighting dimensions

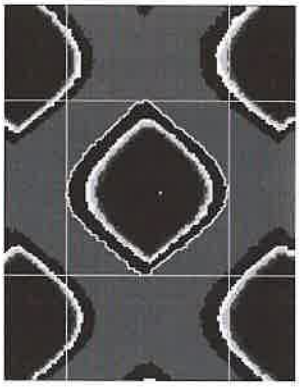

Figure 14: Top view of 3D profile, highlighting dimensions calculated by the software

In Figure 15, 16, 17 the results are plotted against each other showing a good agreement of two techniques. The compared cells were engraved with a 130° stylus angle tool, 60° Screen angle and 60 lines/cm screen ruling.

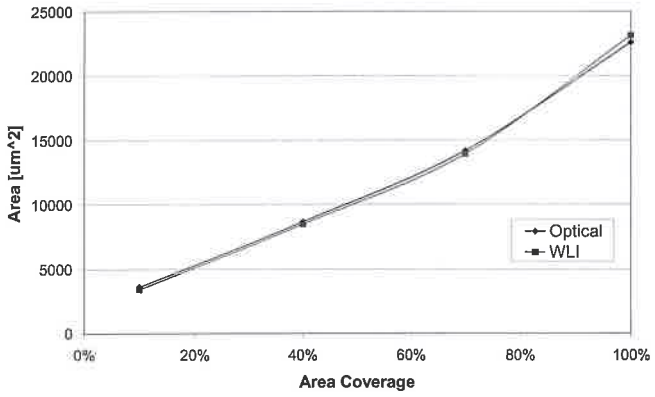

Figure 15: Cell top open area vs. nominal area coverage

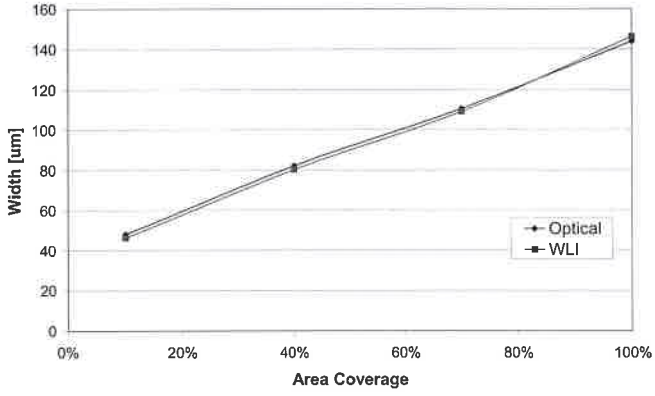

Figure 16: Width vs. nominal area coverage

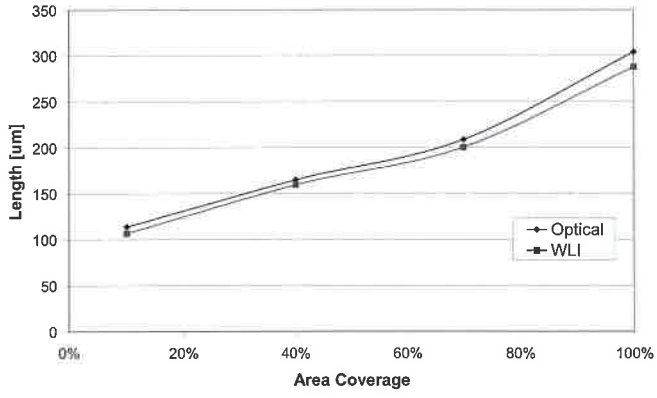

Figure 17: Length vs. nominal area coverage

4. Application

Cells of different shapes and sizes have been analysed, the software proved to give reliable results in all cases, Figure 18 - 19. The software was shown to be robust, being able to deal also with poorly engraved cells, Figure 19.

Figure 18: Examples of results from mechanical engraved cells with different area coverage

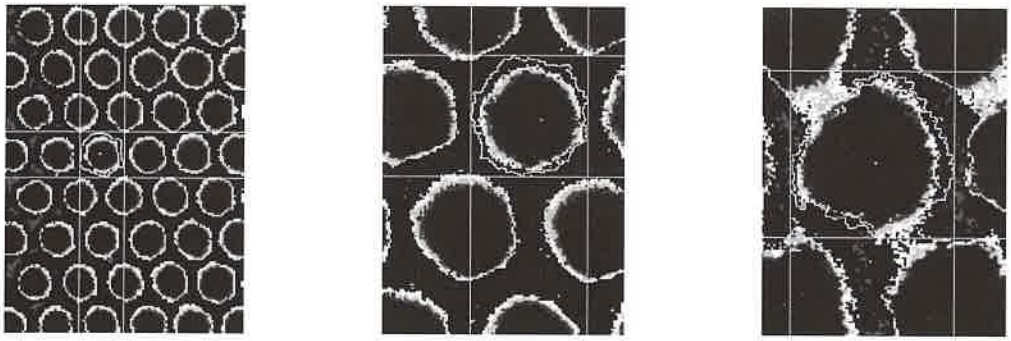

Figure 19: Anilox cells with different screen ruling.
On the far right: a poorly engraved cell with an extremely rough land area

An example of the capabilities and possible applications of the software is a study of the effect of chromium plating on the size and shape of the engraved cells. Mechanical engraved cells were measured before chromium plating and then after. In Figure 20 and Figure 21 the effect of a chromium plating process on cell volume and the stylus angle is shown. The cells were engraved with 55 l/cm screen ruling, 45° compression ratio at 12 nominal area coverage levels.

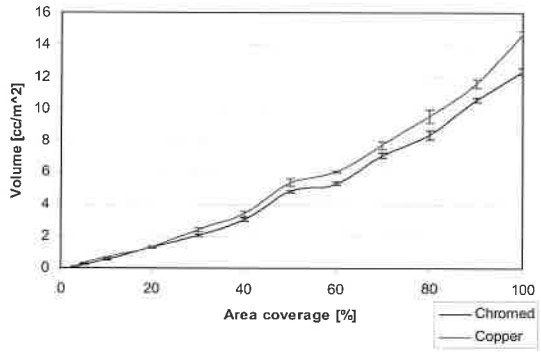

Figure 20:
Volume variation due to chromium plating

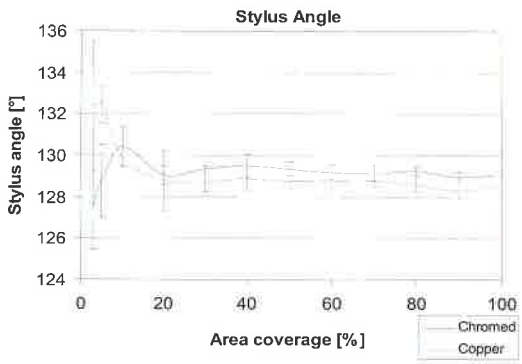

Figure 21:
Stylus angle variation due to chromium plating

In these measurements, the software was able to assess value of volumes with 1% accuracy.

5. Conclusions

Robust and accurate operating procedures and software have been developed for characterising engraved cells that enables white light interferometric data to be rapidly processed achieving better than 1% accuracy in terms of cell volume independent of the operator and being able to deal with a large range of cells, independently from the engraving technique and quality of engraving. Analysing each engraved cell separately, the software is able to automatically identify the cell and its border over a tri-dimensional profile using a newly developed watershed algorithm; it calculates then a large number of geometric parameters, which completely identifies the cell.

The software has greatly improved the process of analysis of the engraved cells allowing large-scale extensive accurate characterisations of gravure cylinders and anilox rolls, process previously time consuming and trained-labour intensive.

References

[1] Bohan M. F. J., Clist A. M., Claypole. T C., Gethin D. T., (2001), *"Characterisation of gravure Cylinders" TAGA Proc 2001, pp 1 - 12*

[2] Cherry J., Hamblyn S. M., Bohan M. F. J., Claypole T. C. and Gethin D. T., (2005), *"Measurement of the cell volume of anilox rolls" TAGA Proc 2005, pp 188 - 201*

[3] Roerdink J. B. T. M. and Meijster A., (2001), *"The Watershed Trasform: Definitions, Algorithms and Parallelization Strategies", Fundamenta Informaticae, 41, 2001 ,pp 187 - 228*

Effects of elevated temperature on flexographic printing

Robert Olsson [1], Li Yang[2], Jan van Stam[3], Magnus Lestelius[2]

[1] Holmen Paper AB, Hallsta Paper Mill
SE-763 81 Hallstavik, Sweden
E-mail: Robert.Olsson@holmenpaper.com

[2] Karlstad University, Department of Chemical Engineering
SE-651 88 Karlstad, Sweden
E-mails: Li.Yang@kau.se; Magnus.Lestelius@kau.se

[3] Karlstad University, Department of Physical Chemistry
SE-651 88 Karlstad, Sweden
E-mail: Jan.van.Stam@kau.se

Abstract

A modern flexographic printing press very often runs at a high speed (above 400 m/min). Accompanying the high running speed, the press generates more heat per time unit, which results in a higher working temperature of the printing units of the press. This, in turn, requires knowledge of ink performance at temperature above room temperature since properties like viscosity and surface energy are altered. This investigation aims to study the effect of temperature on ink performance in a printing press and its final print quality. Viscosity and temperature curves of different inks are measured. Measurements show that viscosity decreases with shear rate and temperature. Printing trials have been performed with a roll-to-roll laboratory printing press, equipped to heat the ink to mimic a real working condition and to evaluate the effect of temperature elevation on print quality. It is shown that the print density increases with temperature as an effect of the lower ink viscosity. Mottling at shorter wavelength is reduced at high temperature. At longer wavelength, the mottling is unchanged or even marginally increased, as the consequence that the ink becomes immobilised before variations are levelled out. Nevertheless, the degree of mottling at long wavelength is very small. Dot gain is slightly reduced at higher temperature as a consequence of faster immobilisation of the ink.

Keywords

Flexographic ink, ink transfer, print quality, temperature, viscosity

1. Introduction

During printing, the temperature in the flexographic printing press rises as a consequence of friction between the doctor blade and the anilox roll, pumping of ink and friction in the different nips between the cylinders in the printing press. This affects the ink performance and most likely the print quality. Podhajny (1990) reported that the temperature at the surface of an anilox roll may be higher than 50°C due to friction between the doctor blade and the anilox roll. Nordström (2000) studied temperature changes in waterless offset presses and concluded that the temperature in the inking station increases after a few minutes and levels out after roughly 30 min from the time when the press is started. For other parts in the press, the temperature increase may prevail for as long as several hours. An increased temperature of the ink influences ink properties that are important for printing, e.g. viscosity and surface tension [Nordström and Johnson, 2002].

The ink viscosity and the surface tension influence ink transfer and ink setting on a substrate [Davies and Claypole, 2006]. Studies on the relationships between ink viscosity and ink transfer have been in focus for a long time. An early study, often referred to, was made by Walker and Fetsko (1955). They introduced an ink transfer equation describing the amount of ink that will be transferred in a printing nip. The equation is based on the ink's possibility to immobilise, the ink thickness on the printing plate and that a certain fraction of the wet ink will be transferred. The effect of ink vehicle viscosity on ink immobilisation is also briefly discussed, a lower vehicle viscosity seems to favours ink transfer, but this process was not entirely covered by the investigation. Information of how wet ink transfer is affected by changes in physical and chemical properties of the ink was not encompassed by the study, though. Taylor and Zettlemoyer (1958) further investigated how the wet ink film splits between the printing plate and the substrate at the printing nip exit. It was suggested that the ink film split

is promoted by viscosity variations within the ink film. These variations are produced by higher temperature or/and higher shear rate that makes the ink film "weaker" closer to the substrate surface and hence, transferring less amount of ink. In another investigation the ink transfer was investigated through studies of the ink-paper interaction of different inks and papers, Schaeffer, et al. (1963). It was concluded that ink transfer increases with increasing print speed, pressure and ink viscosity, which qualitatively follows the theory of capillary flow. They also noted that at lower printing speed the substrate compression may negatively affect the ink transfer due to a decrease in effective capillary diameters. De Grâce and Mangin (1983) studied ink transfer in connection to substrate properties and press conditions. They found that the surface roughness of the substrate influenced the ink transfer so that a rougher surface accepts more ink. But if the surface gets too rough the contact area is reduced which also reduces the ink transfer. However, for newsprint the print density was relatively unaffected by surface roughness. Also, investigating the printing pressure they found that a higher pressure forces more ink into the substrate (newsprint) but too high pressures close off some of the pores, thereby, reducing ink transfer.

Ercan and Bousfield (2000) investigated the effect of ink rheology on filament size at the printing nip exit. They found that a higher elastic component of the ink, or test fluid, contributed to form smaller filaments, while for offset inks a low tensile pressure tended to produce larger filaments. Both Fernández, et al. (1998) and Rentzhog and Fogden (2005) investigated inks rheological behaviour when temperature changes and found that the response followed the Arrhenius relationship [Barnes, et al., 1989]. Rentzhog and Fogden also noticed differences in behaviour between different ink pigments: the cyan ink was much more sensitive to temperature variation than the carbon black. Fernández, et al. found that the offset inks, to a greater extent, flocculated at higher temperatures than lower temperatures due to the polymers' chains that promote bridging between small particles, i.e. heteroflocculation.

Systematic studies on how an elevated temperature influences the final print quality are, unfortunately, scarce in the literature. The aim of the present study is to investigate the effects of an elevated temperature in a flexographic printing press on ink transfer, ink setting and print quality. Printing trials with three inks and different temperatures were performed on a roll-to-roll laboratory printing press. The quality of the prints were evaluated through density, gloss, mottle and ink transfer. The inks were characterised rheologically, by measuring viscosity curves and temperature curves.

2. Materials and methods

2.1 Printing

Three water-based flexographic inks (with different binders, see *Table I*) have been printed at different temperatures and printing speeds with a roll-to-roll laboratory printing press, Rotary Koater, from RK Print Coat Instruments Ltd., UK. A commercially produced (Stora Enso Fors, Sweden) fully coated multilayer folding boxboard, 220 g/m^2, with a coat weight of 20 - 22 g/m^2 was used as substrate for printing. The inks and anilox roll were heated to 25, 40 and 70°C, respectively, prior printing. Surface temperatures were monitored using a handheld IR-thermometer (Optris Minisight, Optris GmbH, Berlin, Germany). The employed anilox roll was a ceramic roll with 220 l/cm and a volume of 4 ml/m^2. A heater was installed to the ink feeder to be able to keep the ink at a certain temperature during printing. Two different printing speeds were used, 30 and 60 m/min. The printing press setup, nip pressure, drying fans, etc., remained constant throughout the trial. The printing plate, DuPont HIQ with a thickness of 1.7 mm and a hardness of 71° Shore A, was produced by Flexopartner, Sunne, Sweden. The print form layout was composed of a large full-tone area and smaller areas (25 cm^2) of tone values from 0 to 90% (the 50% tone value had an area of 50 cm^2), in steps of 10%, situated next to each other. The screening ruling of the 10 to 90% areas was 42 lines/cm.

Table I: The ink characteristics, SPB and EPB are abbreviations for solution polymer binder and emulsion polymer binder respectively

	S1	E1	E2
Binder	SPB	EPB A	EPB B
T_g of binder [°C]	101	-23	110
Solid content [%]	43.5	46.4	45.3
pH	8.2	7.7	8.2
Surface tension [mN/m]	35.6 ± 0.2	38.8 ± 0.2	40.0 ± 0.2

2.2 Ink properties

Two of the three inks, denoted as E1 and E2 respectively, employs different types of emulsion-polymer binders (EPBs, T_g = -23 and 110°C) and the third (S1) a solution-polymer binder (SPB, T_g =101°C). All of the binders are acrylate type. All of the inks contain the same type and amount of ink pigment, cyan, and were characterised using a rheometer for viscosity curves and a FibroDAT 1100, FibroSystems AB, Sweden, for surface tension analysis (pendant drop). The binders and pigments were supplied by Sun Chemical Inks A/S, Skovlunde, Denmark.

2.3 Viscosity curves

Viscosity curves of the inks were obtained by employing a MCR 300 rheometer from Physica Messtechnik GmbH, Ostfildern, Germany. The inks were first sheared at 1 s^{-1} for 10 s, then rest for 60 s. This was followed by a ramp log profile of shear rates from 0.01 to 2.000 s^{-1}, over a period of 1200 s. The measurement was sampled at an interval of 30 s, and the temperature was held at 23°C throughout the measurement.

To measure the effect of temperature elevation on viscosity a USD 200 rheometer from Physica Messtechnik GmbH, Ostfildern, Germany was employed. The measurement procedure was as follows: first a shear rate of 1 s^{-1} is applied to the ink for 30 s at 20°C, and then rest for 60 s. This was followed by a linear increase in temperature from 20 to 80°C and a constant shear rate of 100 s^{-1} for 3.000 s with a sampling interval of 50 s.

2.4 Print characterization

After printing, the prints were stored in a climate controlled room (23°C and 50% RH) prior to analysis. Different measurements were performed on the prints to evaluate the print quality. The print density and overall dot gain were evaluated with a GretagMacbeth densitometer. Roughness of the substrate and that of the fulltone print were measured with an interference profilometer (WYKO NT3300 from Veeco Instruments Inc., AZ, USA). The optical magnification of the profilometer was 20 and the scanning depth, the distance from top to bottom of the vertical scan, was 75 µm. 6 randomly selected sampling points within a scanning area of 1.49 x 1.14 mm^2 were measured, with a scanning resolution of 2 µm/pixel. The size of image was 736 x 480 pixels. The roughness values were calculated using the in-built software, Vision 32 (version 2.303, Veeco Instruments Inc., AZ, USA) of the profilometer. The Tappi gloss values of the prints and substrate were measured at 75° with a glossmeter from Zehntner GmbH Testing Instruments, Switzerland. A Perkin Elmer atomic absorption spectrophotometer 3300, (Perkin Elmer, Wellesley, MA, USA) has been employed to measure the relative ink (cyan) transferred, the copper amount, for all printing conditions according to SCAN-CM 38:05. To collect data for evaluating mottling, a scanner, Duoscan T2500 from AGFA, was used with a scanning resolution of 300 dpi. Mottling was evaluated on the solid tone areas employing a STFI Mottling v.2.41 software (Swedish Pulp and Paper Institute, Stockholm, Sweden).

3. Results and discussion

Ink viscosity affects the ink transfer [Schaeffer, et al., 1963] and is therefore an important parameter for printing. The viscosity curves of the three inks shown in Figure 1 reveal that the inks have different characters. The E1 and E2 (EPB based inks) display a clear shear thinning behaviour while S1 (SPB based ink) is only slightly affected by the increase in shear rate. These are the typical behaviours of the ink as previously described [Olsson, et al., 2007]. The ink viscosity is also affected by the temperature, Figure 2. At room temperature the inks exhibit similar viscosity, at a shear rate of 100 s^{-1}. As temperature increases the viscosity decreases. The ink response to the temperature's variation is slightly different: E1 is less sensitive while E2 is most sensitive.

Generally, the print density increases with temperature, as shown in Figure 3. This behaviour is readily seen for S1, whereas for E2 the trend is less obvious. Ink E1 follows the trend of S1 when the temperature is low, but at a higher temperature the ink probably undergoes a phase shift of the emulsion binder leading to a heteroflocculation, as described by Fernández, et al. (1998), which results in a drastic decrease of ink transferred and print density. Another possibility, less likely though, is that E1 starts film forming at the ink surface in the press as a result of its low T_g and high temperature. A film forming process starting too early in

the printing press may negatively affect the ink transfer since the ink viscous behaviour shifts drastically. From Figure 3 it is also seen that the print densities increase with printing speed for all three inks. This was also seen by Schaeffer, et al. (1963), they attributed this phenomena to deformation of the paper meaning that at low speeds the paper may deform (compress) to a larger extent due to longer dwell time in the pressure nip. When the paper is deformed the average pore diameter will be reduced, and thereby the ability to absorb the ink vehicle is also reduced.

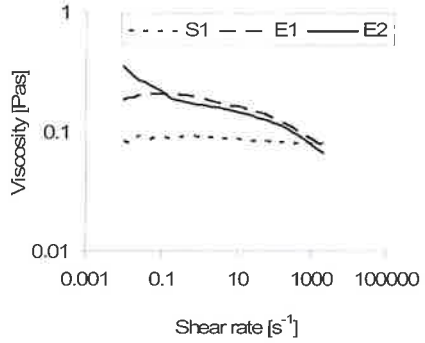

Figure 1: Viscosity curves for the inks (not diluted for printing)

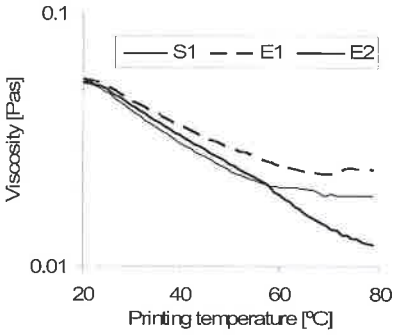

Figure 2: The viscosity as a function of the temperature, at a constant shear rate of 100 s^{-1}, for the different inks (diluted for printing)

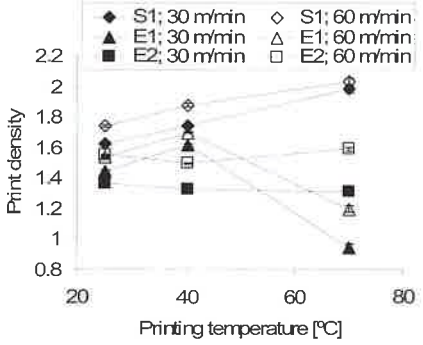

Figure 3: Print density (full tone) at different temperatures and printing speeds. Error bars are the 95% confidence interval of 100 measurement points

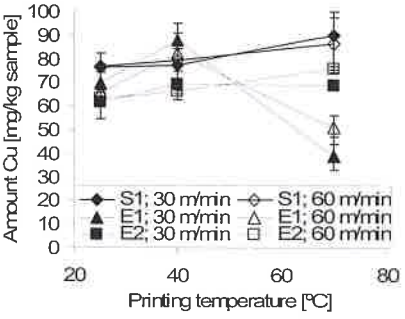

Figure 4: Amount of copper on the printed samples

In the printing nip, the pressure pulse forces ink vehicle into the substrate partly immobilising the ink. With increasing temperature the ink viscosity reduces, which should promote ink dewatering. A higher ink dewatering leads to a thicker immobilised ink layer in the printing nip [Cozzens, et al., 1965]. Since the film split occurs in the non-immobilised ink film [Walker and Fetsko, 1955], a thicker immobilised layer promotes a greater ink transfer. This may explain the higher print density as well as the higher atomic absorption values, Figure 4, obtained at higher temperatures.

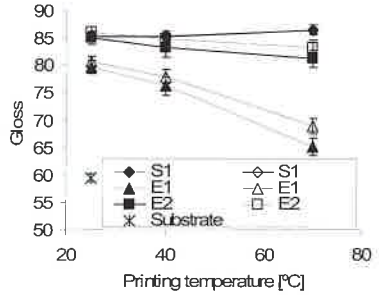

Figure 5:
Tappi gloss of the prints printed at different temperature and speed.
Filled and unfilled character represents the print speed 30 m/min and 60 m/min, respectively.
Error bars indicate 95% confidence interval from 40 measurement points

The effect of temperature on Tappi gloss of the prints with S1 and E2 inks is rather marginal, *Figure 5*. The print gloss has, nevertheless, a tendency to decrease with increasing temperature. In the case of E1, Tappi

gloss decreases significantly, however. This is probably influenced by the lower ink transferred at high temperatures (Figure 4). Generally, as temperature increases the ink sets quicker, which allows shorter time for the ink components to set in a favourable manner which affect the print gloss negatively [Olsson, et al., 2007]. Ink film surface roughness, R_a, was measured using profilometry to investigate if gloss changes were coupled to roughness. The R_a values varied between 0.9 and 1.4 μm for the inks at different temperatures, but statistical analysis indicated that the differences were not significant. Thus observed gloss changes were not a product of roughness changes.

A tendency for lower dot gain was observed for all of the inks as temperature increases, regardless the quantitative differences (Figure 6a - c) between the inks. A possible explanation is that a lower viscosity of the ink at higher temperature makes the ink vehicle more easily absorbed thereby immobilising the ink faster. This, in combination with an increased evaporation, also leads to faster immobilisation and a reduced dot gain. There are nevertheless clear differences between the inks, which may reflect different chemical compatibilities (e.g. wetting and spreading) between the surface and the inks. Lagerstedt and Kolseth (1995) investigated the effect of surface energy in flexographic printing. The effect of surface energies on ink transfer was clear for smaller tone values but for full tone areas only small influences could be detected. Considering that the surface tension varies with temperatures, Cini, et al. (1972), this may enhance the effect seen in Figure 6. As in Lagerstedt and Kolseth study the effect is more dominant at lighter tones than darker ones. The clear difference between E1 (Figure 6b) and the other inks (Figures 6a and 6c) may be a consequence of different chemical compatibility to the surface. An increased temperature may further affect the compatibility between ink and paper than for the other inks. However, one should not forget that the ink transferred is less for E1 at higher temperatures (Figure 4). This makes the ink even easier to immobilise, causing even further dot gain reduction.

Mottling describes the optical heterogeneity of a print and is closely related to ink transfer and absorption [Hallberg Hofstrand, 2006; Johansson and Norman, 1996]. Ink transfer and absorption are affected by the substrate, ink and printing press condition. Mottling are usually evaluated employing image analysis methods based on frequency analysis where the optical signal is divided into various spatial frequencies.

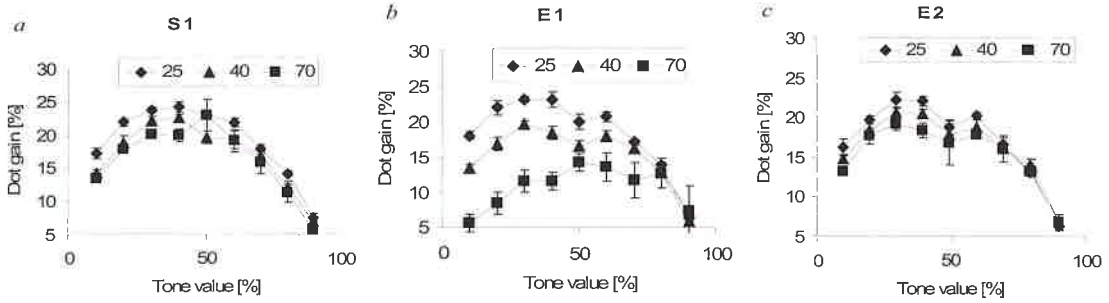

Figure 6: Dot gain at different temperatures (25, 40 and 70°C) of the inks printed at 30 m/min. There are no large deviation in dot gain between the printing speed 30 and 60 m/min. The error bars are standard deviation of 7 randomly selected measurement points. The indexes a, b and c indicates different inks

Mottling decreases with increasing temperature at short wavelengths (< 1 mm), Figure 7a and b, but increases with increasing temperature, at long wavelength interval (1 - 8 mm), Figure 7c. The change in mottling at shorter wavelengths may reflect the ink's possibility to heal and level out irregularities at the ink surface. This possibility increases as temperature increases because the ink becomes more mobile. However, at the long wavelength interval the ink is incapable of spreading and fully levelling out irregularities at relevant lengths, > 1 mm, before immobilisation occurs, resulting in higher or similar degree of mottling, as at lower temperatures, with an elevated temperature. In addition, at long wavelengths local difference in absorptive behaviour of the coating may produce differences, on a local scale, in transferred ink amount as a consequence of different capacity to immobilising ink in the printing nip [Shen, et al., 2004]. Since the transferred ink amount increases with increasing temperature, the differences between the local positions also increase, producing larger degree of mottling. Another aspect also seen in *Figure 7* is that mottling, at all wavelengths, is reduced at higher printing speed. A probable cause for this is that at higher printing speeds the viscosity of the ink is reduced due to a larger induced shear rate, and this reduction in ink viscosity, together with the induced motion in the ink film, may further help the levelling of the ink and thereby reducing the mottling, especially at shorter wavelengths. It is, however, important to point out that the degree of mottling is fairly small for all prints in this study, especially for the long wavelength interval, as a consequence of the smooth paperboard printed upon.

It is also interesting to note that for all wavelengths, the SPB ink generally has the lowest degree of mottling. This was also seen by Rentzhog and Fogden (2006). They attributed this phenomenon to an increase in low shear viscosity and a decreased surface tension for the solution polymer binders. Ink E1, Figure 7a and b, shows a peculiar behaviour in that mottling is reduced at the highest temperature although a lower amount of ink was transferred (Figure 4). For some reason, the induced phase change (possible heteroflocculation) in ink E1 as temperature increase (Figure 3) is advantageous for some aspects of print quality (small scale properties, Figure 7 a - b and Figure 6b, but not all as in Figure 5) and press conditions investigated here.

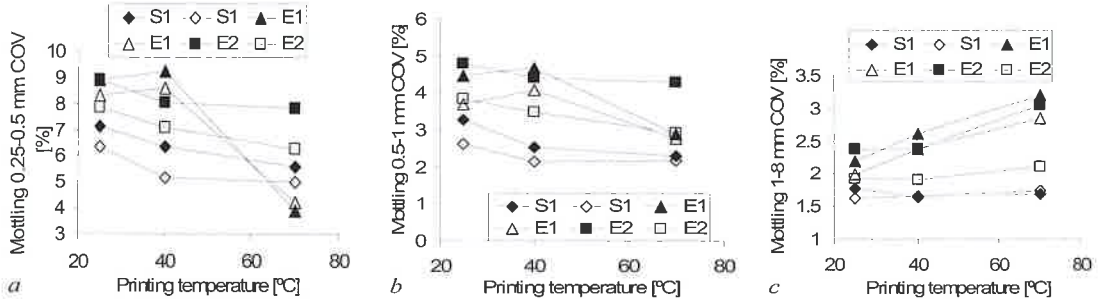

Figure 7: The effect of temperature on mottling separated into different wavelengths. Filled and unfilled characters represents the print speed 30 m/min and 60 m/min respectively. The indexes a, b and c indicates different length interval

Similar to dot gain, Figure 6, which has a tendency to reduce at increasing temperature, the mottling at shorter wavelengths (< 1 mm), Figure 7, also reduces with increasing temperature. Both these parameters are influenced by the inks ability to level and spread. A reduction in viscosity of the ink, and thereby the ink vehicle, caused by a higher printing temperature also increases the inks' ability to level and spread. This could be beneficial for production printing, but would require a minute control of temperatures on the press and in the press room. It would also add to the conditions needed to be controlled when profiling the press in preparation of prepress. This is accompanied by the ambitions of the papermakers to produce a paperboard with greater homogeneity so as to reduce variations, from millimetre scale down to microscopic attributes. It should however be remembered that the spreading of a fluid and penetration into a porous substrates (such as coated paperboard) is also affected by other parameters such as surface tension, which varies with temperature [Cini, et al., 1972], of the fluids and the substrate, roughness. The interplay of these materials, substrate and ink, in the printing press is not yet fully understood and requires further investigations.

4. Summary

It is shown, as expected, that an increased temperature affects the ink rheology, and thereby the print quality. The print density increases as a consequence of more ink transferred at high temperature. The higher degree of ink transfer is likely caused by the lower ink viscosity that promotes ink vehicle penetration into the coating, forming a thicker immobilised ink layer under the printing nip. Dot gain is simultaneously reduced at higher temperature as the consequence of faster immobilisation that competes against ink spreading in x-y directions. Mottling decreases at short wavelengths as a consequence of a more mobile ink at increasing temperature, levelling out local variations before it becomes immobilised. However, this helps little to variations of a larger scale, causing unchanged or slightly increased mottling at long wavelengths, since the ink becomes immobilised before the large variation is levelled out.

Acknowledgments

The financial support from the Swedish Pulp and Paper Research Foundation, the Knowledge Foundation and the Swedish Agency for Innovation System (VINNOVA) is gratefully acknowledged. We would also like to thank Sun Chemical Inks A/S for supplying the flexographic inks and Stora Enso Fors AB for providing the paperboard. For performing the surface tension analysis of the inks Ms. Irene Olsson, Stora Enso Skoghall AB, is also gratefully acknowledged.

References

[1] Barnes, H. A.; Hutton, J. F.; Walters, K., (1989), *An Introduction to Rheology, 7 ed.; Elsevier, p 199*

[2] Cini, R.; Loglio, G.; Ficalbi, A., (1972), *Temperature Dependence of the Surface Tension of Water by the Equilibrium Ring Method, Journal of Colloid and Interface Science, 41, 2, 287-297*

[3] Cozzens, S. L.; Butto, A. M.; Schaeffer, W. D.; Zettlemoyer, A. C., (1965), *Ink Penetration During High-Speed Printing of Uncoated Paper, Paper in the Printing Process, Aulanko, Finland,1 - 24*

[4] Davies, G. R.; Claypole, T. C., (2006), *Effect of Viscosity on Ink Transfer in Gravure Printing, IARIGAI, Leipzig*

[5] De Grâce, J. H.; Mangin, P. J., (1983), *A Mechanistic Approach to Ink Transfer Part I: -Effect of Substrate Properties and Press Conditions, 17th International Conferance of Printing Research Institutes, Saltsjöbaden, Sweden, Banks, W. H., Ed. Pentech Press, London, 312 - 332*

[6] Ercan, S. N.; Bousfield, D. W., (2000), *Influence of Fluid Rheology on Filament Size, International Printing and Graphic Arts Conference, Savannah, GA, USA, TAPPI Press, 121 - 132*

[7] Fernández, M.; Muñoz, M. E.; Santamaría, A., (1998), *Rheological Analysis of Highly Pigmented Inks: Flocculation at High Temperatures, Journal of Rheology, 42, 2, 239 - 253*

[8] Hallberg Hofstrand, E., (2006), *Flexographic Post-Printing of Corrugated Board, Dissertation, Karlstad University, Karlstad, Sweden*

[9] Johansson, P.-Å.; Norman, B., (1996), *Methods for Evalauating Formation, Print Unevenness and Gloss Variations Developed at STFI, Tappi Process & Product Quality Conference Proceedings, Cincinnati, OH, USA, TAPPI Press, 139 - 145*

[10] Lagerstedt, P.; Kolseth, P., (1995), *Influence of Surface Energetics on Ink Transfer in Flexo Printing, Advances in printing science and technology: proceedings of the 23rd research conference of IARIGAI, Paris, France, IARIGAI, 269 - 299*

[11] Nordström, J. - E. P., (2000), *Thermal Changes in a Waterless Sheet-Fed Offset Inking Station, International printing and graphic arts conference, Savannah, GA, USA, TAPPI Press, 153 - 165*

[12] Nordström, J.-E. P.; Johnson, J., (2002), *CSWO (Cold Set Waterless Web Offset) Using Standard Tmp/Dip Newsprint, International Printing & Graphic Arts Conference, Bordeaux, France, pp. 11*

[13] Olsson, R.; Yang, L.; Lestelius, M., (2007), *Water Retention of Flexographic Inks and Its Influence on Final Print Gloss, Nordic Pulp and Paper Research Journal, 22, 3, 287 - 292*

[14] Podhajny, R. M., (1990), *Critical Ink/Press Performance Parameters in Flexo and Gravure, Polymers, Lamination & Coatings Conference, TAPPI Proceedings, Boston, MA, USA, 581 - 583*

[15] Rentzhog, M.; Fogden, A., (2005), *Rheology and Surface Tension of Water-Based Flexographic Inks and Implications for Wetting of PE-Coated Board, Nordic Pulp and Paper Research Journal, 20, 4, 399 - 409*

[16] Rentzhog, M.; Fogden, A., (2006), *Correlation between Properties of Water-Based Flexographic Inks and Their Print Uniformity on PE-Coated Boards, Nordic Pulp and Paper Research Journal, 21, 3, 403 - 410*

[17] Schaeffer, W. D.; Fisch, A. B.; Zettlemoyer, A. C., (1963), *Transfer and Penetration Aspects of Ink Receptivity, Tappi, 46, 6, 359 - 375*

[18] Shen, Y.; Vyorykkä, J.; Bousfield, D. W.; van Heiningen, A.; Donigian, D., (2004), *Linkage between Coating Property Uniformity and Back Trap Mottle, International Printing and Graphic Arts Conference, Vancouver, Canada, 71 - 76*

[19] Taylor, J. H., JR; Zettlemoyer, A. C., (1958), *Hypothesis on the Mechanism of Ink Splitting During Printing, Tappi Journal, 41, 12, 749 - 757*

[20] Walker, W. C.; Fetsko, J. M., (1955), *A Concept of Ink Transfer in Printing, American Ink Maker, December, 38 - 44, 69-71*

Time-dependent rheology effects on print quality using water-based ink compositions

Scott Williams, Stephanie Pieruccini

Rochester Institute of Technology, School of Print Media
69 Lomb Memorial Drive, Rochester, NY 14623, USA
E-mail: sawppr@rit.edu

Abstract

An investigation into the dependence of water-based gravure ink rheology on image quality was conducted. We prepared a dilution series of a water-based process red gravure ink system ranging from 20 (fast ink) to 60 (slow ink) seconds (#2 Zahn Cup). Upon gravure printing using a range of screen resolutions from 110 to 200 LPI, we found that print defects exhibited as long streaks devoid of ink within the image area increased as the gravure cell volume decreased. We initially attributed these results to pigment agglomeration. The process red ink, more so than the other two process colors, bodied significantly over a short period of time. Sedimentation experiments suggest that this increase in viscosity may be do more to pigment: resin associations rather than simple pigment agglomeration. A rheology and thermodynamic investigation continues to explore the reasons for this bodying reaction on the molecular level.

Keywords

Bodying reaction, pigment agglomeration, styrene-acrylic resin, water-based gravure ink

1. Introduction

The motivations, pros and cons, to the development of water-based gravure (WBG) ink have been well documented[1-4]. Over nearly four decades of research and development, WBG inks still only capture 5% of the gravure ink market. This is in contrast to nearly 37% for the flexography ink market[5]. The barrier that WBG inks must overcome has been high. Literature and industry reports reference to WBG ink development was prevalent in the 1980-90's, and then seemed to give way to advancements in the incineration and solvent recovery options in the current decade[5-8].

The unforgiving behavior of WBG ink was best summarized in a four part series published in the TAGA Proceedings by Ryszard and Sprycha of Sun Chemical[9-12]. Development trials and challenges over a 15 year period was also documented by the US Bureau of Engraving and Printing in 1986[13]. A common theme emerges from these reports and articles; WBG inks are difficult to control on press. Print mottle[13] and poor overprint trapping are the result of high dynamic ink surface tension[9,10], unpredictable rheology[10], dot gain[12], and ink-substrate interferences from changes in interfacial pH[11]. As if these challenges were not enough of a barrier to market entry, we observed an undocumented property which may be a root cause of some of the aforementioned issues - ink bodying upon storage.

Bodying, a term used in the ink industry, refers to the static increase in viscosity over time. We observed that a commercially available styrene-acrylic WBG proofing process red ink substantially bodies over a short period of time. Of the four process colors, only process red bodies over a period of time as short as 24 hours. Process yellow bodies the least, but tends to exhibit pigment sedimentation. Process blue was found to be the least prone to bodying and appears to be the most stable dispersion of the process inks. We began a study to investigate the bodying reaction mechanisms and their corresponding impact on print quality.

2. Methods

2.1 Water-based commercial ink dilution study

Commercially available water-based proofing process red gravure ink was obtained for our study. Zahn cup (#2) readings were taken as the average of three trials per dilution condition. The ink was reduced with glass distilled water until the low shear viscosity endpoint was obtained.

2.2 Gravure printing trials

A J. M. Heaford Single Cylinder Proofing Press (HA custom model) located within the Print Science Laboratory at RIT was used for this study. Southern Graphic Systems of Phoenix, New York engraved a 30-inch long, 21-inch repeat hollow-core cylinder with a portion of the target design shown in figure 1. This 55 to 100% Percent Tint Target was replicated five times by varying the line screen to 110, 150, 165, 180 and 200 LPI across the cylinder. Impression pressures were approximately 600 Kg. A commercially available LWC gravure paper stock was selected for the prints.

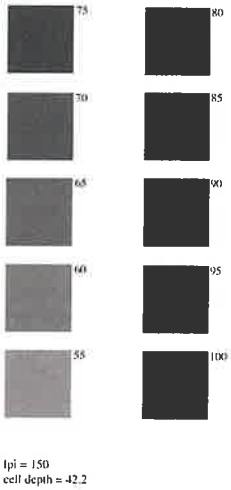

Figure 1:
RIT gravure print quality target

2.3 PAL normal peel scan procedure

A method was developed in order to compare ink coverage over a substantial print area. We borrowed a proprietary process developed at the Printing Applications Laboratory (PAL) at RIT. A print area was identified and scanned at high resolution, and then converted to a gray scale image. Using a proprietary procedure, the gray image is then integrated and compared to the percentage of exposed paper white. Essentially, a densitometric value is obtained over a larger area than can be obtained using any desktop spectrophotometric device. PAL uses this procedure, for example, to measure ink adhesion using ISO and TAPPI tape procedures.

2.4 RIT Water-based bravure ink formulation

A two-step formulation process was used to prepare RIT water-based gravure inks. A master grind was prepared that contained about 20% pigment, 56% Joncryl 60 (Johnson Polymer), 2% Zetasperse 1.400 (Air Products) and 20% glass distilled water. All weights are wet-weight percent. Pigment to resin ratio was about 1:1 within the grind. This master grind was ball milled using three mm chrome-plated steel media for 24 hours at 120 RPM. The master grind was then letdown using a resin preparation prepared by adding 72% Joncryl 77 (Johnson Polymer), 20% Jonwax 26 (Johnson Polymer) and 8% distilled water using gentle stirring. Pigments selected for the study were CI Pigment Blue 15:3 (Fastogen Blue 5380E, Sun Chemical), CI Pigment Red 122 (Sunfast Magenta 122) and CI Pigment Yellow 138 (BASF Paliotol Yellow L0960HD). A defoaming agent was required when preparing the RIT Process Red and Yellow preparations. Surynol DF-110D (Air Products) defoamer was typically added at a 1 - 1.5% amount at the letdown stage.

2.5 Sedimentation experiment

Ink sedimentation experiments were performed using three 50 ml burets suspended on buret stands. The inner diameter of each buret was six millimeters. These burets were then filled up to an identical level with freshly letdown RIT Process Red, Yellow and Blue ink formulations. The time-zero column of ink measured 37.7 mm from stopcock to the meniscus liquid level. Sedimentation (Rs) was measured in a similar manner as Rf is measured in thin-layer chromatography. The sedimentation level was measured from the top of the settled

pigment residue to the bottom of the liquid meniscus (d*p*(mm)). The time-zero column length of ink was di(mm). The sedimentation value was calculated as shown in equation 1.

$$Rs = \frac{di(mm) - dp(mm)}{di(mm)} \quad (1)$$

Rs values approaching one (1) would indicate no sedimentation with time, a stable dispersion of ink components. The lower the value of Rs, the more settlement of pigment components from the ink. Using this method, the value of Rs would be a quantitative measure of ink dispersion stability.

2.5 TGA analysis

Thermogravimetric analysis (TGA) was performed using a TA Instruments Model TGA 2050 located at the Department of Chemistry (RIT). About 10 milligrams of commercial water-based process red and yellow were prepared onto 100 µl platinum sample boats for the analysis. A survey temperature ramp of 20°C/min over a temperature range of room temperature to 800°C was analyzed. The TGA profiles were collected in a nitrogen atmosphere.

3. Results and Discussion

3.1 Commerical ink dilution series

The catalyst, for this study, was the observation that a commercially available water-based magenta gravure ink formulation significantly bodied with time. In order to survey the bulk composition of bodied ink, a dilution series was prepared. Figure 2 illustrates the gravure print trial results using the commercial proofing ink dilution series from 60 to 20 seconds.

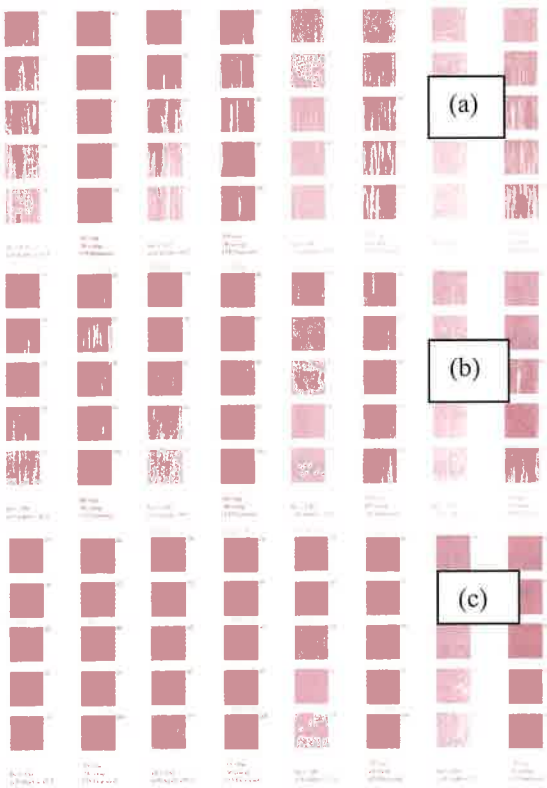

Figure 2:
Gravure prints produced with a commercially available water-based process red proofing ink diluted to a #2 Zahn Cup viscosity of 60 (a), 45(b) and 20 (c) seconds. Each print segment comprises eight tints ranging from 55 to 100% in 5% increments. The 21 inch repeat gravure cylinder was engraved with five screen rulings and cell depths (Left to Right) ranging from 110 (not shown), 150 (42.2 µm), 165 (59.7 µm), 180 (25.5 µm) and 200 (23.5 µm) LPI (cell depth in microns). Substrate was a LWC gravure publication stock. The black rectangular box represents the PAL Normal Peel scan area used in the analysis discussed below

Although there are print anomalies that require analysis and discussion, our initial conclusion was that agglomerated pigment structures caused the print void streaks. We noticed that the apparent frequency of void

streaks decreased as the low shear viscosity decreased to a 20 second minimum value (figure 2c). If the frequency of void streaks increased as the result of increasing pigment agglomerate size, we should have observed differences in the shear properties of each dilution.

We supposed that the bodying was the result of larger and complex structural assemblies that would form as the pigment agglomerated. If these agglomerates were weakly assembled; then, they should break down with the increasing shear force. If weakly assembled agglomerates were the cause of the bodying, the rate of viscosity change would directly vary with viscosity. That is, the larger, weakly associated, agglomerates formed within the higher bodied ink, would disassemble at a slower rate as compared to smaller structures under similar shear force. Figure 3 is a power log plot of viscosity as a function of shear rate.

The viscosity rate of change does not vary with changes in low shear (Zahn Cup) viscosity over the range 20 - 35 seconds. Rheology profiles were not obtained with higher low shear viscosity conditions. Using our method of analysis, the viscosities were outside of the measurable range using a SV-1 Brookfield spindle. We elected not to change to another spindle for the analysis. Figure 5 results would suggest that the bulk ink structures are similar in the viscosity range measured. A low shear viscosity of 35 seconds would be well outside the typical range of a typical gravure ink, even for a proofing application. We do not have however, rheology data for viscosities higher than 35 seconds.

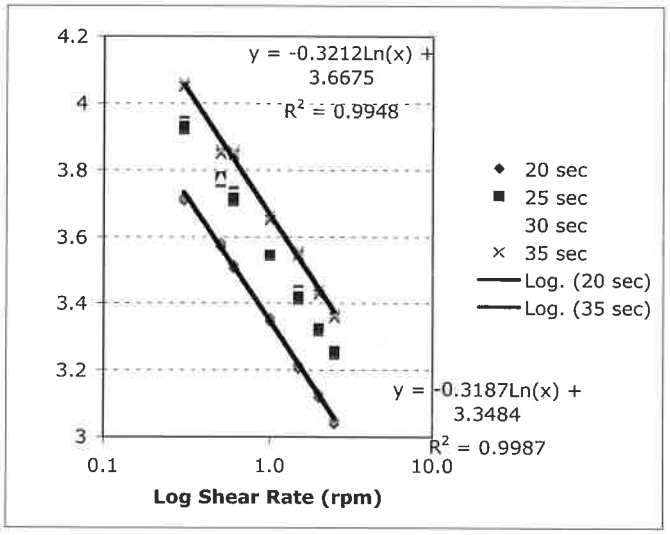

Figure 3: Power log viscosity plot as a function of low shear viscosity over the range 20 - 35 seconds

We further analyzed the gravure print data to see if we could correlate the print void streaks as a function of low shear viscosity. What we found illustrated the need to extend our rheology analysis to the higher low shear values.

Figure 4 illustrates the ink coverage area as a function of low shear viscosity as measured using the PAL Normal Peel Scanning procedure. The area coverage values represent the average over four trial prints and target tint ranges from 80 to 100% at 150 LPI line (see figure 2 for an illustrated representation of the scanned area). The trend roughly follows the amount of water added to reduce the viscosity to 20 seconds (Data not shown). That is, small water additions caused large changes in ink viscosity, and leveled out as the ink thins. At 20 seconds, we had added nearly the same weight of water as ink; and therefore, the area value of around 50% was expected. What was not expected were the three distinct transitions in coverage area observed (figure 4).

Comparisons between figures 2 - 4 all seem to suggest the formation of weakly associated pigment agglomerates. At very high low shear viscosity, the printed tint areas corresponding to larger cell volumes appeared to contain the fewest print defects (figure 2). The number of print defects increases substantially from 150 to 200 LPI screening, and from 100 to 55% within the 150 LPI area.

The ink coverage areas measured from prints made with 45 to 20 second ink viscosities all appeared to have the same value with some mottle and ink non-wetting as the primary print defects. The number of print

streaks decreased with the thinner inks. The ink rheology, over the same range, also correlated with the print area data. The inks decreased in viscosity over a series of water reductions, but the rate of change remained the same throughout the sample set. These results would suggest similar ink structures.

Overall the observed print and ink rheology pointed to an ink bodying mechanism associated with pigment agglomeration. We needed to obtain more direct and controlled evidence of this bodying mechanism.

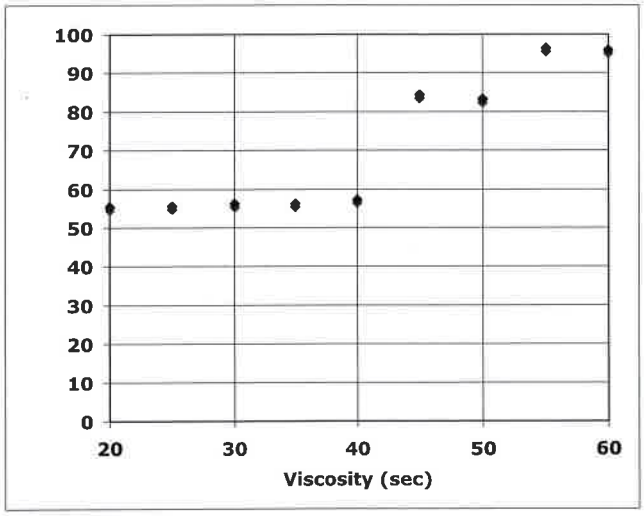

Figure 4: Percent PAL normal peel area averaging 80 to 100% tint target at 150 LPI

3.2 Sedimentation experiments

If pigment agglomeration was the main bodying reaction mechanism, we might be able to observed agglomerate growth with time using a sedimentation procedure. The RIT Process Red, Blue and Yellow formulation was used for this study. The solids content for all RIT inks were about 35% with the pigment being about 7% by weight of total solids. If the pigment fraction, with a typical particle size distribution of about 0.5 to 5 microns (determined by SEM, data not shown), was unsupported by the resin matrix; then, a sealed column of ink would sediment to the bottom third of a sedimentation tube. The more pigment support the matrix provides within the suspension, the less the sedimentation. The Rs value is a measure of the sediment distance from the bottom of a ink solution meniscus. A unitless value of one (1) would indicate no pigment sedimentation. Values less than one would indicate the percent of pigment sedimentation. Figure 5 illustrates the differences in sedimentation rates over a 17 day period.

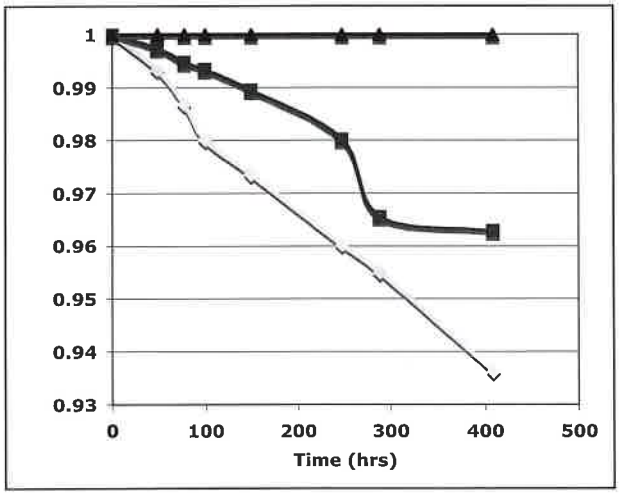

Figure 5: RIT process red, blue and yellow sedimentation experiment. The line colors correspond to the ink formulation color

Figure 5 confirms the observed bodying results in the commercial and RIT inks. The ink dispersions are all particularly stable over a 17 day period. The most striking result was the immediate bodying of magenta pigment within the RIT and Commercial Process Red formulations. The Process Red ink bodies and doubles in viscosity over just a 24 hour period (data not shown). No magenta sedimentation was observed suggesting the rapid formation of a supporting resin: pigment matrix structure as opposed to pigment agglomeration.

RIT Process Yellow showed a relatively rapid sedimentation rate. In all cases, however, the overall rate of sedimentation was less than 10%. The sedimentation rates are also extremely slow. Process Yellow sedimentation rate would be about 59 μm/hr, for example (figure 5).

RIT Process Blue result was equally interesting. The sedimentation rate was slow and settled to a Rs value of 0.96. The viscosity, however, does not significantly change over the experiment time (data not shown). Sedimentation profiles for the three process colors, analyzed together, would suggest that the resin: pigment matrix structures are being formed that cause physical changes within the ink bulk volume.

3.3 TGA analysis

If the process inks are forming different pigment or resin:pigment structures, the differences may be resolved through thermal analysis. Figure 6 illustrates the results of two survey scans with commercial WBG ink process yellow (figure 6A) and red (figure 6B) completed before the submission of this paper. The weight loss percentages approximately correspond to the ink composition. These inks were roughly 33% solids with 8% pigment and 25% resin loads. Although more careful scan and scan analysis will be forthcoming, there was a difference in the transition associated with the pigment decomposition. The process red pigment uniformly decomposes over a range starting at 310°C to 382°C (figure 6B).

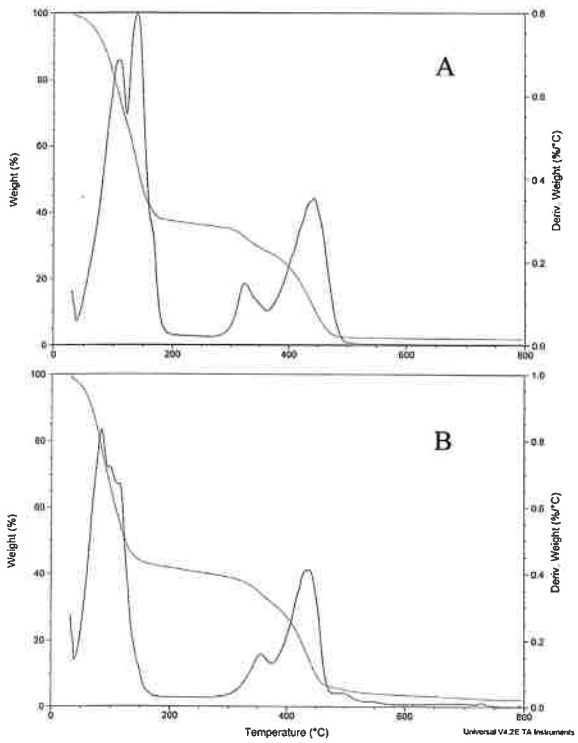

Figure 6:
TGA analysis of commercial WBG process yellow (A) and red (B) ink. This was a survey scan using a 20°C/min temperature ramp over a range of room temperature to 800°C. The plots are displayed as the weight loss and derivative of the weight loss percent

That is, the derivative of the weight percent change for process red pigment is nearly Gaussian-like in shape. The process yellow, however, showed evidence of two distinct populations of pigment decompositions starting from 297°C to 364°C (figure 6A). One can imagine the decomposition range for this pigment could be curve fitted using a pair of similar Gaussians-like profiles. The resin decomposition range appears to be nearly the same for both samples as would be expected. Both samples were let down with the same resin composition and in the same amount. We are intrigued by the two corresponding peaks of the derivative curve between the two ink pigments at about 350°C. Whether this peak corresponds to a yellow aggregate, and the magenta peak corresponds to uniformly

dispersed pigment will only be resolved through a more careful study. If the magenta pigment is uniformly dispersed, the bodying reaction may result for pigment:resin structure formation rather than pigment agglomeration. Yellow aggregate formation would explain the faster sedimentation rate observed (figure 5).

4. Conclusion

We are investigating the mechanism of water-based gravure ink bodying with time on the molecular level. Our focus is to ascertain whether the reaction is a pigment agglomeration process, as is typically assumed, or if there are pigment:resin structures forming that greatly alter ink performance. Printing trials with ink that has been reduced over a range of low shear viscosities point to a pigment agglomeration mechanism. The predominant print defect was streaks that increase over several subsequent impressions of the same run. The streak number also increases as the image cell size decreases.

What counters this possible conclusion was while process yellow pigment, in particular, settles over a period of weeks, the magenta pigment does not. In fact, we consistently find that the bodying reaction with magenta was rapid, occurring over the course of just 24 hours. We also do not find any evidence of pigment de-wetting at the nip and doctor blade; that is, the percent solids of the applied ink and the ink recovered at the printing nip are equal to within one percent (data not shown). If agglomerates were being dragged between the doctor blade and cylinder, we would expect to find a higher solids content at the nip after printing.

Equally intriguing was the result that this rapid bodying reaction occurs with several different pigment magenta compounds and has not been observed with yellow or cyan pigment derivatives (work in progress). The pigments, for all three colors, have many available sites for hydrogen bonding with themselves and with the acrylic resin side groups. What makes magenta particularly susceptible to these associations remains a mystery at present. Further investigation using high resolution imaging, separation methods and thermal analysis will be used to resolve the mechanisms responsible for these bodying processes.

References

[1] Kasunich, C. L., April 1986, *Using Water-Based Inks Can Be a Sticky Matter*, Package Printing, 33:4, pp 24 - 28

[2] GAA Conference on Water-Based Inks Proceedings, May 1992

[3] GAA Western Regional Gravure Symposium on Water-Based Gravure Inks Proceedings, October, 1995

[4] Chudolij, A., February 1999, *Success of Water Technologies In Gravure Printing*, GAA Pressroom Conference Proceedings, pp. 199 - 207

[5] *Despite Europe's Economic Upswing, Ink Manufacturers Remain Wary: Improved performance, government regulations are key to future gains* (2000). Retrieved June 20, 2007 from Ink World Web site: http://inkworldmagazine.com/articles/2000/02/water-based-inks.php

[6] The Gravure Report (2001). Retrieved June 20, 2007 from Ink World Web site: http://inkworldmagazine.com/articles/2001/05/gravure-market-update.php

[7] The Gravure Report (2004). Retrieved June 20, 2007 from Ink World Web site: http://inkworldmagazine.com/articles/2004/05/the-gravure-report.php

[8] The Gravure Report (2005). Retrieved June 20, 2007 from Ink World Web site: http://inkworldmagazine.com/articles/2005/05/the-gravure-report.php

[9] Spyrcha, R. and Hruzewicz, J. N. (1994) *Impact of Ink/Paper Interactions on Printability of Aqueous Publication Gravure Inks Part I: Dynamic Contact Angle and Paper Wetting*, TAGA Proceedings, pp 433 - 458

[10] Spyrcha, R. and Hruzewicz, J. N. (1995) *Impact of Ink/Paper Interactions on Printability of Aqueous Publication Gravure Inks Part II: Soprtion of Liquids by Paper During Ink Setting and Drying*, TAGA Proceedings, pp 228 - 250

[11] Auerbach, R., Hruzewicz, J. N. and Spyrcha, R. (1996) *Impact of Ink/Paper Interactions on Printability of Aqueous Publication Gravure Inks Part III: Acid/Base Interactions at the Paper/Ink Interface*, TAGA Proceedings, pp 143 - 158

[12] Spyrcha, R. and Krishnan, R. (1997) *Impact of Ink/Paper Interactions on Printability of Aqueous Publication Gravure Inks Part IV:Ink Transfer and Spreading on Paper*, TAGA Proceedings, pp 829 - 843

[13] Mercer, J. W. (1986) *Bureau of Engraving and Printing Experience with Water-based Gravure Postage Stamp Printing*, Tappi Journal v. 69, pp. 30 - 34

Study of the rheological behaviour of conventional, hybrid and UV offset inks

Marie Kaplanová, Katarína Remenárová, Bohumil Jašúrek, Jan Vališ

University of Pardubice, Faculty of Chemical Technology, Department of Graphic Arts and Photophysics
Studentská 95, Pardubice 532 10, Czech Republic
E-mail: marie.kaplanova@upce.cz; st8922@student.upce.cz; bohumil.jasurek@upce.cz; jan.valis@upce.cz

Abstract

The UV markets have been growing over last two decades. Hybrid inks are less than six years old and growing rapidly. They represent a hybrid between conventional and UV curing inks, because their drying process includes both drying mechanisms. This work was focused on the one process colour ink. Seven process magenta inks from different suppliers were tested, two conventional, two hybrid and two UV inks. Two different types of fountain solutions one without alcohol and one with the addition of 5% IPA were used for preparing emulsions. The emulsions were determined by the amount and rate of water pick-up.

The shear-load dependent flow and time-dependent behaviour of neat inks and emulsions were measured at different temperatures by rotational rheometer RV1 HAAKE. Tackmaster-92 was used to measure the tack and misting characteristics.

Keywords

Emulgation, hybrid ink, offset ink, tack, thixotropy

1. Introduction

The rheological properties of inks can determine processibility, help drive technology to better product quality, performance, and eventually growth in consumer acceptance. The amount of inks available on the market is still increasing, motivated by newer printing technologies, demands of the printers and the end-users. The current problems of ink manufacturers are of course faster printing speeds, a more cost-effective processes and environmental regulations.

The most important properties of inks are cohesion and adhesion. Printing is possible in consequence of the ink is more inclined to adhere to different substrates then to it self. The two main components of offset ink, are a solid and a liquid, the solid being the pigment providing the colour, and the liquid being the vehicle to carry the pigments in a printable medium and make them adhere to a substrate. In the case of conventional inks, the vehicle is a combination of binders and solvents. The solvents not only keep the ink in enough of a liquid state through the time needed for printing, but also control how the ink dries after. Almost all solvents used in conventional formulations are volatile substances. As the ink dries solvents evaporate and leaving the rest of the ink on the substrate.

Ultraviolet (UV) curable ink systems are an expanding area of the printing industry with expectations to develop significantly within the next few years. This printing technology is applicable in various areas, including the field of packaging, safety and security, the production of smart cards, CDs/DVDs and on printed circuit boards. The only major difference in this printing process, in comparison with conventional web or sheet fed printing, is the mode of ink drying. UV ink systems contain photoinitiators which when activated with the correct wavelength of radiation, undergo a rapid free radical reaction causing the ink to set rapidly forming a dry hard resin film. Vehicles consist of oligomers and monomers and do not contain VOCs. This system, give a number of advantages, namely rapid drying with no ink set off or smearing, high print gloss and an abrasion resistant surface. There is also less problem of sample blocking, where none dried ink films cause the sheets to stick together. The process is reported to be relatively cost effective, clean and environmentally friendly, however the printed material may be a little more difficult to recycle.

Hybrid inks are based on conventional offset printing inks, but contain part of UV curable components as well and are able to run on conventional press machine refitted with UV lighting stations. One of the major

advantages of hybrid ink technology is that smaller commercial printers can add inline UV varnishing to their operations at relatively low cost. The hybrid inks should be printable with blankets that are also suitable for conventional inks. The change-over between conventional and hybrid inks is not so simple, and there are a lot of unanswered questions about, what are the best practices for operators and what are the expectations of the quality and performance will be.

2. Experimental

In this work, seven magenta process inks were tested, three conventional, two hybrid and two UV inks, listed in table I. Two different types of fountain solutions were used for preparing emulsions, one without alcohol (Supreme 250, Inchema) and one (V 45) with addition of 5% IPA.

Table I: Process magenta offset inks tested in this work

Name of product	Type of ink	Manufacturer
Rapidon Magenta	coldset offset ink	SI COLOR Drükfarben
OPTIMA ECO PLUS OPE27	coldset offset ink	Coates Lorilleux
Arrow Star Fast Setting 3030	coldset offset ink	FLINT - SCHMIDT
SICO - BRITE Magenta 78000026	hybrid ink	SI COLOR Drükfarben
REFLECTA–HYBRID Magenta, 42UH 8900	hybrid ink	Michael Hüber München
SICURA DEO 456, 12 QM 236648 Magenta	UV ink	SIEGWERK INK Packaging
LITHOCURE UO 330080-409	UV ink	X SYS Print Solutions

Duke Ink Water Emulsification Tester Model D-10 (HDuke Enterprises, USA) was used for preparing the emulsions. The emulsion was determined by the amount and rate of water pick-up.

The flow behaviour and the viscosities of neat inks and emulsions were measured on rotational rheometer RV1 HAAKE. All the tests were done with a one cone-plate measuring system. For high viscosity samples, a titanium cone with radius 20 mm and angle 1° was used. For temperature control during the test a temperature dependent flow behaviour thermostat DC 30 was used. Experiments for flow characteristics were run for shear rates 0.1 to 1620 s^{-1}.

The yield stress and the dynamic mechanical analysis were performed on a rheometer, HAAKE RS 150 RheoStress, with the same cone-plate measuring system.

The dynamic analysis of neat inks was performed by a test from 0.1 to 100 $rad.s^{-1}$ with constant strain $\gamma = 0{,}01$ in LVE region of each ink.

The Tackmaster-92 (Kershaw Instrumentation, USA) was used to measure the tack and misting characteristics. The tackmaster rollers temperature was set to 32°C for all measurements. The ink was applied to the tackmaster with a small pipette that holds approximately 1.2 cubic centimetres and left in low speed (290 rpm) for 50 seconds to equilibrate. Then the speed was increased to 800 rpm. The tack value was taken after a 120 seconds at 800 rpm. Misting was performed by way of placing a white piece of paper behind the tackmaster and collecting the mist for 5 minutes at 800 rpm. The ink layer thickness was triplicate.

3. Emulsions

The flow behaviour of the offset ink is altered when a dampening solution is emulsified within it. The fountain solution feed rate is controlled by the type of plate and fountain solution efficiency.

In Table II are summarized the results of the densities of neat and emulsified inks and the percentage of the decrease in density of the emulsified inks. Also there are the parameters E_{max}, the maximal amount of emulsified fountain solution and k, the emulgation coefficient. These parameters were evaluated based on the relation:

$$E = E_{max}(1 - e^{-kt}) \quad (1)$$

UV inks are less able to pick-up fountain solution than conventional inks, but their rates of water pick-up are the fastest. The decreases in density of the emulsions compared to neat inks are greater for UV inks.

With emulsification, the viscosity is decreased. For comparison, a value of viscosity of $\dot{\gamma} = 50s^{-1}$ was chosen. For all the inks, the viscosity decreased to 35% of original value. In Table III are shown the values of the viscosity of neat and emulsified inks and the percentage of mutual ratio. Coldset inks being more thixotropic than UV and hybrids cause larger values of viscosity.

Table II: Duke water take-up

	neat	emulsion without IPA				emulsion with IPA			
ink	ρ [g/cm^3]	ρ [g/cm^3]	decrease [%]	E_{max} [g/100g ink]	k [10^{-3} s^1]	ρ[g/cm^3]	decrease [%]	E_{max} [g/100g ink]	k [10^{-3}s^1]
SICO BRITE hybrid	1.2687	1.1687	7.88	48.83	9.81	1.1602	8.55	55.49	7.28
REFLECTA hybrid	1.2972	1.2525	3.44	30.18	33.28	1.2233	5.69	39.83	19.98
SICURA DEO UV	1.2991	1.1889	8.49	26.21	30.95	1.2373	4.76	26.03	23.78
LITHOCUR E UV	1.2903	1.2097	6.25	34.15	23.8	1.2020	6.85	36.61	17.8
SI COLOR coldset	1.1058	1.0611	4.04	49.68	9.54	1.0808	2.26	49.02	14.88
OPTIMA ECO coldset	1.1505	1.1052	3.94	63.84	6.5	1.0946	4.86	54.91	11.2
FLINT SCH. coldset	1.1169	-	-	-	-	1.0899	2.42	90.00	4.38

Table III: Viscosity values at $\dot{\gamma} = 50s^{-1}$

ink	neat ink η[Pa.s]	emulsion (IPA) η[Pa.s]	decrease to [%]
SICO BRITE hybrid	15.2	5.8	37.9
REFLECTA hybrid	15.5	5.6	36.3
SICURA DEO UV	19.6	6.8	34.9
LITHOCURE UV	12.1	3.6	29.7
OPTIMA ECO coldset	29.4	9.2	31.4
FLINT SCH. coldset	30.1	14.0	46.6

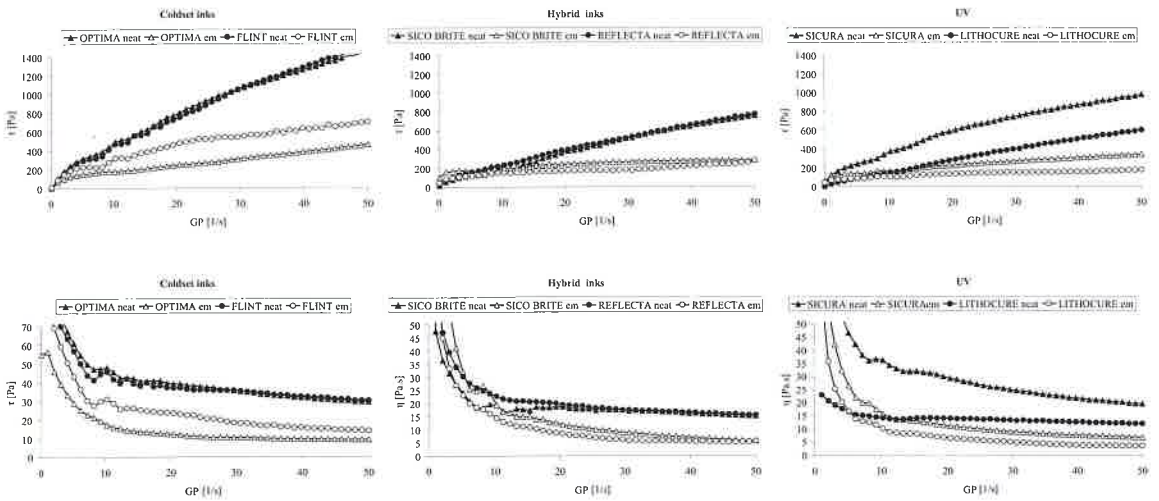

Figure 1: Flow and viscosity curves of neat and emulsified inks (with IPA content)

4. Flow curves

To determine the character of the behaviour of the inks at medium and high flow velocities, rotational tests were run from shear rates 1 to 1620 s^{-1} and a curve fitting with rheological model functions was applied. Characteristics of hybrid and UV inks were evaluated by means of Casson and Herschel-Bulkley model functions, which includes the apparent yield point, table IV.

Casson: $\sqrt{\tau} = \sqrt{\tau_{0C}} + \sqrt{\eta_{\infty C}\dot{\gamma}}$ Herschel-Bulkley: $\tau = \tau_{0HB} + c_{HB}(\dot{\gamma})^p$

UV and hybrid offset inks have a different flow behaviour compared to the conventional ones. Viscosity curves are plotted in logarithmic scale in figure 2.

Table IV: Characteristic of neat and emulsified hybrid and UV inks evaluated from flow curves

Ink		Casson		Herschel-Bulkley		
		$\eta_{\infty C}$ [Pa.s]	τ_{0C} [Pa]	c_{HB} [Pa.s]	τ_{0HB} [Pa]	p
REFLECTA hybrid	neat	4.91	107.39	37.04	30.28	0.74
	emulsified	0.62	132.04	27.06	24.99	0.59
SICO BRITE hybrid	neat	6.88	130.75	33.75	29.29	1.62
	emulsified	0.14	119.55	47.08	29.28	0.34
SICURA DEO UV	neat	4.33	139.80	27.61	75.37	0.78
	emulsified	1.87	129.00	8.84	190.70	0.83
LITHOCURE UV	neat	4.07	42.58	13.72	8.67	0.85
	emulsified	0.44	69.11	4.33	81.04	0.75

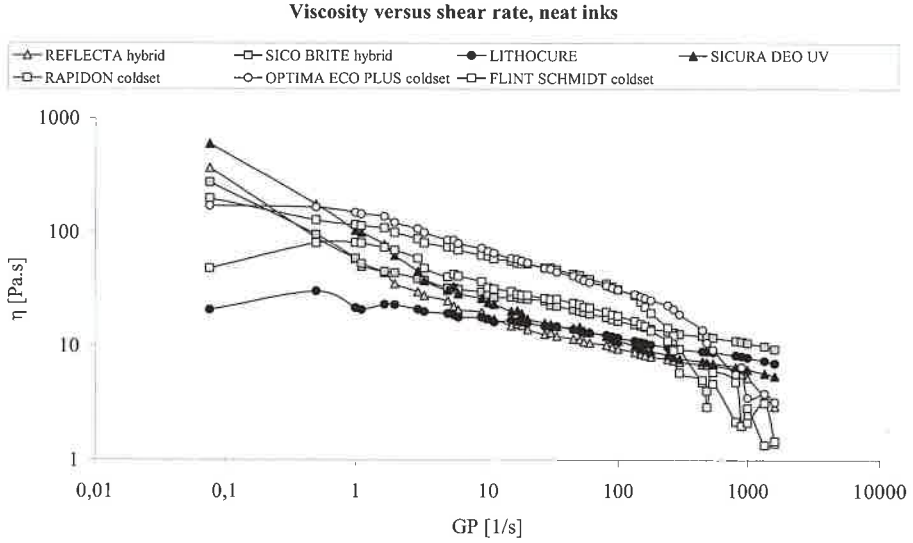

Figure 2: Steady shear test, viscosity versus shear rate

The temperature heavily influences the behaviour of the ink flow. Thus, during measurement it is very important to control the temperature. The viscosity of a liquid generally decreases with increased temperature.

5. Thixotropy

Thixotropic behaviour means the reduction in structural strength during the shear load phase and complete structural regeneration during the subsequent rest phase. Thixotropy is a decrease in the apparent viscosity under shearing, followed by a gradual recovery when the shear is removed. The effect

is time dependent. If the viscosity reduces and immediately returns after shearing, the material is not thixotropic but just 'shear thinning'.

Substances change from a high viscosity gel to a much lower viscosity sol under exerted high shear during a test period. For real thixotropic substances the transformation from a gel to a sol and conversely is reversible.

In this work, thixotropy of neat and emulsified inks was provided by four different methods. One method was the measurement of the percentage of regeneration; the test was divided into three intervals, the first interval with $\dot{\gamma} = 5s^{-1}$ for one minute, the second interval with $\dot{\gamma} = 1000s^{-1}$ for 30 seconds and the last interval with $\dot{\gamma} = 5s^{-1}$ again for three minutes. From the first interval, when the viscosity was almost constant, determined at η (100%) value. At four time points from the third interval the percentage of regeneration was calculated. The rate of recovery is an essential factor for levelling of the ink on the substrate.

The second method to determine the extent of thixotropy, was calculated from the same tests as the difference between the minimum viscosity at the end of second interval under high shear, and maximum viscosity at the end of the test under low shear rate, $\Delta\eta = \eta_{max} - \eta_{min}$. The results are summarized here in Tables V and VI.

Table V: Percentage of regeneration for neat inks

ink	RAPIDON conventional		OPTIMA ECO PLUS conv		SICO BRITE hybrid		REFLECTA hybrid		LITHOCURE UV		SICURA DEO UV	
	η[Pa.s]	reg.[%]	η[Pa.s]	reg.[%]	η[Pa.s]	reg.[%]	η[Pa.s]	reg.[%]	η[Pa.s]	reg.[%]	η[Pa.s]	reg.[%]
low shear	50	100	63	100	25	100	25	100	14	100	32	100
high shear	2.4	4.7	5.1	8.1	8.2	32	5.7	23	5.7	41	6.0	19
after 30 s	25	44	27	43	21	82	23	94	12	83	26	80
after 60 s	31	59	33	52	21	85	24	98	12	87	27	83
after 120 s	33	63	36	56	22	85	23	97	13	89	28	85
after 180 s	35	66	37	58	22	86	24	99	13	94	28	86
Δη	32.6		31.9		13.8		18.3		7.3		22	

Table VI: Percentage of regeneration for emulsions

ink	RAPIDON conventional		OPTIMA ECO PLUS conv		SICO BRITE hybrid		REFLECTA hybrid		LITHOCURE UV		SICURA DEO UV	
	η[Pa.s]	reg.[%]	η[Pa.s]	reg.[%]	η[Pa.s]	reg.[%]	η[Pa.s]	reg.[%]	η[Pa.s]	reg.[%]	η[Pa.s]	reg.[%]
low shear	40	100	22	100	34	100	19	100	14	100	26	100
high shear	1.1	2.7	1.5	6.9	0.5	1.5	1.1	6.1	0.7	5.0	1.9	7.4
after 30 s	15	38	15	68	8	24	16	86	9	64	18	70
after 60 s	17	42	15	70	8	23	15	82	8	60	19	71
after 120 s	19	46	15	70	8	23	14	76	7	53	19	74
after 180 s	19	47	16	74	8	22	14	75	7	53	19	74
Δη	17.9		14.5		7.5		12.9		6.3		17.1	

Neat UV and hybrid inks show an almost complete regeneration after 30 s, but with emulsification, the regeneration decreases. Faster regeneration facilitates the ability to achieve the required layer thickness, as the ink film strength is reached in shorter time. A slower rate of structural regeneration offer a good levelling behaviour, but a too slower rate can cause an increase in dot gain.

Other tests to compare thixotropy of different inks were based on measurement of hysteresis loop. In these tests, the sample is subjected to increasing shear and then reducing shear. A loop between the UP and DOWN curve means, that the samples behave differently before and after shearing and are more or less thixotropic. The value of thixotropy is determined as a difference between two areas, between $\dot{\gamma}$ axis and UP curve and area between $\dot{\gamma}$ axis and DOWN curve. This hysteresis area is proportional to the energy required to break down the thixotropic structure. The first test consisted of three parts, up-ramp, constant upper shear rate and down-ramp. The results are shown here in figure 3.

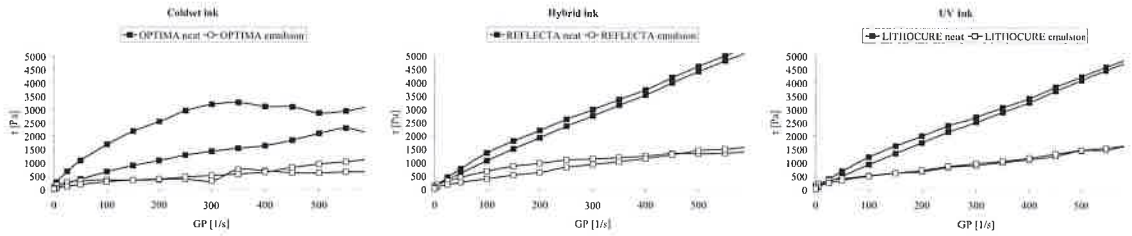

Figure 3: Thixotropic area of coldset, hybrid and UV neat inks and emulsions

Second test contained three up-ramp and down-ramp curves, shown in figure 4.

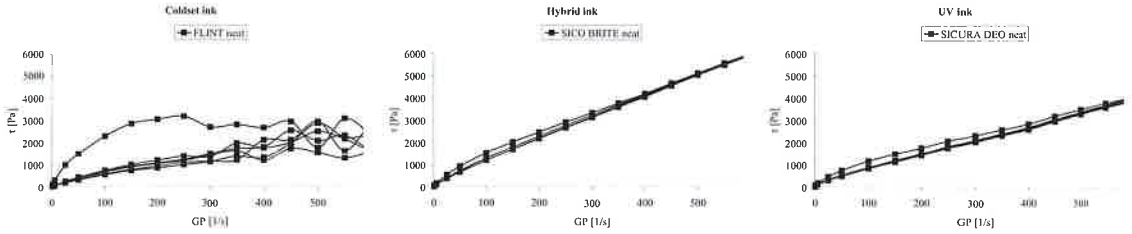

Figure 4: Thixotropic area of neat inks

It is important to recognise thixotropy in materials otherwise; the shear history of the sample may adversely affect the accuracy and reproducibility of the test. The hybrid and UV inks appear to have only a shear thinning nature, as the UP and DOWN curves almost overlay each other. From the structure regeneration test, was obtained a more meaningful insight about the thixotropy phenomenon of offset ink application.

6. Yield stress

The yield stress is defined by the stress at which a fluid starts to move and a big change in viscosity happens. The Herschel–Bulkley model describe this phenomenon simply, given by

$$\sigma = \sigma_y + f(\dot{\gamma}) \text{ if } \sigma > \sigma_y \text{ and } \dot{\gamma} = 0 \text{ if } \sigma \leq \sigma_y,$$

where σ is the applied shear stress, σ_y yield stress and $f(\dot{\gamma})$ function of the shear rate. This model predicate that the flow is always homogenous at all shear rates. In reality happens that at low shear rates, the shear localises in small regions with high shear rate while the remaining part of the liquid behaves like a solid.

The yield stress is very difficult to measure. Large number of test methods to determine the yield point was developed, but different methods give different results. The most direct methods for measuring the yield values provide CS viscometers, which are able to apply small stresses and measure very low shear rates.

The yield point of samples was measured by the limit of the linear elastic range. The shear stress value at which the elastic deformation range is exceeded and the range of irreversible viscoelastic flow begins. The measured data were plotted in a double logarithmic scale with log τ on x-axis and log γ on y-axis. The yield point was identified as a crossover of two tangents. The first tangent was set at the interval of the elastic deformation range with low τ values and second interval with high τ values. The second tangent shows a higher slope increase, when the sample flows. In Table VII are summarized the yield points of neat inks for two temperatures. The rates where the yield point is exceeded are very low; in case of UV and hybrid inks, it is because the macromolecules are able to disentangle, even under small shear forces. Yield stress prevents uncontrolled flow from ink duct, but a too higher value of yield point can cause a big amount of remaining ink in the ink duct. Yield stress and thixotropy together with capillarity of ink influence dot sharpness and penetration to the substrate. The higher the yield point, the lower the amount of spread of the ink onto the print medium.

Table VII: Yield points of neat inks

ink	τ_A [Pa] 25°C	at $\dot{\gamma}$ [s^{-1}] 25°C	τ_A [Pa] 32°C	at $\dot{\gamma}$ [s^{-1}] 32°C
SICO BRITE hybrid	113.6	0.136	52.3	0.029
REFLECTA hybrid	99.9	0.651	90.5	0.529
SICURA DEO UV	114.3	1.567	95.6	1.069
LITHOCURE UV	20.4	4.332	19.5	1.384
OPTIMA ECO coldset	168.3	33.505	164.1	73.29
FLINT SCH. coldset	28.5	7.378	27.8	14.930
RAPIDON coldset	188.7	48.970	140.0	57.265

7. Tack and misting

Tack is by definition the force required to split an ink film between two rollers. The values are given in units, which depend on the instrument and the method used. Tack is an important property in the inking system as well as in the ink/paper interaction and in the ink trapping for multi-colour printing. In order to trap properly, the ink printed first should have a higher tack than that of the following one.

High tack is generally desirable, but too higher tack will result in picking, when fibres are pulled out of the paper.

Table VIII: Tack values in gram/meters of neat and emulsified inks

ink	RAPIDON conventional Tack [g/m]	OPTIMA ECO conv Tack [g/m]	SICO BRITE hybrid Tack [g/m]	REFLECTA hybrid Tack [g/m]	LITHOCURE UV Tack [g/m]	SICURA DEO UV Tack [g/m]
neat ink	9.3	10.5	14.5	16.4	9.7	10.9
emulsion	8.7	9.1	15.8	16.7	10.9	11.5

Another property which was evaluated on tackmaster was misting, the tendency of ink to fly away from the rollers. Misting can result in colour contamination and servicing problem for the operator. Papers with misted ink on it were scanned and subjected to an image analysis. For characterization of the image, a mean value of luminance was used. Conventional ink mists much less than a hybrid or a UV ink, with the conventional inks the paper was whiter at a velocity of 1200 rpm compared to the UV and hybrid inks at a velocity of 800 rpm. Emulsion limits the misting and the mist droplets are smaller compared to those of neat inks.

8. Dynamic test

Offset inks are viscoelastic fluids. Hook's law defines the elastic portion: $\tau = G\gamma$

The viscous portion behaves according Newton's law: $\tau = \eta\dot{\gamma}$

A frequency sweep test was carried out with all neat inks. The frequencies were stepwise increased and each step provided G', G'', η^* and δ. For the inks with G' > G'' the elastic behavior dominates and they show a certain form stability. The G' value is greater for Reflecta hybrid ink, Sicura Deo UV and Flint Schmidt conventional ink. When G' < G'', the viscous behavior dominates and the samples show the character of liquid. For the highly viscous materials this means that the molecule chains are entangled, without chemical and physical forces.

9. Conclusions

The rheological properties of three types of offset inks were investigated, with the aim to describe some of the peculiar characteristic of hybrid inks. This rheological study has shown that in some aspects hybrid ink seem to be similar to conventional inks (water take-up and ink/water balance) and also in some aspects similar to UV inks (flow curves, thixotropy and misting).

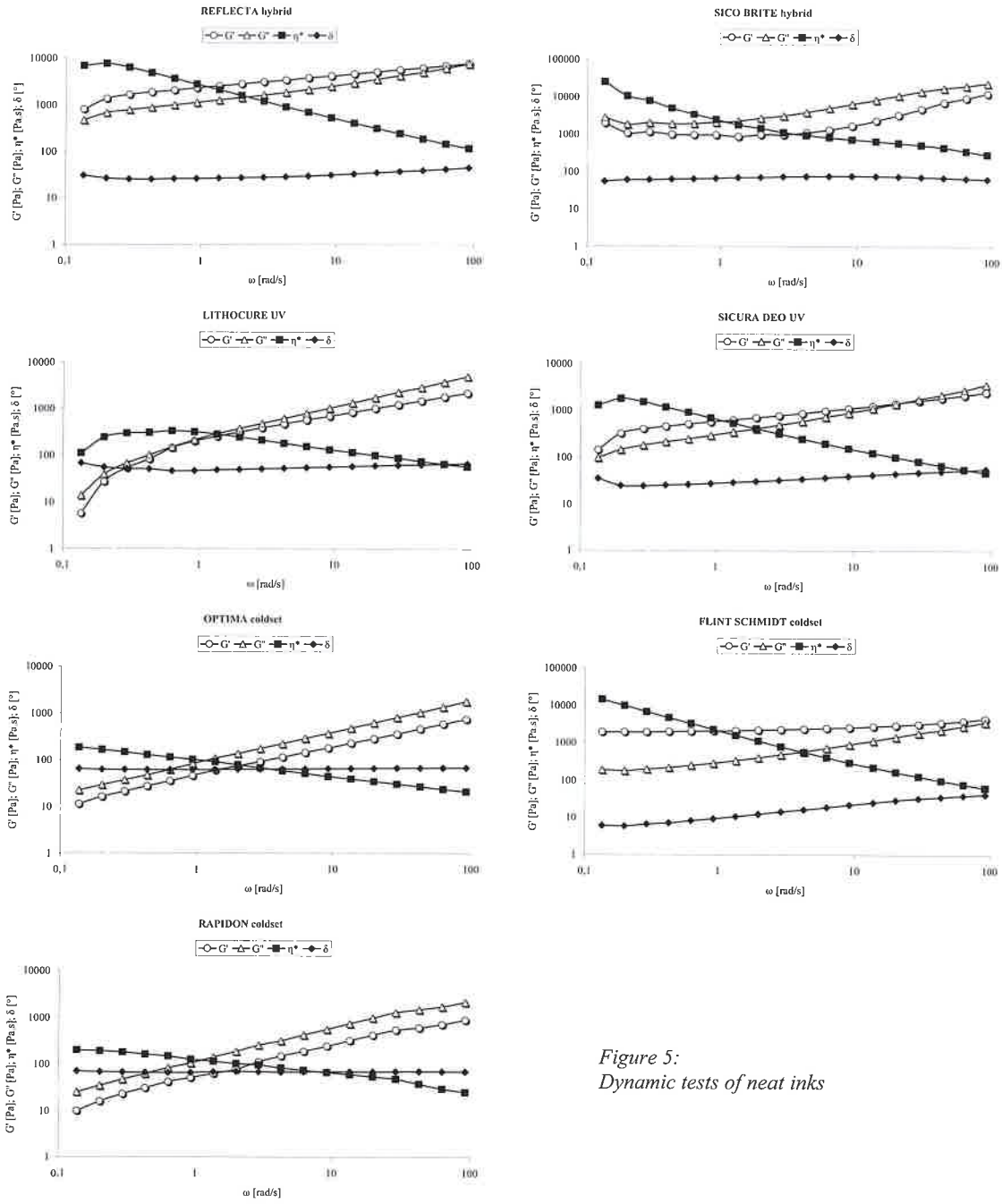

Figure 5:
Dynamic tests of neat inks

All emulsions have viscosities at a high shear rate within required region. Thixotropy of emulsions is also improved in cases of hybrid and UV inks compared to neat inks.

The misting is higher for UV and hybrid inks and this is why it is recommended to run them at lower speeds.

References

[1] Barnes H. A., (1999), *The yield stress - everything flows?, J. Non-Newtonian Fluid Mech.,vol. 81, pp. 133 - 178*

[2] Maurer A., Wozniak G., Hübler A.C., Beier W., (2005), *Über das Zerstäuben von Offset-Druckfarbe, Forsch Ingenieurwes, vol. 69, pp. 223 - 229*

[3] Mezger T., (2002), *The Rheology Handbook, Curt R. Vincentz Verlag, Hannover, ISBN 3-87870-745-2*

[4] Schramm G., (1998), *A Practical Approach to Rheology and Rheometry, Gebrueder HAAKE GmbH, Karlsruhe*

Wavelet automatic classification system of substrates in flexography

Amparo Sánchez-Alandí, Susana Otero, Vicente de Gracia

AIDO, Technologic Institute of Optics, Colour and Image
Nicolás Copérnico, 7 - 13, Parque Tecnológico, Paterna, Valencia, Spain
E-mail: asanchez@aido.es

Abstract

Packaging printing quality has been greatly improved in recent years, small changes in colour and substrates are not anymore accepted by manufacturers. At the same time as its importance has been increased, automatic processes are needed to obtain better profitability. This paper describes an automatic system to grade the type of substrates in packaging. The target of this system is being able to detect changes in substrate while it's being printed.

This system takes profit of the different Near Infrared Spectrum of the substrates. These spectrums can be obtained easily by AOTF technology. The data are processed online by a wavelet algorithm. The main characteristic of wavelets is their noise immunity and its easy handling.

Keywords

Flexography, substrates, quality, wavelet

1. Introduction

Flexography is more and more competitive and demanding, customers want more details, more complicated designs, cleanest and most brilliant colours and mainly consistency, that is, higher quality in printing along the print run. On the other hand, considering also the existing competitiveness in flexographic market, high speed is important.

Clearly with more quality and faster productions, more sophisticated equipment is needed in order to control the printing process. Nowadays there are many control devices to make easy the printing. This kind of devices give secure, continuous and systematic controls, being helpful to the machine operator, giving him a signal to proceed to the needing corrections, avoiding material lost.

Among the different variables to control in flexographic process, such as quality of inks, coatings, pressures, superficial tension, etc. one of the most important variables is the type of material to print.

Flexography has its main market in packaging, where almost 90% of materials are plastics, most of them used to be polyethylene (PE) and polypropylene (PP) and this materials need to receiving a special superficial treatment in order to make them more moisturizing, that is, more ink and coatings receptive. Nowadays, we can still hear customers not happy with the print job because inks were not able to stick on the printed material. This error could be produced, for instance, because of different surface energies or different absorption properties of the inks.

Normally, flexo workers check the material using visual and manual methods: by touch, by politex pencils and by micrometer. So, an automatic method could be useful in high volume productions or when two materials are connected in same productive job. Infrared spectroscopy is a powerful qualitative and quantitative tool for this purpose.

Infrared spectroscopy provides the ability to study the interactions of the vibrational and rotational energies of atoms or groups of atoms within molecules. Infrared spectra reflect vibrational motions that produce a change in the permanent dipole moment of the molecule. There is a large amount of information that can be gained by using IR spectroscopy for the analysis of polymers. Minor changes to the molecular structure usually result in a spectrum that is clearly distinguishable from the spectrum of the original compound. Thus, they can be used to identify the presence of a specific chemical compound or mixture of compounds and advise us if there's any change in the productive chain.

2. Methods

2.1 The infrared spectrum

Infrared spectrum is one of the most characteristic properties of a compound: each compound has its individual and unique spectrum, IR spectrum is like a fingerprint. Inside IR fundamental spectrum there are two regions: functional groups and fingerprint, the former ranges from 4.000 cm^{-1} to 1.300 cm^{-1} and the later from 1.300 cm^{-1} to 640 cm^{-1}.

Table I: Infrared spectrum

IR spectrum	cm^{-1}	µm
Near IR	12500 - 4000	0,8 - 2,5
Medium IR	4000 - 660	2,5 - 15,15
Far IR	660 - 50	15,15 - 200

In the functional group region the absorption peak of the compound depends only on the chemical functional group whereas in the fingerprint region depends on the full molecular structure. However, it's necessary to identify firstly the functional groups because, if a spectrum doesn't have a typical absorption value from the functional group, then the molecule doesn't include this group and it means this is a different material. Once the functional groups from the molecule have been detected, the fingerprint region analysis is made in order to find the characteristic strips from each compound.

2.2 Description of experimental measurement device

The system is made of several halogen lamps to illuminate the plastic. The reason for using halogen lamps is because they work efficiently in the near infrared and they are quite cheap. An aluminium reflexive surface is placed on the back of the plastic so that, the spectrum detected will be a mix of reflected and transmitted light, giving a higher signal without disturbing the information relevant to the identification of the type of material.

The reflected light is picked up by a specially developed measurement device, which will give as output the spectrum of the compound. This measurement device is based in acusto-optical filter. This filter works as diffraction net determined by the vibration frequency. Its big wide band let us obtaining the spectrum at a second fraction.

The measurement device is made of four main components [Barcala, JM]. The first one is the set of collimation lenses, used to collect the reflected light and guiding it to the following elements in a correct way. Afterwards there is a filter that limits the visible light whereas it let the pass of infrared. This filter consists in a silicon plate, material what absorbs wavelengths until 1.200 nm, where all the measurements starts. The transmitted beam reaches a polarizer which let linear polarized light crossing it depending on the direction and refusing the rest.

The second element is the acusto-optic filter. It chooses a specific wavelength that goes out in a beam 7.3° deviated respecting the incident line. Besides, due to a non lineal effect of the acusto-optic filter, stopping some wavelength is possible using additional polarizer.

At the end, there is the sensor that is a germanium photodiode connected to A/D converter that will generate an output signal, that will be managed and interpreted by a PC. The device currently developed is able to analyse the IR spectrum within the functional group range.

2.3 Wavelet analysis

A wavelet is a short time function with an average value of zero. This function fulfils several mathematic properties and it can be used to create a functional space base to represent functions. It's similar to the Fourier transformed but it hasn't a sinus shape. In wavelet analysis the original signal is split into two signals: one out of phase and one out of magnitude than the original wavelet.

One of the advantages of this method is the possibility to obtain a temporal localization of phenomena. In Fourier analysis only the average of the full result is obtained. To correct this aspect, Dennis Gabor [Gabor, D]

proposed a Fourier transform adaptation, which allows analysing only a small part of the signal each time (STFT Short Time Fourier Transform). This represented not a complete solution because the temporal resolution is limited.

The wavelet transform gives information about time and frequency at the same time, allowing a signal representation on time and frequency. And another reason to use this method is that wavelet analysis is noise immune.

Among all the different wavelet families, the wavelet de Haar was used to filter the values from measurements [Grap, A]. So that, it's possible to analyze all the values for different scales by means of a coefficient sets. These coefficients are:

$$h_0 = \left[\frac{1}{\sqrt{2}}, \frac{1}{\sqrt{2}}\right] \quad , \quad h_1 = \left[\frac{1}{\sqrt{2}}, -\frac{1}{\sqrt{2}}\right] \tag{1}$$

These filters give information of the signal and they can be applied several times in order to split the signal into different levels of information. This kind of analysis gives a multiple resolution response.

The Haar transform lets us to compress more than 150 values of the signal, obtaining only a few coefficients. These coefficients can be combined to form quaternions (like a four-dimensional vector) [Hamilton, WR].

There will be a quaternion for each type of material and each quaternion comes from the average of different measurements in the same film. In the other hand, the quaternion will be used as reference value to comparing it with other films. This comparison is done by the Euclidean distance between quaternions.

3. IR Analysis of substrates

Plastic substrates were analysed using the developed equipment. These are Polyester (PET), Polyethylene (PE) and Polypropylene (PP). These substrates were chosen due to their relevance in the packaging industry. All the plastics were manufactured as films, so it's not necessary a previous preparation of samples.

The Polyethylene (PE) is obtained by ethylene polymerization of gaseous ethylene for different pressures, giving different densities and different types of polyethylene. This material needs a previous treatment for its printing. This treatment consists in a surface oxidation. The average spectrum from a polyethylene sample is shown in figure 1. This spectrum includes values between 1.200 and 1.900 nm with absorption bands in (1.380 - 1.440) nm and (1.740 - 1.820) nm.

The Polypropylene (PP) is obtained by polypropylene gas polymerization. Depending on the manufacture technology, it's obtained in two different types of PP due its physical properties (CPP or BOPP). This polymer is used for high transparency films for packaging. The average spectrum from a polypropylene sample is shown in figure 2. This spectrum includes values between 1.200 and 1.900 nm with absorption bands in (1.380 - 1.520) nm and (1.720 - 1.760) nm.

The Polyester (PET) is used in packaging after a chemistry treatment or corona treatment as the previous polymers. The average spectrum from a polyethylene sample is shown in figure 3. This spectrum includes values between 1.200 and 1.900 nm with absorption bands in (1.600 - 17.000).

In figure 4 is showed the comparison of these spectrums, where is evident that the polyester (PET) spectrum is quite different to the others. It only presents a strong absorption peak around 1.600 nm due to the CH bonds. However, it has a similar response between 1.200 and 1.600 nm and 1.750 and 1.900 in the rest of spectrum analyzed.

The polyethylene (PE) and polypropylene (PP) have a similar response presenting two absorption peaks in similar spectrum regions. The difference between them can be detected in the spectrum out of these absorption peaks and mainly between them. The biggest differences appear between 1.420 and 1.750 where polyethylene (PE) reaches high transmittance values while polypropylene (PP) increases smoothly.
This is well correlated with the chemical structure of these polymers.

Tests were carried out on thin films, with increase of thickness the spectrum peaks appears as wide bands and limiting the resolution and our current ability of analysis. For the analysis of these thicker substrates, a different algorithm should be especially developed.

Figure 1:
Polyester (PET) infrared spectrum

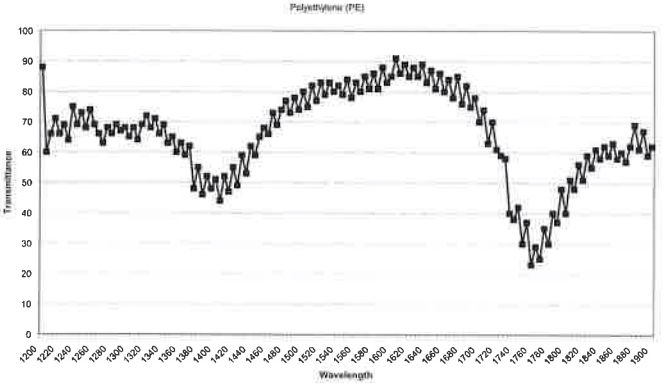

Figure 2:
Polyethylene (PE) infrared spectrum

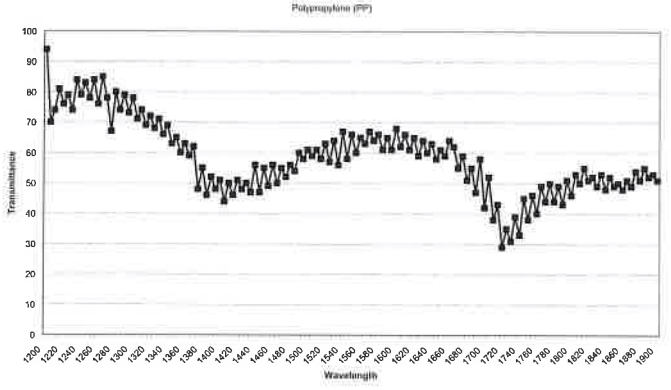

Figure 3:
Polypropylene (PP) infrared spectrum

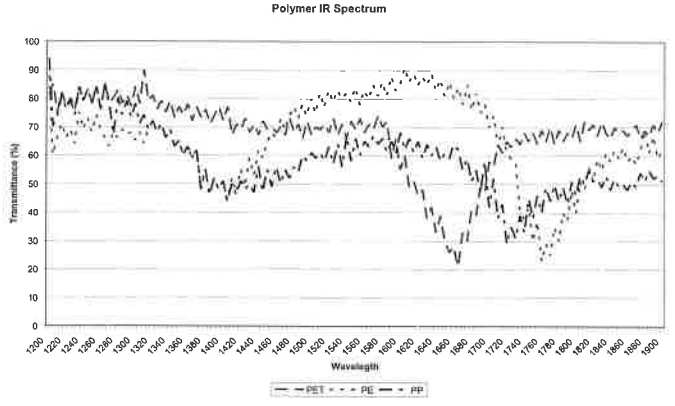

Figure 4:
PE, PET and PP polymers infrared spectrum comparison

4. Conclusions

IR spectrometry has been proven to be able to accurately identify different kind of flexographic films using wavelets analysis. This method gives the ability to produce an automatic, quick and reliable system to detect changes in substrates that affect the printing quality. Substrates have been analyzed in functional spectrum, but an IR Spectrometer working in the fingerprint region should give us more information to classify polymers with almost same composition.

References

[1] Barcala, J. M., Fernández, J. L., Alberdi, J., Molero, F., Oller, J. C.; Jiménez, J., Lázaro, J. C., (2002), Sistema automático de clasificación de plásticos en tiempo real. XXIII Jornadas de Automática. España

[2] Chicharro, J. M., García-Berrocal, A., Balbás, M. and Blázquez, J., (2002), *Pressure transmitter surveillance using quaternion numbers, Mechanical Systems and Signal Processing, 16(6), 1083 - 1091*

[3] Cohen, A., Daubechies, I., and Feauveau, J. C., (1992), *Biorthogonal bases of compactly supported wavelets, Communications on pure and applied mathemathics, Vol. 45, pp. 485 - 560*

[4] Conley, R. T., (1079), *Espectroscopia Infrarroja, Ed. Alhambra*

[5] Eisenrich, N.; Rohe, T., (2000), *Infrared spectroscopy in analysis of plastics recycling, Encyclopedia of analytical chemistry, John Wiley & Sons Ltd*

[6] Fernández, J. L.; Sánchez, J.; Hernanz, A.; Alberdi, J.; Barcala, J. M.; Navarrete, J. J., (1999), *Utilización de la espectroscopia NIR en la clasificación automática de envases plásticos en residuos sólidos urbanos. XX Jornadas de Automática. España*

[7] Graps, A., (1995), *An introduction to wavelets, IEEE Computacional Science and Engineering. IEEE Computer Society*

[8] Hamilton, W. R. (1853), *Lectures on Quaternions: Containing a systematic statement of a new mathematical method; Hodges and Smith*

[9] Siesler, H. W., Holland-Moritz, K., (1980), *Infrared and Raman spectroscopy of polymers, Marcel Dekker. Nueva York*

A lumped parameter model for thermal conductivity of paper coatings

Philip Gerstner, Jouni Paltakari, Patrick A. C. Gane[1]

Helsinki University of Technology
Department of Forest Products Technology, Laboratory of Paper and Printing Technology
Vuorimiehentie 1A, P.O. Box 6300, FIN-02150 Espoo, Finland
E-mail: firstname.lastname@tkk.fi

[1] Omya Development AG
CH-4665 Oftringen, Switzerland

Abstract

The increasing use of coated papers in general, but even more so for the use in digital printing methods, reinforces the need for the properties of paper coatings to be well understood. Especially, a more detailed knowledge of the thermal properties of coatings can contribute to improved print quality and process economy of electrophotography and offset printing. Other finishing and converting operations of coated papers benefit as well. This paper proposes a model to calculate thermal conductivity based on structural parameters and the materials used. The parameters of the model are discussed and a comparison of the model parameters for a talcum and a calcium carbonate coating is given.

Keywords

Coatings, gluability, modelling, thermal conductivity, toner adhesion

1. Introduction

The market for coated papers is growing [Cody, 2005] and so is the importance to understand the properties of coated papers and paper coatings themselves. General properties of paper coatings, including strength, optical and structural behaviour, continue to generate a high profile in research. Thermal properties of coatings, however, have received considerably less attention, partly due to a lack of accepted specifically defined requirements. Nonetheless, many areas of coating, including the study of the application of dry coating, together with end uses in areas such as digital toner adhesion and fusing, all require an increasingly detailed knowledge of the surface response to exposure to heat. In dry surface treatment, for example, binder covered pigment is fused thermally onto the paper surface. Dry coatings can match largely the properties of wet coatings, but in order to achieve a good cohesive fusing, the thermal properties of the coating need to be known [Maijala et al., 2004].

For growth in the higher print quality area, the use of coated papers is almost universally required. Electrophotography, for example, involves a fusing process where small toner particles are thermally fixed onto the substrate surface. This makes the coating layer the toner receiving interface. Better understanding of its thermal properties can help to avoid curling problems and improve toner fixation and increased lifetime of the fixing drums [Sipi, 2002, Williams, 1984].

It is not only the emerging technologies that can benefit from a better understanding of the thermal properties of coatings. Heatset web offset relies on the heating effect of driers to drive the ink on the surface toward setting by increasing the imbibition rate of ink vehicle as its viscosity is lowered by increased temperature together with the evaporation of volatile components.

In order to predict the thermal properties of coatings successfully, a model is needed which takes both material and structural properties into account. This paper describes an approach to developing such a model for a simple three phase system.

2. Methods

Several models for heat conduction in porous media exist. One prominent example is the composite-layer or Krischer-Esdorn model [Krischer, 1978], in which the porous medium is described by serial or parallel layers

of solid and fluid phase. This model has become very popular in paper technology as it enables thermal conductivity to be described as a function of porosity by simply adjusting the ratio of parallel or serial layers. While this was applied successfully for thermal conductivity of papers [Kartovaara, 1985] and for drying of paper [Palosaari, 1965], it does not describe thermal properties of coatings. Guérin et al. [Guérin, 2001] examined the thermal properties of model coating layers and stated that it is not possible to describe paper coatings using the composite layer model. The major drawback of the composite layer model is that it does not reflect the actual structure of the porous medium.

In the lumped parameter model by Hsu et al. [Hsu, 1995], a unit cell is used which represents the simplified structure of the porous medium. The solid phases of the unit cells are finitely connected by a contact plate and surrounded by the fluid phase. We adapt this model (see Figure 1) using a square cylindrical solid phase (k_{s1}), representing the pigment, and introduce a second solid phase (k_{s2}) for the connecting plates, representing the binder, the fluid phase being air when representing a dry coating or a chosen liquid/mix of liquids when considering either a wet coating or one that has absorbed ink vehicle, for example. The width of the binder bridge is c and can be related to the pigment size a as the contact parameter $\gamma = ca^{-1}$. The unit cell can be split up into three parallel layers (Figure 1, I.-III.), consisting of the relative combinations of solid phases and each solid phase with the fluid phase, respectively.

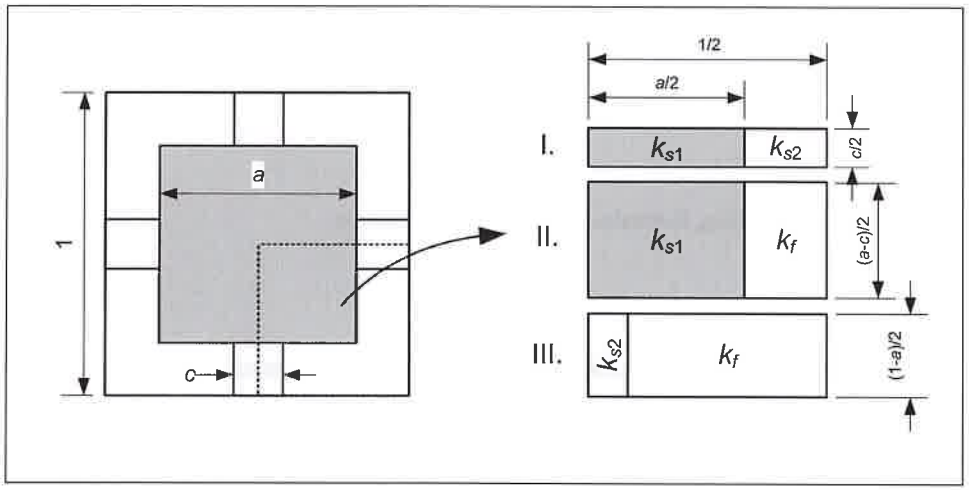

Figure 1: Modified three phase unit cell based on the lumped parameter model /Hsu, 1995 and its decomposition into serial and parallel layers (I. - III.) of thermal resistors

The total thermal conductivity of a unit cell can be calculated using the analogy of thermal and electrical resistance. Whereas the thermal resistance of a single phase within a layer of the unit cell is defined as:

$$R = \frac{\Delta x}{kA} \tag{1}$$

where, Δx is the length of the thermal resistor, k its thermal conductivity and A the area (or width, in the two dimensional case) perpendicular to the heat flow. By combining the thermal resistance of each phase in each layer (analogue to electrical resistors), one gets the overall effective thermal conductivity of the unit cell:

$$\frac{k_e}{k_f} = \frac{\gamma a}{(\lambda-\mu)a+\mu} + \frac{(1-\gamma)a}{(\lambda-1)a+1} + \frac{1-a}{(\mu-1)\gamma a+1} \tag{2}$$

where:

k_e	is the effective thermal conductivity of the unit cell,
k_f	the thermal conductivity of the fluid phase,
$\lambda = k_f/k_{s1}$	the conductivity ratio of the fluid phase to the pigment phase, and
$\mu = k_f/k_{s2}$	the conductivity ratio of the fluid phase to the binder phase.

3. Results and discussion

3.1 Discussion of modelling parameters

When discussing properties of porous media it is common to use the porosity of the medium as the governing parameter. In Figure 1 it can be seen that the porosity of the system is given by:

$$\phi(a,c) = 1 + 2ac - 2c - a^2 \tag{3}$$

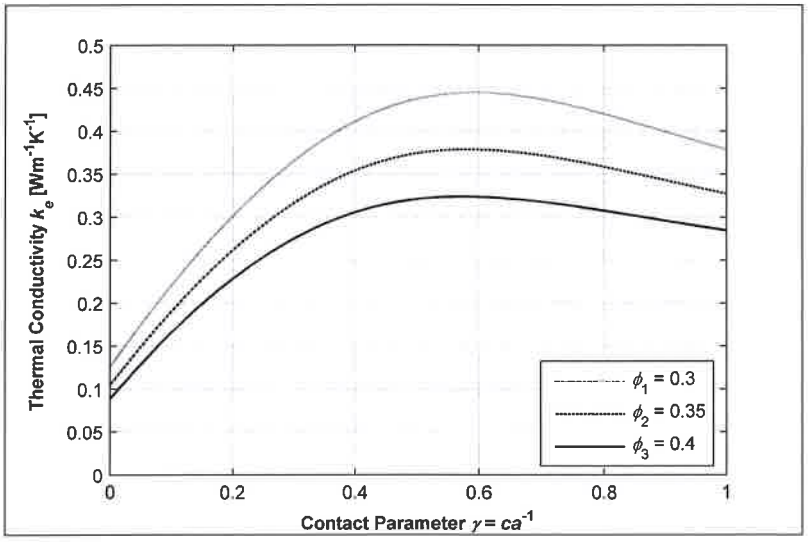

Figure 2: Thermal Conductivity according to the Modified Lumped Parameter model for constant porosities ϕ = 30%, 35% and 40% as a function of contact parameter (γ)

To use porosity as a parameter, Equation 3 needs to be converted to $c = f(a, \phi)$ or approximated (since nonlinear) to $a = g(c, \phi)$, where f and g are appropriate functions. This relationship means that neither a nor c are independent parameters but are mutually dependent, i.e. Equation 3 is not defined for all positive values of c as it does not cover the whole porosity range defined by the variable c alone. In practice this means that it is not possible to model a coating with a given average pigment particle size by setting the particle size parameter a as a constant and using only the binder amount (given by c or γ) to model porosity. For that reason it is better to use the latter and approximate a for a given porosity and contact parameter. It should be noted that the contact parameter itself affects porosity. Therefore, increase in the contact parameter leads not only to the assumption of more binder, but also to less pigment in the unit cell. There is a maximum in thermal conductivity at any given porosity defined by an optimal contact value, such that if the contact parameter rises above this certain value thermal conductivity again drops. Figure 2 shows this effect in a plot of thermal conductivity as a function of the contact parameter for constant defined porosities.

The interconnection of the parameters porosity and contact is a limitation of the model with respect to real coatings. It would be favourable to replace both porosity and contact parameter by a single parameter like binder dosage. For a given pigment particle system, it is essentially the binder that affects porosity and contact parameter. However, the distribution of binder is currently assumed homogeneous, and this is frequently not the case. To model the effect of binder dosage, we would need to discuss its model equivalent in more detail which, given the likely complexity, may not bring too much extra value to the results. Rather it will be illuminating to understand the role of binder amount and then to recognise that binder rich areas will behave differently from binder poor areas.

3.2 Grouped lumped parameter model

The model should be able to cover the whole porosity range starting from a pure air unit cell to pure pigment as well as the whole range of possible binder dosages from no binder to coatings of pure binder. To overcome

the limitations of Equation 3, as discussed above, this is done by splitting up the lumped parameter model and defining three stages (see Figure 3), depending on the amount of binder. For the binder amount, we choose the width of the connections c as a "running" variable for all stages.

In the first stage ($0 < c < a$), the pigment in the unit cell is surrounded by air ($c = 0$). For increasing values of c, connectivity between unit cells and, therefore, thermal conductivity increase by the width of the forming binder bridges. The limit is reached when the binder bridges equal the pigment particle size ($c = a$). This first stage is identical to the previous model:

$$\left(\frac{k_e}{k_f}\right)_{\text{Stage 1}} = \frac{c}{(\lambda-\mu)a+\mu} + \frac{(a-c)}{(\lambda-1)a+1} + \frac{1-a}{(\mu-1)c+1} \tag{4.1}$$

In real coatings, increasing binder amount would continue to fill up the void spaces. This is done in the second stage. The parameter c increases towards the size of the unit cell and replaces the remaining air in layer III (see Figure 1) by binder. The thermal conductivity increases further, by replacing the low conductive air with binder. The limit is reached when layer III is filled with binder, the unit cell becomes then nonporous:

$$\left(\frac{k_e}{k_f}\right)_{\text{Stage 2}} = \frac{a}{(\lambda-\mu)a+\mu} + \frac{1-a}{(\mu-1)c+1} \tag{4.2}$$

When continuing to increase the binder amount, the share of pigment to binder in a unit cell decreases. Therefore, the difference of unit cell width and binder amount (c - 1) is used to lower the "effective" pigment particle size. Since binder has a lower thermal conductivity, the total conductivity decreases because of the increasing influence of binder. The limit is reached when the share of pigment to binder becomes infinitely small, i.e. unit cell consists of binder only:

$$\left(\frac{k_e}{k_f}\right)_{\text{Stage 3}} = \frac{1+a-c}{\lambda(1+a-c)+\mu(c-a)} + \frac{c-a}{\mu} \tag{4.3}$$

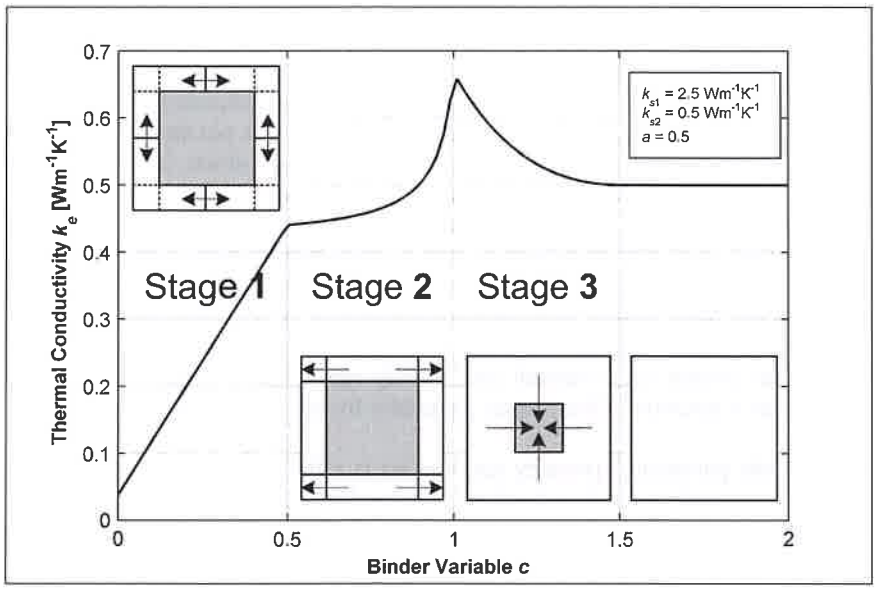

Figure 3: Three stages of the grouped Lumped Parameter Model. In stage 1 binder bridges form, in stage two porosity goes to zero and in stage three the share of binder to pigment increases

3.3 Applicability of the results

Guérin et al. [Guérin, 2001] measured the thermal conductivity of coatings by the temperature rise of a thermal mass through a sample pile. The samples were thin layers of talcum coatings with binder amounts of 5, 10, 15, 20, 25, 30 and 50 parts. They noted that the coatings with 25 parts of binder should be at the critical

pigment particle volume concentration. This refers to point $c = 1$ in our model. We can then use a quadratic correlation of binder variable c and the binder dosage B given in pph:

$$c = -5 \cdot 10^{-4} B^2 + 0.04B + 0.29 \quad (5)$$

Figure 4 shows the model prediction and experimental data obtained by Guérin *et al.*

The calculation example uses literature values [Landoldt-Börnstein, 1980] of $k_{s1} = 3.1$ $Wm^{-1}K^{-1}$ and $k_f = 0.025$ $Wm^{-1}K^{-1}$ for talcum and air, respectively. We assume that a styrene butadiene binder with a thermal conductivity of $k_{s2} = 0.25$ $Wm^{-1}K^{-1}$ [Mark, 1996] was used.

Despite the simple assumption of a quadratic relation between c and binder dosage, the model solution fits the experimental data rather well. There might be some scattering of the results by Guérin et al., but it should also be kept in mind that the measurements were made for thin coating layers. One precondition for modelling of porous media is that the measured structure for the effective properties is large compared to the pore structure [Tsotsas, 1987]. The measurement of thin coating structures might therefore induce some errors due to boundary effects. Furthermore, given the plate-like crystal symmetry of talc particles, thin layer structures will inevitably be preferentially aligned along the basal axes. This is a cause for divergence from the cubic symmetry assumed by the model, and in practice would mean a different thermal conductivity across/through the coating from that in the plane of the coating. Additionally, at high binder dose levels, the spherical nature of a latex binder will disrupt the pigment alignment somewhat and lead to a change from highly aligned structures to less aligned more homogeneous structures, during which the clearer transitions seen in the model will become smeared out. Nonetheless, the correspondence is promising.

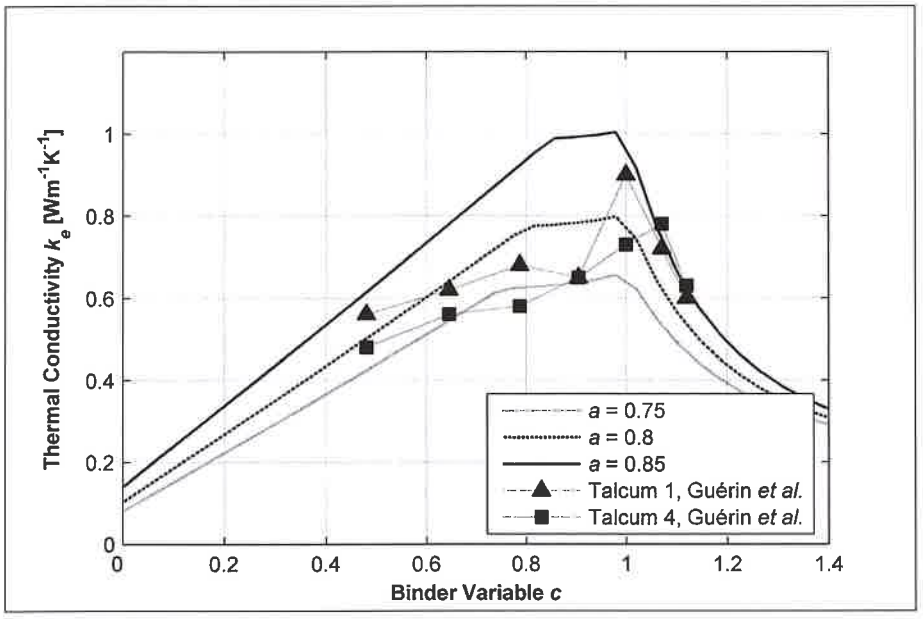

Figure 4: Thermal conductivity predicted by the model as a function of the binder variable c with $a = 0.75$, 0.8 and 0.85. Thermal conductivities of the phases are $k_{s1} = 3.1$, $k_{s2} = 0.25$ and $k_f = 0.025$ $Wm^{-1}K^{-1}$. Results by Guérin et al. [Guérin, 2001] for Talcum 1 and 4 are given for comparison

Figure 5 shows the theoretical temperature response within a coated paper. The paper is 120 µm thick, whereas 20 µm of its thickness is coating. The thermal diffusivity $D_{coating}$ used for the coating layer is based on recent measurements by the author, using a method established by Gane et al. [Gane et al., 2006], for a calcium carbonate coating structure with 8 parts binder. A pigment factor of $a = 0.8$ and a binder variable of $c = 0.52$ are used to match the result for the 8 parts binder calcium carbonate coating structure. For the calculation a thermal conductivity for the calcium carbonate pigment [Landoldt-Börnstein, 1980] of $k_{s1} = 2.0$ $Wm^{-1}K^{-1}$ was used. The thermal diffusivity of the base paper D_{paper} is a literature value of mechanical pulp containing handsheets [Kartovaara, 1985]. The heating temperature is chosen to be in the same order as of the toner fixing drum in electrophotography printing (170°C); the initial temperature of the paper is 23°C. The lines indicate the temperature responses after 1 ms, 5 ms and 10 ms of residence time.

The model parameters a and c, chosen for the coating temperature responses in Figure 5, deliver a thermal conductivity of $k_e = 0.53$ $Wm^{-1}K^{-1}$ for the talcum material properties (see Figure 4). This is the mean of the experimental thermal conductivity values to be expected for the Talcum 1 and 4 in Figure 4. A reverse calculation of the quadratic fitting (Equation 5) used for the correlation of binder variable and binder dosage, shows that the binder variable $c = 0.52$ equals a binder concentration of approximately 6 pph. So in addition to the calcium carbonate coating structure with 8 parts binder, the same model parameters also fit the talcum coating data of Guérin et al. with approximately 6 parts binder. The difference in the binder concentration can be related to the difference in the pigment particle system of the two examples. In both cases the pigment factor was $a = 0.8$. The fact that the binder concentration of the talcum system is predicted lower than that of the calcium carbonate system indicates that the platy and denser packed talcum particles have a higher connectivity as such and therefore require less binder in order to deliver the same thermal conductivity level.

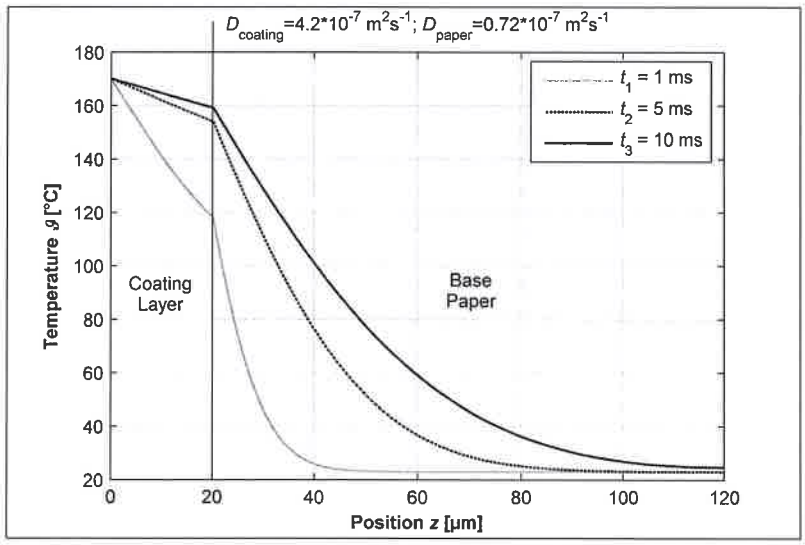

Figure 5: Predicted temperature distributions for different residence times within a coated paper. The heating temperature and maximum residence time are chosen similar to those in an electrophotography fusing nip

If we consider some of the implications for practical applications, we see clearly from Figure 5 that the thermal transfer through the coating layer is significantly faster than through the base paper underlying it. For processes, such as heatset web offset or the need to fuse toner in electrophotography, the efficiency of thermal conduction is likely to be very important, not only with respect to absolute values but also in respect to homogeneity. This model deals only with bulk conductivity and not the efficiency of the interface boundary, with its dependency on roughness and, hence, contact area, and specifically not with the interface conductivity properties necessary to ensure thermal transfer. However, it can be speculated that a rapidly heating surface will provide for a more efficient thermal response in printing applications as well as sheet drying, calendering and hot melt gluing, for example. The wear lifetime of the fusing cylinder in electrophotography could be greatly extended if surface temperature could be reduced, allowed for perhaps by a coating layer of the right design enabling optimal fusing conditions to be reached more quickly. The role of relative pigment and binder distribution is therefore going to be of vital importance, as well as the nature of the materials used. On the other hand, as we observe from the curves in Figure 5, the base paper can be strongly influenced. For example, after 10 ms, the base paper temperature at a depth of 40 µm has reached the boiling point of water. This could act very negatively in respect to base paper curl and fluting, so that the right balance of printing technology parameters (external temperature applied) would need to be achieved if highly conductive coating layers are to be considered. Alternatively, highly conductive coatings may need to be applied as topcoats only onto an otherwise insulating precoat. These aspects all point to the need to undertake further experimental verification of the predicted relevance of the model discussed here, and to investigate further the practical relevance and potential solutions it will predict.

4. Conclusions

A Modified Lumped Parameter Model for thermal conductivity of paper coatings is proposed. The model uses a unit cell resembling the structure of simple paper coatings. It includes the binder phase and distinguishes

between three stages of binder dosage in relation to pigment amount. The parameters of the model suggest that it is favourable to use binder dosage and a pigment size parameter together instead of porosity as the governing parameter, since binder dosage is a command variable in coating colour formulations, and the parameters for the two solid phases are clearly interconnected. This requires an empirical connection to be made between binder dosage and the binder (connectivity) variable of the model. Currently, too little measurement data exist to set up such a relation. Since the model predicts effective thermal conductivities, it requires that measurement data be taken from samples having dimensions that are large compared to their pore structures. Future research is ongoing, therefore, following the tablet forming methods of Gane et al. [Gane et al., 2006] to gather information on thermal conductivities of a macroscopic pigmented system at different parameterisable binder levels.

Acknowledgements

Grateful thanks are given to Omya Development AG for its continuing financial support of this work. A particular thanks also to Dr. Cathy J. Ridgway, Senior Scientist at Omya's R&D Laboratories, Oftringen, Switzerland, for her expertise and support in assisting in the sample construction and determination of coating pore structure.

References

[1] Cody, H. M., 2005, Coated Paper Markets Post Strong Rebound, PaperAge, Mar/Apr, pp. 18 - 19

[2] Gane, P. A. C., Ridgway, C. J., Schölkopf, J., Bousfield, D. W., 2006, Heat Transfer through Calcium Carbonate-based Coating Structures: Observation and Model for a Thermal Fusing Process, Paper presented at the International Printing and Graphic Arts Conference, Cincinnati, Tappi Press

[3] Guérin, D., 2001, Morin, V., Chaussy, D., Auriault, J. L., Thermal Conductivity of Handsheets, Papers and Model Coating Layers, The Science of Papermaking, 12th Fundamental Research Symposium, Oxford, Fundamental Research Society, Bury, UK, pp. 927 - 945

[4] Hsu, C. T., Cheng, P., Wong, K. W., 1995, A Lumped-Parameter Model for Stagnant Thermal Conductivity of Spatially Periodic Porous Media, J. Heat Transfer, 117, pp. 264 - 269

[5] Kartovaara, I., Rajala, R., Luukkala, M., Sipi, K., 1985, Conduction of Heat in Paper, Paper Making Raw Materials, Trans. 8th Fundamental Research Symposium, Oxford, Mechanical Engineering Publications Ltd, London, pp. 381 - 412

[6] Krischer, O., 1978, Trocknungstechnik Band I, Die wissenschaftlichen Grundlagen der Trocknungstechnik, Springer Verlag, Berlin

[7] Landolt-Börnstein, 1980, Zahlenwerte und Funktionen, Band IV Technik, 4. Wärmetechnik b, 6. Auflage, Heidelberg

[8] Maijala, J., Putkisto, K., Grön, J., 2004, Coating layer formation in dry surface treatment of paper substrates, Tappi Journal, 3, 5, pp. 20 - 24

[9] Maijala, J., Putkisto, K., Pietikäinen, R., Grön, 2004, J., Heat transfer during fixation of coating layers in dry surface treatment, Nordic Pulp and Paper Research Journal, 19, 3, pp. 291 - 299

[10] Mark, J. E., 1996, Physical Properties of Polymers Handbook, American Institute of Physics, Woodbury, New York

[11] Palosaari, S., Norden, H. V., 1965, Kemian Teollisuus, 22, 5, p. 359

[12] Sipi, K., 2002 Toner-paper interactions induced by the fixing process in electrophotographic printing, Licentiate's thesis, Helsinki University of Technology, Espoo, Finland

[13] Tsotsas, E., Martin, H., 1987, Thermal Conductivity of Packed beds: A Review, Chem. Eng. Process., 22, pp. 19 - 37

[14] Williams, E. M., 1984, The Physics and Technology of Xerographic Processes, New York, pp. 254 - 257

Digital paper and print surface topography

Pierre Vernhes, Anne Blayo, Bernard Pineaux, Jean-Francis Bloch

EFPG
461 rue de la papeterie, BP 65, F-38402 Saint-Martin d'Hères, France
E-mail: vernhes.pierre@voila.fr

Abstract

Paper is a complex composite material. Its structure and its surface greatly influence its runnability and its printability. The roughness is primordial for the absorption and the spreading of inks. It also plays a major role to determine the amount of coating. The paper surface characterization is crucial for understanding light reflection and scattering that control the level of gloss. The paper surface topography can be approached with different techniques, such as air leakage instrument, stylus technique or optical devices. From this mapping, parameters can be calculated according to a TAPPI standard. However a huge number of parameters exist; the most common is the root mean square of the height distribution of the surface S_q. This paper investigates the digital paper topography by calculating the smallest surface statistically representative of a given paper grade. Two algorithms are compared. In a second part the surface modification due to laser print is studied for different halftoning coverage. Measurements are compared to a model we developed.

Keywords

Electrophography, digital paper, toner, topography, roughness

1. Introduction

Digital printing is getting more and more attractive in terms of price, speed and quality. The two main technologies of the digital printing are electrophotography and inkjet printing.

One of the specificities of electrophotography is to create a toner layer on top of the paper. During the last step of the process, fine solid toner particles are heated and pressed (in the case of the hot roll fusing) onto the paper substrate. The thickness of this toner layer depends on the nature of the toner and of the haltoning, it can vary from a few micrometers up to 100 micrometers.

In the inkjet technology, a liquid ink is ejected at high frequency from a nozzle; then it penetrates and dries on the paper surface. In order to improve print quality, inkjet papers are coated. Those coating layers ensure a good smoothness of the surface. Surface characterisation is therefore of main importance. The gloss is strongly related to the surface topology [1] [2]. Gloss is often associated with high printing quality.

The aim of this study is to investigate the digital paper and print surface topographies. Thanks to an optical profilometer, a mapping of the surface is achieved [3]. From this mapping, parameters can be calculated according to the TAPPI standard [4]. Attention is focused on 3 parameters called amplitude parameters: namely, S_q the root mean square, S_{ku} the kurtosis (characterizing the flatness of the height distribution) and S_{sk} the skewness (characterizing the asymmetry of the height distribution) [5]. Those parameters are often chosen in paper physics to describe the "roughness" of a given surface [6].

The first step of this work was to find the "elementary representative surface" 'ERS', which is the smallest surface characterising the paper (or the print) considered. Two Matlab routine were developed in order to get an extensive statistical analysis of the surface. In the first routine, the parameters chosen were calculated in a sub surface centrally located. Various surface sizes were chosen (from 10µm up to 20.00µm). In the second routine, the sub surfaces used to calculate the roughness parameters are randomly chosen. From the initial (2 x 2) mm^2 surface, sub surfaces were randomly extracted from a size of (10 x 10) μm^2 up to (1.900 x 1.900) μm^2. Thus, the convergence of the amplitude parameters was studied. It gives relevant information on the uniformity of the paper sheets and therefore on paper quality.

In the second part, the evolution of the standard parameters is compared to the halftoning for both electrophotography and inkjet. Numerical simulations of the standard parameters were carried out and compared to the experimental results measured with the profilometer.

2. Materials and methods

2.1 Paper Samples

We chose two electrophotographic papers referenced as Q+ and Q-, respectively. These papers are common office papers: Q+ is assumed to have a better quality than Q-. We also studied an inkjet paper of high quality referenced as Jet. Finally a recycled paper was also analysed (referenced as Green).

The main paper properties (basis weight, thickness and Bentsen roughness) are presented in Table I.

Table I: basic properties of the paper considered in the study

	Grammage (g/m^2)	Thickness (µm)	Bendtsen roughness (ml/min)
Paper Q+	103	116	67.2
Paper Q-	82	103	137
Paper JET	120	105	30.8
Paper Green	80	108	162

Those papers were printed with varying black halftone coverages according to a given chart (Baseline). The attention was focused on 11 halftone coverages: 100%, 90%, 80%, 70%, 60%, 50%, 40%, 30% , 20%,10% and 0%, corresponding respectively to Baseline 1, 3, 5, 7, 9, 11, 14, 17, 19, 23 and 30.Therefore, the samples will be referred as Q+, Q-, Jet and Green completed with the Baseline number (ex: Q+10).

The laser printer used is a Gestetner 3532 (brand Ricoh).

2.2 Light profilometry

Surfaces of real prints were characterised with a Altisurf® profilometer.

This system consists of a white light source, a lens, a spectrophotometre, a signal processing system, coupled with a motorised stage and an appropriate image analysis software (Altimap® expert). The surface analysed was a 2 mm x 2 mm square, with a measurement spacing of 1 µm. The vertical resolution is below 0.01 micrometer. From the raw images, it is not possible to extract relevant information. Consequently, data treatments must be applied. The following protocole was applied to the entire set of samples considered in this study. We applied a central rectification. This operation ensures the flatness of the surface. A threshold is performed in order to maximize the contrast. A refilling of the non measured points is carried out in order to calculate the standard parameters. The last operation consists in a 3D gaussian spatial filtering.

2.3 Roughness parameters chosen for the study

We focused on three parameters, namely Sq, Ssk and Sku.

S_q is a dispersion parameter defined as the root mean square value of the surface departures within the sampling area.

$$S_q = \sqrt{\frac{1}{MN}\sum_{j=1}^{N}\sum_{i=1}^{M}\left|z\right|^2(x_i, x_j)} \quad (1)$$

Where, M is a number of points of per profile, and N is the number of profile. S_{sk} (skewness) is the measure of asymmetry of surface deviations about the mean plane.

$$S_{sk} = \frac{1}{MNS_q^{\,3}}\sum_{j=1}^{N}\sum_{i=1}^{M}\left|z\right|^3(x_i, x_j) \quad (2)$$

This parameter can effectively be used to describe the shape of the topography height distribution. For a Gaussian surface which has a symmetrical shape for the surface height distribution, the skewness is zero. For an asymmetric distribution of surface heights, the skewness may either be negative if the distribution has a longer tail at the lower side of the mean plane or positive if the distribution has a longer tail at the upper side of the mean plane. This parameter can give some indication of the existence of "spiky" features. The knowledge of the asymmetric behaviour of a paper surface is relevant for the control of the friction.

S_{ku} is a measure of the peakedness or sharpness of the surface height distribution.

$$S_{ku} = \frac{1}{MNS_q^{\,4}} \sum_{j=1}^{N} \sum_{i=1}^{M} \left| z \right|^4 (x_i, x_j) \qquad (3)$$

This parameter characterizes the spread of the height distribution. A Gaussian surface has a kurtosis value of 3. A centrally distributed surface has a kurtosis value larger than 3 whereas the kurtosis of a well spread distribution is smaller than 3. By a combination of the skewness and the kurtosis, it may be possible to identify surfaces which have a relatively flat top and deep valleys.

3. Results and discussion

3.1 Parameters convergence based on central growing regions:

In order to determine the 'deterministic' SER size of the papers samples considered, we have performed an analysis of the influence of the surface size on Sq, Ssk and Sku. The length of l, which is the edge of the square, where those parameters are calculated, varies from 10 µm to the entire image with a step of 10 µm. Basically, a central growing of the surface was performed and the influence of the surface size was taken into account. The figure 1 shows the result for the analysed papers.

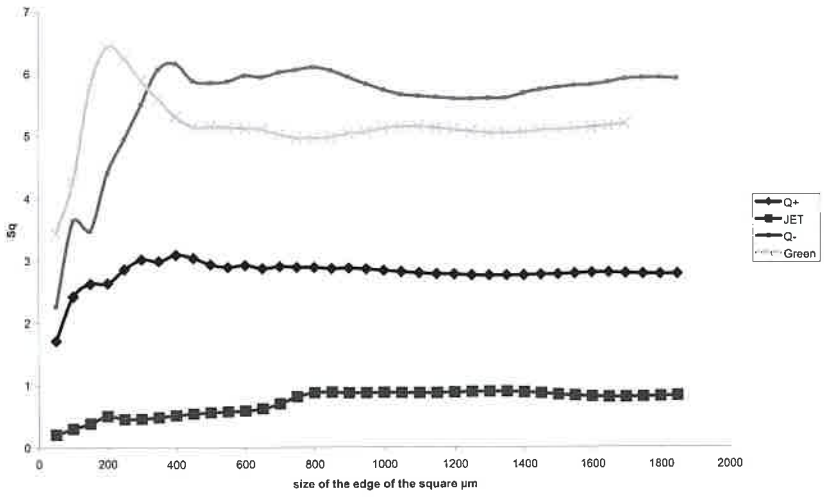

Figure 1: Sq evolution for central growing regionsof 5 samples of Q+, Q- Jet and green respectively

The shape of the curves follows a similar behaviour. There is a sharp increase of the value of Sq when the size of the edge of the square is comprised between 0 and 200 µm. Then, the fluctuations get smaller and eventually a stabilisation is achieved after 400 µm. This conclusion does not fit with the JET grade evolution. As a matter of fact the roughness of such a high quality paper is due to defaults and cracks. Hence, a bigger surface leads to a higher probability of discontinuity.

The figure 2 presents the evolutions of the skewness (Ssk) as a function of the size of the sample. The behaviour of the curves for the different paper grades is far to be stable. Huge variation of the parameters can arise below a size of square edge of 1.000 µm. A clear stabilisation is only achieved for the paper Q+.

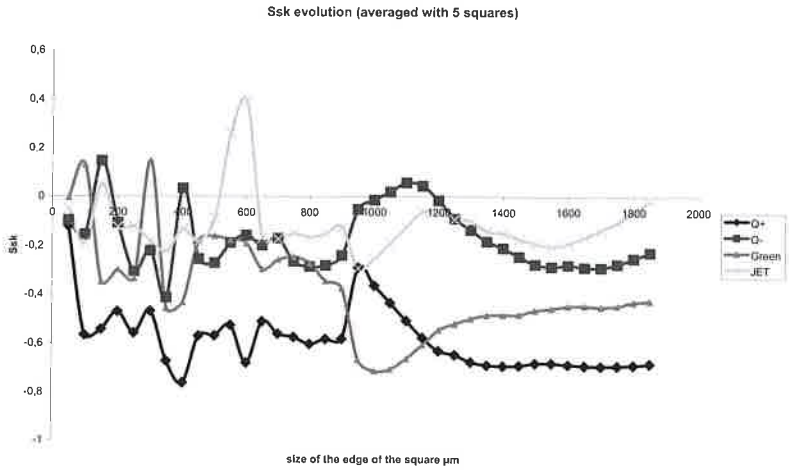

Figure 2: Ssk evolutions for a central growing of 5 samples of Q- with a magnification x10

3.2 Random growing

A second algorithm was built to study the statistical representative size of paper according to the roughness parameters. It needs 3 inputs: the size of the sample measured (it was fixed to 2 x 2 mm^2), the number of measurements for each size of sub surfaces (set at 20) and the step of growth between each size of sub surface (set at 50 µm).

Basically, from the raw surface of (2 x 2) mm^2, the routine randomly extracts 20 squares for each size of subsurface considered. Then it calculates for each square the mean plane, and the three parameters: S_q, S_{sk} and S_{ku}. The variations of S_q for the different papers considered are presented in figure 3.

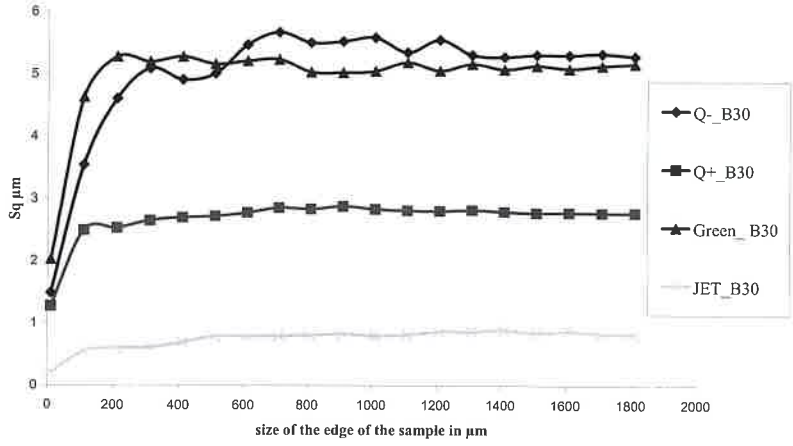

Figure 3: Sq evolution function of the size of the sample (averaged with 20 measurements)

The shape of the curves is the same for all the papers considered. There is a sharp increase of the value of Sq up to an edge of the square of 350 µm. Then a stabilisation occurs. For the 4 samples analysed, a size of 400 µm x 400 µm is representative of the entire surface for the S_q parameter. Indeed, this surface, (400 x 400) μm^2, corresponds to less than 5% of variation of S_q compared to the final value obtained with the full sample (2.000 µm x 2.000 µm).

From these curves relevant information on the paper quality can be deduced. For the papers Q- and Green, the Sq parameter varies much more than S_q of the paper Q+ and Jet. It confirms that papers Q+ and Jet are more uniform than Q- and Green. We get similar results by studying the variation of the S_{ku} parameter according to the size of the surface studied.

The study of the statistical evolution of the parameter S_{sk} was carried out. It has to be noted that the curves do not reach a limit even for a size of sample of (2.000 x 2.000) μm^2 (figure 4).

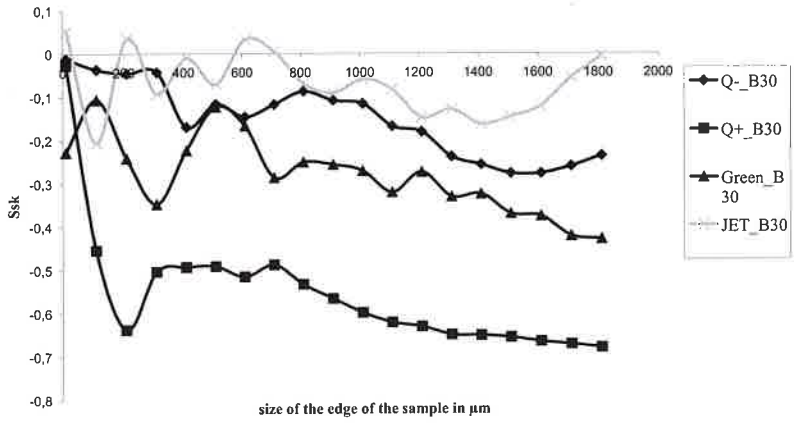

Figure 4: S_{sk} evolution function of the size of the sample (averaged with 20 measurements)

The relevance of the parameter S_{sk} is therefore questioned considering the presented experimental results. Similar results were obtained for different halftoning coverage in the case of a laser printing. The aim of such an experiment was to characterize the modification of the surface causes by the printing process.

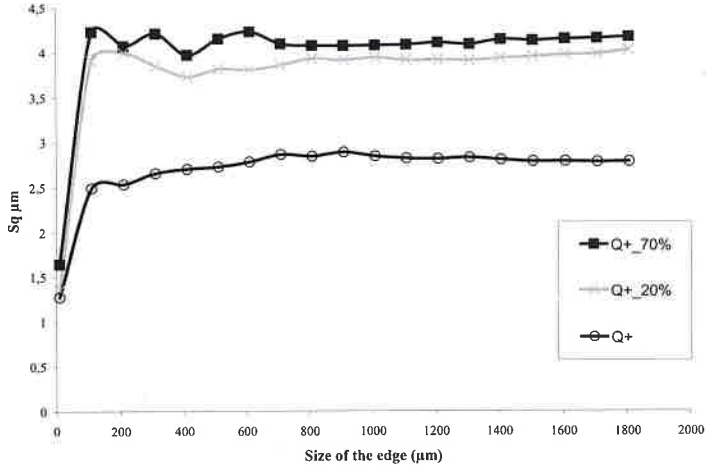

Figure 5: S_q evolution for Q+ for three halftonings: 0%, 30% and 70% respectively

The figure 5 shows that the stabilisation of Sq for an inked paper is also reached for a surface of 350 x 350 μm^2.

3.3 Standard parameters variation as a function of the halftone coverage

The variation of the 3 chosen standard parameters was studied versus the ink coverage of the 4 papers. To illustrate those results, we present the graph for the paper Q+ in Figure 6.

Furthermore, we model the theoretical behaviour of S_q in the case of an electrophotographic print. We first assume that there is no penetration of the toner in the paper structure. We suppose that the filmification is perfect. Under those hypotheses, S_q is calculated as a function of the halftone coverage x, (Eq.4):

$$S_q = S_{qo} + \sqrt{x[(e-ex)]^2 + (1-x)(ex^2)}\,, \tag{4}$$

with S_{qo} the value of S_q of the virgin paper and e the thickness of the ink layer.

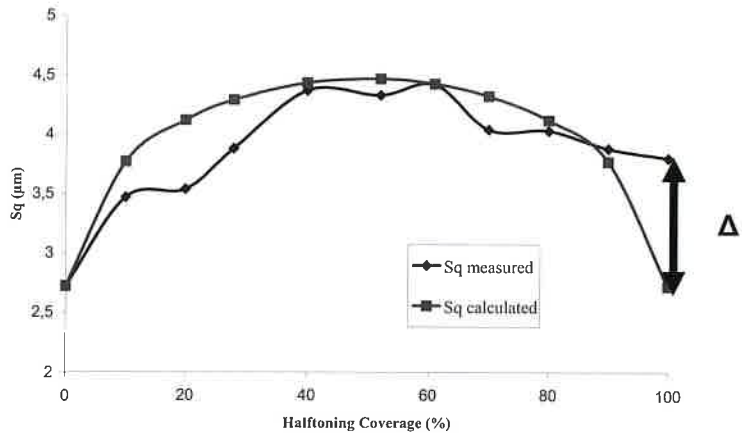

Figure 6: Sq versus black halftoning coverage on Q+ (experimental and simulated results)

The differences Δ between the value of S_q of a solid print and the value of the virgin paper could be used to characterise the print quality. As a matter of fact, a film of an even thickness will ensure a reliable colour quality. Nevertheless such evenness could never be achieved.

In the case of an inkjet printing, the behaviour of a dot on the paper surface is different. The fluid penetration is sought to ensure a good separation between the carrier and the dyes. Hence, default such as bleeding is avoided. Beside, the size of the dyes particles or the pigment used in the inkjet technology has to be as small as possible to flow through the nozzle and permit a good control of the fluid rheology.

Topographical measurements on inkjet prints does not show any difference compared to the unprinted paper.

4. Conclusion

New methods were developed allowing calculating the elementary representative size of a paper surface and its prints. Results do not depend much on the paper quality, neither on the halftoning coverage. An area of (400 µm x 400 µm) seems fully representative of the entire paper for the amplitude parameters. Besides, a statistical analysis can be performed giving information on the paper uniformity.

The parameter S_{sk} is classically used to characterize the paper surface. However, This parameter (the asymmetry parameter) is very sensitive to the measured area size and does not achieve a stabilisation even for a sample size of (2 mm x 2 mm).

Moreover, for a given paper, the variation of the halftone from 0 to 100% greatly influences the amplitude parameters in electrophotographic printing. Simulations of those variations were performed and gave acceptable results. We focused on Sq, and introduced a new parameter to evaluate the quality of the filmification by studying the difference between S_q for a solid print and S_q for the virgin paper.

References

[1] Chinmayanandam, T. K., Phys. Rev. 13:96 (1919)

[2] Béland, M., Bennett, J. Effect of local microroughness on the gloss uniformity of printed surfaces, Applied optics 39, 16, 2000

[3] Arney, J S; Stewart, D, Surface topography of paper from image analysis of reflectance images. Journal of Imaging Science and Technology. Vol. 37, no. 5, pp. 504 - 509. 1993

[4] TAPPI Standard, T 480 Om-92

[5] Mezgahni Saber, Approches multi-échelles de caractérisation tridimensionnelle des surfaces - Applications aux procédés d'usinage, école centrale de Lyon, phD 2005

[6] Chinga, C. Aquadtree decomposition approach for surface assessment, Pattern Analysis & Applications, vol 9, pp 94 - 101, 2006

2

Color and quality

Achieving color agreement: evaluating the options

Robert Chung[1], *Fred Hsu*[2], *Wuhui Liu*[3]

[1] RIT School of Print Media
69 Lomb Memorial Drive, Rochester, NY 14623, USA
E-mail: rycppr@rit.edu

[2] RIT Printing Applications Laboratory
66 Lomb Memorial Drive, Rochester, NY 14623, USA
E-mail: cyhter@rit.edu

[3] Wuhan University
Wuhan, HuBei Province, PRC, 430079
E-mail: wuhui_liu@163.com

Abstract

Color repeatability addresses conformance to standards and process control to ensure color consistency in process color printing. While repeatable color is a virtue, poor color agreement often exists among color printing devices. In this research, a number of image adjustment methods, from applying transfer curves to applying device link profiles, were examined to see if one method would achieve significantly better color agreement than any other methods. We found out that there is no single method that produces significantly better visual agreement when the color differences between the two printing systems are small. On the other hand, the device link achieves the best color agreement when the colorants of the two color printing devices are different.

Keywords

Calibration, color management, color matching, printing

1. Introduction

When sending the same CMYK file to different output devices, the hard copies often appear differently in color. This is because CMYK is device dependent. When print buyers demand color matching between different printing devices, they will not accept the above as an excuse. Thus, printers need a solution to reconcile the color difference between different color output devices. For repeatable printing devices, the reconciliation can be done by means of device calibration and color image adjustment.

1.1 Three levels of color match

Before we delve into color matching solutions, let's take a look at the three levels of color matching expectations: spectral match, colorimetric match, and appearance match. Spectral match, being the most stringent of the three, relies on ink formulation and colorant mixing. The match does not depend on light source and is regularly applied to ink mixing and spot color printing. Colorimetric match relies on the principle of tristimulus integration, i.e., by integrating spectral energy of the light source, the spectral reflectance of the colorant, and the color matching functions of the human eye. The match may exist between dissimilar colorants. Colorimetric match is applicable to proof and press sheet match. Appearance match, being the least stringent of the three, relies on visual judgment of human observers that can be influenced by the viewing conditions and the color vision of the observers themselves. Appearance match is applicable to pictorial color image agreement, e.g., between proof and print, and is frequently exercised by graphic designers and print buyers.

1.2 Objectives

Given that color differences exist between CMYK devices and that color differences can be reconciled using image adjustment methods, this research raises a basic questions, i.e., "Does a particular adjustment method

yield better color agreement than the rest of the methods, and why?" In this research, color agreement of different image adjustments is determined by visual examination in the form of paired comparison.

2. Experimental

This section first describes a situation whereby two printing devices belong to two different color reproduction workflows. The output of the first workflow is the press sheet that serves as the reference. The output of the second workflow is the proof that serves as the sample. Sample proofs need to match the press sheet closely by means of different image adjustment methods. This section then describes input materials and equipment used in the experiment. This is followed by various color image adjustment procedures.

2.1 Two color reproduction workflows

To explore various options in achieving color agreement between two dissimilar color printing devices, we consider the following two workflows: publishing and proofing. As shown in the top row of Figure 1, the publishing workflow involves the conversion of RGB images to the press CMYK space plus printing these images under calibrated press conditions. The press sheet ($CMYK_1$) represents the reference.

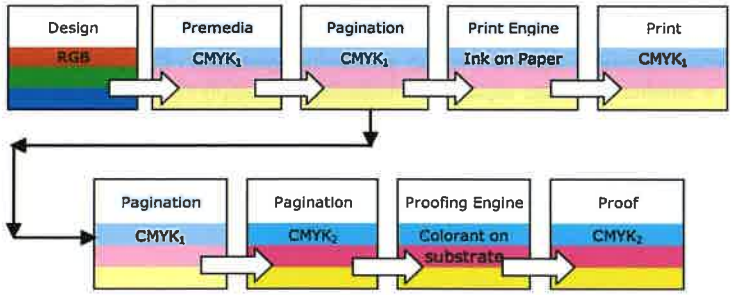

Figure 1: Two workflows involving two color printing devices

The color proofing workflow (bottom row of Figure 1) starts with the press CMYK as the input data. The adjustment of color image data from the press color space ($CMYK_1$) to the proofer color space ($CMYK_2$) is the objective of the study. Adjusted image data are then printed by the proofer under its calibrated conditions.

2.2 Materials and equipment used

The Heidelberg Speedmaster 74 sheetfed offset press is the output device in the publishing workflow. The Kodak NexPress 2100 digital press is the output device in the proofing workflow. Figure 2 depicts the test form used in the initial phase of the experiment. Here, color control bars are used for press calibration and printing process control; IT8.7/3 (basic) color patches are used to analyze color differences between the two color printing devices and are used to reconcile the differences; and pictorial images are used for visual assessment of color agreement between proof and press sheet.

Figure 2:
Test form for visual and quantitative analyses

2.3 Four image adjustment methods

The first adjustment method is gradation adjustment. A transfer curve is derived between the reference gradation and the sample gradation. As shown in Figure 3a, the procedure begins from (1) identifying an input value, e.g., 80% digital dot, and trace through the reference gradation to find out the magnitude of the output (1.0 density); and (2) finding the specific digital dot that produces the same magnitude in the sample device (85%). If we find enough data points, e.g., 80% vs. 85%, using the procedure and construct the transfer curve (Figure 3b), we can reconcile the gradation difference channel by channel.

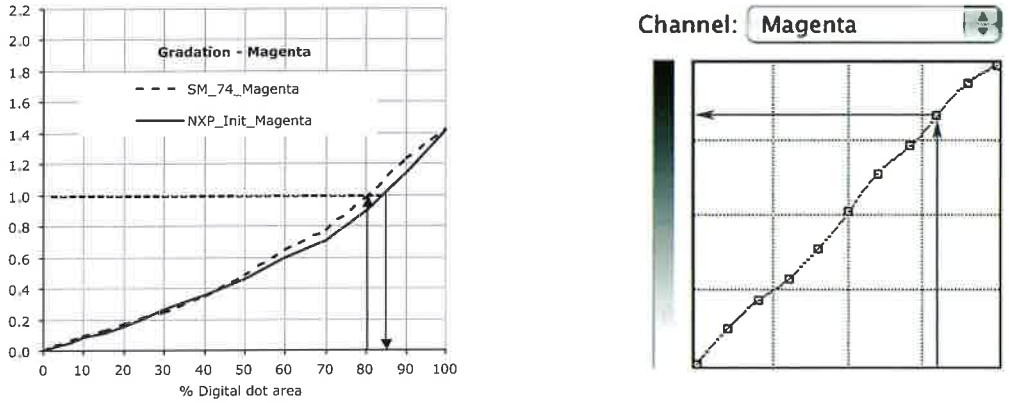

Figure 3: Using gradations (left) to derive a transfer curve (right)

Instead of using density as the gradation, transfer curves may be derived using metric chroma (C*) for chromatic inks and darkness (100 - L*) for black printer. Transfer curves are typically applied at the RIP stage prior to output. In this research, transfer curves are applied at the image editing stage (early device-binding) so that sample prints, prepared by different adjustments, can be printed in a single press run.

The second adjustment method is based on tone reproduction and gray balance (TrGb for short). This is accomplished by deriving three (CMY) transfer curves (Figure 4) that satisfy gray balance and, when added the adjusted black gradation by the first method, also satisfy the tone reproduction between the reference and the sample.

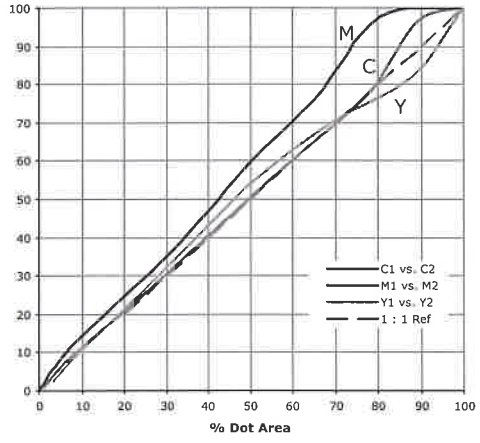

Figure 4: Using gray balance and tone reproduction to derive a transfer curve

To implement the TrGb method, we need to know the combination of CMY that would render a series of neutrals (also known as equivalent neutral dot area) for both the reference and the sample device. One way to obtain equivalent neutral dot area is to construct ICC profiles without the black channel; then use a color management API, such as ColorThink 3.0 Pro, to find out the equivalent neutral dot areas for both the reference and the sample device.

As shown in Table I, the same neutrals are rendered by different CMY amounts between the offset reference and the NexPress. Here, the neutral is represented by Darkness (DK), i.e., (100 - L*). So, Figure 4 is the result of plotting the equivalent dot area of the reference (x-axis) against the equivalent dot area of the sample (y-axis) for each of the cyan, magenta, and yellow channel. As in the gradation adjustment method, these transfer curves may be applied at the image editing stage (early device-binding) or at the RIP (late device-binding) stage prior to output.

Table I: Equivalent neutral dot areas of two printing devices

DK	SM74			NexPress		
(100 - L*)	%DA_C1	%DA_M1	%DA_Y1	%DA_C2	%DA_M2	%DA_Y2
75	89.6	80.6	87.4	96.6	97.7	81.7
65	78.2	65.2	69.6	78.3	76.1	70.4
55	63	50.4	52.7	63.1	60.2	56.7
45	48.3	39.1	41.7	48.7	45.7	44.8
35	35	26.5	30.3	35.4	31	32.1
25	21.6	15.5	19.7	22.2	19.9	20.9
15	8.7	5.5	9.4	10.1	8.9	10.1
5	1.1	0.2	3.5	1.2	0.6	2.8
0	1.2	0.2	3.7	1	0.4	2.7

The third adjustment (A-B-A for short) method converts color image data from the press CMYK (A) space, via the profile connection (B) space, to the proofer (A) color space. We use the Adobe Photoshop as the color management API to specify the two ICC profiles and the absolute colorimetric rendering intent. Depending on workflow considerations, other API, e.g., PDF and RIP, may also be used prior to output.

The fourth adjustment method converts color image data from the press CMYK space directly to the proofer space using a device link profile and the absolute colorimetric rendering intent. We use Alwan LinkProfiler to construct the device link profile by concatenating the source (offset press) profile and the destination (NexPress) profile together while preserving purity of all single ramps and two-color print solids. We use the Adobe Photoshop plug-in by Alwan to perform the device link conversion. Color conversion can also be applied to PDF files using Acrobat plug-in from Callas.

3. Results and discussions

Results of the experiment are organized in the following three sections: (1) verification of adjustment methods, (2) color agreement testing by paired comparison, and (3) further color agreement testing using different colorants. Subsequent discussions are also included to reflect key findings in the research.

3.1 Verification of adjustment methods

Let's begin with the before-and-after comparison of to gradation adjustment method. Figure 5 shows the adjusted NexPress print (dotted line) and the initial print (solid line). The left-hand side of Figure 5 is the overall gradation, expressed as % digital dot area vs. density; and the right-hand side of Figure 5 shows the density differences relative to the offset reference (x-axis). There are two observations: (1) the gradation difference is quite small to begin with (something that we did not envision beforehand), and (2) the experimental error is very small, i.e., we implemented the gradation adjustment well.

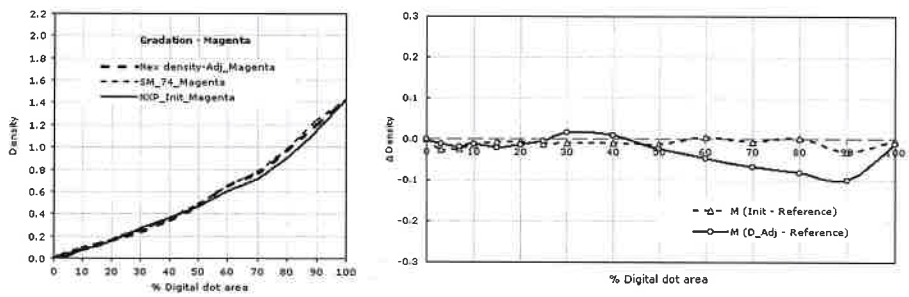

Figure 5: Verification of density-based gradation adjustment

The verification of the TrGb based adjustment is illustrated in Figure 6. Notice that the tone reproduction (solid line) between the initial print and the offset reference, as shown in Figure 6 (left), do not have a one-to-one relation. The adjusted tone reproduction becomes a straight-line at 45 degrees (dotted line).

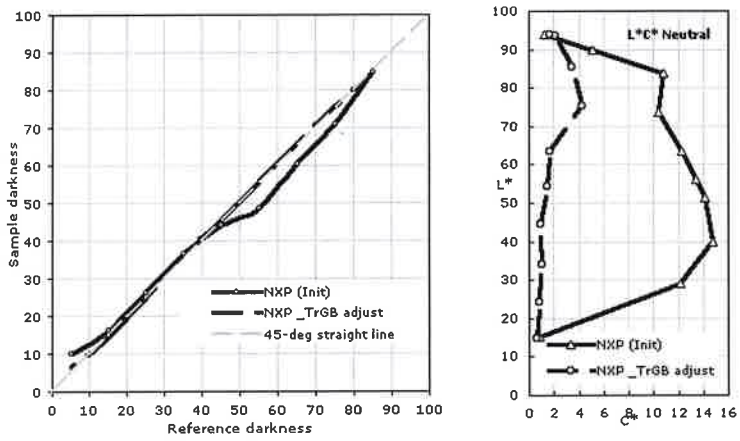

Figure 6: Verification of tone reproduction (left) and gray balance (right) based adjustment

Figure 6 (right) is the L*C* plot of chromatic neutrals indicating neutrality difference between the NexPress and the offset reference. Here, the NexPress, when printed with equivalent dot areas of the offset reference, has fair amount of colorcast (solid line). The result of the TrGb adjustment restores neutrality (dotted line) rather well.

Incidentally, the GRACoL Committee in the U.S. developed a Computer-to-Plate calibration technique, known as the G7 method [IDEAlliance, 2006]. It requires the use of a specially designed gray balance target along with special-purpose software to derive the transfer curves relative to a few pre-defined reference conditions. The TrGb adjustment method, described in the paper, offers a generalized solution for any user-defined reference conditions.

The effect of the A-B-A method can be verified from color gamut of the initial state (solid line) and the adjusted state (dotted line) of the NexPress in comparison to the offset reference. As shown in Figure 7, (1) the color gamut of the NexPress is slightly larger than that of the offset reference; and (2) all corner points of the adjusted color gamut (dotted line), particularly the yellow solid and CMYRGB ramps, are closely aligned to that of the offset reference (gray line).

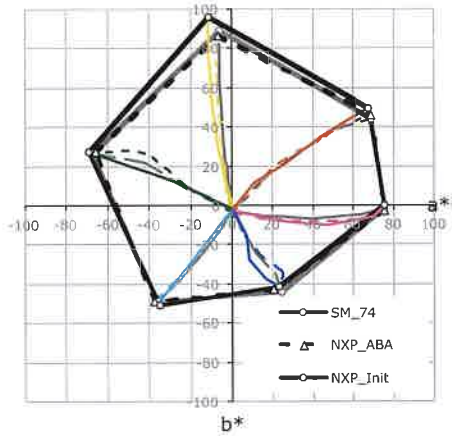

Figure 7: Verification of A-B-A adjustment

A potential drawback of the A-B-A method is that primary colorants, e.g., cyan only pixels, are mapped to pixels with multi-colorants. Consequently, a small amount of magenta or yellow is also printed where the cyan is by the destination device. This effect becomes pronounced when single back type becomes rich

(CMYK) black that challenges the registration ability of the press and causes quality issues in clarity and readability of small types.

The effect of the device link adjustment method is evidenced in Figure 8. Notice how corners of the adjusted color gamut stay unchanged due to the constraints imposed when constructing the device link profile. By preserving the purity of single solids and ramps, it overcomes the printability issues as discussed in the A-B-A method.

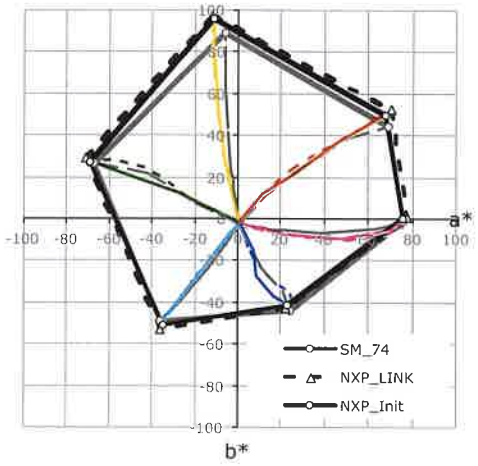

Figure 8: Verification of the device link adjustment

One may wonder what is the downside of using device link profile, particularly in the context of colorimetric accuracy. Our experiences have been none. This is because pixels in real life pictorial images do not have pixels with pure primary chromatic colors. Even though the device link profile trades colorimetric accuracy of the primary colorants for printability, colorimetric accuracy of pictorial images between the reference and the sample is preserved.

3.2 Color agreement testing by paired comparison

We conducted a paired comparison test using two pictorial subject matters, *Old Man* and *Gears* as shown in Figure 1. Each subject matter is prepared by five adjustment conditions: (A) initial or no adjustment, (B) gradation, (C) tone reproduction and gray balance, (D) color management, and (E) device link. Ten observers were asked to pick one from a pair of prints, under standard viewing conditions, which matches closer to the offset reference. The test was conducted one judge at a time (Figure 9).

Figure 9: A judge compares a pair of prints to a reference

By means of non-parametric statistical analysis [Rickmers, 1973], Table II shows that six out of ten judges are consistent in judging a given subject matter. Only four judges who are consistent in judging both subject

matters. Due to similarity of the color gamut of the two devices, there is no real difference in the print samples. In fact, the initial print (A) was not ranked the last in both cases; and the longer one stares at the images, the less certain is about the visual difference between them. The only exception that a print has real difference is the *Old Man* print adjusted by the TrGb method. The TrGb method was ranked as the best match to the offset reference.

Table II: Summary of color agreement by paired comparison

Scene	# of consistent judges	Ranking of adjustment methods from best to worst	Significant agreement among judges at 0.05 risk	Correlation coefficient (R)	Print that has real difference
Old man	6	CBDAE	Yes	0.5	C
Gears	6	BAECD	No	0.1	None

It became clear that color agreement between printing devices with similar colorants is lesser of an issue than color agreement between devices with different colorants. The reason is because there is not much color difference existed between the two devices to begin with. In addition, the magnitude of the process drift and run-to-run variability can easily reduce the effect of the adjustment.

3.3 Further color agreement testing using different colorant conditions

We conducted the experiment using different colorants between the reference and the sample device in order to further test the effect of image adjustment methods. In this case, we used the Heidelberg Speedmaster 74 sheetfed offset press as the reference device and the Epson 4000 inkjet printer as the sample device. Figure 10 illustrates the test from with the pictorial color images used to the color agreement assessment.

Figure 10:Test form for visual and quantitative analyses-Round Two

The ColorBurst 4.1 RIP controls the Epson 4000 inkjet printer by enabling all CMYK primary inks and disabling all light inks. Figure 11 illustrates the color gamut difference between the offset press and the Epson 4000 inkjet printer. Figure 11 suggests that the inkjet color gamut is significantly larger. In addition, the two magenta inks are very different with the printing ink being more reddish and the inkjet ink more bluish. In term, there are sufficient color differences in two-color overprints (red and green).

3.4 Color agreement testing by paired comparison-round two

We conducted a paired comparison test using five pictorial subject matters prepared in five adjustment conditions: (A) density, (B) chroma and darkness, (C) tone reproduction and gray balance, (D) color management, and (E) device link. Ten observers were asked to pick one from a pair of prints, under standard viewing conditions, which matches closer to the offset reference. By means of non-parametric statistical analysis, the results are summarized in Table III.

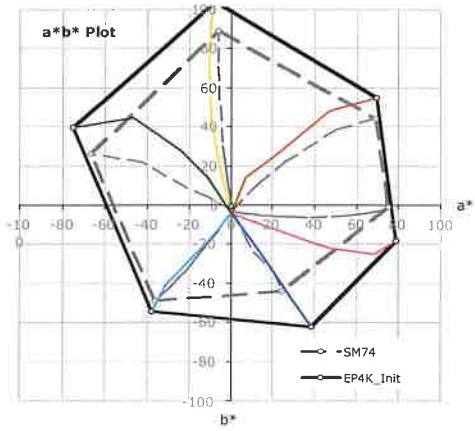

Figure 11: Color gamut comparison between offset press and the Epson 4000

Table III: Summary of color agreement by paired comparison

Scene	Number of consistent judges	Ranking of adjustment methods from best to worst	Significant agreement among judges at 0.05 risk	Correlation coefficient (R)	Print that has real difference
Camel	7	EDCAB	Yes	0.8	E and B
Pink Peony	8	EDCAB	Yes	0.7	E and B
Red Peony	6	EDCAB	Yes	0.9	E and B
Lotus	9	EDACB	Yes	0.8	E only
Pumpkin	7	DEACB	Yes	0.6	B only

To elaborate, six or more judges are consistent in judging a given subject matter. There is good agreement among these consistent judges. Due to large color differences between the two devices, there is real difference in the print samples prepared by the device link method (E) that produces the best match to the reference press sheet. The color-managed (D) print came as a close second. The print sample by tone reproduction and gray balance (C) falls in the middle of the color agreement ranking. The print sample prepared by the chroma adjustment method (B) produces the worst match to the reference press sheet.

4. Conclusions and further research

This research explored various image adjustment options in achieving color agreement between different color printing devices. When colorants are similar, the color difference between the reference and the initial sample print is small; no one color image adjustment method yields better color agreement than other methods. When the color difference between the reference and the initial print sample is large, the print sample adjusted by the device link method produces the best match to the reference. This is followed by the color management method.

To achieve color agreement between similar colorant conditions, e.g., from press run to press run, transfer curves derived from either the gradation adjustment or the tone reproduction and gray balance work well. To achieve color agreement between different colorant conditions, e.g., proof and print, device link method performs the best.

Several follow-up research projects are under way. We want to find out to what extent we can improve the color agreement further by means of profile editing. We want to predict visual assessment outcome by quantitative analysis with the use of a synthetic test image that is image content-based, as oppose to colorant-based, e.g., IT8.7/3 (basic) target. In addition, we want to explore the above research objectives by means of simulation, i.e., using soft proofing to replace hard copy, in order to eliminate process drifts and run-to-run color variations.

Acknowledgments

The authors wish to thank members of the RIT's Color Printing Outreach team and the Printing Applications Laboratory for their collaboration and implementation of the press run. They also want to thank RIT's School of Print Media students for their participation in the paired comparison test.

Reference

[1] Paired Comparison, Course Notes, Albert Rickmers, RIT, 1973

[2] Calibrating, Printing and Proofing to the G7 Method, IDEAlliance, Version 5, June 2006

Comparing corresponding colors

Lidija Mandić, Darko Agić, Maja Strgar Kurečić

University of Zagreb, Faculty of Graphic Arts
Getaldićeva 2, HR-10 000 Zagreb, Croatia
E-mail: lidija.mandic@grf.hr

Abstract

The goal of color management is to reproduce the desired color appearance of an original in a way that is consistently pleasing and acceptable. With so many different media and devices used in image processing it becomes hard to achieve the desired color quality. Conventional CIE XYZ colorimetry is useful for specifying color appearance under a given set of viewing conditions and for determining whether two colors will match in a viewing configuration. Therefore, in recent years, researchers have tried to develop more comprehensive color appearance models (CAM), which are able to predict color appearance accurately across a range of viewing conditions. Most CAMs include a chromatic adaptation transform (CAT). A number of CATs are currently in use. Psychophysical experiments were carried out to collect corresponding-colors data using pictorial images. Corresponding colors are two stimuli, viewed under different viewing condition, that match color appearance. The two most commonly used media, CRT-displays (soft copy) and printed images (hard copy), were included in this research using four complex images. These data were compared with the corresponding data calculated by different CATs: SHARP, CAT02 and HPE. The results show that he SHARP CAT outperforms the other transforms.

Keywords

Chromatic-adaptation transform, color appearance, corresponding data

1. Introduction

The CIE system of colorimetry (based upon *XYZ* tristimulus values) is system for color specification, some advanced color specification models such as CIELAB could be arguably be described as models of color appearance. The distinction between color specification (CIEXYZ) and color appearance (CIELAB) is that the normalization by the illuminant achieves a color space that makes better prediction of color appearance than the tristumulus space from which is derived. The x and y chromaticities of a perfect white surface vary with the illuminant, the CIELAB coordinates remain constant.

If a simple colorimetric match is made between a printed image and a CRT display, the perceived colors in the images typically do not match. This is due to differences in viewing conditions between the two displays. Such differences include changes in luminance level, white point chromaticity and surround relative luminance. Two colors, which are a colorimetric match, can appear quite different if viewed under different viewing condition.

The human visual system has a remarkable ability to maintain the color appearance of an object despite quite large changes in the quality and intensity of the illumination. The human visual system achieves color constancy by chromatic adaptation that allows it to discount the effect of the illumination. Fairchild (1998) has classified chromatic-adaptation mechanisms into two groups: sensitive and cognitive. Chromatic adaptation is the largely independent sensitivity control of the three mechanisms of color vision, those that respond automatically to the stimulus energy. Cognitive mechanisms are those that respond based upon observers' knowledge of scene content. When hard-copy images are being viewed, an image is perceived as an object that is illuminated by the prevailing illumination. Thus both sensory mechanisms, that respond to the spectral energy distribution of the stimulus, and cognitive mechanisms, that discount the known color of the light source, are active. When a soft copy display is being viewed only sensory mechanisms are active because it can not be interpreted as an illuminated object. Most color appearance models include a chromatic-adaptation transform (CAT). A chromatic-adaptation transform (CAT) is a method for computing the corresponding color under a reference illuminant for a stimulus defined under a test illuminant.

In psychophysical studies of chromatic adaptation it is useful to define the concept of corresponding colors. Corresponding colors are defined as two stimuli, viewed under differing viewing conditions, that match in

color appearance. A stimulus specified by the tristimulus values, XYZ_1, viewed in one set of viewing conditions, might appear the same as a second stimulus specified by the tristimulus values, XYZ_2, viewed in a second set of viewing conditions. XYZ_1 and XYZ_2, together with specifications of their respective viewing conditions, represent a pair of corresponding colors. Corresponding-colors data have been obtained through a wide variety of experimental techniques. Most modern CATs are loosely based on the von Kries model of adaptation [Kries, 1902].

CIE tristimulus values are linearly transformed by a 3 x 3 matrix **M** to derive post-adaptation cone responses under the first illuminant, denoted as *R'G'B'* in this paper. The values of **M** are transform dependent. The resulting *R'G'B'* values are independently scaled to get the post-adaptation cone responses *R"G"B"* under the second illuminant. The scaling coefficients are also transform dependent, but most often based on the illuminants' white-point post-adaptation cone responses. If there are no non-linear coefficients, this transform can be expressed as a diagonal matrix. To obtain CIE tristimulus values (*X"Y"Z"*) under the second illuminant, the *R"G"B"* are then multiplied by $\mathbf{M}^{-1}$, the inverse of matrix **M**. Equation 1. describes a matrix notation of this concept:

$$\begin{bmatrix} X'' \\ Y'' \\ Z'' \end{bmatrix} = \mathbf{M}_{CAT}^{-1} \begin{bmatrix} R''_W/R'_W & 0 & 0 \\ 0 & G''_W/G'_W & 0 \\ 0 & 0 & B''_W/B'_W \end{bmatrix} \mathbf{M}_{CAT} \begin{bmatrix} X' \\ Y' \\ Z' \end{bmatrix} \tag{1}$$

Quantities *Rw'* ,*Gw'* ,*Bw'* and *Rw"* ,*Gw"* ,*Bw"* are computed from the tristimulus values of the first and second illuminants, respectively, by multiplying the corresponding XYZ vectors by **M**CAT.

The von Kries CAT assumes that chromatic adaptation is indeed an independent gain control of the cone responses of the human visual system, and that the scaling is based on the ratio of the cone responses of the illuminants. Under this assumption, the matrix **M** of equation 1 needs to linearly transform tristimulus values (*XYZ*) into relative cone responses (*LMS*). Typically, the cone responses are determined from the tristimulus values using the following matrix by Hunt, Pointer and Estevez (HPE), equation 2.

$$\mathrm{M}_{\mathrm{HPE}} = \begin{bmatrix} 0.3897 & 0.6890 & 0.0787 \\ -0.2298 & 1.1834 & 0.0464 \\ 0 & 0 & 1 \end{bmatrix} \tag{2}$$

A widely used newer chromatic adaptation transform is the Bradford transform [Fairchild, 2001]. It was empirically derived by Lam from a set of corresponding colors as determined from 58 dyed wool samples with varying color constancy, evaluated under illuminants A and D65 [Luo and Rhodes]. Because of the varying color constancy of the samples, the experiment was designed so that corresponding colors represented the same appearance under the different illumination sources, and not necessarily the same sample. One implication of the Bradford chromatic adaptation transform is that color correction for illumination takes place not in cone space but rather in a 'narrowed' cone space. The Bradford sensors (the linear combination of *XYZ*s defined in the Bradford transform) have their sensitivity more narrowly concentrated than the cones (see Figure 1). Additionally, the long and medium wavelength Bradford sensitivities are more de-correlated. However, Bradford sensors are not optimally narrow.

Recent research [Finlayson and Süsstrunk, 2000; Susstrunk et al., 2001] has shown that a chromatic adaptation transform based on even sharper sensors performs just as well as the Bradford transform for sets of corresponding color data, and in some cases even better than its linearized form. The SHARP transform is given in equation 3.

$$\mathrm{M}_{\mathrm{SHARP}} = \begin{bmatrix} 1.2694 & -0.0988 & -0.1706 \\ -0.8364 & 1.8006 & 0.0357 \\ 0.0297 & -0.0315 & 1.0018 \end{bmatrix} \tag{3}$$

The chromatic adaptation transform CAT02 is given in Equation 4.

$$\mathbf{M}_{\mathrm{SCAT02}} = \begin{bmatrix} 0.7328 & 0.4296 & -0.1624 \\ -0.7036 & 1.6975 & 0.0061 \\ 0.0030 & 0.0136 & 0.9834 \end{bmatrix} \tag{4}$$

2. Methods

The two most commonly used media, CRT-displays (soft copy) and printed images (hard copy), were included in this research using four complex images. The first image contains house, snow and sky, the second contains neutral colors, the third image contains grass and sky and the fourth contains different hues. These images were continuous tone images printed on mat papers using a large format printer at 254 dpi. The original hardcopies were captured by an Agfa scanner at 72 dpi to provide RGB data for processing the CRT reproduction. The scanner and CRT display were calibrated and characterized using Macbeth software ProfileMakerPro 4. The experiment was taken in dim room that is close to the actual environment in practical viewing condition. Printed hard copies were illuminated and viewed under viewing booth that simulated CIE Standard Illuminants D50. Additionally, images were displayed on Mitsubishi monitor, white point was set to the chromaticity coordinates close to 6500K (CIE Illuminant D65). A cathode ray tube and the light boot with a gray background of luminance factor 0.2 were placed on the table with the same center height. Each printed and each monitor image had a 5 mm white border, which was the reference white for chromatic adaptation purposes. The printed originals and monitor reproduction were used so as to correspond to simultaneous binocular viewing. A total of five observers, all experienced in using Adobe Photoshop, took part in the entire experiment. The observers were skilled operators, who have been worked in graphic industry long time. All the observers had normal color vision as evaluated by Ishihara plates and a Farnsworth-Munsell 100-hue test. Observers sat approximately 25" from the printed originals and monitor screen. Observers adjusted the colors on monitor images to match the color appearance of the printed images [Fairchild and Braun, 1997]. The monitor images adjustments were accomplished using Adobe Photoshop. Observers were allowed to use any of the color adjustment tools in Photoshop, but were not allowed to perform spatial manipulation of the images. The length of each experimental session was left to the discretion of the observers. Each experiment began with the same starting-point image, uncorrected scans. After observers completed the various matching tasks, the images were segmented into several number of object region, depend of image context as it is shown in Figure 1.

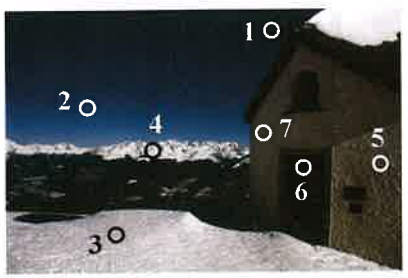

Image 1

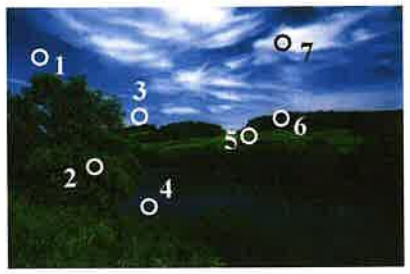

Image 2

Image 3

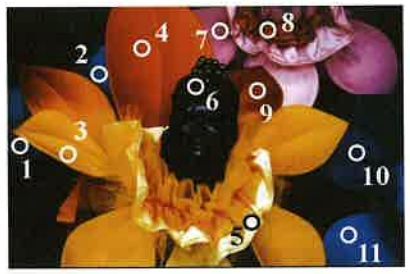

Image 4

Figure 1: The images segmentation

3. Results

The printed images and images displayed on monitor were measured using a Gretag Spectrolino 45/0 spectrophotometer. After measurement, corresponding data were determined. The corresponding color data

from psychophysical experiments were compared with calculated corresponding data (CAT02, SHARP and HPE). The color differences ΔE_{94} are calculated. The results are presented in Figure 2 and Figure 3.

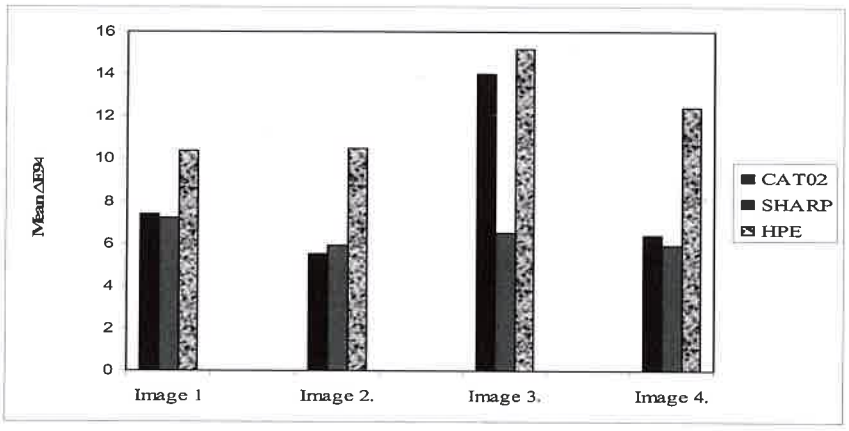

Figure 2: The mean color differences ΔE_{94} for all images

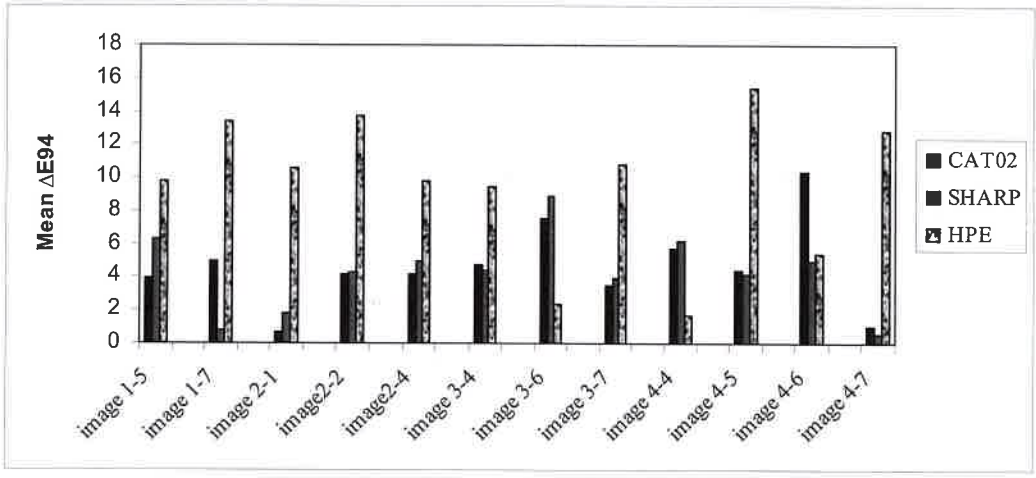

Figure 3: The aberration for different image regions

In Figure 3 are shown greatest aberration between corresponding data. First number determines image and second number region.

4. Discussion

The results shown the best agreement of the corresponding data calculated by using SHARP matrix and those obtained from visual experiment. The large aberration was obtained by using HPE matrix, for all images. The situation is different if the results describe different image areas. The color differences calculated by using CAT02 and SHARP matrices slightly differ for most regions, except for image 1 (house in shadow), image 2 (gray) and image 4 (black). The corresponding data obtained from calculation with HPE matrix are closer to visual data only for dark green (image 3 - 6) and orange (image 4.4). The HPE matrix gives the worst results for other image areas.

5. Conclusions

Psychophysical experiments were carried out to collect corresponding-colors data between printed images and images displayed on monitor. After observers completed matching tasks, images were segmented into several

number of object regions that are measured with spectrophotometer. The corresponding-colors data obtained from visual matching were compared with calculated corresponding colors data by using three transform matrices: CAT02, SHARP and HPE. When comparing SHARP to CAT02, it cannot find statistically significant difference between the two. The HPE matrix is not appropriate to use for calculation corresponding data for different media. The SHARP CAT outperforms the other transforms, but still needs to be evaluated.

References

[1] Fairchild M. D., and Braun K. M., 1997, Investigation of Color Appearance Using the Psychophysical Method of Adjustment and Complex Pictorial Images, *AIC Color 97,* Kyoto,. 179 - 186

[2] Fairchild M. D., 1998, *Color Appearance Models,* Addison-Wesley, Reading, MA

[3] Fairchild M. D., 2001, A revision of CIECAM97s for practical applications." *COL. Res. and Appl.*, 26(6), 418

[4] Finlayson G. D. and Süsstrunk S., 2000, Performance of a Chromatic Adaptation Transform based on Spectral Sharpening, *Proc. IS&T/SID 8th Color Imaging Conference,* 49 - 55

[5] von Kries J., 1902 Theoretische Studien ueber die Umstimmung des Sehorgans. Festschrift der Albrecht Ludwig Universitaet, 145

[6] Luo M. R. and Rhodes P. A., Corresponding Colour Data Sets, *University of Derby,* http://colour.derby.ac.uk/colour/info/catweb/

[7] Susstrunk S., Holm J. and Finlayson G. D., 2001, Chromatic Adaptation Performance of Different RGB Sensors, *SPIE* 43, 72 - 183

Spectral color reproduction versus color reproduction

Jérémie Gerhardt, Jon Y. Hardeberg

The Norwegian Color Research Laboratory, Gjøvik University College
P. O. Box 191, N-2802 Gjøvik, Norway
E-mail: jeremie.gerhardt@hig.no

Abstract

In this paper we compare spectral color reproduction and color reproduction. We use a simulated multi-colorant printer and we compare and eventually combine two approaches to colorant separation: one aiming to reproduce the spectral reflectance, another aiming to reproduce the original color as viewed under a given illuminant. This operation is realized by inverting a spectral printer model: the spectral Neugebauer model. The inversion is an optimization problem in which the difference between the desired spectral reflectance and its estimation by the spectral printer model is minimized. For spectral color reproduction the spectral root mean square difference is used; for color reproduction the CIE 1976 CIELAB color difference is used. Finally we propose to combine the two approaches and use a weighted sum of colorimetric and spectral differences as an optimization criterion. Two test charts are used in our experiments: data from the gamut of the printer and data mapped to the printer gamut. Our results show improvement on both spectral and colorimetric differences for the method combining the two approaches comparing to the only color or spectral color reproduction approaches, especially in case of spectral data originally in the printer gamut.

Keywords

Inverse spectral printer model, multi-colorant printing, spectral color reproduction, spectral colorant separation, spectral printer model

1. Introduction

With a color reproduction system it is possible to make a color acquisition of a scene or object under a given illuminant and to print a color reproduction of it. With proper calibration and characterization of the devices involved, and disregarding the problems related to color gamut limitations, it is theoretically possible to produce a color reproduction which will appear identically to the original. For example a painting and its color reproduction put side by side will appear identical under the illuminant used for its color acquisition even if the spectral properties of the painting pigments are different from the print inks. This phenomenon is called metamerism. On the other hand, if the illumination changes, the reproduction will generally no longer be perceived as equal to the original. This problem can be solved in a spectral color reproduction system.

Multispectral color imaging offers the great advantage to provide the full spectral color information of a surface. While a color acquisition system records the color of a surface under a given illuminant, a multispectral acquisition system can record the spectral reflectance of a surface and allows us to simulate the color of under any illuminant. In an ideal case, after saving a spectral image we would like to display or to print it, from that point we have two options: either to calculate the color rendering of our spectral image for a given illuminant and to display/print it, or to reproduce the spectral image. This is a challenging task when for example we have made the spectral acquisition of a 2 century old painting and the colorants used at that time are not available anymore or we have lost the technical knowledge to produce them.

The introduction of multi-colorant printers in color printing, with the primary goal of increasing printer color gamut and reducing graininess, has offered new possibilities in spectral color reproduction. The first works with a spectral use of a multi-colorant printer were focused on colorant selection [Kohler and Berns, 1993, Tzeng and Berns, 1999, 2000] and spectral printer modeling [Wyble and Berns, 2000, Balasubramanian, 1999]. Then spectral color reproduction of spectral images was introduced [Taplin and Berns, 2001, Berns et al., 2003, Kraushaar and Urban, 2006, Gerhardt and Hardeberg, 2006, 2007]. A complete workflow for spectral color reproduction is existing and research works are caring out to connect acquisition and reproduction of spectral image [Rosen et al., 2003, Derhak and Rosen, 2006] as it could be done in color reproduction system.

Multi-colorant printer offers the possibility to print the same color by various colorant combinations, i.e. metameric print is possible. This is an advantage for colorant separation [Ostromoukhov, 1993, Agar, 2001], it allows for example to select the colorant combination minimizing the colorant coverage or to optimize the separation for a given illuminant. In spectral colorant separation we want to reduce the spectral difference between a spectral target and its reproduction, i.e. we want to reduce the metamerism. This task is performed by inverting the spectral printer model.

The spectral Neugebauer model and the Yule-Nielsen spectral modified Neugebauer model (YNSN) are commonly use for spectral printer characterization [Hardeberg and Gerhardt, 2004]. As in color reproduction such system needs to be characterized and spectral printer characterization has been used already for color reproduction since it provided more accurate information [Balasubramanian, 1999].

2. Spectral versus colorimetric printing

In this paper we want to asses the difference between a multi-spectral print and a colorimetric print. The choice of colorimetric versus spectral printing is made during the colorant separation process. The inverse of the spectral Neugebauer printer model is used for the colorant separation. Inversion is performed by optimization technique ending by minimizing a cost function. When a spectral print is desired the colorant separation is performed such that the difference between the spectral target and the estimated print is minimized for the spectral difference. We use the spectral root mean square (sRMS) as spectral difference. For a colorimetric print we will calculate a CIE 1976 CIELAB difference between the spectral target and the estimated print.

Gamut mapping plays an important role in color reproduction when for example the data to reproduce are not totally included in the printer gamut: gamut mapping will map these data toward the printer gamut such that less information is lost. Gamut mapping becomes more complicated for spectral data, due to the dimension of the problem it is likely impossible to apply directly gamut mapping color techniques to spectral data. But with the use of an inverse printer model and optimization it is possible to mapped spectral reflectance to the spectral printer gamut. The spectral printer gamut is defined by the spectral reflectance of the available colorants and all the combination between them, i.e. the Neugebauer primaries (NP) of the printer. According to the Neugebauer printer model the spectral reflectance of a printed colorant combination is the weighted summation of the NP where the weights are the area covered by the NP. It is a convex optimization problem to solve since the summation of the weights is equal to 1. So by inverting the spectral Neugebauer model for the weights we obtain an estimation of the closest printable spectral reflectance according to the desired spectral target and colorants [Alsam et al., 2005].

3. Experiment and results

Two spectral targets are tested: a grid in colorant space and the MacBeth ColorChecker testchart. The grid is made of 463 patches, maximum of 300% coverage is allowed for each patch, spectral reflectances of all colorant combination are estimated by the Neugebauer model. After print estimation noise is added to the spectral reflectances. These data are assumed to be in the printer gamut. Before performing colorant separation the spectral reflectances of the MacBeth ColorChecker are gamut mapped with the technique described above for a simulated six colorants printer.

Colorant separation is performed for spectral print and colorimetric print for a simulated six colorants printer (the same colorants were used for the gamut mapping of the ColorChecker). Four colorant separations are performed for colorimetric print, each of them minimizing CIE 1976 CIELAB difference for the following illuminants: A, D65, D50 and FL11 (CIE 15:2004).

Simulated prints performance of the colorant separation processes are shown in Table I for the grid and Table II for the gamut mapped ColorChecker. Differences between target and prints are calculated in CIE 1976 CIELAB space for illuminant A, D50, D65, FL11 and sRMS.

A second experiment is run where we combine spectral print and colorimetric print. In the colorant separation process the minimized difference is now a weighted summation of a sRMS and a CIE 1976 CIELAB difference as follows:

$$diff = (1 - \alpha)^* \Delta E_{ab}^* + \alpha^* sRMS \quad (1)$$

where the sRMS have been scaled to vary in the same range of value as for the CIE 1976 CIELAB difference. This second experiment is performed four times for the following couple of illuminant and sRMS: A and sRMS, D65 and sRMS, D50 and sRMS, FL11 and sRMS. The colorant separation is then applied for the α parameter varying from 0 to 1. α = 0 means colorimetric print and α = 1 means spectral print. In Figure 1 and Figure 2 are displayed the colorimetric and spectral differences between grid and its reproduction versus the α parameter. In Figure 3 and Figure 4 are displayed the colorimetric and spectral differences between the gamut mapped ColorChecker and its reproduction versus the α parameter.

Table I: Differences between the grid and its reproduction when colorant separation has been performed in order to obtain minimum CIE 1976 CIELAB difference for illuminant A, D50, D65 and FL11 and to obtain minimum spectral difference

Colorant separation		CIE 1976 CIELAB A	D65	D50	FL11	sRMS
A	Av.	0.1408	1.4064	1.0623	1.9905	0.0153
	Std.	0.9895	1.6959	1.4212	1.6959	0.0156
	Max	12.6730	14.3431	13.9292	14.9707	0.1115
D65	Av.	1.1342	0.1003	0.3940	1.7224	0.0162
	Std.	1.2183	0.8489	0.8326	1.4183	0.0173
	Max	12.9279	14.1823	13.8367	11.9511	0.0895
D50	Av.	0.8606	0.4137	0.1092	1.6859	0.0152
	Std.	1.1013	0.9732	0.9287	1.4775	0.0167
	Max	12.8183	14.1949	13.8256	17.1687	0.1109
FL11	Av.	1.9861	1.8293	1.7921	0.1055	0.0188
	Std.	1.5294	1.3657	1.3230	0.4941	0.0197
	Max	12.1259	9.1764	9.4035	6.0788	0.1506
Spectral	Av.	0.5528	0.5644	0.5623	1.0689	0.0027
	Std.	0.7866	0.7305	0.7325	1.1477	0.0004
	Max	8.5982	6.0682	6.6017	7.2685	0.0072

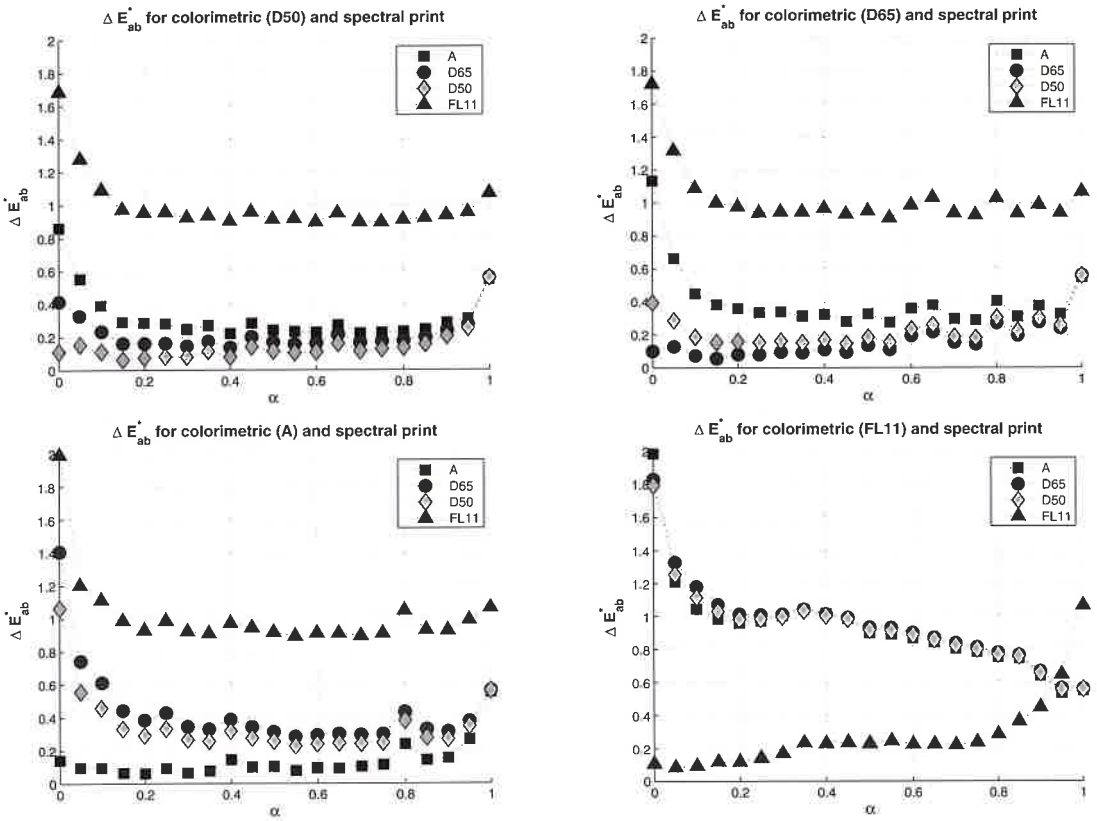

Figure 1: Colorimetric difference between the grid and its estimated reproduction for the colorant separation minimizing a weighted summation of CIE 1976 CIELAB difference and spectral difference versus the parameter α, where α = 0 corresponds to a colorimetric print and α = 1 corresponds to a spectral print

Table II: Differences between the gamut mapped ColorChecker and its reproduction when colorant separation has been performed in order to obtain minimum CIE 1976 CIELAB difference for illuminants A, D50, D65 and FL11 and to obtain minimum spectral difference

Colorant separation		CIE 1976 CIELAB A	D65	D50	FL11	sRMS
A	Av.	0.1805	1.6003	1.2192	0.9366	0.0145
	Std.	0.5617	1.1423	0.8956	0.8087	0.0109
	Max	2.5107	3.8634	2.8296	3.2950	0.0418
D65	Av.	1.6916	0.2163	0.6487	1.5082	0.0227
	Std.	0.9990	0.6937	0.6297	1.1751	0.0149
	Max	4.0173	2.5044	2.6079	4.1605	0.0515
D50	Av.	1.2459	0.6577	0.2216	1.3627	0.0194
	Std.	0.8160	0.6367	0.6974	1.1057	0.0125
	Max	2.7843	2.5174	2.5943	3.9325	0.0497
FL11	Av.	1.0788	1.4498	1.2743	0.1656	0.0191
	Std.	0.8207	1.1886	0.9441	0.5185	0.0126
	Max	3.4596	3.7389	2.8626	2.1389	0.0521
Spectral	Av.	1.2494	1.5776	1.4764	1.3400	0.0059
	Std.	1.4022	1.7560	1.6326	1.3567	0.0051
	Max	4.7051	5.7461	5.6895	4.4655	0.0178

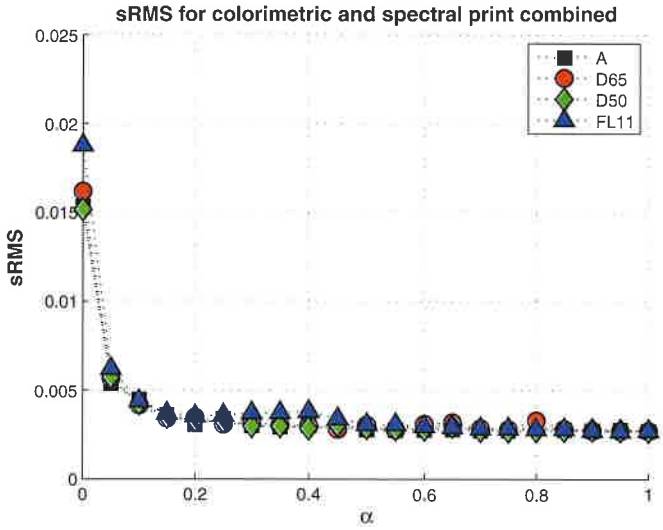

Figure 2: Spectral difference between the grid and its estimated reproduction for the colorant separation minimizing a weighted summation of CIE 1976 CIELAB difference and spectral difference versus the parameter α, where α = 0 corresponds to a colorimetric print and α = 1 corresponds to a spectral print

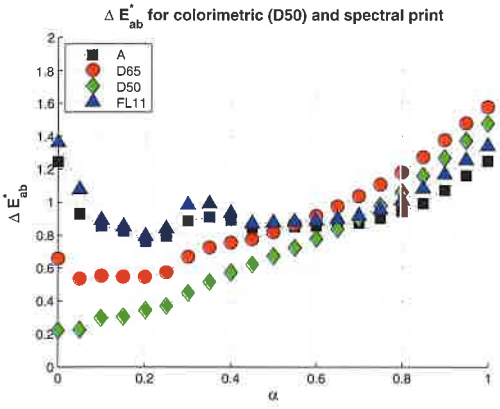

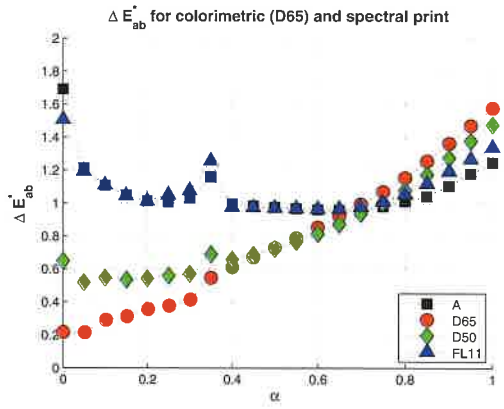

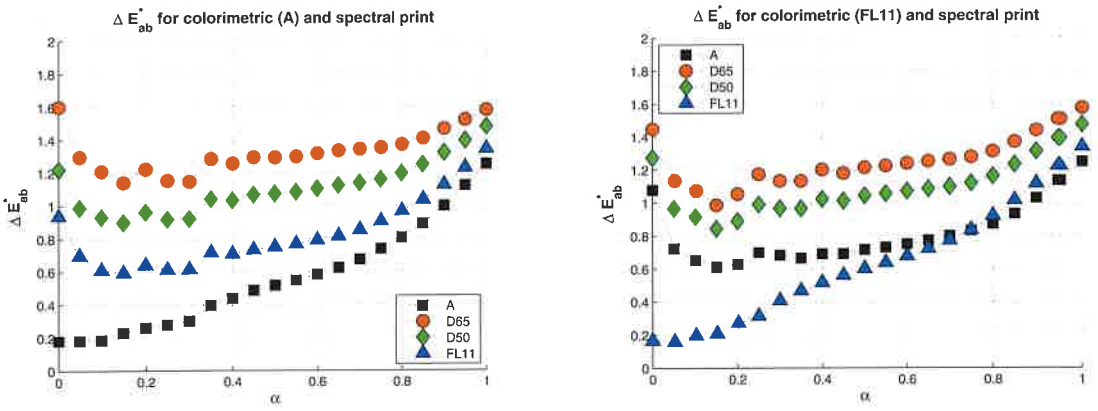

Figure 3: Colorimetric difference between the gamut mapped ColorChecker and its estimated reproduction for the colorant separation minimizing a weighted summation of CIE 1976 CIELAB difference and spectral difference versus the parameter α, where α = 0 corresponds to a colorimetric print and α = 1 corresponds to a spectral print

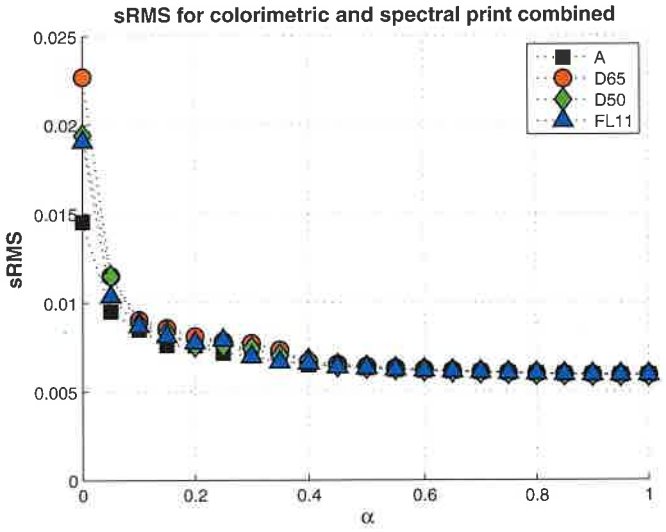

Figure 4: Spectral difference between the gamut mapped ColorChecker and its estimated reproduction for the colorant separation minimizing a weighted summation of CIE 1976 CIELAB difference and spectral difference versus the parameter α, where α = 0 corresponds to a colorimetric print and α = 1 corresponds to a spectral print

4. Conclusion

In case of reproduction of data included in the printer gamut, we can see that a colorimetric print will give better results in term of color difference for the chosen illuminant during the colorant separation process, this comparing to colorimetric difference for the same illuminant after spectral print, see Table I. The spectral print gives more homogenous colorimetric difference (except for fluorescent illuminant FL11) than for the colorimetric print and better spectral difference.

The second experiment which combines colorimetric and spectral approaches for colorant separation brings interesting results. We can see that the parameter α increasing (more weight put on spectral difference during the colorant separation) the sRMS is decreasing toward a minimum for α = 1 which was expected, but all colorimetric differences reach also a minimum for mid α value and colorimetric differences are all smaller than for a colorimetric print.

It is not possible to generalize the previous results for the second tested test chart. Colorimetric differences are better for color print for all illuminant than for colorimetric differences for spectral print, but these colorimetric

differences are more homogenous for the later. A spectral print tends to not favour a given illuminant and then to reduce metamerism. We can also see that the spectral difference is minimized for the spectral print. In case of colorant separation with both colorimetric and spectral difference it is more difficult to find the best α parameter, but we can observe that the sRMS is always decreasing, first rapidly to mid α value and slowly to $\alpha = 1$.

In that paper we have presented a comparison of spectral color reproduction and color reproduction, two approaches for colorant separation by minimization of CIE 1976 CIELAB difference or spectral sRMS were experimented. Colorant separation was done by inverting the spectral Neugebauer printer model. The combination of colorimetric difference and spectral difference has improved the results for data included in the printer gamut. Other targets and set of colorant should be tested for the colorant separation process. Also the use of the inverse YNSN should provide better results since it improves the spectral Neugebauer model.

References

[1] Ufuk Agar A., 2001, *Model based color separation for cmykcm printing. In The 9th Color Imaging Conference: Color Science and Engineering: Systems, Technologies, Application*

[2] Alsam A., Gerhardt J. and Hardeberg J. Y., 2005, *Inversion of the Spectral Neugebauer Printer Model. In AIC Colour 05, pages 44 - 62*

[3] CIE, 2004, *Publication CIE 15:2004 Colorimetry, 3RD edition*

[4] Balasubramanian R., 1999, *Optimization of the spectral Neugebauer model for printer characterization. Journal of Electronic Imaging, 8(2):156 - 166*

[5] Berns R. S., Taplin L. A. and Liang T. Z., 2003, *Spectral color reproduction with six color output. US patent 0098896A1*

[6] Derhak M. W. and Rosen M. R., 2006, *Spectral colorimetry using LabPQR: an interim connection space. Journal of Imaging Science and Technology, 50(1):53 - 63*

[7] Gerhardt J. and Hardeberg J. Y., 2006, *Spectral colour reproduction by vector error diffusion. In Proceedings CGIV 2006, pages 469 - 473*

[8] Gerhardt J. and Hardeberg J. Y., 2007, *Controlling the error in spectral vector error diffusion. In Color Imaging: Processing, Hardcopy, and Applications XII, Electronic Imaging, Symposium, SPIE Proceedings, San Jose, California*

[9] Hardeberg J. Y. and Gerhardt J., 2004, *Characterization of an eight colorant inkjet system for spectral color reproduction. pages 263 - 267*

[10] Kohler T. and Berns R. S.. 1993, *Reducing metamerism and increasing gamut using five or more colored inks. IS&Ts Third Technical Symposium On Prepress, Proofing, and Printing, pages 24 - 29*

[11] Kraushaar A. and Urban P., 2006, *How to linearise a multispectral printing system for graphic arts uses? In IARIGAI Proceedings 33rd International Research Conference*

[12] Ostromoukhov V., 1993, *Chromaticity gamut enhancement by heptatone multi-color printing. In IS&T SPIE, volume 1990, pages 139 - 151*

[13] Rosen M. R., Hattenberger E. F. and Ohta N., 2003, *Spectral redundancy in a 6-ink ink-jet printer. IS&T 2003 PICS Conference, pages 236 - 243*

[14] Taplin L. A. and Berns R. S., 2001, *Spectral color reproduction based on a six-color inkjet output system. The Ninth Color Imaging Conference, pages 209 - 212*

[15] Tzeng Di-Y. and Berns R. S., 1999, *Spectral based ink selection for multiple-ink printing II. optimal ink selection. The Seventh Color Imaging Conference: Color Science, Systems, and Applications, pages 182 - 187*

[16] Tzeng Di-Y. and Berns R. S., 2000, *Spectral-based six-color separation minimizing metamerism. In IS&T/SID Eight Color Imaging COnference, pages 342 - 347*

[17] Wyble D. R. and Berns R. S., 2000, *A critical review of spectral models applied to binary color printing. Color Research Application, 25(1):4 - 19*

An evaluation of colour differences and tolerances in soft proofing

Janne Laine

VTT Technical Research Centre of Finland
P.O. Box 1000, FIN-02044 VTT, Espoo, Finland
E-mail: janne.laine@vtt.fi

Abstract

The perceptibility and acceptability of colour differences in soft proofing were evaluated in psychometric experiments. In the first part of the study the perceptibility and acceptability of colour differences between systematically modified versions of photographic images displayed on an LCD monitor were examined. An interval scale of perceived colour differences was derived from the results of a paired comparison experiment. The acceptability threshold for the colour differences of a contract proof was located on that scale based on the results of a category experiment. Significant but incomplete correlation was found between the perceived colour differences and predictions of colour difference equations, as calculated from the instrumental measurements of uniform colour patches. The threshold of acceptability corresponded to approximately 2 CIELAB ΔE units on average, but the threshold depended considerably on the image content and the type of modifying function. Furthermore, the magnitude and acceptability of colour differences between proofs produced by two commercial soft-proofing systems and the corresponding reference prints were judged visually in another set of psychometric experiments. The results were comparable to the results of an earlier study with hardcopy proofs, and the proofs of the both soft-proofing systems were on average found to be sufficiently close in appearance to the reference prints to be acceptable as contract proofs.

Keywords

Acceptability, colour difference, colour tolerance, psychometry, soft proofing

1. Introduction

Although not completely replacing hardcopy proofing at this point in time, the new soft-proofing systems are starting to be more widely used in the graphic arts industry in different phases of the publishing process for pre-visualization of the printed product. Soft proofing offers a number of benefits over hardcopy proofs, including more efficient workflows. Although hardcopy proofs are still seen to be better suited to certain kinds of print jobs and processes, soft proofing can in principle be used in all the tasks that a hardcopy proof has conventionally been used in, including checking the text content and layout, as well as critical evaluation of colour reproduction and contract proofing. This paper concentrates on the perceived colour differences in soft proofing.

The visual tolerances for colour differences between hardcopy proofs and reference prints were examined in an earlier work [Laine et al., 2006]. The experiments reported in this paper extend those studies to colour differences in pictures seen on computer monitors and to the perceived differences between soft proofs and printed reference pictures. Specifically, the perceptibility and acceptability of colour differences in the case of softcopy contract proofing were investigated in a psychometric study. The performance of the CIELAB ΔE as an objective metric of colour difference was evaluated by comparing it to the perceptual data resulting from the psychometric experiments with the display images. An objective definition for colour tolerances would be a useful tool for validating the colour accuracy of proofs or proofing systems.

In the previous work the average threshold for the acceptability of colour differences in hardcopy contract proofs was found to be approximately 4 ΔE units [Laine et al., 2006]. That result is in line with the recommendation of 4 ΔE as the tolerance for the average deviation of all the colour patches in the Media Wedge [Schmitt and Dolezalek, 2004]. The Ugra/FOGRA Media Wedge CMYK Version 2.0 is a control strip comprised of 46 uniform colour patches and is meant for validating digitally printed proofs. The Media Wedge patches were also used by Laine et al. for calculating the ΔE values between the proofs and the reference prints, while the perceived colour differences were judged between proofs and reference prints of three photographic images from the Altona Test Suite. Similar figures have also been obtained when the acceptability of colour differences in

colour reproduction in general has been studied. Johnson and Green (2001) suggest 4 ΔE as the threshold of acceptability for critical visual evaluation in graphic arts applications, based on their experiments on perceived colour differences of uniform printed colour patches. Stokes et al. (1992a, 1992b) found an acceptability threshold of approximately 6 ΔE for pictorial images displayed sequentially on a CRT monitor. In experiments carried out by Song and Luo (2000) perceived colour differences between pairs of images shown on a CRT display, again one image at a time, were evaluated, the average threshold of acceptability in that case being 4.5 ΔE. Their later study suggested that the threshold is in the same range for printed images [Song and Luo, 2001].

Stokes et al. and Song and Luo calculated the abovementioned ΔE values as averages over all pixel-wise colour differences between the original and the modified image. That is a common approach to predicting the perceived colour differences between digital images, although it is well known that the perception of colour and colour differences in colour patches seen on a uniform background (the situation for which colour difference equations like CIELAB ΔE were developed) is considerably different from the perception of colour in complex images. Algorithms such as spatial CIELAB (S-CIELAB) have been proposed in order to obtain a better correspondence with perceived colour differences in images or other spatially variable stimuli [Zhang and Wandell, 1996]. Currently models that combine features of colour appearance models like CIECAM02 with modelling of various spatial visual effects are being developed and considered as tools for specifying the appearance and perceived differences of images, among other tasks; Johnson and Fairchild (2001) outline directions for the development of that kind of colour image difference metrics and later describe a framework around an image colour appearance model, iCAM, that could be used for specification of colour image differences [Fairchild and Johnson, 2003].

Here, however, the main interest is in the validation of proofing systems, and in practice the colorimetric image data required by such image difference metrics is not readily available. A certain set of colour patches is measured instead, and the validity of the proof or proofing systems is verified by checking that the colours of the patches reproduced by the proofing system are sufficiently close to the known colorimetric reference values. This is the idea behind including control strips such as the Media Wedge in hardcopy proofs. Colorimetric predictability and accuracy of a soft-proofing system can be similarly verified by displaying a series of colours on the monitor used for proofing and checking that the measured output is sufficiently close to the given target values and that the current display colour profile predicts the actual response of the display accurately enough. Automated calibration and verification procedures are included in some of the soft-proofing systems aiming for contract-proof-level colour accuracy, and Ugra offers an Ugra Display Analysis and Certification Tool for verifying the suitability of a display for proofing colours. The question of the appropriate colorimetric tolerances for proofing applications has not been conclusively answered, however. The experiments documented below add to the publicly available data of the perceived colour differences and their acceptability in soft-proofing.

Furthermore, soft proofs produced by two different commercial soft proofing systems were visually compared to the printed reference images, in order to evaluate the suitability of soft proofing to critical evaluation of colour reproduction in practice. The colour accuracy of the soft proofs was also evaluated against the perceived colour difference scale of hardcopy proofs, generated in the earlier study.

2. Experiments

A total of 21 colour-normal persons (5 women, 16 men) participated in the psychometric experiments as observers. 11 of them were from various companies in the graphic arts industry, and 10 were research personnel at VTT. All experiments were carried out in a special room that is shielded from outside light and whose walls are painted 20% reflecting gray. The room was dimly and indirectly illuminated by fluorescent tubes simulating the D50 standard illuminant. The illuminance measured at the table-top level was approximately 10 lx and the chromaticity coordinates of the ambient illumination were (x, y) = (0.347, 0.357), reasonably close to those specified for D50.

The paired comparison and category scaling experimental methods were used for testing the perceptibility and acceptability of colour differences in a set of photographic images displayed on an Eizo ColorEdge LCD monitor. The display white point was set to the luminance 120 $cd \cdot m^{-2}$ and to the chromaticity coordinates of the D50 standard illuminant. The display was regularly calibrated and its colour profile updated throughout the experiments. Three images from the ISO 12640-2:2004 standard XYZ/sRGB images were used as reference images: "N1 - Woman with glass" (referred to as picture A in this text), "N2 - Flowers" (picture B), and "N8 - Silver" (picture C). The images were transformed from the sRGB colour space to the monitor colour space. 21 variations of the sRGB profile were made by modifying the tone reproduction curves of the RGB channels. The

modifications were intended to approximate typical errors in display calibration and characterization. Three kinds of modifying functions were used, each with seven different parameter levels, resulting in the total of 21 profile variations. Using each of the modified profiles in turn as the source profile in transforming into the destination monitor colour space produced three sets of 21 image samples with systematic colour variations. The transformation method corresponded to the ICC's media-relative rendering intent [ICC.1:2004-10].

In the profile versions from 1 to 7 the tone reproduction curves were modified by raising the normalized tone reproduction curve values to the powers of 0.9, 0.95, 0.98, 1.0, 1.02, 1.05, and 1.10, respectively. The same power was used for all three of the RGB channels in these profile versions. Thus the modifications increased (versions 1 - 3) or decreased (versions 5 - 7) the luminance of the mid-tones and decreased (versions 1 - 3) or increased (versions 5 - 7) the purity of colours without significantly affecting colour balance. Profile version 4 was identical to the original.

In the profile versions 8 - 14 a constant value of -0.02, -0.01, -0.005, 0.0, 0.005, 0.01, or 0.02, respectively, was added to all values of the tone reproduction curves of all three RGB channels. The effect was to decrease (versions 8 - 10) or increase (versions 12- 14) the luminance of all tones. Profile version 11 remained identical to the original.

Finally, in versions 15 - 21 the same power function modifications as for versions 1 - 7 were used but in this case they were applied to the B channel only. This modification affected the colour balance of the resulting images. Versions 15 - 17 were bluish and versions 19 - 21 were yellowish compared to the original, while version 18 was identical to the original. There were thus three versions, numbered 4, 11 and 18, among the test images that were identical to the original image, serving as hidden references in the test image set.

All possible pairs of the 21 images were shown to each observer in random order by an automated test procedure in the paired comparison experiment. The samples were displayed side by side on a 20% gray background. The corresponding reference image, converted with the unmodified sRGB source profile, was displayed above the pair. The size of the images on screen was approximately 10 cm by 8 cm. The task of the observer was simply to indicate which one of the samples was closer in appearance to the reference. An interval scale representing the perceived distance of the samples from the reference image was derived from the experimental results as described in the next section.

In the category experiment the sample images were shown on the monitor one by one, in random order, below the reference image. The observers were instructed to assign each of the samples, understood as soft proofs of the reference image, into one of three categories based on how closely they resembled the reference image in appearance, assuming the reference image was an ideal soft proof that exactly matched the colour appearance of the print being simulated. The class definitions were identical to those used in the earlier work with hardcopy proofs [Laine et al., 2006]:

Category 1: Excellent Proof. *The difference between the colours of the reference print and the proof is not noticeable or is just barely noticeable.*

Category 2: Acceptable contract proof: *There is a noticeable difference between the reference print and the proof, but the difference is small enough to be still acceptable for a contract proof.*

Category 3: Not contract proof level. *The proof differs significantly from the reference print, and is not acceptable as a contract proof.*"

An ordinal scale for the samples was derived by simply calculating the average of category values assigned to each sample, as described in the following section. The purpose of this experiment was to locate the transition point from acceptable to unacceptable contract proofs in the scale derived from the paired comparison experiment. The ordinal scale derived from the category experiment cannot by itself be assumed to indicate the relative perceptual distances between the samples as accurately as the interval scale.

An sRGB equivalent of the Ugra/FOGRA Media Wedge and 21 modified versions of it, corresponding to the 21 image versions, were created. The colour patches of each version of the wedge were displayed on the monitor and their spectral power distributions were measured with a Minolta CS-1000 telespectroradiometer. CIELAB ΔE colour differences were calculated between the patches of each modified version of the wedge and the reference wedge, which was converted to the monitor colour space from the colour space of the

unmodified sRGB profile. The values given by the CIELAB colour difference equation are compared to the perceived differences between the samples below. This procedure corresponds to the one used with hardcopy proofs in the earlier work, making the results straightforward to compare; this was the main reason for using the Media Wedge also in this way here.

Finally, the sheets from the Altona Test Suite were proofed with two commercial soft-proofing systems. The soft proofs of two pictorial images (picture 21, a portrait of a woman, and picture 25, low-key image of an egg with various shades of brown, in the Altona Visual sheet) were compared visually to the corresponding reference prints. The printed 10 cm by 10 cm pictures, cut out of the sheet, were viewed in a Just Normlicht Pantone Color Viewing Light booth. With the illuminance of approximately 2500 lx, chromaticity coordinates approximating those of the D50 standard illuminant, and a gray background the viewing conditions fulfilled the requirements set in ISO 3664 for conditions P1 meant for critical evaluation of prints. A simultaneous binocular viewing technique, in which the observers were free to move their view between the print in the light booth and the soft proof shown on the monitor next to the light booth, was used. Only the soft-proof picture and an approximately 1 cm wide gray border around it were visible on the monitor, the rest of the screen being masked by gray cardboard. The simultaneous binocular viewing technique is somewhat problematic from the colour reproduction point of view because the observer's state of chromatic adaptation, and thereby the perceived colour, varies as she moves her view from one image and media to another, and the effect is difficult to predict reliably. It was still chosen in these experiments as the aim was to evaluate the magnitude of perceived colour matching error found in practical use of soft proofing, and these kinds of mixed viewing conditions are common in the industry. A part of the experiments was repeated with lower illuminance (500 lx) viewing conditions for the reference print, corresponding to the P2 conditions defined in ISO 3664.

The two soft-proofing systems were judged in a category experiment, with the same user instructions and category definitions as in the previous experiment with the systematically modified image samples. In another experiment the observers judged the colour difference between the soft proof and the print relative to the difference between the same print and four hardcopy proofs shown in the light booth next to the print. The best and worst hardcopy proofs, and two intermediate proof samples were chosen based on the perceptual scale built in the earlier work, and were used as physical proof quality rulers in this work. This experiment thus allowed the soft proofs to be located on the perceptual colour difference scale of the hardcopy proofs. The results are described in the following section.

3. Results

An interval scale representing the perceived distance of the systematically modified samples from the reference image was derived from the experimental proportions for each sample pair with Morrisey's least squares solution, assuming the distribution of judgments follows the Case V of Thurstone's Law of Comparative Judgement, as described by Engeldrum (2001). Samples with the highest scale values (z-scores) were perceived to be closest in colour to the reference, the perceived colour difference increasing with decreasing scale value. The scale values for the 21 versions of each of the three pictures are shown in Figure 1. The scale values of samples produced with different parameter levels of the same modifying function are connected in the graph. As expected, there are no significant differences between the scale values of the three samples (4, 11 and 18) identical to the reference, and the perceived difference increases on either side of the references with increasing magnitude of modifications, as indicated by the decrease in scale values. The scale values for pictures A and C follow roughly similar curves for each of the three modifying functions, but the scale values of picture B show some significant departures from these trends. Especially notable is that in the case of the third modifying function (colour balance modification, samples 15 - 21) no significant differences between the scale values of any of the seven versions of picture C were found. This indicates that the colour balance modifications that were easily noticeable in the case of pictures A and C were mostly imperceptible in the case of picture B.

A second scale of perceived colour difference was formed for the same samples by simply calculating the average of category values assigned to each sample in the category experiment. This ordinal scale cannot be assumed to indicate the relative perceptual distances between the samples as accurately as the interval scale. However, by comparing the psychometric scales from the paired comparison and category experiments the acceptability limit for contract soft proofs could be set in the interval scale. This was done by mapping the average category value of 2 to the interval scale, as shown by the dotted lines in Figure 2. The combined results of all three test images are shown here. As was the case in the earlier work with hardcopy proofs, the two scales are again in relatively close agreement with one another, which supports the validity of the results.

The simulated soft proof samples included in the experiment were thus located on a perceptual interval scale with a tolerance limit for contract proofs. About one third of the sample images were found to differ from the reference more than visually acceptable for a contract proof, on average.

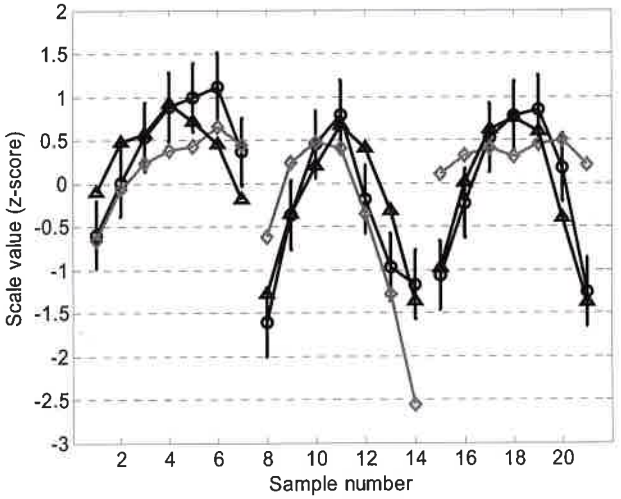

Figure 1: Interval scale values (z-scores) for the sample picture. Scale values for picture A are marked with circles, scale values for picture B with diamonds, and scale values for picture C with triangles. 95% confidence intervals for the scale value differences are shown for the picture A samples

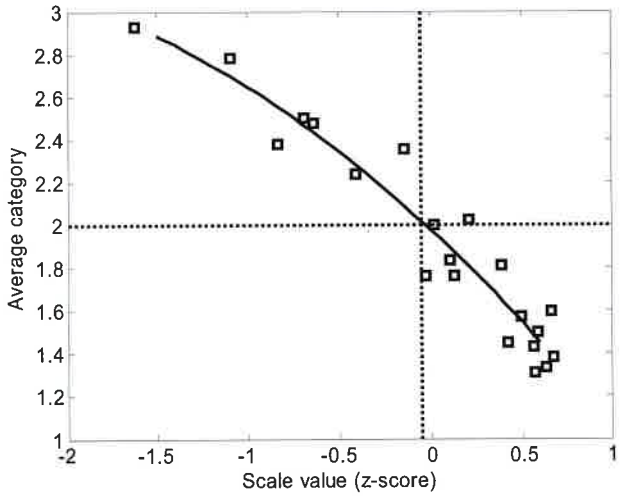

Figure 2: Average category versus interval scale values

The average CIELAB ΔE values calculated for the Media Wedge patches corresponding to the modified images were compared to the perceptual scale values, as depicted in Figure 3. The scatter of the sample points in this graph resembles the graphs for the hardcopy proofs from the earlier work, but with some differences, as discussed below. The correlation coefficient between the ΔE 's and scale values was in this case r = -0.78, comparable to the values of r = -0.62 and r = -0.77 obtained with the hardcopy proofs and indicating significant but incomplete negative linear correlation between the ΔE and scale values.

If the perceptual scale values of samples corresponding to one type of modifying function only are plotted against the average ΔE a more regular graph with less scatter than in Figure 2 results. This can be seen in Figures 4, 5 and 6, which also show that the acceptability threshold, whose location on the perceptual scale is again indicated by the dotted line, could be mapped to a wide range of different average ΔE values, depending on the type of the modifying function.

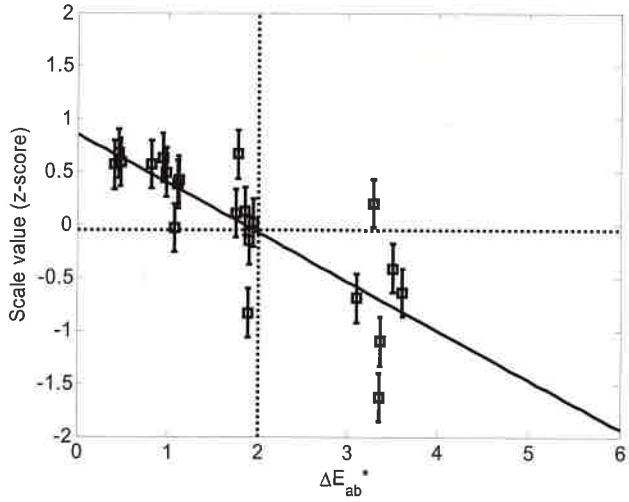

Figure 3: Interval scale values versus average CIELAB ΔE

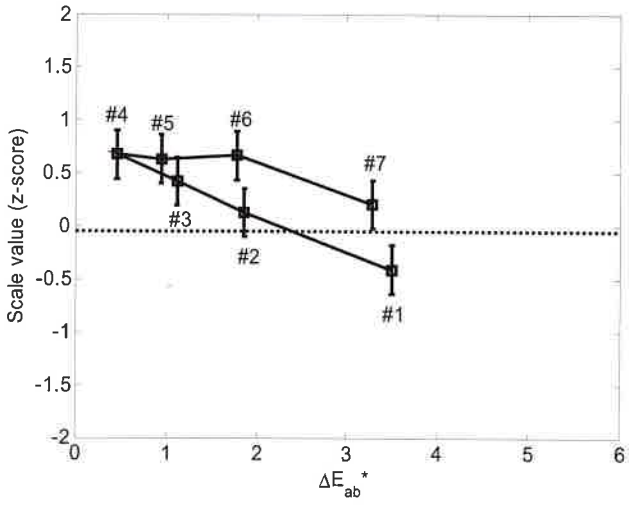

Figure 4: Interval scale values versus average CIELAB ΔE for samples created with the power function modification of the source profile tone reproduction curves. Sample numbers are shown next to the data points

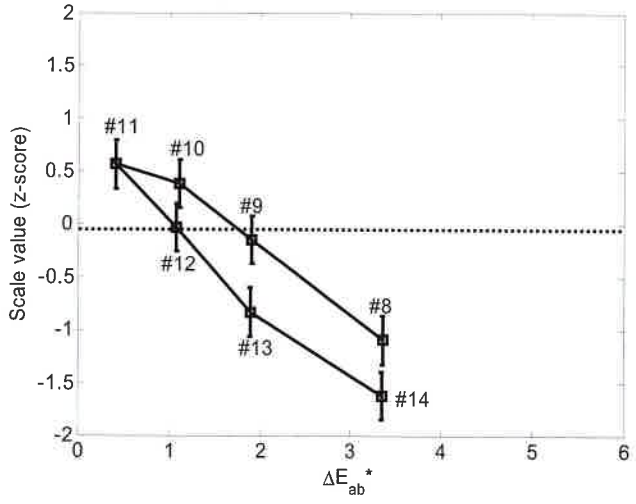

Figure 5: Interval scale values versus average CIELAB ΔE for samples created with the additive constant modification of the source profile tone reproduction curves

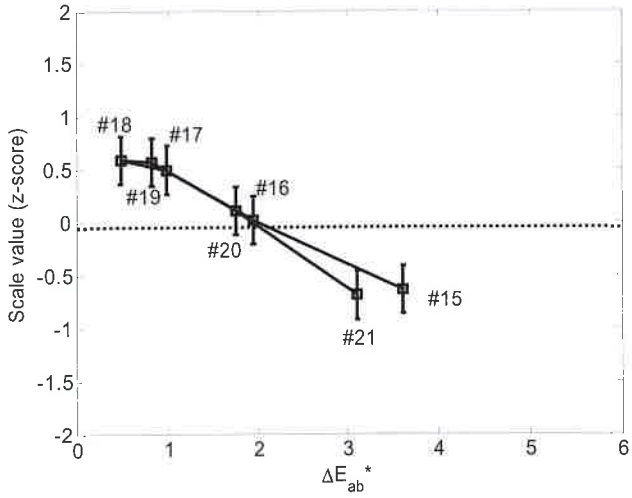

Figure 6: Interval scale values versus average CIELAB ΔE for samples created with the power function modification of the source profile blue channel tone reproduction curves

Finally, the tests with the two commercial soft-proofing systems suggested that both are capable of simulating the perceived colours of the reference prints accurately enough to be used in contract proofing. The average categories for both systems were below 2 for both images when the reference print was viewed under the 2500 lux illumination (but not so for the other system when 500 lux illumination was used). In comparison to the four hardcopy proofs, regarding the magnitude of perceived difference to the reference print, both soft-proofing systems were on average positioned between the best and the second best hardcopy proof. This position falls on the acceptable range of colour difference also on the perceptual scale of hardcopy proofs established in the earlier study [Laine et al., 2006].

4. Discussion

The significant but incomplete correlation between the perceived differences and the average ΔE values was expected, as it is known that average CIELAB ΔE, or values given by other colour difference equations for uniform colour patches, can roughly indicate the magnitude of perceived differences in images but cannot be expected to give accurate predictions of perceived colour differences in individual images, due to higher-level perceptual effects related to the image content and its interpretation by the human visual system.

The acceptability threshold of only 2 ΔE units, mapped by the dotted lines from the perceptual scale to the ΔE scale in Figure 2, is surprisingly low when compared to the value of approximately 4 ΔE found for the hardcopy proofs. Other studies do not indicate significant differences in colorimetric acceptability thresholds for prints and computer display images [Song and Luo, 2000, 2001]. Two main factors are thought to have caused this difference here. The first is that the colour differences in the experimental image sample set were limited to a relatively narrow range, as a compromise in the experiment design. The fact that no very large colour differences were present in the sample set may have made the observers more critical to the smaller differences. Such effects are well known in psychophysics generally.

Another factor emerges when analyzing how the three different types of modifications used in creating the samples affected the perceived differences, as was seen in the graphs of Figures 4, 5 and 6. The location of the acceptance threshold on the ΔE scale was found to vary significantly depending on the modifying function used. This indicates that the type of modification affects the magnitude of perceived colour differences, although such effects are not reflected in basic colorimetry as measured from separate control patches. It was not analyzed here how calculation of ΔE averages directly from the image data would have affected matters, but it is unlikely that the dependency of the acceptability tolerance in terms of ΔE on the modifying function would have disappeared. In fact, the studies of perceptibility and acceptability performed by Stokes et al. (1992a, 1992b) and Song and Luo (2000, 2001), who calculated ΔE values as averages of pixel-wise colour differences, as well as the perceptibility experiments carried out by Sano et al. (2003), who calculated ΔE values from colour patches chosen from the image colours, all show same kind of dependency of the acceptability, and perceptibility, thresholds on the type of modification.

Content was also found to affect the susceptibility of an image to the effects of a given type of modification, as evidenced by the case of picture B and the colour balance modification in Figure 1 above. These results underline the complexity of the colour and colour difference perception in pictures. As the acceptability tolerance is a function of both the image content and the type of colour variation, the value of average ΔE, measured from a set of colour control patches, that corresponds to the perceptual acceptability threshold is to be accepted to vary over a certain range. With the systematically created samples used in this study that range was from slightly above 1 to beyond 4 ΔE units, as evaluated visually from Figures 4, 5, and 6. In practice different types of colour variations are bound to be present in both soft proofs and hardcopy proofs. This was also the case with the hardcopy proofs used in the earlier study [Laine et al., 2006]. Expectations for the proof quality are also known to vary from one type of print job to another, which is another factor that makes it difficult to find a single objective tolerance for all cases.

Setting a tight limit close to the minimum of the tolerance range, which may be difficult to achieve in practice, should guarantee the visual acceptability of all proofs, while the risk of unacceptably large colour differences increases as the tolerance limit is placed towards the upper end of the range. Especially in the case of soft-proofing systems it is good to also keep in mind that there are multiple sources for possible perceived colour differences between the proof and the print. While the capability to reproduce given colour stimuli on the monitor with appropriate colorimetric accuracy is a pre-requisite for matching the colours of the soft proof and the printed image, some compensation, beyond the colorimetric matching, for the perceptual effects related to the mixed adaptation of the viewer to the different viewing conditions of the print and the display may be required in order to produce a perceptually accurate colour match.

The results of the experiments with the two commercial soft-proofing systems suggest that the perceptual colour accuracy of soft proofing systems is comparable to the accuracy of hardcopy proofs. It should be noted, though, that in this test only a very limited soft proof sample group was used and that there can be considerable variation between different proofing systems.

5. Conclusions

The acceptability of perceived colour image differences in soft-proofing applications was studied in a series of psychometric experiments. A perceptual scale of colour differences for the image samples whose colours had been systematically modified with varying parameter levels of three different modifying functions was derived from the experimental results. Comparison of the perceptual scale with the average CIELAB ΔE colour difference values calculated between a set of similarly modified colour patches and unmodified reference colour patches revealed a relatively strong dependency of the acceptability threshold, in terms of ΔE, on the type of modifying function. The acceptability tolerance was located on the value of approximately 2 ΔE units when all the samples were considered together, but varied from slightly over 1 to beyond 4 ΔE units when the samples created with different modifying functions were considered separately. The susceptibility of the image to certain kinds of modifications was also found to vary with image content: a modification that is imperceptible in a certain image may cause an unacceptably large colour difference in another image.

These results add to the pool of data concerning perceived colour differences and are of interest when specifying colorimetric tolerances and developing objective metrics for proofing, or other colour imaging applications. The digital image sample set, with its colorimetric specification, can also be used with the perceptual data for future testing of advanced colour image difference algorithms.

The acceptability of colour differences was also evaluated between the proofs produced by two commercial soft-proofing systems and the corresponding reference prints. The results, although not conclusive due to the limited test set, suggested that a colour-matching accuracy comparable to that of hardcopy proofs and sufficient for contract proofing can be achieved with soft proofing systems.

References

[1] Altona Test Suite Application Kit (2003), *Documentation.* http://www.altonatestsuite.com

[2] Engeldrum, P. G. (2001), *Psychometric Scaling: A Toolkit for Imaging Systems Development*, Imcotek Press

[3] Fairchild, M. D., Johnson, G. M. (2003), *The iCAM framework for image appearance, image differences, and image quality*, Journal of Electronic Imaging, Vol. 13. p. 126 - 138

[4] ISO 12640-2:2004, *Graphic technology-Prepress digital data exchange-Part 2: XYZ/sRGB encoded standard colour image data (XYZ/SCID)*, ISO

[5] ISO 12646:2004, *Graphic technology-Displays for colour proofing-Characteristics and viewing conditions*, ISO

[6] ISO 3664:2000, *Viewing Conditions-Graphic technology and photography*, ISO

[7] Laine, J., Koivumäki, K., Leppänen, T. (2006), *Colour tolerances in contract proofing*, Advances in Printing and Media Technology: Proceedings of the 33th International Research Conference of iarigai, Leipzig, Germany. p. 389 - 398

[8] ICC.1:2004-10, *Image technology colour management - Architecture, profile format, and data structure*, ICC

[9] Johnson, A. J., Green, P. J. (2001), *The CIEDE2000 colour difference formula and its performance with a graphic arts data set*, Advances in Colour Reproduction: 28th Conference of iarigai, Montreal, Canada

[10] Johnson, G. M., Fairchild, M. D., *Darwinism of Color Image Difference Models*, IS&T/SID 9th Color Imaging Conference, Scottsdale, 24 - 30 (2001)

[11] Schmitt, U., Dolezalek, F (2004), *UGRA/Fogra Media Wedge CMYK V2.0: Instructions for use.* http://www.mediawedge.com

[12] Sano, C., Song, T., Luo, R. (2003), *Colour Differences for Complex Images,* The Proceedings of the 11th IS&T/SID Color Imaging Conference, p. 121 - 126

[13] Song, T., Luo, R. (2000), *Testing Color Difference Formulae on Complex Images Using CRT Monitor*, The Proceedings of the 8th IS&T/SID Color Imaging Conference, p. 44 - 48

[14] Song, T., Luo, R. (2001), *Colorimetric Thresholds for Printed Images*, The Proceedings of the 9th IS&T/SID Color Imaging Conference, p. 219 - 223

[15] Stokes, M., Fairchild, M. D., Berns, R. S. (1992a), *Precision Requirements for Digital Color Reproduction*, ACM Transactions on Graphics, 11(1992)4, p. 406 - 422

[16] Stokes, M., Fairchild, M. D., Berns, R. S. (1992b), *Colorimetrically Quantified Visual Tolerances for Pictorial Images*, TAGA/ISCC Proc., Vol. 2, p. 757 - 777

[17] Zhang, X. M., Wandell, B. A. (1996), *A spatial extension to CIELAB for digital color image reproduction*, Proceedings of the SID symposium 27. p. 731 - 734

The development of a six colour separation algorithm

Eifion Jewell[1], *Tim Claypole*[1], *Barry Palmer*[2]

[1] Welsh Centre for Printing and Coating, University of Wales Swansea
Singleton Park, Swansea, Wales, UK
E-mail: e.jewell@swan.ac.uk

[2] Only the First Ltd.

Abstract

A algorithm is described which can be used for 6 colour separation of complex photographic images in order to maximise image gamut. Using a custom set of 6 colour process inks a Yule Nielsen modified Neugerbauer equation is used to produce a colour model to predict colour mixing using 65 Neugerbauer primaries. Over 60% of the model predictions were within a ΔE of 5, while some larger errors could be associated with the optical brighteners in the paper substrate. This model was considered sufficiently accurate for the basis of a colour separation model. To reduce computational effort at the separation stage a 24^3 pure lookup table was created to store the results of the colour model. The "one to many" mapping from XYZ to 6 colourants was dealt with by enabling a rule based system and a smoothing function. To incorporate the possibility of a black separation for some dark images, a system was developed where the "in gamut" of any image is calculated in order to maximise output colour gamut.

Keywords

Colour separation

1. Introduction

The limitations of the 4 colour gamut are well known and numerous multi colour systems have been developed which allow a better rendition of saturated images. The use of 4+ colour printing is likely to increase in the future as it offers printers and ink makers a number of advantages. For the printer the colour gamut and perceived quality of the print is increased and the number of pantone and spot colours obtainable within a standard ink set is increased. This reduces the need for spot colours allowing the same colours to be kept in the press, eliminating mixing and clean up times. For the ink maker, the reduced number of the spot colours which need to be supplied to the printer is the primary advantage.

These benefits must be balanced by the economic constraints of additional print units and plate materials. A further additional cost which must be met in multi colour halftone printing is the pre press time associated with colour separation. Historically this has been achieved by skilled pre press operators who develop a sense of colour separations required to produce the best image. This subjective method can be slow, inconsistent and tends to be costly due to the time required by skilled labour. In order to reduce the financial burden associated with the pre press and improve consistency, then this colour separation needs to automated.

This paper builds on a previous IARIGAI paper, ref. [1], to examine the development of an automatic colour separation algorithm for a 6 colour set which contains two yellows (an orange shade yellow and green shade yellow), two reds (orange shade red and blue shade red) and two blues (green shade blue and red shade blue), ref. [2]. Before describing the separation algorithm the paper summarises the main technical challenges from the literature.

2. Summary of relevant literature

A number of methods have been developed for the separation of 3 channel images into multi colour separations. They key issues these have addressed are the colour mixing model, separation colourant selection, data storage and interpolation method and gamut mapping for out of gamut colours. These challenges are well summarised by Stollnitz et al [3].

The modified Neugerbauer approach to colour model development have been used successfully by a number of authors. Modifications to standard Neugerbauer include the Yule-Nielsen correction for scattering, [3, 4, 5 & 6]. The issue of gamut mapping between RGB and other colour gamuts has been examined on numerous occasions and is well reported in 4 colour printing applications. Ostromoukov [4] ignored this issue as it was stated that the larger gamut of multi colour spaces did not require mapping; thus eliminating one of the most difficult challenges. Stollnitz et al [3] describe a co-ordinate system which can be varied from a cylindrical mapping system to a circular mapping system

One unique problem which arises in multi colour separation is the "one to many" mapping from XYZ to multi colour device space, [3, 4]. In 3 colour process printing, this issue does not arise since the number of colourants and the colour co-ordinates of any pixel are equal. With multi colour separation there a number of possible solutions to achieve a specified colour. The choice of solution is critical to the printability of the separation as artefacts and discontinuities can be created in the image. Separations containing discontinuities and artefacts impose extreme requirements on tone gain and register on the printer. Wang et al [6] overcame this by fixing colour components which could be used in separate areas of colour space. Chen et al [7] describe a system where the choice of colourants is made based on colour constancy such that metamerism is minimised.

One method which is increasingly being used in the commercial packaging industry for multicolour halftone printing is the use of ICC colour profiles. Commercial packages such as Gretag Macbeth Profilemaker pro, ref [8], offer the ability to produce test forms and generate profiles for multi colour separation. While this offers a commercial means of utilising multi colour halftone printing it is a "black box" approach and it is likely to be even more problematic than 4 colour profiling, ref [10].

3. Colour prediction model

The prediction of the XYZ colour within the algorithm is based on Neugerbauer equations which predict the colour based on the concentration of the Neugerbauer primaries (the base colours and overprints). It was decided that the effect of trapping as described by Stollnitz [3] would be ignored. his was felt to be justified as it added additional complications (particularly with six colours), requires further assumptions and as the end application of the technology is UV flexography where printing is wet on dry then the added complications could not be justified.

For a 6 colour system there are 65 Neugerbauer primary coefficients (64 single colours and overprints plus the substrate). The XYZ colour values can be calculated from

$$\begin{bmatrix} X_{tot} \\ Y_{tot} \\ Z_{tot} \end{bmatrix} = \sum_{1}^{64} a_i \begin{bmatrix} X_i^{\frac{1}{n}} \\ Y_i^{\frac{1}{n}} \\ Z_i^{\frac{1}{n}} \end{bmatrix} \quad (1)$$

Where the subscript tot represents the total colour, the subscript i is the i^{th} Neugerbauer primary, a represents the percentage area of the i^{th} primary and n is the Yule-Nielsen factor. Given the XYZ values of the Neugebauer primaries then for given percentage areas of each of the 6 colours, then the total colour can be calculated.

In order to test the model for colour prediction the data from a previous offset lithographic printing trial, ref. [1], was used. This provided the necessary 65 Neugebauer primaries together with another 12384 patches which contained various combinations of printed percentages of the 6 colours. Thus, it was possible to compare the predicted colour against the measured colour. A parabolic dot gain curve was applied to the dot areas of each of the colours reaching a maximum at a 50% tone. This maximum value varied between 10% and 20% depending on the colour. The Yule- Nielsen correction factor was calculated by measuring the tone strip using a densitometer and by image capture through a microscope. Image segmentation at a fixed grey value (mid point between peaks at nominally 50% coverage) through the tonal scale allowed the true physical percentage coverage to be calculated. The Yule-Nielsen factor was chosen at 1.2 such that it gave the minimum mean error between the measurement from Yule Nielsen modified Murray Davies equation and the physical measurements.

Figure 1 shows a cumulative distribution of ΔE_{ab} (between the predicted and measured colour) as a function of the percentage of patches. 60% of the patches are within ΔE_{ab} of 5 while 90% within ΔE_{ab} of 10. This represents reasonably good agreement between measurement and prediction.

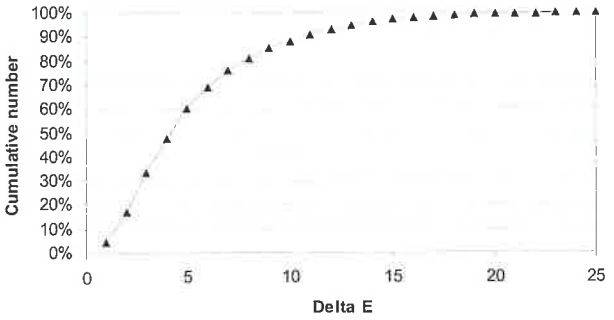

Figure 1: The cumulative number of points plotted against the colour difference between the predicted and measured colours for the 12384 measurement points

Further analysis the colours which were not well predicted (those where the ΔE_{ab} were larger than 10) showed that there was a pattern in these colours which was associated with the optical brighteners in the substrate whose colour was measured at L* = 94.2, a* = 3.5, b* = -13.53. The large ΔE_{ab} were concentrated in areas where no yellow was printed, Figure 2. All predictions were accurate when the yellow was present as the yellow had the effect of filtering the strong blue nature of the paper.

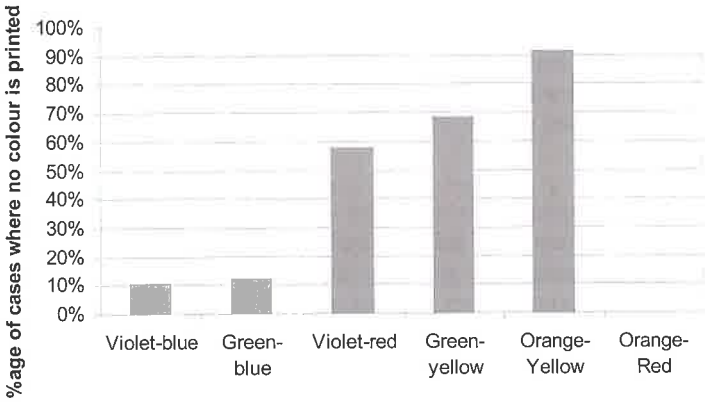

Figure 2: An analysis of the colour deviations greater than 10 between the predicted and measured colour

Given that the model produced reasonable agreement between the predicted and measured values, it was decided that this would form the basis of a colour separation algorithm for 6 colours.

4. Implementing a colour separation model

Preliminary discussions with the packaging industry showed that they were impressed by the colour rendition but highlighted that they would appreciate the ability to substitute one of the 6 colours for black. This makes it easier to print detailed text and reduces the total ink amount when printing dark colours. If a particular image required a great deal of shadow and had little colour in the orange yellow part of the spectrum, then it would make sense to sacrifice the yellow-orange ink to make way for the black. Thus, a strategy needed to be developed which accommodated the black as a possible substitute colour for any of the primary colours used in the ink set.

At the initial stages of model development a similar principal to that used by Ostromoukov [4] was applied to the issue of gamut mapping, in that it was felt justifiable to ignore it due to the large colour gamut of the process set. The implications of this are given in the discussion section of the paper.

In separating an image, the XYZ of the pixel is known and the percentage coefficients (a_i) must be calculated. The direct mathematical solution of these equations is extremely difficult since there are 6 unknowns (the percentage of each colourants) and 3 equations (one for X, Y and Z). This would require some predetermination of the solution and / or iterative techniques to find a solution. The equations are also highly non linear and thus any mathematical techniques would need highly complex and impractical.

Given this scenario, an alternative strategy was devised. This involved looping through every possible combination of the seven ink colours from 1% to 100% in 1% steps (100^6 combinations) and calculating the XYZ and subsequently L*a*b* coordinates of the predicted colour. Thus, a table representing the possible colour gamut is developed over time. The most practical method for storing the data was to store 1 bytes for each colour channel for each possible L*, a* and b* value with a byte representing each L*a*b* value. This allows a three dimensional table containing the 6 colourants required for 256^3 entrees.

Given a RGB pixel value it is then possible to calculate L*a*b* and then directly point the algorithm to the relevant colourant combinations required to create this colour in the table. The algorithm is therefore a direct LUT and not an lookup, find neighbours and interpolate table. The advantage of this strategy is that it is quick at the separation stage since no LUT nearest point finding and interpolation is required during separation. The disadvantage of this strategy is that it is computationally intense at the table creation stage, since all 100^6 combinations are calculated, and it requires the table of 2^{24} entries containing a byte for each of the 6 colourants to be stored in memory, approx 100 Mb. This is memory, but not computationally, expensive at the separation stage. At the table creation stage this computation takes approximately 4 hrs on a dual Pentium PC.

There are two major issues relating to this strategy. One is the limited colour gamut of the 6 colour system compared to L*a*b* colour space, which results in null records being calculated for many L*a*b* colours. The other is associated with the "one to many" mapping. In some instances there were in excess of 10,000 combinations of the 6 colourants which would produce the necessary colour. By simply looping through all the possible combinations of the 6 colourants then it is not possible to control which combination is chosen. Although the separations are colourimetrically correct, they tend to include discontinuities and bands in smooth transitions, as the choice of colourant is effectively dependent only on the order of the search. In order to overcome this limitation, a rule based system which aimed to apply logic to the criteria was developed coupled with an array smoothing function.

The rule based system can be prioritised for minimum ink use, preferential colours and dot size limits. The minimum ink use compares the amount of ink required to achieve a colour and selects the combination of colorants with the lowest total ink usage. The preferred colours was achieved by giving each colour a ranking as its preferred use, largely based on pigment cost, loading and ink film thickness required to achieve the standard densities. By examining the sum of the ranking, the combination which achieved the highest rank would then be chosen. The dot size limits ensured if a colourant required deep shadow (> 95%) or light highlight (< 5%) then it would not be the preferred option. Before a colourant combination is stored in the array it is checked against the incumbent value using these rules and if it answers these rules more fully, it replaces the current value.

The smoothing function minimises any individual values which are in the array but are significantly different from near neighbours. An algorithm was adapted which examined each entry in the array and compared the constituent colourants to its 8 near neighbours. If the percentage differences between the central entry and its near neighbours is excessive then a smoothing function is applied to the entry.

Much of the testing of the separation was carried out using a test image obtained from ref. [10] which provides a challenging test of the system as it contains smooth blends, saturated colours, grey areas and fine detail. Separations for the violet blue with and without the rule based system and smoothing are shown in Figure 3. Although the modified separation is not completely free of discontinuities in tone, it is a much more amenable to printing than the initial separation.

In order to offer the possibility of black substitution for one of the colours, an additional 6 colour tables were generated for black substitution for each of the colours. The Neugebauer primary data for this was made by overprinting the 65 patches with a black overprint. This yields 130 patches with all combinations of 6 colourants.

If all 7 colour combination tables were to be kept in memory, then approximately 700 Mb would need to be allocated for table storage, substantially reducing computer operation. In practice, this is unacceptable. To overcome this issue 7 single bit data tables were created representing each possible colour combination. Each table entry bit represents whether the RGB colour can be achieved using the chosen colour combination. Upon

loading an image, the "in gamut", RGB colours can be directly examined and a total of in gamut and out of gamut colours created. By comparing the percentage of "in gamut" colours for each colour combination, the ideal separation colours can be calculated. Typical examples of this are shown in Table I where the percentage of colours obtainable (irrespective of the area of colour) within each of the images (Figure 4) are shown for each colour combination.

(a)

(b)

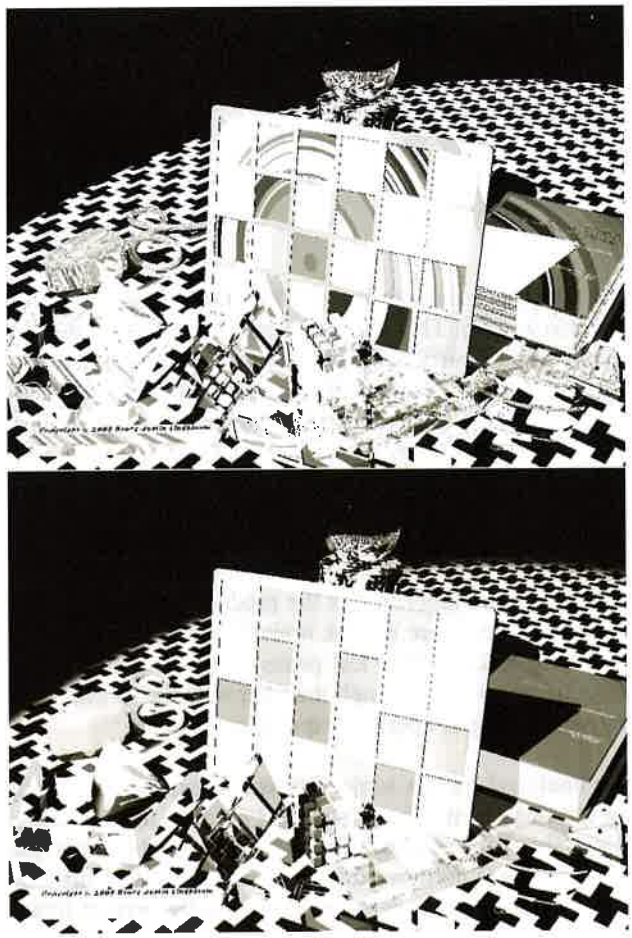

Figure 3: Separations created (a) without and (b) with the rule based and smoothing functions

Figure 4: Sample test images used to examine the optimum ink colourant solution

Table I: Results of "in gamut" for the images in Figure 4.
Each row represents the percentage "in gamut" where black substitutes the noted colour

	Peppers	Romeo & Juliet	Delta E	Dog	Virgin Mary	Sports car
Original 6 colours	87	76	56	95	46	95
Violet Blue	94	85	63	99	97	97
Green Blue	75	82	60	92	98	96
Violet Red	77	81	62	99	98	97
Green Yellow	88	87	64	98	99	97
Orange Red	76	82	63	99	99	97
Orange Yellow	94	86	64	97	99	97

In almost all instances the 6 original colours are not the most appropriate (i.e. they do not give the largest percentage coverage within the gamut). This is most noticeable in images with a higher degree of shadow and shows the difficulty in laying down a sufficiently dark colours using a high total ink coverage of the 6 original colorants. The analysis shows the usefulness of the technique in choosing the optimised ink colours for any image in terms of colour gamut. In the software implementation of the technique, the out of gamut section of images are shown visually.

5. On press testing

The real test of any colour separation algorithm is the production of plates and printed material. During the development of the algorithms, a number of test prints were made on an 8 colour Speed Master offset lithographic press at Heidelberg UK. Several test prints of the original ink colours (no black substitution) were run at preset ink densities (measured through the filter with the largest response) with adjustments being made to the ink key settings according to operator experience.

The complex images were analyzed from a subjective assessment by the printers based on running the jobs and by observers viewing the final print. The printers did not find the job difficult to run although the initial make ready was approximately twice that of normal 4 colour jobs. This was partly associated with the additional plates and ink but the large portion could be attributed to the time associated with manipulating the ink keys to balance the need for set solid densities and visually correct image attributes. This is likely to reduce as press operators become more experienced with the system. The main concern amongst the printers was the high ink coverage which was being printed in the shadow areas. This did not cause any set off problems but printers felt that dark neutral regions with over 400% ink lay down was excessive. Visually, all observers felt that the increased colour gamut produced by the six colour set enhanced the appeal of the image, particularly for the packaging type images of foodstuffs. It was difficult to come to any subjective value added perception to the image.

In order to provide more objective analysis of the prints, then custom written software was developed which read a scanned CIE RGB file and the image to an a*b* gamut plot. The 6 colours prints were compared to traditional 4 colour images printed under normal test conditions, Figure 5. In all instances the 6 colour print shows increased chroma.

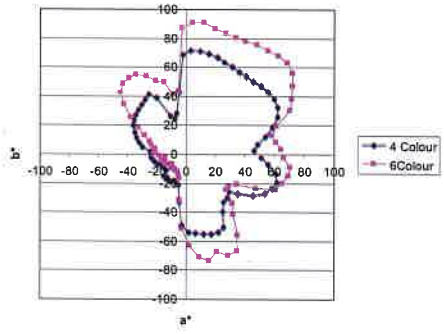

Figure 5: Comparison of colour gamut of 4 and 6 colour printing

6Discussion

The algorithm developed operates well. It is robust and takes minimal computation at the separation stage; being a true LUT and not a look up, find nearest neighbour and interpolate system. This approach is novel but is not elegant and is only possible due to the computational power and storage capacity of modern desktop computers.

Although the system has been developed for the 6 colours described, the authors see no reason why it could not be used for other 6 or more colour systems. The system has been designed to be "open" in that it has not been hardwired to operate with the currently selected colourants. The increase in computational effort for additional colourants at the table creation stage would be significant, a factor of 50 or 100 dependent on the number of percentage steps considered. Instead of the full factorial approach used in the current algorithm, intelligent selection of the colourant combinations could reduce the wasted computational effort considerably. A 7 colour system may then increase run time by approximately twice the 6 colour system.

The inclusion of gamut mapping to compress the original's gamut into the available 6 colour gamut is needed to ensure that colour differences in the original close to the gamut edge are maintained in the print. Although observers were not visually aware of extreme gamut compression in high chroma colours, the separations clearly showed some high chroma regions whose pixels where numerically different in the original L*a*b* but which were of equal colourant concentration. The limited sensitivity of the eye in high chroma regions are likely to the key reasons for this.

The difficulty in rendering dark neutral colours without excessive total ink coverage using 6 colours is a fundamental issue which is likely to cause practical problems in implementing the 6 colour system. The addition of the black reduces the total film thickness substantially but has an impact on the number of printing units required. Before the 6 colour system can be placed in the market a valid economic model needs to be created which examines the balance the financial penalty of the system with the potential increased revenue from new markets, value added printing and reduction in costs associated with spot colours. The economic argument is increasingly important in a world where print is seen as commodity. This requires more rigorous studies to be undertaken on financial added value and costs associated with spot colours to be more accurately modelled.

For scientific completeness and ease of data presentation, the workflow currently converts any RGB image (from most common RGB colour spaces) to XYZ and subsequently to L*a*b* and examines an L*a*b* LUT.

In many instances the XYZ to L*a*b* step can be removed and an RGB LUT created. This would reduce a computational step in the data workflow and improve productivity. The RGB space chosen would need to have a colour gamut larger than that of the 6 colour gamut.

7. Conclusions

The system developed provides a robust way of converting an RGB image to the six colour separations. The six colour system provides a wide colour gamut which can be used for chroma rich presentation of complex images. Utilising a modified Neugerbauer model, there is sufficient agreement between the predicted colour and the measured colour to enable colour separation software to be based on the model. The software created utilises a true LUT, dispensing with the need for interpolation. The software is computationally expensive during the production of the LUT but rapid during the separation process. It is likely that the system developed could be used for alternative colour systems and even be extended for additional colours.

Acknowledgements

The authors would like to acknowledge the help of "Only the First Ltd" for supporting the work and for Heidelberg UK (Brentford) for providing printing facilities

References

[1] Wilcox M., Claypole T. C. & Jewell E. H. - "The development of a six colour ink system for enhanced colour gamut", Proceedings of IARIGAI September 2005

[2] GB patent number GB 0300640, US patent number 0321979,518

[3] Stollnitz. E. J, Ostromoukhov V and Saliesin. D. H - "Reproducing color images using custom inks", proceedings of Sigraph 1998 computer graphics annual conferemce 1998

[4] Ostromoukhov V.. "Chromaticicty gamut enhacement by heptatone multi colour printing", International Symposium on Electronic imaging science and Technology, IS&T/ SPIE Jan 1993

[5] Pobboravsky I. & Pearson M. - "Computation of dot areas required to match a colorimetrically specified color using the modified Neugebauer equations", Proceedings of TAGA 1972

[6] Chen Y., Berns R, Taplin L. A, Imai F. H - "A multi ink colour separation alogorithim maximising colour constancy", published at IS&T, Eleventh colour imaging conference

[7] Wang, X. H, XIU X. J, Zhu, W. H & Tang H. J - "Colour control of multi colour printing device", Journal of Zheijiang Univsersity Science A 2006 pp 1187 - 1192

[8] Gretag Macbeth Profilemaker Pro

[9] Sharma A. and Fleming P. D. "Evaluating the Quality of Commercial ICC Color Management Software" p. 336. Proceedings of TAGA, 2002

[10] Bruce Lindbloom website: www.brucelindbloom.com

A micro-scale study of optical dot gain in color halftone

Daniel Nyström, Björn Kruse, Li Yang[1]

Dept. of Science and Technology, Linköping University
SE-60174 Norrköping, Sweden
E-mail: danny@itn.liu.se, bjokr@itn.liu.se

[1] Dept. of Chemical Engineering, Karlstad University
SE-65188 Karlstad, Sweden
E-mail: li.yang@kau.se

Abstract

Modeling the color reproduction of color halftones is difficult, because of light scattering, causing optical dot gain. Most available models base on macroscopic color measurements, the average value over an area that is large relative to the dot size. The aim of this study is to go beyond the macroscopic approach, to study optical dot gain on a micro-scale level, using colorimetric images of printed halftones. The main focus is to study how the reflectance values of the printed dots and the paper between the dots, $R_i(F_i)$ and $R_p(F_i)$, vary with the dot area fraction, by using color histograms. A previously proposed extension of the Murray-Davies equation, incorporating $R_i(F_i)$ and $R_p(F_i)$, is evaluated. The model is further extended to handle color prints, predicting tristimulus values, using 3D color histograms in CIEXYZ color space. To reduce the complexity, projection from XYZ coordinates into one-dimensional color distributions are used. The prediction errors of the model were found to be close to equivalent to that of the Yule-Nielsen model with an optimal n-factor. However, unlike Yule-Nielsen, the extended Murray-Davies model preserves the linear additivity of reflectance, thus providing a better physical description of optical dot gain in color halftones.

Keywords

Color halftone, color reproduction, optical dot gain, Yule-Nielsen effect

1. Introduction

Over the years, many models have been proposed to predict the outcome of color halftones. This is a difficult task, partly because of light scattering within the halftone image, causing optical dot gain, also known as the Yule-Nielsen effect. On the other hand, optical dot gain often co-exists with the so called physical dot gain caused by the physical dot extension. Understanding the physical nature and accurate models of optical dot gain in color halftone are essential for accounting for the effect in order to improve print quality.

In the 1930s Murray and Davies published the first model to predict the output reflectance of a halftone print [Murray, 1936]. The mean reflectance R, is simply given by the linear superposition of the reflectance of the bare paper, R_p, and the full tone, R_i, weighted by the dot area fraction, F_i, as:

$$R(F_i) = F_i R_i + (1 - F_i) R_p \tag{1}$$

The famous Neugebauer model is then a relatively straightforward extension of Murray-Davies, to handle the multiple colorants in color printing. Since the reflected light from different areas is added to predict the overall reflectance, both these models preserve the linearity of photon additivity. It is, however, well known that the performance of these linear models is very limited. The relationship of R versus F_i is in fact non-linear, due to light scattering in the paper substrate, causing optical dot gain.

In the 1950s, Yule and Nielsen published their famous work on light penetration and scattering in paper [Yule & Nielsen, 1951]. It was then showed that the nonlinear relationship could be approximated by a power function, as:

$$R(F_i) = \left[F_i R_i^{1/n} + (1 - F_i) R_p^{1/n} \right]^n \tag{2}$$

The Yule-Nielsen (Y-N) *n-factor*, accounting for light scattering in the paper, is an empirically derived constant, selected to provide the best fit to experimental data. Values of n between 1 and 2 are physically meaningful, with $n = 2$ corresponding to a highly scattering substrate. It has been suggested that an average n value of 1.7, should be satisfactory when the real value is unknown [Pearson, 1980]. However, with modern high-resolution printers, values of n greater than 2 are often required [Wyble & Berns, 2000]. The Y-N model is still commonly used, because it works relatively well. However, it does not physically describe or explain the phenomenon of optical dot gain, and the conservation of energy is lost when the nonlinear transform is applied to the reflectance values. Notice that the fundamental assumption in all these models is that the color for the substrate and the ink is both uniform and constant, which is rarely the case in reality.

In the 1990s, it was showed that the color of the halftone dots and the paper between the dots is not constant, but in fact dependent on the dot area fraction, F_i. [Engeldrum, 1994]. The reflectance of the printed halftone dots, as well as the paper between them, decreases with increased dot area coverage, due to the light scattering in the substrate. En expanded Murray-Davies model was proposed, with the constants for paper and ink reflection replaced by the functions $R_i(F_i)$ and $R_p(F_i)$, [Arney, et al.1995]:

$$R(F_i) = F_i R_i(F_i) + (1 - F_i) R_p(F_i) \tag{3}$$

This model preserves the linear additivity of reflectance while the non-linear relation between R and F_i caused by optical dot gain, is now accounted for by using the functions $R_i(F_i)$ and $R_p(F_i)$. Naturally, the difficulty with this approach is to derive $R_i(F_i)$ and $R_p(F_i)$, i.e. the way that the "colors" of the ink and paper shift with varying dot area fraction. It is clear that it is not possible to derive these components using macroscopic measurements, giving only averaged reflectance of the print. Accurate color measurements on a micro-scale level are in hence needed.

Previous attempts to measure and characterize $R_i(F_i)$ and $R_p(F_i)$ have been limited to point wise measurements using a spectroradiometer equipped with magnification lenses [Engeldrum, 1994]. Spectral and colorimetric values for the halftone dots and the paper between the dots were measured, using a field of view corresponding to a circle of 0.13 mm in diameter. Clearly, the method is not sufficient to derive measurements on a microscale level, for today's high resolution prints. Furthermore, the limited numbers of measurements will not necessarily be representative for a large population of halftone dots. Later on, histogram data from grayscale images have been used to compute the micro-reflectance values for the dots and the paper [Arney, et al.1995]. The results were promising, but the application was limited to monochrome grayscale prints only, and the maximal print resolution was only 330 dpi.

In this work, we continue the approach of micro-scale studies of the reflectance of the halftone dots and the paper between them. An experimental imaging system, combining the accuracy of color measurement instruments with a high spatial resolution, is used to capture micro-scale images of halftone prints. The aim of this study is to investigate if histogram data from such images can be used to measure and characterize $R_i(F_i)$ and $R_p(F_i)$, for both grayscale and color prints. The validity of Eq. 3 will be also evaluated for today's high resolution prints, and an extension to tristimulus values is proposed, using 3D histograms in CIEXYZ color space.

2. Experimental setup

The image acquisition system

An experimental image acquisition system is used, specially designed for acquiring micro-scale images of prints and substrates. The images are captured using a monochrome CCD camera, with a resolution of 1360 x 1024 pixels and 12 bit dynamic range. The CCD, specially designed for scientific imaging, is of grade 0, which means no defective pixels, and uses digital temperature compensation to reduce noise. It has previously been verified that the camera response is linear with respect to the intensity of the incident light [Nyström, 2006]. The optics used is a macro system, designed for scientific applications, allowing for images of various magnifications, up to a maximal resolution of 1.2 μm/pixel.

The substrate is placed on a table which allows for controlled translations in two directions and for rotation around the optical axis. The illumination is provided using a tungsten halogen lamp through optical fibers, which offers an adjustable and well-controlled angle of incidence, as well as the possibility of using a backlight setup. Color images are captured sequentially, using filters mounted in a filter wheel in front of the light source. By

using this color sequential method, there is no need for any interpolation or de-mosaicing scheme, as is the case in conventional digital cameras. Besides the ordinary RGB-filters, the filter wheel also contains a set of 7 interference filters, which allows for the acquisition of multi-channel images. The image acquisition system has previously been thoroughly calibrated and characterized. Models have been developed, allowing for the device dependent images to be converted into the (device independent) colorimetric representations CIEXYZ and CIELAB, and also to reconstruct spectral reflectance data [Nyström & Kruse, 2006].

Processing of the images

Grayscale and RGB images of various test prints have been captured using the 45°/0° measurement geometry. The field of view was 2.7 x 2 mm, giving a resolution corresponding to 2 μm/pixel. All images are first corrected for dark current and CCD gain. After calibration against a white reference, the pixel values for the grayscale images correspond to true reflectance values. The conversion to CIEXYZ color space was made by polynomial regression from RGB images, using characterization functions individually derived for each print. The method has previously been verified to be sufficient, with a mean CIE 1976 color difference of 1.7 ΔE_{ab} and a maximum of 3.3 ΔE_{ab} [Nyström, 2007].

Printed samples

The printed samples used in this study consisted of offset prints on three different paper grades, with both conventional halftoning (AM) and stochastic halftoning (FM). The details on the print samples are given in Table I. Macroscopic measurements of the spectral reflectance and the CIEXYZ tristimulus values of the printed color patches were derived using a spectrophotometer, under the CIE standard illuminant D65.

Table I: The printed test samples

	Paper	Halftone
Print 1	Silk, 130 gr/m^2	AM 175 lpi
Print 2	Gloss, 130 gr/m^2	AM 175 lpi
Print 3	Gloss, 130 gr/m^2	FM 1200 dpi
Print 4	Matt, 130 gr/m^2	AM 150 lpi

3. Method

The possibility to acquire colorimetric and multispectral images of color prints opens up possibilities to properly characterize the microstructure of color halftones. Micro-scale images, i.e. when the resolution of the images is high in relation to the resolution of the halftone, allow for colorimetric and spectral measurements of the individual halftone dots, as well as the paper between them. To capture the typical characteristics of a large population of halftone dots, which may differ in their appearance, we compute histograms from the micro-scale images. A histogram is merely a probability density function for the occurrence of different colors or reflectance values in the image and contains nominally no spatial information. However, with the a priori knowledge that the image represents a halftone print captured in micro-scale, one can relate properties of the histogram to spatial properties of the halftone, such as the edges of the halftone dots [Arney & Wong, 1998; Nyström & Kruse, 2005].

Reflectance histograms

Figure 1 displays an example of a normalized histogram of reflectance values computed from grayscale images, for the full tone $F_i = 1$; the bare paper, $F_i = 0$; and a 60% tint. The two peaks of the solid line curve correspond to the ink dots and the paper between the dots. The valley between the peaks corresponds to the edges of the halftone dots. It is clear from the positions of the peaks, for the 60% tint, that the reflectance values of the ink, $R_i(0.6)$, and paper, $R_p(0.6)$, have shifted from their original positions (the peaks in dashed lines). As matter of fact, the shifts depend on the dot area coverage, F_i.

From the histogram it is possible to derive the mean reflectance of the print, R, as well as the reflectance for the dots, $R_i(F_i)$, and that of the paper between the dots, $R_p(F_i)$. The mean reflectance, R, corresponding to the macroscopic measurement, is given by integral:

$$R = \int_0^1 R \cdot H(R)dr \tag{4}$$

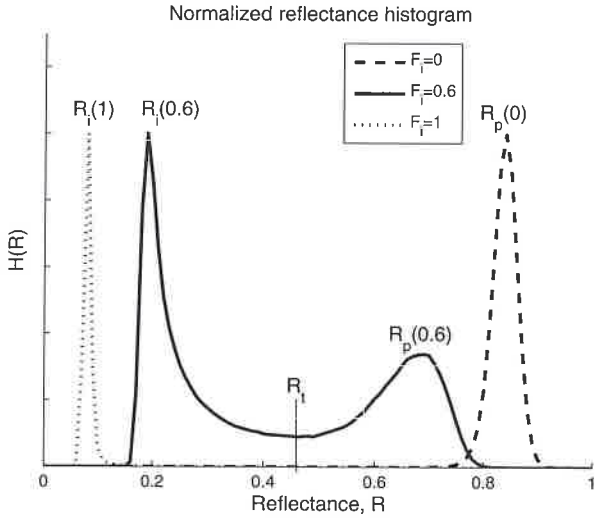

Figure 1: Normalized reflectance histogram for grayscale halftone prints of Fi = 0, Fi = 0.6 and Fi = 1

The integral can be divided into two parts, corresponding to the contribution from the ink and from the paper, respectively:

$$R = \int_0^{R_t} R \cdot H(R)dr + \int_{R_t}^1 R \cdot H(R)dr \tag{5}$$

where R_t is a reflection threshold value, defining the transition between the printed dot and the paper. If the reflection of the ink and the paper is approximated by the peak values from the histogram, $R_i(F_i)$ and $R_p(F_i)$, then Eq. 5 becomes:

$$R = R_i(F_i)\int_0^{R_t} H(R)dr + R_p(F_i)\int_{R_t}^1 H(R)dr \tag{6}$$

The integrals in Eq. 6 correspond to the area fractions for the ink, F_i and the paper, $F_p = (1 - F_i)$, and Eq. 6 thus reduces to the expanded Murray Davies according to Eq. 3. [Arney, et al., 1995]

In this study, we use the straight forward approach of defining R_t as the midpoint between the peaks corresponding to $R_i(F_i)$, and $R_p(F_i)$, for each F_i. It is important that the dot area fraction, F_i, used in Eq. 3 should be the effective dot area fraction, which may differ from the commanded F_i, due to physical dot gain in the printing process. The effective dot area fraction is computed from the histogram, using the threshold value R_t as the limit between the ink and the paper, as:

$$F_i = \frac{\int_0^{R_t} H(R)dr}{\int_0^1 H(R)dr} \tag{7}$$

Extension to color

When extending the method to handle color printing, the reflectance values in Eq. 3 are replaced by the CIEXYZ tristimulus values for the ink and the paper, $XYZ_p(F_i)$ and $XYZ_i(F_i)$. After converting the images into

CIEXYZ color space, 3D color histograms are computed. In the 3D histograms, the paper and the inks will appear as clusters, with the transitions between the clusters corresponding to the edges of halftone dots. Figure 2 illustrates a visualization of a 3D histogram for a magenta tint of 50% nominal ink coverage. The tristimulus values of the paper and the ink, $XYZ_p(F_i)$ and $XYZ_i(F_i)$, can then be computed as the centers of gravity of the clusters corresponding to the paper and ink, for each area coverage, F_i. The threshold value R_t, is now replaced by a threshold plane located at the midpoint, orthogonal to the vector between the clusters.

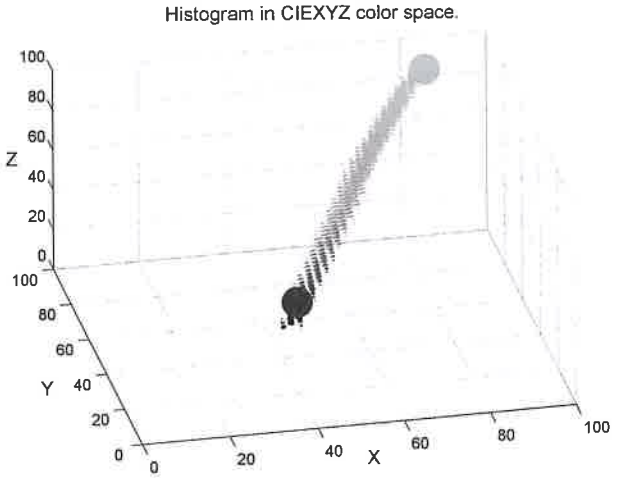

Figure 2: Visualization of a 3D histogram in CIEXYZ color space, for a 50% magenta print

However, computing full 3D histograms and performing all computations in 3D, is computationally heavy. Since the transitions occurring between the clusters are found to be close to one-dimensional, we suggest a projection into one-dimensional color distributions [Nyström & Kruse, 2005]. The centers of gravity for the clusters of full-tone ink and bare paper are used to create a projection-vector between the clusters. Then, an orthogonal projection of all color coordinates in the XYZ images are made onto the vector. The resulting 1D color distributions are normalized so that 0 and 1 correspond to the centers of gravity for the unprinted paper and the full ink coverage, respectively. Figure 3 illustrates an example of projections to one-dimensional color distributions, for magenta tints of various ink coverage.

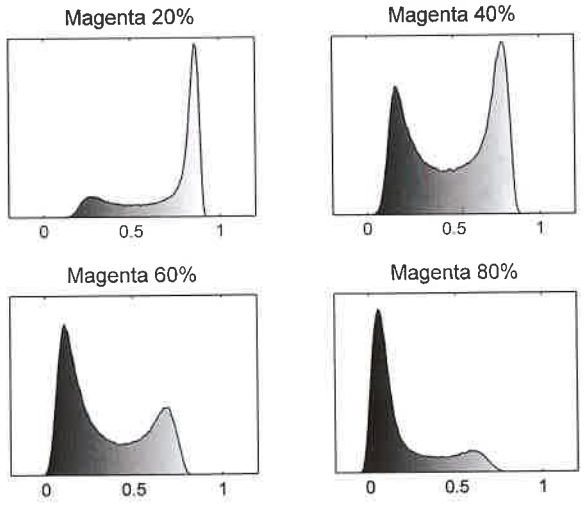

Figure 3: One-dimensional color distributions for magenta prints, projected from CIEXYZ color space

After computing the one-dimensional color distributions, the same methodology as described for the reflectance case, can be applied to compute R, $R_p(F_i)$ and $R_i(F_i)$. These values are then simply converted back to CIEXYZ tristimulus values, by using the known vector of projection.

4. Experimental results

Reflectance values

Table II lists the RMS errors between the measured reflectance and the reflectance values computed from grayscale histograms using the extended Murray-Davies model given in Eq. 3. Computations with the Murray-Davies model (Eq. 1), the Y-N model (Eq. 2) with a fixed n-value of 1.7, and the Y-N model with the optimal n-value that minimizes the RMS error are also included. The results by employing the extended Murray-Davies model are equivalent to the Y-N results using the optimal n-value, and clearly outperform the results for the ordinary Murray-Davis and the Y-N with the fixed n-value.

Table II: RMS errors between measured and predicted reflectance values

	MD	YN (optimal)	n-value	YN (n=1.7)	Extended MD
Print 1	0.065	**0.013**	1.86	0.034	0.014
Print 2	0.080	0.014	1.70	0.015	**0.012**
Print 3	0.133	**0.013**	2.92	0.031	0.020
Print 4	0.060	0.012	2.11	0.031	**0.011**

Figure 4 displays the measured reflectance values compared to the predicted reflectance using the model, and the reflection for the ink, $R_p(F_i)$, and the paper, $R_i(F_i)$, estimated from the histograms. Clearly, the largest variation for both $R_p(F_i)$ and $R_i(F_i)$ occurs for Print 3, reflecting the strongest optical dot gain effect resulted from its high resolution (1200 dpi) FM halftone. The variation of the reflectance of the paper, $R_p(F_i)$ is generally larger than that of the ink $R_i(F_i)$. To study and model the asymptotic behaviors of $R_p(F_i)$ and $R_i(F_i)$ when F_i approaches 0 and unity, test prints containing more intermediate levels of F_i, close to 0 and 1 are needed.

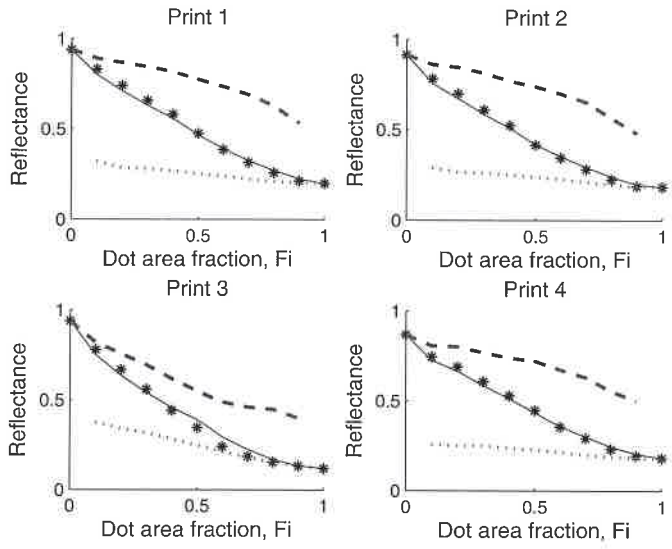

Figure 4: Measured reflectance (solid), predicted reflectance (*), $Rp(F_i)$ (dashed) and $Ri(F_i)$ (dotted)

The largest errors clearly occur for Print 3, using FM halftoning with a resolution of 1200 dpi. The reason is that with the high resolution FM halftone, there is no longer possible to distinguish the paper from the small, closely spaced dots when ink coverage is high. The result is that the bimodal properties of the histogram is lost, making it difficult to find the proper values of $R_p(F_i)$, $R_i(F_i)$ and R_t, using histogram data. As an example, images of 80% black tints using AM and FM halftoning for the same paper grade (Print 2 and Print 3) are displayed in Fig. 5, along with the corresponding histograms. Clearly, the FM halftone appears more like a homogeneous gray even in micro-scale, as also suggested by its histogram.

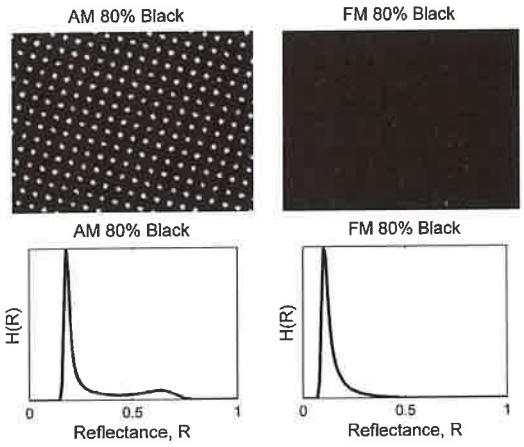

Figure 5:
Images and reflectance histograms of two 80% black tints, using AM and FM halftoning

Tristimulus values

Table III lists the results when the model is used to predict tristimulus values, based on the one-dimensional color distributions projected from CIEXYZ color space. The results are evaluated using the Euclidian distance in CIEXYZ color space, ΔXYZ, as well as the CIE 1976 color difference ΔE_{ab}, between the measured and predicted colorimetric values. Again, the largest estimation errors occur for Print 3, using the FM halftone, where the correct values for $XYZ_i(F_i)$ and $XYZ_p(F_i)$ is difficult to derive from histogram data.

Table III: Estimation errors between measured and predicted colorimetric values

		ΔXYZ max	**ΔXYZ mean**	**ΔE_{ab} max**	**ΔE_{ab} mean**
Print 1	Black	5.73	3.42	5.29	2.99
	Cyan	3.30	1.95	2.92	2.09
	Magenta	4.75	3.44	6.84	4.28
	Yellow	4.98	1.98	5.64	2.54
Print 2	Black	6.50	3.34	5.39	2.73
	Cyan	6.44	3.50	6.13	3.23
	Magenta	4.44	3.16	8.12	4.47
	Yellow	7.60	4.57	7.42	5.27
Print 3 (FM)	Black	12.0	3.58	10.6	4.47
	Cyan	10.2	4.74	12.7	5.85
	Magenta	13.5	6.62	15.4	6.29
	Yellow	18.4	8.74	25.2	8.49

Figure 6 displays the measured and predicted tristimulus values for the black print, as well as how the tristimulus values for the ink and the paper, $XYZ_i(F_i)$ and $XYZ_p(F_i)$, varies with the dot area coverage, F_i. The measured and predicted tristimulus values for Print 2 are displayed in Figure 7, for the cyan, magenta, yellow and black colors.

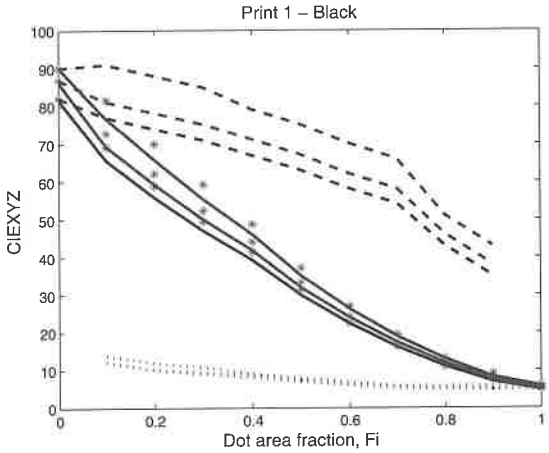

Figure 6:
Measured CIEXYZ values (solid), predicted (*), $XYZ_p(F_i)$ (dashed) and $XYZ_i(F_i)$ (dotted)

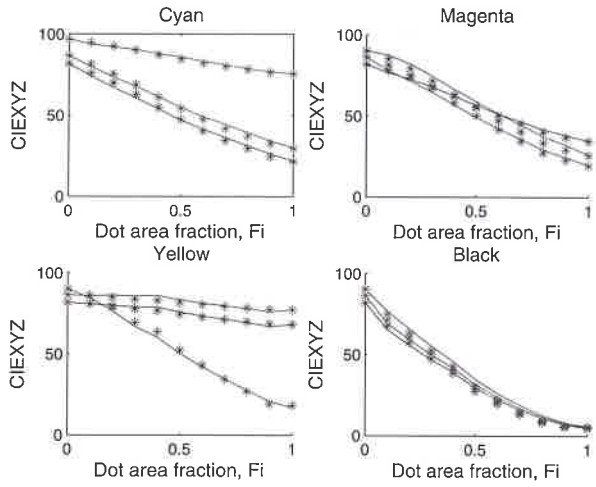

Figure 7: Measured (solid line) and predicted (*) mean CIEXYZ tristimulus values, for Print 2

5. Discussion

The proposed model may be further improved by using more sophisticated methods to estimate the threshold value, R_t, which is used to derive the effective area coverage. One alternative could be to perform line scans in the images over a number of halftone dots, and defining R_t as the region of maximal rate of change in reflectance values [Arney, et al., 1995]. Another is to use the backlight setup to capture transmissive images of the same printed samples. It would then possible to perform the same measurements without the involvement of optical dot gain, providing measurements of the true dot area fraction. The third option may be to incorporate a previously proposed model, separating the optical dot gain from the physical dot gain [Yang, 2004].

For the color case, predicting tristimulus values, preliminary results indicate that the accuracy can be further improved when using the full 3D histograms to compute $XYZ_i(F_i)$, $XYZ_p(F_i)$ and F_i. A possible way to improve the proposed method of projection onto one-dimensional color distributions that will be further investigated is to use principle component analysis, PCA. Defining the projection by the most significant eigenvector from the covariance matrix of all XYZ coordinates in the prints, will most likely provide a more robust method, compared to that using only the coordinates for the full tone and bare paper.

The problems arising for the high resolution FM prints is due to the difficulty in finding the proper peaks and threshold values from the histograms. A possible way to overcome this problem could be to incorporate an improved model for histogram analysis, developed specially for the case of noisy histograms from halftone images [Arney & Wong, 1998].

6. Summary and future work

This work focuses on micro-scale studies of color halftone, especially how the reflectance of the printed dots and the paper between them, vary with respect to the dot area fraction. An experimental imaging system is used to acquire colorimetric micro-scale images of halftone prints. The reflectance values of the ink, $R_i(F_i)$, and paper, $R_p(F_i)$, are estimated for each area coverage, using histogram data for both grayscale and color prints. The validity of the extended Murray-Davies model, utilizing the varying reflectance $R_i(F_i)$ and $R_p(F_i)$ to account for the non linearity of optical dot gain, has been evaluated. It is shown that the model is valid, even for prints of considerably higher print resolution than those were previously tested, and it is appropriate to extend the model to color printing, predicting CIEXYZ tristimulus values. Beside from the problematic high resolution FM print, the prediction errors of the model were found to be equivalent to the results of the Yule-Nielsen model, using optimal n-values. However, unlike the Yule-Nielsen model, the extended Murray-Davies model preserves the linear additivity of reflectance, thus providing a better physical description of the optical dot gain in color halftone.

The study has so far been limited to offset prints and verifications by a larger collection of print samples, using various paper grades, halftone patterns and print technologies will be performed. The current study has

included only single color prints, and the natural continuation will be to extend it to include the more complex cases of multiple colorants. This will involve characterizing and modeling the variations in reflectance and colorimetric values also for overlapping inks, using 3D color histograms.

By using high-resolution colorimetric images of halftone color prints, it is possible to measure and characterize $R_i(F_i)$ and $R_p(F_i)$, i.e. how the color for the halftone dots and the paper between the dots varies with dot area fraction. The future studies should be to model the color shift phenomenon, especially with the focus to relate it to properties of the substrate, the print method and the halftone used. We believe that the combination of micro-scale imaging with colorimetric and spectral accuracy, provide a powerful tool for the development of a deeper understanding of the complex phenomenon of optical dot gain. An understanding, crucial in the development of more sophisticated models of halftone color printing, which can benefit the print quality.

References

[1] Arney, J. S., Engeldrum, P. G. and Zeng, H., (1995). *An Expanded Murray-Davies Model of Tone Reproduction in Halftone Imaging, Journal of imaging science and technology, Vol.39, No. 6, pp 502 - 508*

[2] Arney, J. S., Wong, Y-M, (1998). *Histogram Analysis of the Microstructure of Halftone Images*, Proc. *IS&T's 1998 Image Processing, Image Quality, Image Capture, Systems Conference, Portland*

[3] Engeldrum, P. G, (1994). *The Color between the Dots, Journal of imaging science and technology, Vol.38, No. 6, pp 545 - 551*

[4] Murray, A., *(1936),Monochrome reproduction in photoengraving, J Franklin Institute, 221, 721*

[5] Nyström, D. (2006). *Colorimetric and Multispectral Image Acquisition. Licentiate Thesis No. 1289, Linköping University, Sweden*

[6] Nyström, D. (2007). *Reconstructing Spectral and Colorimetric Data Using Trichromatic and Multi-channel Imaging, Proc. Ninth International Symposium on Multispectral Color Science and Application, Taipei, pp 45 - 52*

[7] Nyström, D., Kruse, B. (2005). *High resolution properties of color prints. Proc. CSIST/IS&T Beijing International Conference on Imaging, Beijing, pp 242 - 243*

[8] Nyström, D., Kruse, B. (2006). *Colorimetric Device Characterization for Accurate Color Image Acquisition. In Advances in Printing and Media Technology, Vol. 33, pp 349 - 360*

[9] Pearson M., (1980),. *n Value for General Conditions, TAGA Proc., pp 415 - 425*

[10] Wyble, D. R., Berns, R. S. (2000). *A Critical Review of Spectral Models Applied to Binary Color Printing, Color research and application, volume 25, pp 4 - 19*

[11] Yang, L., (2004), *A Unified Model of Optical and Physical Dot Gain in Print Color Reproduction, Journal of imaging science and technology, Vol. 48, No. 4, pp 34 7 - 353*

[12] Yule J. A. C., Nielsen W. J. (1951), *The Penetration of Light Into Paper and Its Effect on Halftone Reproductions. TAGA Proc., 3, pp. 65 - 76*

Correcting method of optical dot gain to full color halftone image printed on white paper

Michitaka Nonaka[1], *Susumu Kitazawa*[2]

[1] Faculty of Engineering, Tokyo Polytechnic University
1583, Iiyama, Atsugi-shi, Kanagawa, 243-0297 Japan
E-mail: nonaka@mega.t-kougei.ac.jp

[2] Yamatoya Co., Ltd
5-9-7, Toranomon, Minato-ku, Tokyo, 105-0001 Japan
E-mail: sumkit@yamatoya.co.jp

Abstract

Verification of correcting optical dot gain to full color image print was performed for CK, MK, YK and CMYK with color chart by systematically comparing the calculated value with our measured value.

Keywords

Color reproduction, correcting method, optical dot gain, printed dot

1. Introduction

A color printing image is made up of four color halftone dot superimposed on the white paper. Calculated reflectance of the print using Pollak's equation disagrees with reflectance measured by the densitometer because of optical dot gain. Yule-Nielsen introduced the correcting value "n" to the Murray-Davies's equation for correcting dot gain to the single color print.

But the correcting method for optical dot gain is not exited on a full color print. So we established a method of correcting the effect of optical dot gain to full color print by introducing a correcting term into Pollak's equation. The method is that the image of halftone dots superimposed on white paper through red filter is seen as black dot to both a cyan and black dot. So we take the black halftone dot as a cyan halftone dot and the amount of correcting for the effect of optical dot gain is applied to the cyan area combined with the black dot area. We can similarly correct the effect of optical dot gain on green reflectance and blue reflectance. By this method we can approximately correct the effect of optical dot gain to full color print.

In this study we systematically show the effect of correcting optical dot gain to full color print by our method.

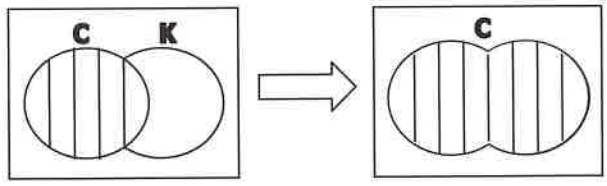

Figure 1: Scheme of black halftone dot considered as cyan halftone dot

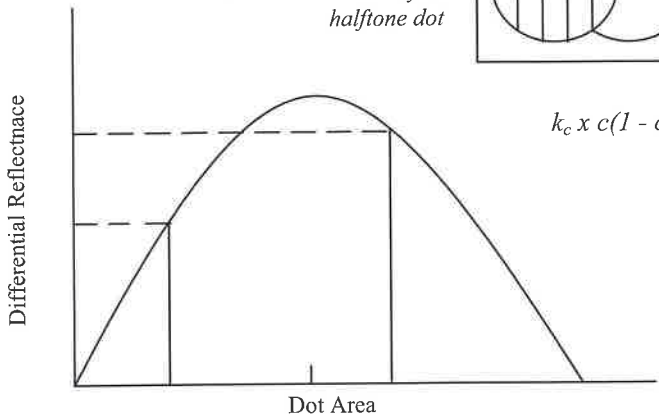

Figure 2: Scheme of correcting amount of optical dot gain adopted at the point of C + K - C x K

2. Experimental

2. 1 Verification of accuracy to Demichel's equation

We prepared the color chart that is used at prepress work to prepare the color produced by printing variously combined dot areas of C, M, Y, K. We call the chart "Kyodo Chart."

The technical deta of process and printing conditions to Kyodo Chart is given below.
Original: Screen Tint Positive Film
Screen Angle: C 15°, M 45°, Y 90°, K(BL) 75°
Press Plate: Positive PS Plate, Printing Machine: Four Color Lithographic Press
Printing Speed: 8000 sheets/ hour, Ink: Standard Color Ink for Kyodo Printing Co.
Order of Printing: K→C→M→Y
Paper: "Tokubishi Art" 135kg/1000 sheets (788mm x 1091mm) made by Mitsubishi Paper Mills Co.Ctd
Density: C 1.50 ~ 1.55, M 1.40 ~ 1.45, Y 1.50 ~ 1.55, K 1.70 ~ 1.80 (Measured with Macbeth RD-918 Densitometer)

Pollak's equation is based on Demichel's equation. So we first verified the dot areas (divided into 16 parts) by superimposing the C, M, Y, K dot with the image processing device incorporating the microscope. For measuring, the frame is set to containing 4 x 4 dots. By color dividing function in the device color image is separated into gray image of R, G, B. The ratio of halftone dot is calculated by counting pixels in the frame. We confirmed the Demichel's equation by application to dot areas of superimposed by C, M, Y, K dots. The ratio of halftone dots agreed well with the multiplication rule of probability appreciably.

The confirmation was indirectly done to the ratio of white paper part of halftones by superimposed dot areas on the print. We selected the dot areas of 20%, 40%, 60% on C, M, Y, K and select patch printed by these dot areas on the color chart for verification of calculated value with measured value. The number of patches was 81 (3 x 3 x 3 x 3). The ratios of the halftone dot superimposed with CM, CMY, CMYK were measured and the values were compared to calculated value with the measured dot area of C, M, Y, K. And the adaptability of multiplication rule of probability (Demichel's equation) to the superimposed dot area was proven.

The results are shown in Table II. The largest difference between measured value and calculated value was 4%. So Demichel's equation is appropriate to apply to superimposed dot areas.

Table I: Measured dot areas of C, M, Y, K

	Measured Value			
	C(%)	M(%)	Y(%)	K(%)
20%	21	21	22	19
40%	40	42	42	39
60%	66	66	67	65

Table II: Calculated and measured dot areas of CM, CMY, CMYK

	Calculated Value			Measured Value		
	CM(%)	CMY(%)	CMYK(%)	CM(%)	CMY(%)	CMYK(%)
20%	37	51	60	38	55	58
40%	65	80	88	65	77	89
60%	89	96	99	88	93	98

Ex. Calculated value (40%, CM(%)): $(1 - (1 - C/100)(1 - M/100)) \times 100 = (1 - (1 - 40/100)(1 - 42/100)) \times 100 = 65$

2.2 Correcting method of optical dot gain and the results for CK, MK and YK

We introduced the correcting term for optical dot gain to Pollak's equation. The correcting term in the case of R is

$$k_c (c + k - c\,k)\,[1 - (c + k - c\,k)] \quad (1)$$

Pollak's equation with above term is

$$R = R_p [(1 - c + c R_{SC})] (1 - m + m R_{SM}) (1 - y + y R_{SY}) (1 - k + k R_{SK}) - k_c (c + k - c k) [1 - (c + k - c k)]. \quad (2)$$

c, m, y, k: The dot area of C, M, Y, K, R_P: Reflectance of the paper through red filter. (In this paper $R_P = 1$). R_{SC}, R_{SM}, R_{SY}, R_{SK}: Reflectance of solid C, M, Y, K print through red filter. k_C: The correcting coefficient of optical dot gain of C through red filter.

For G or B, R in the equation (2) is converted to G or B. In the case of C and K, reflectance R is expressed by the equation (2) in which m and y are zero. In the case of MK and YK, calculated reflectance values G or B were derived in a similar way. In these cases the calculated values correlated well with the measured values. This means that our correcting method is essentially correct.

We show the comparison of the calculated dot area values to the measured dot area values in the case of CK in Figure 3. There is good correlation. Also we show the comparison of the calculated reflectance to the measured red reflectance in Figure 4 in the case of CK.

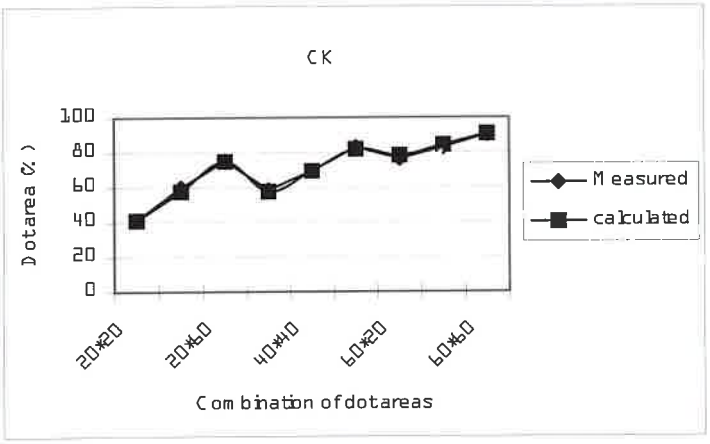

Figure 3: Comparison of measured and calculated dot areas in the case of CK

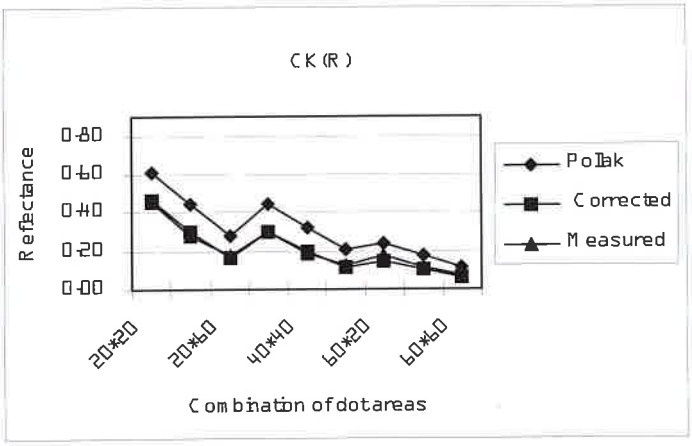

Figure 4: Comparison to Pollak, corrected by our method and measured reflectance in the case of CK(R)

2.3 Verification to full color image

Next we consider the comparison of the calculated value by the equation (2) with the measured values in the case of full color (C, M, Y, K).

The number of combinations of halftone dots at full color was 81. The calculated dot areas for full color were well correlated with the measured values as was the case for two color halftone dots.

But the calculated reflectance of full color was not so well correlated with the measured values as was the case for two color halftone dots. We suspect the cause of optical dot gain to be optical absorbance of ink film to scattering light in the paper. So we expect that the effect of optical dot gain is proportional to the amount of light entering from the paper part of the halftone print. In the case of four color print unexpected absorbance exists at M and Y halftone dot in the case of R. So the amount of light entering from the paper part decreases because of unexpected absorbance. Therefore, we correct for that effect by calculating the amount of unexpected absorbance. The correcting coefficient to R, G, B are I_R, I_G, I_B. They are as follows.

$$I_R = [(1 - c)(1 - m)(1 - y)(1 - k) + T_{MR}(1 - c)\, m\,(1 - y)(1 - k) + T_{YR}(1 - c)(1 - m)\, y\,(1 - k) + T_{MR}\, T_{YR}(1 - c)\, m\, y\,(1 - k)]/[(1 - c)(1 - k)]$$

Where T_{MR} is $\sqrt{D_{SMR}}$, T_{YR} is $\sqrt{D_{SYR}}$. (3)

$$I_G = [(1 - c)(1 - m)(1 - y)(1 - k) + T_{CG}\, c\,(1 - m)(1 - y)(1 - k) + T_{YG}(1 - c)(1 - m)\, y\,(1 - k) + T_{CG}\, T_{YG}\, c\,(1 - m)\, y\,(1 - k)]/[(1 - m)(1 - k)]$$

Where T_{CG} is $\sqrt{D_{SCG}}$, T_{YG} is $\sqrt{D_{SYG}}$. (4)

$$I_B = [(1 - c)(1 - m)(1 - y)(1 - k) + T_{CB}\, c\,(1 - m)(1 - y)(1 - k) + T_{MB}(1 - c)\, m\,(1 - y)(1 - k) + T_{CB}\, T_{MB}\, c\, m\,(1 - y)(1 - k)]/[(1 - y)(1 - k)]$$

Where T_{CB} is $\sqrt{D_{SCB}}$, T_{MB} is $\sqrt{D_{SMB}}$. (5)

I_R, I_G, I_B are multiplied to k_c, k_m, k_y (Correcting coefficients of optical dot gain), and excessive correction is relaxed. The improvement was achived.

The measured values and derived values from the printing sample are shown in Table III.

Table III: Solid density of C, M, Y, K (the measured way of zero density with paper)

	C	M	Y	K
R	1.44	0.04	0.01	1.40
G	0.40	1.28	0.02	1.56
B	0.09	0.48	1.40	1.56

$K_C = 0.59$, $K_M = 0.40$, $K_Y = 0.41$

Table IV: The calculated values of I_R, I_G, I_B

	I_R	I_G	I_B
c20m20y20k20	0.99	0.92	0.90
c40m20y20k20	0.99	0.83	0.88
c60m20y20k20	0.99	0.75	0.86
c20m40y20k20	0.98	0.92	0.82
c40m40y20k20	0.98	0.83	0.80
c60m40y20k20	0.98	0.75	0.72
c20m60y20k20	0.97	0.92	0.72
c40m60y20k20	0.97	0.83	0.71
c60m60y20k20	0.97	0.75	0.69

Figure 5 shows the comparison of measured and calculated dot areas. The number of figure is 1 sheet among 9 sheets.

Figure 6 - Figure 11 are comparison to Pollak, corrected by our method and measured reflectance and the pairs of having not fine correction and fine correction. Each of figures is 1 sheet among 9 sheets.

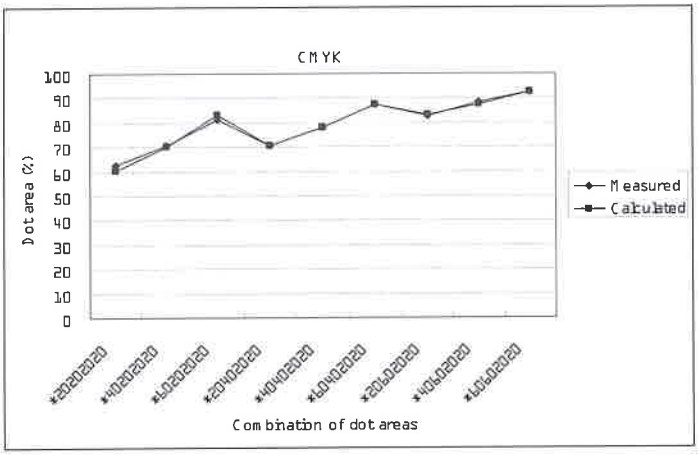

Figure 5: Comparison of measured and calculated dot areas for the case of CMYK

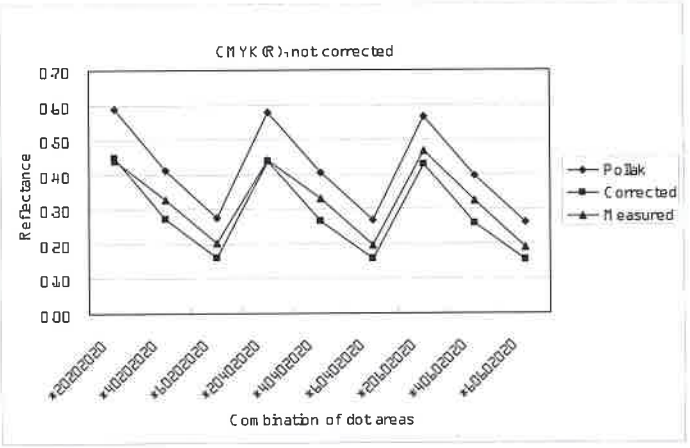

Figure 6: Comparison of Pollak, corrected by our method and measured reflectance in the case of CMYK(R) not additionally corrected

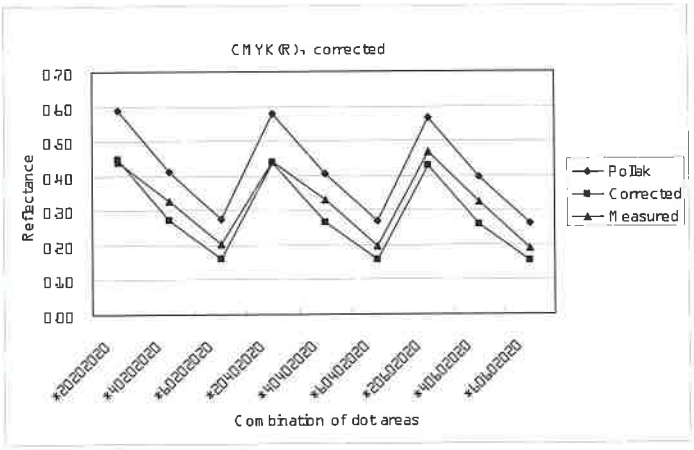

Figure 7: Comparison of Pollak, corrected by our method and measured reflectance in the case of CMYK(R) additionally corrected

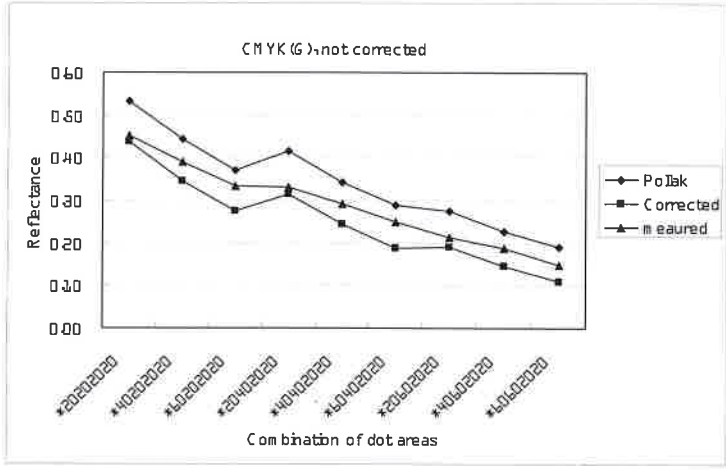

Figure 8: Comparison of Pollak, corrected by our method and measured reflectance in the case of CMYK(G) not additionally corrected

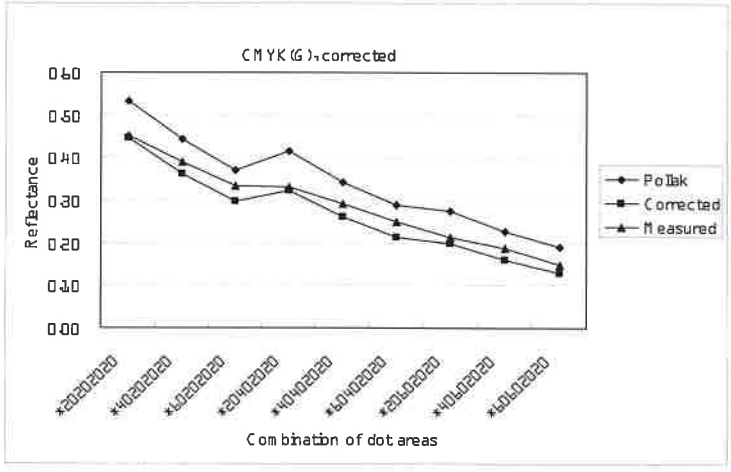

Figure 9: Comparison of Pollak, corrected by our method and measured reflectance in the case of CMYK(G) additionally corrected

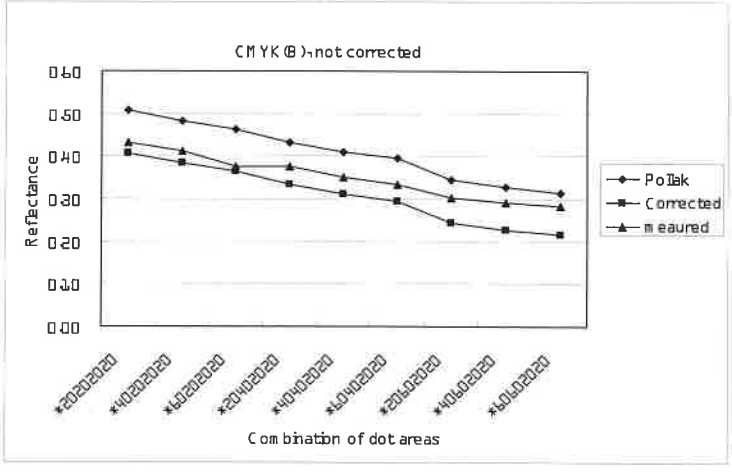

Figure 10: Comparison of Pollak, corrected by our method and measured reflectance in the case of CMYK(B) additionally not corrected

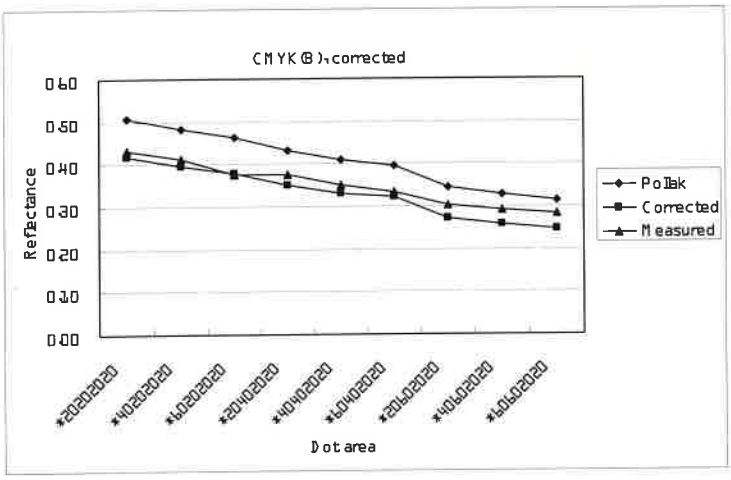

Figure 11: Comparison of Pollak, corrected by our method and measured reflectance in the case of CMYK(B) additionally corrected

3. Conclusion

We confirmed the adaptability of the multiplication rule of probability on the ratio of dot area in the case of full color print. This fact shows the stability of color reproduction on color print. And we enabled approximate correction of optical dot gain at full color print.

References

[1] Pollak F., *J.Photogr.Sci.*, **3**, 112 (1952)

[2] Yule J. A. C., *Principles of Color Reproduction*, John Willy and sons, New York, 1967, p. 263

[3] Nonaka M., Isoda M., *J.imag. Sci. Technol.*, **43**, 120 (1999)

[4] Demichel M. E., *Pro'ed're*, **26**, 17 (1924)

Deriving optimal spectra for standard offset primaries

Philipp Urban[1], *Andreas Kraushaar*[2]

[1] RIT
Color Science Building, 54 Lomb Memorial Drive, Rochester, NY 14623-5604
E-mail:urban@cis.rit.edu

[2] Fogra
Streitfeldstrasse 19, 81673 München
E-mail: Kraushaar@fogra.org

Abstract

Based on a set of ISO 12642-2 compliant offset prints gathered at Fogra, characteristic spectral reflectance curves were measured representing different ink-paper-press-combinations. Aiming for spectral reflectance curves that are spot on the ISO 12642-2 CIELAB values (D50/2°) for coated paper stock three different methods have been encountered. A linear regression technique, a quadratic programming technique and a Bayesian estimate were used to calculate possible candidates. The resulting spectral reflecting curves are well within the variability of typical offset printing but change slightly in their spectral reflectance curves. These techniques could be a basis for creating spectral characterization data, which is demanded e.g. for high quality off-press proofing.

Keywords

Bayesian estimate, ISO 12647-2, spectral characterization data, spectral reconstruction

1. Introduction

The trend for higher quality print products is continuing unabated. In standard offset printing process control therefore plays a very vivid role. Online and offline colour measurement systems are increasingly used for setting up the press and monitoring quality. This is done by the means of densitometry, colorimetry or spectral information. In the advent of new technologies one can measure the whole print image spectrophotometrically. The major task for a process control system is to tell the operator what adjustments are needed in order to reach the proof or other aim values. These adjustments are approved and sent to the press, which then regulates the ink zones in all the printing units simultaneously. But often the printers must print without a contract proof or even only with the given data. In this case the process norm ISO 12647-2 defines CIELAB values for the primary colours depending on the paper type used in the pertinent print run. Due to the metameric character of the current printing technologies there are many spectral reflectance curves possible all aiming towards the same CIELAB value. Having both the current CIELAB value of the print sheet and the CIELAB aim value one can quantify the colour difference but direct control means for cyan, magenta, yellow and black colour units can't be unambiguously derived. In fact spectral information (e.g. including infra red) is necessary to analyse the underlying ink composition. Having the spectral reflectance curves of the primaries printers will benefit in many aspects. Using spectral based control software the user will get direct means for adjusting the coloration of the press. Simultaneously the press operator gets the closest colour differences toward the wanted aim value (e.g. ISO 12647-2) using the pertinent paper-ink-combination. This information will save time- and cost-consuming work at the most expensive place in the printing site.

This paper describes how to derive reflectance curves for the CMYK offset primaries yielding in perfect CIELAB values (according ISO 13655) with respect to ISO 12647-2. Three methods are proposed: A linear regression technique, a method using quadratic programming and a Bayesian method. All methods are based on representative print runs utilizing different paper, presses and printing inks. These methods are already applied on other problems in the field of colour science: The regression technique is widely used with some modifications for colour correction [König, 2001; Hardeberg, 1999]. Quadratic programming is used for camera sensitivity reconstruction [Finlayson, G. D., Hordley, S. and Hubel, 1998]. The Bayesian method is used for reflectance and illuminant reconstruction from sensor responses and colour correction in image acquisition systems [Brainard, 1994; Brainard and Freeman, 1997; Zhang and Brainard, 2004].

2. Terminology and requirements

In the following paper we will denote by r1x, ..., rmx ∈ [0, 1] N, (x = cyan, magenta, yellow, black, red, green, blue, paper white) a set of sample primary spectra of different ink-paper-combinations measured on ISO 12647-2 compliant print sheets according ISO 13655. Here N is the number of sampling wavelength and m is the number of sample measurements. These training spectra were derived using measurements of the print sheets out of the Fogra shoot-out called DNS [Kraushaar 2006].

2.1 Training Dataset

In 2006 Fogra conducted two printing shoot-outs called DNSI and DNSII symbolizing "Drucken nach Standard" - printing according to the standard. Here printers were asked to print an offset sheet based on a PDF-X1a file and an associated contract proof aiming for the ISO 12647-2 - the international standard for commercial offset printing. The characterisation data set FOGRA39 was used to fully reflect the printing condition defined in ISO 12647-2:2004 /Amd 1 namely a screen ruling corresponding to 60/cm and a matt or glossy coated paper stock. While 26 participants joint DNSI, 10 print houses sent their sheets in for DNSII. These prints do represent many different setups comprising different printing presses, CtP-imagers, paper types and printing ink. A detailed overview can be found at the Fogra webpage [Kraushaar, 2006]. This open database is subject to be extended in order to facilitate upcoming printing evaluations of all kind.

The CIELAB aim values defined in ISO 12642-2:2004 /Amd 1 on coated paper (paper type 1/2) are given in Table I. These represent the colour centres of the previous figures. Here only these spectra were used in which their D50/2°-CIELAB values met the CIELAB tolerance of $\Delta E = 5$ around the pertinent aim values defined in ISO 12647-2. This is shown in Figure 1 for cyan, magenta, yellow and black (CMYK) and in Fig. 2 for red, green, blue and the paper white (RGBP) respectively.

In the following text sxISO ∈ CIEXYZ corresponds to the CIELAB value defined in ISO 12647-2. We denote by

$$\Omega_{D50} = \begin{bmatrix} \bar{x}(\lambda_1)L_{D50}(\lambda_1) & \dots & \bar{x}(\lambda_N)L_{D50}(\lambda_N) \\ \bar{y}(\lambda_1)L_{D50}(\lambda_1) & \dots & \bar{y}(\lambda_N)L_{D50}(\lambda_N) \\ \bar{z}(\lambda_1)L_{D50}(\lambda_1) & \dots & \bar{z}(\lambda_N)L_{D50}(\lambda_N) \end{bmatrix} \quad (1)$$

the lighting matrix where $\bar{x}$, $\bar{y}$ and $\bar{z}$ are the colour matching functions and LD50 represents the CIE D50 illuminant both stipulated in the ISO 13655.

2.2 Requirements

The aim of this article is to derive reflectance spectra for each of the given colour centre defined in ISO 12647-2 that satisfy the requirements.

1. The D50/2° CIELAB values of these reflectances shall be identical to the colour centres defined in ISO 12647-2, see Table I.

Table I: CIELAB Aim values for the primaries and secondaries according ISO 12647-2, white backing

	ISO 12647-2:2004 / Amd 1 – Paper Type 1/2		
	L*	a*	b*
Cyan	55,0	-37,0	-50,0
Magenta	48,0	74,0	-3,0
Yellow	89,0	-5,0	93,0
Black	16,0	0,0	0,0
Red	47,0	68,0	48,0
Green	50,0	-68,0	25,0
Blue	24,0	17,0	-46,0
Paper White	95,0	0,0	-2,0

2. The reflectances should represent a generic printing condition characterizing the average of all offset printing presses in compliance with ISO 12647-2.

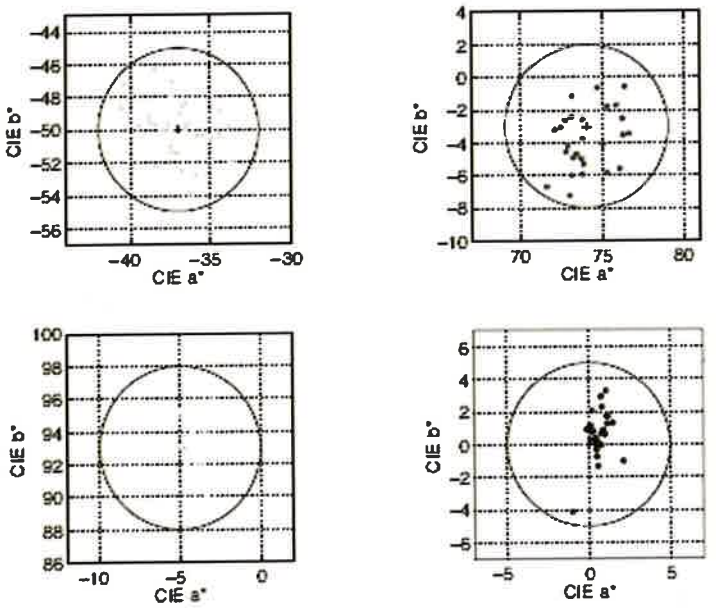

*Figure 1: ISO 12647-2 Aim Values as well as the CIE a*b* values of the conformant spectra - CMYK*

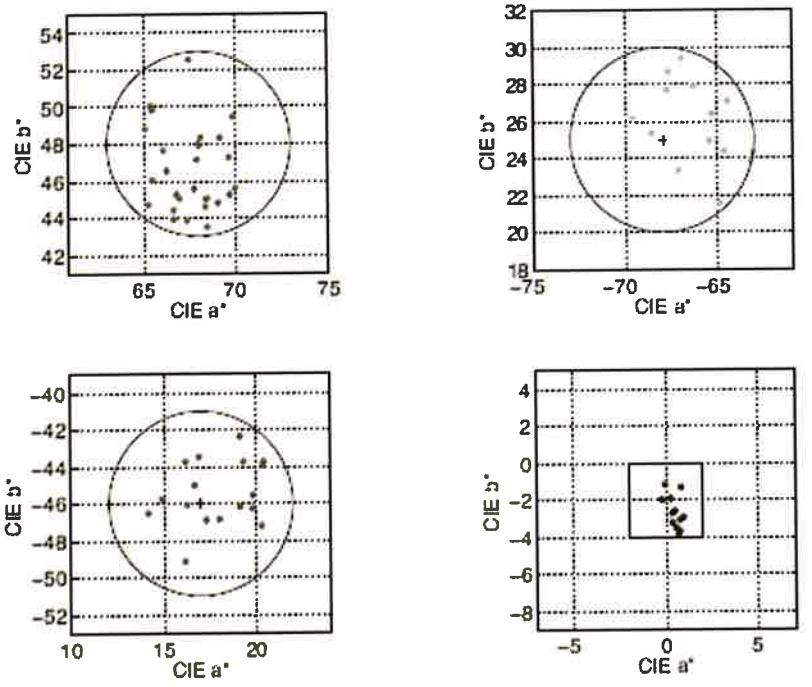

*Figure 2: ISO 12647-2 Aim Values as well as the CIE a*b* values of the conformant spectra - Red, Green, Blue and Paper (Note that the tolerance for the substrate is CIEa*b* < = 2)*

3. Regression technique

For the first approach we arrange the sample measurements r1x, ..., rmx $\in$ [0, 1] N into a matrix Rx = (r1x, ..., rmx). We want to find a linear combination of the trainings spectra within Rx in a way that it matches the aim value sxISO (ISO 12647-2). For this purpose the following equation system has to be solved

$$s_{ISO}^{x} = \Omega_{D50} R^{x} \cdot a \tag{2}$$

Since m > 3 this equation system is under-determined and the solution is ambiguous. One possible solution is given by the pseudo inverse, i.e.

$$a = ((\Omega_{D50} R^{x})^{T} \Omega_{D50} R^{x})^{-1} \Omega_{D50} R^{x} s_{ISO}^{x} \tag{3}$$

The resulting reflectance spectrum

$$r_{ISO}^{x} = R^{x}((\Omega_{D50} R^{x})^{T} \Omega_{D50} R^{x})^{-1} \Omega_{D50} R^{x} s_{ISO}^{x} \tag{4}$$

leads to the desired CIELAB values but may have not the smallest possible RMS difference to the mean spectra of the pertinent characteristic training spectra because the linear regression method minimizes the RMS error in the CIEXYZ colour space.

This method can be visualized by the means of a weighted combination of tristimulus values ΩD50Rx (eg. 2) around the ISO aim value sxISO in the CIEXYZ colour space. The weights for each tristimulus value represents the weights of the spectral reflectance factors Rx building up the resulting reflectance curve rxISO with spot on ISO CIEXYZ values. Richter used this technique in order to derive practical metamers [Richter, 1970].

4. Quadratic programming (QP)

The aim of the quadratic programming approach is to find a reflectance spectrum that leads to the ISO CIELAB value and minimizes the root mean square distance to the mean of the measured samples.

$$\bar{r}^{x} = \frac{1}{m} \sum_{i=1}^{m} r_{i}^{x} \tag{5}$$

For this purpose we have to solve the following QP problem

Minimize $\left\| r - \bar{r}^{x} \right\|_{2}^{2}$ (6)

subject to

$$\begin{aligned} \Omega_{D50} r &= s_{ISO}^{x} \\ r &\geq 0 \\ r &\leq 1 \end{aligned} \tag{7}$$

5. Bayesian estimation (BE)

The determination of optimal spectra for standard offset primaries is a typical inverse problem:

An ISO CIELAB value and the transfer function (lighting matrix) are given and a reflectance spectrum has to be reconstructed that exactly leads to the ISO value. It is moreover an underdetermined inverse problem, since CIELAB is three-dimensional and the reflectance space has more than three dimensions. Therefore additional information, included within the measured samples, have to be used to obtain a spectrum that satisfies also requirement 2 stated in section 2.

The Bayesian method uses a priori knowledge of the probability distribution of offset primaries to determine the best estimate of the reflectance spectrum that match exactly the CIELAB value given in ISO 12647-2.

The Bayesian estimation uses a probability distribution and a likelihood model:

The probability distribution is the distribution of the spectra *r* of all offset presses matching the tolerances of ISO 12647-2. This distribution is called in Bayesian terminology "prior distribution" and we denote it by p(r). We assume that p(r) is a multivariate Gaussian distribution (Central Limit Theorem):

$$p(r) \sim N(\mu_r, K_r) \tag{8}$$

The mean μr and covariance matrix Kr can be estimated using the trainings samples. Figure 3 shows the histogram of the reflectance values for the cyan samples at a wavelength of 550 nm and a fitted Gaussian density distribution.

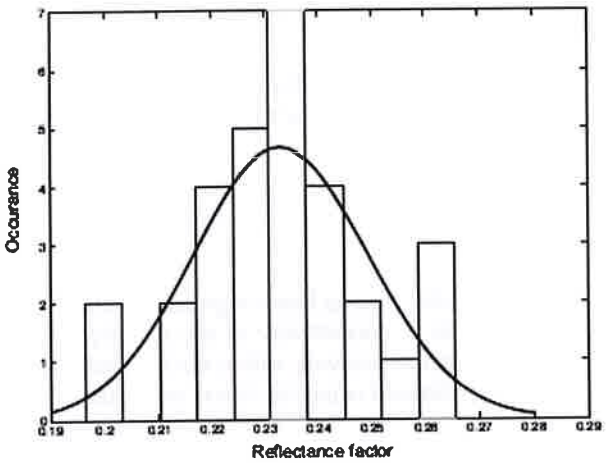

Figure 3: Histogram of the reflectance factors at 550 nm of cyan trainings spectra and the fit of the Gaussian density distribution

The likelihood model is based on the lighting matrix that is the transfer function from spectral reflectance to tristimulus value S, i.e.

$$s = \Omega_{D50} r + \varepsilon \tag{9}$$

where ε is the noise of the visual system, which is assumed as a multivariate Gaussian distribution with zero mean and a diagonal covariance matrix Kε:

$$p(\varepsilon) \sim N(0, K_\varepsilon) \tag{10}$$

The likelihood model is the probability distribution of the tristimulus values under the condition of a given reflectance spectrum, i.e.

$$p(s \mid r) \sim N(\Omega_{D50} r, K_\varepsilon) \tag{11}$$

Given the prior distribution and the likelihood model we are able to determine the so called posterior distribution p(r|s). The posterior distribution describes how likely a reflectance spectrum is under the condition of a given tristimulus value (in our case the tristimulus values derived from the ISO CIELAB values). To calculate the posterior distribution we apply Bayes rule, i.e.

$$p(r \mid s^x_{ISO}) = \frac{p(s^x_{ISO} \mid r)\, p(r)}{p(s^x_{ISO})} \sim N(\Omega_{D50} r, K_\varepsilon) N(\mu_r, K_r) \tag{12}$$

Here p(sxISO) is the so called normalizing factor since it is independent of r. The posterior distribution is again Gaussian [Zhang and Brainard, 2004; Gregory, 2005]

$$N(\Omega_{D50} r, K_\varepsilon) N(\mu_r, K_r) = N(\mu, K)$$

where

$$\mu = K_r \Omega_{D50} (\Omega_{D50} K_r \Omega_{D50}^{\ T} + K_\varepsilon)^{-1} (s^x_{XYZ} - \Omega_{D50} \mu_r) + \mu_r, \tag{13}$$

$$K = (K_r^{-1} + \Omega_{D50}{}^T K_\varepsilon \Omega_{D50})^{-1} \tag{14}$$

The reflectance spectrum with the highest probability that leads to the desired ISO CIELAB value is the mean μ of the posterior distribution (minimum mean square estimator). For an ideal human observer the noise of the visual system is zero and we can omit the covariance matrix Kε. This leads to the final reconstruction

$$r_{ISO}^x = \mu = K_r \Omega_{D50} (\Omega_{D50} K_r \Omega_{D50}{}^T)^{-1} (s_{XYZ} - \Omega_{D50} \mu_r) + \mu_r \tag{15}$$

If the offset reflectance follow the prior distribution than the Bayesian approach is optimal in the sense that the estimation fulfils Requirement I and minimizes the expected mean square error to the offset reflectance satisfying the ISO 12647-2 tolerances.

6. Results

The spectra to be derived by using methods utilizing linear regression techniques, quadratic programming and a Bayesian estimator are all well within the uncertainty of the underlying training data. Again these are spectral measurements of offset prints, which are well within the ISO tolerances. A closer inspection of the spectral curves reveals that the spectra derived using the linear regression and the Bayesian estimator look more similar to each other than the one derived by the quadratic programming.

As stated all spectra meet the first requirement namely the perfect match with the aim value given in ISO 12647-2, although all methods changed slightly in the way, how to represent the most likely representative candidate. The linear regression technique tries to find the smallest RMS difference in the CIEXYZ colour space. Since the linear equation system is underdetermined an arbitrary spectrum is found that leads exactly to the ISO value but is not necessary the best representation of the underlying training prints. The quadratic programming yields also to a reflectance that matches the ISO CIELAB value. Moreover this reflectance has the minimal RMS distance to the average of the training spectra. A drawback of this method is that the shape of the determined reflectance is not necessarily representative to a typical press spectrum, because only the information of the mean spectrum of the trainings data is used. Therefore a reflectance that oscillates around this mean spectrum is imaginable. However, we could not observe this behaviour in our results.

The Bayesian estimator produces spectra that have the highest probability with respect to the training spectra. The results are shown in Figure 3 for CMYK and in Figure 5 for RGBP. Here the average curve is always plotted using a solid black line in combination with its 95th percentile. The derived spectra are coloured in dashed lines of red, green and blue. Note that the scaling of the y-axis differs for the black and white colour.

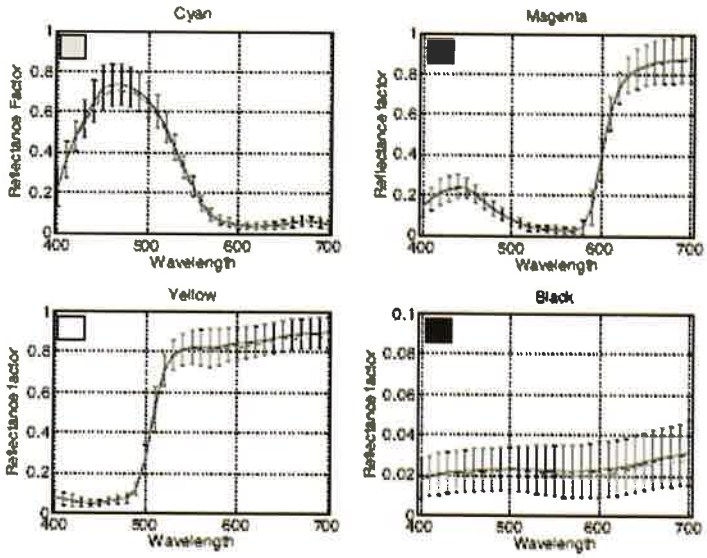

Figure 3: Comparison of the average of the training spectra (solid black line)

and the results of the three methods plotted in dashed lines (red, green and blue); CMYK

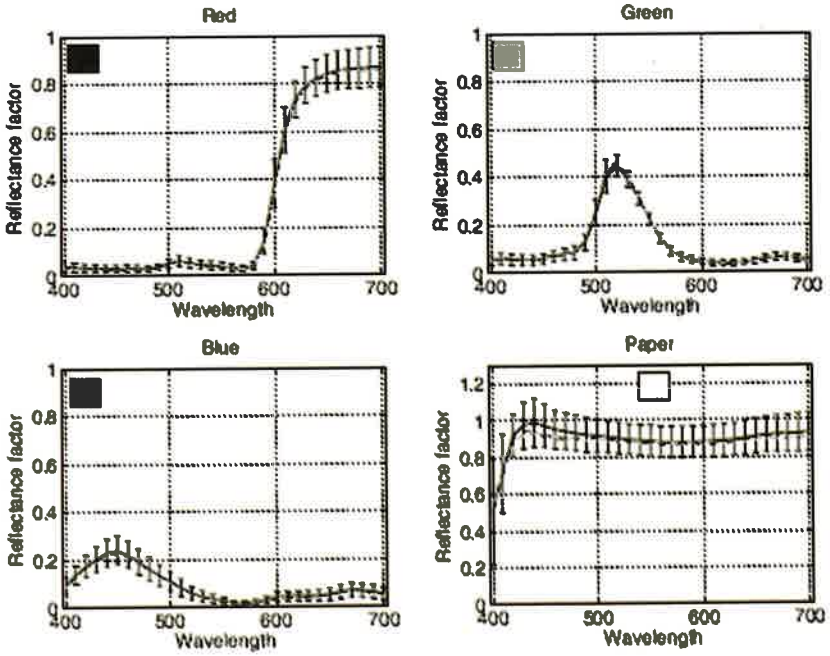

Figure 4: Comparison of the average of the training spectra (solid black line) and the results of the three methods plotted in dashed lines (red, green and blue); Red, Green, Blue, Paper

The spectral difference by the means of the RMS error between the calculated curves and the mean reflectance of the pertinent training samples is shown in Table II. As expected, one can see that the spectra calculated with the quadratic programming technique end up having the smallest RMS. The differences between the results gathers using Regression method and the Bayesian estimator are not significantly different from each other.

Table II: RMS error between the new spectra and the average spectra of the pertinent training dataset

RMS in %	Regression	Bayesian Estimator	"min RMS" using quadratic programming
Cyan	1,75	1,78	1,68
Magenta	0,51	0,51	0,36
Yellow	1,32	1,17	0,86
Black	0,18	0,18	0,14
Red	0,92	0,82	0,69
Green	0,68	0,78	0,53
Blue	0,55	0,63	0,46
Paper_White	2,82	2,77	2,31

7. Discussion/conclusion

If one considers the smallest RMS error between each spectrum and the average reflectance of the underlying training dataset as the best metric than the quadratic programming method performs slightly better that the other two. Considering the probability distribution of typical offset press the method using the Bayesian estimator is favourable.

All spectral reflectance curves are spot on the wanted ISO 12642-2 aim values and can be used for a multitude of applications beyond the offset printing process and primary and secondary colours. The most significant are certainly the so-called "best match" function, which tells the operator what the closest colour difference is using the headroom of over- and under inking and the creation of spectral characterization data, which is more and more demanded by high quality off-press proofing manufactures. It is planed to extent these methods in order to derive spectral curves for many tone value combinations such as the set defined in ISO 12642-2.

References

[1] Brainard D. H., (1994) Bayesian method for reconstructing color images from trichromatic samples, Proceedings of the IS&T 47th Annual Meeting, pp. 375 - 380

[2] Brainard D. H. and Freeman W. T. (1997), Bayesian color constancy, J. Opt. Soc. Am. A 14, 1393 - 1411

[3] Finlayson, G. D., Hordley, S.and Hubel, P. M.(1998):Recovering Device Sensitivities with Quadratic Programming. In: IS&T/SID. Scottsdale Ariz.,, S. 90 - 95

[4] Gregory P., (2005), Bayesian Logical Data Analysis for the physical Sciences, Cambridge University Press

[5] Hardeberg, J. Y. (1999) Acquisition and reproduction of colour images: colorimetric and multispectral approaches. France, Ecole Nationale Superieure des Telecommunications, Dissertation,

[6] ISO 12647-2:2004, Graphic technology - Process control for the production of half-tone colour separations, proof and production prints - Part 2: Offset processes

[7] ISO 13655:1996, Graphic technology - Spectral measurement and colorimetric computation for graphic arts images

[8] König, F. (2001), Die Charakterisierung von Farbsensoren. Deutschland, Rheinisch-Westfälische Technische Hochschule Aachen, Dissertation

[9] Kraushaar A. (2006), DNS - "Drucken nach Standard", http://www.fogra.org/research-de/dns/home/

[10] Matlab (2001), The Language of Technical Computing, Language Reference Manual. 7.0.The MathWorks Inc.

[11] Richter M, (1970), Die Berechnung von Metameren, Die Farbe

[12] Zhang X., and Brainard D. H., (2004), Bayesian color correction method for non-colorimetric digital image sensors, IS\&T/SID, Scottsdale Ariz., 308 - 314

Implementing process color printing by colorimetry

Robert Chung

RIT School of Print Media
69 Lomb Memorial Drive, Rochester, NY 14623, USA
E-mail: rycppr@rit.edu

Abstract

Standards-based printing is shifting from densitometry-based specifications to colorimetry-based specifications. Similar to switching rules in the middle of the game, this has caused confusions in pressrooms worldwide. This paper reviews how standards-based printing began, describes underlying reasons for shifting process control aims from densitometry to colorimetry, and addresses issues in implementing colorimetry in the pressroom. Analysis of ink drawdown samples and a sheet-fed lithographic press run were conducted to develop procedures that would allow pressmen to adopt colorimetry in the pressroom. In doing so, this paper also elaborates on how conformance to printing standards can be verified by colorimetry.

Keywords

Colorimetry, densitometry, ISO, printing standards, process color

1. Introduction

Print media has been an effective mass communication media for centuries. Contents were printed and print quality was in the hands of the printer. As printing technology developed, process color printing became possible to render pictorial color images in the form of editorial contents and advertisements. Due to market conditions and technology advancements, print buyers and content creators started to demand color accuracy and consistency in printing.

Standards-based printing began evolving from craft to science. Specifications Web Offset Publication (SWOP) was the first printing standard developed in 1970s. Densitometric parameters, e.g., solid ink density and tonal value increase (TVI) were used to specify aim points and tolerances for process color printing. Portable densitometers were also developed in the 1970s to help pressmen implement color control in the pressroom. The process of adopting densitometers to aid pressmen in ink key settings and maintaining color consistency was a slow process. It took 15 years to transform the publication printing industry from eyeball-based color adjustment to instrument-based control because print-by-number involves not only capital investment, but also training and cultural change in the pressroom.

Printing technology mainly addresses the output side of the graphic arts industry. Print buyers need a total solution that encompasses content creation, prepress, printing, and distribution. Digital color management became a solution that addresses the integration of prepress and press to make color portable and predictable in the early 1990s. International Color Consortium (ICC) is the standardization body that specifies the file format for look-up tables that describe the relationship between the device color space and the device-independent color space. The metrology for device-independent color space is colorimetry.

The effectiveness of color management depends on color repeatability of the printing device. Device color repeatability begins from the color of the ink in the can. ISO 2846 specifies colors of process inks by colorimetry. It became evident that printing process control aims, such as ISO 12647, are shifted from densitometry to colorimetry. Therefore, the integration of prepress and press by means of color management is the main driver for implementing colorimetry in the pressroom.

2. Objectives

Densitometry has proven to be effective for process control in the pressroom. But density numbers do not correlate to colorimetric numbers directly. Thus, the issue at hand is how to apply colorimetry in the pressroom.

There are four issues: (1) how to verify ink, (2) how to achieve press make-ready, (3) how to exercise process control, and (4) how to verify printing conformance by colorimetry.

3. Experimental

A pressman has to place the right amount of process color (CMYK) inks in register with one another on the substrate during the press make-ready. He also has to maintain the control of the press run so that all products printed conform to colorimetric requirements. This paper addresses that: (1) the correct inks are used, (2) the correct amount of ink is printed, (3) color control is maintained throughout the press run, and (4) color quality assurance is documented colorimetrically.

1. Verifying ink

How does a pressman know he uses the correct process color inks? Process color inks are specified in ISO 2846-1 and ISO 12647-2. In this case, colorimetric values (L*/a*/b*) of CMYK solids are specified as K: 16/0/0; C: 54/-36/-49, M: 46/72/-5, and Y: 88/-6/90. Instead of sending inks to a laboratory, we verify the correctness of process inks by ink drawdown with a grind gauge block on a Little Joe proofer with inks supplied by Kohl & Madden. A single impression from the grind gauge block produces a range of ink film thicknesses. Color measurements were made at various ink film thicknesses. Color differences were calculated relative to the ISO specified aim points. ISO 12647-2 also specifies that deviation of CMYK solids should be less than 5 ΔE.

2. Conforming to colorimetric aims

We organized a press run with the following equipment, materials and procedures. From the input side, a customized test form was used for the press run. As shown in Figure 1, the test form can be used for calibration, press capability study and characterization.

The Creo Prinergy 3 CTP system was used to produce a set of linear plates at 170 lpi AM screening. A 6-color Heidelberg Speedmaster 74 sheet-fed offset press was used to print the test form on Sappi Lustro, Grade 1 coated paper, at the speed of 8.000 impressions per hour. The printing sequence for the 6-color press was blank-blank-K-C-M-Y-aqueous coating. Because of the use of aqueous coating, press sheets were delivered dry and color measurement can be done without delay. We measured color control bars, located at the perimeter of the test form, to set ink keys.

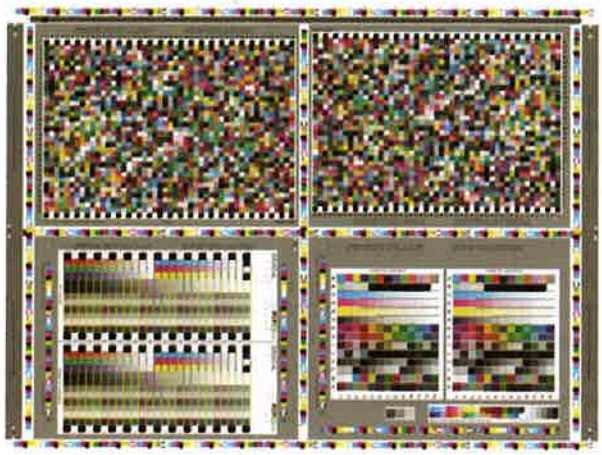

Figure 1: Test form printed in the first press run

In order to print by colorimetry, we used the IntelliTrax, a scanning spectro-densitometer from X-Rite, capable of measuring multiple color control patches width-wise in density and color. Any color measurement system capable of providing densitometric and colorimetric values must collect spectral data from the press sheets and compute density and color by formulation.

Solid ink densities of K: 1.69, C: 1.45, M: 1.52, Y: 1.00 were initially set using the X-Rite IntelliTrax scanning spectro-densitometer as the aim points (Figure 2). Press sheet densities were converted to CIELAB values in

IntelliTrax and compared to ISO 12647-2 colorimetric aim points. Densities that correspond to the smallest ΔE for each of the CMYK keys were selected as the new aim points. In other words, pressmen are able to use familiar density for initial ink setting and ink key adjustments while conforming to colorimetric specifications.

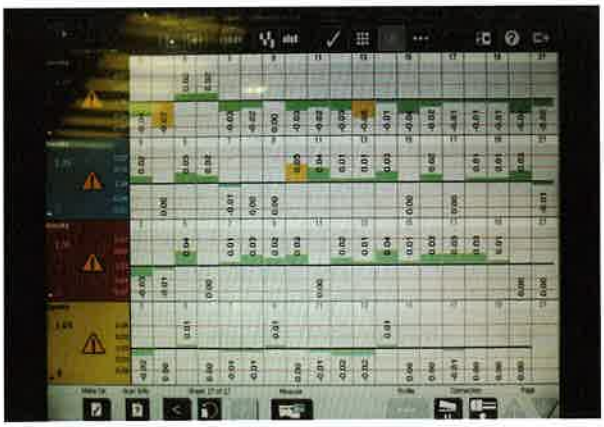

Figure 2: Spatial uniformity across the sheet as displayed by IntelliTrax

3. Controlling color

When spectral reflectance data are collected, we can compute Status T (D_T) density per CGATS.4. We can compute spectral (D_{nm}) density at the wavelength having the maximum light absorption. As shown in Figure 3, the wavelength with the maximum absorption for cyan ink is at 630 nm; the wavelength of the magenta ink is at 570 nm; and the wavelength of the yellow ink is at 430 nm. We can also compute metric chroma (C*) from the spectral data per CGATS.5. The question we want to answer is, "Which metric provides the best signal for detecting process change?"

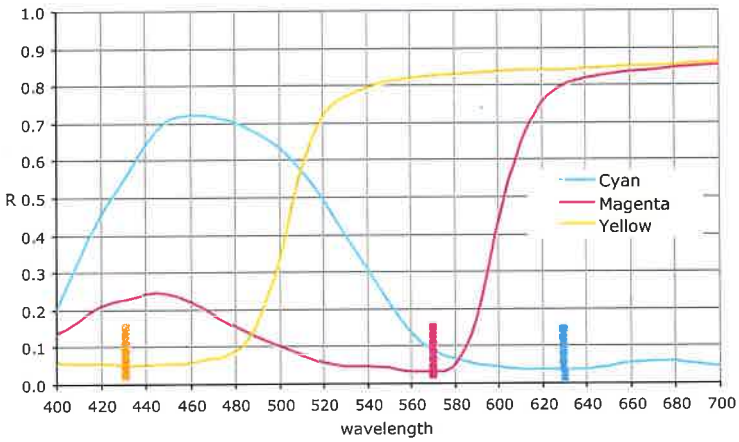

Figure 3: Spectral reflectance curves of process inks

In this study, we answer the above question by (1) selecting an ink film thickness (IFT) from the drawdown sample that matches the colorimetric aim point closest as the new reference, (2) calculating ΔD_T, ΔD_{nm}, and ΔC* between the new reference and a range of ink film thickness of interest, and (3) studying the linearity and magnitude of change for each of the three metrics.

4. Assuring process quality

Printing specifications only provide aim points and tolerances. Press make-ready only provides evidence of initial conformance. Neither the specification nor the make-ready stipulates the spatial uniformity and the temporal consistency of the entire press run. In this study, we measure a pre-determined CMY chromatic gray patch over the width of the press sheet and over time to document the uniformity and the stability of the press run.

4. Results and discussions

Below are results with discussions relative to major findings and experiences gained in ink verification, press make-ready, process control, and press run quality assurance based on colorimetric analyses.

1. Ink verification

Figure 4 shows color difference as a function of relative ink film thickness. We collected multiple measurements from the drawdown sample plus trend lines in order to smooth out the noise. Notice that ΔE values at the ink film thickness at 5.5 relative IFT are less than the allotted tolerance of 5 ΔE for all three inks. This provides evidence of ink conformance.

Even though we did not know the exact ink film thickness, we know that the grind gauge block indicating the ink film thickness at 5.5 μm has been split twice. The first ink split is between the gauge and the blanket and the second ink split is between the blanket and the paper. Assuming that the ink split ratio is 45:55, the resulting ink film thickness is 5.5 x 0.45 x 0.45 or about one μm.

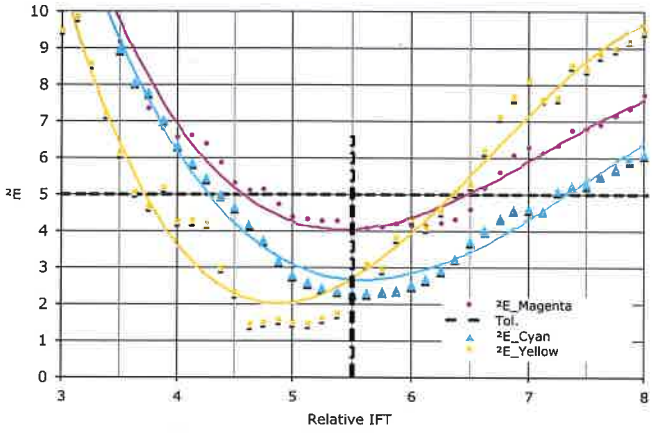

Figure 4: Color difference as a function of relative ink film thickness

Conformance to ink specification is the first step in implementing printing process control by colorimetry. Measuring ink drawdown samples with a spectrophotometer and the prescribed ink verification method in-house encourages us. We can extend the ink verification method to verifying spot color accuracy prior to the press run.

2. Colorimetric conformance

Putting the correct amount of process inks quickly and accurately is the goal of press make-ready. ISO 12647-2 stipulates a window of 5ΔE for CMYK solid plus RGB overprints as the conformance rule. As shown in Table I, all solid ink patches, except the (M + C) blue overprint, are in conformance. Achieving correct overprint color is a printability issue, e.g., adjusting ink sequence or ink tack. The tolerance of 5 ΔE on primary chromatic inks may be used strategically to encourage conformance of two-color overprint RGB colors.

Table I: Colorimetric conformance of process color printing

ID	Location	K	C	M	Y	²Eab
1	A1	0	100	0	0	1.8
2	A2	0	0	100	0	2.5
3	A3	0	0	0	100	4.1
4	A4	0	100	100	0	7.8
5	A5	0	100	0	100	2.1
6	A6	0	0	100	100	4.3
25	B12	100	0	0	0	3.1

In addition, current ISO 12647-2 also stipulates that tonal value increase (TVI) of each of the tonal ramps be conformed. TVI, traditionally defined densitometrically, has been redefined from using tristimulus values in ISO 12647-1. We find the TVI aspect of the printing standard confusing, adding no value, and is difficult to implement.

Instead of using the seven solid ink patches and TVI as conformance criteria, we propose the use of metric chroma (C*) to calibrate tonal ramps of CMY via transfer curves. Figure 5 shows the magenta gradation in terms of C* between the initial press run and the ISO 12647-2. For the black printer, Darkness (100 - L*) can be used to calibrate the black ramp.

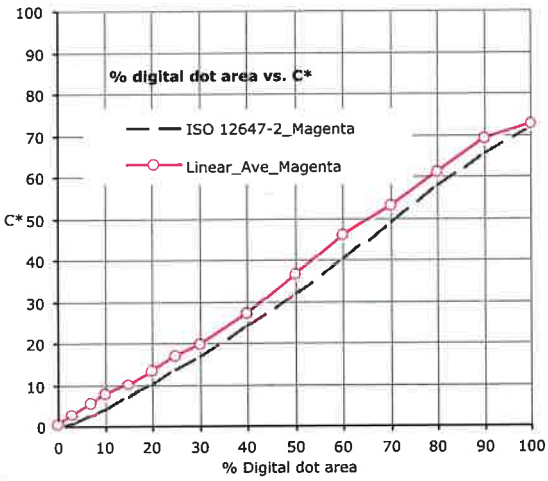

Figure 5: Magenta gradation in terms of C (left)*

To answer the question of colorimetric conformance, we compare a significantly larger number of color patches instead of the seven solid ink patches as specified in the current ISO 12647-2 standard. TVI should be eliminated from being a part of the standards because TVI is a calibration issue, and not a conformance issue.

As an example, color differences of the IT8.7/3 basic data (182 patches) between the OK sheet and that from FOGRA39 where ISO 12647-2 aim points are compared. Figure 6 shows the CRF of ΔE between the two data sets. As a rule of thumb, process conformance threshold (the gray dotted line) is when the median ΔE is 3, the 90 percent tile ΔE is 6, and the maximum ΔE is 12 [Chung, 2001]. In Figure 6, the median ΔE is at 4 which exceeds the conformance threshold. This is where printing conformance just missed out; color image differences are visually noticeable if press sheet were compared with the standard press sheet.

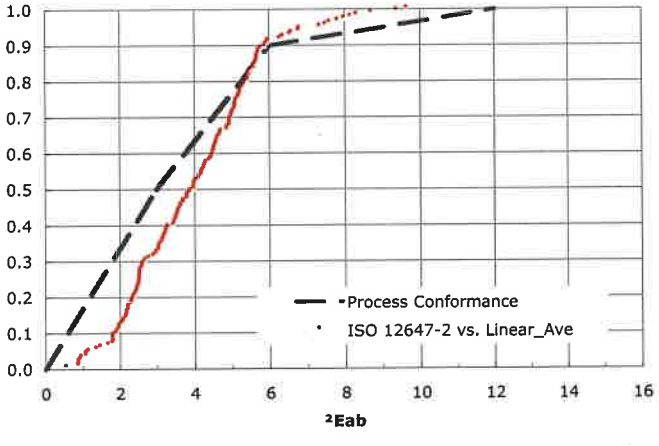

Figure 6: CRF of ΔE based on IT8.7/3 basic

3. Process control metrics

Regarding the choice of metric for printing process control, Figure 7 is graph of ΔD_T, ΔD_{630}, and ΔC* as a function of ΔIFT for cyan ink. Here, the status T density has a linear response to changes in cyan ink film thickness. Spectral density is only sensitive to changes in high cyan IFT region and metric chroma (C*) is only sensitive to changes in low cyan IFT region. Status T density would be the metric of choice for cyan inking control.

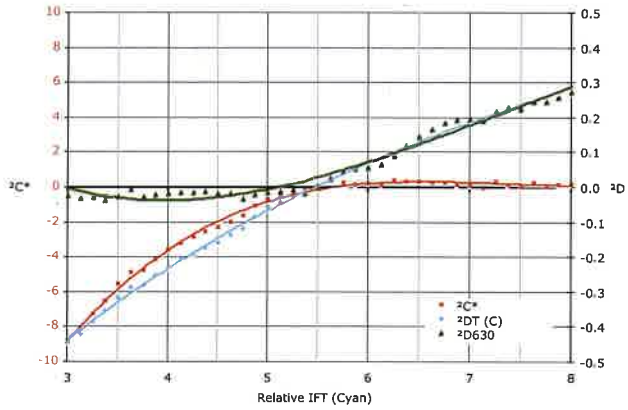

Figure 7: Three metrics in detecting changes in cyan ink film thickness

Figure 8 is graph of ΔD_T, ΔD_{570} and ΔC^* as a function of ΔIFT for magenta ink. Here, all three metrics are linear and behave similarly to changes in magenta ink film thickness. Any one of the three metrics would be useful for magenta inking control.

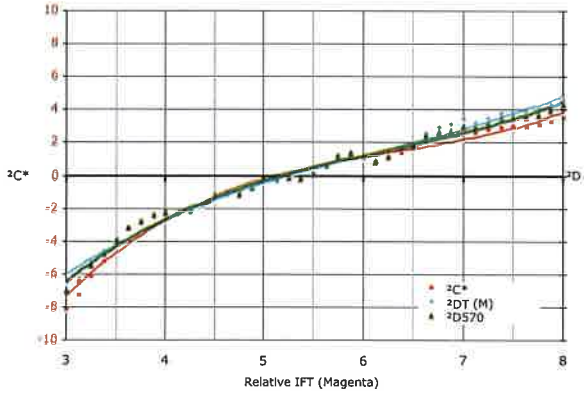

Figure 8:Three metrics in detecting changes in magenta ink film thickness

Figure 9 is graph of ΔD_T, ΔD_{430}, and ΔC^* as a function of ΔIFT for yellow ink. Here, all three metrics are linear to changes in yellow ink film thickness. The slope of the spectral density of yellow ink is higher than that of the status T density. In addition, metric chroma has the largest change in yellow ink in comparison to the same range of ΔIFT in cyan and magenta inks. Thus, status T density is the least useful metric for controlling yellow ink.

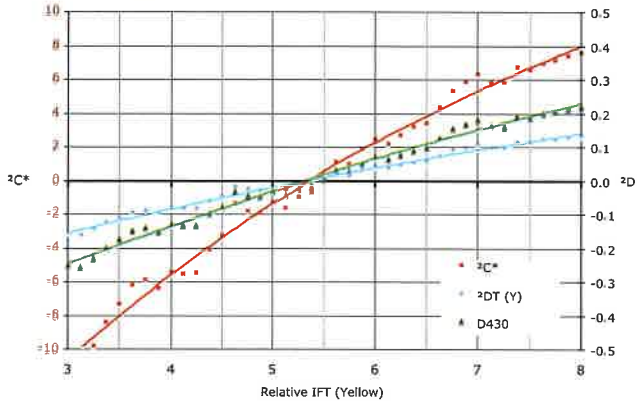

Figure 9: Three metrics in detecting changes in yellow ink film thickness

By judging from Figure 7 - 9, there is no single metric that demonstrates the best sensitivity and linearity over the ink film thickness of interest for all three chromatic process inks. If process control is implemented in a closed-loop environment, different metrics may be used without human intervention.

4. Printing quality assurance

Instead of assuming that inking is uniform across the sheet, we can investigate the spatial uniformity of the printing system. The spread of the data from its average can then be compared with the tolerance. In this case, we measured a chromatic gray bar plus a black tint across the sheet relative to its average (Figure 10). Notice that there is larger variation at either edge of the sheet. The data could have been removed from the analysis if this is the trim or non-image area of the sheet. While ISO 12647-2 specifies that variation of CMYK solids should be less than 4 ΔE, the spatial uniformity of the printing system, based on 3-color neutrals or black tints, is around 2 ΔE units.

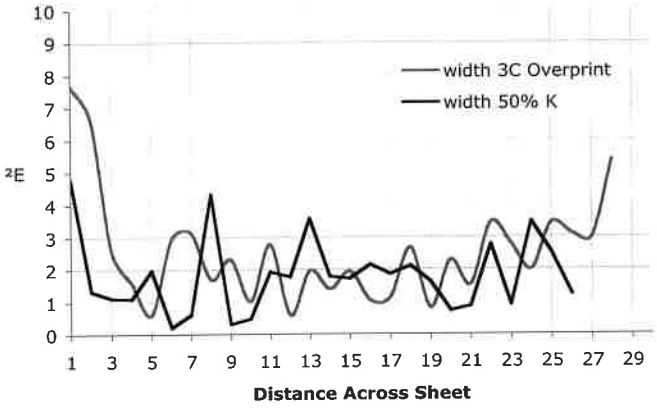

Figure 10: Spatial uniformity as assessed by 3-color gray and black tint

Instead of assuming that process does not drift after its make-ready, we investigate how to document the temporal consistency of the press run. Quality assurance of a press run begins with sampling and measuring multiple press sheets collected over time. We can depict the temporal consistency of a press run by depicting the colorimetric variation of a chromatic gray patch. If the chromatic gray is pre-determined, e.g., 75C, 63M and 60Y, the spread of the data points in a*b* diagram as shown in Figure 11, may be off-centered. In this case, the tighter the spread is, the more consistent the printing process is.

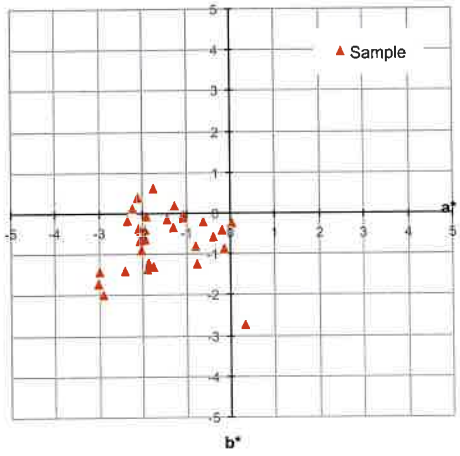

Figure 11: Temporal consistency of a chromatic gray patch

5. Summary

Density-based printing standards and using densitometry in the pressroom have facilitated color consistency since 1970s. As the demand for colorimetric accuracy and consistency in process color printing continues, it is

inevitable that CIELAB-based printing standards will become the norm. Not only densitometers will be replaced by spectral-based color measurement devices, all density-based specifications, including TVI, will be replaced by colorimetric parameters.

We explored the use of colorimetry for ink verification. Since density only specifies ink amount and not color, colorimetry is here to stay. We explored the use of colorimetry for achieving printing aims. Since printing aims are specified colorimetrically, colorimetry is essential for implementing standard-based printing. In addition, the knowledge of the prepress for gradation adjustment and the knowledge of the press are essential to achieve closer printing conformance.

We explored three metrics (status T density, spectral density, and metric chroma) as process control parameters, we did not find a single metric suitable for monitoring all three process inks significantly better than other metrics. Finally, we looked at how a press run may be certified to assure its spatial uniformity and temporal consistency with the use of colorimetry. The results have been encouraging, but more work and user feedback are necessary.

Acknowledgments

The author wishes to thank members of the RIT's Color Printing Outreach team and the Printing Applications Laboratory for their collaboration and implementation of the press run. He also wishes to express his sincere appreciation to Bill Birkett and David McDowell for their review of the paper.

References

[1] ISO 12647-1:2004, Graphic technology - Process control for the production of half-tone colour separations, proof and production prints - Part 1: Parameters and measurement methods

[2] ISO 12647-2:2004, Graphic technology - Process control for the production of half-tone colour separations, proof and production prints - Part 2: Offset processes

[3] ISO 2846-1: 2006, Graphic technology - Colour and transparency of ink sets for four-colour-printing - Part 1: Sheet-fed and heat-set web offset lithographic printing

[4] Chung, R. and Shimamura, Y. 2001 "Quantitative Analysis of Pictorial Color Image Difference," TAGA Proceedings, pp. 381 - 398

Influence of paper and printing process on the visual perception and colorimetric characteristics of newsprint

Timothy C. Claypole, Eifion H. Jewell, Nigel Wells[1], Paul Casey[2]

Welsh Centre for Printing and Coating
School of Engineering, University of Wales Swansea
Singleton Park, Swansea SA2 8PP, UK
E-mail: t.c.claypole@swansea.ac.uk

[1] Virtual Industrial Marketing

[2] Sun Chemicals

Abstract

There is increasingly intense media and revenue competition for the newspaper industry. Adding value to newsprint by improved substrate or printing process is seen as a way of attracting higher revenues or achieving product differentiation. VAPoN is a Print City sponsored cross industry project evaluating the Value Added Printing of Newspapers. A bespoke eight-page sample was printed on five different newsprint substrates with a combination of cold and heat set inks. These was assessed visually and the results compared with quantitative colorimetric measurements obtained sphectrophotometrically and using bespoke software to obtain the gamut from scanned images. A direct correlation was found between the value added and both the chroma of individual colours and colour gamut of the printed product. This relationship will allow the direct assessment of the fiscal benefit of using improved newsprint substrates and heat set offset printing compared with traditional newsprint.

Keywords

Colour, gamut, newsprint, offset, visual assessment

1. Introduction

There is increasingly intense media and revenue competition for the newspaper industry. Adding value to newsprint by improved substrate or printing process is seen as a way of attracting higher revenues or achieving product differentiation. VAPoN is a Print City sponsored cross industry project evaluating the Value Added Printing of Newspapers. Market research has indicated the following as means of producing innovative and differentiated newspaper products:

1. High impact cover pages without marking;
2. Special interest editorial supplements;
3. High impact ROP advertising pages;
4. Pre-printed advertising inserts;
5. Magazines & guides;
6. More & better colour;
7. Upgraded paper;
8. Multiple versions of same newspaper;
9. Reader-market profile drives format, binding, paper & process.

Means of achieving these are through pre-press, such as alternative screening technologies, improved materials, post press such as stitching and inserts and changing formats. Equipping a newspaper paper press with a dryer enables the press to be used to print commercial work, magazines, directories & some newspaper products, thus allowing better utilisation of the press.

In order to study the impact of ink printing method and substrate, a bespoke eight-page sample was printed on five different newsprint substrates with a combination of cold and heat set inks. A cross section of the industry from production to purchasing drawn from four continents visually assessed each sample using standard newsprint printed with coldset inks as the base reference. In parallel, the physical characteristics of

the prints such as the colorimetric properties were measured. This paper reports the findings of the visual assessment and compares them with the colorimetric characteristics of the print. These are discussed in the context of an associated questionnaire completed by those completing the assessment on the future developments for newsprint. This was undertaken for comparison to the perceptions described above.

2. Visual assessment

An eight page supplement with images and text designed to represent a newspaper supplement were produced at the DELO printing plant in Ljubljana, Slovenia. The cold set on a Mann Roland Colorman press and the heat set on a Mann Roland Uniset press. Production quality control during the trials was carried out by IFRA, as a body independent of the manufacturers and suppliers involved in the trial. Five different papers were printed by heatset or coldset to give seven samples sets for visual comparison (Table I). Standard newsprint printed cold set was used as the reference paper.

Table I: Paper grades and print processes used

Paper	Heatset	Coldset
54 gsm LWC printed	X	
54 gsm SC-B ISO 67 printed	X	
52 gsm Matt C (VAC) ISO 80 printed		X
45 gsm Improved Newsprint ISO 72 printed	X	X
45 gsm Standard Newsprint ISO 58 printed	X	X

The visual assessment and questionnaires was completed by 77 participants from 13 countries. While it is unrealistic to split the responses into countries, the responses were analysed in terms of the geographic groupings of Europe (non Scandinavian), Eastern Europe, India, North America and Scandinavia. Most of the respondents (over 90%) were companies producing daily newspapers, with over 60% also producing supplements. The visual assessments were performed in the field, by a variety of personnel; generally at the production site. Whilst realising the limitations of the conditions under which the assessment was performed, the assessments should give a reasonable estimate of trends and relative value of the prints produced.

The survey was analysed in terms of the professional responsibility of the person completing the questionnaire. There was a similar distribution of the professional responsibility of those performing the visual perception across all five geographic groups allowing meaningful results to be obtained. The professional groups to reflect the different interests as a customer (advertising), owner (publisher) and production.

- ◊ Advertising (newspaper advertising sales, newspaper marketing, advertising agency and purchaser of advertising space) - 27 questionnaires.
- ◊ Publisher (newspaper publisher/general manager, newspaper editor) - 12 questionnaires.
- ◊ Production - 32 questionnaires.

There are several features related to production and quality that were considered to have the potential to differentiate newspaper products. Those surveyed were asked what would be most important in the future, ranking the responses from low through medium and high to very high (Figure 1). The most important development for the future would be more four colour pages. This was rated as high or very high by over 80% of the respondents and was ranked "very high" by most Europeans. Quality of the front and back pages were also seen to be quite important.

Some respondents also saw the printing of magazines and advertising to be important, though this was not a view universally shared. However, the potential for a trend to newspapers becoming more like magazines was seen by most to be unlikely.

The most important future features were examined for each region by combining the "very high" and "high" scores for each professional grouping. There are some distinct differences between the future expectations of the advertising, publisher and production groups (Figure 2) that reflect their expectations and interests. The

quality of the front and back page were more important to the advertising group, they felt the ROP (Run of Paper) paper grade and print quality was, at their highest score of over 80%, twice as important as was thought by production. The publishers and production felt more four colour pages was the most important future trend, probably because of the implications for production. More compact form was of least consequence to the advertisers, compared to the publishers and production. This infers it does not effect their perception of the news papers, whilst a compact form is of commercial cost significance to the other group. The advertising group also rated the importance of printing supplements far higher than production or the publishers.

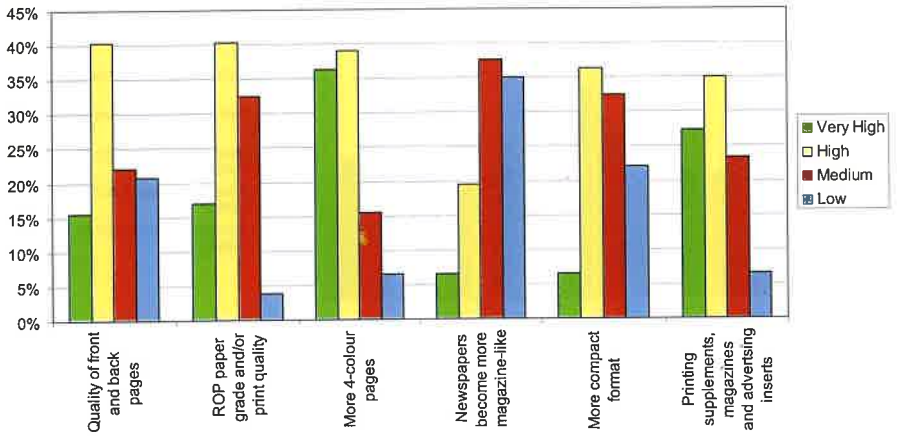

Figure 1: Future expectations in answer to the question "In your opinion how important will the following be in the future?"

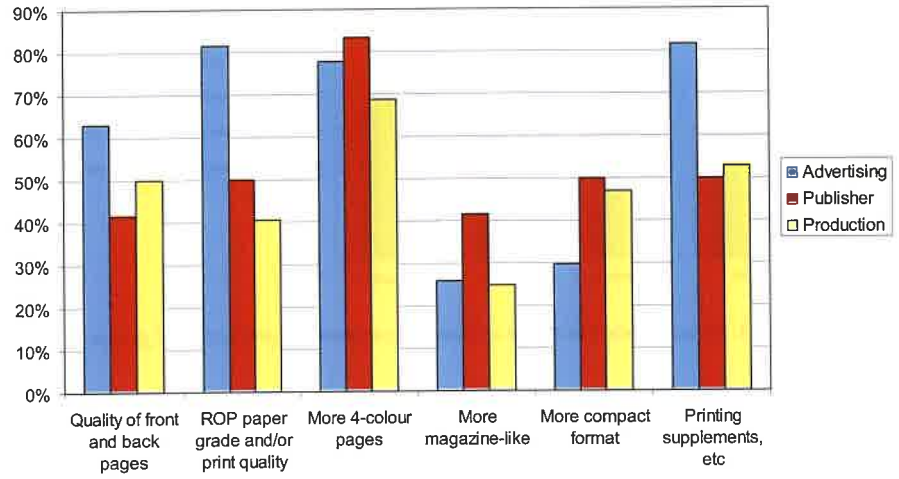

Figure 2: Most important future features by professional group

The papers were being ranked in ascending order of quality, i.e. starting with the base reference paper, successive rows in the form represent the paper quality improving. The papers were ranked by awarding 7 as the top score, even if only one paper was ranked higher than the base reference paper. On this basis 54 gsm LWC printed Heatset and 54 gsm SC-B ISO 67 printed Heatset papers achieved the best results (Figure 3).

There were some regional variations when the results were analysed in of the geographic groups. The 52 gsm matt C (VAC) printed coldset, rated highest by the Eastern European group and place second by the Scandinavian group. The European and the Indian groups rated the papers in descending paper weight and in quality from heatset to cold set. A similar trend is also seen when the results are analysed in terms of professional groups for the printers and the publishers (Figure 4). This could reflect the print knowledge of these groups influencing their perception. The advertisers ranked the 52 gsm matt C (VAC) printed coldset second highest and almost as high as the 54 gsm LWC printed Heatset samples.

As not all papers were rated better than the base paper, another analysis is to look at the number of highest scores (7's) through to the lowest (1's). The paper 54 gsm LWC printed Heatset was seen to be the best with the highest number of times. Paper 54 gsm SC-B ISO 67 printed Heatset had a reasonably score predominantly by the number of times it was ranked second and received 6 points. Similarly, paper 52 gsm Matt C (VAC) ISO 80 printed Coldset had most third places. Thus, despite the concerns with regard to the visual assessment, the results would appear to be consistent.

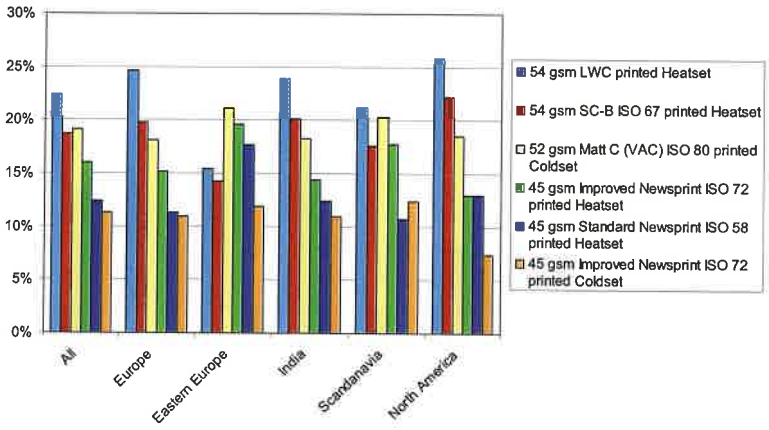

Figure 3: Paper ranked in terms of visual assessment in geographic groups

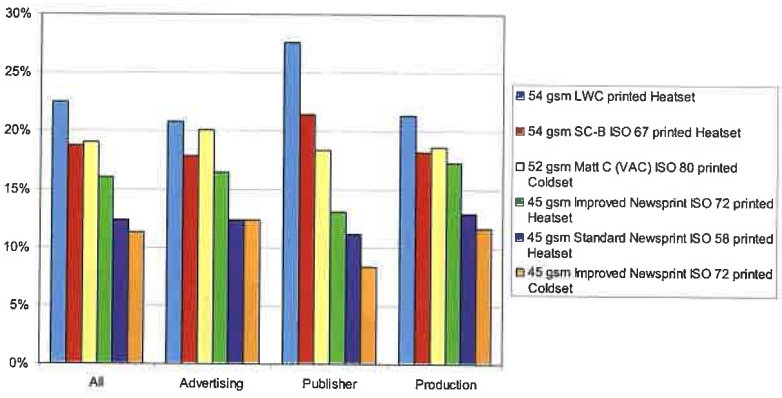

Figure 4: Paper ranked in terms of visual assessment in professional groups

The visual ranking of the prints only gives the order of merit. However, each of those completing the assessment were asked to estimated the percentage sales premium for ROP for products using value added newsprint (Figure 5). The average, maximum, minimum and range are show below as percentage price more than the base paper (Table II). The average over standard newsprint for the 54 gsm LWC printed Heatset was 34%, but this value had a large range. The advertising professionals (purchasers), would be prepared to pay only half the premium the publishers (sellers) feel the improved product could command (Table III).

Table II: Additional amount (% of base paper rate) the additional quality might command

Paper	Average	Max	Min	Range
54 gsm LWC printed Heatset	34	200	-15	215
54 gsm SC-B ISO 67 printed Heatset	23	100	-30	130
52 gsm Matt C (VAC) ISO 80 printed Coldset	20	80	-5	85
45 gsm Improved Newsprint ISO 72 printed Heatset	12	60	0	60
45 gsm Standard Newsprint ISO 58 printed Heatset	9	45	0	45
45 gsm Improved Newsprint ISO 72 printed Coldset	6	50	0	50

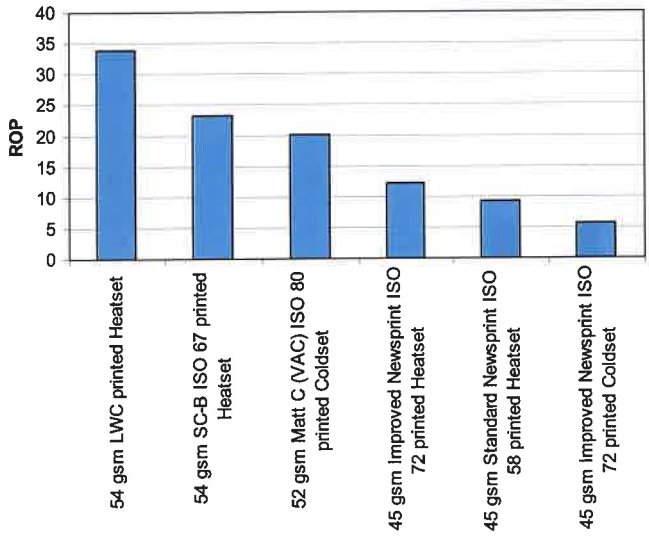

Figure 5: Percentage sales premium for Run of Paper (ROP)

Table III: Additional amount (% of base paper rate) the additional quality might command by professional group)

Paper	Advertising	Publisher	Production
54 gsm LWC printed Heatset	29	56	28
54 gsm SC-B ISO 67 printed Heatset	19	37	20
52 gsm Matt C (VAC) ISO 80 printed Coldset	19	24	17
45 gsm Improved Newsprint ISO 72 printed Heatset	12	15	11
45 gsm Standard Newsprint ISO 58 printed Heatset	9	10	8
45 gsm Improved Newsprint ISO 72 printed Coldset	7	6	4

3. Print characterisation

The whiteness of the substrates used in the trial does not directly correlate with the ranking of the visual assessment (Figure 6). The 54 gsm LWC is the whitest, but the second ranked paper, the 54 gsm super calendared is only as white as the improved newsprint. The difference between the whiteness measured over white and over black gives a measure of the opacity. In this case the LWC paper is the least opaque, while the standard newsprint is the most, the complete reverse of the ranking. This suggests that opacity and hence show through is not considered a major issue in print quality.

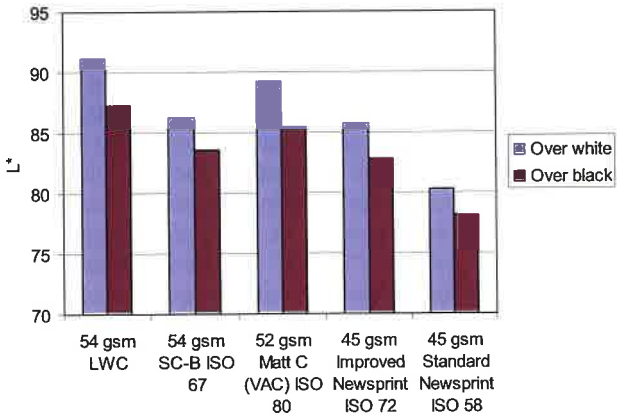

Figure 6: Paper whiteness

The gloss of the two best performing prints is far higher than the other paper grades (Figure.7). This would suggest that the paper gloss is more important. However, when one considers the inks there is not such a clear correlation. The two highest ranked prints have high ink gloss, whilst the two lowest ranked prints have the next highest ink gloss.

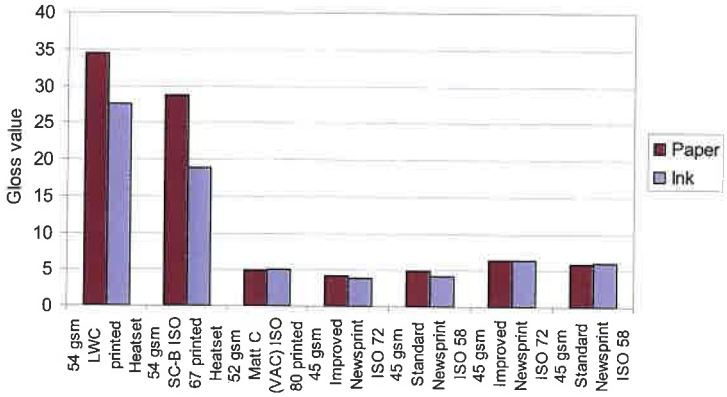

Figure 7: Substrate and ink gloss

As the prints contained no formal test targets, the chroma of the printed inks was assessed by measuring with a spectrophotometer in selected solid areas of flat tone where there was no colour printed on the reverse side (to prevent the results being influenced by show through). Four patches met this criteria, two of which, a yellow and a red, were strongly saturated colours. All the patches show a correlation for higher chroma with ranking of the prints (Figure 8).

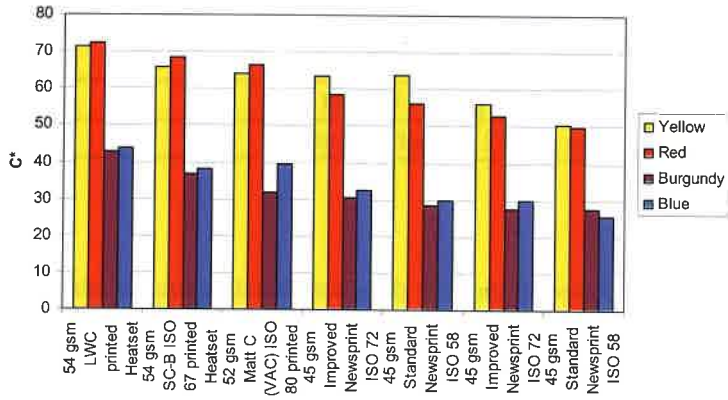

Figure 8: Ink chroma for selected areas on the different test prints

Selected images on the print were scanned and using bespoke software, the colour gamut for the each image on each substrate was obtained. The location of each pixel in the image was used to establish the largest chroma in arcs of 5° hue angle. These were then plotted in $a^* b^*$ colour space. In order to obtain the full gamut then it was necessary to evaluate several images, as the gamut obtained was highly dependent on the image. Each image was selected to try to ensure an overall coverage of the full colour space. In each case, the size of the gamut corresponded with the preferences expressed by the panel. The gamut from all the images were combined to establish the full gamut of the images on the newsprint (Figure 9). The gamut of the standard newsprint has a reasonable correlation with the "SNAP" standard, whilst that of the LWC coated printed heatset corresponds with the "SWOP" in the yellow-red, red-blue quadrants. However, despite the images that were scanned for their green content ("cyclists" and "lime bike", the gamut in the green yellow quadrant is less than "SWOP". These results highlight the difficulty in using half tone images to obtain the gamut, in that there are few saturated colours. However, the results obtained by this method will allow qualitative assessments of the printing process for quality control and development purposes. The rank obtained from the visual assessment corresponds with the progressive enlarging of the printed gamut. The two best performing ink and paper combinations having the widest gamut. The two heat set inks printed on the standard and

improved newsprint produce the next widest gamut, which is of a similar size to the cold set ink on 52 gsm stock. The cold set ink on 45 gsm newsprint (standard or improved) produces the smallest gamut.

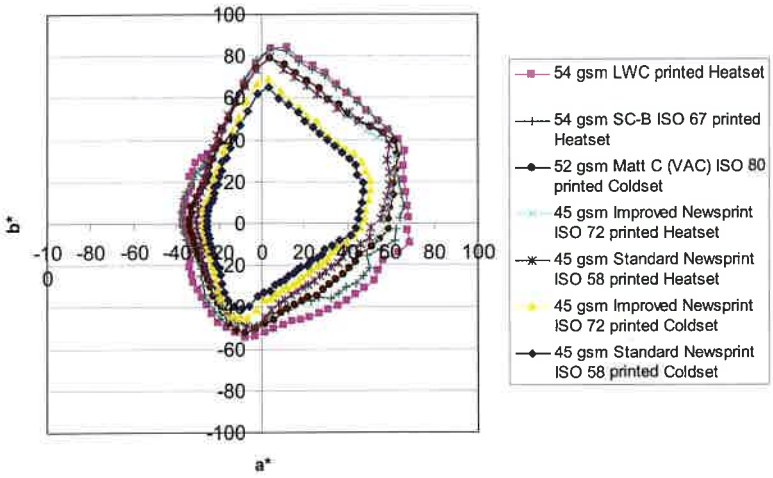

Figure 9: Combined Colour Gamut of image for the different prints

There is a direct correlation between the chroma of added value of the improved newsprint products and the additional amount those who performed the assessment were prepared to pay. In Figure 11, the percentage the assessor would have been prepare to pay is plotted against the chroma of the four colours assessed on each print. The correlation coefficients in each case for the linear fit to the data is over 0.9, indicating a strong relationship between the parameters. There was a difference between the sellers and buyers (publishers and advertisers), in that a linear relationship was obtained between chroma and added value in both case, except the publishers expected the purchaser to pay almost twice what the advertisers expected to pay for the same quality of print.

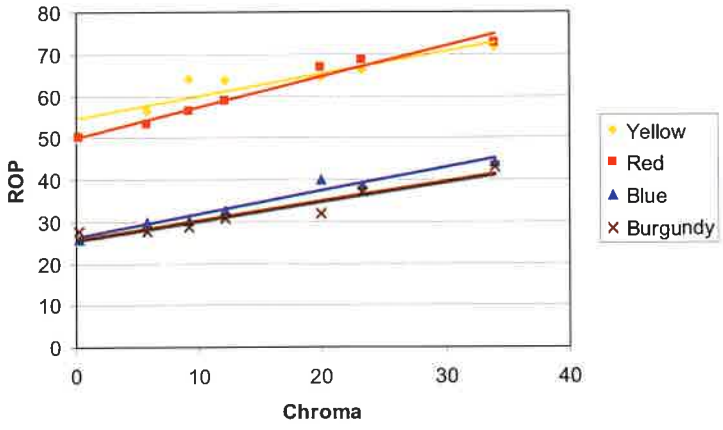

Figure 11: Chroma vs. Percentage sales premium for Run of Paper (ROP)

4. Conclusions

The assessors thought the most important development for the future of newsprint would be more four colour pages and the quality of the outside pages. There is a tendency for the perceived improvement in the newsprint to reflect an increase in paper weight and also a preference for heatset over coldset. A marked contrast was found in the results of the professional groups. Those who purchased advertising tended to make a more subjective assessment compared to those who produced prints who tend to evaluate the prints from a more technical perspective. There is a distinction between the advertising who tended to purchase and the publisher who can be viewed as the seller, the latter expecting a higher rate of return for the improvements compared to the buyer.

The results of the visual perception analysis and associated questionnaire have been compared with physical measurements of colour that were obtained on the prints. This has involved using bespoke software to gather data from scanned printed images. This has highlighted the difficulties in obtaining the gamut from half tone images, but has proved to be sufficient for process development and quality control. A direct correlation was found between the value added and both the chroma of individual colours and colour gamut of the printed product. This relationship will allow the direct assessment of the fiscal benefit of using improved newsprint substrates and heat set offset printing compared with traditional newsprint.

Acknowledgements

The authors wish to acknowledge the financial support of Print city for this work. In particular the VAPoN project sponsors Adphos-Eltosch, MEGTEC, MAN Roland, Sun Chemical and UPM. Also to acknowledge the support of IFRA in running of the press trial. Also, James Claypole, Swansea Printing Technology for the analysis of the survey and print measurement.

Improved proofing method for postage stamps

Erzsébet Novotny

Papír- és Nyomdaipari Műszaki Egyesület (PNYME)
H-1027 Budapest, Fő utca 1, Hungary
E-mail: novotny@any.hu

Abstract

Colour Management System requires constant and sophisticated maintenance. Challenges crop up every day for printers: new materials, new devices, higher quality demand of customers for contract proofs. At the contract proofing of the postage stamps the digital proof and the paper differ significantly from the point of luminescence. The proof is highly brightened, while the print substrate is lightly brightened optically or not brightened at all. The visual difference causes serious problems in connection with the production due to the yellow shades of pressroom print. We decided to use a UV-emission filter for the colorimetry of proof calibration to stamp paper. It was suggested for this type of problem, however the exact kind of colour modification caused by using it for stamp papers was not known. At the State Printing Company we had made proofs using the ICC profiles of real operating conditions printed test charts. The test charts were printed on two types of stamp papers: Shil and Tropimatic. The proofs were measured with a UV-emission filter and without this filter by the SpectroScan measuring instrument; for our examinations we used the dates given by the ProfileMaker software package. The aim of these examinations was to compare ΔE values of two different methods and to evaluate the comparison. We concluded that it is necessary to-, and worth-, improving the perceptual colour rendering with appropriate (modified) ICC profiles for better (within the tolerance) quality.

Keywords

Digital proof, security stamp paper, UV emission filter

1. Introduction, the objectives of the research

New materials, design technologies and colour rendering requirements represent great challenges for printing companies producing postage stamps. The key issue of today's printing tasks is whether colours appearing on the displays of a stamp designer and colours determined by post offices are the same on all devices of the manufacturing. Moreover, the customer must have a subjective impression when looking at the printed colours that they are "original-like" prints.

The Colour Management System, - which encapsulates pieces of information into the software system of the colour image processing received from each input and output device -, offers an overall solution to these problems.

We have used colour management with stamp production for many years. Our aim was to ensure correct and predictable colour reproduction through harmonizing our devices and security stamp papers with different characteristics. In spite of using colour management we realised that there was sometimes a significant difference - especially in the highlights, due to the shades of yellow - between the contract proof and the press-room prints. We therefore had to correct the ICC profiles at the CtP device then make new printing plates, which required a new press set up and resulted in high costs.

The reason of our problems was hidden in the materials which we used in contract proofing and in the features of the stamp paper.

The postage stamps are printed on special paper which is glued or self-adhesive, may consist of safety fibres, and has a low level of optical brightening.

Approval of stamp design-reproduction is implemented through digital proofs before printing, just like with our company's other products. We use the same proof paper (Fuji IPPSG) for approval of every type of product and for economical production. However, in the case of stamp paper, the digital proof and the substrate of print differ significantly from the perspective of luminescence. The proof is highly brightened,

while the print substrate is lightly brightened optically, or for example, the security stamp paper is optically not brightened at all. (Figure 1) This visual difference causes serious problems in contract proofing, in ICC profile making and also in the pressroom.

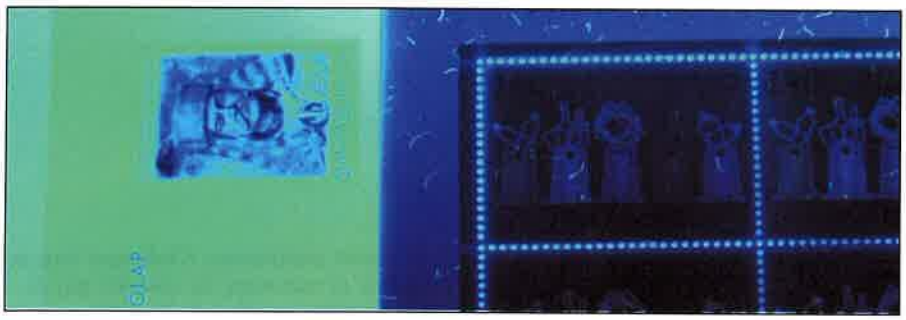

Figure 1: Proof (left) and postage stamps printed on special stamp paper (right) by UV-including radiation

Practice in digital colour management generally suggests the usage of a UV emission filter for the colorimetry of the proof's test charts. However, it is not known what level of colour modification is caused to the system by UV emission filters as regards to stamp paper, or how it will change the colour rendering and colour gamut.

We had to look for an answer to this issue with our investigations.

2. Research methods

Firstly, we studied the influence of optical brightening since optically brightened proof paper shows a high level of luminescent radiation while the stamp paper shows a low level (Figure 1). We examined the reflection spectrum of coated and uncoated stamp paper with a spectrophotometer and chose the ones from both types that had the lowest level of luminescent radiation (Figure 2).

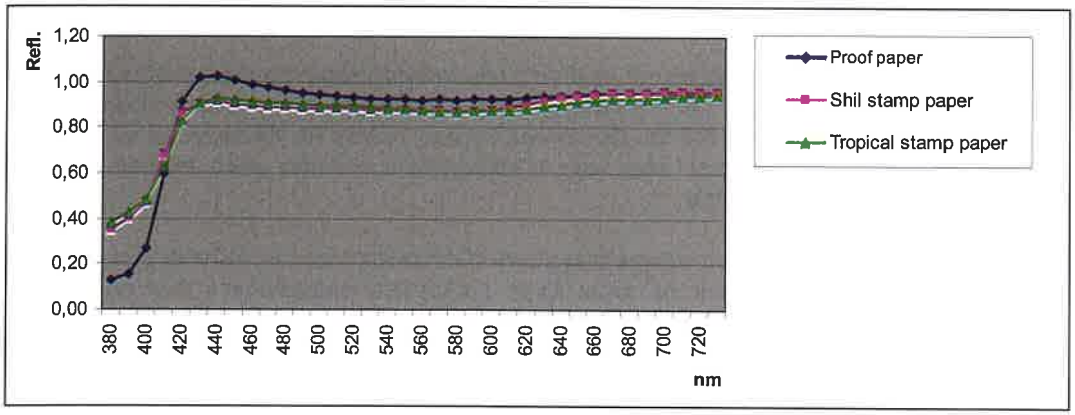

Figure 2: Reflection curves of different types papers (Fuji IPPSG proof paper, Shil and Tropimatic stamp papers)

Following this we made - using the Epson Stylus Pro 4000 Proof-Printer - proofs with ICC profiles of real operating conditions printed TC 6.02 CMYK test charts. The test charts were printed on the chosen two types of stamp paper: Shil and Tropical. The proofs were measured with the UV-emission filter, then without the filter on the SpectroScan measuring instrument. The aim of these examinations was to compare ΔE values calculated from L^*, a^*, b^* values measured in two different ways and to compare the results.

We used the ProfileMaker 3.1.5 software package for our examinations, which consists of the *MeasureTool, ProfileMaker, ProfileEditor* and *ColorPicker* programmes.

MeasureTool controls the gauge implementing scanning and saves the result in a .txt file. The gauge lights the sample with D50 beam scattering and its observer scans with 45/0 scattering geometry and 2°.

ProfileMaker makes a colour profile on the basis of the measured results. It presents them in a .txt file. On the basis of the colour profile prepared by ProfileMaker custom-made for the given printing machine and paper, the graphic image can be checked visually and chromatically with ADOBE Photoshop before printing.

ProfileEditor is applied if the colour separation of the prepared colour profile doesn't match the original copy to be reproduced. This programme allows the modification of the profile. The programme can check and adjust the grey balance, colour gamut and gradation curve of the measured test chart. If the profile changes the consequent change in the artwork can be followed directly in the Photoshop programme. A monitor without colour defects must be used for the perfect colour reproduction. The colour profile can be changed until the required shades are achieved.

ColorPicker allows the implementation of manual measurements. When implementing manual measurements, the measuring block can be removed from the device and can be used independently of the testing desk.

Measuring results are given in the CIELAB colour space. When the required colour profile is preset, the programme also makes suggestions pertaining to the best CMYK components of the measured colour in the given colour space, and it indicates the ΔE value between the colour measured and the colour producible. Components of CMYK can be changed manually in order to decrease the ΔE value.

We got the highest and the lowest ΔE^* values on the basis of X, Y, Z and L^*, a^*, b^* data saved by ProfileMaker 3.1.5. In the case of the Shil stamp paper the highest value was $\Delta E^*_{max} = 3.91$, while the lowest was $\Delta E^*_{min} = 0.05$. The average of the colour differences was: $\Delta E^* = 1.41$. With the Tropimatic stamp paper these values were higher; the maximum value was $\Delta E^*_{max} = 4.17$, the lowest was $\Delta E^*_{min} = 0.05$ and the average of the colour differences was: $\Delta E^* = 1.76$ (Figure 3).

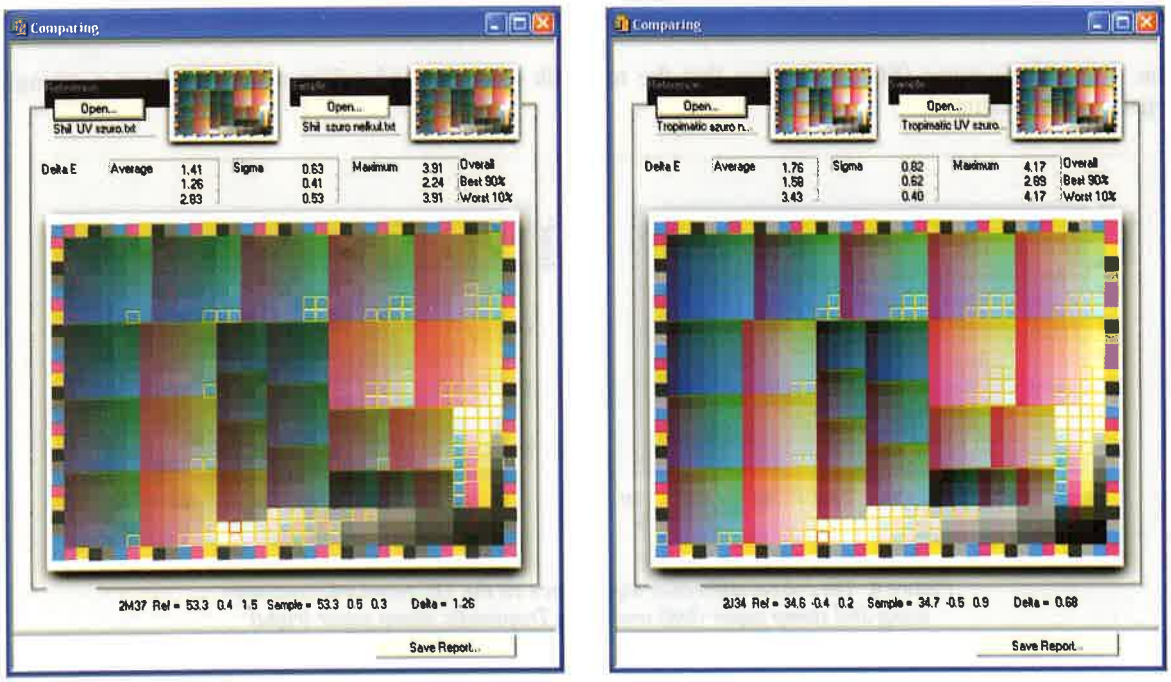

Figure 3: The greatest colour differences of proof measured with UV-emission Filter and without filter, using Shil and Tropimatic stamp paper

3. Digital proof evaluation

Firstly, we arranged our measuring results given by *ProfileMaker* software package in tables then made diagrams for digital proof evaluation.

Tables I - IV show some of the chart-patterns which have the lowest and highest colour differences as compared to total ink coverage in the case of Shil and Tropimatic stamp paper.

Table I: ΔE^* and CMYK values of fields with high total ink coverage (Shil)

Field	2A25	2J34	2K35	W21	2C27
TIC (%)	470.98	500	400	460	470
ΔE^*	0.37	0.44	0.46	0.47	0.47

Table II: ΔE^* and CMYK values of fields with low total ink coverage (Shil)

Field	O25	2L36	2I33	N25	2J34
TIC (%)	9.42	0	2.75	14.13	7.06
ΔE^*	3.91	3.89	3.85	3.84	3.84

Table III: ΔE^* and CMYK values of fields with high total ink coverage (Tropimatic)

Field	W21	X21	W22	2J25	2L26
TIC (%)	280	360	280	200	400
ΔE^*	0.09	0.33	0.28	0.29	0.16

Table IV: ΔE^* and CMYK values of fields with low total ink coverage (Tropimatic)

Field	N25	N26	P25	2L15	2K16
TIC (%)	9.4	9.4	18	0	2.7
ΔE^*	4.13	4.17	4.11	4.09	4.07

The TIC-ΔE^* diagrams (Figure 4) show that the total ink coverage and colour difference have a strongly negative relationship.

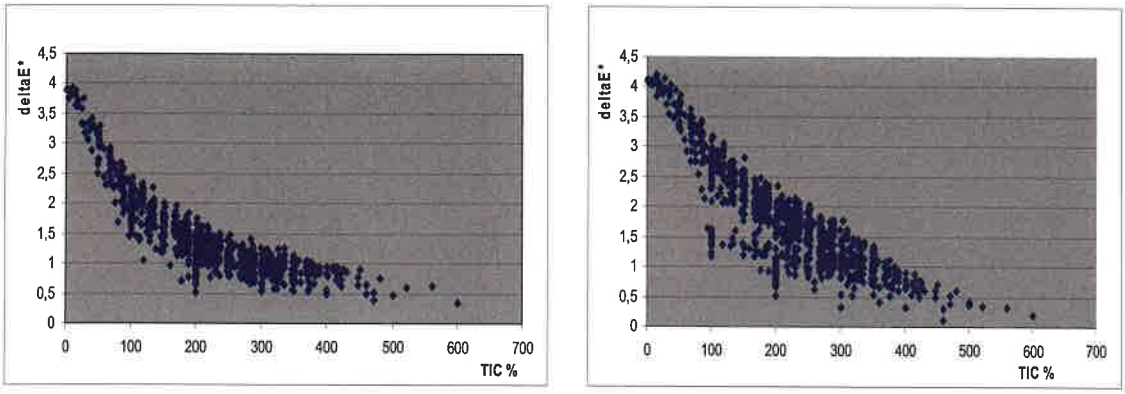

Figure 4: The colour difference dependence on the TIC (total ink coverage) using Shil stamp paper (left) and using Tropimatic stamp paper (right)

The results show that colour difference values decrease exponentially where the total ink coverage is growing. This result corresponds to our initial expectations since the effect of optical brightening of the print substrate must be necessarily higher in the case of low total ink coverage. The visual optical brightening of the substrate has less effect where the total ink coverage is higher than in the case of fields with lower total ink coverage.

Tables V and VIII contain ΔE^* and L^* values of dark and light shades of the Shil and Tropimatic stamp paper. In this case the colour difference with Tropimatic was also higher than with Shil stamp paper.

The results of Table V - VII show that low ΔE^* values belonging to the lowest L^* values belong to the fields of the dark shade. The highest ΔE^* values, belonging to the highest L^* values which belong to the fields of the lightest shades, are in Table VI - VIII.

Table V: ΔE^* values of dark shades (Shil)

Field	2A25	2J34	2K35	W21	2C27
L^*	33.89	28.01	34.99	31.23	32.56
ΔE^*	0.37	0.44	0.46	0.47	0.47

Table VI: ΔE^* values of light shades (Shil)

Field	O25	2L36	2I33	N25	2J34
L^*	92.8	96.56	94.94	93.41	96.21
ΔE^*	3.91	3.89	3.85	3.84	3.84

Table VII: ΔE^* values of dark shades (Tropimatic)

Field	W21	X21	W22	2J25	2L26
L^*	25.12	19.55	28.22	20.18	13.07
ΔE^*	0.09	0.33	0.28	0.29	0.16

Table VIII: ΔE^* values of light shades (Tropimatic)

Field	N25	N26	P25	2L15	2K16
L^*	95.95	96.92	96.21	97.64	97.62
ΔE^*	4.13	4.17	4.11	4.09	4.07

According to our L^*-ΔE^* diagrams the features of the results are similar for both kinds of stamp paper but the Tropimatic paper has the higher colour differences. The ΔE^* colour difference values increase when the metric value of brightness increases.

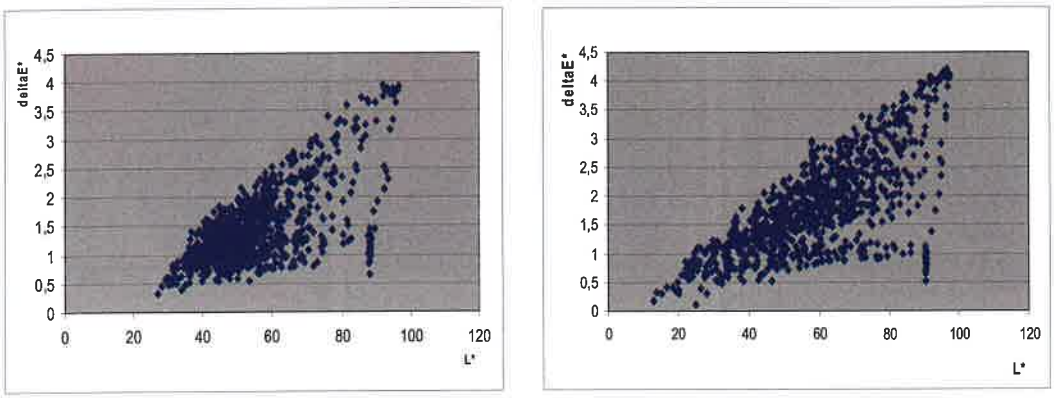

Figure 5: The colour difference dependence on the L^* metric value of brightness, using Shil stamp paper and Tropimatic stamp paper

The Figures show that depending on the growing L^* metric value of brightness, the ΔE^* values also increase. In the case of Shil paper (Figure 5, left) the values are in the interval between $L^* = 35$ and $L^* = 60$ with the highest density. Their value is in the interval between $\Delta E^* = 0.5$ and $\Delta E^* = 2.5$.

Using Tropimatic paper (Figure 5, right), the values are in the interval between $L^* = 35$ and $L^* = 70$ with the highest density. Their value is also in the interval between $\Delta E^* = 0.5$ and $\Delta E^* = 2.5$.

4. Results

The difference between the values measured with and without the UV-emission filter must be great in the case of lighter shades namely of high lightness value, since the effect of optical brightening is stronger where lighter shades are printed to the printing substrate.

It was however also important to compare the colour gamut of digital proofs measured with and without using the UV-emission filter and to check the degree of white point shifting. For a better visual comparison, all of the gamut view diagrams (xy, ab, u'v') have been examined.

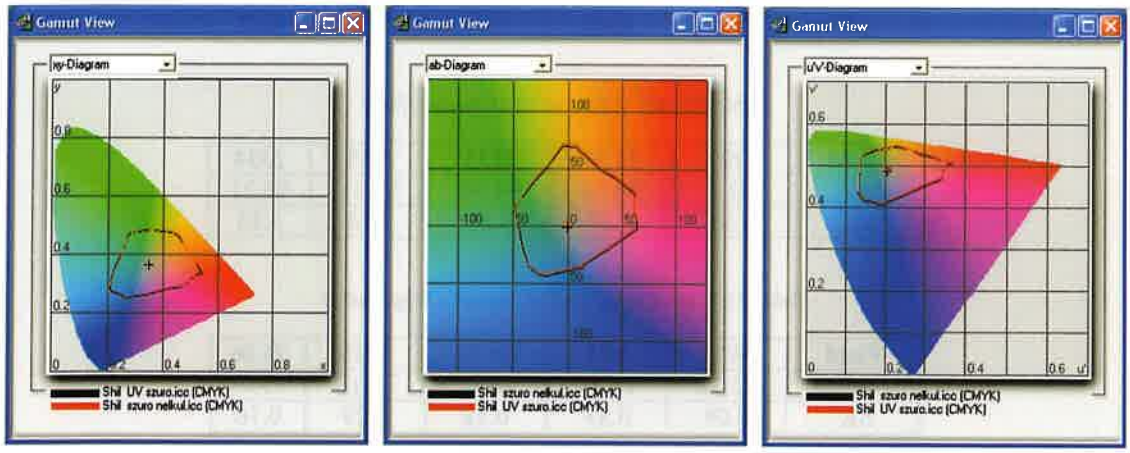

Figure 6: Colour gamuts of Shil paper's digital proof measured without UV-emission filter and with UV-emission filter

It was found that the white point is shifted significantly towards yellow direction in the case of using UV-emission filter, due to the colour transformation of the measurement method. The shape of the colour gamut also changed and the gamut itself shifted to yellow direction especially with blue and violet colours. It caused the altering of the colour of the pressroom-print by the highlights compared with the proof.

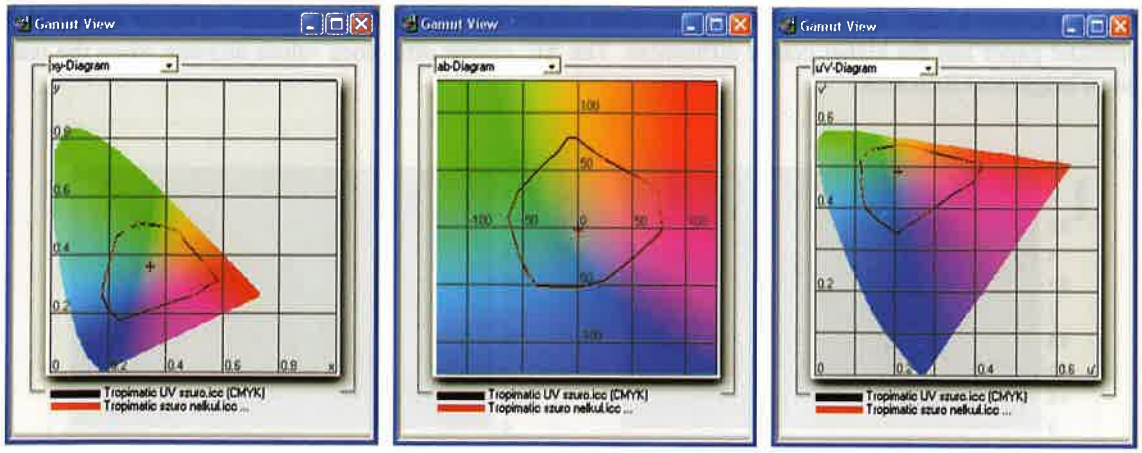

Figure 7: Colour gamuts of Tropimatic stamp paper digital proof, measured with UV-emission filter and without UV-emission filter

It is clear from the tests that if the colour fields of a test chart are printed and measured on an optically brightened digital paper when preparing the ICC profile for the proof printer, it is worth applying the UV-emission filter in order to be able to define the required colour profile with the possible greatest accuracy for contract proofing of postage stamps which are printed on low optically brightened paper. Only in this way can we avoid the yellow shades of print compared to the contract proof. Additionally, we have to use *ProfileEditor* software as the colour gamut shifting and shape altering was not uniform. The colour gamuts gained by using UV-emission filter were smaller and shifted unequally to the yellow shades (Figures 6 and 7). We checked the modification of the colour profile directly in the Photoshop programme then saved the appropriate ones. The pressroom prints later proved the correctness of this method too.

5. Conclusions

We realised that the Colour Management System requires constant and sophisticated maintenance, even though this would be expensive for printing companies.

The aim of our examinations was to compare the two different methods of colour measurement for proof calibration and to evaluate this comparison, check ΔE colour differences, and colour gamut deformation.

From our results we concluded that we have to use a UV-emission filter when measuring the test charts for proof calibration in the case stamp paper. We also have to modify the colour profiles of stamp printing technology to reach better colour rendering using the Profile Editor software. Only in this way can we achieve a better quality of colour rendering at stamp printing and reduce the colour difference between the contract proof and the pressroom prints under the tolerance-limit of our quality control system.

Acknowledgements

Special thanks to Dr. Péter Schulz and Mr. Miklós Jármai for contributing in measuring, and to the CEO of State Printing Company, to György Gyergyák for the permission of publishing this paper.

References

[1] Malacara, D.: Color Vision and Colorimetry, Theory and Applications, SPIE Press, Bellingham, WASINGTON, 2002

[2] http://www.color.org

[3] Kutasi T.: Könnyűipari enciklopédia II/1, Papírgyártási technológia. BMF, Budapest, 2003

[4] http://www.paper.clariant.com

Effect of drops interactions on ink-jet print quality

Christophe Mercier[1], *Magalie Peralba*[1,2], *Martin Dubé*[1], *Jean-Francis Bloch*[2], *Patrice J. Mangin*[1]

[1] Centre Intégré en Pâtes et Papiers, Université du Québec à Trois-Rivières
3351 Boul. Des Forges, Trois-Rivières, Québec Canada G9A 5H7
E-mail: christophe.mercier@cipp.ca, martin.dubé@cipp.ca, patrice.mangin@cipp.ca

[2] EFPG, Laboratoire Génie des Procédés Papetiers,
BP 65, 38402 Saint-Martin-d'Hères Cedex, France
E-mail: magalie.peralba@efpg.inpg.fr, jean-francis.bloch@efpg.inpg.fr

Abstract

Non-impact ink-jet printing is steadily becoming more and more popular, whether it is for home or commercial printing. It is also used by researchers in printing field as a printing technology of reference to study print quality perception. This is due in part to an increase in reliability and also to the continuously improving quality of the print itself. Further understanding on what defines print quality is important to find solutions to improve print technologies. To test these developments, a printer model has to be developed. It should have two parts: one about on an image formation and one about spectral interactions. By combining theses two parts, prediction of the mottling, raggedness or detail rendering can be achieved. A coupled model, spectral reflectance and ink repartition is our ultimate goal. In the present communication, we explore some aspects of drop interactions in ink-jet printing, concentrating mostly on tone reproduction and mottle as well as ink-jet printer models. Results are used as an input in a inkjet printer model aiming at produce a printed area. At this time, only one color is integrated in the model. From this printed area, mottling, edge, raggedness and detail rendering can be virtually studied.

Keywords

Ink-jet, print quality, printer model

1. Introduction

Non-impact ink-jet printing is steadily becoming more and more popular, whether it is for home or commercial printing. It is also used by researchers in printing [Lindberg 2005] as a printing technology of reference to study print quality perception. This is due in part to an increase in reliability and also to the continuously improving quality of the print itself. Further understanding on what defines print quality is important to find solutions to improve print technologies.

Print quality is a controversial subject. For some, it has to be defined as a result of a print without considering paper properties or printing technologies. By doing so, it hides the aspect of best quality achievable with a given paper and printer. In a press room or at home, users have only a finite number of papers and machine printing. In order to clarify print quality, several objective attributes have been isolated. Their number itself is already a debate. The standard ISO 13660 is the first international standard to include a wide range of print quality attributes for monochrome prints. The attributes included in ISO 13660 can be divided in character and line attributes and large area quality attributes. The standard presents the advantage of being device independent. Mangin [Mangin & al, 2007] proposes fives items: color, uniformity, rendering, interface, frequency. Uniformity gathers mottle and graininess. The standard ISO 13660:2001 defines aperiodic fluctuations of print density at spatial frequencies higher than 0.4 cycles/mm as graininess whereas frequencies lower than the limit are mottling. However, following Buczynski [Buczynski 1999], printing presents specific image quality attributes which should be added to ISO 13660. These are satellites, linear resolution, linearity, stepping, circular uniformity and overlapping. Moreover, a psychosensorial aspect makes the final judgement dependant of vision properties and sensitivity of individuals. Nyman [Nyman G & al 2006] stated that the correlation between subjective and objective estimations is often poor. In its study, the image ranking by participants is explained at 80.16% the image sharpness. Sharpness is the subjective impression of density differences that is made upon the mind of an observer when examining the boundaries of well-resolved elements of image detail [Field G.G. 2004]. Acutance is the physical measure of image sharpness. Colour account for 7.21%.

To test developments in dithering algorithms [Ostromoukhov 1996], or in paper grades, which are related to print quality, a printer model has to be developed. It should have two parts: one about on an image formation and one about spectral interactions. The first part should focus on the physical repartition on ink at the surface and in the volume of paper. Ink positioning by the printer and ink spreading, or mechanical dot gain, are of interest because they influence geometrical dot shape and hence its sharpness. The second part concerns optical interactions between the light, the ink, the paper, or light and paper. Lateral spreading of light in paper can be studied independently of the ink. Optical ink spreading due to paper optical diffusivity, called optical dot gain have to considered [Gustavson 1997, Rogers 1997]. Reflectance of IJ printed paper has been widely studied [Emmel 1998, Yang & al 2001, Yang 2004]. Yang [Yang L. 2004] proposes an unified model based on a quadratic form of mechanical dot gain. It imposes a symmetric form to the curve, which is not always verified with the type of halftoning. By combining theses two parts, prediction of the mottling, raggedness or detail rendering can be achieved. A coupled model, spectral reflectance and ink repartition is our ultimate goal. In the present communication, we explore some aspects of drop interactions in ink-jet printing, concentrating mostly on tone reproduction and mottle as well as ink-jet printer models. Results from printed papers are used as an input in a inkjet printer model aiming at produce a printed area. At this time, mottling and sharpness in one colour is integrated in the model.

2. Image formation in Ink-jet printing

Ink-jet printing relies on deposition of ink droplets on paper. From a digital image, to a printed image I(x, y), there are two operations where image is deteriorated: halftoning and printing. Haltoning takes numerical image as input and gives analogical image as output. Ink-jet printing consists in sending droplets from the spatial data of previous analogical images. To achieve full tone coverage, diameter of the ink dot has to be at least equal to the length of the diagonal of the printing resolution [Shu J. 1995]. Figure 1 shows the three mains stages: grey scaled images at 128, haltoned image and printed image with ideal radius. For example, to achieve a resolution of 2880, 1440, 720 and 360 dpi respectively, pixel size must be 8.8, 17.6, 35.3, 70.7 µm, and, hence dot diameter will be 12.5, 25, 50, 100 µm.

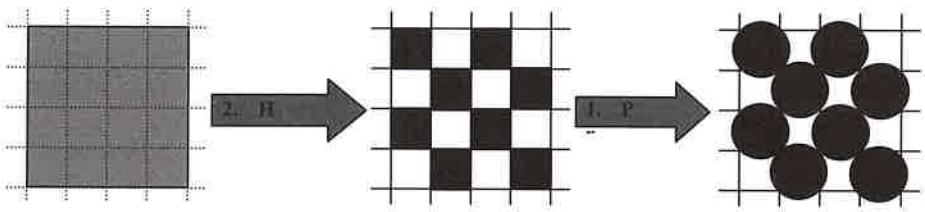

Figure 1: Principle of ink-jet printing: 50% coverage without ink spot superposition

Once on the substrate, the physical shape of a droplet, deduced from the Young equation [Adamson 1984], is given by:

$$r=\left(\frac{3V_0}{\pi(2-3\cos\theta+\cos^3\theta)}\right)^{\frac{1}{3}} \quad (1)$$

where r: diameter of hemispherical cap, V_o: initial ink volume, and θ: contact angle which usually ranges between 20 and 60 degree. Inkjet inks generally have pigment contents of 1 to 10% by weight, based on the ink. Based on water, 90 to 99% of the ink as to be either evaporated or absorbed. If evaporation and absorption occur without modification of initial diameter, an effective ink film thickness H, can be evaluated using:

$$H=\frac{V_0-\alpha V_0}{\pi r^2} \quad (2)$$

where α part of volatile content in ink. We concentrate on ink containing pigments. In table 1, α is set to 0.9.

Dot circular shape implies than ink spots will superpose for a diameter corresponding to the printing resolution. Figure 2 shows the amount of superposition in print ranging from 0 to 100% of coverage. For 100% of coverage, more than 50% of the surface will be composed of two layers of ink. Superposition happens in two different ways. For ideal dot diameter, it is in the cardinal direction North, South, East, West. If spot size diameter is wider than expected for a given resolution, it happens in the diagonal direction North

East, North West, South East, South West. Figure 3 illustrates the proportion of cardinal and diagonal connected points.

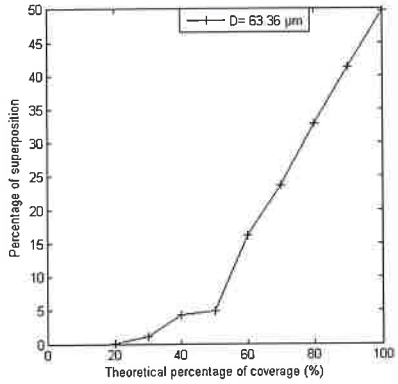

Figure 2: Printing resolution of 360 dpi, simulation resolution of 9600 dpi, dot radius of 19 pixels

There is a big difference between offset with amplitude modulation haltoning and ink-jet printing with frequency modulation haltoning, considering ink dot interactions. In offset printing with AM halfoning algorithms and without taking account for mechanical dot gain, dots come in contacts at 78% coverage (ratio of disc area $\pi a^2/4$ by cell area a^2). For ink-jet printers, using error diffusion halftoning algorithms, the number of 8-connected pixels can be evaluated. Above 30%, it follows the percentage of coverage. Thus, even without colour reproduction, ink superposition is a subject of importance

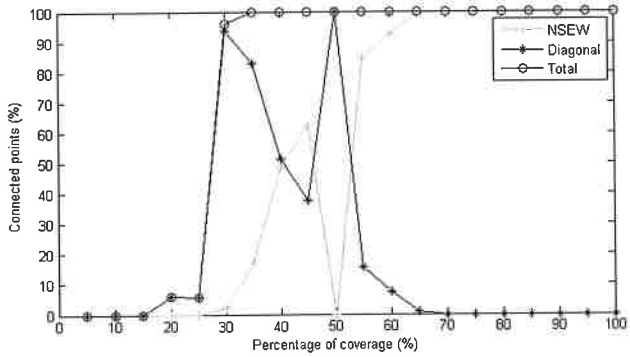

Figure 3: Fraction of connected points in function of percentage of coverage

Most of the drop-on-demand ink-jet printers on the market today are using either the thermal or piezoelectric principle [Hue 1998]. For the former, the spacing between nozzle is 600 dpi, as the latter the spacing is 180 dpi [Smouse & al 1999]. To achieve higher resolution in paper transport direction and to reduce instructions stored in memory, multiple printing passes are necessary. It is also due to the amount of memory needed to store instruction to send ink. Actual printers are able to send different sizes of ink droplets as small as 1 pl. A noisy spatial positioning can increase local area of superposition. While the ideal spot size is circular, it is in reality ellipsoidal with small droplets, called satellites. Besides knowing factors influencing ink spreading on paper, it is then also important to understand what happens when ink spreads on previous printed area.

3. Materials & methods

3.1 Materials

An Epson Stylus 4800 PRO inkjet printer is used. The nozzle configuration is designed with 180 lines and 8 rows, corresponding to the number of colours. Epson 4800 PRO printer works with droplets of 3.5, 5 and 7 pl. Table I gives diameter of ink spot and an effective thickness.

In order to investigate the manufacturer choices of dots sizes and placement rules, papers printed at 1% coverage and different resolution are presented figure 4. They all have been scanned with same resolution to compare their size.

Table I: Diameter of ink droplets

Droplet volume: V_0 (pl)	Ink dot diameter (µm)	Ink film thickness (µm)
3.5	48	0.18
5	54	0.21
7	61	0.23

(a) *(b)* *(c)* *(d)* *(e)*

Figure 4: Depending on paper and resolution selection, three different dots have been noticed on a printed paper with 1% of coverage: (a) draft plain paper, (b) 360 dpi plain paper, (c) 720 plain paper, (d) 720 photo paper, (e) 1440 photo paper

The figure 4 shows that there are three dot sizes, and that dots are often printed on above the other in order to give different resolution in the x- and y-direction (eg., 360 x 720 dpi). Moreover depending of coverage, large and small dots are simultaneously printed.

At printing resolution of 1440 dpi, a two dots aggregation technique is used. Figure 5(a) shows a portion of paper printed with a black ink at 1% coverage with a resolution of 1440 dpi. Original image is 6 mm² with scanning resolution of 9600 dpi. Close visual examination reveals that ink spots seem to be composed of two dots.

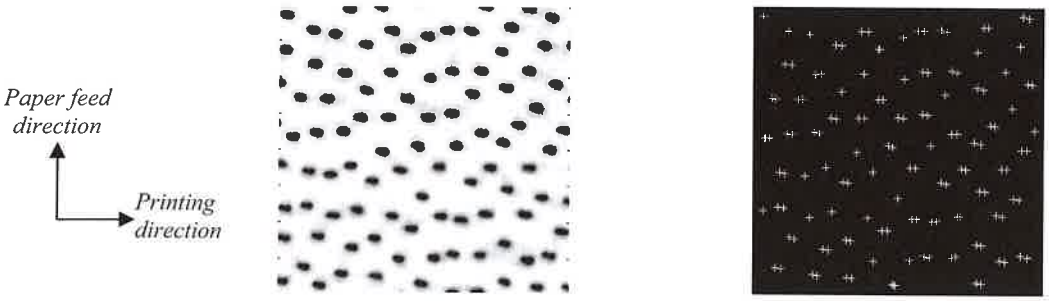

(a) *(b)*

Figure 5: (a) image printed at 1440 dpi with 1% coverage, (b) summits detection for the ink dots

To verify it, two analyses are done. First, a "grain analyse" is performed to isolate ink spot, starting from a binarized image. Next, a filter is built to detect summits. Superposition of these results in given in figure 5(b). For ink spots exhibiting two summits, the mean distance between them is 37.6 µm with coefficient of variation 18.5%. Mean area of ink spot with one summit is 1003.2 pixels (variation 9.8%) , mean area of ink spot with two summits is 1007.1 pixels (variation of 11.16%). Intensity of summit higher is superior to the intensity. Radius of upper summit is 25.3 µm (variation 7.62%) and radius of lower summit is 21.3 µm (variation 9.81%). In this case, ink spots are formed of two droplets with a volume of 5 and 3.5 pl.

Four printing modes are used: plain paper at 360(vertical) x 360(horizontal) dpi, plain paper at 720 x 360 dpi, photo paper at 720 x 720 dpi and photo paper at 1440 x 720 dpi. The first one is used by Lindberg [Lindberg 2005] and corresponds to resolution used in offset printing of magazine. Others are resolution used for colour image printing in ink-jet. Specifications in term of droplets volume for each mode are not known.

Three different papers are used, called A, B and C. First one is high quality ink jet printing, the two others are light weight coated. B has been calendared from C. In term of physical properties, permeability are of 835 ml/min for C, 500 ml/min for B, and the roughness PPS are of 7 µm for C and 4 µm for B.

3.2 Ink-jet printer model

First, an image with a grey level between 0 and 100% is halftoned. The error diffusion algorithm, developed in the "Digital halftoning" Matlab toolbox [Lau 2001] is used. The resulting image is magnified to scanning resolution. Dot are then deposited. The dot placement can be perturbed by a gaussian noise. The range for the standard deviation of that gaussian distribution is calculated from print structure.

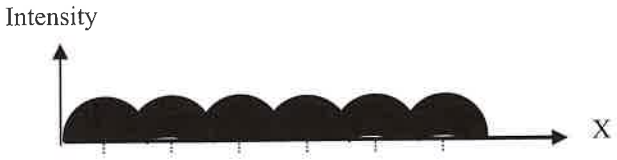

Figure 6: Ink density profile for circular dots on a regular grid

The model needs radius of ink spot and the shape of the ink dot. Dot shape can be modulated. As example, it can be spherical as presented figure 6. Colour scaling is done by using a decreasing exponential law. As only black ink is considered, grey level (GL) follows the equation:

$$GL=255*e^{-\frac{t}{t_0}} \quad (3)$$

where t is ink thickness and t_0 is a constant fixed to 200. For t = 0, the paper is white. Optical dot gain is simulated by convolving spatial ink repartition with a gaussian filter. A typical value for lateral light spreading is used. Comparison between measured and virtual printed paper is done with power spectrum function (PSF):

$$PSF(k_x,k_y)=\left|\tilde{m}(k_x,k_y)\right|^2 \quad (4)$$

where $\tilde{m}$ is the Fourier transform of grey level intensity I(x, y).

4. Results and discussion

4.1 Printing structure

In this section, the influence of the printing technology on printed papers is studied. In ink-jet printing, the print structure is influenced by multi-pass techniques, shown figure 7. To print at 360 dpi with a printing head where nozzles are spaced of 180 dpi, several passes are used. In the case presented figure 7(a), five passes are detected. To configure our printer model, evaluation of importance of printing has to be evaluated.

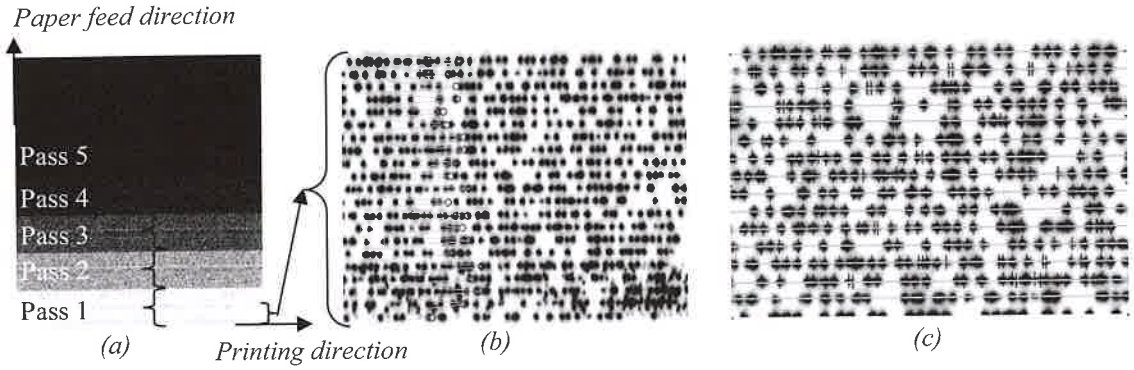

Figure 7: (a) Multi-passes printing ink-jet for print at 360 dpi, 37 x 37 mm , (b) first passe at 180 dpi with horizontal projection (green) and summits detection (red), (c) summits detection and line finding

By summing grey level intensities in the printing direction, an intensity profile is obtained, line figure 7(b). Summits of this curve are detected, circle in figure 7(b). Mean spacing is 140 µm with coefficient of variation 5.3 µm. It can be deduced than the first pass prints at 180 dpi. In the passes from two to five, intensity is

equalized in each line printed at 360 dpi. Final mean spacing between horizontal lines is 70.1 µm, with a coefficient of variation of 16.5%. If horizontal lines of are detectable, vertical resolution is harder to detect by that method. As number of passes increases, standard deviation of distance between lines increases. Mean of standard deviation around each line is 4.23 µm. Standard of standard deviation is 0.47 µm.

Extraction of a grey level intensity in paper feed direction can provide information on the print structure. A part of one dimension power spectrum of grey level intensity along the paper feed direction is represented figure 8, taken from A paper printed at 360 dpi. A peak at near 200 µm, can be observed. Similarly, for print at 720 dpi a pike appears toward 92 µm. Intensity for these particular wavelength has been computed for the three papers printed at 1440 dpi and 720 dpi plain paper. Instead of using one pixel width, a narrow band is summed is the printing direction.

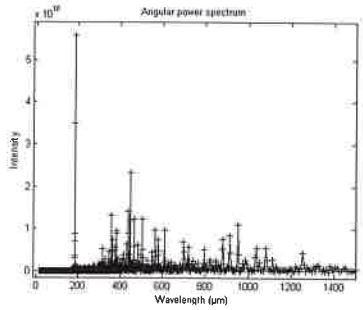

Figure 8: Power spectrum of density profile in paper direction for A paper at 100% black with printed at 360 dpi resolution

A paper has the strongest intensity at this particular wavelength, compared to the two others papers. Moreover, the intensity is maximum near 50% of coverage.

4.2 Reflectance curves

Information on ink density can be obtained from reflectance curves. We measure those (figure 9) at various coverage and resolution for the three papers using a colorimeter For the three papers, reflectance curves are similar. For each of them, photo paper at 720 dpi and 1440 dpi are nearly superposed. Lowest reflectance for 100% coverage is obtained with A paper at 720 or 1440 dpi. Stronger interval between highest and lowest reflectance for the four printing modes is seen with A paper. The printing mode plain paper 720 dpi is an intermediate between plain paper at 360 dpi and photo paper at 720 dpi. Reflectance curve of A paper printed at 360 dpi plain paper, exhibits a linear part between 20% and 70% of coverage. Also A paper printed 360 dpi plain paper shows a linear part between 10 and 50%. Compared to B and C papers, the linear part is not observable, neither 360 dpi plain paper, nor 720 dpi plain paper.

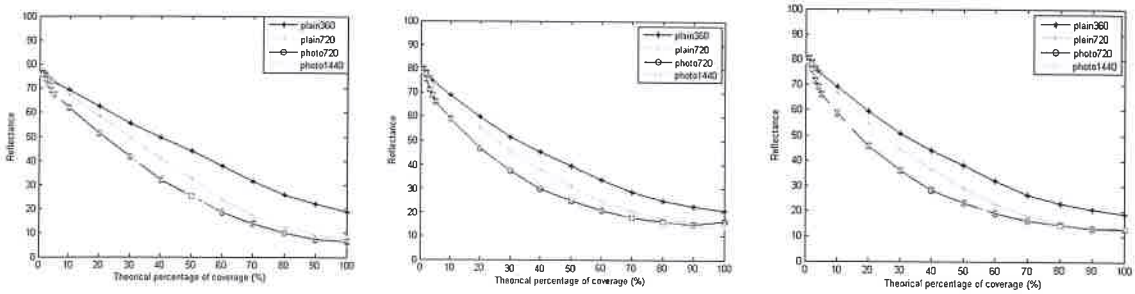

Figure 9: Reflectance (a) A paper, (b) B paper, (c) C paper

Reflectance curves show a major difference at 100% coverage between 360 dpi resolution and others resolution. It may be due to smaller ink dot diameter than expected for this resolution.

4.3 Edge raggedness

Edge raggedness is an evaluation on the roughness of a line delimiting an inked and a non-inked area, evaluated at 100% coverage. Without taking into account technical implementation, it depends on printing resolution and dot size. Moreover , printers can intensify that distortion. In IJ printing, due to moving of the printing head and multipasses printing, vertical edges can present distortion of different wavelengths. In horizontal edges, due to noisy setting of dots around horizontal line can lead to uneven edges. Finally, in both cases, paper can increase edge unevenness by ink spreading.

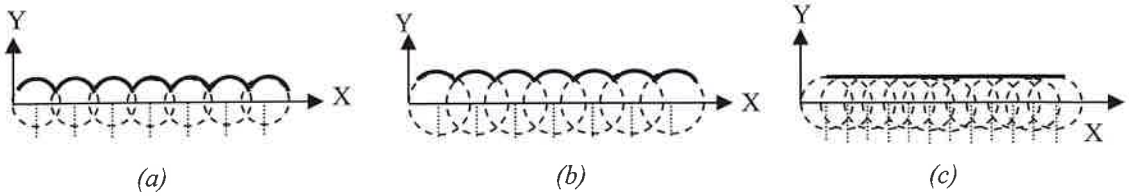

Figure 10: External perimeter of dots an a regular grid: (a) with radius equal to pixel length, (b) with dot radius wider than resolution, (c)same dot radius than (a) but resolution is multiply by two

Printings on the three papers with the four modes can be sum up by the figure 10. Table II presents results of edge raggedness for the three papers used.

Table II: Edge raggedness evaluated on a length of 30 mm, values are given in micron metre

		360 dpi plain	720 dpi plain	720 dpi photo	1440 dpi photo
A	Horizontal	4.76	0.74	0.74	0.57
	Vertical	6.72	0.86	0.83	0.80
C	Horizontal	2.92	1.6	1.73	1.78
	Vertical	3.67	1.5	1.57	1.23
B	Horizontal	3.70	2.34	2.43	1.90
	Vertical	3.77	1.77	2.12	1.74

A paper has the worst edge raggedness at 360 dpi, however at 1440 dpi, it is the best. For A paper, paper feed direction presents the more important root mean square deviation, as for the papers "B and C", it is the opposite. In term of print quality, A is better than C which is better than B for the three printing modes plain paper 720 dpi, photo paper 720 dpi, photo paper 1440 dpi. However, for a given paper, by example, C the best print mode resolution is 720 dpi plain paper.

The printer model is used to simulate the cases presented in figure 10. Setting printing resolution and dot diameter, it enables to calculate edge raggedness. For a resolution of 720 dpi and a dot diameter of 50 µm, RMS of raggedness is 0.74 µm. For an ink dot of 65 µm, with same print resolution, raggedness is 0.55 µm. Increase of ink dot diameter decreases edge raggedness.

4.4 Mottling and graininess

It has been shown than edge raggedness can be simulated for the A paper. By gathering in-plane and X-Intensity simulation in one model, mottling of ink jet papers can be studied.

Visual examination of solid print done with a resolution of 360 dpi, figure 11, shows paper without ink. At this resolution, spacing between line is 70.7 µm and biggest drop give a diameter of 61 µm. The same resolution is used for scanning and for simulation of printing. For a printing at 360 dpi, scanning is done at 4800 dpi. Figure 12 shows the PSF of the A paper printed at 360 dpi, from 20 to 100% coverage.

The curves are similar in the range 0 - 171 µm. In the interval between 171 and 350 µm, there are a slight difference between percentage of coverage. Figure 13(a) shows the PSF of the simulation of the A paper printed at 360 dpi, from 20 to 100% coverage with ink dot diameter of 116 µm. We first show on figure 13(a)

how the PSF is reproduced by the printer model with dots of constant diameter and without deposition noise. The shape of relative intensities at various coverage is reasonably well reproduced.

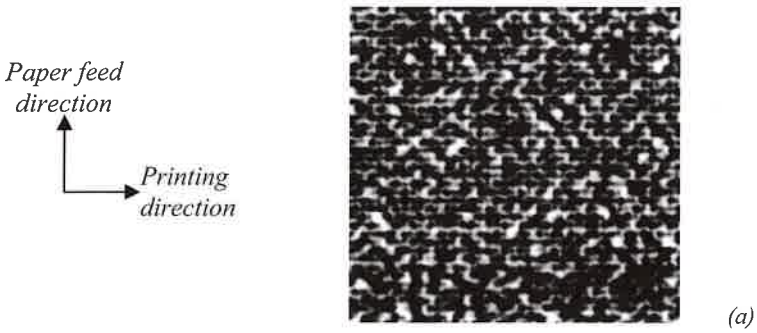

Figure 11: 100% coverage printed at 360 dpi resolution and scanned at 4800 dpi, size is 2.8 x 2.8 mm

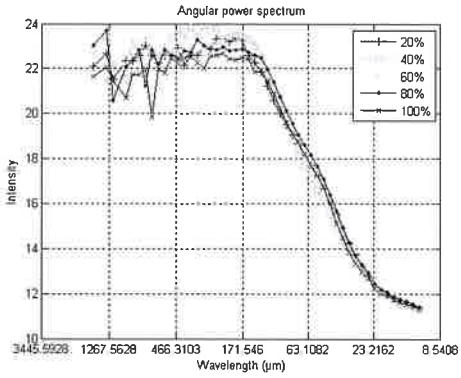

Figure 12: Power spectrum of A paper printed at 360 dpi, from 20 to 100% of coverage

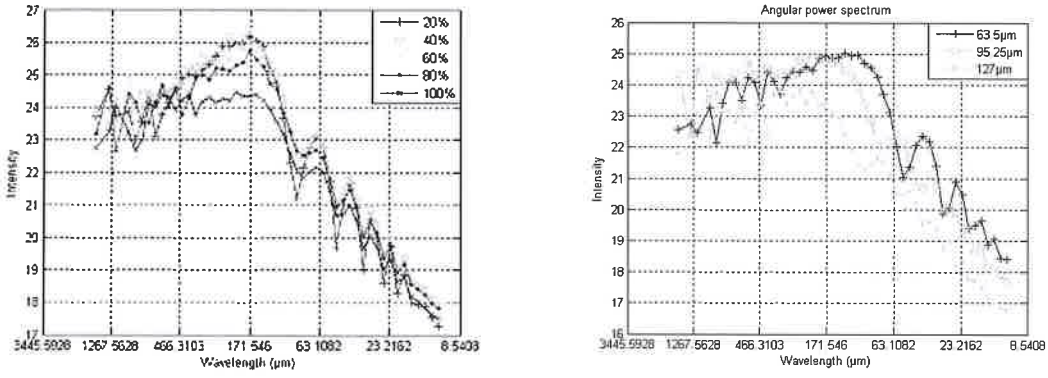

Figure 13: Power spectrum for round dots: (a) with a diameter of 116 µm from 20% to 100% coverage, (b) with diameter from 63.5 to 127 µm at 100%

The difference between 100% coverage and percentage of coverage below is also reproduced. Influence of ink dot diameter on mottling via the power spectrum is presented at figure 13(b). As the dot diameter increases, the length of the correlated part of the spectrum increases.

Including noise and dot shape modification, the A paper is printed. Figure 14(a) present the comparison between simulation and measured printed paper. A fair agreement is obtained. Typical dot used in the simulation is presented figure 14(b).

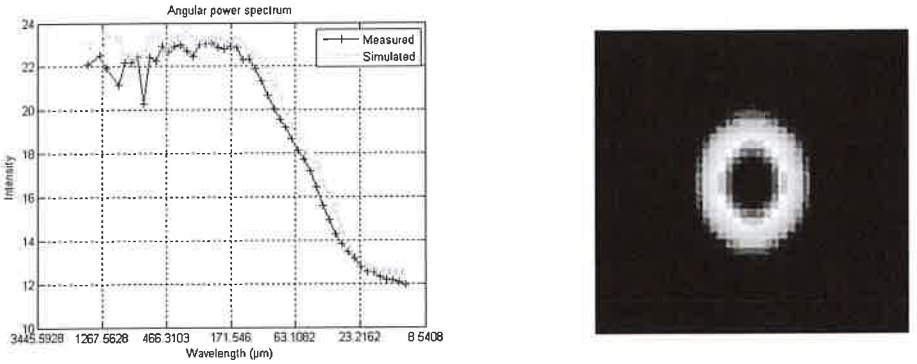

(a) *(b)*

Figure 14: (a) PSF of the simulated and printed papers at 360 dpi resolution and 100% coverage, (b) typical ink dot used in the simulation

5. Conclusion

We have studied ink-jet printed papers, from theirs reflectance curves, edge raggedness, intensity profile in paper feed direction and mottling. A recent three droplet sizes inkjet printers has been used. Reflectance curves show a major difference at 100% coverage between 360 dpi resolution and others resolution. It may be due to smaller ink dot diameter than expected for this resolution. Power spectrums of the intensity profile in paper feed direction proves that print structure exist on papers studied. Absolute values of power spectrums are nevertheless higher on A paper. Edge raggedness results have revealed that the behaviour of high quality ink jet paper can be interpreted by dot diameter and printing resolution. Mottling of high quality in-jet paper has been studied. In the case of ink dot diameter corresponding to printing resolution, mottling has been simulated. Power spectrum of the measured and simulated printings have been compared and fair agreement has been obtained. Next stages of the model will take into account surface topography measured by optical profilometry in order improve ink spreading.

Acknowledgements

C. Daneault and J.-P. Lamothe, from CIPP are gratefully acknowledged for interesting and stimulating discussions.

References

[1] Adamson A. W. 1984 Physical chemistry of surfaces 4th ed. Wiley-Interscience, New. York

[2] Buczynski L. 1999 Special print quality problems of ink jet printers. Recent progress in Ink jet Techonologies II p 538 - 544

[3] Emmel P. 1998 Modèles de prédiction couleur appliqués à l'impression jet d'encre. Thèse EPFL, no 1857 (1998). Dir.: Roger-David Hersch

[4] Field G. G. 2004 The Field Guide to Color Reproduction Editor: TECHNICAL ASSOCIATION OF THE GRAPHIC ARTS

[5] Gustavson S. 1997 Dot Gain in Colour Halftones. PhD thesis, Dept. of Electrical Engineering, Linköping University, September 1997

[6] Hue P. Le 1998, Progress and Trends in Ink-jet Printing Technology Part 3, Journal of Imaging Science and Technology Volume 42, Number 1, January/February 1998

[7] Lau D. L. and Arce G. R. 2001 Modern digital halftoning, Marcel Dekker, New York NY, USA 2001

[8] Lindberg S., Fahlcrantz C-M. 2005 Perceptual assessment of simulated print noise with random and periodic structure. J. Vis. Commun. Image R. 16 (2005) 271 - 287

[9] Mangin P. J., and Dubé M. 2006 Fundamental questions on print quality, International Printing and Graphic Arts Conference

[10] Nyman G., Radun J., Leisti T., Oja J., Ojanen H., Olives J-L, Vuori T., Häkkinen J. 2006 What do users really perceive: probing the subjective image quality Proceedings of SPIE - Volume 6059, Image Quality and System Performance III

[11] Ostromoukhov V., Emmel P., Rudaz N., Amidror I, Hersch R.D., 1996 , Dithering Algorithms for Variable Dot Size Printers, *IEEE Signal Processing Society, 1996 Intl. Conf. on Image Processing,* Proceedings, Vol. 1, pp. 553 - 556, 1996

[12] Rogers G. 1997 Optical dot gain in a halftone print. Journal of Imaging Science and Technology, 41(6):643 - 656, November/ December 1997

[13] Shu J. 1995 Error diffusion with ink reduction for high quality and high resolution inkjet printing Proceedings of the 1995 International Conference on Image Processing (Vol. 3) page: 3121

[14] Smouse E., Nigro S., 1999 Hewlett-Packard Inkjet Printing Technology: the state of the art

[15] Yang L. 2004, A unified model of optical and physical dot gain in print color reproduction The Journal of Imaging Science and Technology, , vol. 48, no. 4; p. 347 - 353

[16] Yang L. 2004 A unified model of optical and physical dot gain in print color reproduction, The Journal of Imaging Science and Technology, 2004, vol. 48, no. 4; p. 347 - 353

[17] Yang L., Gooran S. and Kruse B. 2001 Simulation of optical dot gain in multichromatic tone reproduction. Journal of Imaging Science and Technology, 45(2):198 - 204, March/April 2001

New ink absorption method to predict inkjet print quality

Taina Lamminmäki, Pasi Puukko

KCL Science and Consulting
P.O. Box 70, FIN-02151 Espoo, Finland
E-mail: taina.lamminmaki@kcl.fi, pasi.puukko@kcl.fi

Abstract

Inkjet print quality depends strongly on ink-paper interactions in the ink setting. A high print quality requires an optimal ink solvent absorption speed, the right absorption direction, and a high absorption volume. There are several methods for studying inkjet ink absorption speed, but there is still a need for an efficient and quick ink absorption speed testing method, which can simulate the situation where several ink drops act together, as in the practical case where an inkjet printer nozzle array moves across the paper surface. In this study, a new ink absorption speed measurement device, DIGAT, was designed. The device was tested using kaolin-coated papers. The variables in the coatings were the binder type (swelling and non-swelling) and the binder content. The absorption speed of inkjet inks was compared with the print quality factors. The results showed that the bleeding tendency of non-swelling surfaces can be predicted based on the DIGAT absorption time. Different kinds of coating layer structures, as well as inkjet inks setting phenomena, can be effectively studied using the DIGAT device.

Keywords

Ink absorption, ink drying, ink setting, inkjet printing

1. Introduction

The popularity of inkjet printing is constantly increasing. The possibility to print changing information has been utilized in the applications of packaging and transactional mail. In addition to desktop printing, inkjet is utilized increasingly for production scale printing. Four colour prints and graphical pictures have already been applied on bills. In the package area, digital printing is used for labels, cartons, corrugated and flexible packaging destined for test markets, sales samples, promotional campaigns, new product introduction, production of entertaining features. Digital printing is used for applications that require mass customization and personalization. One growing application area is private labeling. Inkjet printing is evidently participating in this progress.

In the future, printing speed increases, drop size gets smaller, and higher resolution is achieved. How do these changes influence the drop setting process? Table I illustrates an estimate (speculation) on how a decrease in the drop size and an increase in printing speed theoretically affect the ink amount on a compact printed surface. The table also contains an estimate about the absorption speed - how much ink solvent the surface must absorb not to leave any more free solvent on the printed media. For drop-on-demand (DOD), a drop size decrease to 2 pl, a resolution increase to 2440 x 2440 dpi, and a speed increase to 2 m/s means a dramatic increase in the solvent absorption speed. The surface must absorb almost ten times as much ink solvent as presently.

Table I: An estimation of the inkjet ink amount on the paper surface, the printing speed and the solvent absorption speed requirement. The ink in the estimation is water-based, with a 96% solvent content

Ink	Drop size, pl	Resolution, dpi	Ink amount, g/m²	Printing speed, m/s	Solvent absorption speed, g/s
DOD, Today	15	1200 x1200	33	0,12	3,9
DOD, ***Future***	2	2440 x2440	18	2	35
CIJ, Today	15	300 x 1200	8,4	2	16
CIJ, ***Future***	6	600 x 600	3,3	5	16

In today's continuous jetting (CIJ), there is clearly more solvent on the surface than for the DOD inkjet. Present and future CIJ printing (drop size 6 pl and resolution 600 x 600 dpi) gives same absorption speed of a 16 g/s requirement. One way to affect the ink absorption speed is to use dryers after the ink application to evaporate the solvent faster from the surface. Thus, in DOD inkjet printing, the speed increase increases the demand for solvent absorption speed. For CIJ, a lower resolution compensates for the speed effect, but if the resolution is higher, the amount of ink solvent also increases.

Inkjet print quality depends strongly on ink-paper interactions - how inks set onto the surface. A high print quality requires optimal ink solvent absorption speed, absorption volume, and absorption direction. On a surface with a low absorption volume and speed, inks can mix together, resulting in bleeding, halftone dots spread, dot gain and mottling. On the other hand, if the surface is too porous, ink colorants penetrate too deep into the paper structure, causing a reduction of print density and increased print-through.

The setting and drying speed of inkjet inks has been studied using different modified set-off measurements. The traditional set-off based measurements (Figure 1, set-off time) which have been developed mainly for evaluating the offset ink setting process are too slow for inkjet inks. There are several published methods, which measure the penetration speed and drop spreading of one ink drop [3, 6, 12]. Desie and Kerdraon [4] studied coalescence of two inkjet ink drops. In their device, two ink drops from two print nozzles were applied. They showed that drops that are applied side by side onto the PET surface coalesce, and may or may not move over the substrate, depending on the liquid properties and the drops size, and they concluded that this affects print quality formation in that way. However, measuring one or two drops does not give information about interactions between several ink drops. Thus, there is a need for an efficient and quick ink penetration speed method, which can simulate a situation where several ink drops affect together - as in the practical case when an inkjet printer nozzle array moves across a paper surface. In this paper, ink absorption time refers to the time between a drop being applied on the surface until disappearing into the surface structure.

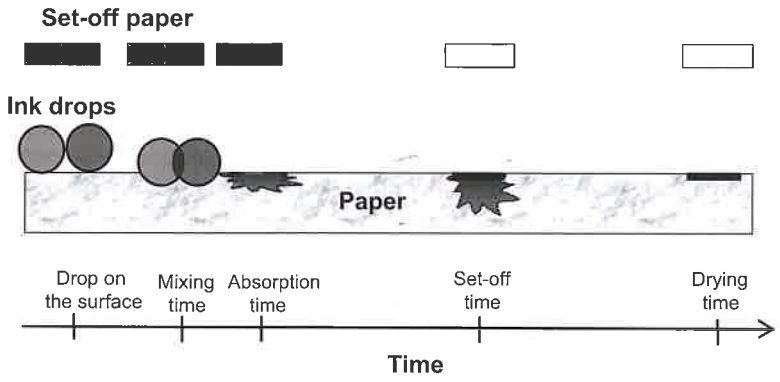

Figure 1: Used terminology

1.1 Objectives of the research

The objective of this work was to develop a new test environment for studying the absorption speed of different inkjet inks. A requirement for the method was for it to operate over short time periods, less than 10 sec. In order to make sure that right phenomena are measured, the connection between results of the new environment and the final inkjet (DOD) print quality was monitored.

2. Materials and methods

2.1 Testing methods

DIGAT (Dynamic Ink Gloss and Absorption Tester) measures the absorption time using a laser beam to detect changes in the gloss level (Figure 2). The measurement starts from the moment when the ink arrives at the surface, and lasts until the gloss of the ink has reached an equilibrium value. Ink is applied on the surface with a glass capillary tube, using the ejector principle, and the ink forms an even layer on the paper surface. The application system makes it possible to use different inks, soluble and pigment inks, as well as other low viscosity liquids. By

using this application method the liquid amount on the substrate varies between 6 and 12 g/m^2. The detector, which is a part of the DIGAT, measures the voltage as a function of time. The laser beam and the detector are both fixed at an angle of 20°. The result is given as absorption time (t 90- > 10, Figure 2, lower part), corresponding to the time between 90% of the maximum gloss value and 10% of the saturation gloss value.

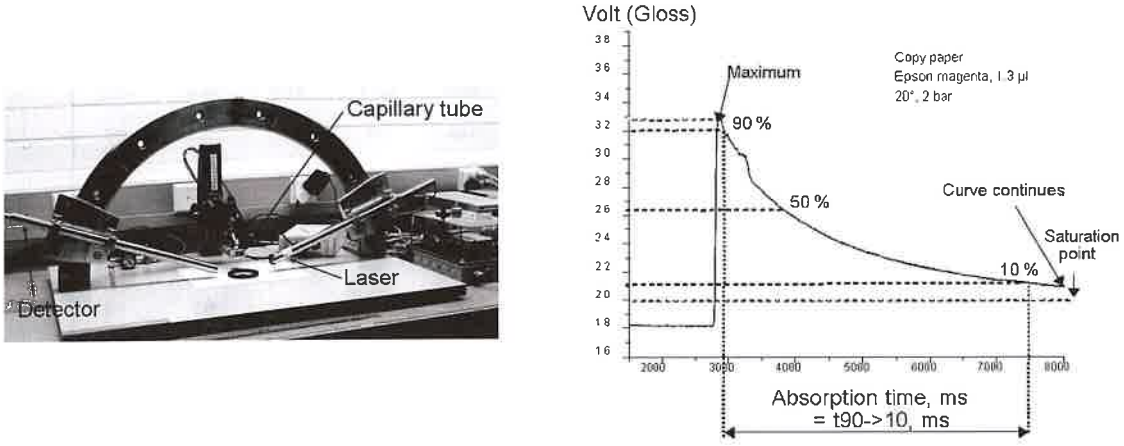

Figure 2: DIGAT device and result curve

The measuring principle of the DIGAT device has also been utilized in other measuring environments. At KCL, the first and second critical points of coating colours during color consolidation have been studied in laboratory scale as well as in pilot scale using same measurement principle.

The following paper tests were used for coating surface evaluation: grammage (EN ISO 536:95 modf.), roughness (ISO 8791-2:90), air permeability (ISO 5636:3:92), opacity (ISO 2471:98), contact angle (Internal, Fibro DAT 1100 instrument), and absorption coefficient with nozzle applicator (Internal). In the contact angle measurement, a 2 µl water drop was applied on the surface and filmed with a CCD camera. The contact angle was measured 0.5 s after the drop was applied on the surface. In the nozzle applicator, water was applied onto the surface with a 1.2 mm slit nozzle using ten different nozzle speeds. The amount and the area of applied liquid were measured, and the final absorption coefficient was calculated. All tests were made at a relative moisture content of 50% RH and a temperature of 23°C.

The pH of the ink was measured with a glass-composite electrode. The surface tension of ink was measured using the so-called Du-Nouy ring method, based on a surface balance, Sigma 703. The method is based on the release force between the liquid and a flat, circular platinum-iridium ring. The density of the ink was analyzed using the Paar DMA 45 density meter, at a constant temperature. The kinematic viscosity was measured using a Cannon-Fenske type capillary viscometer. The method is based on liquid trickling in a narrow calibrated capillary tube. All the ink measurements were made at a constant temperature of 23°C.

The papers were printed using an Epson Stylus Color 900 printer. The print density was measured with a Macbeth RD 1252 densitometer. The bleeding and the properties of halftone dots were measured with a Digital camera which was integrated in an Olympus BX60 light microscope. The figures were analyzed using the AnalySIS Pro program. The bleeding was measured from a grey level profile as a normal edge width.

2.2 Papers and inks

In order to test the applicability of the DIGAT method, model coatings were prepared. Polyvinyl alcohol (PVA) and styrene acrylate (SA) latex were used as binders. The idea was to compare coatings with swelling and non-swelling binders - PVA absorbs more water (swells) at certain time than SA. The PVA was Airvol 107 and SA Raisional 212. The binder amount was also used as a variable in the coatings, varying from 5 parts to 20 parts, causing a reduction in porosity. The pigment of the coating colors was 100 parts of SPS kaolin. The PVA coatings contained 1 pph of carboxyl methylcellulose (Finnfix 10). The coating trial was carried out on a pilot coater using a short dwell time applicator and a coating speed of 700 m/min. The base paper was surface-sized fine paper (80 g/m^2). The applied coating amount was 10 g/m^2. The coated surfaces

were analyzed using two commercial dye-based inks (HP and Epson magenta) and DIGAT. The same Epson magenta ink was used in printing. The properties of the coated surface are shown in Table II.

Table II: Properties of papers

Property	Coatings							
	Base paper	5 pph PVA	10 pph PVA	15 pph PVA	5 pph SA latex	10 pph SA latex	15 pph SA latex	20 pph SA latex
Grammage, g/m²	81,4	91,9	92,7	92,0	92,1	91,9	91,9	92,5
Bendtsen roughness, ml/min	215	90	100	140	75	60	105	85
Bendtsen air permeability, ml/min	1220	27	15	8	30	24	14	4
Opacity, %	91,5	94,6	94,5	93,9	94,7	94,7	94,3	94,0
Contact angle (water), °	106,2	45,5	54,1	69,0	42,0	51,4	60,3	65,8
Absorption coefficient, ml/m²/s^{0,5} (water)	2,9	5,9	3,2	3,8	11,3	10,1	6,9	4,4

The studied inks were commercial inks from Epson Stylus Color 900 (Epson) and Hewlett Packard DeskJet 850 (HP). The properties of the inks are shown in Table III.

Table III: Ink properties

Ink	pH	Surface tension, mN/m	Density, kg/dm^3	Viscosity kinem. Mm^2/s
HP, Magenta	6.9	25.0	1.04	2.07
Epson, Yellow	8.6	33.7	1.04	2.46
Epson, Magenta	9.0	34.1	1.06	2.53
Epson, Black	8.9	34.9	1.06	2.60

3. Results

3.1 Ink absorption speed

The coated papers were analyzed with DIGAT using commercial magenta ink from Epson Stylus Color 900 and HP Deskjet 850 printers. The applied ink amount was 10 g/m^2. The DIGAT results showed that the absorption time of inks was longer when the coating contained more binder (Figure 3). When the coating contained 15 pph PVA, the absorption time of the Epson magenta ink was more than 80 seconds, indicating a very slow ink absorption into the coating layer. As for the PVA amount, an increased latex content increased the absorption time. However, the increase in the absorption time of SA coatings was lower than that of PVA coatings. The maximum absorption time of SA coating was 43s, while PVA coating was as high as 98s.

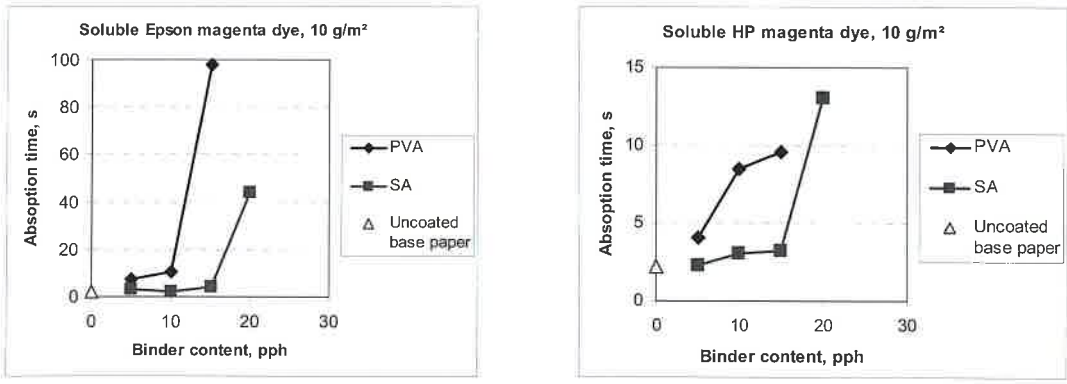

Figure 3: Epson and HP magenta ink absorption speed on polyvinyl alcohol (PVA) and styrene acrylate (SA) latex coating layers

HP magenta ink was evidently more quickly absorbed into the studied coating structure than Epson magenta, when the coating contained 15 pph PVA and 20 pph SA (Figure 3, right side). At a lower binder content, both inks had similar absorption times. The effects of paper porosity and ink properties on ink absorption speed are shown in Figure 4.

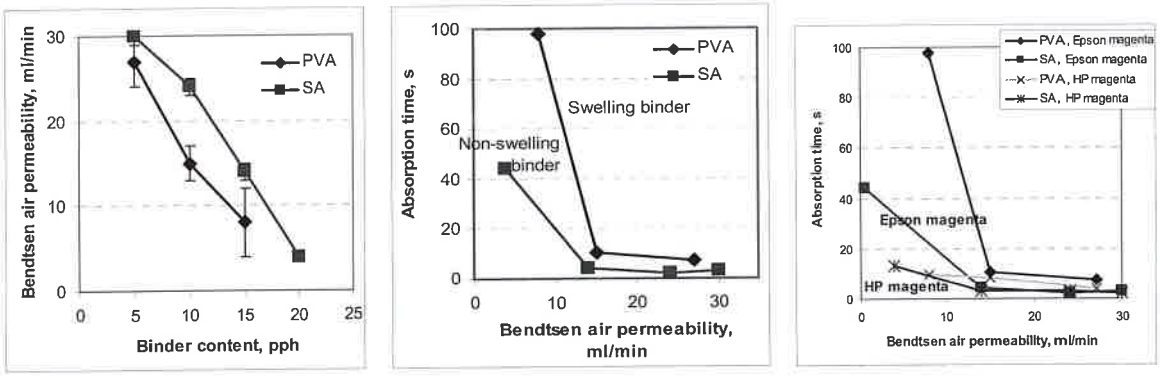

Figure 4: The effect of binder content on air permeability (Bendtsen) and air permeability vs. absorption speed (DIGAT). The absorption time was measured with DIGAT using Epson Stylus Color 900 magenta ink and HP Deskjet 850 magenta ink

3.2 Print quality

The results of the Epson Stylus Color 900 printer are presented in this paper. The difference between the measured print quality properties of swelling and non-swelling surfaces was smaller when HP Deskjet 850 printing was used.

PVA coatings produced a higher print density (Figure 5) and higher bleeding (Figure 6) than SA coatings. Moreover, the halftone dots spread more on the PVA coatings at same grey level than the dots on SA coatings.

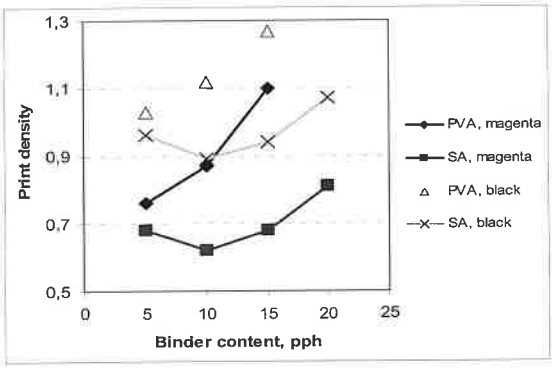

Figure 5: Print density of polyvinyl alcohol (PVA) and styrene acrylate (SA) latex coatings. Dye-based magenta and black inks from Epson Stylus Color 900

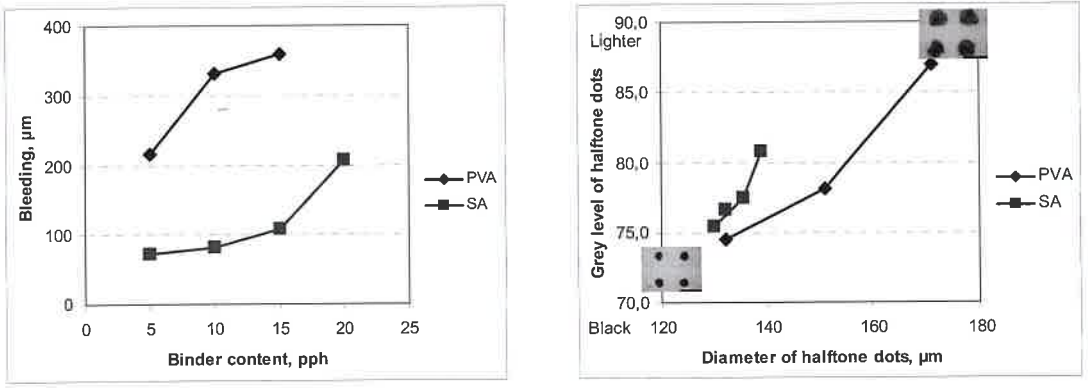

Figure 6: Print density, bleeding and halftone dot properties of PVA and SA latex coating surfaces. Dye based magenta/yellow and black inks from Epson Stylus Color 900

4. Discussion

4.1 Effect of coating layer porosity

When the ink touches the coating surface, the ink starts to penetrate into the porous structure. The dominating phenomena in the ink solvent movement are pressure and capillary penetration. Simultaneously, there is a sorption of ink solvents into the paper components, as well as solvents movement along the paper components through diffusion.

The pressure penetration is caused by the speed of the ink drop. Drops reach the substrate surface at a speed of 5 - 9 m/s, for piezo-inkjet [13, 14, 15] and thermal inkjet at 12 m/s [16]. The pressure is proportional to the speed, which means that a higher speed makes pressure penetration more important in the ink drop setting process.

The capillary flow is caused by the coating porosity itself. The ink flows from the large pores to the smaller ones because of the differences in capillary pressure between the pores. The penetration into the capillaries is usually described by the Lucas-Washburn equation, which takes into account the surface contact angle, the pore radius, and the viscosity and the surface tension of the liquid [11]. A pore diameter reduction means that the capillary pressure increases and the liquid speed in the pore increases. The Lucas-Washburn equation does not take into account the fact that a filter cake can form on top of the coating. Consequently, in the case of pigment inkjet inks, this model is not the best equation to describe the ink setting phenomenon onto the paper surface. The liquid penetration phenomenon has been studied by many researchers [5, 8, 11].

Figure 4 illustrates how the increase of binder content decreases the air permeability of paper. At the same time, absorption time got longer when paper was more closed. PVA binder produced a closer structure than SA, at the same binder content. The DIGAT results showed that SA coating absorbs ink quicker than PVA coating. The porosity difference affects the absorption time. The other effecting phenomenon is binder swelling, which will be discussed in the next chapter.

The open structure of SA coatings also affected the print density results. A lower print density was achieved with SA coatings. This indicates that the soluble colorant follows the solvent into the coating layer, and the surface does not have any chemical component on the coating top layer that can bind the colorants. The grey values of halftone dots were in line with the print density results.

4.2 Binder swelling

As described above, capillary penetration plays an important role in the inkjet inks setting process. The other important phenomenon in this context is the swelling of binders. As a binder swells on top of coating pigments, the pore diameters decrease, causing a slowdown of ink movement in the capillaries. The question is how important the role of swelling has in a real inkjet ink setting process.

All the studied inkjet inks were water-based. Water affects the coating structure, both in liquid and vapour form. As water makes contact with the binders, the water molecules interact strongly with the hydrophilic groups on the binder surface, such as hydroxyl (-OH), carboxylic acid (-COOH), amino ($-NH_2$), amide ($-CONH_2$ or $-CONR_1R_2$, where R_1 and R_2 are H or acrylic), and sulfonic acid ($-SO_3H$) groups. Hydrophobic groups like $-CH_3$, $-SiOSiCH_3$ and $-CH_2F$ reject water molecules [1, 2, 7]. The number and type of hydrophilic groups determines how much solvent the binder absorbs.

In a dynamic situation, the binder film swells and part of the binder dissolves. Dissolving influences the viscosity of the ink and reduces the ink penetration speed. However, the dissolving must clearly be a slow phenomenon compared with absorption. In fact, complete drying of inkjet ink takes quite long time and this enables the existence of binder dissolving phenomenon. Consequently, binder swelling influences ink setting via two mechanisms, both of which reduce the ink penetration speed:

- ◊ It decreases capillary diameter;
- ◊ It increases the viscosity of the ink.

PVA has more hydrophilic groups which absorb more water than styrene acrylate, and this causes pores to close and pore diameter to diminish during solvent absorption. When the PVA and SA coatings were compared at the same porosity level (see Figure 4), a longer absorption time was reached for PVA. Without

swelling the absorption speeds would have been identical. Thus, the smallest pores are closing and diminishing in PVA coating during solvent absorption.

4.3 Ink properties in ink setting

Von Bahr et al. [10] concluded that the degree of inkjet ink spreading and penetration onto the top layer of the substrate depends on ink properties such as the surface tension relaxation and rheology of the ink. In addition, the kinetic energy the drop - drop impact, drop delivery time and predeposition of drops - have an effect on drop behaviour on the surface.

A low viscosity ink is usually absorbed quicker than a high viscosity ink [8]. The role of ink surface tension on the ink setting process is a more complicated phenomenon, as ink drop setting depends strongly on the surface tension of the printed layer. Moreover, dissolving of surface compounds occurs during the ink setting process, which affects the dynamic situation on the surface. If the ink forms a small contact angle on the printed media, the wetting of the surface is good [9]. This means that the ink stays on the surface only for a short time, and the ink sets quickly. The effect of surface tension was beyond the scope of this research work.

For PVA coating, longer absorption times were reached with Epson magenta ink than with HP magenta (Figure 4, right figure). It seems that the slightly higher viscosity of the Epson ink slows down ink penetration. However, there is a small difference in the surface tension of inks, which affects the absorption speed. HP ink had a lower surface tension. The situation is quite similar on top of styrene acrylate coating, especially when the coating is more closed.

4.4 Bleeding vs. DIGAT results

The SA coatings had lower bleeding values than the PVA coatings (Figure 7, left side). The faster ink absorption was reflected on the bleeding results as a narrower ink colorant mixing length. The SA paper reached a bleeding level of 200 µm at a Bendtsen air permeability of 5 ml/min, whereas the value for PVA paper was 27 ml/min. Binder swelling reduces the pore diameter, and smaller pores close up, causing the ink solvent movement into the structure to slow down. A more closed surface produces more bleeding and spreading than a porous surface. The inks stay longer on the top of the coating layer and this enables mixing of different colour inks.

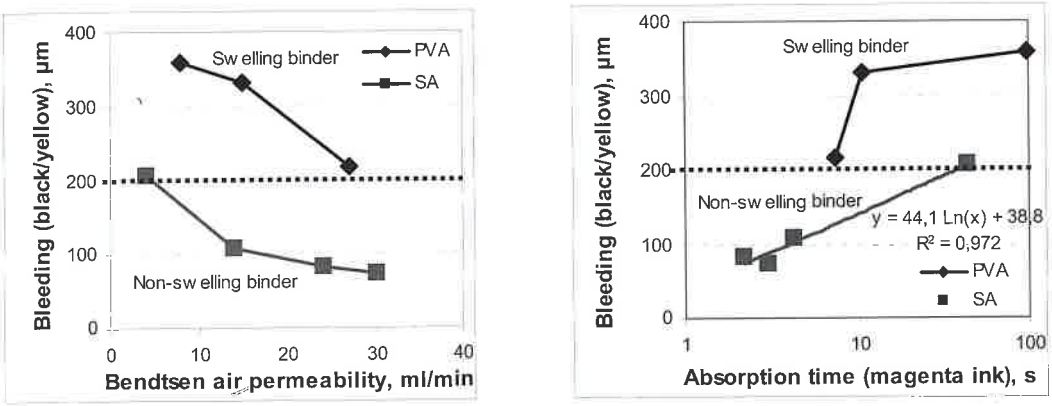

Figure 7: Bleeding presented as a function of porosity on PVA (swelling) and SA (non-swelling) coatings. The ink is Epson Stylus Color 900 printer standard ink

When the DIGAT results are compared with the bleeding results (Figure 7, right side), it can be noticed that, for a non-swelling binder coating, the absorption time and the bleeding results clearly have a logarithmic correlation. With a DIGAT device it is possible to predict the bleeding tendency of a non-swelling surface.

At a certain absorption time level, PVA coating gives a higher bleeding value than SA coating. If the only difference between the surfaces is porosity, all the results should be on the same curve. The effective porosity in the SA coating case originates only from the porosity of the coating layer. In the PVA coating case, it

consists of coating porosity and swelling of the binder. At the same absorption time level, different phenomena dominate, depending on the swelling capability of the binder. How does this reflect the ink setting process? It seems that the swelling of PVA prevents the penetration of ink into the inner coating structure. The same amount of ink on a PVA coating can only spread in the x, y-direction, whereas the ink penetrates deeper in the z-direction of the layer for SA coating (Figure 8). This reflects on the print quality of PVA coating, providing a higher print density, darker and more spread halftone dots, and more bleeding. Thus, for DIGAT it is possible to study inkjet ink setting phenomena and predict the print quality formation.

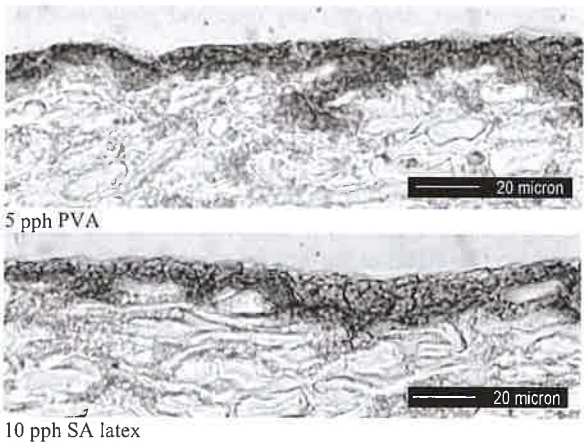

Figure 8: Cross-section figures from PVA and SA coating layers printed with soluble magenta ink

5. Conclusions

A new device for studying inkjet ink absorption speed was designed. DIGAT (Dynamic Ink Gloss and Absorption Tester) measures the absorption time using a laser beam to detect changes in the gloss level from the moment the inkjet ink arrives at the surface until it has disappeared into the structure. With DIGAT it is easy to simulate the attraction between several ink drops. Different ink types can be studied very easily and quickly. Based on the results it was concluded that the absorption time enables a good prediction of the dynamic situation on the surface. The DIGAT device can be used for studying how the binder type or the binder amount in the coating layer affects the ink absorption time. The absorption time is evidently also linked to the print quality properties.

In the future, the use of high-speed inkjet will increase and new types of surfaces will be printed using inkjet. Research is needed, especially for fine paper, and offset paper for hybrid printing, where offset is combined with inkjet, and in packaging and labelling (sentence slightly confusing, needs rephrasing!). The development work needs to be made alongside ink development. In this research work, the basic information about how ink absorption speed affects the printing result is also needed.

Acknowledgements

The authors thank the National Technology Agency (Electronic publishing and printing program) for the financial support.

References

[1] Berthold, J., *Water Adsorption and Uptake in the Fibre Cell Wall as Affected by Polar Groups and Structure. Thesis for the degree of doctor. Royal Institute of Technology, Stockholm, 1996, 41 p*

[2] Finch, C. A., *Chemistry and Technology of Water-Soluble Polymers. Plenum Press, New York 1983, 358 s*

[3] Desie, G., Deroover, G., De Voeght, F., Soucemarianadin, *A., Printing of dye and pigment-based aqueous inks onto porous substrates, Journal of imaging science and technology 48(2004)5, 389 - 397*

[4] Desie, G., Kerdraon, P., *Multi-color printing, NIP20: International conference on digital printing technologies, 31.10.- 5.11.2004, Salt Lake City, Utah, The Society for Imaging Science & Technology, 820 - 827*

[5] Desjumaux, D., Bousfield, D., Glatter, T., Donigian, D., Ishley, J., Wise, K., *Influence of Pigment Size on Wet Ink Gloss Development, Journal of pulp and paper science 24(1998)5, 150 - 155*

[6] Heilmann, H., Lindqvist, U., *Effect of drop size on the print quality in continuous inkjet printing, Journal of imaging science and technology 44(2000)6, 491 - 494*

[7] Jönsson, B., Lindman, B., Holmberg, K., Kronberg, B., *Surfactants and Polymers in Aqueous Solution. John Wiley & Sons Ltd, West Sussex, England 1998, 438 s*

[8] Salminen, P. *Studies of water transport in paper during short contact times, Thesis for the doctor of technology, Åbo Akademi, Turku, 1988, 94 p*

[9] Triantafillopoulos, N., Rosinski, J., Serafano, J., *The role of ink and paper chemistry in water based publication gravure, International printing and graphic arts conference, 18-21 Oct. 1992, Pittsburg, PA, USA, TAPPI Press, 1992, 279 - 289*

[10] Von Bahr, M., Kizling, J., Zhmud, B., Tiberg, F., *Spreading and penetration of aqueous solutions and waterborne inks in contact with paper and model substrates, Advances in printing science and technology, 27th Research conference of the international association of the research institutes for the printing, Information and communication institutes, Graz, Austria, 10-13 September 2000, PIRA International, 87 - 102*

[11] Xiang, Y., Bousfield, D., *Influence of Coating Structure on Ink Tack Dynamics. Journal of Pulp and Paper Science 26(2000)6, 221 - 227*

[12] Yip, K. L., Lubinsky, A. R., Perchak, D. R., Ng, K. C., *Measurement and modelling of drop absorption time for various ink-receiver systems, IS&T's NIP18: 2002 International conference on digital printing technologies, 29th September - 4th October 2002, San Diego, California, 378 - 382*

[13] http://www.flow3d.com/pdfs/tp/micro_tp/FloSci-Bib01-07.pdf (4.6.2007)

[14] http://konicaminolta.com/inkjethead/products/inkjethead/index.html (4.6.2007)

[15] http://agfabeint01.net.agfa.com/bu/gs/dms/Marketing.nsf/AllDocs/B3786CC2FC9D8153C125701200329B0A/$FILE/LFT_UPH_GB_20050523l%201.0.pdf (5.6.2007)

[16] http://ieeexplore.ieee.org/xpl/freeabs_all.jsp?arnumber=1215356 (5.6.2007)

3

Special printing and printed functionality

The problem of a quantitative evaluation of adhesive strength in printing on polymer films

Evgeny Bablyuk, Vadim Bakanov, Konstantin Farenbrukh

Moscow State University of Printing Arts
2a, Pryanishnikova St., 127550, Moscow Russia
E-mail: BabliukEvgen@mtu-net.ru; Vadim.A.Bakanov@gmail.com

Abstract

The article demonstrates the experimental results on feasibility study of the normal fracture method for a quantitative evaluation of adhesive strength on the interface "polymer film-ink". Evaluation of the adhesive strength level has been made for water-based and solvent-based inks spread on BOPP film surface.

Keywords

Adhesive strength, polymer films, printing inks

1. Introduction

Printing with the use of polymer films as a substrate has recently received an intensive development. In the first place, this is due to rapid industrial development dealing with the production of consumer goods in colorful packaging of polymer materials. Moreover, there will be growing interest for printing on polymer films in connection with the introduction of new technological processes in making electronic microcircuits using graphic methods. Objective information concerning the level of adhesive strength on the interface "polymerized product-ink" is required while developing the new processes, connected with printing on polymer films.

For many research workers in the adhesion area, the methods of quantitative evaluation of adhesive strength are known and used for research of various systems [Minford J. D., 1981]. They are a splice shearing test method, a splitting method, and a normal fracture method. Schematically these methods are presented in Figure 1.

As it appears from the presented schemes, the first two methods (**a** and **b**) are being applied only for evaluation of adhesion on model compounds, while carrying out research works. The normal fracture method (scheme **c**) can be used for evaluating adhesive strength on actual products, for example, on samples of packaging materials.

The present work demonstrates the experimental results on development and practical run-up of the normal fracture method for a "polymer film-printing ink" system. The method allows comparing several ink systems, to evaluate the technique effectiveness of surface polymer films activation, to set up the effect of process variables on adhesive strength connected with ink drying and curing.

This method can be used not only for printing inks but also for varnishes, primers, inks with any technique of curing. Restrictions for this method are certain requirements as for substrate thickness and rigidity as well as for flatness of an ink film (without nonprinted areas).

2. Methods

The evaluation of adhesive strength has been carried out using a fracture testing machine supplied with a tensometer registering maximum load up to 500 H. After sticking a metal stub, a sample of a polymer film with an ink coated on it has been fastened in a special cell as it is shown in Figure 2.

By carrying out numerous experiments it became possible to optimize the design of a cell concerning a definition of its dimensions, a diameter of a stub, a diameter of a port hole in a laying-in metal plate. The

significant part of an experimental work has been devoted to selection of glue for adhesion of a metal stub to the surface of an ink layer. As a result we have made the optional halt on a cyanoacrylate adhesive. The preparation procedure of samples for testing has been as following.

Samples of films with an ink layer of the size 15 x 50 mm are cut out. Then the conditioning of film samples is carried out at the temperature of (23 ± 2)°C and at the relative air humidity of (50 ± 2)%. The duration of conditioning is at least 2 hours.

Tests are carried out under the same conditions as for conditioning of samples. The preparation of a sample for tests is conducted on a special compression unit (Figure 3).

The optimal quantity of cyanoacrylate adhesive is uniformly applied on the stub. The present stub is fastened in clamps of a compression unit (Figure 3). A sample with a testing side upwards is placed on a sample stage. Then pressing up to full contact with the sample is conducted. This pressure is being held till the absolute dryout of adhesive (approximately 5 - 7 s).

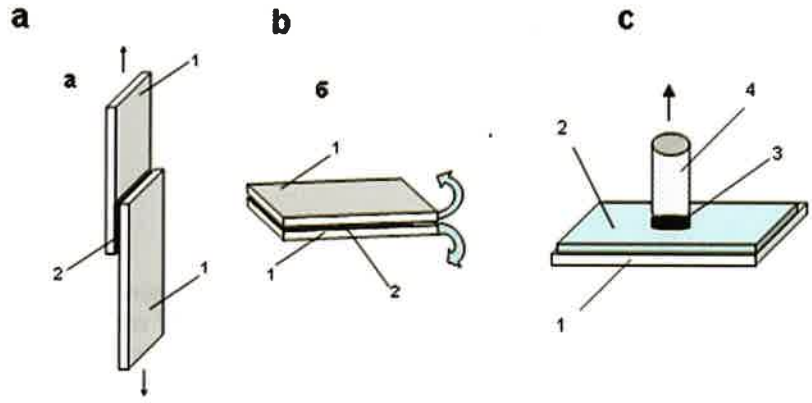

*Figure 1: Schemes of evaluation methods of adhesive strength of printing inks on polymer films: **a** - a splice shearing test method, **b** - a splitting method, **c** - a normal fracture method; where 1 - polymer film, 2 - printing ink, 3 - glue, 4 - metal stub*

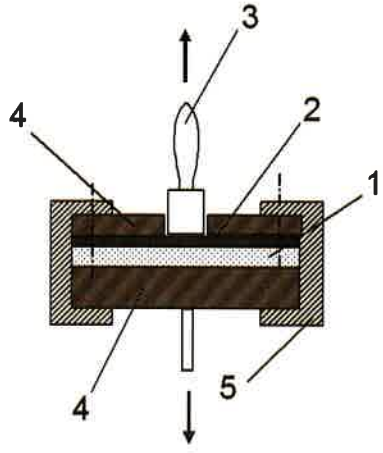

Figure 2: A cell for evaluation of an adhesive strength by a normal fracture method, where 1 - polymer film, 2 - printing ink, 3 - metal stub, 4 - metal plates, 5 - clamps

The stub together with a affixed sample are taken away from the compression unit and are laid on the lower plate of the cell for definition of adhesion (Figure 2). A pressure plate is laid over. Then the centering of the stub is carried out relative to the upper pressure plate. After that the pressure plates are fixed hard by clamps. Assembled in such a way the cell is fastened in the clamps of a fracture testing machine.

It is necessary to pay special attention to the strict observance of verticality when fastening the cell during the test. Then tearing off is fulfilled in the fracture testing machine. The traverse speed of a movable clamp was 100 mm/min.

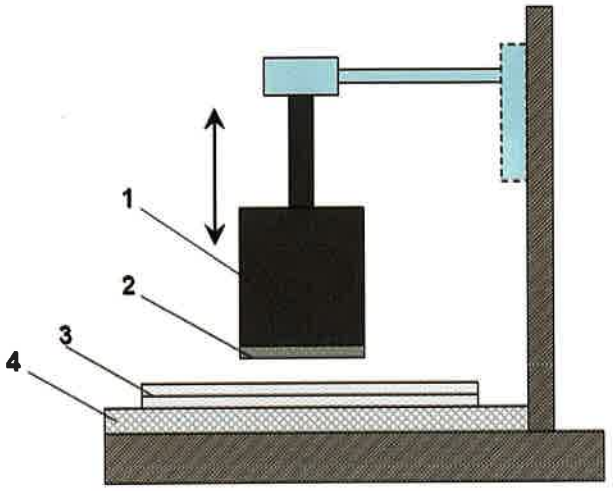

Figure 3: A compression unit: 1 - metal stub, 2 - glue, 3 - polymer film with coated ink layer, 4 - tympan material

Before putting on an ink layer, roughness parameters of the polymer film surface have been evaluated using the laser-beam profilograph Micro Measure 3D station.

After carrying out tests relative to the wetting edge angle of water, evaluation methods of surface film hydrophilic behavior have been applied to identify the adhesive compound destruction character (it can be adhesive, cohesive and mixed). For the same purpose the method of ATR FT-IR spectroscopy has been used.

3. Results

Preliminary work through of methods on evaluation of adhesive strength according to the scheme (Figure 1**c**) has shown that it is necessary to take into consideration both the surface of an adhesive contact and the area of this contact.

Taking into account the fact that participants in adhesive reciprocal action (inks, polymer films, various glues) have different levels of adhesion and cohesion, it is necessary to identify the destruction character during tests and so to determine whether the destruction has been purely adhesive, cohesive or mixed.

Also ATR FT-IR spectra of three types have been recorded (film surface without ink, film surface with an ink layer coated on it and film surface after adhesive compound destruction). Indicated spectra for water-based inks and organic solvent-based inks are represented in Figures 6 and 7.

a

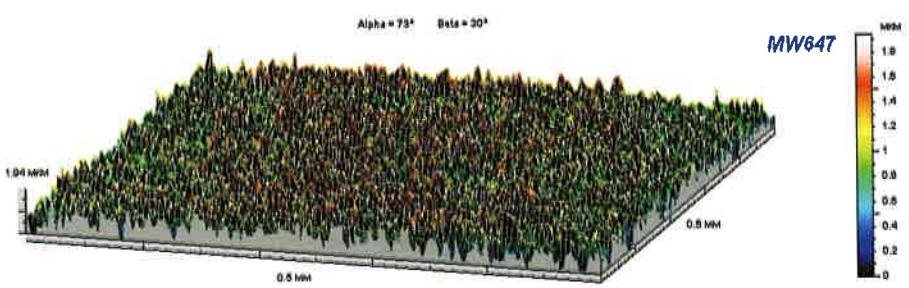

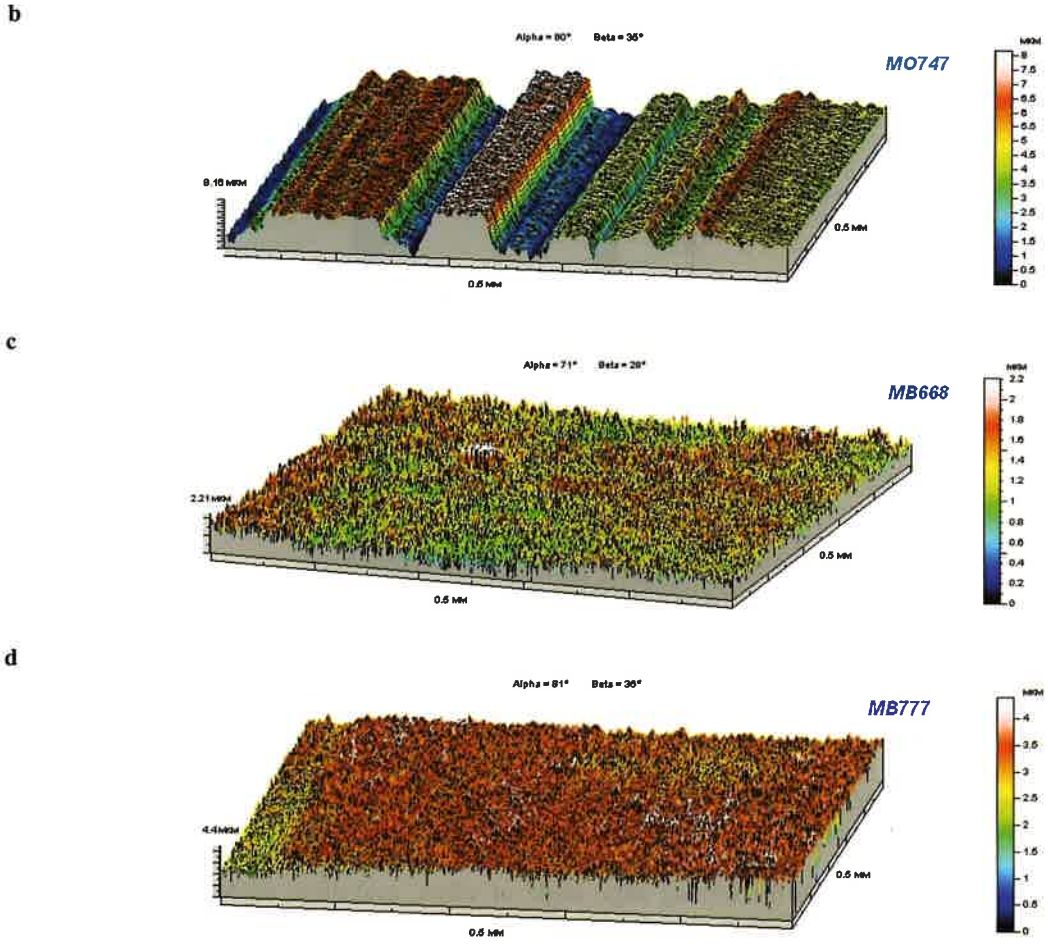

Figure 4: Three-dimensional image of surface polymer film morphology: a - MW647, b - MO747, c - MB668, d - MB777

During the evaluation of roughness parameters of polymer film surface, the arithmetical mean surface deviation (R_a) and the middle depth (R_z) have been determined. Three-dimensional profiles of researched polymer film surfaces are represented in Figure 4.

Figure 5 represents the experimental results on evaluation of adhesive strength level of FlintGroup Co. inks on BOPP films produced by ExxonMobil Co. In the present Figure the results are represented which have been obtained on the samples where destructions had an adhesive character.

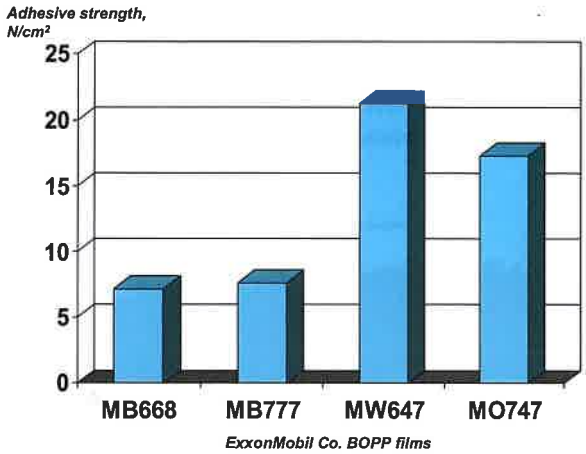

Figure 5: Adhesive strength of flexographic printing ink of FlintGroup Co. on BOPP films

Calculated values of R_a and R_z parameters for researched films in comparison with the evaluated adhesive strength level are represented in Table I.

Table I: Comparison characteristics of roughness and adhesive strength for BOPP films produced by ExxonMobil Co

Film type	Adhesive strength, N/cm^2	Roughness parameters	
		R_a, μm	R_z, μm
MW647	21.3	0.261	2.74
MO747	17.3	0.205	1.74
MB668	7.2	0.128	0.248
MB777	7.5	0.108	2.06

Also ATR FT-IR spectra of three types have been recorded (film surface without ink, film surface with an ink layer coated on it and film surface after adhesive compound destruction). Indicated spectra for water-based inks and solvent-based inks are represented in Figures 6 and 7.

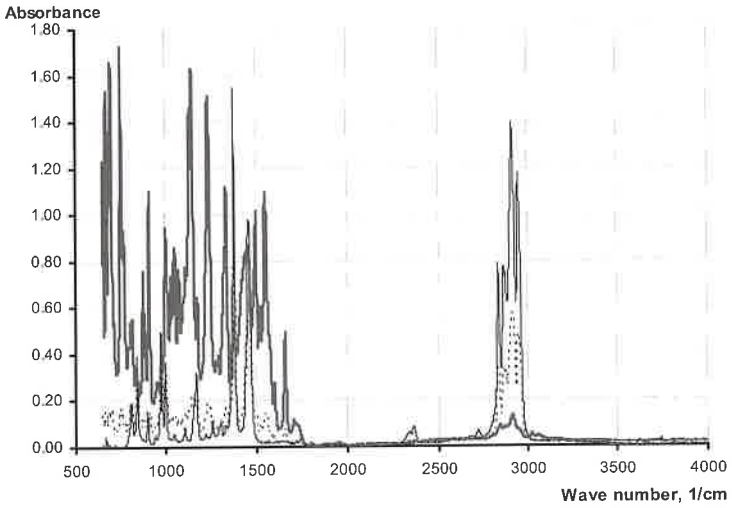

Figure 6: ATR FT-IR spectra of BOPP film without ink (solid line), water-based ink surface (bold line) and surface after adhesive compound destruction (dot line)

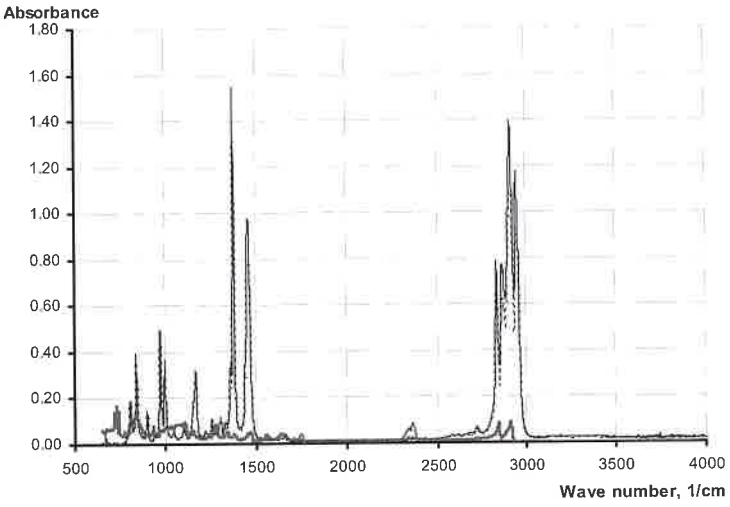

Figure 7: ATR FT-IR spectra of BOPP film without ink (solid line), surface of solvent-based ink (bold line) and surface after adhesive compound destruction (dot line)

In the present case IR spectra of BOPP film samples are represented on which the figure of full exfoliation of ink from the film surface was observed. The lack of curves referring to the spectrum of both water-based and solvent-based inks testifies to adhesive destruction character on the interface "printing ink-polymer film". During research work more complicated cases of adhesive compound destruction have been observed.

For a fuller description of a process picture taking place on the interface "polymer film-printing ink", it is necessary to make a careful analysis of the obtained IR spectra.

The results of evaluation of surface BOPP film hydrophilic behavior at different stages of tests concerning adhesive strength evaluation and the results of IR-spectroscopy researches are well correlated with.

The results of measuring wetting edge angle of water of BOPP film surface, ink surface and film surface after adhesive compound destruction are represented in Table II.

Table II: Values of wetting edge angle on different stages of preparation and test of adhesive compounds

Object of measurement	Wetting edge angle of water (distilled water), degree
BOPP film without ink	79
BOPP film with coated water-based ink	31
BOPP film after adhesive compound destruction	73

Surface BOPP films activation treated by corona discharge reduces the wetting edge angle of water up to 48 - 50 degrees. At the same time an adhesive strength increases up to 30%.

The comparison of results received by evaluation of surface hydrophilic behavior and by recording film samples and inks IR-spectra allows to identify the destruction character as adhesive in most conducted experiments.

4. Discussion of results

During research a number of technical approach problems concerning the quantitative problems of adhesive strength on the interface "polymer film-printing ink" have been solved. By experimental research work the design of the measuring cell has been defined more exactly, the type of glue has been selected and the technology of preparation of adhesive compounds for tests has been perfected.

In cases when destruction on the interface "printing ink-polymer film" is of an adhesive character that is confirmed both by the visual observance and by the research of the surface destruction using microscopic methods, the ultimate conclusion about the adhesive destruction character is given by the evaluation methods of surface hydrophilic behavior and to a greater degree by the use of ATR FT-IR spectroscopy.

In this case a quantitative value of strength under which an adhesive compound had been broken during test with use of a fracture testing machine, we can refer to the area of an adhesive compound, that is to receive a quantitative value of an adhesive strength measured in N/cm^2.

As it can be seen from the results represented in Figure 5 and in Table I, the film MW647 shows the highest level of roughness of researched samples. Its arithmetical mean surface deviation is 0.261 μm and middle depth is 2.74 μm (Figure 5). The surface of this film is characterized as uniform, with a highly developed structure. And in this case we are to certify that fastness of ink retention on this film turned out considerably higher in comparison with other researched samples and formed 21.3 N/cm^2.

Analyzing profilogramm of the film MO747, it should be noted that its parameters are close to the film MW647. The parameter R_a is least of all on 0.056 μm and R_z is least of all on 1 μm, but as for a structure the film is nothing of the kind. It can be seen in Figure 5**b**. The surface here and there represents highly developed parts which are abruptly changed with deep downfalls. Such high overfalls and heterogeneity of surface have slightly reduced an adhesive strength level-17.3 N/cm^2.

BOPP film MB668 shows the roughness parameter $R_a = 0.128$ μm, its roughness middle depth R_z is 0.248 μm that is approximately by 8 - 10 times less in comparison with other samples. The surface represents micro-

serrated structure with outside inclusions in the kind of small holes or craters apparently formed in consequence of surface film treating by corona discharge (Figure 5**c**). Judging by the ideal structure of the film MB668 it is possible to wait for high printing quality. But in this case due to low value R_z the adhesive strength level has made only 7.2 N/cm^2.

The arithmetical mean surface film MB777 deviation (Figure 5**d**) is 0.108 μm. As for the depth roughness R_z, its index was 2.06 μm that is on 0.68 μm less than for MW647 and the more than for films MO747 and MB668. As a whole the film structure is uniform enough as for the sample MB668, shows small outside craters on the surface stipulated by the same reasons. Adhesive strength for this film has constituted 7.5 N/cm^2. It is explained by low value of index R_a.

Under the adhesive compound mixed destruction character that one can see during microscopical observance of the surface after tearing off the stub, it is necessary to calculate the area of the surface which is free of ink and divide it on the measured value of the stub tearing off strength.

As a rule the ink image on a polymer film surface is more contrasting in comparison with the image on a polymer film without ink. Areas of contrasting objects on the image can be easily calculated using programs Adobe Photoshop.

5. Conclusions

The developed approach to the quantitative evaluation of adhesive strength can be used in making any systems, where a polymer film and a polymer layer coated on it are involved.

For researched polymer films the continence strength of printing inks, other things being equal, is defined in many respects by the surface roughness parameters.

The ATR FT-IR spectroscopy method can be successfully used for destruction character evaluation on the interface "polymer film-printing ink".

References

[1] Minford J. D., 1981, Treatise on Adhesion and Adhesives. N. Y.: Marcel Dekker, v.5

Colour differences on offset printed PET and PVC shrink sleeve labels

Gorazd Golob[1], Diana Gregor Svetec[1], Dejana Đorđević[1], Boštjan Žorž[2]

[1] University of Ljubljana, Faculty of Natural Sciences and Engineering
Snežniška 5, 1000 Ljubljana, Slovenia
E-mail: gorazd.golob@ntf.uni-lj.si; diana.gregor@ntf.uni-lj.si; dejana.djordjevic@ntf.uni-lj.si

[2] KRO d.o.o., Medvode
Barletova 4, 1215 Medvode, Slovenia
E-mail: bostjan.zorz@gmail.com

Abstract

Shrink sleeve labels have been well known for over 30 years. They are printed on oriented PVC using gravure or flexo printing technique. PVC is still very popular with 70% market share. Today the use of environment friendly PET, PETG and other oriented plastic films is recommended and they are increasing their market share. For cost effective production of small series of shrink labels the web digital printing technique (HP Indigo) and variable format offset printing with UV inks have been introduced.

The dimensional changes of shrink sleeves causes higher concentration of pigment on smaller area. The result should be higher optical density of colour and colour differences on the print sample. The goal of our investigation was a comparison test of PVC and PET shrink sleeve labels printed on Mueller Martini Alprinta 74V prototype offset press with flexo print or varnishing unit. For both substrates we used UV inks, cured on chill rollers to prevent shrinking. We measured dimensional changes of printed labels and colour differences on both materials after shrinking.

Keywords

Colour differences, PET, PVC, shrink sleeve label, variable format offset printing

1. Introduction

Labels compete with other technologies such as direct-printed bottles and cans, laminated cartons, and flexible packaging in product decoration and identification. Of 33 billion square meters estimated worldwide consumption Europe has a 36% market share and North America an estimated 28% with growing rates on both continents at around 3 to 5%.

Shrink sleeve labels have been well known for over 30 years, their growth rates excess 15% and only wrap around film labels have higher growth rate at around 20%. Heat shrink sleeves offer highly graphical decoration, with the ability to present large volumes of information because of their 360-deg, head-to-toe container coverage. Dominant substrate for shrink sleeve labels are oriented polyvinyl chloride (PVC) films with market share over 70%, followed by oriented polystyrene (OPS), PET, PETG films, and even PP grades, in response to environmental concerns and the growing issue of recyclability [Llewellyn, Thomas].

At the production of thin films using calender, blown or castfilm extrusion the film gets an orientation of the molecule structure by tensile stress. This stored molecule structure can variously trigger oriented shrinking of the film during warming. The orientation of the molecule structure and depended shrinking can be in machine direction (typical for wrap-around shrink labels), in cross direction (shrink sleeve labels) or in both directions. Typical shrinking characteristics of some suitable oriented plastic films are shown in Figure 1.

Traditional printing techniques for shrink sleeve label production are gravure and flexo. For cost effective production of small series of shrink labels the web digital print technique (HP Indigo) and variable format offset printing with UV inks has been introduced. Drying process of printing ink and varnish on oriented plastic film is critical in all mentioned printing techniques because of unwanted heat inducted dimensional changes of substrate. Hot air drying process is limited to about 50°C in flexo conventional printing and use of chill rollers is necessary in UV drying systems [Vainstein 2005, Bolte].

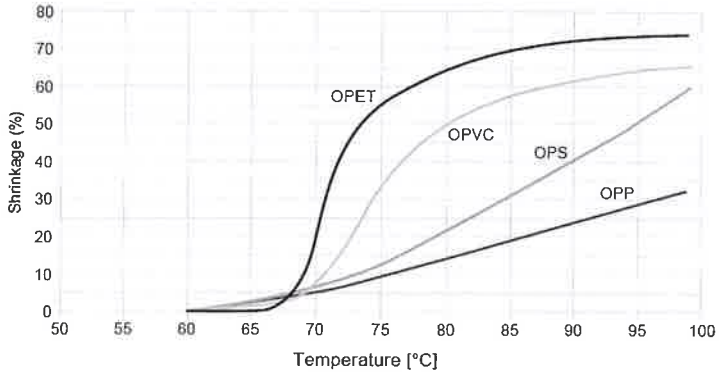

Figure 1: Shrinkage dependance on temperature (Breil)

Shrink labels require the use of inks specially formulated for this application. Inks used to print on pressure-sensitive substrates are not suitable. These inks must be flexible enough to withstand the shrinkage up to 70% with high resistance to cracking and delamination. Because heat is involved in the process, these inks need to be formulated with pigments that won't change color or fade when heat is applied. Some inks are specially formulated for particular substrates [Polischuk, Vainstein 2005].

The dimensional change of shrink sleeves causes higher concentration of pigment on smaller area. The result should be higher optical density of colour and colour differences on the print sample. The goal of our investigation was a comparison test of PVC and PET shrink sleeve substrate printed and white varnished on Mueller Martini Alprinta 74V prototype offset press with flexo print or varnishing unit. For both substrates we used UV inks, cured on chill rollers to prevent shrinking.

2. Methods

Our investigation was included into test printing for potentional buyer of new web press Mueller Martini Alprinta 74V and shrink sleeve label market research project. The configuration of the press included four offset print units and flexo print unit with UV dryers and chill rollers. For investigation we prepared testforms with measurement patches and sample labels. We used clear PVC and PET cross oriented films from Klockner Pentaplast and UV offset inks with white varnish overprint from Zeller+Gmelin. Because of a small quantity of substrates we printed only label samples. There were no clear solid CMYK patches available for measurement.

After printing we performed dimensional measurements of substrates and colour measurements of some typical inks on printed labels with and without white varnished layer. All colour measurements were made using GretagMacbeth Spectrolino spectrophotometer with settings D50/2° on the same white plastic backing material. For density measurement the instrument was set to Status E.

Then we used hot water to shrink labels. We took samples for dimensional and colour measurements at 60 and 80°C. We repeated colour measurements of typical colours on all samples and calculated colour differences.

During rub resistance test we found out good characteristics on unshrinked and shrinked labels. Rub resistance of the prints was good enough for use on the seaming and packaging machines. At seaming process there were no problems with seam quality. Because of some unexpected results in colour differences we performed additional analyses under SEM and optical microscope that lead us to some conclusions and opened some interesting new questions.

3. Results

On the press we achieved good dimensional stability of prints during UV curing process with dimensional changes under 1% on PVC and PET substrates. Then we observed dimensional changes of prints after

warming of prints in hot water from 50°C. Shrink process started at 60°C for PVC and PET substrate. At 90°C we achieved maximum dimensional change. For PVC it was about 50% and for PET about 70%. Shrinked substrates had uneven wrinkled surface and became more rigid.

In Table I the average values of 10 measurements and calculated colour differences of the first set of measurement are presented.

Table I: CIELAB colour values and differences for labels printed on PVC and PET substrates

	Blue	Red	Yellow	Green	ΔE_{ab}^*							
	PVC ref.				PVC 60°C				PVC 80°C			
L^*	48.4	46.6	81.5	71.7	2.5	1.7	1.3	1.4	1.5	2.0	1.0	1.0
a^*	-25.9	67.4	-2.0	-31.0								
b^*	-42.1	-6.6	84.4	66.7								
	PVC white varnish ref.				PVC white varnish 60°C				PVC white varnish 80°C			
L^*	42.3	45.5	79.4	66.6	1.4	1.1	1.0	0.8	0.6	0.9	0.9	0.9
a^*	-16.1	66.0	2.2	-32.3								
b^*	-43.8	5.0	87.0	64.5								
	PET ref.				PET 60°C				PET 80°C			
L^*	47.3	49.4	81.5	71.2	0.6	1.5	0.5	0.7	9.5	16.2	7.7	7.9
a^*	-26.6	62.4	-2.2	-28.8								
b^*	-41.9	-7.3	88.8	70.1								
	PET white varnish ref.				PET white varnish 60°C				PET white varnish 80°C			
L^*	39.8	48.3	80.3	61.3	1.8	1.3	0.6	0.6	7.2	4.8	5.8	3.9
a^*	-14.9	64.1	1.3	-36.9								
b^*	-44.8	1.1	84.6	52.7								

SEM images of printed shrinked PVC substrate show us interesting regular wrinkled structure of the ink (Figure 2). On the images of PET the structure was different and some artifacts were present on the film surface as a result of surface energy treatment process performed by substrate manufacturer.

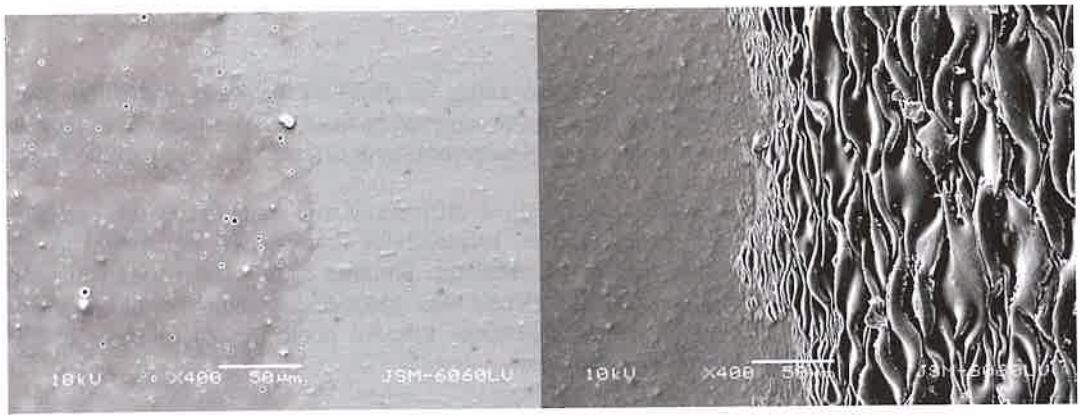

Figure 2: SEM images of printed PVC substrate before (left) and after shrinking process (right)

During first part of experiment there was extremely high colour difference on red PET sample shrinked at 80°C and in general higher ΔE_{ab}^* values on PET prints shrinked at 80°C. We decided to repeat a part of the tests and measurements. Colour differences of blue and green colour of prints, white varnished, on PVC and PET substrates, shrinked for 30% and 50% are presented in Table II. The SEM images of the same samples are presented in Figure 3.

Table II: CIELAB colour values and differences for labels printed on PVC and PET substrates, shrinked for 30% and 50%

	Blue	Green	Ref. to shrink ΔE_{ab}^*			
	PVC ref. 0% shrink		PVC 30% shrink		PVC 50% shrink	
L^*	47.4	72.9	13.8	12.6	23.0	18.8
a^*	-35.2	-23.8				
b^*	-45.3	65.1				
	PET ref. 0% shrink		PET 30% shrink		PET 50% shrink	
L^*	42.6	64.3	14.6	12.3	24.6	18.9
a^*	-32.3	-38.0				
b^*	-50.9	50.3				

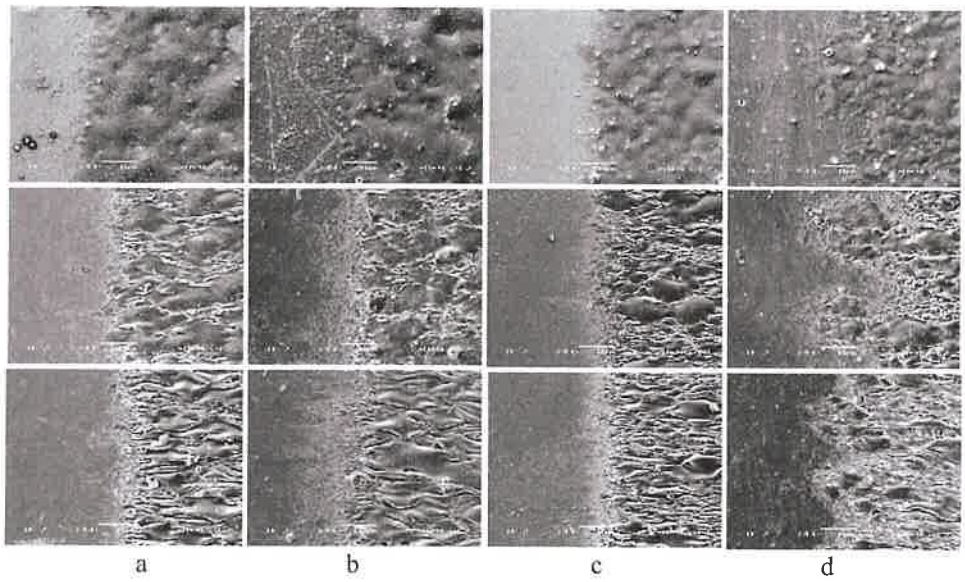

Figure 3: SEM images of unshrinked (top), shrinked 30% (middle) and shrinked 50% (bottom) of blue PVC (a), blue PET (b), green PVC (c) and green PET (d) samples, printed area on right

4. Discussion

As we expected UV ink based offset printing process is suitable for shrink sleeve labels production. The visual apperance of typical label colours was different than colour achieved in flexo printing technique. This problem should be solved by using proper ICC profiles in colour management system and in the design of the labels.

The first set of measurements shows us relative small colour differences with some exceptions and in general higher changes for PET substrate. We chose samples, prepared for first part of experiment at different temperature level and not according to percentage of shrinkage. Samples were uneven with wave structure caused by different shrinkage of areas covered with different inks. Molecular structure possibly played a role too. The quality of the results of first set of measurements was not good enough to make useful final conclusions. Therefore we decide to repeat the experiment.

For second set of measurements we chose large smooth areas of blue and green label colours. The samples were white varnished. We prepared PVC and PET labels shrinked for 30% and 50% using hot water. We repeated the measurements and got colour differences very similar for PVC and PET substrate. Maximum colour differences ΔE_{ab}^* were 24.6 for blue and 18.9 for green, both on PET substrate. Measured optical density, chroma and hue angle give us interesting results. For blue colour on PVC and PET value L* and D_c decreased by shrinking but for green colour on PVC and PET value L* decreased and D_y increased (Table III). We see that for most critical blue colour, shrinked for 50%, on PET substrate we achieved $\Delta L^* = -9.6$, $\Delta C^* = -12.5$, $\Delta h = +18.4$ and $\Delta D_c = -0.43$. Decreased optical density seems to be a result of the not suitable filter for cyan and change of chroma and hue angle during shrinking process.

Table III: Colour values: lightness, a^*, b^*, chroma, hue and optical density for blue and green samples printed on PVC and PET substrate

	Blue			Green		
	PVC 0%	PVC 30%	PVC 50%	PVC 0%	PVC 30%	PVC 50%
L^*	47.4	40.7	35.9	72.9	65.5	59.6
a^*	-35.2	-23.0	-15.4	-23.8	-27.4	-27.3
b^*	-45.3	-44. 5	-42.4	65.1	55.6	52.3
C^*	57.4	50.1	45.1	69.3	61.9	59.0
h	232.2	242.6	250.0	110.1	116.2	117.5
D	1.64	1.53	1.51	1.19	1.25	1.36
	PET 0%	PET 30%	PET 50%	PET 0%	PET 30%	PET 50%
L^*	42.6	38.3	33.0	64.3	65.2	51.3
a^*	-32.3	-18.7	-10.8	-38.0	-27.8	-37.8
b^*	-50.9	-47.5	-43.4	50.3	57.1	36.7
C^*	60.2	51.1	44.7	63.1	63.5	52.7
h	237.6	248.5	256.0	127.1	116.0	135.9
D	1.98	1.57	1.55	1.19	1.28	1.31

SEM images show us different surface structure of unshrinked and shrinked printed samples. On the images we see only surface covered with white varnish, because on SEM we see only surface of the sample. We can see differences between blue and green colour and between PVC and PET substrate. The correlation of the surface structure and achieved colour differences is unknown. We are still working on the print surface analysis to find out the reason for big colour change which depends not only on higher concentration of the pigment in the ink but on the deformations of the ink layer on the substrate too.

5. Conclusions

During our investigation we opened some interesting questions and didn't get all the answers. Because of unsuitable label samples we had to repeat our experiment in the future using CMYK solids and their combinations on standard patches. The use of printability tester (like IGT) in combination with lab UV dryer should give us more standardized prints for measurements.

SEM images of the printed surface are very interesting but they don't give us enough information. We should add colour images from optical microscope with cross section of the prints to find out the influence of shrinking process on colour changes.

It seems that colour differences are partly influenced by thermocromaticity of some inks. We have to find out colour changes of different inks in the future.

Colour changes in shrink sleeve label production have been mentioned in published works but only in the case of flexo or gravure printing process but no differences using different ink colours and substrates were discussed, known to the authors. We intend to continue our work in the future to find out the reasons for differences using different UV inks on PVC or PET substrates and to describe the model of colour changes during shrink process.

Acknowledgements

The authors want to express their gratitude to the Mueller Martini GmbH, Klockner Pentaplast Group Zeller+Gmelin GmbH and KRO d.o.o. for technical support.

References

[1] Bolte G., *UV-PRINTING OF THIN FILMS*, IST-Metz GmbH, www.radtech-europe.com/files_content/boltepaperjune.pdf

[2] Breil J., 2004, *Speciality Oriented Films: Speciality Plastic Films*, Brückner Maschinenbau GmbH, www.brueckner.com/pdf/spf_2004%20.pdf

[3] Llewellyn W., 2003, *Europe: Label's Leader*, AWA Alexander Watson Assoc. http://pffc-online.com/tapes/paper_europe_labels_leader/

[4] Polischuk T., *Printing Inks That Shrink*, http://www.packageprinting.com/story/story.bsp?sid=36772&var=story

[5] Thomas A. (Editor), *Global Label Market*, Labels & Labeling, www.labelsandlabeling.com

[6] Vainstein J., 2005, *A Study Of The Conditions And Variables That Affect The Printing Of Shrink Films On Waterbased Flexography,* School of Print Media in the College of Imaging Arts and Sciences of the Rochester Institute of Technology

Quality control for printed interference colours - investigation for a basic measuring geometry

Heike Hupp, Edgar Dörsam

Technische Universität Darmstadt, Fachgebiet Druckmaschinen und Druckverfahren
Magdalenenstrasse 2, 64289 Darmstadt, Germany
E-mail: hupp@idd.tu-darmstadt.de; doersam@idd.tu-darmstadt.de

Abstact

Special effect colours, such as pearlescent/interference colours, get more and more important in printing industry. Until now, process control is restricted to conventional absorption colours (CMYK). Here, measuring devices and procedures have proved good practice. In contrast, print quality of interference inks is controlled only by visual inspection.

This paper presents the investigation regarding the necessary quantity of measuring geometries and suitable angles, that build a measuring device for an appropriate quantification of printed interference inks.

Starting from a literature study concerning special effect colours, the proceeding of the investigation is derived. As measuring results, colour values CIELAB and colour differences are compared. Regarding the results achieved by this investigation, recommendations for a basic measuring geometry to determine the change in colour appearance related to a varying ink film thickness is presented.

Keywords

Colour measurement, interference colour, measuring geometries, offset printability tests

1. Introduction

In order to highlight ones print products within those of competitors, especially from low cost countries, it is necessary to use additional technologies, such as printing special effect colours. The appearance of these colours is based on physical effects that differ from the principle of absorption colours, such as the process colours Cyan, Magenta, Yellow and Black (CMYK). The group of special effect colours comprises metallic colours, pearlescent and interference colours of first and second generation. This wide variety of inks poses new challenges in assuring print quality. While spectrophotometers and densitometers, connected directly to the printing press or as standalone devices, are state of the art for controlling the quality of conventional absorption colours, for most effect colours, especially for pearlescent/interference inks (in the following called interference inks), no measuring devices and procedures have been established until now. Consequently, in these cases print quality is controlled by visual inspection only.

Overcoming this unsatisfactory state, purpose of this paper is to find a basic measuring geometry, which allows determining the change in colour appearance with respect to a varying ink film thickness of printed interference inks. Evaluation concentrates on measurements of Datacolor Multi FX10, a multi-angle measuring instrument, known from quality control in manufacturing process of interference pigments.

In this report, an introduction on colour appearance of interference colours related to different measuring geometries is given. Secondly, the research procedure is described. Observed changes in colour values, which are related to the different measuring geometries and the increasing ink film thickness, are then discussed. In conclusion, recommendations for a suitable measuring device are presented.

2. Methods

2.1 Literature study

Process colour inks (CMYK), high fidelity and spot colour inks belong to the group of absorption colours. Their pigments absorb particular wavelengths of the illuminating light. Colour appearance is determined by

the remaining wavelengths of the reflected light. Since the pigments are of irregular shape, the resulting reflection is diffuse. That means that colour appearance is almost constant for all combinations of illumination and viewing angles [Völz, 2001].

The group of special effect colour inks represents the second class of printing inks and varnishes. Typically, they are used for design, highlighting and finishing purposes. This group can be subdivided according to special effect pigments and their physical principles, which determine colour appearance (Table I).

Table I: Classification of pigments used in printing inks with respect to physical principles, which determine their colour appearance [Klein, 2004; Cramer, 2001]

Pigments	**physical behaviour of colour appearance**
Luminescent pigments	Selective absorption and emission in a different (usually longer) wavelength. Differentiation between fluorescence and phosphorescence pigments.
Thermochromatic pigments	Selective absorption related to temperature.
Metallic pigments	Metallic (mirror) reflexion.
Pearlescent/interference pigments of the first generation (mica based pigments)	Interference effects caused by light refraction at thin layers of different refration indices. Simulation of pearlecent gloss, pearl luster effects from silky matte to highly glittery. Various color effects from pearl white to interference colour. Examples: yellow, red, blue, green and gold
Interference pigments of the next generation (e.g. coated synthetically produced silicon dioxide platelets or cholesteric liquid chrystals)	Interference effects caused by light refraction at thin layers of different refration indices or liquid chrystals. Intense colour shifts, multicolour effects (angle-dependent colour changes) and intensive chrystal effects.

For this paper, only interference colours of the first generation are of interest and will be described in the following. Information about other special effect colours can be gleaned in literature [Cramer, 2001; Klein, 2004].

Most interference pigments of the first generation are mica flakes coated with single or multiple thin layers of metal-oxide (e.g. TiO_2). They are transparent and acquire the colour effects through interference with little or no absorption [Rodrigues, 1995; Huber, 2000]. The interference is caused by the interaction of the part of light which is reflected at the surface and the refracted part of the light, which is reflected at the interfaces of the layers (see figure 1). According to the simplified interference equation, the resulting reflection colour is a function of the layer thickness of the titanium dioxide, of its refraction index and of the angle of incidence of the light [Cramer, 1999].

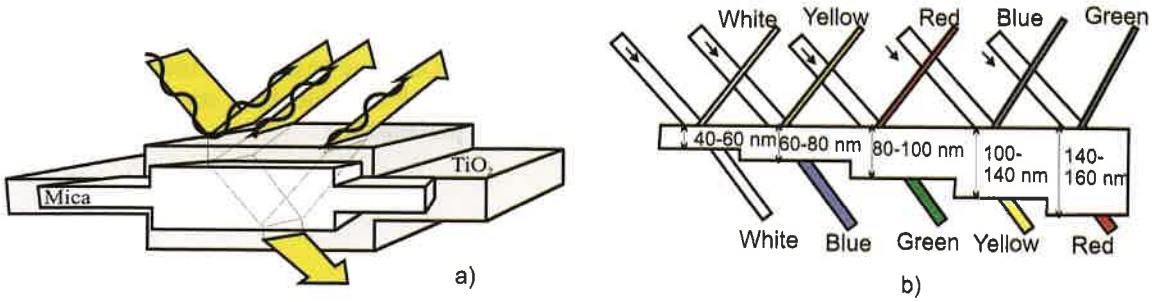

Figure 1: a) Schematic cross-section through a mica flake pearl lustre pigment, b) Changes in colour, with respect to thickness of the TiO_2 layer [Maisch, 1991]

Furthermore, colour appearance depends on the viewing angle. According to Cramer [Cramer, 2001] an interference ink applied on a white underground shows the interference colour only at angles within a range of 30° for the aspecular angle ($\gamma < 30°$). Under all other viewing conditions, the complementary colour, determined by the reflection of the transmitted light on the white underground superposed by the reflection of the white underground itself, is perceived [Cramer, 2001]. Thereby, the gloss angle is another expression for the reflection angle, given by the laws of reflection (angle of incidence equals the angle of reflection) and the aspecular angle are illustrated in figure 2.

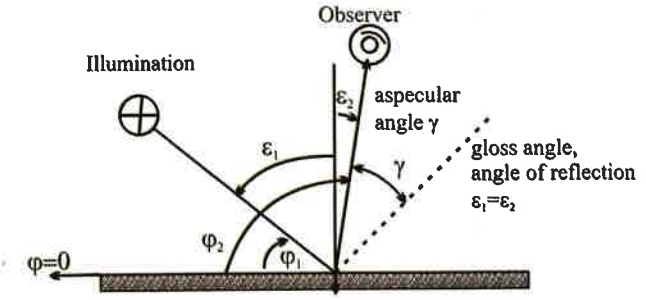

Figure 2: Definition of the illumination, observing and aspecular angle [Datacolor, 2006]

This leads to the conclusion, that measuring devices for determining the colour appearance of interference colours require more than one illumination angle and more than one viewing angle.

In a previous paper an overview of the state of the art of measuring devices for the printing industry and for measuring interference colours was presented [Hupp, 2006]. As result of this paper, the multi-angle measuring device of Datacolor, named Multi FX10, is the only measuring device available, which meets the demands of various illumination and viewing angles. However, this measuring device cannot be adapted to the requirements of the print process. As conclusion, further investigations on this device were recommended, which are presented in the following.

2.2 Experiments

With regard to quality control of interference colours, the relation between ink film thickness and colour appearance has to be specified. Therefore, it is necessary to manufacture samples, which provide a defined ink film thickness. Since offset printing is a very complex process, it is advantageous to reduce the sample manufacture to a simpler process, where the parameter ink film thickness can be monitored. With the IGT Test Equipment [IGT, 1972] (see figure 3), the production process of the samples satisfies standardisation ISO 2834:1999.

For the test series, a paper of Scheufelen, called "Phoenix Imperial II/II, APCO" was used. This paper is glossy coated and free from optical brighteners. The two offset printing inks used are colourless oil coatings enriched with red and blue interference pigments respectively (LithoRed and LithoBlue, Huber Druckfarben, München). For each colour, two test series were performed, applying an aluminium printing form, which provides full tone. In the first test series, the ink film thickness of the samples ranges between 0.05 and 1.4 µm, while the ink film thickness of the samples of the second series was increased up to 5 µm for LithoRed and 5.5 µm for LithoBlue. Furthermore, samples were produced using an applicator bar which allows applying increasing ink films in ten steps with a thickness of 10 µm up to 200 µm. Since this process is not accurately reproducible and such high ink film thicknesses are not feasible in offset printing, these samples were only considered for an appraisal of the trend in colour appearance for very thick ink films.

2.3 Measurements

For the measurements the multi-angle measuring device Datacolor Multi FX10 was used. Datacolor Multi FX10 is the only industrial measuring device today, which allows to rate special effect colours [Hupp, 2006]. It is equipped with ten sets of illumination/viewing angles, thus ten different measuring geometries. Figure 2 illustrates illumination and viewing angles which define the different measuring geometries of Datacolor

Multi FX10. These measuring geometries are defined in 4b) according to different normenclatures. Figure 4a) illustrates the implementation of these measuring geometries in the measuring device. The nomenclature for measuring geometries at the measuring device differ from standardized nomenclature ASTM WK 1164. In the following, the nomenclature of the measuring device and the values of the aspecular angle are used. For nomenclature according to ASTM WK 1164, figure 4 can be consulted.

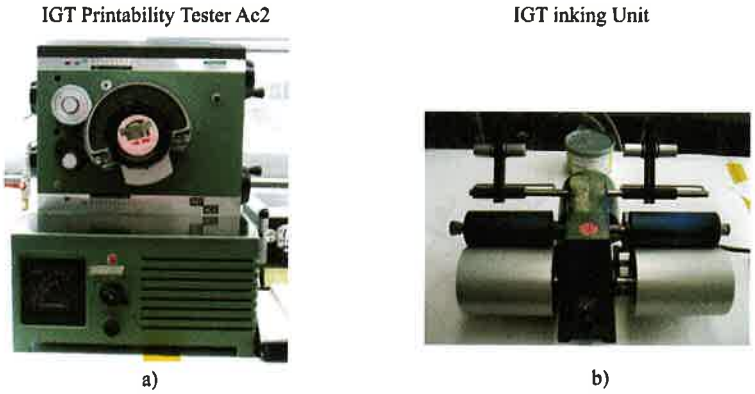

Figure 3: IGT Printability tester and inking unit

As measurement data, Datacolor Multi FX10 can display calculated values, such as CIELAB, or spectral data. To unify the calculation, only spectral data was used for the following researches. Furthermore, the recommendations to measure leastwise three times for one sample [Hupp, 2006] were followed.

a) Datacolor Multi FX10:
Moving half pipe, with fixed positions for illumination and viewing optics

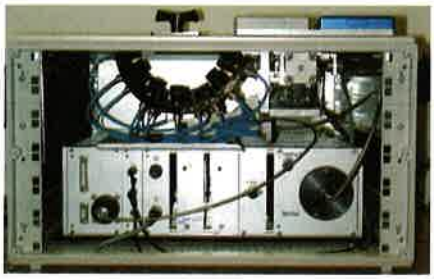

b) Measuring geometries of Datacolor Multi FX10:

Nomenclatur of the measuring device (counted from horizontal)			Nomenclature according to ASTM WK 1164 (2006)			
	illumination angle [°]	viewing angle [°]		illumination angle [°]	viewing angle [°]	aspecular angle [°]
	ε_1	ε_2		φ_1	φ_2	γ
25°/170°	25	170	65/-80 (as -15)	65	-80	-15
25°/140°	25	140	65/-50 (as 15)	65	-50	15
45°/150°	45	150	45/-60 (as -15)	45	-60	-15
45°/120°	45	120	45/-30 (as 15)	45	-30	15
75°/120°	75	120	15/-30 (as -15)	15	-30	-15
75°/90°	75	90	15/-0 (as 15)	15	0	15
45°/110°	45	110	45/-20 (as 25)	45	-20	25
45°/90°	45	90	45/0 (as 45)	45	0	45
45°/60°	45	60	45/30 (as 75)	45	30	75
45°/25°	45	25	45/65 (as 110)	45	65	110

Figure 4: a) View into measuring device Datacolor Multi FX10, illustrating the moving half pipe, with fixed positions for illumination and viewing optics b) Measuring geometries of Datacolor Multi FX10 according to nomenclatures of the measuring device and ASTM standard WK 1164 respectivel. Naming of the angles, see figure 2 [Datacolor, 2005; ASTM, 2006]

2.4 Calculations

The measuring results depend not only on the varying ink film thickness, but also on the measuring geometry used. Therefore, the spectral data was transferred to a self-designed calculation tool, whose target was to calculate colour and density values. For this research work only the CIELAB colour values (L^*, a^* and b^*), calculated according to DIN ISO 13655:2000, were taken into consideration.

Based on this calculation the changes in lightness L^*, green-red-axis a^* and blue-yellow-axis b^* were displayed. To examine the influence of the colour appearance of the print substrate (paper), the colour differences in

lightness ΔL^*_{paper}, green-red-behaviour Δa^*_{paper} and the blue-yellow-behaviour Δb^*_{paper}, as well as the overall colour difference $\Delta E^*_{ab,\ paper}$ were calculated, see equation (1). Furthermore, two measuring geometries were selected in order to distinguish the changes that are related to the variation of viewing/illumination angle. The chosen measuring geometries were 45°/90°, as standard for measurements in printing providing an aspecular angle $\gamma > 30°$, and 45°/120°, providing an aspecular angle $\gamma < 30°$. For these two geometries, the colour differences were calculated according to equation (1).

$$\Delta L^*_{nominal} = L^*_{actual\ value} - L^*_{nominal}$$
$$\Delta a^*_{nominal} = a^*_{actual\ value} - a^*_{nominal}$$
$$\Delta b^*_{nominal} = b^*_{actual\ value} - b^*_{nominal}$$
$$\Delta E^*_{ab,\,nominal} = \sqrt{\Delta L^{*\,2}_{nominal} + \Delta a^{*\,2}_{nominal} + \Delta b^{*\,2}_{nominal}}$$

with

- "nominal" as wild-card either for the colour values of the paper, the colour values of 45°/90°-measuring geometry or colour values of 45°/120°-measuring geometry
- "actual value" as wild-card either for the colour values of the samples with respect to the same measuring geometry or the colour values for the same sample but for the different measuring geometries.

(1)

3. Results

First, samples with high ink films, that were manufactured with the applicator bar, were analysed. For different measuring geometries, figure 5 illustrates the changes in lightness as well as in a^*-b^*-values (CIELAB) of the applied ink LithoRed (thickness d = 180 µm), as example.

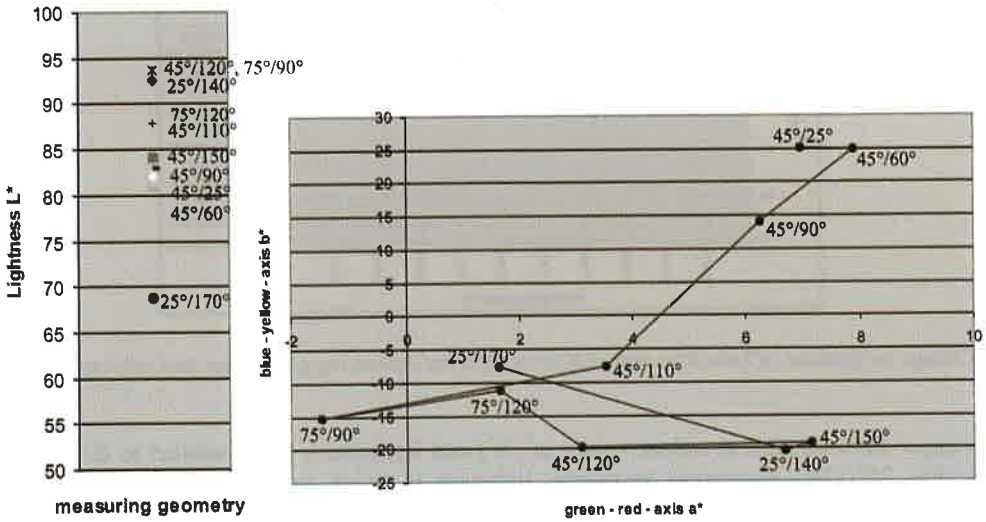

Figure 5: Chroma diagram of LithoRed with an ink film thickness d = 180µm. Lightness (left) and a^*-b^*-values (right) change, depending on the measuring geometry applied

At high ink film thickness, LithoRed shows a yellowish colour, indicated by positive b^*-values and low a^*-values, at measuring geometries with an aspecular angle $\gamma > 25°$ (as 45, as 65 and as 110). For geometries with an aspecular angle $\gamma = \pm 15°$ (as 15 and as -15) it shifts to a colour that is influenced by the interference colour (here red and blue, respectively). Only measuring geometry 25°/170° shows deviant behaviour: the colour is much darker and shifts to an achromatic colour appearance, indicated by low absolute values of a* and b*.

For measuring geometries with constant aspecular angle ($\gamma = \pm 15°$), changes in colour appearance depending on varying angle of incidence, have "bellied" character. Thereby, measuring geometry 45°/120° marks a

turning point. The colour values of the other measuring geometries vary from this turning point perpendicular to "interference"-direction. As it can be seen in figure 4, the "interference"-direction of LithoRed is determined by a change in $+a^*$-direction (increasing red colour appearance). The perpendicular direction is a change in b^*-direction, which is a shift to a more bluish colour appearance. Same behaviour, but with different "interference"-direction can be observed for LithoBlue, see figure 6.

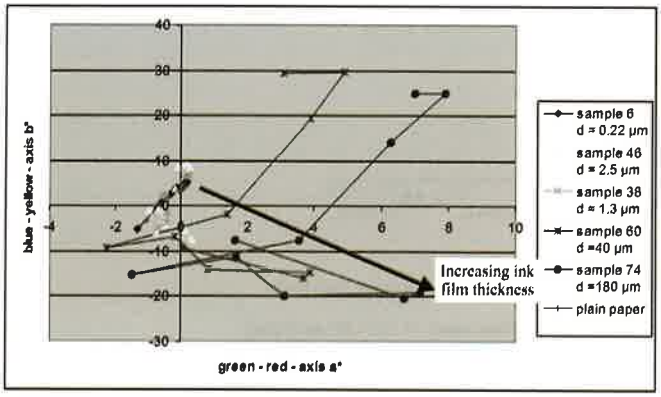

Figure 5: Colour appearance of LithoBlue with subject to different measuring geometries and varying ink film thickness

For printing purposes, much thinner ink films are of interest. Therefore, in the next step, changes in colour appearance with subject to lower ink film thicknesses were examined. In comparison to the colour appearance of plain paper, figure 5 and figure 6 exemplify colour shifts in a^*-/b^*- and L^*-direction of LithoBlue for thin ink films: two ink film thicknesses that are applicable in printing ($d \approx 1.3$ µm and $d \approx 2.5$ µm) and two higher ink film thicknesses.

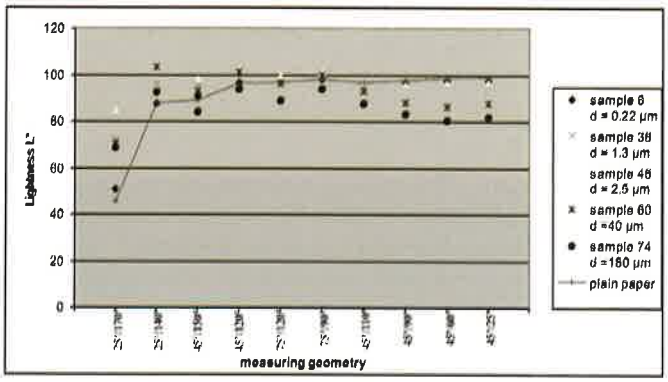

Figure 6: Change in lightness of LithoBlue with subject to different measuring geometries and varying ink film thickness

Even plain paper shows a shift in colour values (a^*, b^*) and lightness L^* with subject to different measuring geometries. For 25°/170°- measuring geometry, lightness is much lower than for the other measuring geometries. With steeper illumination angles and increasing aspecular angles, lightness increases up to almost 100 lightness units, see figure 7 solid line for plain paper. Regarding a^* and b^* (figure 8a), solid line), again a deviant behaviour for the 25°/170°- measuring geometry can be observed. In colour values, paper shows a slight greenish colour for measuring geometries 45°/150° and 45°/120°. For a steeper illumination angle and an aspecular angle bigger than 25°, colour shifts to a more yellowish appearance.

The characteristics of plain paper influence strongly the colour appearance of samples with an ink film thickness smaller than 0.3 µm, see figure 8a). The colour difference $\Delta E^*_{ab,\ paper}$ for this range of ink film thicknesses is smaller than 2 ($\Delta E^*_{ab,\ paper} < 2$). For higher ink film thicknesses (0.3 µm up to 5 µm) the influence of the ink film increases, see figure 8b). The hitherto yellowish colour appearance for measuring geometries with an aspecular angle $\gamma > 25°$ changes to a colour which is determined by the interference colour, as it can be seen for as ± 15-measuring geometries. Additionally, the influence of the angle of incidence increases with rising ink film thickness, see figure 7b).

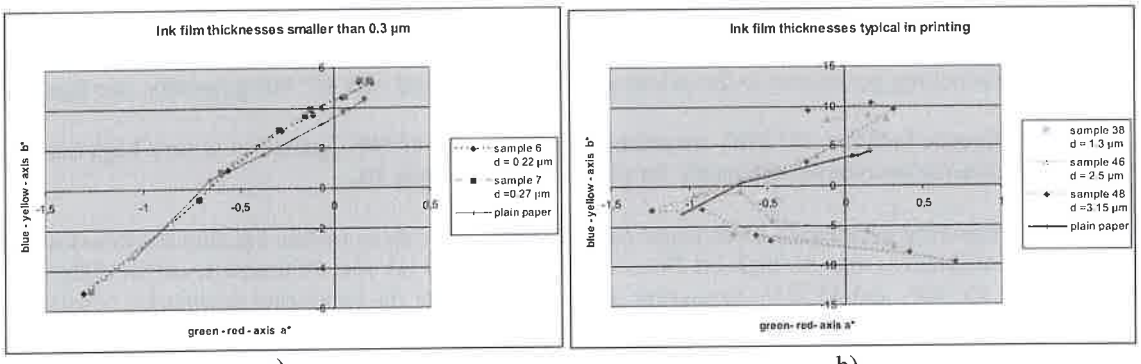

a) b)

Figure 7: Colour appearance of LithoBlue with subject to different measuring geometries and varying ink film thickness. a) Ink film thicknesses smaller than 0.3 µm; b) Ink film thicknesses typical for printing

The increasing influence of the ink applied, can also be seen when relating the colour difference $\Delta E^*_{ab,\ paper}$ to the colour values of the paper, see figure 9a) for LithoRed and figure 9b) for LithoBlue.

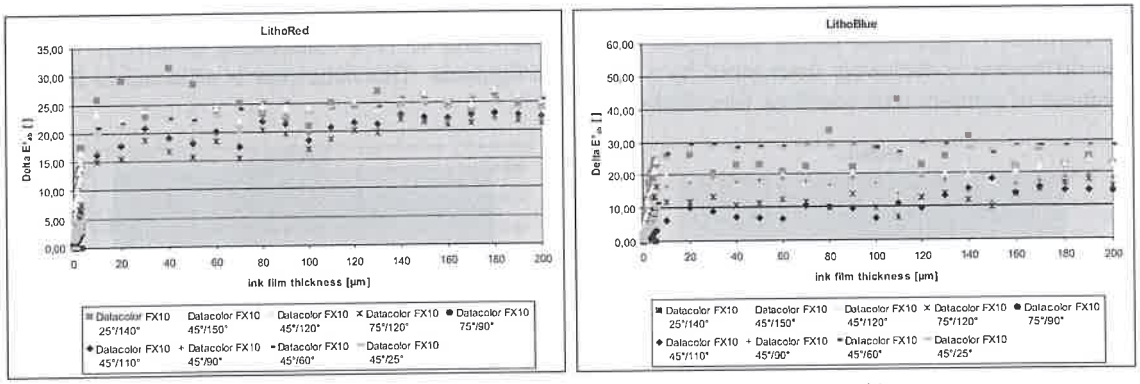

a) b)

Figure 8: Colour difference $\Delta E^*_{ab,\ paper}$ of samples with increasing ink film thickness to the colour values of the paper. a) LithoRed; b) LithoBlue

For increasing ink film thicknesses, the colour difference $\Delta E^*_{ab,\ paper}$, between printed ink and plain paper, increases as well, for all measuring geometries. Reaching very high ink film thicknesses (d > 60 µm), colour appearance is not changing noticeably, a kind of saturation can be observed. Colour difference between several measuring geometries can be characterised by different effects on colour appearance. For instance, geometries with an aspecular angle $\gamma > 25°$ show a darker and more yellowish colour, hence colour values change substantially along the lightness and the a^*-axis. For geometries with an observation angle near gloss ($\gamma = \pm 15°$), colour difference derives from a rising influence of the interference colour.

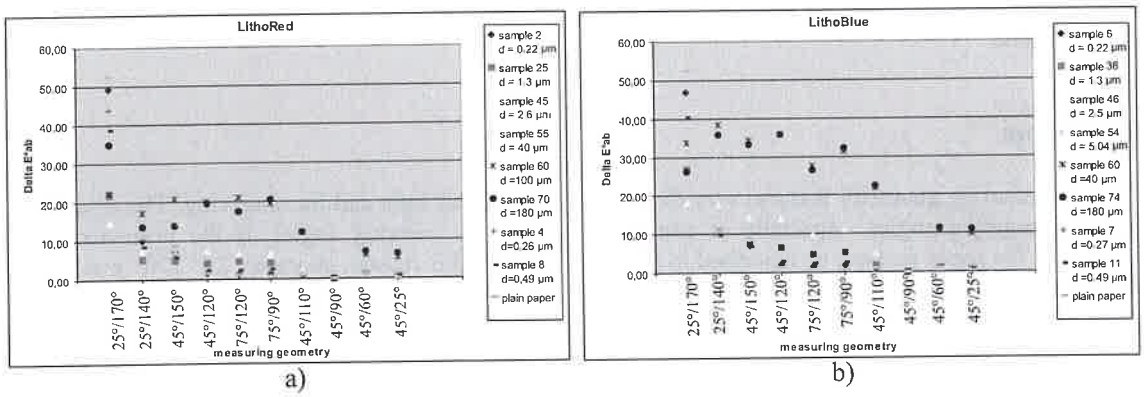

a) b)

Figure 9: Colour difference $\Delta E^*_{ab,\ 45°/90°}$ of samples with increasing ink film thickness to the colour values of the 45°/90°-measuring geometry. a) LithoRed; b) LithoBlue

Since measuring geometry 45°/90° marks turning point for colour appearance of interference colours, the colour shift in interference colour direction can be seen best, when relating the colour appearance observed with the other measuring geometries to the colour appearance observed with 45°/90°-geometry, see figure 10.

The colour difference between 25°/170°- measuring geometry and 45°/90°- geometry is very high compared to the other measuring geometries, especially for plain paper, see figure 10.

For all other measuring geometries, plain paper and samples of low up to middle ink film thicknesses, show smaller colour differences than for high ink film thicknesses. For all ink film thicknesses, colour difference is smaller for the 45°/60°- and 45°/25°- measuring geometries than for the measuring geometries consisting of an aspecular angle smaller than 25° ($\gamma < 25°$). Overall, LithoBlue reveales higher colour differences than LithoRed and a wider distribution related to the measuring geometries. Measuring geometries with an aspecular angle smaller than 25° ($\gamma < 25°$) show a higher colour difference, which is determined by a change to the interference colour and in lightness. Differences between the as ±15 - measuring geometries are ascribable to differences in direction perpendicular to interference, that is along a^*-axis for LithoBlue and along b^*-axis for LithoRed.

The overall differences between the measuring geometries of an aspecular angle of $\gamma = \pm 15$ were examined next. Thereby, investigations were based on colour values of the 45°/120°- measuring geometry, see figure 10. Plain paper reveales a significant colour difference for 25°/140°- and 45°/150°-measuring geometry, while this colour difference is decisively determined by a change in lightness. This behaviour is reflected in the colour differences of samples with small ink film thicknesses.

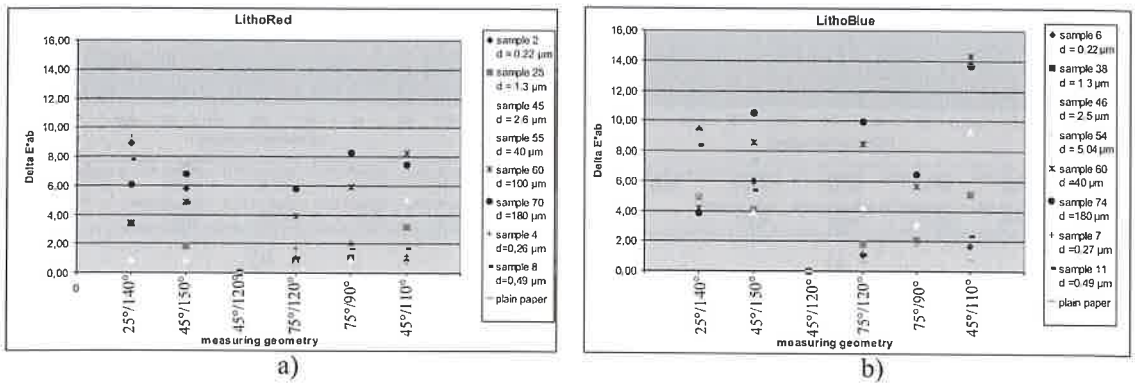

Figure 10: Colour difference $\Delta E^*_{ab,\ 45°/120°}$ of samples with increasing ink film thickness to the colour values of 45°/120°-measuring geometry

For samples providing an ink film thickness, which is typical in printing, the colour difference to the 45°/120°-geometry is almost constant for all as ± 15 - measuring geometries, within a tolerance of $\Delta E^*_{ab,\ 45°/120°} < 5$. For very high ink film thicknesses, colour difference reaches a value of $\Delta E^*_{ab,\ 45°/120°} < 10$. Concerning the colour difference to the 45°/120°-measuring geometry, especially the change in a^*-direction for LithoBlue and b^*-direction for LithoRed, that is the perpendicular direction to the "interference"-direction, influences the colour difference most.

4. Discussion

25°/170°-measuring geometry features very flat angles for incident light and for observing. The disadvantage of flat illumination angles, especially in combination with flat viewing angles, is the influence of light scattering at the paper surface, as described in [Pohl, 1963]. For this reason, geometry 25°/170° was excluded from draft standard WK 1164 [ASTM 2006]. Beside this measuring geometry, measurement device Datacolor Multi FX10 provides nine feasible measuring geometries.

Additionally, the colour characteristics of paper had to be considered, because plain paper showed a very high colour difference compared to the samples ($\Delta E^*_{ab,\ 45°/120°} \approx 9$ for measuring geometry 25°/140° and $\Delta E^*_{ab,\ 45°/120°} \approx 7.5$ for measuring geometry 45°/150°). Unlike these measurement results, a visual inspection (not standardized)

of the plain paper did not reveal such a strong colour shift. Therefore, these measurement results cannot be supported. Nevertheless, the results of measurements showing the light scattering effect at very flat illumination and viewing angles, as mentioned before, are ascribable. Since, for measuring geometry 25°/140° both angles are very flat, and for the 45°/150°-measuring geometry the viewing angle is very flat as well, the light scattering at the paper surface could have influence on the measuring results. For rising ink film thicknesses, this effect decreases, because of the increasing reflection at the surface of the ink and the increasing smoothness of the surface due to the ink film.

Since a measuring device for printing industry has to be as simple as possible, and the time frame for measuring is very short, it is necessary to reduce the number of measuring geometries. From these preconditions, the necessary quantity of measuring geometries and suitable angles had to be derived, that build a measuring device for an appropriate qualification of printed interference inks.

First of all it is necessary to comprehend the colour shift of the printed interference colour. As mentioned in literature [Cramer, 2001] and improved by this investigation, the colour appearance of interference inks changes with subject to the aspecular angle. The turning point, where the appearance of the ink changes from the interference colour to the transmission colour, given in literature as aspecular angle 30° ($\gamma < 30°$) is confirmed by this research work. While colour values for 45°/110°- measuring geometry ($\gamma = 25°$) indicate the interference colour, measuring geometries with an aspecular angle $\gamma \geq 45°$ show the transmission colour superposed by the reflection at the surface of the printing substrate.

Beyond this, the influence of the illumination angle is described in literature. The results of the experiments showed, that within the range of ink film thicknesses, typical for offset printing (1 - 3 µm), the angle of incidence does not strongly influence the results. In contrast to the results of the 45°/120°-measuring geometry, the other geometries, consisting of a variable angle of incidence and a constant aspecular angle of $\gamma = \pm 15°$, showed colour differences of $\Delta E^*_{ab,\ 45°/120°} < 5$. Measuring geometries 75°/120° and 75°/90° revealed an even smaller colour difference of $\Delta E^*_{ab,\ 45°/120°} < 2$. Hence, it is not necessary to implement more than two measuring geometries.

Second criterion arises from the fact, that the new measuring geometries should be installed easily into existing measuring devices. Nowadays the 45°/90°-measuring geometry is the standard geometry for measuring tasks in printing (DIN ISO 13655). This geometry provides an observing position far away from gloss direction, which means an aspecular angle bigger than 25° ($\gamma > 25°$). Hence, for interference inks, it is possible to measure the colour values of the transmission colour, given by the pigment of the interference ink, superposed by the reflection at the surface of the printing substrate. For measuring the interference colour, an additional measuring geometry is necessary, which provides an observing angle near gloss. The two geometries 45°/150° and 45°/120° satisfy both requirements, observing conditions near gloss ($\gamma = \pm 15$) and easy implementation into existing devices, because only one additional observing sensor is needed and it is not necessary to install an additional lighting. The experiments of this research showed, that the influence of light scattering is stronger for the 45°/150°- than for the 45°/120°-measuring geometry. Furthermore, the colour values for measuring geometry 45°/120° are placed in between the colour values of the other as ± 15 -measuring geometries for almost every ink film thickness. Hence, measuring geometry 45°/120° features the best conditions and can therefore be recommended as additional measuring geometry.

5. Conclusion

Focus of this paper was the enhancement of quality control of printed interference inks. A literature study showed, that it is essential for interference pigments to be viewed/measured under different illumination and viewing conditions. From these requirements, the necessary quantity of measuring geometries and suitable angles was searched, that build a measuring device for an appropriate qualification of printed interference inks. Therefore, samples with varying film thicknesses of interference inks (LithoBlue and LithoRed) were examined, using the multi-angle measuring device Datacolor Multi FX10. As measuring results, colour values CIELAB and colour difference were compared.

Based on these examinations, it could be demonstrated, that the influence of the interference colour increases with thicker ink films and reaches saturation at very high ink film thicknesses ($d > 60$ µm). Beyond this, the increasing influence of the angle of incidence for high ink film thicknesses could be demonstrated. For ink

film thicknesses typical in offset printing (1 - 3 µm), a colour shift towards the interference colour with subject to the aspecular angle was determined. This colour shift increases with increasing ink film thickness. Furthermore, it was discovered that the influence of the illumination angle for ink film thicknesses typical in printing is very small. Hence, only two different measuring geometries are necessary to describe the behaviour of printed interference inks in an appropriate way.

Since measuring geometry 45°/90° (which provides an observing angle far away from gloss) is state of the art in measuring printed colours, only an additional measuring geometry, which consists of an aspecular angle $\gamma \leq 25°$, has to be installed. Here, measuring geometry 45°/120° was found to be a good solution.

As conclusion, it can be recommended to install the two measuring geometries 45°/90° and 45°/120° in new measuring device to enhance the quality control of printed interference inks.

This conclusion is valid only for the interference inks (LithoRed and LithoBlue) and the printing substrate (Phoenix Imperial APCO II/II) examined, though most probably, it can be applied on other interference inks and substrates as well. This has to be proved in further researches. Additionally, it is necessary to investigate the repeatability of the results achieved in this paper to prove their statistical firmness.

References

[1] ASTM (2006), *WK 1164 Standard Practice for Multiangle Color Measurement of Interference Pigments, USA*

[2] Cramer (1999), *Magical Mixtures, Paint & Coatings Journal 9, 72*

[3] Cramer (2001), *Measuring Special Effects, Paint & Coatings Journal 7 - 8, 36 - 42*

[4] Datacolor (2006), *Multi FX10 Operation Manual*

[5] DIN ISO 13655 (2000), *Spektrale Messung und farbmetrische Berechnung für graphische Objekte*

[6] Hupp (2006), *Measuring special effect colours - first experiences with the MultiFX10 spectrophotometer, Iarigai XXXIII conference*

[7] Huber (2000), *Effektpigmente in Lacken, Phänomen Farbe 7 + 8*

[8] IGT (1972), *Operation Manual*

[9] ISO 2834 (1999), *Test prints preparation for offset and letterpress inks*

[10] Klein (2004), *Farbenphysik für industrielle Anwendungen, Springer, Berlin*

[11] Pfaff (2007), *Spezielle Effektpigmente, Vincentz, Hannover*

[12] Pohl (1963), *Optik und Atomphysik, 11. Auflage, Springer, Berlin*

[13] Rodrigues (1995), *Color and Appearance Measurement of Metallic and Pearlescent Finishes, ASTM standardisation News*

[14] Schröder (2002), *Technische Optik, Vogel Verlag, Würzburg*

[15] Völz (2001), *Industrielle Farbprüfung, WILEY-VCH Verlag, Weinheim*

Photoacoustic study of varnished solids printed by different techniques

Markéta Držková, Jiří Hejduk, Klára Grolichová

University of Pardubice, Faculty of Chemical Technology, Department of Graphic Arts and Photophysics
Studentská 95, Pardubice 532 10, Czech Republic
E-mail: marketa.drzkova@upce.cz; jiri.hejduk@upce.cz; klara.grolichova@seznam.cz

Abstract

The aim of the study was to establish the methods utilising the non-destructive photoacoustic depth profiling for investigation of varnished solid prints, to gain the information inaccessible by common thickness or gloss measurements. Two theoretical models describing the dependence of photoacoustic signal on modulation frequency were considered and their validity for individual types of samples was verified. Varnish layers with varying thicknesses coated over one-colour solids printed on diverse substrates by offset lithography and flexography were examined. The reason for choosing different printing and coating techniques and various commonly used combinations of substrate, ink and varnish was to explore the limits of the photoacoustic method with respect to its application for varnished solid prints. The study proved the applicability of photoacoustic investigation in this field and determined both theoretical and experimental limitations for respective types of samples. The varnish thermal diffusivity was calculated from thickness and photoacoustic measurements for samples with higher thickness of varnish layer.

Keywords

Flexography, offset lithography, photoacoustics, varnishing

1. Introduction

One of the important parameters influencing the quality of printed product is the thickness of individual layers which form the resulting image or change its appearance, resistance etc. Usually printed colour ink layers are the former and transparent layers created by varnishing or film laminating are the latter. This study is focused on varnish layers with varying thicknesses coated over solids printed on different substrates by offset lithography and flexography. The aim is to establish methods for investigation of varnished solid prints, based on non-destructive photoacoustic depth profiling.

Generally, in case of printed products, reliable determination either of overall thickness or particular layer thickness is complicated due to number of reasons. The use of the most common methods and devices is significantly limited, as variations in substrate thickness are usually of the same order as thicknesses of ink or coating layers and the dependence between optical properties like density or gloss and thickness of respective layers becomes quite soon saturated. Thus, more sophisticated methods were recently used for depth profiling of printed samples or other materials common in the field of graphic arts. As an example, studies utilizing step-scan FTIR spectroscopy with photoacoustic detection and confocal Raman measurement [Vikman, 2000; Sipi, 2001] or confocal laser scanning microscopy, cross section analysis with optical microscopy and photoacoustics [Muck, 2006] can be mentioned.

Comparing these methods, probably the main advantage of photoacoustic or more generally photothermal techniques is their versatility, enabling to setup the experiment suitable for given conditions. On the other hand, except the limiting cases when the theory of photoacoustic effect in condensed matter [Rosencwaig, 1980] is reasonably simple, planning the experiments and proper interpretation of measured data requires deeper understanding of all aspects influencing both intensity and phase of the photoacoustic signal. For brief introduction to theory of indirect photoacoustic effect and references on photoacoustic studies in printing see for instance [Držková, 2004].

Recently published studies [Kaplanová, 1997; Walther, 2001] dealing with selected varnish layers in printing and packaging assumed for the additional phase lag caused by non-absorbing varnish layer the simplified modulation frequency dependence for thermally thick regime. In the present study of varnished solid prints,

theoretical modelling of photoacoustic signal in dependence on modulation frequency was based on generalized theory of the photoacoustic effect in a multilayer material [Hu, 1999].

2. Materials and methods

For the theoretical modelling, matrix expressions of the photoacoustic signal were evaluated in Wolfram Research's Mathematica.

The experiments were aimed to explore the limits of the photoacoustics with respect to its application for varnished solid prints, so different printing and coating techniques were used for sample preparation and various commonly used combinations of substrate, ink and varnish were investigated.

2.1 Substrates

Six types of the substrates commonly printed by offset lithography and flexography were chosen for the study. Characteristics and parameters of the individual substrates are given in Table I and II, respectively.

Table I: Characteristics of the substrates

Designation	Description
GC	Gloss two-side triple-coated wood-free paper
MC	Matt two-side triple-coated wood-free paper
OF	Uncoated wood-free offset paper
CP	One-side coated wood-free paper
PE	Transparent polyethylene foil
PP	White polypropylene foil

Table II: Parameters of the substrates

	GC	MC	OF	CP	PE	PP
Mass-per-area (g/m^2)	166	96	82	49	54	93
Thickness (μm)	116	80	114	68	60	100
Bulk (cm^3/g)	0.70	0.98	1.19	1.39	1.12	1.07
PPS Roughness (μm)	0.95	1.83	6.87	3.56	0.82	0.84
Gloss (DIN 16537)	7.4	2.7	3.9	5.9	10.5	9.4

2.2 Inks and varnishes

Oxidatively drying process yellow offset ink (Athlon Intensiv, Sicolor GmbH) was used for offset lithography prints. For flexographic printing, solvent-based process magenta ink (ZMR 110-1, Siegwerk) was diluted with 1:1 ethanol-methoxypropanol solution (303 g of ink and 18 g of thinner).

Offset lithography prints were varnished with two dispersion varnishes (Varn, Day International GmbH), one gloss (designation VG) and one matt (designation VM). Flexographic prints were varnished with two gloss varnishes (Siegwerk); water-based dispersion varnish ZW 50 (designation FD) was used without dilution, solvent-based varnish 10-613608-8 (designation FS) was diluted with ethoxypropanol (154 g of varnish, 10 g of thinner). Parameters of the individual varnishes are given in Table III.

Table III: Parameters of the varnishes

	VG	VM	FD	FS
Density (kg/m^3)	1043	1064	1045	937
Dry content (%)	40.0	45.9	42.3	29.0

2.3 Printing and coating equipment

Printability tester for conventional and UV-curing offset inks, IGT C1 (IGT Testing Systems), was used for preparation of solid prints with elastomer top rollers, rubber printing disc (65 shore A, coated, printing width 35 mm, printing length 210 mm) and following printing unit settings: printing speed 0.3 m/s, printing force 400 N.

Phantom Proofer (HarperScientific, Printing and Coatings Supplies Division) is the hand proofer intended for coating and flexographic printing. Anilox rolls with four different screens were chosen for coating; designation of varnish layers from K to N corresponds to 79, 102, 197 and 217 l/cm.

Saueressig Flexo Proofer F. P. 100/300 (Saueressig GmbH + Co. KG) was used both for preparation of solid prints and for coating. Solids were printed with the 100 l/cm anilox roll (printing speed 0.3 m/s). For coating, the anilox roll divided into eight strips was employed; designation of varnish layers from A to H corresponds to 48, 54, 60, 70, 80, 100, 120 and 140 l/cm.

Sheen four sided applicator (Sheen Instruments Ltd) enables preparation of films with wet coating thickness of 30, 60, 90 or 120 μm.

2.4 Sample preparation

First, standard prints with yellow offset ink on gloss two-side triple-coated paper (GC), matt two-side triple-coated paper (MC) and offset uncoated paper (OF) were prepared on IGT C1 printability tester and subsequently varnished by means of Phantom Proofer using anilox rolls with four different screens (79 to 217 l/cm). Next, multiple varnish layers (up to five) were applied using the roller with 102 l/cm. In both cases commercial gloss (VG) and matt (VM) dispersion varnishes were compared.

Second, Saueressig Flexo Proofer was used to produce standard prints with solvent-based magenta ink on three other substrates – transparent polyethylene (PE), white polypropylene (PP) and one-side coated wood-free paper (CP). Dispersion (FD) and solvent-based (FS) varnishes (both gloss) were applied using anilox roll divided into eight strips with fineness varying between 48 and 140 l/cm. After drying, part of the sample prints was varnished for the second time (in the same way).

Finally, Sheen four sided applicator was used to create on the above mentioned magenta prints varnish layers with higher thicknesses (comparable to those printed by serigraphy), again using both dispersion and solvent-based varnish. The thickness of the wet film was 30, 60 and 90 microns, respectively.

2.5 Sample measurement methods

All studied samples were measured with a thickness gauge and a gloss-meter and then by photoacoustics. The thickness gauge used (Schröder) allows to measure thicknesses up to 1 000 μm with resolution of 1 μm. Gloss measurements were performed with Viptronic Vipgloss-I; according DIN 16537, value 0.0 corresponds to totally diffuse and value 10.0 to totally reflective reflection (perfect gloss). Values above 10.0 are out of range defined in DIN 16537 and are usually measured for metallic or strongly reflective materials.

The photoacoustics is generally understood as a measurement of the photoacoustic signal in the frequency domain at constant wavelength of the exciting radiation. To cover the region with high absorption of yellow and magenta ink, respectively, two laser modules were used for measurements - DPBL 9020 with wavelength 473 nm and DPGL 3020T with wavelength 532 nm (both Photop Suwtech Inc.). The experiments utilized whole frequency range feasible for modulation of both laser modules, from 10 Hz to 1 kHz. The light beam impinged on the surface of the sample placed inside a closed cylindrical photoacoustic cell. Generated acoustic signal was detected by a 1/2" condenser microphone [Brüel and Kjaer, type 4137] and preamplified. Output signal was fed to a DSP lock-in amplifier (Stanford Research Systems, model SR830). The laser light was modulated using the internal oscillator of the lock-in amplifier. All measurements were controlled and processed by PC.

The samples for the photoacoustic measurement (10 mm in diameter) were cut from the sheets and mounted on the plexiglass backing using two-sided adhesive tape. As a reference, polypropylene foil with thin gold layer deposited via evaporation in high vacuum was used.

3. Results and discussion

3.1 Thickness

Comparing the overall thickness of the solid print with the thickness of the respective substrate, the values lie within ± 3 μm. Differences between thicknesses measured for sets of prints varnished with varying screen on Saueressig Flexo Proofer and thickness of bare solid print are shown on Figure 1. Analogical results were obtained for samples varnished by means of Phantom Proofer with four different anilox rolls (not shown here). In case of multiple varnish layers, thickness increases only for prints on gloss coated paper with gloss dispersion varnish (Figure 2).

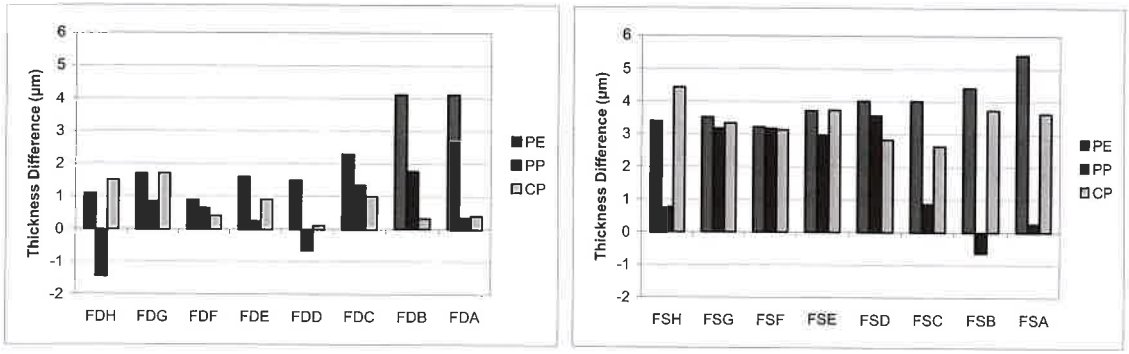

Figure 1: Change in thickness measured by a thickness gauge for solid magenta prints with dispersion (left) and solvent-based (right) varnish layers coated once using divided anilox roll (amount of transferred varnish increasing from H to A)

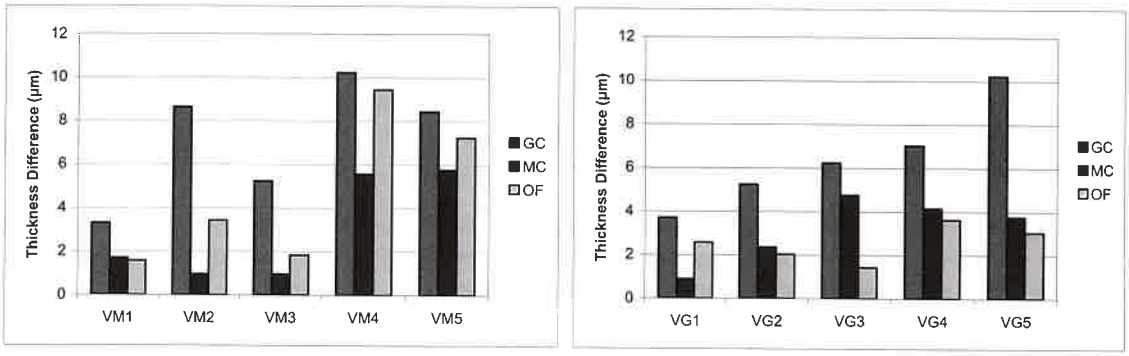

Figure 2: Change in thickness measured by a thickness gauge for solid yellow prints with multiple matt (left) and gloss (right) dispersion varnish layers coated by Phantom Proofer

Thus, both in case of papers and polymer foils it isn't possible to determine the thickness of the coated layers as the difference between the overall thickness and the thickness of the printed substrate, or not with sufficient reliability. Reasonable values might be gathered only by averaging great number of thickness measurements in sufficiently large area; however, in this manner it is impossible to evaluate the amount of varnish transferred to particular place.

Such results would be also influenced by the substrate roughness and character of the coating, as in dependence to these factors the coating builds into the substrate structure to different extent. This is clearly shown for the set of samples coated using Sheen applicator (Figure 3).

The quite large amount of varnish applied to the prints should ensure measurable increase of thickness; however, the increase of thickness resulting with given varnish somewhat differs for individual substrates and for combination of solvent-based varnish and one-side coated paper is the thickness nearly the same as before coating. The maximum increase in thickness for dispersion varnish was about 30 μm. For solvent-based varnish on polymer foils it was between 15 and 20 μm; in case of paper, the measured thickness was within 5 μm from thickness of uncoated print. Omitting values for this combination, the ratio of both dry content and mean layer thickness is roughly 1.5 comparing dispersion and solvent-based varnish used.

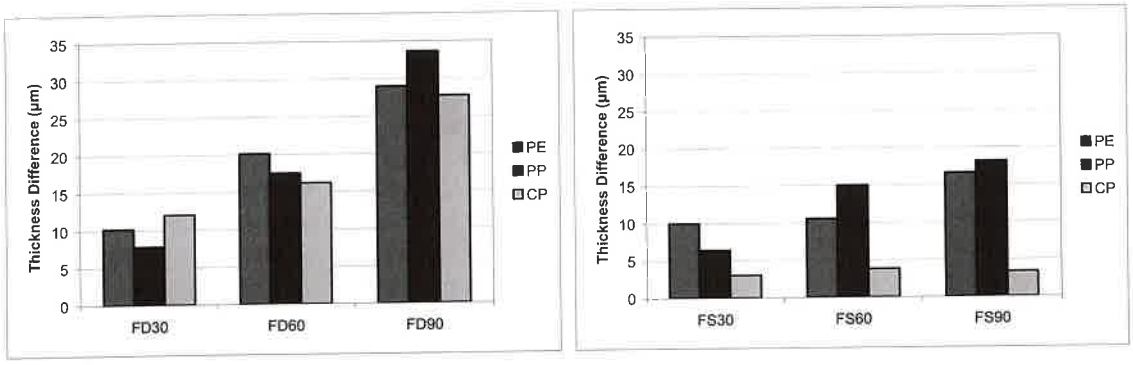

Figure 3: Change in thickness measured by a thickness gauge for solid magenta prints with dispersion (left) and solvent-based (right) varnish layers coated using Sheen applicator (thickness of the wet film 30, 60 and 90 µm, respectively)

3.2 Gloss

The results of gloss measurements for individual types of samples are depicted in Figures 4 - 8. Similarly to findings based on thickness measurement, the gloss of varnished solid prints can be used to estimate the thickness of varnish layer or amount of varnish applied only in certain cases.

Distinct increase in gloss was measured only for prints on paper coated with higher amounts of dispersion varnish using Sheen applicator (up to 3.2) and for prints on offset paper with multiple layers of gloss dispersion varnish (up to 2.6); slight increase for the set of prints on paper with dispersion varnish coated with varying screen for two times on Saueressig Flexo Proofer and for prints on offset paper with multiple layers of matt dispersion varnish (both up to 1.0). Distinct decrease in gloss appeared for prints on gloss coated paper with multiple layers of matt dispersion varnish (up to -3.9). In case of all other sample sets measured, the change in gloss with increasing amount of transferred varnish is not monotonic, or the changes in gloss are negligible.

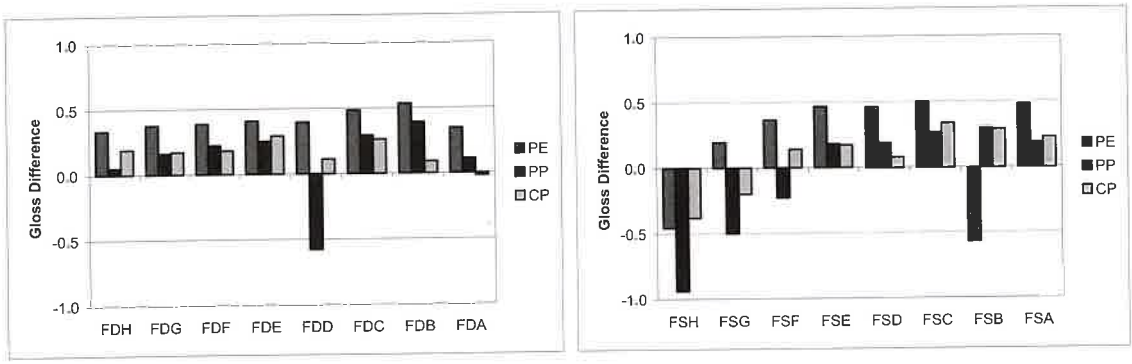

Figure 4: Change in gloss according to DIN 16537 for solid magenta prints with dispersion (left) and solvent-based (right) varnish layers coated once using divided anilox roll (amount of transferred varnish increasing from H to A)

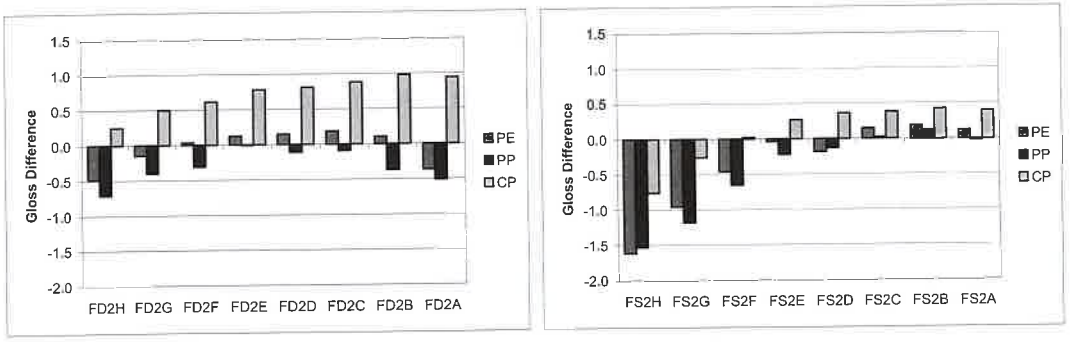

Figure 5: Change in gloss according to DIN 16537 for solid magenta prints with dispersion (left) and solvent-based (right) varnish layers coated twice using divided anilox roll (amount of transferred varnish increasing from H to A)

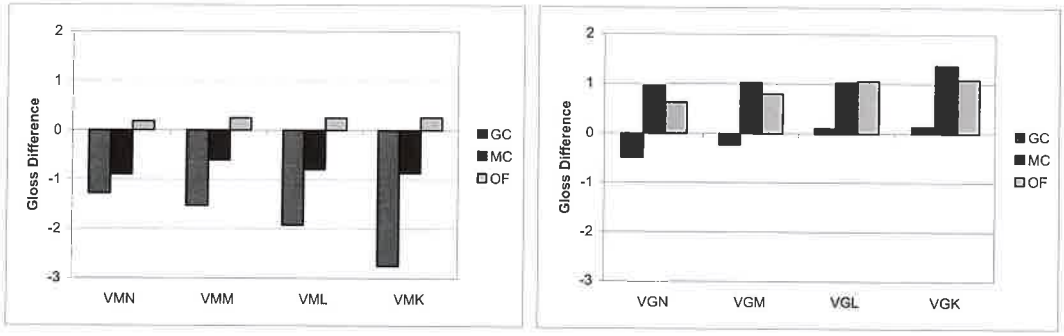

Figure 6: Change in gloss according to DIN 16537 for solid yellow prints with matt (left) and gloss (right) dispersion varnish layer coated by Phantom Proofer using anilox rolls with four different screens (amount of transferred varnish increasing from N to K)

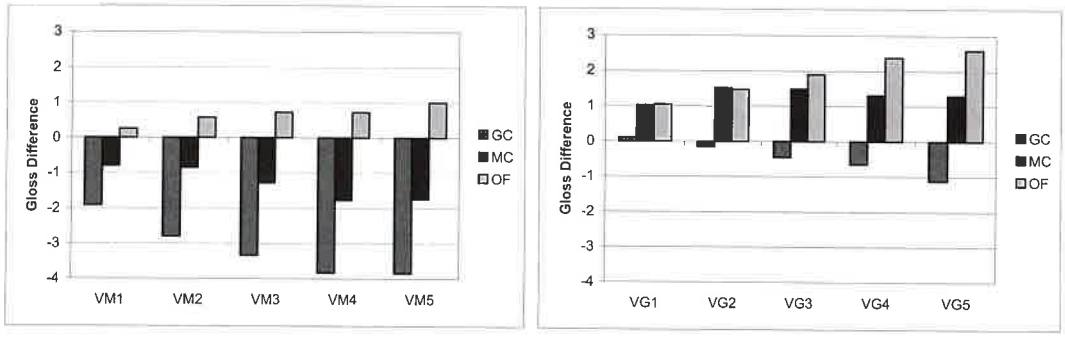

Figure 7: Change in gloss according to DIN 16537 for solid yellow prints with multiple matt (left) and gloss (right) dispersion varnish layers coated by Phantom Proofer

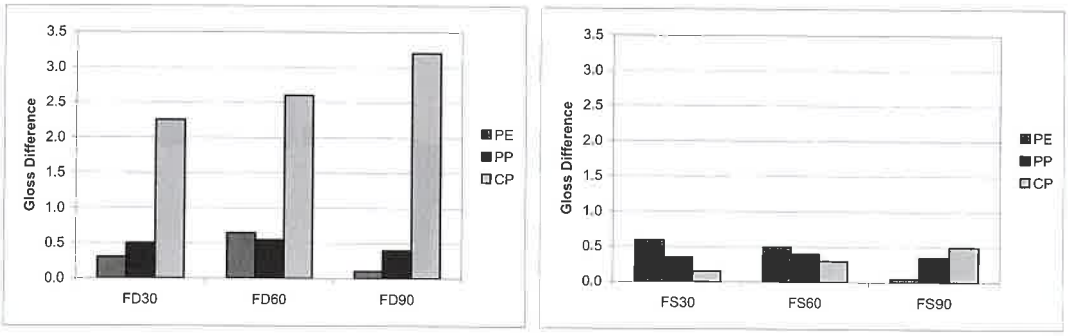

Figure 8: Change in gloss according to DIN 16537 for solid magenta prints with dispersion (left) and solvent-based (right) varnish layers coated using Sheen applicator (thickness of the wet film 30, 60 and 90 µm, respectively)

3.3 Photoacoustics

Using the photoacoustic depth-profiling, the increasing amount of transferred varnish results in changes of the measured signal for all sets of samples.

On the low end of the scale are differences between varnish layers coated using anilox rolls with varying screens (Figures 9 and 10). Both for samples printed with conventional offset ink and with solvent-based flexographic ink, changes in the phase of the photoacoustic signal are relatively small, but still distinguishable, with exception of solids printed by offset lithography and varnished using similar screens, which would need even higher modulation frequencies, not achievable with laser modules used. For samples varnished using divided anilox roll (48 to 140 l/cm) and printed on polymer foils the maximum phase delay measured for 1 kHz ranges between 6 and 17 degrees for dispersion varnish and between 5 and 11 degrees for solvent-based varnish (comparing to uncoated solid print). In case of samples printed on one-side coated paper the additional phase lag decreases with

increasing amount of transferred varnish, which will be discussed later on. For samples varnished by means of Phantom Proofer (anilox rolls with 79 to 217 l/cm) the maximum increase in phase delay measured for 1 kHz was up to about 5 degrees both for gloss and matt dispersion varnish; slightly higher values were measured for set of samples with matt dispersion varnish on gloss coated paper (up to 9).

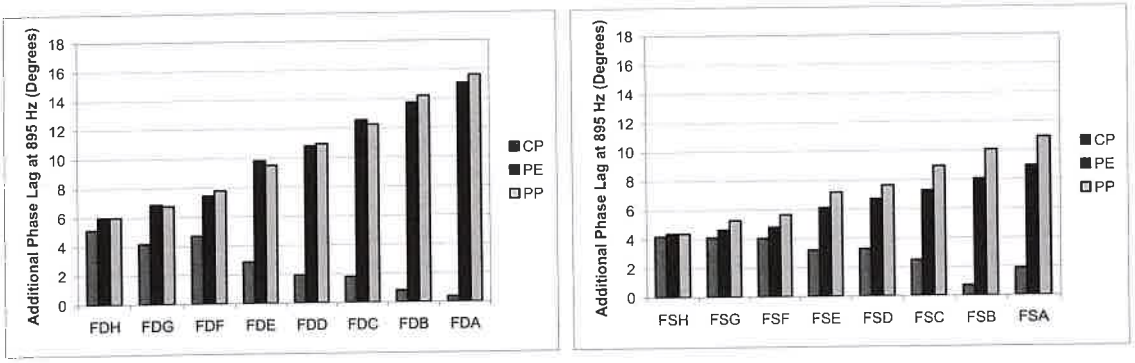

Figure 9: Additional phase lag of the photoacoustic signal measured at 875 Hz for solid magenta prints with dispersion (left) and solvent-based (right) varnish layers coated once using divided anilox roll (amount of transferred varnish increasing from H to A)

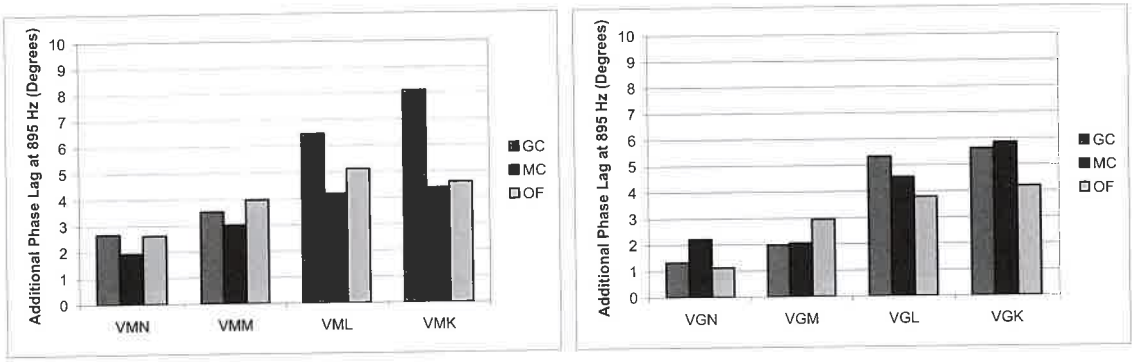

Figure 10: Additional phase lag of the photoacoustic signal measured at 875 Hz for solid yellow prints with matt (left) and gloss (right) dispersion varnish layer coated by Phantom Proofer using anilox rolls with four different screens (amount of transferred varnish increasing from N to K)

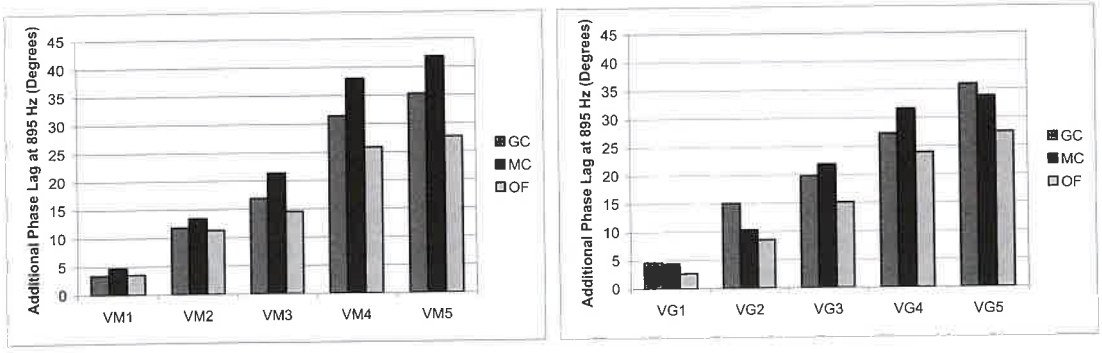

Figure 11: Additional phase lag of the photoacoustic signal measured at 875 Hz for solid yellow prints with multiple matt (left) and gloss (right) dispersion varnish layers coated by Phantom Proofer

In measurement of multiple varnish layers, both the intensity and phase of photoacoustic signal can be used for evaluation, however, the phase information is more suitable. Comparing bare solid print and sample coated with five layers, the maximum phase delay measured for 1 kHz ranged between 30 and 45 degrees. The relation between the number of layers and increase in the phase lag is approximately linear for the set of samples coated with gloss dispersion varnish; in case of matt dispersion varnish, the increase for second and fourth layer is bigger than for third and fifth ones (on all three substrates; see Figure 11). With Saueressig

Flexo Proofer, only two layers of varnish could be applied. Again, in case of polymer foils, the phase delay approximately doubles with the second varnish layer; the values for 1 kHz are roughly 30 and 20 degrees in case of dispersion and solvent-based varnish, respectively. In case of samples printed on one-side coated paper the additional phase lag increases more markedly only with second varnish layer.

Finally, the upper limit of the method with respect to varnish thickness is demonstrated through the results for prints coated using Sheen applicator (Figure 12). For largest amounts of transferred varnish and higher modulation frequencies, the photoacoustic signal originating in strongly absorbing ink layer is fully attenuated and both the intensity and phase lag measured are influenced only by minimal absorption in varnish layer. In case of dispersion varnish and thickness of the wet film of 90 μm, this behaviour is observed from modulation frequency around 400 Hz both on polymer foils and coated paper.

The smallest phase delays were measured for combination of solvent-based varnish and one-side coated paper, but in contrast to the thickness measurement where both negative and positive changes took place with increasing thickness of the wet film, the photoacoustics shows increase of the phase delay and decrease in the intensity of the signal. Comparing the values for the samples with thickness of the wet film of 30, 60 and 90 μm, significant increase in the phase delay takes place first with the thickest varnish layer. This is in agreement with the appearance of respective samples, indicating that the solvent-based varnish applied in larger amounts first builds into the whole volume of the paper and - as appears from the photoacoustic depth-profiling - thicker varnish layer remains on top of the sample only in case of 90 μm wet film.

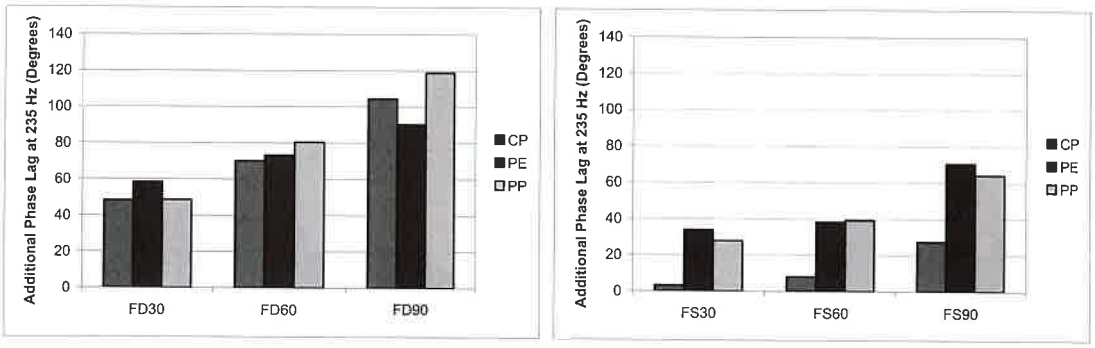

Figure 12: Additional phase lag of the photoacoustic signal measured at 235 Hz for solid magenta prints with dispersion (left) and solvent-based (right) varnish layers coated using Sheen applicator (thickness of the wet film 30, 60 and 90 μm, respectively)

In respect to theoretical treatment, two models were considered. First, the simplified model of two homogeneous layers, where the photoacoustic signal generated in the bottom layer absorbing the excitation light is both attenuated and delayed by the upper layer transparent to given wavelength. Second, the generalized expression, taking into account the thermal and optical properties as well as the geometry of multilayer structure.

As demonstrate the experimental data on Figure 13 for solids coated once by divided anilox roll, the simplified model can be applied if the substrate is sufficiently smooth, but fails, if the structure made by printing and coating is more complex, as is the case of papers. The simplified model proposes linear increase of the phase delay proportional both to the thickness of varnish layer and to the square root of modulation frequency. This behaviour was observed for polymer foils, but in case of paper the phase delay with increasing varnish thickness starts to decrease, and begins to grow first with second layer of the varnish, still only at higher frequencies. The factual structure of these samples is not known, so the calculation of the theoretical course of the photoacoustic signal using generalized theory was not possible.

Concerning the varnish layers with higher thickness, simple dampening of the intensity and increase of the phase lag was observed for coating thickness up to approximately ten microns. For thicker varnish layers, modulation frequency dependence of both intensity and phase of the photoacoustic signal differs from the course corresponding to the simplified model (see Figure 14). Upon previous experiences, the probable reason of the deviations is the weak absorption in the varnish layer. To verify this, the generalized theory was used for the calculation of respective photoacoustic signal. The exact parameters of the individual layers are not

known, however, even with the estimated values there is reasonable agreement between the experimental data and the theoretical curves.

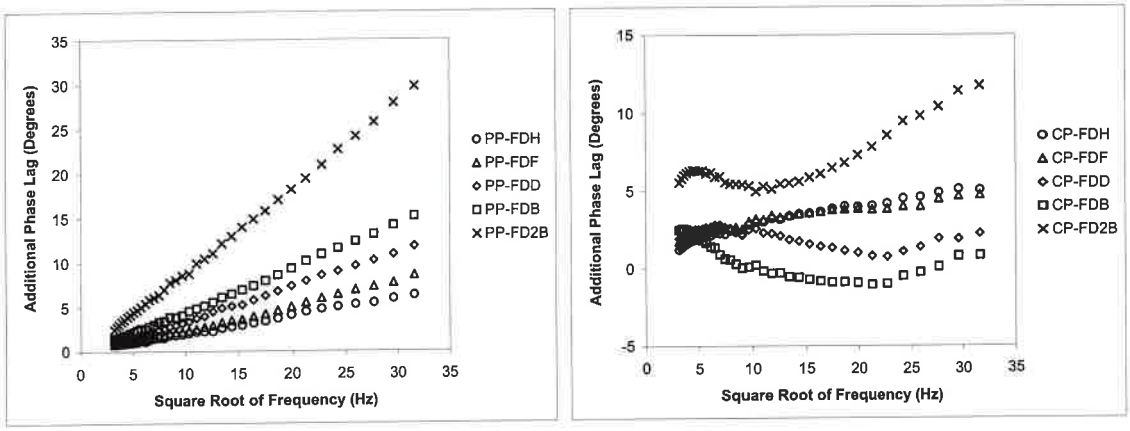

Figure 13: Additional phase lag of the photoacoustic signal versus square root of the modulation frequency for solid magenta prints on polypropylene foil (left) and one-side coated paper (right) with selected dispersion varnish layers coated using divided anilox roll once (amount of transferred varnish increasing in the order H, F, D, B) and twice (2B)

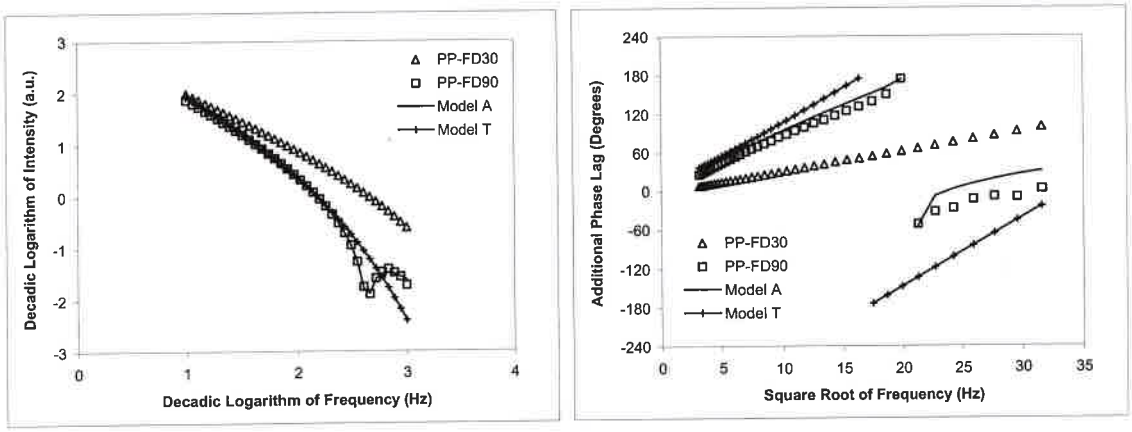

Figure 14: Modulation frequency dependence for intensity (left) and additional phase lag (right) of the photoacoustic signal for solid magenta prints on polypropylene foil with dispersion varnish layers coated using Sheen applicator (thickness of the wet film 30 and 90 μm, respectively), the latter compared with theoretical curves for transparent (Model T) and weakly absorbing (Model A) varnish layer

The thermal diffusivities were estimated from thickness and photoacoustic measurements for samples on polymer foils with higher thickness of varnish layer. For dispersion varnish, the result 1.4×10^{-7} m^2/s is in good agreement with the literature value [Walther, 2001]. The thermal diffusivity of solvent-based varnish was determined as 1.8×10^{-7} m^2/s. Both values are in the range common for polymer materials.

4. Conclusion

As expected, the values resulting from common thickness and gloss measurements generally do not show any clear dependence on amount of varnish coated over solid prints. In case of photoacoustics, the study has verified the anticipated possibilities and benefits of photoacoustic investigation of varnished solids as well as the validity of the theoretical models under consideration for individual types of samples. The measured curves of the photoacoustic signal in the frequency domain have shown that the simplified model has only limited application for evaluation of photoacoustic response as far as samples common in printing industry are concerned. Among the suitable types of samples belong namely varnish layers with medium thickness coated on smooth substrates and usually higher frequency range must be used. To describe the course of the

photoacoustic signal especially in case of once coated prints on paper, or on the contrary products with varnish layer thicknesses in tens of microns, the general theory for multilayer materials is needed.

For the future research, two areas are concerned. First, the determination and comparison of thermal properties of all types of commercially used varnishes is necessary to make the measurement of varnish layer thickness possible without need to make calibration sets. Second, the research aimed to find the models corresponding to the structure created by substrate, ink and varnish with respect to their optical, thermal and geometrical properties for all main printing techniques, allowing to calculate the theoretical courses of the photoacoustic signal to more detail.

Acknowledgement

This work was supported by the Ministry of Education, Youth and Sports of the Czech Republic, project Nr. MSM 0021627501.

References

[1] Držková M., Otáhalová L., Kaplanová M., (2004), *Photoacoustic Study of Printed Samples, Proceedings of The Second European Conference on Color in Graphics, Imaging and Vision (CGIV), Aachen, Germany, pp. 307 - 310. ISBN/ISSN: 0-89208-250-X*

[2] Hu H., Wang X., Xu X., (1999), *Generalized Theory of the Photoacoustic Effect in a Multilayer Material, Journal of Applied Physics, vol. 86, no. 7, pp. 3953 - 3958. ISSN 0021-8979*

[3] Kaplanová M., Černý J., (1997), *Photoacoustic Study of the Ink-Paper Interactions, Advances in Printing Science and Technology, Ed. J. A. Bristow, John Wiley & Sons Ltd., vol. 23, pp. 301 - 314. ISBN 0471971588*

[4] Muck T., Lozo B., Otáhalová L., Držková M., Kaplanová M., (2006), *Non-destructive methods in the study of IJ ink - substrate interaction, Advances in Printing and Media Technology, Ed. N. Enlund and M. Lovreček, iarigai with Acta Graphica Publishers, Zagreb, vol. XXXII, pp. 225 - 232. ISBN 953729201-0*

[5] Rosencwaig A., (1980), *Photoacoustics and Photoacoustic Spectroscopy, Chem. Analysis V57, John Wiley & Sons, New York, pp. 104 - 107. ISBN: 0471044954*

[6] Sipi K. M., (2001), *Toner Layer Structure and Toner Adhesion on Coated Paper, NIP17: International Conference on Digital Printing Technologies, Fort Lauderdale, Florida, vol. 17, pp. 145 - 150. ISBN: 0-89208-234-8*

[7] Vikman K. J., Sipi K. M., Oittinen P. T., (2000), *Applicability of FTIR and Raman Spectroscopic Methods to the Study of Ink Jet and Electrophotographic Prints, NIP16: International Conference on Digital Printing Technologies, Vancouver, Canada, vol. 16, pp. 408 - 413. ISBN: 0-89208-230-5*

[8] Walther H. G., Christ A., (2001), *Photoacoustic study of layer thickness and moisture content from varnished packaging materials, Journal of Applied Physics, vol. 89, no. 7, p. 4124 - 4127. ISSN 0021-8979*

Flip flop and spatial (3D) graphics in lenticular technique

Ivana Žiljak[1], *Jana Žiljak Vujić*[2], *Klaudio Pap*[1]

[1] Faculty of Graphic Arts
Getaldićeva 2, 10000 Zagreb, Croatia
E-mail: ivana.ziljak@vip.hr, klaudio.pap1@zg.t-com.hr

[2] Polytechnic of Informatics and Design
Vrbik 8, 10000 Zagreb, Croatia
E-mail: janazv@tvz.hr

Abstract

The research work presented in this paper refers to printing techniques used in spatial (3D) and flip flop graphics, and to multi-layer graphics carried out in lenticular micro-lens technique. Such research work makes way for new contemporary and future areas linked with the topic "New developments in printing materials" and to new manners of visual communication, modern graphic design and product protection. The possibility to carry out the work by means of dynamic micro-lens technology is a challenge to any graphics designer. Playing with words and messages they convey, joining of certain meanings, blending of photographs, three-dimensional graphics and portraits are examples of the numerous possibilities of visual communication and contemporary advertising, graphic product improvement and protection of documents.

Keywords

Contemporary design, holography, lenticular technology, new technologies, protection, spatial 3D graphics flip flop graphics

1. Introduction

Contemporary documents: identification cards, passports, diplomas, certificates, packaging material for various products, especially medicaments all have security elements with individualized data designed and carried out in lenticular technique. Whereas this is considered in the first two cases as a high level of security, in the latter cases lenticulars enable top modern design.

Spatial and flip-flop graphics are most often present in holographic products. Those are high resolution smaller format graphics (in documents, securities and bills) that include micro-text, and numerous security contents. During the past conferences we reported on spatial and flip-flop graphics, especially on holography as a means for protection on packaging material [Iarigai 2004]. Micro-lenses open a new designer sequence of 3D spatial design and flip flop graphics depending on the position and angle of viewing. We have studied a graphic work in lenticular technology that is observed from a greater distance. We have achieved extraordinary results where multi-layer graphics and multi-layer messages are in the depth of our perception and some tens of centimeters above and below the print's surface. With these designs the viewer himself plays a large role participating actively in producing the impression, depth, spatial characteristics and the speed of visual message altering depending on the position he has taken.

2. Research methods

Spatial and alternating graphics computer models enable effective working out of the design for which it is necessary to first carry out testing and to set realization standards. The standards apply to parameters that determine the angle of viewing, the number of flip flop graphics, the number of deep layers (3D graphics), the height and depth of the image (3D portrait), the ratio of alternating certain levels, blending, colors, contrasts.

Designing of lenticulars is followed up with keeping documentation on graphics, layers and colors. The lenticular technique, also called micro-lens technique may be carried out in digital printing. The print containing two or more

incorporated images represents a high level of security. Only those who possess the original image parts can carry out and reproduce the original image. Experiments with lenticular images on security elements coming out from our laboratory have already been applied in practice and they proved to have extraordinary results. The method was applied on identification cards, certificates, diplomas, in advertising products, as direct mailing, advertisements in newspapers or on posters. The innovations are in the flip-flop design, alternating graphics or in two or more graphics, floating graphics, and imitation of object movement and in the three dimensional - 3D display. Experiments covered small and larger formats on different micro-lens liniatures: from 20 to 120 LPI. The printing background was paper, foil and glass. The most important printing technique is direct digital print on the micro-lens plastic material itself (on its smooth side) with application of contact film in spray form.

The example chosen for this paper's discussion is a 3D sign with a floating background (Figure 1). The method for extending lenticular analysis after printing is determined. Scanning is done with a reflected white light, with UV light of selected wave lengths UV254, 312, 365 nm and with IR light. High quality scanning in the UV area is carried out under an angel parallel in a line of micro lenses and perpendicularly to the micro-lenses.

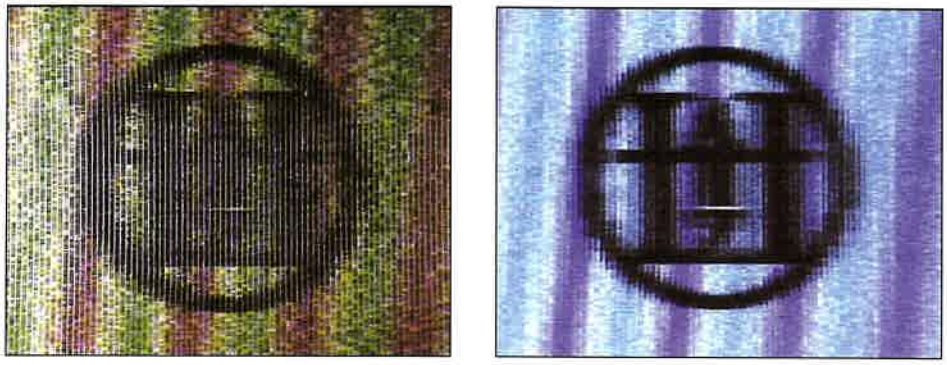

Figure 1: Lenticular HATZ1 original, and in HATZ1 under UV 365nm

Besides the quality of being three dimensioned, lenticular, the sign for Croatian Academy of Technical Sciences has a security color. A color has been designed that changes the response of red RIv500 in daylight into purple RIv365 under UV light with wave length 365 nm with the condenser for LUMI illumination in values 5 and 6, and also from green GIv500 into blue Biv365 under UV light with wave length 365 nm with condenser for LUMI illumination in values 5 and 6.

On basis of results up till now it may be concluded that it is useful to use black, blue and red linear background. They react differently under UV lighting and IR lengths. If UV invisible color is introduced, it is necessary to print it after the lenticular printing. The case with the uncontrolled background is simpler due to the fact that the graphic's parallel quality is not apparent. UV paint with a visible tone must be positioned under the UV light. UV invisible paints for inkjet printing directly onto the lenticular plastic have not been offered yet.

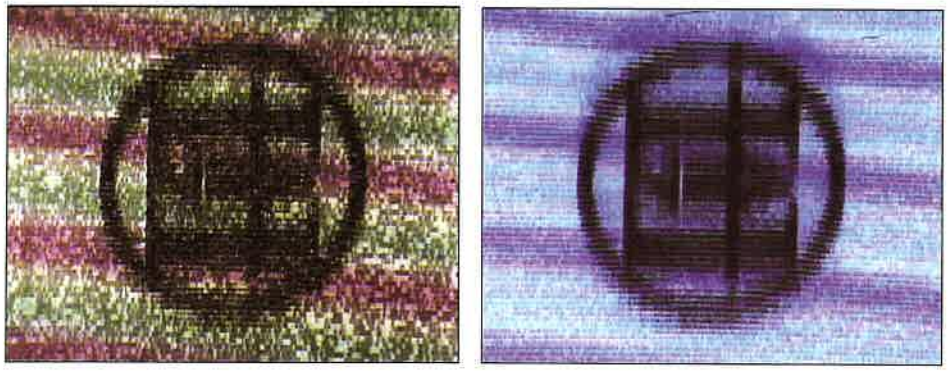

Figure 2: Lenticular HATZ 90°, lenti HATZ 90° UV365

The scanned lenticular (Figure 2) image in day light and UV light under the angle of 90° in respect to the lens direction is shown in the figure. The optical scanner for UV area does not create the impression of a 3D image nor flip-flop, but it recognizes multi-layer graphics only.

Special research work was carried out in respect to the problem of typography for the described communication and carrying it out in lenticular technique. It was determined that in order to carry out the typography by using this technology it is necessary to respect certain rules. On basis of analyzing and carrying out different designs, parameters were determined for setting the standardization and for new directions of testing. Liniature and resolution, and the very micro-lens structure set certain limitations. On the other hand there is a goal to make the maximum out of spatial experience. It was determined that due to a certain set liniature amounting to 20 - 120 lpi it was not possible to reproduce letters smaller than 8 pt, i.e. that "small" typography would not be legible. But the most important thing is that through such reduction i.e. simplifying to the most essential, it is quite evident how a large quantity of text is left out, such, as for instance, product descriptions, and a great deal of space is left to the visual graphic and designer intervention. In a certain way the ordering party is forced to give its consent to simplicity, sharpness and clearness of visual messages. Large formats have not been studied due to difficulties in bringing into coordination the parallel quality of micro-lens miniature and the printed graphics liniature as this must be in full coordination.

The text example carried out in 3D technology (Figure 3): *graphics and typology with micro-lenses* was designed in sizes ranging from 10 to 20 typographic dots. The text was designed for three dimensional executions on micro-lenses where the sense of height ranged up to 8 mm above the print's surface. When carrying out the design it is possible to plan precisely and determine what the sense of height will be even in cases of up to several centimeters above the surface, depending on the liniature, dimensions and lenticular thickness. A low resolution of 50 lpi was deliberately given in this example for purposes to illustrate the display. This lenticular as a separate 3D graphic work in spot colors may be applied over various vector floating lenticular graphics, as in the example "iz" (Figure 4).

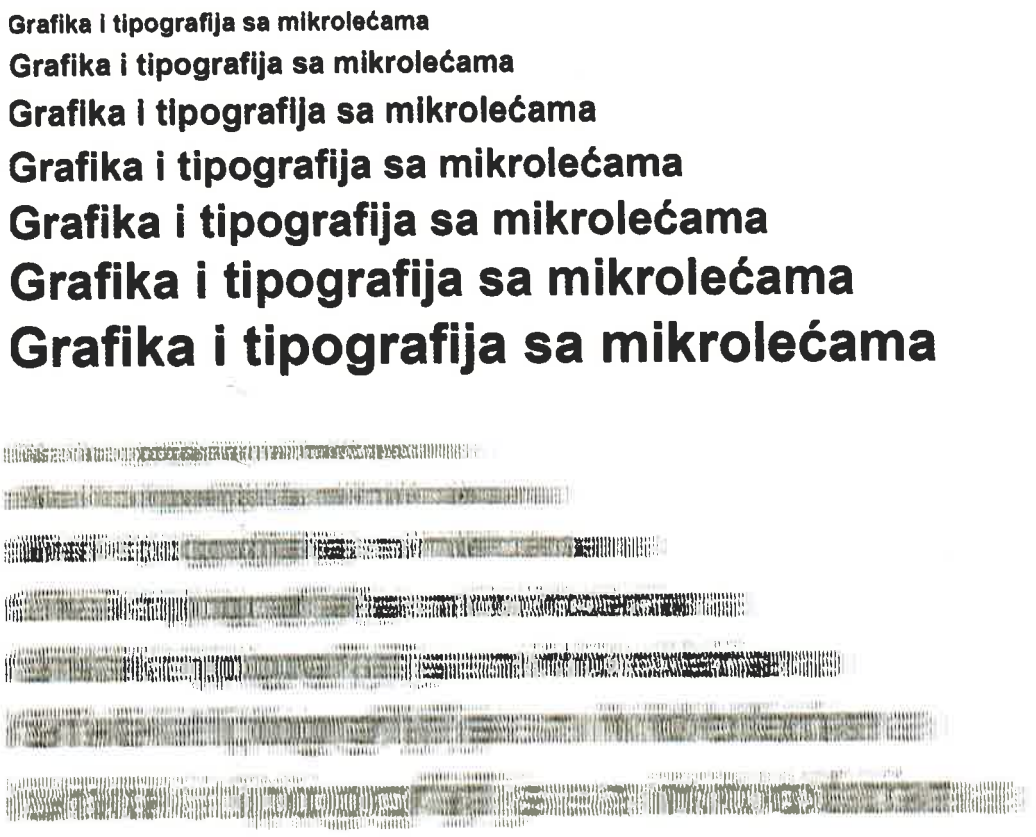

Figure 3: Graphics and typography with microlenses for 50 lpi microlens

The relations between the graphics, typography and background, i.e. the color and the background contrast are also important. In case black typography is alternating on a white basis and in case the words are long, there is possibility that with vertical movements (viewing from left to right) there will be black "remaining residue", i.e. the previous image in relation to the new image will not disappear in full. A color background is much

better (red, black), especially if it is carried out in the spot color technique, and the alternating typography is in the negative - white. In this case the possible "traces" are covered with the very color of the background and an impression is gained of total covering capacity. A good combination is also the one with black letters on a color background. Testing has proved that the best results are achieved by spot color application.

We have tested various graphics that simultaneously function in the same space but are of different height and depth in direct contact, as for instance, the effect of the floating typography. The effect is greater if there is contact, i.e. the relationship, contrast between two different letter heights.

3. Results

Lenticular technology and micro-lenses set a limitation in resolution, and this applies especially to vector graphics thickness values and typography size, as well as vector graphics thickness values. Spatial and flip flop graphics carried out in the micro-lens technology are applied in documents such as ID cards, i.e. on cards that have a certain thickness required by such technology due to optical laws.

Resolution is firmly set and we have carried out the testing and analyzing on 20 to 120 lpi micro-lenses. The smaller liniatures (20 lpi) are more suitable for 3D designs; - their structure and the height of three-dimensional effect are stressed. Such designs on 20 lpi micro-lenses are good for larger formats, posters and material that are placed in large interiors or on jumbo posters. Such designs are not suitable for carrying out smaller formats due to the very micro-lens size being up to 5 mm. Flip flop alternating graphics are formed in the application of smaller format promoting material and thinner micro-lenses; promotion material. The 50 to 75 lpi to 120 lpi lens structure has proven excellent for application on wrapping material 5 to 15cm in size. The number of alternating images may be from 2 to 12 or even 24 horizontally or vertically in respect to the viewer. The effect of printing animation is achieved and this improves significantly the wrapping material graphics. However, in case of more than four images in an alternating sequence there is blending of contents. This paper describes successful cases with two to three image changes.

In order to prove the authenticity of the lenticular graphic element scanning has been done under different lighting conditions, under precisely determined angles of slanting EPI light with precisely determined wave lengths of 254 nm from the UV are to 1.000 nm from the IR area. For proving the authenticity of the lenticular, first the make ready is done by designing security graphics. The following are taken into consideration at the beginning of planning: flip flop, floating graphics, three dimension quality, lenticular thickness, resolution, direction of observation, color, transparency, printing technique with which the lenticular will be carried out. In case the project for making the graphic product did not anticipate the use of various and wide events with visible altering of the above listed parameters, it will not be possible to check nor prove anything later.

Figure 4: a) Slanted light EPI

b) IR 780 nm

Figure 4: Three-dimensional design for IŽ sign in lenticular technique, three-dimensional design for personal initial sign in lenticular technique with altering digital printing colors.

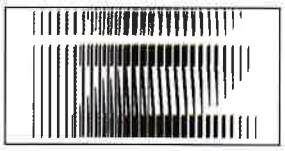

Figure 4: c) IŽ 3D

Reproductions of 3D lenticulars give only the print plane regardless of whether the figure was taken in EPI position with a small angle of the light beam or the light falls perpendicularly onto the lenticular. The small angle provides additional shading due to the light refraction on the micro-lenses. This is uncontrollable in the micro-structure, but the graphics are, nevertheless, recognizable. The example of a background with colors that do not respond in IR light has been enclosed on purpose. The graphics of the floating in-depth background consists of magenta, cyanogens and yellow color. 3D initials IZ are visible under IR light as the security element where only the security IR black color is seen in wave lengths of 780 nm, 830 nm and 850 nm.

Figure 5. a) UV 254 nm *b) UV 365 nm pseudo* *c) UV 365 nm*

The figure IZ Lenticular figure scanned in the UV area with pseudo color interpretation. The pseudo color effect has been applied in the figures and so the index color arrangement has been added to the UV area. It is a well-known method from early interpretations of "heat images", where the programmed line of index colors is copied allowing visual demarcation in the rich color system.

In Figure 6 the "hp" flip flop lenticular is shown containing two alternating images. The typography appears or vanishes completely. The red background executed in spot red color is excellent for visual coverage of images alternating from one to the other.

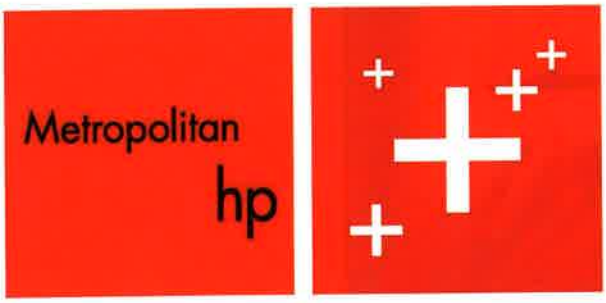

Figure 6:
a) Design for HP flip flop image 1 and image 2

Figure 6: b) HP flip flop Lenticular, 75 lpi

Flip-flop lenticular figures can be taken with digital cameras from longer distances so as to provide dividing of incorporated figures. Such digital records do not have known values of all shooting parameters so the experiment can not be repeated in the quantitative sense. Such figures are information on quality only. Lenticular technique is already incorporated into money bills as *micro-lens of dome form* with thin-layer materials and a liniature above 120lpi. This novelty provides the impression of a moving figure from all viewing angles. Due to the very high liniature it is almost impossible to produce outside a laboratory.

The next example is designing the lenticular sculpture (Figure 7). The sculpture has been photographed with the designed technique of 3D photographing that consists of six cameras placed under a precisely set angle of shooting in respect to the object to be taken. The first and last figures have been enclosed as examples. Six figures are programmed and merged into a lenticular whole for 3D execution on a 50 lpi lenticular.

Figure 7: a) Original Skulpture 1/6

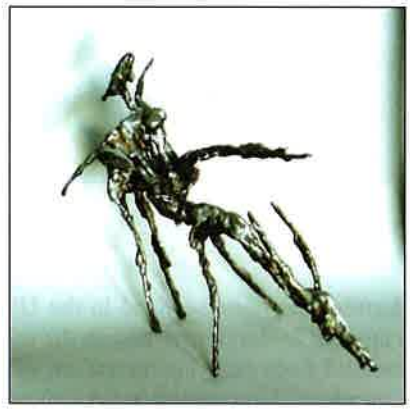

b) Original Skulpture 6/6

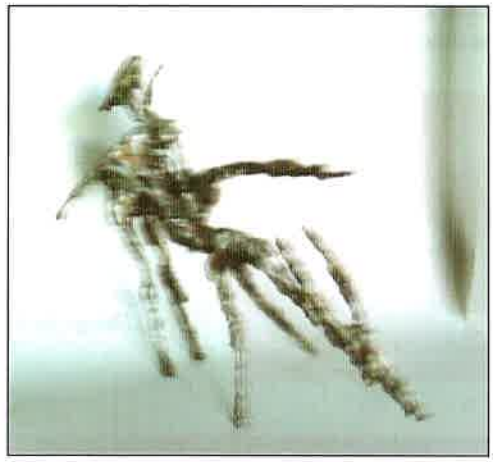

Figure 7: c) Lenticular Skulpure 3D 50 lpi microlens

Sophisticated methods of the 3D portrait are proposed as the ultimate security level, photographed with 6 cameras, programmed and printed in 3D lenticular micro-lens technology. The 3D lenticular portrait is combined with flip-flop elements and floating 3D graphics in a 120 lpi resolution, with security Ultraviolet 254 nm, 312 nm and 365 nm and infrared colors. Colors are used for infrared checking that in day light give the impression of color and black, whereas under infrared 780 nm to 1.000 nm are not visible, the portrait vanishes completely and the security graphics appear in its place. It is impossible to scan and fake such a portrait on identification cards and in passports because its initial record had been made in the technique of 3D photographing with six cameras, and is stored in the database.

4. Discussion

An extreme area in the printing business is the lenticular graphics design that can not be imitated or faked. This paper is on further development and extending of printing practice, graphic design and demanding

printing practice. The scientific contribution in this paper is the fresh knowledge on graphics' transformation carried out in the lenticular flip flop technology and 3D manner and their quantitative measurements. Merging of lenticular technology with ultra-violet and infrared colors in relief digital printing is a proposal for future wide application in the area of document and securities protection.

The quantitative method of designing, execution and checking of the lenticular print is an excellent application in security printing, where there is a database for each element that is further used for checking of color, designed graphics, materials and provides the possibility of repeating the whole procedure.

Attached to this paper is our proposal for classification of printed matter promotion using spatial images, as part of instructions for appearing in the new graphics market. The classification covers the design technology, the limitations of contemporary printing technique precision, limitations of digital printing trial prints. The future application of dynamic and deep computer graphics in lenticular technique is not only a means of protection (personal identity number, initials, and identification digits) but also promotion, advertising and top design as additional product values. Wrapping material is an excellent type of media, as are all kinds of credit cards, for which a new visual event may be applied for each new edition. Then there is packaging material, promotion material such as promotion cards, direct individualized parcels sent to address (mailing), magazine covers, and advertisements in magazines - where the design in micro-lenses may be applied in segments, business and promotion material, planners (covers), covers of yearly reports, calendars, and posters. The application may be also applied to all graphic products, and also to products from the product design area (advertisements in sale spots), all aimed at having a noticeable visual communication, great possibilities in design and promotion design as well as in product security. Lenticular graphics carried out in order to present the various possible applications are in the attachment to this paper.

5. Conclusion

The most frequent application of graphics designed in the lenticular technology is in the field of advertising, in 3D flip flop lenticular design consisting of two or more images. The most significant application is in the field of security documents where flip flop protection is applied in personal identification cards, and the sophisticated method of the 3D portrait is proposed as the highest level of protection in combination with flip flop elements and floating 3D graphics, UV and IR colors.

The set and proposed methods comprised lenticular technology in flip flop and three dimensional executions, from 20 till 120 lpi in digital printing with conventional spot and process paints, protective ultraviolet and infrared colors responding in precisely determined wave lengths. Related databases are created as a basis for software type analysis. This is the first time that such analysis is approached systematically, with quantitative measuring on facilities with precisely determined lighting angles and determined wave lengths ranging from 254 to 1000 nm. Printing of lenticular graphics with UV and IR paints by means of digital techniques has extended the design complexity protection of securities and prevention of counterfeiting. Research results have been transferred to the field of practical and security digital printing on micro-lenses. This is a completely new way of protecting graphic products.

The value of such research work is in the new quantitative procedures for proving the authenticity of a lenticular graphic product. A new system of design and marking with precisely coded micro-lens structure has been implemented, providing different behavior depending on the different viewing angles and in various lighting. This work has extended the knowledge and practice of designing security graphics and using digital printing with application on micro-lenses. This paper is a contribution to extending graphic design and printing practice and opening possibilities of further investigation in the field of lenticular graphics.

Visual communication through spatial and flip flop graphics in lenticular technique is an original method. The graphic design consists of two or several different messages, visual, typographic, illustrations or photos that are alternating in a precisely determined sequence or blending in different combinations, having different depths and heights and coming out into the third dimension. By passing by the graphic design carried out in the spatial and alternating graphic technology or by moving a graphic product; flyer, mailing, advertisement add, packaging material, the viewer changes the angles of viewing and thereby takes part in creating the visual message. Such a graphic product or segment is interesting as an "eye catching" product, and is very soon singled out from other products. The value of a graphic product designed in this manner is that it remains preserved during time and in the majority of cases it is not destroyed or wasted as a single-use printed product.

Its additional value is in its property to protect a product. It is impossible to copy, reproduce, photograph or counterfeit lenticular technique spatial and flip flop graphics. The ordering party remains permanently protected and its product or campaign remains in one's memory as original. This kind of approach to graphic design through new lenticular technology is linked to other contemporary technologies in multimedia. The reason for lagging behind in this area up till now is only because the area for application has not been fully researched. This paper is a contribution to expanding knowledge through practical application of spatial and flip flop graphics in lenticular techniques and is aimed at having not only scientific research goals, but commercial ones as well.

References

[1] Žiljak I., Žiljak-Vujić J., Pap Kl.;.Modeling of screening elements in stochastic multi-color reproduction // 33rd International Research Conference IARIGAI, Leipzig, Germany, 2006

[2] Žiljak I., Design of documents with visible and unvisible graphics DESIGN 2006 9 th INTERNATIONAL DESIGN CONFERENCE Zagreb, Glasgow, Dubrovnik, 2006

[3] Žiljak I., Holography on packaging material and an estimate on the rising trend of its application // The 31st International Research Conference Iarigai. Copenhagen, Denmark, 2004

[4] Žiljak I., Designing and customising new screening elements for digital printing technologies - Tools for graphic designers // INTERNATIONAL CONFERENCE ON INNOVATIVE EDUCATIONAL CONTENT MANAGEMENT AND DIGITAL PRINTING CustomDP., Athens, Greece, 2003

Carbon black loaded paper: an intelligent substrate for electronic sensors design

Rodolphe Koehly[1], Denis Curtil[2], Theodorus G. M. van de Ven[3], Marcelo M. Wanderley[1]

[1] Music Technology, McGill University
550 Sherbrooke W, Eastern tower, Suite 500, Montreal, Quebec, H3A1E3, Canada
E-mail: rodolphe.koehly@mail.mcgill.ca; marcelo.wanderley@mcgill.ca

[2] LGP2, EFPG, INPG Grenoble
461 rue de la Papeterie - BP 65 38402 St Martin d'Hères Cedex, France
E-mail: denis.curtil@efpg.inpg.fr

[3] Pulp and Paper Research Centre, McGill University
3420 University Street, Montreal, Quebec, H3A2A7, Canada
E-mail: theo.vandeven@mcgill.ca

Abstract

Pressure and position sensors are usual components of many electronic devices. They equip cars and planes for security and presence sensing, industrial automated systems and many other Human-Interface Devices for medicine and kinesiology robotics, video games, etc. We present alternative ways to develop our selves these sensors using a low cost material: conductive paper loaded with carbon black pigments.

We show that such a paper can be easily used to develop position, pressure and flexion sensors and that it is a good basis to develop more refined sensors such as accelerometers or tilt sensors for shock sensing with smart packaging. We last compare a few trials to produce oneself this paper using conventional fibers such as TMP, chemical or recycled pulp using classic laboratory handsheet formers and mixing those with industrial carbon black loaded papers.

Keywords

Conductive pigments, human computer interface, intelligent substrates, piezoresistivity

1. Introduction

The most massively used flat pressure and position sensors are the Force Sensing Resistors (FSR) from Interlink Electronics Company, Camarillo, USA. FSRs are printed components and are composed of mixed polymers, organic pigments and metals. Unfortunately, due to their production process, they cannot be easily recycled. Moreover one can only have such sensors produced for minimal quantities corresponding to large-scale productions, and so, Interlink or most equivalent companies only develop sensors solutions for the massive industries introduced earlier.

Researchers and designers of Human Interface Devices who need only a few sensors have to find the appropriate one among those that were developed by major brands. They have to adapt their design to available sensors but they would prefer some customizable piezoresistive material that would enable them to design the size and shape of the sensor itself. This material would be inherently sensitive, available in rolls or sheet and so completely open to any shape or dimension for the user.

We have been looking for such materials [Koehly, 2005] and we have found that conductive paper would be an ideal candidate here. Loading paper with electrically resistive pigments such as carbon black provides us with an elastic and flexible volume resistive material, which simply needs to be placed between metallic electrodes (A1 and A2) to be used as a pressure (Figure 2), position or flexion sensor depending on the chosen design. Loading paper with conductive pigments does not prevent its re-use, as most papers are loaded with white pigments for optical properties, and we can recycle them similarly to produce cardboard or newspaper.

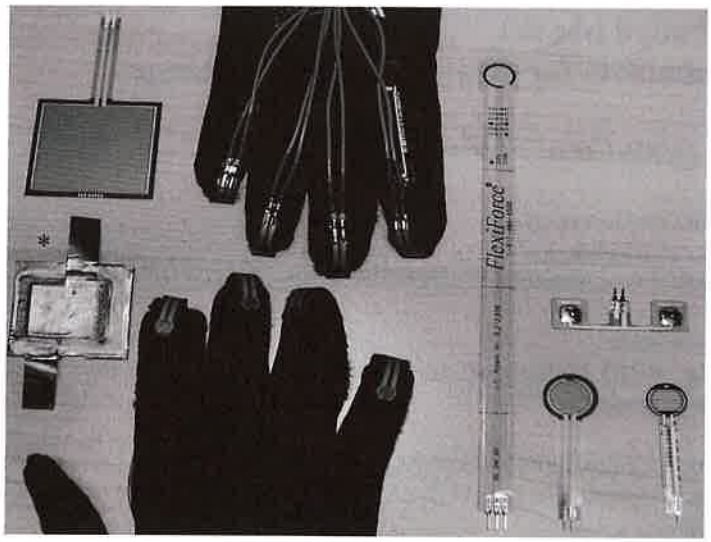

*Figure 1: Various pressure sensors to be used or mounted onto a glove for musical application. One can also notice an example of homemade paper FSR on the left **

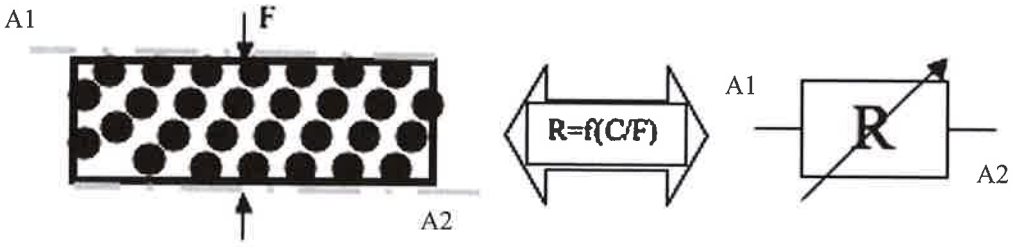

Figure 2: The resistance of carbon black loaded paper between two electrodes (A1 and A2) is function of the dimension of the electrodes (constant C) and is inversely proportional to the force applied onto the paper: R = f(C/F)

In a research project between EFPG in France and the department of Music Technology at McGill University in Canada, we have been studying conductive paper to be used as position and strain sensors. Our goal is to provide digital musical instrument designers with straightforward means to circumvent the limited offering of commercial sensors, which are restricted to a few technologies with predefined electrical characteristics, shapes and sizes [Jensenius, 2005]. Our goal is also to define the basis of possible applications of our sensors for advances in printing and media technology. For instance, we can imagine developing smart packaging for fragile packages that would integrate force sensors and tilts in case of shock. We also think on the development of printed conductors as far as connections are concerned.

2. Minimal considerations for building paper sensors

Carbon black loaded paper is a conventional paper that can be made using various types of fibers. The difference with other papers is mainly that it is loaded with carbon black pigments instead of the usual whitening pigments such as clay or $CaCO_3$. If one wants to develop a paper for a position sensor, the best paper will be highly refined and calendered to decrease as much as possible the surface porosity and roughness, as the aim will be to get a linear variation of electrical resistance along the surface. In reality, and as shown in figure 3, even a rough paper (industrial sample, thickness e = 0.275 mm, basis weight W = 160 g/m^2) can provide sufficient linearity to develop a position sensor with a few mm resolution.

Position sensors [Koehly, 2006] are made using three electrodes along a linear conductive sample. This sample can be any flexible support, inked or coated with an electrically conductive component or it can be a volume conductive material such as a band of conductive paper. One electrode is then fixed on each end of the band (figure 4). The resistance between the two electrodes A1 and A2 is then fixed and depends on the

volume resistivity of respectively the ink coat or the whole conductive paper. The third electrode A3 is placed all along the conductive length, and provides a variable output proportional to the volume of resistive material that the current has to cross.

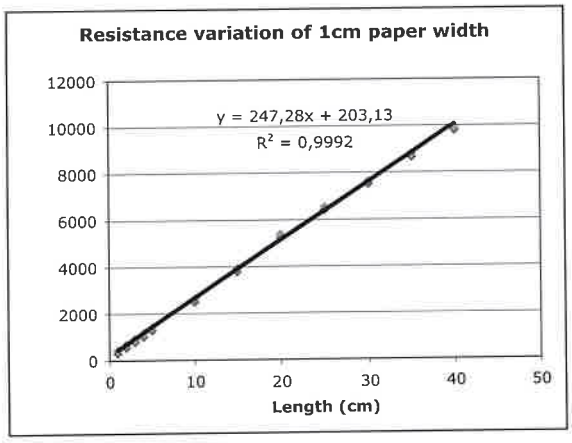

Figure 3: Even a rough paper provides sufficient linearity to develop a position sensor with a resolution under the pressure exerted by a human finger (2 mm resolution equals around 50 Ohms)

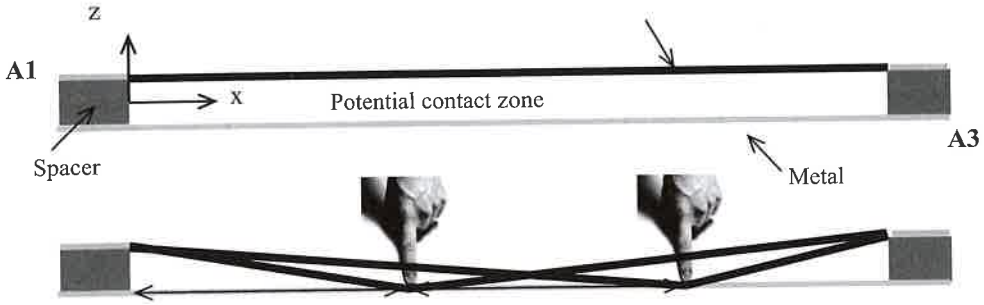

Figure 4: Schematic of a one-axis position sensor: pressing with the finger along the flexible resistive material creates a contact with the anode A3 that enables to obtain a value of the position of the sensor along the x-axis

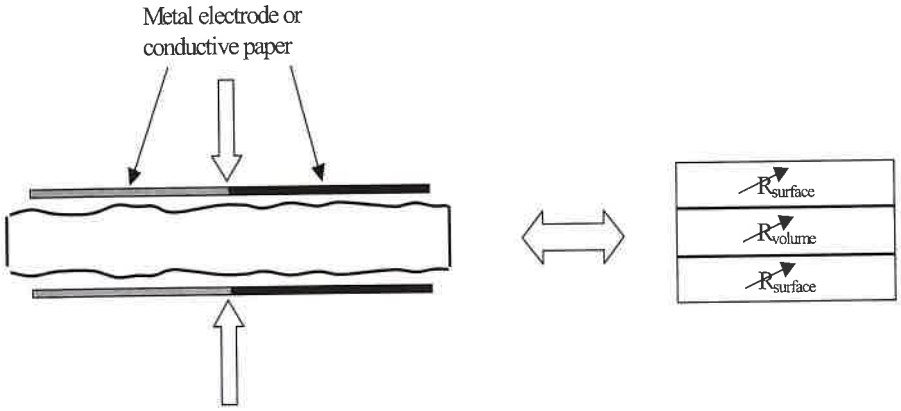

Figure 5: A conductive paper in between electrodes or other sheets of paper is equivalent to variable resistances in series, the variations of resistance being mostly due to surface contact variations (see figure 8: the variation of resistance due to contact surface is 100 times more important than the one in volume)

To develop efficient force or flexion sensors [Koehly, 2006], it is better to provide high roughness and porosity, because the volume resistivity and the surface contact variation mainly affect the resistance of the paper under

strain. Pressure sensors are made using one or a stack of sheets of conductive paper between 2 electrodes. This sandwich would then act as a variable resistance, decreasing with compression. We show that this variation is partially due to the compression of the material along its thickness, and most mainly to contact surface variation between each sheet.

A few sensors were developed using this configuration for which two conductive papers were investigated: One (paper G) was loaded with carbon and was thick (thickness e = 0.275 mm, basis weight W = 160 g/m^2, 12.6% ash content for an ash test at 450°C) and the other (paper F) with graphite and was thinner (0.160 mm, 100 g/m^2, 8.4% ash content). We varied the number of sheets stacked in order to see how we could extend the range of those pressure sensors; each stack was inserted between 2 copper plates used as electrodes. The paper samples were squares of 2.5 cm^2 and the copper electrodes were 2 cm^2 extended by a 1cm width plate to solder a wire. The whole was covered with some plastic film to prevent moisture variations and copper oxidation. Figure 1 shows one of these sensors (*). Two laboratory sheets were made from some repulped paper G with an English Sheet Former to increase its bulk.

Table I shows the range for each of those sensors. For instance, a sensor called 4G3F is composed of a stack of 4 sheets of G and 3 sheets of F. The table enables one also to compare the range of the paper sensors to the range of 2 industrial sensors. For each sensor we give a comparative value of its range normalised by the mean value of the resistance. This enables to better compare the range efficiency between sensors.

Table I: Comparison of the range for various homemade sensors to two industrial sensors for loads of 100 g and 5 kg. The samples were placed onto a weighing machine (compressed zone: 2 cm^2) while the resistance was measured. It is possible to reproduce the same sensor using the same number of sheets stacked in a sandwich under 2 copper electrodes

Paper	3G	3G	3G	7G	4G +3F	4G +3F	4G +3F	Round FSR	Square FSR	1R	2R
R at 100g (Ω)	550	450	500	1100	7, E 06	8, E 06	6, E 06	50, E 06	55000	2000	4000
R at 5000g (Ω)	18	17	22	41	28000	24000	30000	3400	200	19	42
ΔR (Ω)	532	433	478	1059	6972k	7976k	5970k	49996k	54800	1981	3958
ΔR/Rmean	1.87	1.85	1.83	1.86	1.98	1.99	1.98	1.99	1.98	1.96	1.96

We can first notice that we obtain a good reproducibility of the sensors looking at the samples 3G or 4G3F that were duplicated three times and all provide results in the same range. We can also notice that industrial sensors can have quite a much wider range than the homemade ones. Last, we can see that increasing the number of sheets stacked enables one to improve the range, but here again, there is a limit to the number of sheet one can stack for optimal results. It is also interesting to notice that stacking the 2 sorts of papers (F and G) together provided the best results.

The industrial paper G was repulped and some new sheets were made in order to provide a thicker fibrous mat and so to increase the range of resistance variation. The new paper was around 2.1 mm thick for W = 1200 g/m^2. The bulk then increased from 1.67 cm^3/g to 1.75 cm^3/g. Experiments show (paper 1R and 2R) that we increased the possible range in this way (ΔR/Rmean went from 1.85 to 1.96), but we can not know if this is due to the difference in pigments concentration (11.2% ash content for an new ash test at 450°C), the increase of the bulk or simply the increase of the basis weight or the thickness. We have then produced a series of paper based on paper G and three types of pulps: TMP and chemical pulp to see how this could vary the results in resistance variation.

3. Results and discussion

We tried to improve paper G, changing the pigment concentration and adding new virgin fibres to increase the elasticity of the fibrous mat. The major parameter that would influence the paper conductivity is the Carbon Black concentration. Preliminary ash tests (ISO 1762:1974) at 400°C on some samples showed the pigment concentration of the paper is between 15 to 20%. However, according to the papermakers, there is also some CaCO3 pigments in this paper, and an ash test does not able to differentiate carbon black pigments from the other ones. We then chose to produce new papers, increasing their thickness and their bulk by using bigger

and less refined fibres. We used unbleached chemical pulp at 11°SR, and mechanical pulp at 66°SR to check that high refining would really be bad for paper elasticity.

Starting from some repulped paper G, we made 10 different pulps adding each time from 10 to 50% of each new pulp to the industrial one. From those pulps, we made each time two 500 g/m^2 hand sheets (ISO 5269:1998) to check the influence of forming, pressing and drying. We expected to have higher bulk and lower pigment concentration for the "a series" than for the "b series". Table II shows some of the results.

Table II: influence of the sheet formation and addition of new fibres into the conductive paper G

Paper	% Paper G	%other pulp	Basis weight (g/cm²)	Thickness (mm)	Bulk (cm³/g)	% Pigments	% Porosity	Gram-mage (g/cm²)	% Moisture	Resist. 10cm (W)
0a	100		630.8	1686	2.67	15.20%	74.0%	598.3	5.1%	575
0b	100		509.3	1019	2.00	12.10%	66.5%	476.4	6.5%	1500
1a	90	Chemical	660.8	1688	2.55	13.70%	73.1%	626.2	5.2%	
1b	90	Chemical	459.7	1039	2.26	10.30%	70.8%	429.9	6.5%	4700
2a	80	Chemical	658.2	1878	2.85	12.10%	76.2%	622.8	5.4%	
2b	80	Chemical	492.5	1162	2.36	9.50%	72.2%	460.5	6.5%	6000
3a	70	Chemical	645.9	1872	2.90	10.30%	76.9%	611.4	5.3%	1600
3b	70	Chemical	478.4	1193	2.49	7.60%	74.0%	447.8	6.4%	17000
6a	90	TMP	609.3	1615	2.65	13.30%	74.3%	574.7	5.7%	
6b	90	TMP	451.0	1061	2.35	10.60%	71.9%	421.3	6.6%	3700
7a	80	TMP	543.0	1331	2.45	11.80%	72.4%	514.4	5.3%	
7b	80	TMP	441.7	1033	2.34	9.60%	72.1%	410.2	7.1%	8200
8a	70	TMP	567.1	1325	2.34	10.10%	71.5%	534.5	5.7%	
8b	70	TMP	434.9	1012	2.33	7.50%	72.3%	405.9	6.7%	18500

3.1 Pigments concentration

Carbon black particles that are present in the paper enable it to be conductive. These pigments have the advantage to be very fine and very inexpensive. We can assume that the more pigments a paper contains, the more conductive it will be. However, this is not the only parameter that will influence the conductivity. Indeed, we can also imagine that an increase in thickness, bulk or porosity will decrease the conductance. Figure 6 plots the resistance of the various samples.

We can see that there is a clear but not direct link between pigment concentration and resistance value, and an exponential decrease of the resistance value with an increase of the pigment concentration. The variations are certainly due to the variations of the bulk and porosity between the samples (see Table II).

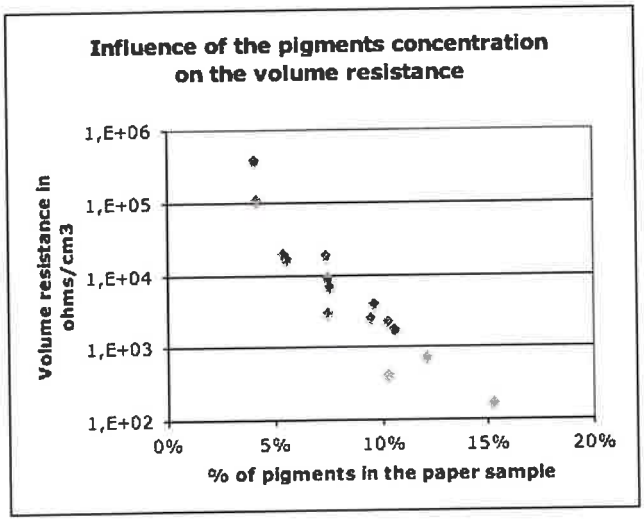

Figure 6:
Variation of the volume resistance of various samples with pigments concentration. The resistance was measured over samples of 10 cm length and 2 cm width. The thickness varied between 1 and 2 mm, the values of resistance were normalised to the volume of the samples. Extracted from table II and other samples tested at lower pigments concentration

3.2 Repeatability

A fundamental parameter for a sensor is its repeatability: the device should provide the same result in terms of resistance variation for the same applied compression. Conductive papers can provide such a characteristic because of their high compressibility and memory-shape property. If calibrated, i.e. if the paper is submitted to an excess of compression before its use, one can expect to obtain excellent results with a paper force sensor for various forces as long as one does not exceed the compression load.

We mentioned earlier that the resistance variation would mainly be due to surface contact variations and much less to the volume compression of the paper. We then developed an apparatus (figure 7) enabling one to control the pressure on a defined zone of the paper (4 or 10 cm^2) and measure the variation of conductivity. The sample was placed on a high sensitivity pressure sensor that sends the pressure value applied on the sample to the computer. A pneumatic system was controlled by the computer to apply a force of 0 to 60 Newton through a pneumatic jack on which was screwed a flat contact piece (5 x 2 cm^2) that would distribute the pneumatic force along a defined zone over the paper sample (4 or 10 cm^2 depending on the contact piece orientation). The contact piece in metal will vary the conductivity of the paper sample and provide information on the variation of resistance due to contact surface variations. This apparatus does not work efficiently for less than 4 Newton, because of some friction forces in the pneumatic jack. This system enables one to plot the variation of Force vs Conductance on a scale of 4 to 60 N.

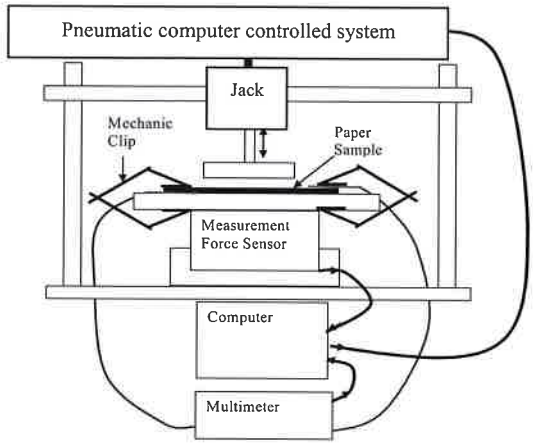

Figure 7: Sensor testing apparatus developed at the EFPG by the LGP2

A first trial was made on paper G to determine the influence of the resistance variation in volume and the one in surface in surface. For the test in volume, the contact piece was covered with an insulator. Figure 8 shows the results: while the variation of resistance in volume is only a few ohms, the variation in surface is around 300 ohms.

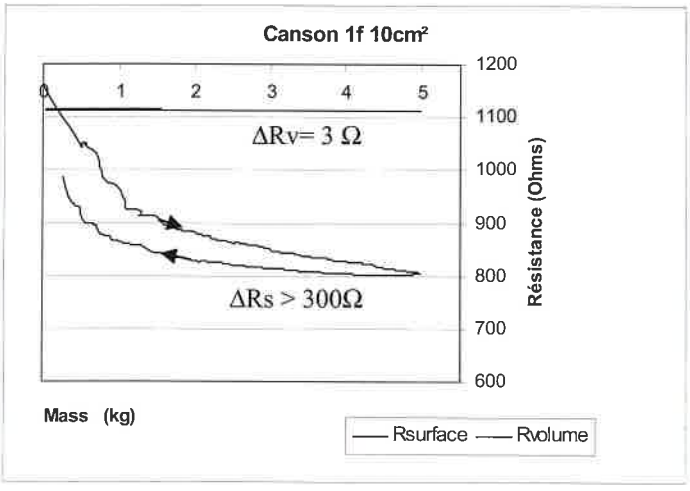

Figure 8: Variation of resistance for sample G tested with the apparatus of figure 7. When the contact piece is insulated, we can only notice a few Ohms resistance variations, whereas when it is not, the resistance variation drops from more than 1100 ohms to 800 ohms for a load gradually applied from 0 to 5 kg and return (compressed zone 4 cm^2)

We can also notice the hysteresis that is generated when compressing and releasing the force applied which is inherent to any material in compression that is not purely elastic. Other industrial sensors would suffer the same drawback. Also, the variations at the beginning of the test are due to the apparatus: when the friction force of the jack is passed a sudden load is applied onto the paper and the system has to readjust to the setting. However, it is interesting to see the results given over a few trials to check the repeatability of the measurements for the same load setting. The test of figure 9 shows that, after a first loading, that is different from the following (i.e. calibration test), the other trials are very similar thus providing a good repeatability for the measurement of varying force from the paper G.

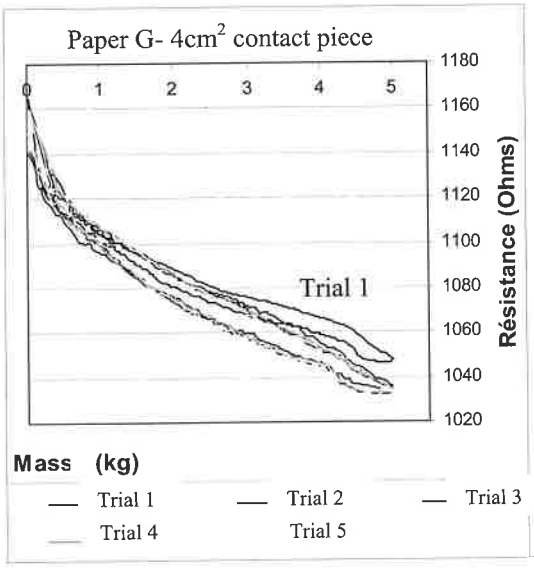

Figure 9: Repeatability test: after a calibration load the paper will provide the same resistance variation for the same applied force, and this as much when loading than when unloading

3.3 Influence of the fibres

The influence of the fibres is not easy to determine. Indeed, we did not make sheets with various pulps and having the same pigment concentration, except for samples 3b and 8b:

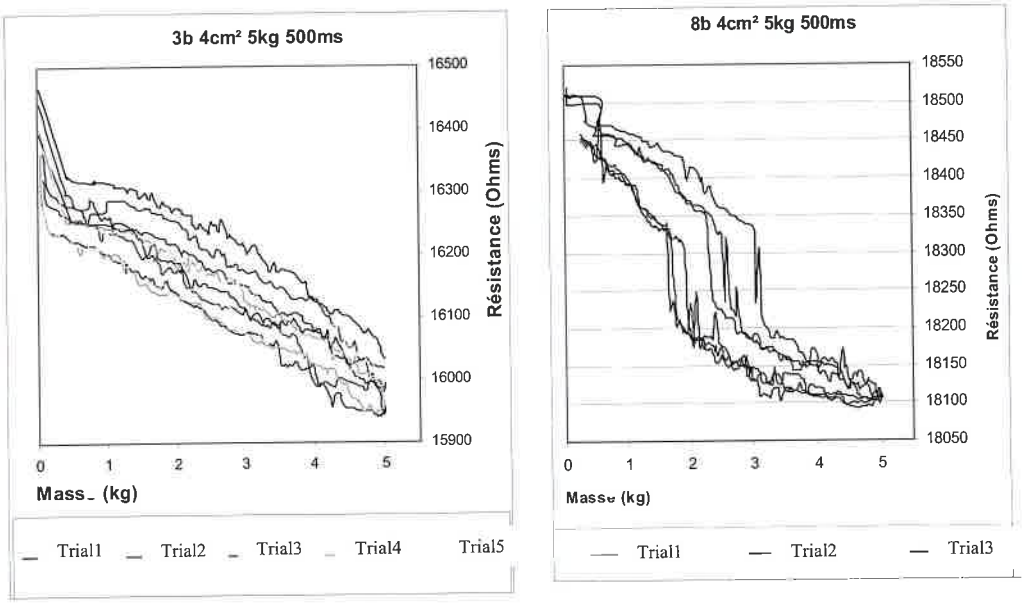

Figure 10: Influence of the fibres on the linear response of the resistance variation. 30% of chemical pulp and TMP were added respectively for papers 3b and 8b. We can see that long and less refined fibres yield better linear results and elasticity

Sheets 3b being made with chemical pulp and sheet 8b with TMP, we can notice the importance of using long and less refined fibres to obtain linear results and fibre elasticity. Indeed, the results for sheet 3b is much better than for 8b in terms of linearity for the $4cm^2$ loading surface.

4. Perspectives and conclusion

We could notice that some industrial papers such as paper G already provided good results in terms of repeatability for various applications. Another important point to use sensors for "expert" control gesture or dynamic measurement is its time-response, which means the time the material takes to come back to its original position and conduction response after being loaded. We measured this with an oscilloscope and noticed that it takes 75 ms for the sensor to come back to a steady conductivity value when the pressure is released. This means that we can not measure with precision two data below this time interval. Then, if we build for instance an electronic percussion, the sensor will enable to detect around 13 hits per second. A professional percussionist might go faster than the sensor when he drums, but for toys and no professional quality, this time-response would be sufficient for such an application. As far as tilts sensing for packaging applications is concerned, it is also interesting to have a low time response as the sensors should detect quick shocks due to bad manipulation during transportation.

New papers will be developed as well as another method to measure the content of pigments such as using a thermogravimetric analyer. Paper G will be kept as a basis of material and lower concentrations of long fibres such as chemical pulp will be added to improve its bulk, trying to find a compromise between an optimised range, good repeatability and low hysteresis for the optimised sample.

Another machine will also be built to enable better measurements, replacing the pneumatic jack by an electrically driven worm, thus eliminating the problem of friction and bad measurements under 4 Newtons.

References

[1] Jensenius, A. R., R. Koehly and Wanderley. M. M. 2005. "Building Low-Cost Music Controllers." In R. Kronland-Martinet, T. Voinier, and S. Ystad (Eds.): CMMR 2005 - Proc. of Computer Music Modeling and Retrieval 2005 Conference, LNCS 3902. Berlin Heidelberg: Springer-Verlag, pp. 123 - 129, 2006

[2] Koehly, R. 2005. "Study of Various Technologies for Home-Made Sensors." Masters Thesis. Master AST 2004 - 2005, Grenoble, France. Available by request to the author

[3] Koehly, R. et al. 2006. "Paper FSRs and Latex/Fabric Traction Sensors: Methods for the Development of Home-Made Touch Sensors." Proceedings of the International Conference on New Interfaces for Musical Expression (NIME'06), IRCAM, Paris, France, pp. 230 - 233

Printing of functional layers using flexography

Ulrike Herzau-Gerhardt, Henning Nagel

University of Applied Sciences Leipzig, Department of Media
Gutenbergplatz 2-4, D-04103 Leipzig, Germany
E-mail:uherzau@fbm.htwk-leipzig.de

Abstract

The advantages of printing processes to realise low thicknesses not only in continous layers (full tone) but in structured (half tone) suggest that the printing technology could solve the problem of coating functional layers with a high quality and economy.

The objectives of the scientific research consist in testing the possibilities of conventional flexographic printing to transfer special conductive metal dispersions or polymeric systems to plane glass surfaces. In a first step a special testing proofer based on flexographic process is to be choosen. Secondly it has to be investigated how the rheological properties of the fluids should be defined for the coating of an even distribution of the liquid on the plane glass surfaces.

Keywords

Flexographic printing, functional layers, rheological properties

1. Introduction

In present time investigations of using printing processes for coating of very thin functional layers on the surfaces of different substrates are carried out with the aim to introduce a more effective production technology with lower costs. Such layers are used for applications as well as in security packaging printing and bank note printing and out of the printing industry for the coating of defined layers of special conductive organic and inorganic components (e. g. LED, OLED, RFID).

But the printing processes differ in the optimal usability for those tasks because of their differences of the fluid transfer processes inside of the printing machines. The possible printing or coating results depend on the properties of the transferred inks or liquids, the substrates and the printing conditions (printing pressure, printing speed). Especially the physical and chemical properties of the liquids and the substrates which have to be coated and the reactions at the interfaces between the liqids and the substrates influence the results of the transfer. All printing processes offer techological possibilities to transport special coatings but only in their process limits. To find out the limitations and to define the necessary process conditions is the applied research work for printers and customers.

A comparison of the present output of a standard printing press to the manufacturing of microeelctronics shows a big difference. As well as the annual production of highly automated silicon chips could be realized in a real printing press extremely faster the costs for the investment of the printing press are definitely lower than for the production engineering of semi-conductor techniques.

But not only these general descriptions of the different technologies leads to a final decision if printed electronics could be substitute the former technologies. It is necessary to understand that there are principle differences in the demands of traditional printing of multicoloured images and on the other site of functional structures with fully changed properties of the transferred layers. Only the detailed description of the transfer phenomena in the printing presses leads to an applicable solution for printing of functional layers.

2. Basic conditions for printing of functional layers

In the last years all printing processes are optimized for the application in printing of traditional products like newspapers, journals, books, advertising materials and packagings (for instance cardboards and labels). The

slow resolution of the printed images is depending on the facilities of the human eyes. The resolution limits of the human eyes are defined as about 150 µm. To reach a reproduction of an image in an acceptable quality (necessary steps of grayness) the smallest pixels have a dimension of about 15 µm. For transferring special functional layers it is necessary to appplicate structures in a range of about 100 nm. So the finesse of the present manufacturing of electronic materials is much lower than in printing and is a very important advantage of this industry. In Table I is shown which criteria have to be compared in the qualification for printing images and functional layers.

Table I: Criteria for the evaluation of printing processes [Hübler2002, Rost 2005]

Criteria of printing processes	Traditional printing	Printing of functional layers
Resolution	> 15 µm	< 5 µm
Thickness of the layer	≈ 1µm	0,1 - 0,2 µm
Homogenity of the layers	No problem	Very important
Chemical pureness of transfer	No problem	Very important
Chemical recipe (solvents)	Well developped	Very important but less experience
Drying	Important	Very important
Special pure conditions in the pressroom	No problem	If necessary
Speed	Important (up to 15 m/s)	Not so important

In present time the printing processes could be characterized with the capacity values wihich are shown in Table II.

Table II: Capacity values of the different printing processes [Hübler2002, Rost 2005]

	Functional layers	Offset	Flexo-graphy	Gravure	Screen printing	Inkjet	Electro-photo-graphy
Resolution [µm]	0,1 - 10	> 10	> 30	> 15	> 50	>50	> 30
Thickness of the layers [µm]	0,05 - 1	0,5 - 2	0,8 - 3	0,8 - 8	3 - 15	0,3 - 10	1 - 10
Viscosity of the liquid [Pa s]	different	30 - 100	0,03 - 0,5	0,03 - 0,5	0,5 - 50	0,001 - 0,05	10 - 20 (liquid toner)

To print functional layers it is necessary to analyse the special conditions for the liquid transfer. So the following questions have to be answered:

1. How do the solvents change the rheological properties of the functional liquid?
2. How do the surface properties of the used plates and substrates influence the coating of the functional liquids?
3. How do the functional liquids dry?
4. Is there any chemical interaction between the different layers which are printed in a multilayer system?

But not only the liquid properties of the functional layers are of interest for the printing process which have to be used. Because of the special behaviour of the substrates transporting through the printing press investigations have to be planned to find out the most effective transport conditions in the printing press.

3. Flexography

First investigations with flexographic printing machines are known [Schmidt 2005]. The advantages of the flexographic printing process for the application of functional layers are the low costs (in general) and the possibilities to transfer inks or liquids with low viscosities. So the flexographic printing process seams to be suitable for the transfer of fluid layers with a film thickness of less than one micrometer to solid substrates or to webs.

The following investigations are dealing with the coating of thin functional liquids on substrates like glass and polymeric materials using the flexographic printing process.

3.1. Printing proofer

In a first step a special testing proofer based on flexographic process is to be choosen. The existing printing proofers for flexographic printing (K-Lox-Roller by Erichsen shown in Figure 1, Flexoprinting proofer F1 by

IGT shown in Figure 2) have been analysed. Both are not able to transfer the special functional liquids on formatted pieces of glass and to simulate the defined printing conditions.

Figure 1: K-Lox-Roller (Erichson)

Figure 2: F1 (IGT)

It was decided to design an new flexographic printing proofer to realise the necessary printing conditions. The following demands have to be fullfilled:

◊ Transport of formatted plane pieces of glass;
◊ Using a standard flexographic printing unit;
◊ Using standard photopolymeric plates and tapes;
◊ Realising of repeatable printing results.

In Figure 3 is shown the scheme of the basic printing unit. A special chamber coating unit is used to transport the liquid to the surface of the ceramic anilox roller. The plate cylinder is prepared with photopolymeric plates by adhering with special tapes.

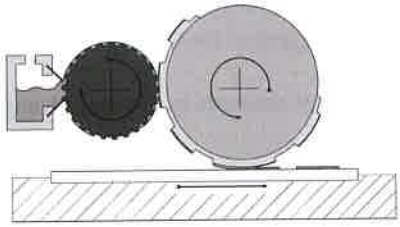

Figure 3: Scheme of the flexographic printing unit

After designing and manufacturing the special printing proofer printing tests were prepared and carried out to test a range of dispersions with different compounds and different chemical solvents and concentrations. The printing results were evaluated with special optical measuring systems to characterize the realised liquid film thickness and the topography of the surface.

3.2. Rheological properties

Before printing the rheological properties of the dispersions were controlled by measuring the viscosity depending on the deformation rate and the time. The measuring conditions in the rotational viscosimeter (Physica, Germany) were defined due to the real conditions in the printing proofer (simulation of a printing speed of about 1 m/sec).

The results of the measurements of the viscosity of the used dispersions with different solvents are in a range between 100 to 180 m Pas. These viscosities are comparable with the viscosities of waterbased flexographic printing inks (Figure 4). Special rheological phenomena like thixotropy could not be observed.

4. Conclusions

In general the printing results have showed that the transfer of a thin liquid layer with defined functional properties with a flexographic printing unit is possible. The realized liquid film layers of about 0,8 to 1,0 µm meet the demands for transferring the special functional dispersions. However the eveness of the surface has

to be improved in further investigations. Special efforts will be developped to reach more continous layers because of the next aim to print structured layers too.

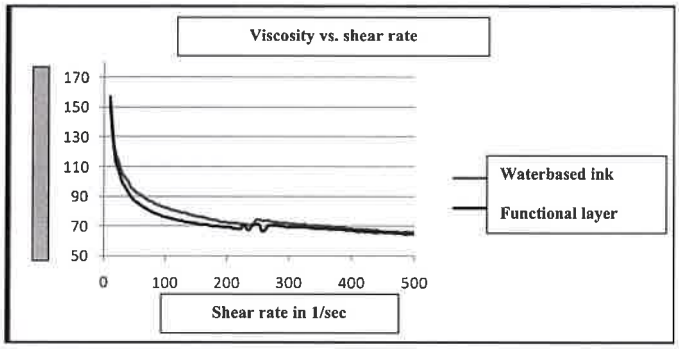

Figure 4: Characteristic curves of vicsosity

With the discribed basic results it was found out that the flexographic printing process is suitable for transferring special functional dispersions with conductive properties on plane surfaces.

References

[1] Hübler 2002: High volume printing technologies for the production of polymer electronic structures, Proceedings of the 2nd IEEE Conference, Hungary, 2002

[2] Rost 2005: Vom Polymertransistor zur gedruckten Elektronik, Kunststoffe 10(2005), 209 - 214, Carl Hanser Verlag München

[3] Schmidt 2005: Realization of electronic structures by means of flexographic printing, Printing Future Days, Chemnitz, Germany, 2005

Rotogravure and pad printing of microstructures for electronic applications like oFETs

Gunter Hübner, Werner Till

Hochschule der Medien Stuttgart, Institut für Angewandte Forschung (IAF)
Nobelstr. 10, D-70569 Stuttgart, Germany
E-mail: huebner@hdm-stuttgart.de; till@hdm-stuttgart.de

Abstract

Within the last years many companies, universities and research labs worldwide have begun to work in the field of organic electronics. Materials which are electrically conductive, semi-conductive or insulating are available in fluid form and it is common sense that these materials can be used to form very cheap electronic devices by using the patterning techniques of the printing processes. In order to produce electronic circuits with acceptable performance it is necessary to print extremely fine structures.

Thus, the subject of the research work is to explore the limits of the printing processes in the region of microstructures for organic electronics. One of the most challenging examples of this printronic application is the printing of source-drain structures for organic Field Effect Transistors. (oFET).

Rotogravure and Pad Printing are two closely related technologies which are capable to print high quality and fine lines. Both processes are well known for their reliable and stable printing process. Therefore they were chosen to investigate their potential for printing organic electronics. Gravure printing is a technology that is capable of printing high volumes in very good quality. Pad Printing is a related technology which is much easier to handle and findings from there can be transferred to other processes.

Keywords

Microstructures, OFET, organic electronics, pad printing, rotogravure

1. Introduction

In the field of Rotogravure and Pad Printing major technological progress has been made in the last years. In Rotogravure Printing the advancements in Laser and engraving technologies for example have made it possible to produce cylinders with fine, smooth lines. Compared to conventionally engraved printing cylinders the etched cylinders show much finer outlines. But as a result of the etching process the geometry of the cell is different to that of traditionally engraved cylinders.

When a cylinder is etched the depth of the cell can be chosen independently from the width. This is not, or only within restricted limits, possible with engraving technologies. When etching a fine line or a cell, the depth of the line can vary in a very wide range almost without changing the width of the line. Hence the volume of a cell or line can vary too.

Consequently, within certain limits, the volume of ink transferred to the substrate can be chosen independently from the width of the cell or line too. The use of etched cylinders therefore seems to be very promising in the field of printed electronics. Different from the requirements in traditional printing the basic needs of printed electronics are mainly exact outlines, smooth surfaces and preferably a volume of transferred ink that can be chosen as free as possible. The last requirement results from the great variety of electric active polymers and other materials which in some cases have just about 5% electrical active material which is dissolved for example in water and alcohol.

To achieve a conductivity that is good enough for electrical purposes it is desirable to transfer an exactly defined volume of the material to the substrate.

The ink transfer from the gravure cell to the substrate is a very complicated process which is still a subject to theoretical research from different sides, even in traditional printing.

We therefore began with some experimental works to find the boundaries of our printing systems and to analyze the feasibility of printing some electrical active materials with our special technologies.

2. Methods

Prior to the printing itself there are a few steps which are of course well known in the printing industry, but for the needs of microstructure printing they have to be questioned again. Without that a survey about the problem would not be complete.

When trying to print fine structures in the scale of 10 or 20 microns, the first question is: Is the traditional Software that is used for the graphic industry capable to create such structures reliably?

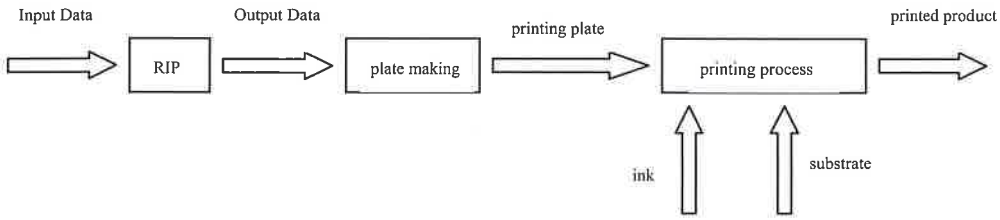

Figure 1: A simplified scheme of the process steps in printing

The problem of the reproduction of lines in the micron-range already starts with the creation of the data. It can be said that CAD-software (vectorised data) is accurate at least down to 1µm but standard layout software used in graphic arts applications usually comes to its reliability limits at structures smaller than 10 microns. The exchange of data from one software package to another must be avoided due to unpredictable results. Here vectorised data was used as long as possible in the process. In the next step, in plate making, the Raster Image Processor (RIP) converts the data usually into pixel-oriented bitmaps. RIPs in the graphical industry are optimised in general for the needs of rendering halftone images to precisely coloured rasterised prints. In electronic printing only solid tones are needed. However, in gravure and pad printing, certain screening methods must be applied because even in solid tones cell walls are needed to support the doctor blade.

2.1 Target: oFETs

One of the most challenging examples of such an extremely fine lined printronic application is the printing of source-drain structures for oFETs (organic Field Effect Transistor). Figure 2 shows a schematic top-view of such an S/D-structure which is the lowermost layer of a so called top-gate oFET consisting in total of 4 layers. Three more layers have to be printed on top of the S/D-structure.

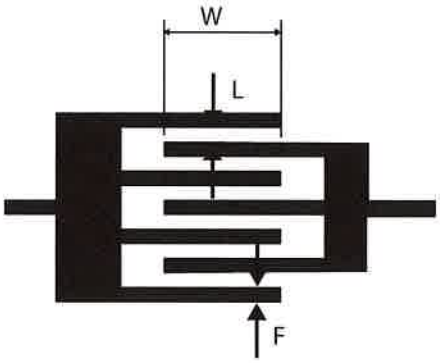

Figure 2: Source-Drain structure

Typical requirements for satisfying performance of the Transistor are 20 µ < F < 150µm, L < 20 µm and 100 µm < W < 500 µm. The Source-Drain Structure has to be printed with conductive material.

Further, these structures have to be smooth, without internal failures and the outline boundaries have to be sufficiently even.

The process of printing form making has been investigated both for pad printing (flat forms) and for rotogravure (cylinder preparation).

2.2 Pad printing

Pad printing, like gravure printing, normally requires screening. Between the screened cells that are filled with ink the cell walls are needed to support the doctor blade. The RIP produces this structure according to the standard procedures of the graphic industry. When fine lines should be printed and the cell sizes are in the same order of magnitude as the lines, these lines may be heavily distorted (see Figure 3). Thus, for the requirements of printed electronics the question must be: Can fine structures be printed in pad or gravure printing without screening, at all and from what line width on is screening necessary?

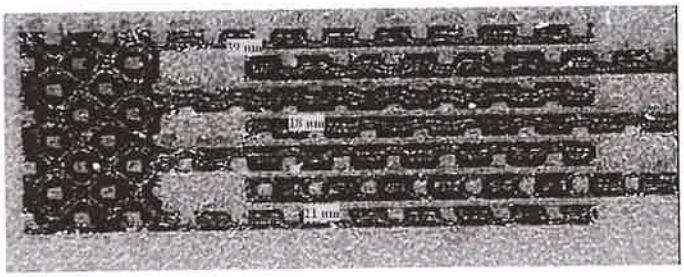

Figure 3: Image of a pad printing plate (LAMS-technology). Line width was 20 microns in the original data and is about 25 microns on the plate. The line pattern is heavily distorted by the screening technology

The laser imager that exposed the plate from Figure 3 is typically used in security printing and has a resolution of 8000 dpi.

Distorted or interrupted lines are no problem in traditional printing because the eye merely is not able to see such textures but in the field of printing electronics such a structure will not be conductive and fails.

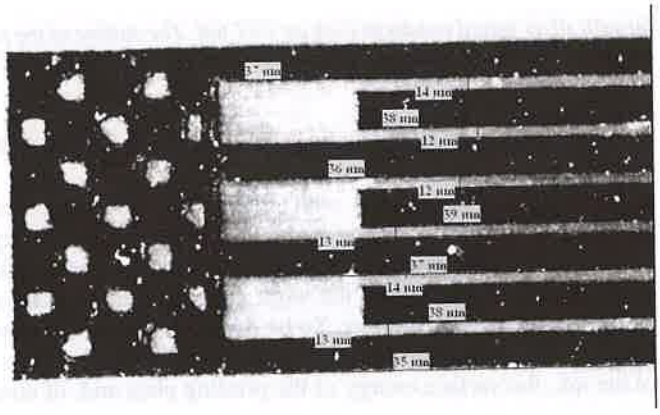

Figure 4: Image of pad printing plate. The same pattern as in Figure 3. Before imaging the single bit data coming from the Rip was manually modified by removing the cell pattern in the fingers. The plate is ablated only, but not processed. Positive and negative line width was 20 micron in the original data; however, the positive lines are approximately 35 micron on the plate

In order to test the image quality without the screening the single bit data coming from the Rip were manually modified by removing the cell pattern in the fingers. The result is shown in Fig 4. Within the larger solids at the end of the fingers the "lands" are needed to support the doctor blade but may probably cause pinhole-type failures in the print.

Now (Figure 4 shows it much better than Figure 3), another problem of the RIP processing and exposing system is revealed. The positive and negative lines which had both a width of 20 microns in the original data (F and L in Figure 2) show different dimensions!

In Figure 4 the positive lines are much wider than they should be. The negative lines are, as a consequence of that, much too narrow. This effect does appear in almost any exposing system that is used in the graphic industry today. The effect is changing with the angle between the structure and the laser moving direction.

The corresponding printing experiments that were carried out with standard pad printing ink (for comparison) and carbon black conductive ink showed that very fine positive and negative lines with a width of 20 microns can be printed reproducible in rather good quality without "shorts", see Figure 5.

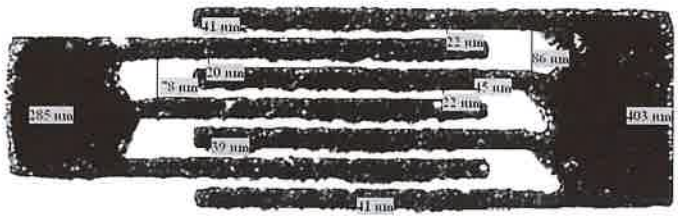

Figure 5: Pad print with carbon based conductive ink on PET foil. Printed from a plate without screening as shown in Figure 4. The negative lines have a width about 20 microns, the positive lines about 40 microns

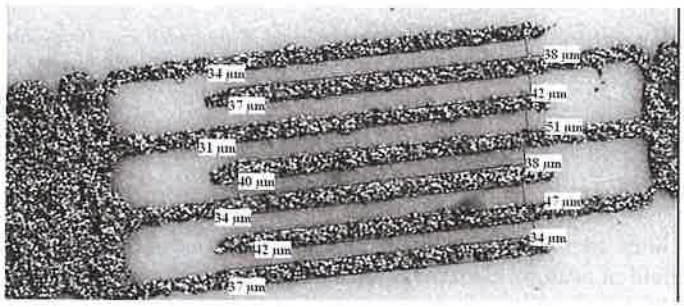

Figure 6: Pad print with silver based conductive ink on PET foil. The outline of the print is good but the surface roughness is rather high because of the silver flakes. The negative lines are about 34 microns wide

Some other printing experiments were carried out with silver based ink as shown in Figure 6.

The print samples both with carbon black and with silver ink show that printing without screening respectively with modified screening in pad printing is possible, thus, the feasibility of the method has been proven. Even the unusual conductive inks which are not yet optimised for pad printing can be processed well with that technique. The results are promising and the work is being continued in order to further define the operating windows and necessary parameter settings. To be explored are the ink transfer from the lines to the substrate, the geometry (depth) of the lines, the rheology of the ink, the particle sizes (surface evenness) in the ink, the surface tension of the ink, the surface energy of the printing plate and, of course, the surface energy of the substrate.

2.3 Gravure printing

After it was shown that printing without screening is possible in pad printing the next step is to investigate the possibility of printing fine structures without screening in rotogravure printing.

In the last decades cylinders for rotogravure printing were almost exclusively engraved with diamond styluses. In the last years technologies based on etching the cylinders were developed. The mask for the etching process is ablated with a laser into an etch-resistant coating of the cylinder.

Direct laser engraving in the copper or in copper/zinc presently is either not available yet or has an insufficient resolution.

Etching a rotogravure cylinder has the advantage that any geometrical structure (for example lines) can be etched and the depth of the structure is almost independent of the line width. Thus, the volume of ink that is stored in the cylinder and consequently the volume of ink that is transferred to the substrate can be chosen in a rather wide range. The cylinders can be etched completely without any screening or with modified screening that is adapted to the structure that shall be printed. These are considerations which make an etched cylinder promising for printing electronics.

The experiments with rotogravure printing were mainly carried out with cylinders with modified screening on an experimental narrow web lab printing press (70 mm diameter, 160 mm width) and a few experiments with an industrial size cylinder (300 mm diameter, 1.300 mm width for a packaging press). The printing experiments were performed both with standard gravure ink and with the conductive polymer PEDOT using the small cylinder and with gravure ink using the industrial cylinder.

Similar as in pad printing the cylinder preparation process revealed that there were deviations from the original structure dimensions to the ones imaged onto the cylinder by the laser imager or by etching. Positive lines always showed gain in line width.

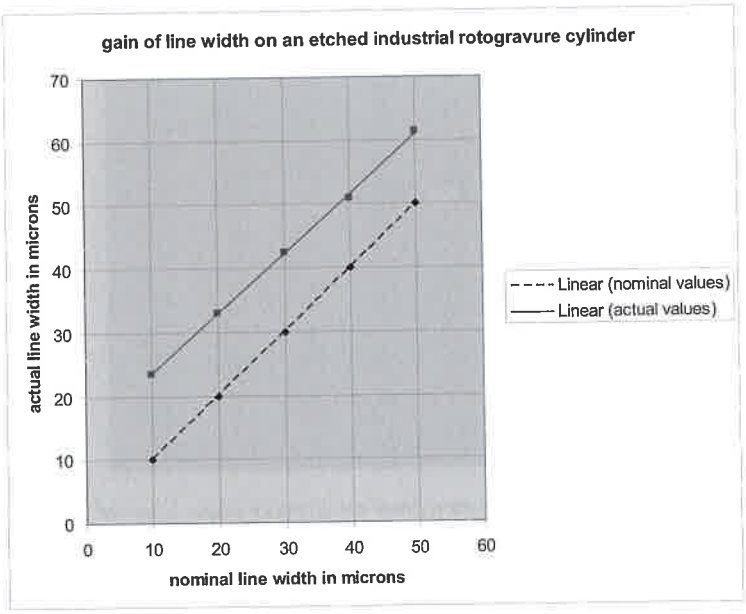

Figure 7: Gain of line width on an etched rotogravure cylinder. The lines are 10 to 14 microns wider than they should be

The gain of line width on the small cylinder is slightly greater than on the industrial type cylinder because it is technologically difficult to mount such small cylinders in the imager and to control the etching process.

The readings from the industrial rotogravure cylinder show that the technology of making a cylinder with such accuracy is bringing the technology close to its limits although the methods used here are normally used for security printing.

3. Results

The following paragraph describes the results of printing experiments on a proof press and on an industrial rotogravure press.

It is well known in the printing industry and it has been proved by other research works [3] that the quality and the width of line on the substrate in gravure printing highly depend on the angle to the doctor blade. The

best results are made with lines that are perpendicular to the doctor blade. Fig 8 and 9 show such lines. Both lines had a nominal width of 50 microns. The actual line width on the etched cylinder was 60 microns (50 microns data, see Figure 7).

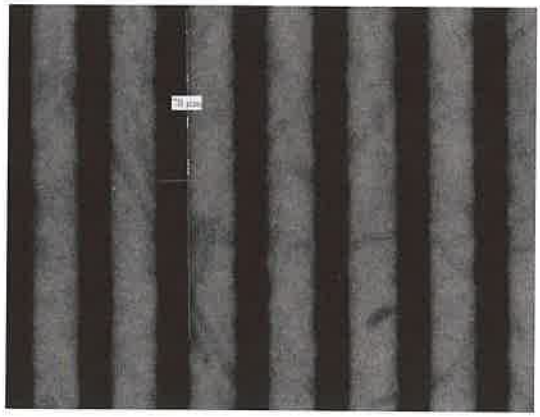

Figure 8: Print with gravure ink on PE foil on a proof rotogravure press. Nominal width of lines: 50 microns - actual width of lines in print 78 microns. Direction of lines is perpendicular to the doctor blade. The depth of etched lines is 15 microns. The lines on the cylinder were without cell walls. Viscosity of the ink was 35 sec measured with a 3 mm DIN cup

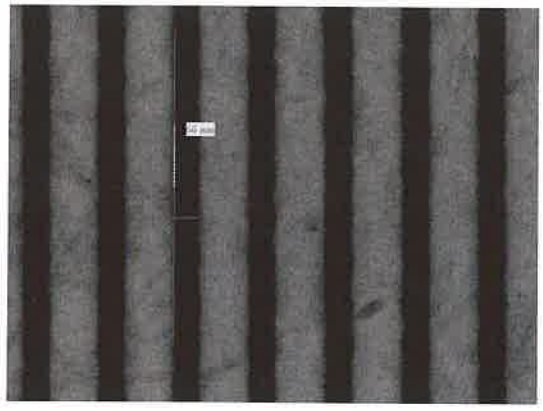

Figure 9: Print with gravure ink on PE foil on a proof rotogravure press. Nominal line width: 50 microns - - actual line width in print: 66 microns. The direction of lines is perpendicular to the doctor blade. The depth of etched lines is 10 microns. The lines on the cylinder were not completely without cell walls but with modified screening. Viscosity of the ink was 35 sec measured with a 3 mm DIN cup

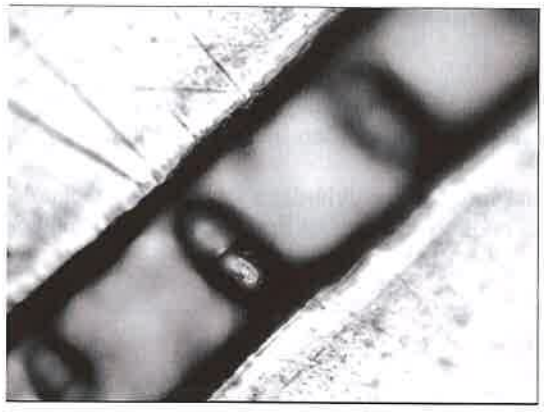

Figure 10: Microscopic photograph of an etched line. Nominal width should be 50 µm, actual width is 60 µm, depth 15 µm. The prints in Fig. 8 and 9 were made with such lines

The difference between the two patterns in Figure 8 and Figure 9 is the depth of the etching.

The depth for the sample from Figure 8 was 15 microns and for Figure 9 was 10 microns. With a depth of 10 microns the cell walls can still be seen in the print, whereas with a depth of 15 microns the influence of cell walls is completely eliminated. However, the deeper cells result in a wider line.

In Figure 11 the results from a printing experiment on an industrial gravure press are shown. The line width was measured for lines parallel and perpendicular to the doctor blade and an etching depth of 10 microns. The lines on the cylinder were not completely without cell walls but with modified screening as described already for Figure 9 and 10. The substrate used in this experiment was significantly more rough than the substrate that was used on the proof press.

The parameters on the press were set to standard production conditions (ink viscosity, speed, angle of doctor blade, corona treatment) best suitable for the PE-substrate.

Due to the patterns on the cylinder that were already wider than the intended width and the further gain during the printing process the minimum line width that could be printed was 35 microns.

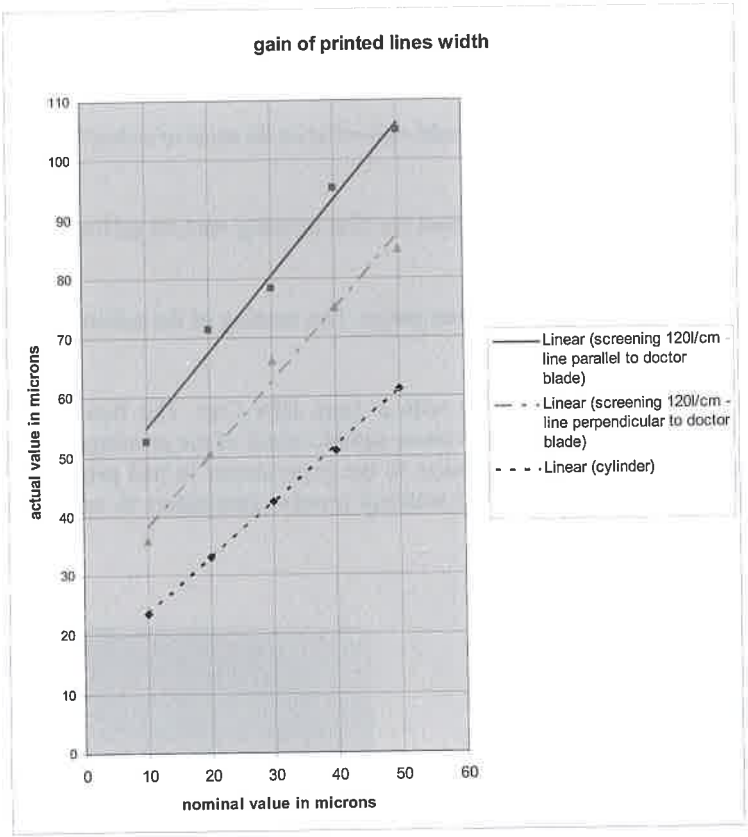

Figure 11: Comparison of actual and nominal line width values for print with gravure ink on PE foil in industrial rotogravure press. Etching depth 10 microns

Figure 11 compares the gain in line width for lines with 10 and 15 microns deep etching, perpendicular and parallel to the doctor blade. The gain of the line width of the 10 micron deep lines seems not to increase further depending on the line width itself, whereas the gain of the 15 micron deep lines still increases up to the measured 61 µm value. Responsible for these effects are the capillarity of the ink in the printing cylinder nip, the angle, the wetting properties, the printing speed and the ink volume in the deepenings of the cylinder and maybe more.

3.1 Printing with PEDOT

One important electrical conductive polymer today is PEDOT which is water soluble. Although water soluble inks are not easy to process in gravure printing on plastic foil it was possible to print lines with 60 microns width on our narrow web rotogravure press.

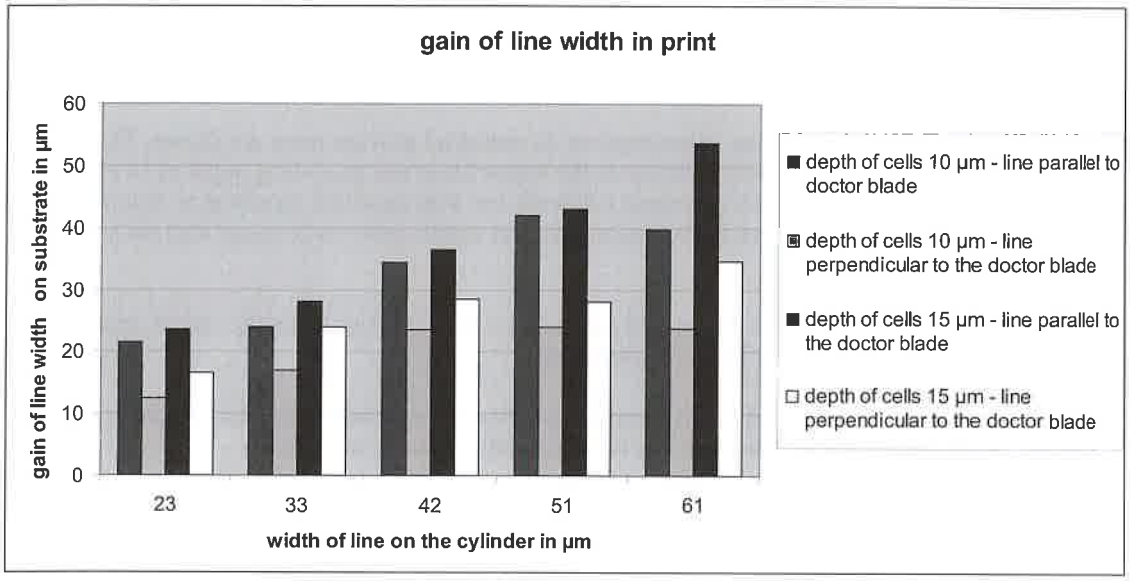

Figure 12: Gain of line width depending on the depth of etched lines

The surface energy of the PET foil that was used for that printing was 50 mN/m, the polar component was 21 mN/m.

The surface tension of the PEDOT is in the same range. The wetting of the substrate therefore is possible but it is critical.

The viscosity of the PEDOT was determined with a 3mm DIN Cup. The flow out time was 35 seconds. Printing speed was 27 m/min. Figure 13 and 14 show sample result of the printings. Obviously it is possible to print lines with at least 60 microns width. Similar to the experiments in pad printing we are continuing our work in order to determine more cylinder and printing process parameters to make reliable industrial print production feasible.

Figure 13: Gravure printing with PEDOT on PET foil. The line width is about 60 micron

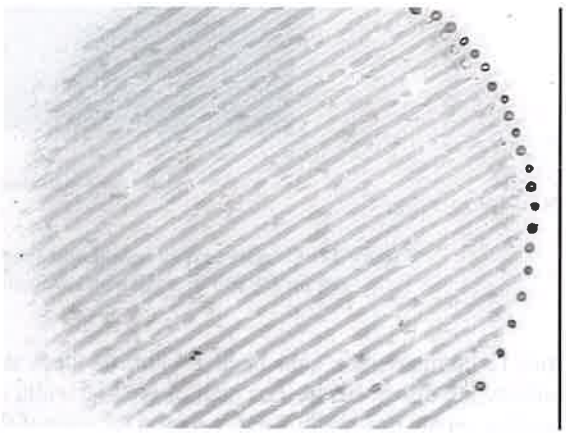

Figure 14: Gravure printing with PEDOT on PET foil. Printing conditions were the same as in Figure 12

4. Conclusions

An experimental investigation about the feasibility of microstructure printing with traditional ink and with electrical conducting inks was made:

◊ The experiments with gravure ink showed that fine lines can be printed in rotogravure printing.
◊ The process of etching the cylinders still can be optimized, so that the actual width of the etched lines comes closer to the nominal width.
◊ In pad printing positive lines with a width about 20 microns can be realized with conductive inks. Negative lines can even be smaller.
◊ The printing performance of presently available conductive inks is still not as good as the one of conventional inks. Further work has to be done to analyze and adjust the relevant printing process parameters for the conductive inks. It is not likely that the inks presently on the market in short term will achieve satisfying performance. Hopefully there will be material developments that the conductive inks come closer to the conventional ones.

References

[1] Reuter K., Kempa H, Brandt N., Bartzsch M., Huebler A. C., "Influence of process parameters on the electrical properties of offset printed conductive polymer layers", Progress in Organic Coatings 58 (2007), pages 312 - 315

[2] Fenoll M., Catusse R., Rousset E., "Gravure Printing: Material Characterisation for All-organic Capacitor", Taga Proceedings 2005, pages 83 - 92

[3] Claypole T., Jewell E. Davies G. Vigne V., "The Effect of Speed and Viscosity on Line Quality in Rotogravure", Taga Proceedings 2005, pages 93 - 99

[4] Fenoll M., Catusse R., Rousset E., "Gravure printing: formulation and characterisation of polymer conductive inks", iarigai- International Research Conference Proceedings 2006, pages 147 - 152

[5] Davies G., Claypole T., "Effect of viscosity on ink transfer in gravure printing", iarigai- International Research Conference Proceedings 2006, pages 235 - 244

Printing process for Lithium-ion electrodes elaboration

Franck Medlege[1], *Anne Blayo*[2], *Hélène Rouault*[1], *Naceur Belgacem*[2]

[1] CEA Commissariat à l'Energie Atomique
17 rue des martyrs, 38054 Grenoble cedex 9, France
E-mail: franck.medlege@cea.fr; helene.rouault@cea.fr

[2] EFPG Ecole Française de Papeterie et des industries Graphiques
461 rue de la papeterie, 38400 S[t] Martin d'Hères, France

Abstract

A new ink based on a polymeric binder system was elaborated in order to produce patterned Lithium-ion electrodes using a flexographic technique. The printed electrodes obtained presented a thickness higher than 40 µm and were efficient in comparison with standard Lithium-ion electrodes.

Keywords

Electrodes, flexography, inks, lithium batteries, printing process

1. Introduction

The strong market driven for a safe room temperature and high-energy rechargeable battery has fuelled the development of lithium-ion (Li-ion) technology. The Li-ion battery has the highest energy density of any rechargeable one and the improvement of its performances has been spectacular. The Li-ion battery with significant higher energy density has replaced the Ni-MH technology as soon as production capability was available. It is today the technology used for portable electronic devices and now it is challenging the Ni-MH for the hybrid vehicle application. Today, there are over 30 manufacturers, worldwide with production ranging from approximately 4.000 to 100.000 cells per day.

In the lithium-ion battery, there is no lithium metal lithium is found only in ionic form or in atomic state when it is in electrolyte or intercalated into the electrode active materials. The first commercial Li-ion cells was designed and sold by Sony in 1991, shortly after the publication of Tazawa and Nagaura (1990), who described the first commercial cell, its construction and its performances. The cell has a carbon/graphite anode, a lithium-cobalt oxide $LiCoO_2$ cathode and an organic electrolyte of lithium hexafluorophosphate ($LiPF_6$) salt with ethylene carbonate based organic solvent mixture. The principle of working of such a lithium cell is based on intercalation mechanisms. Thus in discharge, the Li^+ cations produced by the oxidation of the negative electrode (anode) intercalate into the positive one (cath ode), the phenomenon being inversed in charge, (see Figure 1).

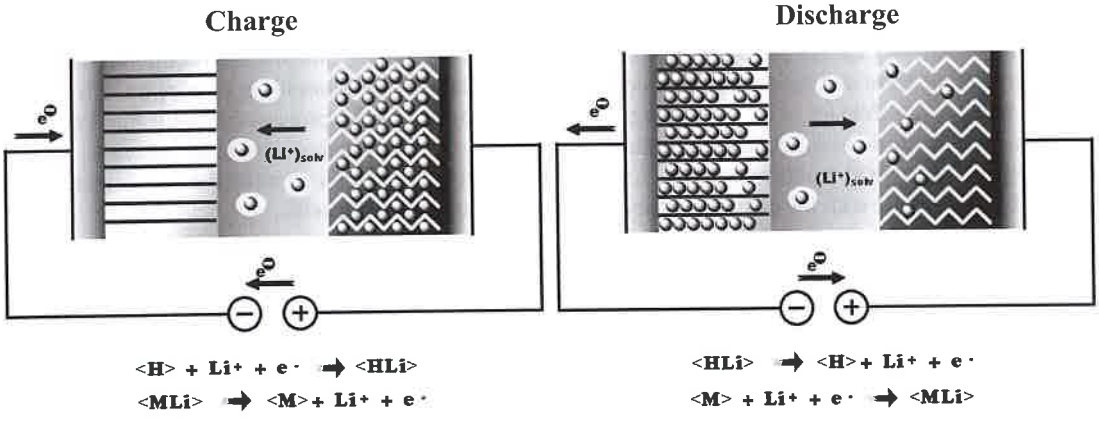

Figure 1: Principle of working of lithium-ion system

The Li-ion cells are assembled in the discharge state. It is the reason why the lithium-ion battery has to be charged to be made operational. Indeed, lithium is thus transferred from the lithited cobald oxide based positive electrode to the graphite based negative one. The lithiated cobalt oxide active material practically delivers about 145 mAh/g and may be doped with Al, Mg, etc ... to stabilize its structure against oxygen evolution [Jang et al., 1998]. Cobalt oxides constituted materials of choice and are used in the majority of commercial cells. However, there are a lot of lithium intercalation compound which could be use in Li-ion cells, namely manganese oxides, vanadium oxides, iron phosphate ... The anode material is generally a carbon/graphite material. However it can be replaced by a lithiated titanium oxide $Li_4Ti_5O_{12}$ when performances at high rates in charge or in discharge are required.

The conventional electrode manufacturing processes use coating techniques for applying a paste constituted by the anode or cathode active material, one or more conductive additives, usually acetylene black, graphite or carbon powders, a polymeric binder, such as poly-vinylidene-difluroride (PVDF) or Styrene-Butadiene Rubber (SBR) with Carboxy Methyl Cellulose (CMC), and an a solvent, usually N-methyl-pyrrolidone (NMP) or water, on a current collector like aluminium or copper foils, for example. Common types of coaters include extrusion, reverse roll coating and knife over roll or doctor blade. The coating process is a critical step ensuring a high capacity, high reliability product. If the coatings are of poor quality, only low performance batteries will be produced.

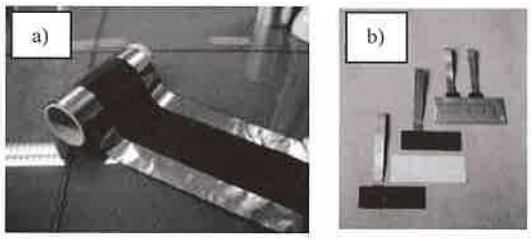

Figure 2: a) Coated electrode, b) Patterned electrode

A typical coated electrode is shown on figure 2a. Growth in demand of specifically designed electrodes in medical, military or miniaturised applications requires the fabrication of patterned electrodes as shown on figure 2b. Coating techniques are not adapted for manufacturing such electrodes because patterned electrodes has to be cut in the continuous coated electrode (cf. figure 2a) and a non negligible part of the coating is definitively loss in such operation. The best way for manufacture patterned electrodes is to deposit the coating paste on the considering metallic folder just on specifics areas with the desired shapes.

Consequently, printing techniques offer all the advantages in order to produce these electrodes. The consumption of the ink, and especially of the electrode active materials (with their high cost) can be reduced, the time spent for implementing the electrodes is saved and then the battery production can be increased. Note that in Lithium-ion technology, electrode layers exhibits high thickness comprised between 20 and 120 µm depending on the surface area and the desired final cell capacity.

To produce such electrodes thicknesses, some printing processes could be mentionned, namely the screen printing technique, flexography, gravure, intaglio or ink-jet. Gravure required an expensive operation to engrave a copper cylinder and allow only a metal/metal contact due of the use of a metallic folder substrate in our case which seems to be difficult to realise. Nevertheless this technique could be envisioned. The intaglio process is no more used in the industry except for a few fields of applications. Otherwise this process required a high pressure between the printing form and the substrate which is not possible with the aluminium or copper foils used in the lithium-ion technology. Ink-Jet is an interesting technique but is not really processable with highly pigmented and viscous inks of lithium-ion electrodes without using additives like wetting agents, dispersants, defoamers, levelling agents, rheological modifiers agents ... etc. These additives are often combined in the formulations and are susceptible to interact with the electrochemical reactions occurring in the cells.

This paper presents the investigations engaged for manufacturing shaped Li-ion electrodes by a flexographic technique. This process has been chosen because it can be used in a large range of ink viscosities, the printing forms are easily adaptable, the process can work with very low pressures and it is possible to adapt the anilox volumes in order to transfer the appropriate amount of ink. Otherwise screen printing is used in many organic electronic printing applications but printing plates are quite expensive. This technique is being now evaluated in order to compare the results with those obtained with the flexography technique. These experiments are in progress and will not be dealt in the present paper.

One kind of electrode was studied: a $LiCoO_2$ positive electrode conventionally manufactured with PVDF binder dissolved in NMP.

2. State of the art

Printed electrodes for lithium-ion batteries are a newest field of application for printing processes. Unfortunately, there is no useful information in the literature data. Therefore, the first step of the study was to identity the similarities and differences in properties between a standard electrode coating paste and the printing inks. Table I gives an overview of the relevant properties. The main difference is the low surface tension of the electrode coating paste containing a PVDF binder, compared to the surface tension of a printing ink (between 35 and 45 mN/m).

Table I: Electrode coating paste and printing inks properties

	Electrode coating paste	**Printing inks**
Solid phase	Anode or cathode active material + Conductive-material(s)	Black or coloured pigments
Vehicle : Polymers + Solvents	Polymeric binder Solvents	Polymeric binder Solvents
	Aqueous or organic	Aqueous or organic
Viscosity	0.1 to 1 Pa.s	A few mPa.s to Pa.s
Rheological behaviour	Shear-thinning	Newtonian or shear-thinning
Surface tension	PVDF: **23 mN/m**	35 to 45 mN/m

In order to increase the surface tension, PVDF was mixed with another polymer containing polar groups, susceptible to increase the polar contribution of the surface tension. The behaviour of polymer blends was studied using the Flory-Huggins theory [Flory-huggins, 1941, 1942].

3. Materials and methods

3.1 Materials

For the cathode composition, a cobalt oxide $LiCoO_2$ provided by ITOCHU© was chosen and mixed with a high specific area carbon powder (Printex EX2, Degussa©) and carbon fibers. For the binder, a PVDF 1015 provided by Dyneon™ was used whereas the second polar polymeric material which can be a polyvinyl-alcohol for example was provided by Aldrich©. For the cell assembly, lithium metal counter electrode was used.

3.2 Methodology

Traditional coated electrodes and printed electrodes were performed with the new binder. Then, they were electrochemically tested and compared with standard coated PVDF electrodes.

The electrodes were prepared by mixing the polymeric binder (PVDF or polymer blends of the study) with carbon conductive materials and $LiCoO_2$ positive material in N-methyl-pyrrolidone (NMP), using a Dispermat® apparatus. The slurries obtained were then coated with a Braive-Instrument coating table and/or printed with a home-made flexography proofer on aluminium foils. After evaporation of the NMP, dried electrodes were obtained.

The porosity of the electrode layer, often comprised between 30 and 40%, has great consequences on the performances of the electrodes. It was adjusted by calendering.

For the electrochemical tests, coin cells were built as shown on figure 3. The cells used a polypropylene microporous separator (Celgard®), an electrolyte [1*M* $LiPF_6$ dissolved in a 1:1 (v/v) mixture of ethylene-carbonate and dimethyl-carbonate] and a metallic lithium counter electrode. The cells were assembled and crimped in a dried argon glove box, (see figure 3).

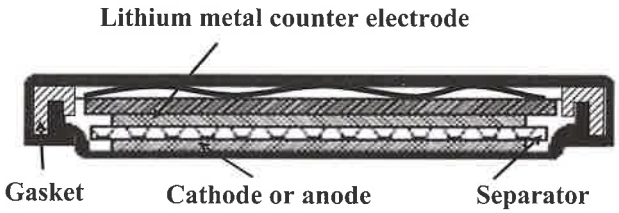

Figure 3: Coin-cell architecture

Rate capability tests were conducted in order to evaluate the electrochemical performances of the cells. A so-called "signature curve" is generated to determine the ability of the cell to deliver current at different rates, [Doyle et al., 1994]. After two cycles of formation (discharge/charge at very low current), the cell is first discharged at the highest test current (or rate) to the low cut off voltage. This voltage depends on the used active materials and is equal to 2.5 V versus Li^+/Li for $LiCoO_2$. The cell is then kept in rest briefly on open circuit and then discharged at a lower current to the same cut-off voltage. The sequence is thus repeated until the lowest current is reached. Each current is defined by a specific "D/n" rate, which is corresponding to a current susceptible for discharging the nominal capacity of the cell in n hours. Thus, discharge rates comprised between D/50 and 30D were applied. The capacity at each rate was then determined from the accumulated capacities of the previous rates. In this way, the rate capability over a wide range of currents was calculated without recharging the cell.

4. Results and discussion

Electrode inks formulated with the new binder were printed successfully with the home made flexographic proofer. The Thickness of the ink films obtained is close to 50 µm.

Highest performances were reached on coated electrodes with the new polymeric binder, in comparison with a standard PVDF binder which is the reference for our study. Figure 4 represents the rate capability test profiles at room temperature for coated and printed $LiCoO_2$ electrodes. The coated electrode prepared with the new binder is able to release a higher capacity percentage for higher discharge rates than those obtained with PVDF binder.

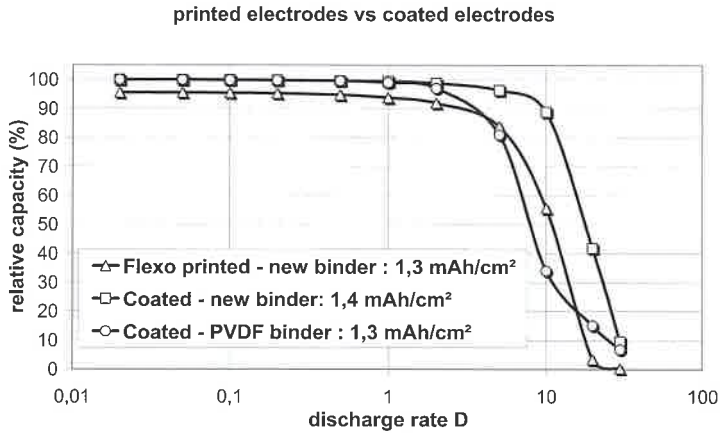

Figure 4: Signature curve for 1.3 mAh/cm² $LiCoO_2$/Li cells

Nevertheless losses of expected capacity were observed at low rates with printed electrodes, compared to coated electrodes. This phenomenon may be due to the surface roughness of the printed electrodes, as shown on figure 5. It is not possible to calender efficiently such electrodes and there is probably some porosity

heterogeneity in the layer. Adjustments on the formulation, rheological and chemical modifications of the electrode ink should allow a better levelling of the printed surface.

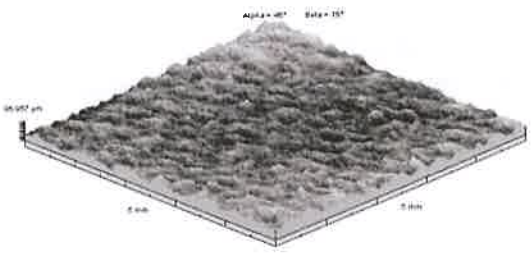

Figure 5: Surface representation of a printed electrode realised with an Alti-Surf® Profiler

Thus, printed electrodes with smoother surfaces can be obtained, through slight modifications of the solid content, only by solvent addition. As a matter of fact, various inks with different solid contents ranged between 49% and 55% were printed in the same conditions. As expected, the surface active material content of each layer decreases with the solid content. For example, the capacity decreases from 1 to 0.7 mAh/cm^2 when the solid content decreases from 55 to 49%. Besides, it is normal to observe that the relative capacities discharged on the whole domain are higher. Nevertheless, it does not justify the loss of relative capacity for the electrode of 1 mAh/cm^2, which should be closed to 100% at low discharge rates (see Figure 6). This effect can be attributed to the quality of the levelling of the electrode surface, together with the relative heterogeneity of the porosity, due to an excessive solid content. The resistivity of the electrode increases and a portion of the active material is not used.

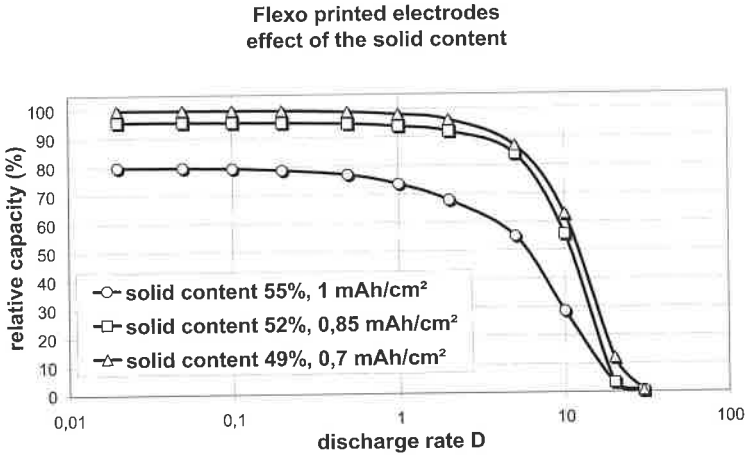

Figure 6: Effect of the solid content on printed electrode performances

Up to now, investigations have been done by keeping the same solid content, used for the traditional coated electrodes, and only by replacing PVDF by the new binder. Now, work is being engaged in order to optimise it, giving a best quality of the electrode in term of surface, cohesion and porosity. In the same time, technological improvements are in progress in order to increase the thickness of the layer, compared to traditional thicknesses obtained by printing process (for example, modification of process parameters and equipment).

5. Conclusion

An increase of the polar contribution to the total surface tension of the binder allowed to print efficient electrodes and had a significant effect on the performances of these electrodes. The printed electrodes layers have a thickness higher than 40 µm and the considered electrodes are efficient comparatively with standard coated PVDF electrodes. The improvement of the performances of the electrodes is still in progress.

References

[1] Doyle M., Newman J. and Reimers J., 1994, *J. Power sources, **52**, p. 211*

[2] Flory P. J., 1941, *J. Chem. Phys., **9**, p. 660*

[3] Flory P. J., 1942, *J. Chem. Phys., **10**, p. 51*

[4] Nagaura T. and Tozawa K., 1990, *Progress in batteries and solar cells, **9**, p. 209*

An experimental study to identify key factors affecting the performance of RFID tag antennas

Yung-Cheng Hsieh, Hui-Wen Cheng

Department of Graphic Communication Arts, National Taiwan University of Arts, Taipei, Taiwan
59, Section 1, Ta-Kuang Rd., Pan-Chiao City, Taipei County, Taiwan R.O.C.
E-mail: t0803@mail.ntua.edu.tw; s9211520@mail.ntua.edu.tw

Abstract

The study used screen printing method with a silver-based conductive ink (Ag) to print REFID tag antennas on the three most commonly used substrates for RFID tags in Taiwan's packaging industry. The three substrates were PET, coated paper, and wet strength paper. An UHF (902 - 928 MHz) antenna was designed for the experiment; the reader is an Impinj Speedway provided by a major RFID tag testing center in Taipei. The research was an experimental research in nature and aimed to investigate how "the distance between the reader and the RFID tags (reading distance, d)", "reading angle between the reader and the tags (reading angle, θ)", "numbers of tags per unit space (tag number)", and "tag moving speed (tag speed)" influence the performance of the RFID tag antennas. The operational definition of RFID tag antenna performance (dependent variable) in this research is the percentage of being read and the number of times of being read per second of the tags by the reader. The purposes of the study were: 1). to identify significant factors influencing the performance of the RFID tags, 2). to study how those significant factors affect the performance of the RFID tags, 3). to establish the optimum combination to achieve the maximum performance, and 4). to compare the tag antenna performance for the three substrates being printed. This study utilized a randomized 2^4 factorial design in which every factor was run at two specified levels (fixed effects) determined based upon the practical operating conditions using screening printing method to print RFID tag antennas with Ag ink at a major RFID tag manufacturer and testing center in Taiwan.

Keywords

Factorial experiment, RFID, RFID tag antenna, screen printing

1. Introduction

RFID technology has been around for many years, but it is only in the past few years that we have seen a surge in its acceptance and a massive growth in its use. However, RFID has not been able to replace the current bar code system yet because of the high production cost of RFID tags, especially the cost of printing RFID tag antennas. Printing the antennas is the most critical part of producing an RFID tag. The high production cost problem of printing RFID tag antennas can be eliminated if the conventional screen printing process can be applied to perform the printing tasks effectively. According to literatures, screen printing technology can be used for RFID tag printing, providing significant time and cost savings compared to traditional etching technology. Therefore, there is a great need to investigate the possibility of applying screen printing method to print RFID tag antennas to perform the task of automatic identification and data capture.

RFID systems provide an automatic means to identify physical objects without the need for line-of-sight communication. The main components of a RFID system are tags, readers, and host computer as shown in Figure 1. RFID tags are attached to physical objects as a means to identify them. RFID readers convert the radio waves sent from the tags to get the digital data and send the collected data to the host computer. RFID tags used in supply chain carry a unique serial number called Electronic Product Code (EPC). [Nikitin, Rao, Lam, Pillai, Martinez, & Heinrich, September 2005]. Passive RFID tags are attached to objects and the RFID tags contain an identification code (ID). EPC-compliant tags used in the supply chain are programmed with an ID called as electronic product code (EPC). EPC generally consists of a unique identifier, a cyclic redundancy check, and a short password [Auto-ID center, November 14, 2004]. Physically, a passive RFID tag is composed of a chip, an antenna on top of a substrate, and may contain a label (adhesive paper for attaching to the product). Figure 2 shows the components of a sample passive UHF RFID tag.

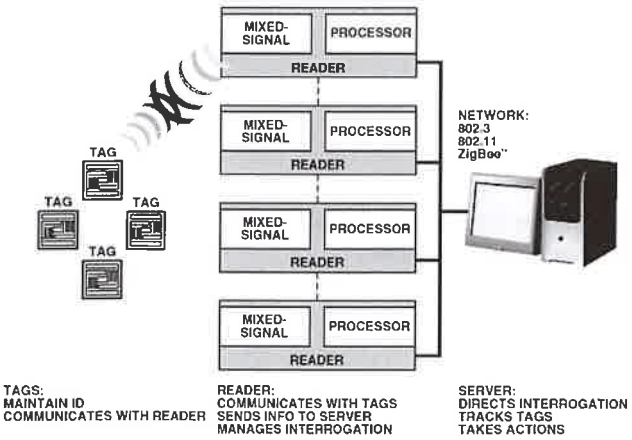

Figure 1:
The main components of a RFID system [ref. Katz et al.]

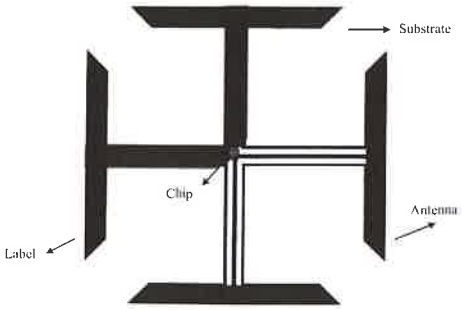

Figure 2: Sample passive RFID tag

2. Objectives

The study used screen printing method with a silver-based conductive ink (Ag) to print REFID tag antennas on three most commonly used substrates for RFID tags in Taiwan's packaging industry. The three substrates were PET, coated paper, and wet strength paper. An Ultra High Frequency (UHF, 902 - 928 MHz) antenna was used for the experiment; the reader is an Impinj Speedway provided by a major RFID tag testing center in Taipei.

The study was an experimental research in nature and aimed to investigate how "the distance between the reader and the RFID tags (reading distance, d)", "reading angle between the reader and the tags (reading angle, θ)", "numbers of tags per unit space (tag number)", and "tag moving speed (tag speed)" influence the performance of the RFID tag antennas. The four variables were chosen based on the request of a local major RFID tag printer in Taipei. The printer suspected that the four variables were the dominant factors influencing their tag antenna performance according to their experience. The operational definition of RFID "tag antenna performance" in this research is *the percentage of being read* (read rate) and *the number of times of being read per second* (read times) of the tags by the reader.

This research was funded by the National Science Council (NSC) of Taiwan (NSC 94 - 2622 - E - 144 - 001 - CC3) in the year of 2006. The purposes of the study were: 1). to identify significant factors mentioned above that influence the performance of RFID tags, 2). to study how those significant factors affect the performance of RFID tags, 3). to establish the optimum combinations of the four variables to achieve the maximum performance of tag antennas, and 4). to compare the tag antenna performance for the three substrates being printed (PET, coated paper, and wet strength paper).

3. Methods

This experimental study utilized a randomized 2^4 factorial design in which every factor was run at two specified levels (1 = high level, - 1 = low level, fixed effects). The factorial levels were determined based upon the practical operating conditions using screening printing method to print RFID tag antennas with Ag ink at a major RFID tag manufacturer and testing center in Taiwan.

The two levels of the factor "reading angle (X_1)" are 0 degree and 67.5 degree; 0 m/sec. and 0.5 m/sec. for the "tag speed (X_2)"; 1 m and 4 m for the "reading distance (X_3)", and. 1/m^2 and 71/m^2 for the "tag number (X_4)". This resulted in a total of sixteen treatment combinations for the experiment, and the run order for the sixteen treatment combinations was randomly determined by computer (randomized design) to reduce possible biases introduced by unplanned changes in the experiment. Each printed tag was imbedded with a chip and was then read ten times for each of the sixteen combinations, and the experiment was replicated five times, therefore, a total of 800 (10 x 16 x 5) readings were collected for each of the three substrates. The data was recorded and analyzed using Minitab 14.0 and SPSS 14.0 statistical software package.

3.1 Variables of the study

There is a great variety of variables affecting RFID tag antenna performance. It is not possible to study all the variables at the same time. One delimitation of this study was that only those variables suspected of significantly affecting RFID tag antenna performance were investigated (experimental variables), and those variables controlled in everyday practice were held constant. The independent variables of the study are "the distance between the reader and the RFID tags (reading distance, D)", "reading angle between the reader and the tags (reading angle, θ)", "numbers of tags per unit space (tag number)", and "tag moving speed (tag speed)". The dependent variables were the percentage of being read and the number of times of being read per second of the tags by the reader. In addition, there were three types of substrates being printed using screen printing process; they were PET, coated paper, and wet strength paper.

3.2 Experimental design

Table I depicts the 2^4 factorial design which includes sixteen treatment combinations. The run order of the sixteen treatment combinations was randomly determined by computer (randomized fixed-effect design) to reduce possible biases introduced by unplanned changes in the experiment.

Table I: 2^4 factorial design of the sixteen combinations

Treatment Combination		0m/sec tag motion (-1)		0.5m/sec tag motion (1)	
		1m reading distance (-1)	4m reading distance (1)	1m reading distance (-1)	4m reading distance (1)
0 degree reading angle (-1)	1/m^2 tag number (-1)	(-1, -1, -1, -1)	(-1, -1, 1, -1)	(-1, 1, -1, -1)	(-1, 1, 1, -1)
	71/m^2 tag number (1)	(-1, -1, -1, 1)	(-1, -1, 1, 1)	(-1, 1, -1, 1)	(-1, 1, 1, 1)
67.5 degree reading angle (1)	1/m^2 tag number (-1)	(1, -1, -1, -1)	(1, -1, 1, -1)	(1, 1, -1, -1)	(1, 1, 1, -1)
	71/m^2 tag number (1)	(1, -1, -1, 1)	(1, -1, 1, 1)	(1, 1, -1, 1)	(1, 1, 1, 1)

Factors	Factor Level	
	-1	+1
reading angle (X_1)	0 degree	67.5 degree
tag motion (X_2)	0 m/sec	0.5 m/sec
reading distance (X_3)	1 m	4 m
tag number (X_4)	1/m^2	71/m^2

3.3. Experimental process and data collection

A single color test form for the tag antenna was designed for this study (shown in Figure 3). The antenna was designed for the frequency of UHF (902 - 928 MHz) RFID tags. Each of the tag antennas was printed with silver-based ink using screen printing ink. A chip, as shown in Figure 3, was then imbedded into every tag antenna printed with Ag ink. A total of fifty tags was printed with imbedded chips, and then they were randomly selected for tag performance test by an Impinj Speedway reader using the parameters of sixteen combinations shown in Table I to determine what the significant factors affecting the tag performance are in terms of percentage of being read (read rate) and number of times of being read per second (read times) of the tag antennas. The tag performance test was conducted in "free-air" environment which means that there was no presence of a material that changes the characteristics of the antennas. To improve the reliability and validity of the experiment, the same experiment was replicated five times in the same day.

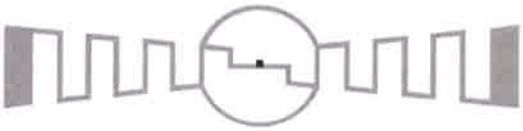

Figure 3: Impinj Single Antenna

The side view, top view, front view of the testing environment arrangement as well as the testing parameters is displayed in Figure 4, 5, 6 respectively. If the tag located in the center is being read by the reader, we call it a good one, and its actual number of times being read per second would be recorded. If the center tag is not being read, its number of times being read is recorded as zero.

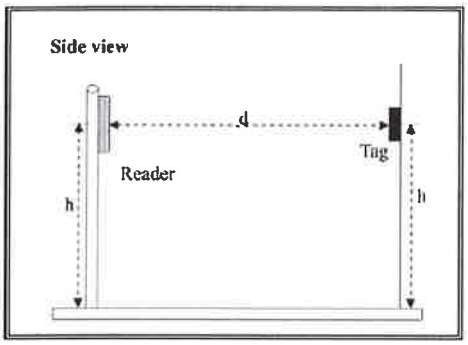

Reader = Impinj Speedway
Reader Antenna Type = CP
Reader Output Power = 1 W
d = 1 m, 4 m
h = 130 cm (held constant)

Figure 4: Side view of the testing arrangement

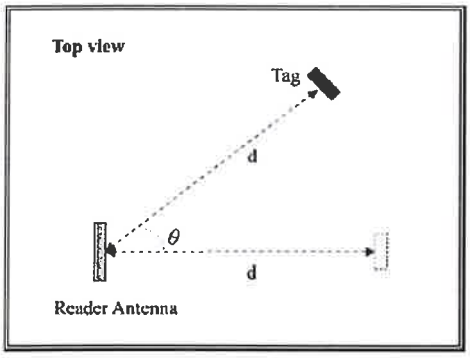

Reader = Impinj Speedway
Reader Antenna Type = CP
Reader Output Power = 1 W
d = 1 m, 4 m
θ = 0°, 67.5°
h = 130 cm (held constant)

Figure 5: Top view of the testing arrangement

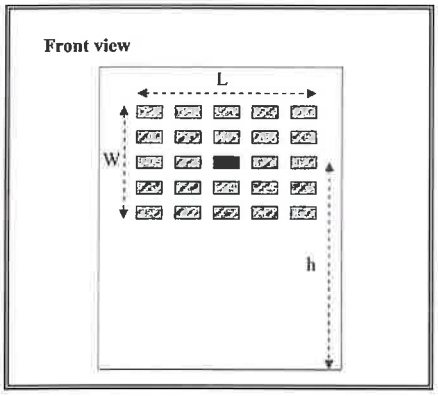

Reader = Impinj Speedway
Reader Antenna Type = CP
Reader Output Power = 1 W
L = 70 cm
W = 40 cm
θ = 0°, 67.5°
h = 130 cm (held constant)
NOTE: If the tag located in the center is being read, we call it a good one

Figure 6: Front view of the testing arrangement

4. Results and discussion

This section reports the results and findings gained through analyses of the experimental data. The software packages employed to analyze the data were SPSS 14.0 and Minitab 14.0.

4.1 Basic Statistics

All of the factors and their levels, the sixteen treatment combinations and their run orders, and the average antenna performance (denoted as $\overline{Y}$), in terms of *the percentage of being read* (read rate) and *the number of times of being read per second* (read times) of the tags by the reader, are listed in Table II.

Table II: Treatment combinations and their tag performance on the three substrates

Items	Factor				Treatment Combinations	Run Order (Random)	PET substrates		coated paper		wet strength paper	
	A Angle	B Speed	C Distance	D Number			% of being read per second ($\overline{Y}$); Read Rate	No. of times of being read per second ($\overline{Y}$); Read Times	% of being read per second ($\overline{Y}$); Read Rate	No. of times of being read per second ($\overline{Y}$); Read Times	% of being read per second ($\overline{Y}$); Read Rate	No. of times of being read per second ($\overline{Y}$); Read Times
1	-	-	-	-	(1)	6	1.00	93.5	1.00	95.7	1.00	96.0
2	+	-	-	-	a	3	1.00	65.4	1.00	48.9	1.00	22.8
3	-	+	-	-	b	8	1.00	19.0	1.00	17.8	1.00	20.0
4	+	+	-	-	ab	5	0.76	14.1	0.46	8.2	0.36	7.0
5	-	-	+	-	c	9	1.00	74.2	0.00	0.0	0.54	1.0
6	+	-	+	-	ac	2	0.14	1.2	0.00	0.0	0.00	0.0
7	-	+	+	-	bc	7	0.86	16.7	0.00	0.0	0.00	0.0
8	+	+	+	-	abc	14	0.00	0.0	0.00	0.0	0.00	0.0
9	-	-	-	+	d	16	1.00	43.9	1.00	42.2	1.00	49.2
10	+	-	-	+	ad	11	1.00	39.0	0.00	0.0	1.00	41.7
11	-	+	-	+	bd	1	1.00	9.2	1.00	9.9	1.00	10.0
12	+	+	-	+	cd	15	0.86	5.8	0.14	0.8	0.58	5.8
13	-	-	+	+	abd	13	0.00	0.0	0.00	0.0	0.00	0.0
14	+	-	+	+	acd	4	0.00	0.0	0.00	0.0	0.00	0.0
15	-	+	+	+	bcd	12	0.00	0.0	0.00	0.0	0.00	0.0
16	+	+	+	+	abcd	10	0.00	0.0	0.00	0.0	0.00	0.0

Factor	Factor Level	
	-	+
A: reading angle (θ, X_1)	0 degree	67.5 degree
B: tag speed (X_2)	0 m/sec	0.5 m/sec
C: reading distance (d, X_3)	1 m	4 m
D: tag number (X_4)	$1/m^2$	$71/m^2$

4.2 Determining the important effects

This section discusses the results of the ANOVA and Factorial and Regression analyses for the main effects of the four independent variables and their interaction effects on the dependent variables (tag performance). It is important to note that the significant level was set at .05 for all the analyses, i.e., $\alpha = .05$. The full model derived from 2^4 the factorial design is:

$$\hat{Y} = \alpha+\beta_1X_1 +\beta_2X_2 +\beta_3X_3 +\beta_4X_4+\beta_5X_1X_2 +\beta_6X_1X_3 +\beta_7X_1X_4 +\beta_8X_2X_3 +\beta_9X_2X_4 +\beta_{10}X_3X_4 +\beta_{11}X_1X_2X_3 + \beta_{12}X_1X_2X_4 + \beta_{13}X_1X_3X_4 + \beta_{14}X_2X_3X_4 + \beta_{15}X_1X_2X_3X_4 + \varepsilon, \quad (1)$$

Where X_1 = reading angle; X_2 = tag speed; X_3 = reading distance; X_4 = tag number.

The general hypothesis for testing whether the main effects and interaction effects are significant is stated as follow:
Ho: $\beta_i = 0$, Ha: $\beta_i \neq 0$; where i = 1, 2, 3, ...14, 15

Discussion in PET substrate

The summary of the ANOVA and Factorial analyses for the main and interaction effects on tag performance for PET substrate is exhibited in Table 3. The Pareto chart of the standardized effects is displayed in Figure 7 and the cube plot of the sixteen treatment combinations is exhibited in Figure 8.

As shown in Table 3 and Figure 7, the negative effect (-31.54) of "tag speed" (X_2) had the greatest impact on the antenna performance (read times) among the four main factors, followed by the "reading distance" (X_3) with an effect of -24.71, "tag number" (X_4) with an effect of -23.25, and "reading angle" (X_1) with an effect of -16.34. Other significant effects on the tag performance include all the two-way, three-way, and four-way interaction effects except the X_2X_3 (tag speed and reading distance interaction) and $X_2X_3X_4$ (tag speed x reading distance x tag number interaction).

In Figure 8, two cube plots are exhibited; the number on each of the eight corners of the cube represents the average number of times of being read of the tags per second by the reader. The cube plot, therefore, displays the relationships among four factors for two-level factorial at a glance. As shown in Figure 8, the treatment combination to achieve the maximum number of read times for PET is (X_1, X_2, X_3, X_4) = (-1, -1, -1, -1); i.e., when the reading angle is set at 0 degree, the tag speed is set at still, the reading distance between tags and the reader is kept 1 meter, and only one tag was present in the reader's field, the estimated maximum number of read times could be 93.38. The adjusted R^2 value (98.60%) in Table III implies that the significant variables (regression model of *Equation. 2*) collectively explain approximately 98.60% of the total variability in read times.

$$\hat{Y}_{PET} = 23.86 - 8.17X_1 - 15.77X_2 - 12.35X_3 - 11.63X_4 + 5.05X_1X_2 - 3.03X_1X_3 + 7.15X_1X_4 + 8.43X_2X_3 + 7.28X_2X_4 + 1.99X_1X_2X_3 - 4.86X_1X_2X_4 + 4.05X_1X_3X_4 - 2.17X_1X_2X_3X_4 \quad (2)$$

Table III: ANOVA and Factorial Analysis summary for PET

Sig. Level	Significant Effects (listed by the order of significance)	Best Treatment Combinations	Estimated Max. Number of Times of Being Read Per Second	R^2 (adj.)
$\alpha = 0.05$	X_2 = -31.54 X_3 = -24.71 X_4 = -23.25 X_2X_3 = 16.86 X_1 = -16.34 X_2X_4 = 14.55 X_1X_4 = 14.30 X_1X_2 = 10.09 $X_1X_2X_4$ = -9.72 $X_1X_3X_4$ = 8.11 X_1X_3 = -6.07 $X_1X_2X_3X_4$ = -4.35 $X_1X_2X_3$ = 3.98	X_1 (reading angle) = 0degree X_2 (tag speed) = 0m/ses X_3 (reading distance) = 1m X_4 (tag number) = 1/m^2 (-1, -1, -1, -1)	93.38	98.60%

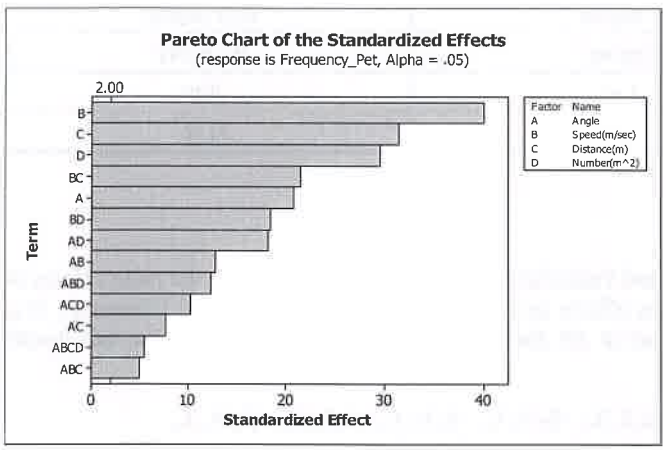

Figure 7: Pareto chart of the standardized effects for PET

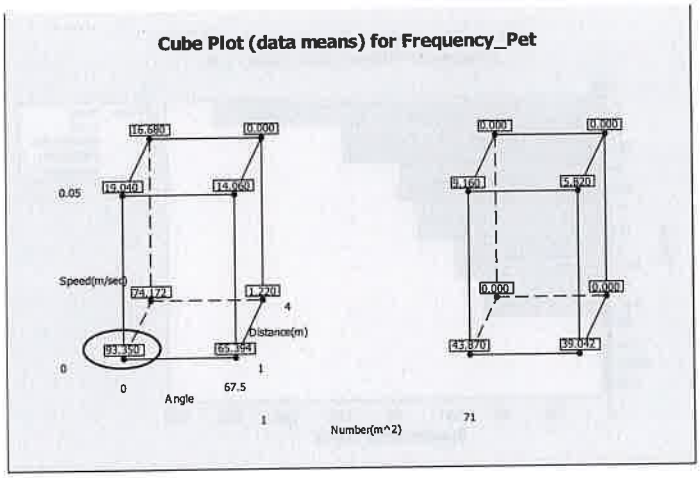

Figure 8: Cube plot of the sixteen treatment combinations for PET

Discussion in coated paper

The summary of the ANOVA and Factorial analyses for the main and interaction effects on tag performance for coated paper is exhibited in Table 4. The Pareto chart of the standardized effects is displayed in Figure 9 and the cube plot of the sixteen treatment combinations is exhibited in Figure 10.

As shown in Table IV and Figure 9, the negative effect (-27.95) of "reading distance" (X_3) had the greatest impact on the antenna performance (read times) among the four main factors, followed by the "tag speed" (X_2) with an effect of -18.76, "tag number" (X_4) with an effect of -14.72, and "reading angle" (X_1) with an effect of -13.47. Other significant effects on the tag performance include all the two-way, three-way, and four-way interaction effects.

The cube plot in Figure 10 displays the relationships among four factors for two-level factorial at a glance. As shown in Figure 10, the treatment combination to achieve the maximum number of read times for coated paper is $(X_1, X_2, X_3, X_4) = (-1, -1, -1, -1)$; i.e., when the reading angle is set at 0 degree, the tag speed is set at still, the reading distance between tags and the reader is kept 1 meter, and only one tag was present in the reader's field, the estimated maximum number of read times could be 95.69. The adjusted R^2 value (99.89%) in Table 4 implies that all the significant variables (shown in *Equation. 3*) collectively explain approximately 99.89% of the total variability in read times.

$$\hat{Y}_{Coat} = 13.98 - 6.84X_1 - 9.38X_2 - 13.98X_3 - 7.36X_4 + 4.39X_1X_2 + 6.74X_1X_3 + 0.31X_1X_4 + 9.38X_2X_3 + 5.44X_2X_4 + 7.36X_3X_4 - 4.39X_1X_2X_3 - 0.26X_1X_2X_4 - 0.31X_1X_3X_4 - 5.44X_2X_3X_4 + 0.26X_1X_2X_3X_4 \quad (3)$$

Table IV: ANOVA and Factorial Analysis summary for coated paper

Sig. Level	Significant Effects (listed by the order of significance)	Best Treatment Combinations	Estimated Max. Number of Times of Being Read Per Second	R^2 (adj.)
$\alpha = 0.05$	$X_3 = -27.95$ $X_2 = -18.76$ $X_2X_3 = 18.76$ $X_4 = -14.72$ $X_3X_4 = 14.72$ $X_1 = -13.47$ $X_1X_3 = 13.47$ $X_2X_4 = 10.87$ $X_2X_3X_4 = -10.87$ $X_1X_2 = 8.79$ $X_1X_2X_3 = -8.79$ $X_1X_4 = 0.63$ $X_1X_3X_4 = -0.63$ $X_1X_2X_3X_4 = 0.51$ $X_1X_2X_4 = -0.51$	X_1 (reading angle) = 0degree X_2 (tag speed) = 0m/ses X_3 (reading distance) = 1m X_4 (tag number) = $1/m^2$ (-1, -1, -1, -1)	95.69	99.89%

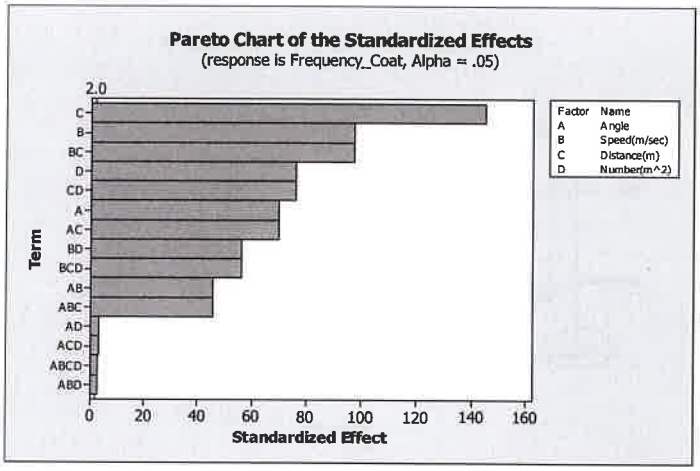

Figure 9: Pareto chart of the standardized effects for coated paper

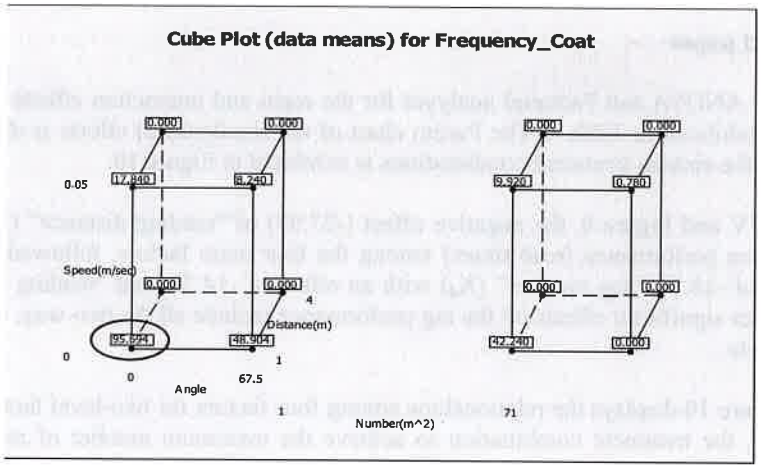

Figure 10: Cube plot of the sixteen treatment combinations for coated paper

Discussion in wet strength paper

The summary of the ANOVA and Factorial analyses for the main and interaction effects on tag performance for wet strength paper is exhibited in Table V. The Pareto chart of the standardized effects is displayed in Figure 11 and the cube plot of the sixteen treatment combinations is exhibited in Figure 12.

As shown in Table V and Figure 11, the negative effect (-31.44) of "reading distance" (X_3) had the greatest impact on the antenna performance (read times) among the four main factors, followed by the "tag speed" (X_2) with an effect of -20.97, "reading angle" (X_1) with an effect of -12.37, and "tag number" (X_4) with an effect of -5.02. Other significant effects on the tag performance include all the two-way, three-way, and four-way interaction effects.

The cube plot in Figure 12 tells that the best treatment combination to achieve the maximum number of read times for wet strength paper is (X1, X2, X3, X4) = (-1, -1, -1, -1); i.e., when the reading angle is set at 0 degree, the tag speed is set at still, the reading distance between tags and the reader is kept 1 meter, and only one tag was present in the reader's field, the estimated maximum number of read times could be 95.99. The adjusted R^2 value (99.90%) in Table V implies that all the significant variables (shown in *Equation 4*) collectively explain approximately 99.90% of the total variability in read times.

$$\hat{Y}_{_Wet} = 15.84 - 6.18X_1 - 10.49X_2 - 15.72X_3 - 2.51X_4 + 4.03X_1X_2 + 6.06X_1X_3 + 4.71X_1X_4 + 10.36X_2X_3 + 1.11X_2X_4 + 2.39X_3X_4 - 3.90X_1X_2X_3 - 3.62X_1X_2X_4 - 4.59X_1X_3X_4 - 0.98X_2X_3X_4 + 3.50X_1X_2X_3X_4 \quad (4)$$

Table V: ANOVA and Factorial Analysis summary for wet strength paper

Sig. Level	Significant Effects (listed by the order of significance)	Best Treatment Combinations	Estimated Max. Number of Times of Being Read Per Second	R^2 (adj.)
$\alpha = 0.05$	$X_3 = -31.44$ $X_2 = -20.97$ $X_2X_3 = 20.72$ $X_1 = -12.37$ $X_1X_3 = 12.12$ $X_1X_4 = 9.43$ $X_1X_3X_4 = -9.18$ $X_1X_2 = 8.05$ $X_1X_2X_3 = -7.81$ $X_1X_2X_4 = -7.24$ $X_1X_2X_3X_4 = 6.99$ $X_4 = -5.02$ $X_3X_4 = 4.77$ $X_2X_4 = 2.22$ $X_2X_3X_4 = -1.97$	X_1 (reading angle) = 0degree X_2 (tag speed) = 0m/ses X_3 (reading distance) = 1m X_4 (tag number) = $1/m^2$ (-1, -1, -1, -1)	95.99	99.90%

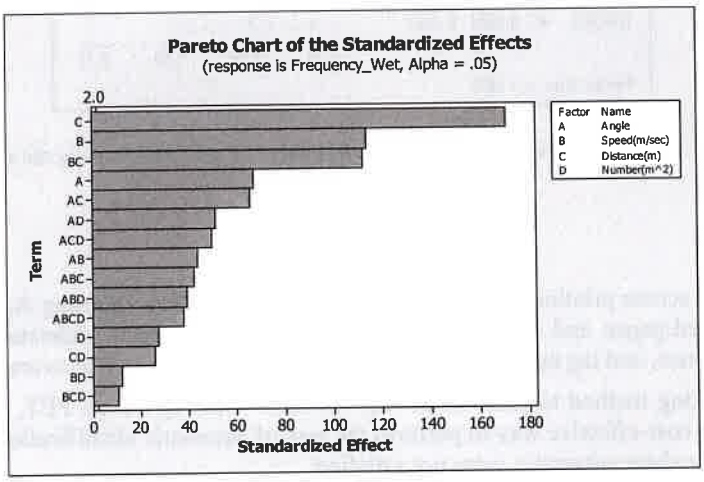

Figure 11: Pareto chart of the standardized effects for wet strength paper

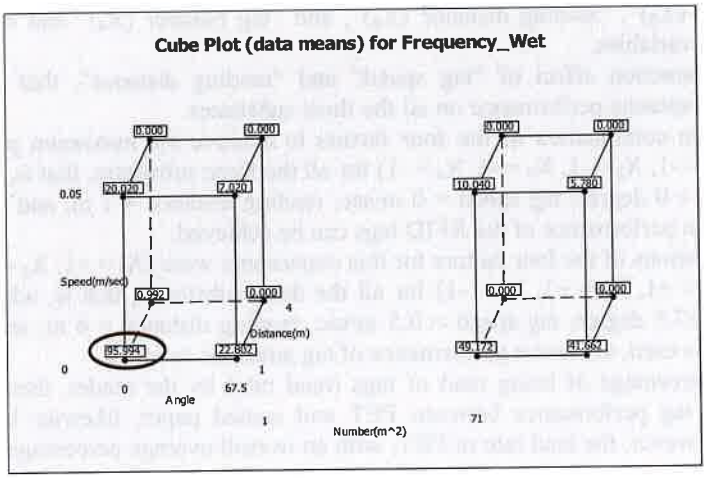

Figure 12: Cube plot of the sixteen treatment combinations for wet strength paper

4.3 Comparisons in read rates among PET, coated paper, and wet strength paper

A one-way ANOVA analysis was conducted to test whether there existed significant differences in the tag performance (*the percentage of being read per second of the tags by the reader, i.e., read rate*) among the three substrates, PET, coated paper, and wet strength paper. The result, as shown in the top part of Figure 13,

reveals that there was a significant difference in the tag performance in at least one pair of the substrates (p value < .05). Examining the 95% confidence intervals (95% C.I.) of the average read rates of the three substrates (bottom part of Figure 13), one can conclude that there was a significant difference in the tag performance between PET and coated paper, likewise, between PET and wet strength paper, no significant difference in tag performance was found between coated paper and wet strength paper. In addition, based on the examination the 95% C.I., one can conclude that the read rate of PET was significantly higher than that of coated and wet strength paper. However, the average read rate of PET was merely over 60%, implying there is a room for improvement.

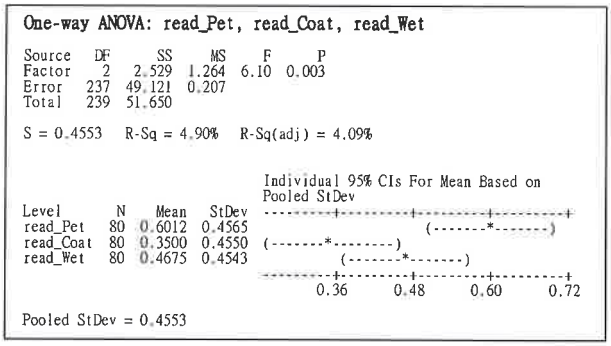

Figure 13: ANOVA analyses to compare the differences in read rates among the substrates

5. Conclusions

The study provides the screen printing industry a practical reference when choosing Ag ink to print RFID tag antennas on PET, coated paper, and wet strength paper, and enables printers understand how reading angle, tag speed, reading distance, and tag numbers affect the antenna performance. The overall results show that:

1. Using screen printing method to print RFID tag antennas with Ag ink on PET, coated paper, and wet strength paper is a cost-effective way to perform the task of automatic identification and data capture, but the read rates of the three substrates were not satisfied.
2. The "tag speed (X_2)" and "reading distance (X_3)" were the most dominant variables affecting the tag antenna performance for all the three substrates, followed by "tag number (X_4)" and "reading angle (X_1).
3. The significant effects on the tag antenna performance included all the main effects of "reading angle (X_1)", "tag speed (X_2)", "reading distance (X_3)", and "tag number (X_4)" and most of the interaction effects of the four variables.
4. The two-way interaction effect of "tag speed" and "reading distance", that is X_2X_3, significantly influenced the tag antenna performance on all the three substrates.
5. The most optimum combination of the four factors to achieve the maximum performance of the tag antennas was ($X_1 = -1$, $X_2 = -1$, $X_3 = -1$, $X_4 = -1$) for all the three substrates, that is, when the combination of "reading angle = 0 degree, tag speed = 0 m/sec, reading distance = 1 m, and tag number = $1/m^2$" is used, the maximum performance of the RFID tags can be achieved.
6. The worse combinations of the four factors for this experiment were ($X_1 = +1$, $X_2 = +1$, $X_3 = +1$, $X_4 = +1$) and ($X_1 = +1$, $X_2 = +1$, $X_3 = +1$, $X_4 = -1$) for all the three substrates, that is, when the combination of "reading angle = 67.5 degree, tag speed = 0.5 m/sec, reading distance = 4 m, and tag number = either $1/m^2$ or $71/m^2$" was used, the worse performance of tag antennas occurred.
7. In terms of the percentage of being read of tags (read rate) by the reader, there existed a significant difference in the tag performance between PET and coated paper, likewise between PET and wet strength paper. However, the read rate of PET, with an overall average percentage of more than 60% for the sixteen combinations, was the best among the three substrates. The tag antennas printed on coated paper yielded the lowest average read rate (35%) among the three substrates.

6. Future Work

Most of the common products used in supply chain have some form of metal or water in them. For example, common products like a bag of chips, dishwashing detergent or toothpaste have some form of metal either in the product or on the packaging. Thus, there is a real need to measure the effects of metal and water on tag

antennas. Questions such as "what is the maximum distance at which a tag is readable in the presence of metal or water is to be measured?", and "Does the presence of metal/water near the tag affect it frequency response?" need to be answered.

The experiments presented in this study was developed using a commercial RFID reader available in the market. There are pros and cons in using a commercial reader. The merit is that one would be able translate all the results directly to real-world. But on the negative side, there are unknown variables with a commercial reader. For example the variation in reader sensitivity is not known for a commercial reader. Also, there is no direct control provided to the end-user for doing a single read attempt. These unknowns in commercial readers are common and these have to be included when interpreting the results. Developing a custom reader would enable us to have more control over all the parameters of the reader and help us in reducing the unknowns.

Also, we have noted that the performance of tags is frequency dependent. Analyzing frequency dependent behavior of tags in detail would enable designing tags that work globally. We have seen that the item tags have more frequency dependent behavior compared to the large tags. A faster way to analyze the frequency dependent performance of tags has to be developed.

Acknowledgement

Sincere appreciation is expressed to the National Science Council of Taiwan who financed this research.

References

[1] Auto-ID center, 860MHz–960MHz Class I Radio Frequency Identification Tag Radio Frequency& Logical Communication Interface Specification Recommended Standard, Version 1.0.0, 14 Nov 2004.

[2] Montgomery, D. C. (1996). *Introduction to Statistical Quality Control (3rd ed)*. John Wiley & Sons, Inc.

[3] Nikitin P., Seshagiri Rao K. V., Lam S., Pillai V., Martinez R. and Heinrich H., Power reflection coefficient analysis for complex impedances in RFID tag design, September 2005

[4] Katz, Ouellette, Gentile and Olivadoti, 2006. Processors Handle Advanced RFID Reader Applications. Analog Dialogue, Volume 40, p. 1

4

Strategic issues in the media industry

Positioning in the printing industry - differentiation in terms of price, lead time, print quality and flexibility

Thomas Mejtoft[1], *Magnus Viström*[2]

[1] STFI-Packforsk/Royal Institute of Technology (KTH)
Järnvägsgatan 3, SE-891 18 Örnsköldsvik, Sweden
E-mail: thomas.mejtoft@stfi.se

[2] STFI-Packforsk/Lund University, Division of Packaging Logistics
Järnvägsgatan 3, SE-891 18 Örnsköldsvik, Sweden
E-mail: magnus.vistrom@stfi.se

Abstract

Differentiation and adding value to the printed product is regarded as important in the low margin, highly competitive commercial printing industry of today. However, there exists a trade-off between the service level and the price the customer has to pay. This quantitative survey study of 136 commercial printing houses sets out to investigate how they are positioning themselves and how they perceive the demand from the customers with respect to *price*, *lead time*, *print quality* and *flexibility*.

In summary the results presented in this paper propose that the commercial printing houses perceived a demand from customers to provide a commodity product with only small differences between price, lead time, quality and flexibility. However, the results also indicate that the printing houses want to sell a more differentiated and customer centric product with focus on flexibility and quality. Although positioning seemed to be independent of printing technology, it was possible to notice that digital printing houses perceived a lower price pressure from the market. These results suggest that using digital printing to enhance customer value was successful since the digital printing houses felt that their customers did not have as high demands for low prices as customers to conventional printing houses.

Keywords

Commercial printing, differentiation, flexibility, strategy

1. Introduction

According to Bunch & Gould (1996, p. 3/1), businesses that seek success have to *"overcome the challenges of very demanding customers seeking high quality, low cost products, responsive to their specific and rapidly changing needs"*. The commercial printing industry is in general considered as a low margin industry, with declining prices, and the competition is regarded as fierce [Birkenshaw, 2004; Smyth, 2006]. Lately, differentiating and adding value to the printed product and becoming a service provider have become widely discussed issues in the printing industry [e.g. PODi, 2003; PODi, 2006; Romano, 2004]. In a production company there exists a trade-off between the level of service and the price the customer has to pay. According to Porter (1996, p. 69), *"positioning trade-offs are pervasive in competition and essential to strategy. They create the need for choice and purposefully limit what a company offers"*. There also exists a trade-off between cost and service/quality [e.g. Brandenburger & Nalebuff, 1996; Herer et al., 2002; Porter, 1980] in a supply chain and Stigler (1939) and Rudberg & Wikner (2004, p. 446) propose that a high level of flexibility can only be achieved at the expense of a higher cost, "*customers have to choose one before the other; low price (productivity) or specific needs (flexibility)*".

To be successful in a changing industry environment, a producing company has to consider the critical success factors - *price*, *quality* and *time* [Blocher et al., 1999; Tan, 1998]. Furthermore companies need flexibility in order to adopt to changing customer needs [Sharifi & Zhang, 1999]. Therefore, the four factors *price, time*, *quality* and *flexibility*, are all important when discussing a supplier-customer relationship. The question is how a company should position itself since there is a trade-off between these factors.

1.1 Research objective

This study sets out to investigate how commercial printing houses are positioning themselves and how they perceive the demand from customers with respect to *price*, *lead time*, *print quality* and *flexibility*. Further this study aims to explore the perceived level of competition in the printing industry.

2. Theoretical framework

The goal of the generic strategies defined by Porter (1980) - *cost leadership*, *product differentiation* and *market focus* is to obtain and sustain competitive advantages. These classic strategies may work well until competitors have copied or outmaneuvered them, which may make them less successful in a dynamic environment [D'Aveni, 1994]. In the theory of competitive strategy, the sustainability of differentiation depends upon continued perceived customer value and the lack of imitation from competitors [Porter, 1985]. However, to be able to continuously deliver value that the customer appreciates, one option is to focus on what Schumpeter (1942/1975, p. 83) refers to as *"creative destruction"*. Collis & Montgomery (1995, p. 124) describes it as *"in a world of continuous change, companies need to maintain pressure constantly at the frontiers - building for the next round of competition"*.

In today's competitive industry environments, it is becoming more difficult to accomplish sustainable competitive advantages [e.g. Dierickx & Cool, 1989; Thomas, 1996; Wiggins & Ruefli, 2005]. The opinions on what strategic path for a company to choose are diversified, and there is no general consensus for how a company should act in order to maintain competitive advantage [Sharifi & Zhang, 1999]. Williams (1994, p. 245) states that *"strategies are inherently self-destructive and thus cannot yield sustainable rents"*. Companies acting in a dynamic business environment have to be agile in spotting new opportunities, developing short cycle strategies and abandoning old cash cows, thus being flexible in meeting customers' current and future needs [e.g. Brown & Eisenhardt, 1998; D'Aveni, 1994; Sanchez, 1995]. According to Narver & Slater (1990) this should be a major goal for companies producing commodity products.

When the general business environment becomes more complex, Evans (1991, p. 85) suggests that *"strategic flexibility is at a premuim [sic] when the rules by which a game gets played are redefined, or when the nature of the game itself changes"*.

2.1 Strategic flexibility and flexibility in production

Strategic flexibility [e.g. Aaker & Mascarenhas, 1984; Evans, 1991; Goldhar et al., 1991; Harrigan, 1985; Johnson et al., 2003; Sanchez, 1995] is a concept with multiple dimensions and can be defined as *"the capability of the firm to proact or respond quickly to changing competitive conditions and thereby develop and/or maintain competitive advantage"* [Hitt et al., 1998, p. 26]. Teece et al. (1997, p. 516) define dynamic capabilities as *"the firm's ability to integrate, build, and reconfigure internal and external competences to address rapidly changing environments"* and this is essential when acting in a dynamic market. Eisenhardt & Martin (2000, p. 1106) suggests that *"dynamic capabilities are necessary, but not sufficient, conditions for competitive advantage"*. The organization and its capabilities are interlinked and Volberda (1996) suggests that being able to have dynamic capabilities is dependent on other factors such as having a flexible organization form.

Two main aspects of strategic flexibility are stressed in the literature - resource deployment and competitive actions [D'Aveni, 1994; Eisenhardt and Martin, 2000; Fombrun and Ginsberg, 1990; Miller et al., 1996; Williams, 1994]. A high flexibility in strategic actions and internal and external capabilities that are dynamic are, as been described, essential for a company that wants (or needs) to act on a dynamic market. However, strategic flexibility has to be put into a context of producing value in a product or service for the company's customers. Sanchez (1995) and Slack (1983) emphasis the importance of flexibility in production, to be able to increase the possibility to produce products that customers really want. Sanchez (1995, p. 143) further suggests that product flexibility is *"more relevant to product competition in dynamic markets"*. This is also stressed by Chang (1993) who proposes that flexibility in manufacturing is a way of protecting the company against uncertainty in future market conditions and fluctuations in customers' taste. The importance of flexibility in manufacturing can be exemplified in the success of the Sony Walkman in the 1980s. Sony created a system to support small design and technological changes, making it possible to launch a large

variety of different products in rapid succession. This was possible due to understanding customers' needs and a *"system of flexible manufacturing so that it could make money on small production runs"* [Sanderson and Uzumeri, 1995, pp. 779].

As has been discussed above, a flexible production to create unique customer solutions is an important ability in becoming a customer-centric company and is an essential part of having high strategic flexibility. However, being able to serve customers to their liking in respect to lead time and product quality is also of great importance.

2.2 Delivery lead times and product quality

Reducing lead times is important in many logistic systems, and is also a source of competitive advantages [e.g. Tan, 1998]. In accordance with Aitken et al. (2002, p. 62), lead time is defined as *"the time taken from a customer raising a request for a product or service until it is delivered"*. Reduced lead time is also an important part of the lean manufacturing approach that derives from the Toyota Production System (TPS) [e.g. Liker, 2004; Liker & Morgan, 2006]. Having short lead times has been deemed as a major order winner and a way of creating short term competitive advantages [Stalk & Webber, 1993].

The quality of a product or service is important in almost every industry [e.g. Normann, 2002], which has been highlighted by the many different concepts that have evolved for improving quality, such as e.g. Total Quality Management (TQM) and ISO9000 [e.g. Conti, 1999; Zhu & Scheuermann, 1999]. Even though these concepts are organization wide and do not in detail guarantee the quality of the end product, they can be used to ensure that high quality business processes have been used. Regarding quality, the most noticeable experience for the end user is the actual product quality, and Cooper (1995) emphasizes the strategic importance of high quality products. Day (1999, p. 173ff.) states that *"boosting quality is now seen as the surest route to creating superior customer value"* and further suggests that high quality is profitable.

When business focus is on the end user, Johansson et al. (1993) suggests that the total customer value can be aggregated as cost, lead time, quality and service. In this paper, the term price will be used instead of cost, since it is the connection between the producing company and the customer that is investigated [e.g. Cooper, 1995]. Also the term flexibility will be used to specify the product flexibility in creating unique services to the customers. Consequently, *lead time*, *quality* and *flexibility* will be regarded in contrast to the trade-off [e.g. Brandenburger & Nalebuff, 1996; Herer et al., 2002; Rudberg & Wikner, 2004] in respect to *price*.

3. Methodology and study design

3.1 Population and sample

This paper is based on a subset of data from a larger survey study of 136 Swedish commercial printing houses carried out during the spring and early fall of 2006. The questionnaire was sent out by letter to 300 companies, which were randomly selected Swedish commercial printing houses from the members' list of the Swedish Graphic Companies' Federation (GFF). It should be noted that this list is not a complete list of all commercial printing houses in Sweden, which limit the possibilities to generalize the results to the whole Swedish commercial printing industry.

An alternative to this list could be e.g. extracted from the telephone directory or a financial information database. However, these other alternatives did not, according to the authors, provide a list with sufficient accuracy. Consequently, the authors believe the list used to be the best directory to constitute the basis for this survey investigation of Swedish printing houses. Although the used list is not complete, it does, according to GFF, include companies covering at least 80% of the volume of invoiced sales of printed commercial products in Sweden [K. Flick, *GFF*, personal communication, January 25, 2007]. Hence, the results should give a good indication of the situation in the Swedish commercial printing industry. CEOs or vice managing directors made up 82% of the respondents. The rest of the respondents were persons responsible for marketing, production or logistics.

The data in the study has been separated and analyzed in different categories depending on the printing technology used at each company (Table I). The categories used were: *all printing houses*, *printing houses with digital printing* and *printing houses with only conventional printing*. The other categories *printing houses*

with only digital printing, *printing houses with both conventional and digital printing* and *printing houses with conventional printing* were also analyzed, but without any interesting results. For a printing house to be regarded as using a specific printing technology in production, it should constitute at least 10% or more of the total production.

Table I: Relative share of printing houses in the survey study according to printing technology used

	Relative share
Digital printers:	39.0% (53)
Only conventional printers:	61.0% (83)
All printers:	100% (136)

3.2 Questionnaire design

The questionnaire was designed to obtain information about the respondents' ranking of *price, lead time, quality* and *flexibility* with respect to how the printing houses perceive the demand from the customers and how they have differentiated their offer. The questionnaire was based on closed questions, with the purpose of measuring opinions. Data was collected using numeric rating scales where the end categories were labeled with appropriate options [Saunders et al., 2003]. Two different scales were used, a 10-point numeric rating scale from 1 to 10 when rating opinions about e.g. perceived pressure. When rating opinions about e.g. differentiation, an 11-point ration scale from - 5 to + 5 (including 0) was used to capture how the companies had chosen to differentiate themselves in relation to, their perceived, market average. However, the companies' ranking of how they had chosen to differentiate themselves does not necessarily reflect on how they actually performed in relation to the market average, because the respondents may have different perceptions about numerical values [Churchill and Brown, 2004]. Furthermore they may tend to set high values when they are evaluating their own performance [Robson, 2002], which was indicated in this study by respondents having a better performance on all factors (besides price) compared to the perceived market average. However, since the purpose was to evaluate the different factors against each other the problem identified by Robson (2002) was not an issue in this case.

All questions were in Swedish, since the questionnaire was completed by Swedish printing houses. To ensure the validity of the questionnaire, an initial pilot testing [Saunders et al., 2003] was performed with three printing houses. Some questions were changed and new questions were formulated according to comments made by the respondents in this pilot test.

3.3 Data collection and analysis

Since this survey was constructed as a self-administrated survey, a covering letter, explaining the survey, was enclosed in the letter to each respondent [Saunders et al., 2003]. The respondents had the choice of responding either by post or through a web interface. The companies that did not respond to the initial survey were reminded by email and/or telephone. While collecting data from the sample, it was found that some of the companies did not meet the research requirements of this study, and they were subsequently omitted. The response rate was calculated, in accordance with the Council of American Survey Research Organizations [CASRO, 1982; Wiseman & Billington, 1984] as:

$$\text{Total response rate} = \frac{\text{Total number of responses}}{\text{Total number in sample} - \text{Ineligible}}$$

Out of a total of 300 companies, 46 were found to be ineligible and 136 eligible companies responded, which constituted a total response rate of 54%. Out of all companies, only six were not possible to reach by personal communication (i.e. telephone or email), implying that practically all ineligible companies in the sample have been identified. The reason for having so many ineligible companies (46) was that the database contained some companies that did not currently own any printing equipment, but were interested in the commercial printing business. In most cases they were working with activities closely related to this business, such as prepress or finishing.

About half of the answering respondents posted their answers without any reminder, whereas the other half sent their response after being given a reminder. According to Armstrong & Overton (1977) people who

respond late are assumed to be comparable with non respondents. In general, no major differences between the two groups were found, thus giving an indication of no significant differences between respondents and non-respondents.

The sample (136 companies) was large (> 30) and approximately normally distributed [Keller, 2005], whereby the t-distribution was used to calculate confidence intervals and p-values. Since the sample also covered a large portion of the studied population (428 companies) a Finite Population Correction Factor (FPCF) was used when calculating the standard deviations for the mean values [e.g. Andersson et al., 2002, p. 257; Keller, 2005, p. 399].

$$FPCF = \sqrt{\frac{N-n}{N-1}} \qquad \begin{array}{l} N = \text{Population size} \\ n = \text{Sample size} \end{array}$$

The significance between different categories in the dataset has been analyzed using an independent sample t-test using a 95% confidence level. The significance of differences between the factors price, lead time, quality and flexibility were determined using a paired sample t-test. Since six comparisons had to be made to find possible significance between the four mean values, the confidence level was adjusted using the Bonferroni adjustment method [e.g. Keller, 2005]. The Bonferroni adjustment stated the confidence level to be set to 99.17% for each t-test, in order to avoid Type I errors (falsely get a significant difference) and implied a 95% confidence level in total. However, using the Bonferroni adjustment might increase the risk for Type II errors (not observing a significant difference) [Keller, 2005]. Due to this, the p-values for factors not showing any significant differences were also investigated without the Bonferroni correction, and in this case none showed any significant difference either. Further the correlation between the fraction of digital printing used in a company against perceived market competition and perceived price pressure was tested. SPSS 15 and Microsoft Excel 2003 were used for the statistical analysis.

A survey study typically gives a good overview over a large population (e.g. an industry), while it is more difficult to get a deeper understanding of specific research questions. To get deeper understanding it is preferable to use in-depth case studies of a few selected companies. However, since the aim of this study was to investigate the positioning of the commercial printing industry, the use of a survey should be regarded as the preferable method. As mentioned earlier, the aim of this survey was to capture opinions of the respondents. Peoples' opinions are, however, always subjective and do not necessarily correspond to reality, which is a limitation of any study concerning the capture of opinions.

4. Results and discussion

In this chapter the results from the survey study will be presented along with a discussion of the interesting results.

4.1 Positioning of printing houses

The printing houses have differentiated their business towards service related factors, such as having a high level of flexibility, good print quality and short lead times (Figure 1). Thus they have primarily focused on giving their customers a high level of service and enhancing customer satisfaction. This increased level of service has been accomplished at the expense of higher prices to their customers [e.g. Brandenburger & Nalebuff, 1996; Herer et al., 2002; Rudberg & Wikner, 2004]. Previous research shows that dynamic strategies and a focus on delivering a high customer value are important to be successful, especially in the digital printing industry [Mejtoft, 2007]. However, it should be noted that there were no significant differences (Table II) at the 95% confidence level between companies with and without digital printing in their positioning with respect to flexibility, which is the factor ranked the highest by the printing houses in this study (Figure 1). Neither was there any difference regarding the other factors, which means that their positions on the market, in respect to these factors, are quite similar.

It should be noted that there were no differences in position for lead times between digital and conventional printers. This is interesting since fast deliveries are something that many digital printing houses regard as important for their business. Further, as can be noted in Table II, the difference in position regarding quality was very close to showing significance at a 95% confidence level. This result illustrates that digital printing houses tended to regard their own position in quality lower than the conventional printing houses. This result

was expected because the print quality of conventional printing technology (in this case mostly offset) is today generally regarded as a "norm".

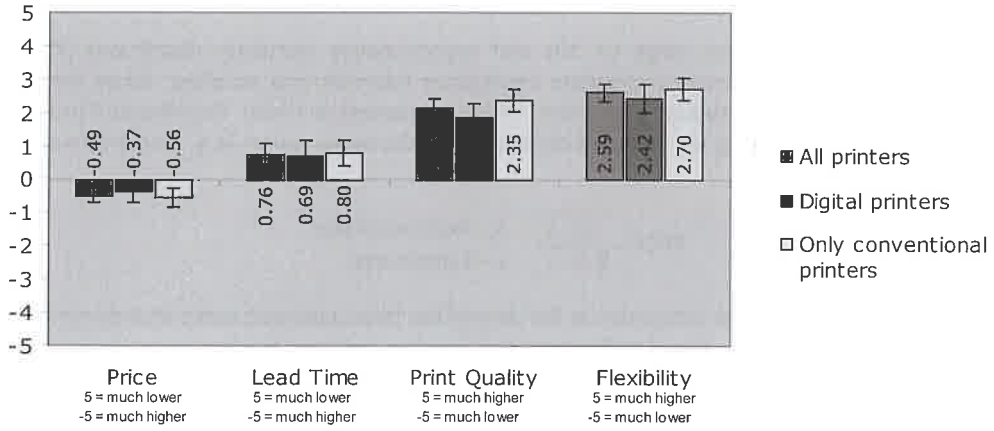

Figure 1: Positioning of the printing houses compared to the industry in general (mean values with a 95% confidence interval)

Table II: Significance of differences between digital printers and only conventional printers in respect to position

	Price	Time	Quality	Flexibility
Mean difference:	0.196	-0.113	-0.527	-0.277
t:	0.855	-0.363	-1.963	-1.031
Degrees of freedom:	132	132	132	130
Significance (2-tailed):	.394	.717	.052	.304

There are no significant differences between means at a 95% confidence level

4.2 Perceived market demand and market competition

It is possible to notice a quite clear difference in how commercial printers have positioned themselves (Figure 1) compared to how they perceive market demand (Figure 2).

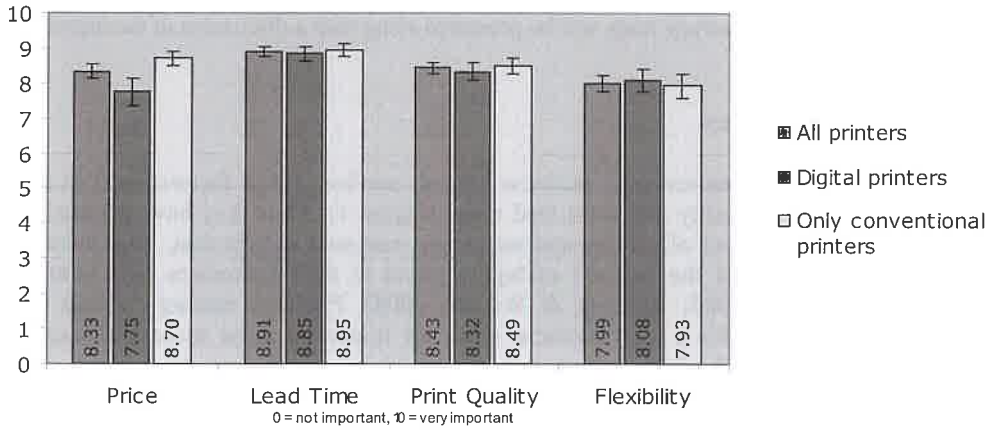

Figure 2: Perceived demand from the market (mean values with a 95% confidence interval)

The printing houses believed that the foremost demand from customers was short lead times, while low prices and high print quality were only second to short lead times. The printing houses have deemed it important to position for a high level of flexibility (Figure 1) even though they do not feel that this is a major demand from their customers (Figure 2). Flexibility was, when investigating all printers, subordinate to both lead time, print quality and for only conventional printers also price. Having a high level of flexibility has been considered

important when acting in any highly dynamic market [e.g. Brown & Eisenhardt, 1998; D'Aveni, 1994; Sanchez, 1995]. However, the results indicate that the printing houses perceived that their customers are demanding a commodity product.

High flexibility and quality are factors that should enhance the possibility to create a high level of customer satisfaction. The printing houses, in general, are differentiating themselves by providing a high level of service to the customer, which can be a way to escape the commoditization of the printed product [e.g. D'Aveni, 1994; Porter, 1985].

Table III: Significance of differences between digital printers and only conventional printers in respect to perceived demand from customers

	Price#	Time	Quality	Flexibility
Mean difference:	-0.944	-0.103	-0.173	0.149
t:	-4.216	-0.757	-0.955	0.610
Degrees of freedom:	87	134	134	133
Significance (2-tailed):	.000*	.451	.342	.543

* Significant difference between means at a 95% confidence level
\# Based on unequal variance of means, all other calculations based on equal variance

An interesting result from this study is how the different respondents believed that their customers valued the price factor. There was a significant difference (Table III) between the pressure digital printing houses and conventional printing houses perceived from their customers regarding the pricing of their products. Printing houses that had digital printing felt a lower price pressure than those without digital printing. This result suggests that differentiating towards a higher level of customer service when using digital printing to add value to the products is a successful concept. These printing houses feel that their customers did not have as high demands for low prices as the customers to conventional printing houses.

The market competition in the commercial printing industry has in general been deemed as fierce [Birkenshaw, 2004; Smyth, 2006]. This statement is further strengthened by the results from this study, where the printing houses have regarded the market competition as very high (Figure 3).

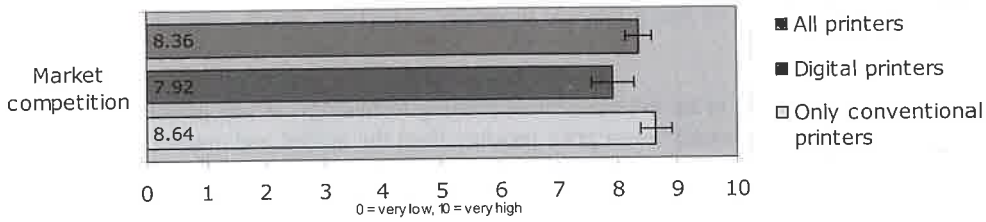

Figure 3: Perceived market competition (mean values with a 95% confidence interval)

Even though both digital printing and conventional printing houses regard the market competition as high, it is possible to notice a significant difference between the two categories. Companies that use digital printing perceived a significantly lower competitive situation on the market than those using only conventional printing technology (Table IV).

Table IV: Significance of differences between digital and only conventional printers in respect to perceived market competition

	Market competition
Mean difference:	-0.715
t:	-3.276
Degrees of freedom:	133
Significance (2-tailed):	.001*

* Significant difference between means at a 95% confidence level

It is also possible to notice a negative medium correlation [in accordance with Cohen, 1977, pp. 79-81] of approximately -.3 between the share of digital printing used in production and the perceived market competition. The same is true for the correlation between the share of digital printing used in production and the perceived demand from customers on providing low prices. Hence, the use of digital printing tends to make the perceived price pressure and market competition lower. This further strengthens the evidence of digital printing having a positive effect, from the printing houses point of view, on the competitive situation and product pricing.

4.3 Strategic positioning

It is easy to argue that to satisfy customers' needs the printing houses should have a focus that is similar to the demand from the market, which is not the case according to the results from this study (cf. Figure 1 and Figure 2). However, the printing industry has a high, or even fierce, level of competition (Figure 3), largely based on price [Birkenshaw, 2004; Smyth, 2006]. This situation does not favor companies active in the industry. However, by shifting focus towards a service oriented organization it should be, in theory, possible to increase the value of the product and accordingly the price. This is what Porter (1980) refers to as having a differentiation approach instead of cost leadership approach or when D'Aveni (1994) discusses to escape the cost-quality area and focus on e.g. timing and know-how. Both the conventional printing houses and the digital printing houses have a similar strategic position (Figure 1). However, it is possible to distinguish in this study that digital printing houses perceived a lower pressure from the market regarding the price and a slightly lower competitive situation. These results indicate that even though the focus is similar, digital printing houses are more successful in their strategic position in having a higher level of service since they can charge a higher price.

5. Conclusions

The positioning regarding price, lead time, print quality and flexibility of the companies and pressure from the market are quite similar regardless of the printing technology used. Previous research [Mejtoft, 2007] has indicated that working closely with customers and being flexible towards their demands, strengthens the possibilities for a successful relationship with their customers and their ability to be competitive. This paper further strengthens this view by illustrating that even though the demand for flexibility is perceived to be significantly lower than e.g. print quality and lead time issues, it is the flexibility that is the differentiating factor that the companies are most intensely focusing on. This result suggests that companies are starting to become aware of the importance of being flexible to satisfy customers' needs, even though customers do not yet value this action.

Although this positioning seemed to be independent of printing technology, it was possible to notice that digital printing houses perceived a significantly lower price pressure from the market and market competition. This result proposes that using digital printing to enhance customer value was successful since these printing houses felt that their customers did not have as high demands for low prices as the customers to conventional printing houses.

Acknowledgements

The authors would like to thank *Ola Karlsson*, *Kaj Flick* and *Hasse Johansson* of the *Swedish Graphic Companies' Federation (GFF)* for valuable input to this survey investigation and sharing their members list. Furthermore, the authors express their gratitude to *the respondents* for their participation in this survey investigation and *Prof. Nils Enlund*, KTH, and *Dr. Marianne Klaman*, STFI-Packforsk for valuable comments regarding this research project. The *Kempe Foundations*, the *EU Structural Fund* and the *industry participants in STFI-Packforsk's DigiPrint project* are gratefully acknowledged for their financial support.

References

[1] Aaker, D. A. and Mascarenhas, B. (1984), *The need for strategic flexibility, Journal of Business Strategy, Vol. 5, No. 2, pp. 74 - 82*

[2] Aitken, J., Christopher, M., Towill, D. (2002), *Understanding, Implementing and Exploiting Agility and Leanness, International Journal of Logistics: Research and Applications, Vol. 5, No. 1, pp. 59 - 74*

[3] Andersson, D. R., Sweeney, D. J. and Williams, T. A. (2002), *Statistics for Business and Economics, South-Western*

[4] Armstrong, J. S., Overton, T. S. (1977), *Estimating Nonresponse Bias in Mail Surveys, Journal of Marketing Research, Vol. 14, No. 3, pp. 396 - 402*

[5] Birkenshaw, J. (2004, Apr.), *The future of print on paper, Prepress and print Technology, Pira International, Retrieved January 26, 2005, from http://pira.atalink.co.uk/pulp-and-paper/163.html*

[6] Blocher, E. J. Chen, K. H. and Lin, T. W. (1999), *Cost Management: A Strategic Emphasis, Irwin/McGraw-Hill*

[7] Brandenburger, A. M. and Nalebuff, B. J. (1996), *Co-opetition, Currency Doubleday*

[8] Brown, S. L. and Eisenhardt, K. M. (1998), *Competing on the edge, Strategy as Structured Chaos, HBS Press*

[9] Bunch, P. and Gould, P. (1996), *From Lean to Agile Manufacturing, IEE Colloquium (Digest), Vol. 278, pp. 3/1 - 3/5*

[10] CASRO (1982), *On the Definition of Response rates, A Special Report of the CASRO Task Force on Completion Rates, Retrieved April 4, 2007, from http://www.casro.org/resprates.cfm*

[11] Chang, M. (1993), *Flexible Manufacturing, Uncertain Consumer Tastes, and Strategic Entry Deterrence, The Journal of Industrial Economics, Vol. 41, No. 1, pp. 77 - 90*

[12] Churchill, G. A. and Brown, T. J. (2004), *Basic Marketing Research, 5e, South-Western*

[13] Cohen, J. (1977), *Statistical Power Analysis for the Behavioral Sciences, Revised Edition, Academic Press*

[14] Collis, D. J. and Montgomery, C. A. (1995, July-Aug.), *Competing on Resources: Strategy in the 1990s, Harvard Business Review, pp. 118 - 128*

[15] Conti, T. (1999), *Vision 2000: positioning the new ISO 9000 standards with respect to quality management models, Total Quality Management, Vol. 10, No. 4 - 5, pp. 454 - 464*

[16] Cooper, R. (1995), *When Lean Enterprises Collide, Competing through Confrontation, HBS Press*

[17] D'Aveni, R. A. (1994), *Hypercompetition - Managing the Dynamics of Strategic Maneuvering, Free Press*

[18] Day, G. S. (1999), *Market Driven Strategy, Processes for Creating Value, Free Press*

[19] Dierickx, I. and Cool, K., (1989), *Asset stock accumulation and sustainability of competitive advantage, Management Science, Vol. 35, No. 12, pp. 1504 - 1511*

[20] Eisenhardt, K. M. and Martin, J. A. (2000), *Dynamic capabilities: what are they? Strategic Management Journal, Vol. 21, pp. 1105 - 1121*

[21] Evans, J. S. (1991), *Strategic flexibility for high technology maneuvers: A conceptual framework, Journal of Management Studies, Vol. 28, No. 1, pp. 69 - 89*

[22] Fombrun, C. J. and Ginsberg, A. (1990), *Shifting gears: Enabling change in corporate aggressiveness, Strategic Management Journal, Vol. 11, No. 4, pp. 297 - 309*

[23] Goldhar, J. D., Jelinek, M. and Schlie, T. W. (1991), *Flexibility and competitive advantage - manufacturing becomes a service business, International Journal of Technology Management, Vol. 6, No. 3/4, pp. 243 - 259*

[24] Harrigan, K. R. (1985), *Strategic Flexibility: A Management Guide for Changing Times, Lexington Books*

[25] Herer, Y. T., Tzur, M. and Yücesan, E. (2002), *Transshipments: An emerging inventory recourse to achieve supply chain leagality, International Journal of Production Economics, Vol. 80, pp. 201 - 212*

[26] Hitt, M. A., Keats, B. W. and DeMarie, S. M. (1998), *Navigating in the new competitive landscape: Building strategic flexibility and competitive advantage in the 21st century, Academy of Management Executive, Vol. 12, No. 4, pp. 22 - 42*

[27] Johansson, H. J., McHugh, P., Pendlebury, A. J. and Wheeler, W. A. (1993), *Business Process Reengineering: Breakpoint Strategies for Market Dominance, Wiley*

[28] Johnson, J. L., Pui-Wan Lee, R., Saini, A. and Grohmann, B. (2003), *Market-Focused Strategic Flexibility: Conceptual Advances and an Integrative Model, Journal of the Academy of Marketing Science, Vol. 31, No. 1, pp. 74 - 89*

[29] Keller, G. (2005), *Statistics for Management and Economics, Seventh Edition, Thomson Brooks/Cole*

[30] Liker, J. K. (2004), *The Toyota Way: 14 Management Principles from the World's Greatest Manufacturer, McGraw-Hill*

[31] Liker, J. K. and Morgan, J. M. (2006), *The Toyota Way in Services: The Case of Lean Production Development, Academy of Management Perspectives, Vol. 20, No. 2, pp. 5 - 20*

[32] Mejtoft, T. (2007), *Creation of Customer Value Using Digital Printing in a Dynamic Business Environment, TAGA Journal, Vol. 3, No. 3, pp. 128 - 143*

[33] Miller, D., Lant, T. K., Milliken F.J. and Korn H. J. (1996), *The Evolution of Strategic Simplicity: Exploring Two Models of Organizational Adaptation, Journal of Management, Vol. 22, No. 6, pp. 863 - 888*

[34] Narver, J. C. and Slater, S. F. (1990), *The effect of a market orientation on business profitability, Journal of Marketing, Vol. 54, No. 4, pp. 20 - 35*

[35] Normann, R. (2002), *Service management, Strategy and Leadership in Service Business, Third Edition, Wiley*

[36] PODi (2003, Jan.), *Best Practices in Digital Printing, Third Edition, Caslon & Company*

[37] PODi (2006), *Best Practices in Digital Print, Sixth Edition, Caslon & Company*

[38] Porter, M. E. (1980), *Competitive Strategy: Techniques for Analyzing Industries and Competitors, Free Press*

[39] Porter, M. E. (1985), *Competitive Advantage: Creating and Sustaining Superior Performance, Free Press*

[40] Porter, M. E. (1996, Nov.-Dec.), *What is Strategy? Harvard Business Review, pp. 61 - 79*

[41] Robson, C. (2002), *Real World Research, Second Edition, Blackwell Publishing*

[42] Romano, F. J. (2004, May 27), *Designing for Digital, Speech presented for the Swedish Graphic Companies' Federation, Stockholm, Sweden*

[43] Rudberg, M. and Wikner, J. (2004), *Mass customization in terms of the customer order decoupling point, Production Planning & Control, Vol. 15, No. 4, pp. 445 - 458*

[44] Sanchez, R. (1995), *Strategic Flexibility in Product Competition, Strategic Management Journal, Vol. 16, pp. 135 - 159*

[45] Sanderson, S. and Uzumeri, M. (1995), *Managing product families: The case of the Sony Walkman, Research Policy Vol. 24, No. 5, pp. 761 - 782*

[46] Saunders, M., Lewis, P. and Thornhill, A. (2003), *Research Methods for Business Students, 3rd Edition, Prentice Hall*

[47] Schumpeter, J. A. (1975), *Capitalism, Socialism and Democracy, Harper Perennial. (Original work published 1942)*

[48] Sharifi, H. and Zhang, Z. (1999), *A methodology for achieving agility in manufacturing organisations: An introduction, International Journal of Production Economics, Vol. 62, pp. 7 - 22*

[49] Slack N. (1983), *The flexibility as a Manufacturing Objective, International Journal of Operations & Production Management Vol. 3, No. 3, pp. 4 - 13*

[50] Smyth, S. (2006), *The Future of European Printing to 2011, Pira International*

[51] Stalk Jr., G. and Webber, A. M. (1993, July-Aug.), *Japan's Dark Side of Time, Harvard Business Review, pp. 93 - 102*

[52] Stigler, G. (1939), *Production and Distribution in the Short Run, The Journal of Political Economy, Vol. 47, No. 3, pp. 305 - 327*

[53] Tan, B. (1998), *Agile Manufacturing and Management of Variability, International Transactions in Operational Research, Vol. 5, No. 5, pp. 375 - 388*

[54] Teece, D. J., Pisano, G. and Shuen A. (1997), *Dynamic Capabilities and Strategic Management, Strategic Management Journal, Vol. 18, No. 7, pp. 509 - 533*

[55] Thomas, L. G. (1996, May-June), *The Two Faces of Competition: Dynamic Resourcefulness and the Hypercompetitive Shift, Organization Science, Vol. 7, No. 3, pp. 221 - 242*

[56] Volberda, H. W. (1996), *Towards the Flexible Form: How to Remain Vital in Hypercompetitive Environments, Organization Science, Vol. 7, No. 4, pp. 359 - 374*

[57] Wiggins, R. R. and Ruefli, T. W. (2005), *Schumpeter's Ghost: Is hypercompetition making the best of times shorter? Strategic Management Journal, Vol. 26, pp. 887 - 911*

[58] Williams, J. R. (1994), *Strategy and the Search for Rents: The Evolution of Diversity among Firms, In Rumelt R. P., Schendel D. E. and Teece D. J. (Eds.), Fundamental Issues in Strategy: A Research Agenda (pp. 229 - 246), HBS Press*

[59] Wiseman, F. and Billington, M. (1984), *Comment on a Standard Definition of Response Rates, Journal of Marketing, Vol. 21, No. 3, pp. 336 - 338*

[60] Zhu Z. and Scheuermann L. (1999), *A comparison of quality programmes: Total quality management and ISO 9000, Total Quality Management, Vol. 10, No. 2, pp. 291 - 297*

Importance of short production runs, variable data printing and web interfaces - a comparison of digital and conventional printing houses

Magnus Vistrom[1], *Thomas Mejtoft*[2]

[1] STFI-Packforsk /Lund University, Division of Packaging Logistics
Järnvägsgatan 3 SE-891 18, Örnsköldsvik
E-mail: magnus.vistrom@stfi.se

[2] STFI-Packforsk /Royal Institute of Technology (KTH)
Järnvägsgatan 3 SE-891 18, Örnsköldsvik
E-mail: thomas.mejtoft@stfi.se

Abstract

In the printing industry overcapacity has resulted in price reductions and decreasing profit margins. These circumstances together with an increasing demand for short production runs have raised challenges for printing houses. In order to be successful, printing houses need to find ways to differentiate themselves. This survey study sets out to investigate: the difference between digital and conventional printers, with respect to (1) the view of the importance of providing short production runs, variable data printing and web interfaces and (2) the difference in usage of web interfaces and in performance of offering short production runs and (3) the performance of offering variable data. The results indicate that digital printers find it more important to provide variable data printing, short production runs and web interfaces compared to conventional printers. Furthermore, digital printers believe they fulfil the need for short production runs better than conventional printers. Hence, their market conditions seem to differ. As a result, digital printers experience a somewhat lower competition. Furthermore, it seems like digital printers to a greater extent need web interfaces in their business. Moreover, short production runs, variable data printing and the usage of web interfaces is expected to increase. Therefore, it seems like the commercial printing industry will experience an even more challenges in the near future, a development that to a greater extent will demand the features that digital printers can more easily provide.

Keywords

Commercial printing, short production runs, variable data, web interfaces

1. Background

In the printing industry overcapacity has resulted in price reductions [Birkenshaw, 2004] and decreasing profit margins. Smyth (2006) argued that profitability in the print market is under huge pressure. These circumstances together with an increasing demand for short production runs bring about many challenges for printing houses. In order to be successful, printing houses need to find ways to differentiate themselves.

The use of a flexible production technology, such as digital printing, gives opportunities for differentiation. Since no printing formes are needed, changeovers between orders are faster and the fixed production costs are considerably lower than with conventional technology. The characteristics of digital printing make it possible to provide every printed copy with a specific design (variable data printing). Hence, it is possible to offer added value that is not possible with conventional printing technology, e.g. by producing personalised advertising material. According to Podi (2006), varying of text, imagery, and design elements is a strategy that is continually being put to use. Documents will serve as a more effective business tool if the information is directed towards the recipient.

As production runs become shorter it gets increasingly important to process orders efficiently. Smyth (2006) argues that the continuing decline in run length of print is advantageous for short run specialists, as long as they can charge accordingly for their services. Handling in particular, needs to be minimised when customers place small orders with low profit contributions. Web applications that offer customers the possibility to order one single printed matter and allow them to customise the content (with text and images) are becoming common.

Hence, web interfaces where customers can place orders directly and specify their printed matters are increasing in importance. Since digital printing is suitable for small production runs it should be beneficial for digital printers to use web interfaces.

On the other hand, drawbacks of digital printing are higher variable costs per printed copy and a lower print speed compared to conventional printing technology. Many companies that have purchased digital printing equipment have actually had a hard time to find suitable applications for their presses. However, the business strategy might have changed for companies that have bought digital presses, since the technology makes it possible to offer value added services. The question is whether the opportunities of digital printing have given these companies a different view on the importance of providing variable data printing, short production runs and web interfaces? Do companies that have purchased digital printing perform differently?

This study sets out to investigate:

- ◊ The difference between digital and conventional printers, with respect to the view of the importance of providing short production runs, variable data printing and web interfaces.
- ◊ The difference in usage of web interfaces and in performance of offering short production runs.
- ◊ The performance of offering variable data.

Hence, this study seeks to contribute to the knowledge concerning the business potential of digital printing.

2. Methodology and study design

Population and sample

This paper is based on a subset of data from a larger survey study of 136 Swedish commercial printing houses carried out during the spring and early fall of 2006. The questionnaire was sent out by letter to 300 companies, which were randomly selected Swedish commercial printing houses from the members' list of the Swedish Graphic Companies' Federation (GFF). It should be noted that this list is not a complete list of all commercial printing houses in Sweden, which limits the possibilities to generalize the results for the whole Swedish commercial printing industry.

An alternative to this list could be e.g. extracted from a telephone directory or a financial information database. However, these two alternatives did not, according to the authors, provide a list with sufficient accuracy. Consequently, the authors believe that the used list is the best directory for constituting the basis of this survey investigation of Swedish printing houses. Although the used list is not complete, it does, according to GFF, include companies covering at least 80% of the volume of invoiced sales of printed commercial products in Sweden [K. Flick, *GFF*, personal communication, January 25, 2007]. Hence, the results should give a good indication of the situation in the Swedish commercial printing industry. CEOs or vice managing directors constituted 82% of the respondents. The rest of the respondents were persons responsible for marketing, production or logistics.

The data in this study has been separated and analyzed in different categories depending on printing technology used at each company. The categories used were - *all printing houses*, *printing houses with digital printing (digital printers)* and *printing houses with only conventional printing*.

For a printing house to be regarded as using a specific printing technology in production, it should constitute 10% or more of the production.

Questionnaire design

The questionnaire was designed to obtain companies' opinion about the importance of providing short production runs, variable data printing and the option to let customers order through web interfaces on a scale from 1 (not important) to 10 (very important). In some cases they were also asked to give their opinion of their performance. Questions about their view of market competition and their expectations about the future were also asked.

The questionnaire was based on closed questions, with the purpose of measuring opinions. Data was collected using numeric rating scales where the end categories were labelled with appropriate options [Saunders et al., 2003]. Two different scales were used, a 10-point numeric rating scale from 1 to 10 when rating opinions about performance and importance and of a certain factor. When rating opinions about e.g. future expectations, an 11-point ration scale from - 5 to + 5 (including 0) was used.

All questions were in Swedish, since the questionnaire was completed by Swedish printing houses. To ensure the validity of the questionnaire, a pilot test [Saunders et al., 2003] was performed with three printing houses. Some questions were changed and new questions were added from the pilot tests.

Data collection and analysis

The questionnaire was printed and sent out to the selected respondents by post. Since this survey was constructed as a self-administered survey, a cover letter, explaining the survey, was enclosed and sent to each respondent [Saunders et al., 2003]. The respondents had the choice of responding either by post or through a web interface. The companies that did not respond to the initial survey were reminded by email and/or telephone. While collecting data from the sample, some of the companies did not meet the research requirements of this study and were classified as ineligible respondents. Therefore, the response rate has been calculated, in accordance with Saunders et al. (2003) as:

$$\text{Total response rate} = \frac{\text{Total number of responses}}{\text{Total number in sample} - \text{Ineligible}}$$

Out of a total of 300 companies, 46 were found to be ineligible and 136 eligible companies responded, which constituted a total response rate of 54%. Out of all companies, only six were not possible to reach by personal communication (i.e. telephone or email), implying that practically all ineligible companies in the sample have been identified. The reason for having as many as 46 ineligible companies was that the database contained companies that did not currently own any printing equipment, but were interested in the commercial printing business. In most cases they were working with closely related businesses, such as prepress or finishing.

About half of the respondents posted their answers without any reminder, whereas the other half sent their response after being given a reminder.

The sample (136 companies) was large (> 30) and approximately normally distributed [Keller, 2005], whereby the t-distribution was used to calculate confidence intervals and p-values. Since the sample also covered a large portion of the studied population (428 companies) a Finite Population Correction Factor (FPCF) was used when calculating the standard deviations for the mean values [e.g. Andersson et al., 2002; Keller, 2005].

$$\text{FPCF} = \sqrt{\frac{N-n}{N-1}} \qquad \begin{array}{l} N = \text{Population size} \\ n = \text{Sample size} \end{array}$$

The difference between the categories in the dataset has been analyzed using an independent sample t-test using a 95% confidence level. SPSS 15 and Microsoft Excel 2003 were used for the statistical analyze.

A survey study typically provides a good overview over a large population (e.g. an industry), while it is more difficult to acquire a deeper understanding of specific research questions. For deeper understanding it is preferable to use in-depth case studies of a few companies. Since the aim of this study was to acquire an overview of the commercial printing industry, the use of a survey was the preferable method. Peoples' opinions are, however, always subjective and do not necessarily correspond to reality which is a limitation of any study seeking to capture opinions.

3. Results and discussion

The results (Figure 1) show that digital printers perceive a lower grade of competition (p-value from independent sample t-test = .002). This might be because digital printers feel that they have a greater opportunity to differentiate themselves through digital printing, which results in less competition.

Short production runs

The importance of meeting the demand for short production runs has in earlier research [Mejtoft, 2006] been stressed as the main argument for using digital printing. This argument is supported by this study as both conventional and digital printers gave rather high rankings on the potential of meeting the demand for short runs by using digital printing (Figure 2). Hence, it seems like there is a reliance on this technology even among conventional printers even though their ranking was significantly lower (p-value = .004). However, digital printers gave a significantly higher ranking on the importance of and on their performance of providing short production runs compared to conventional printers (p-value = .000 for both) (Figure 3 and Figure 4).

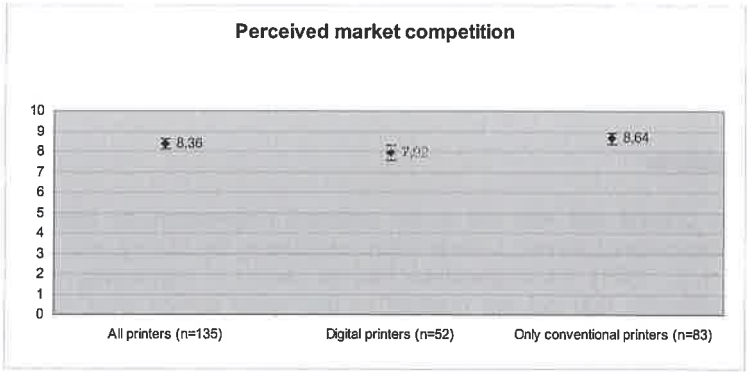

Figure 1: Mean values of perceived market competition (95% confidence intervals)

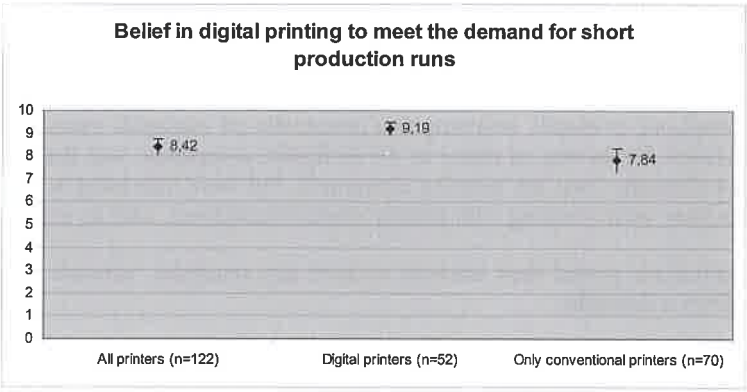

Figure 2: Mean values of the belief in digital printing for meeting the demand for short production runs (95% confidence intervals)

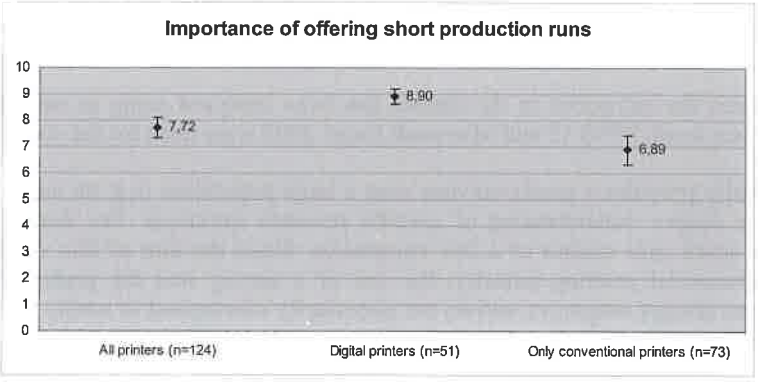

Figure 3: Mean values of the importance of offering short production runs (95% confidence intervals)

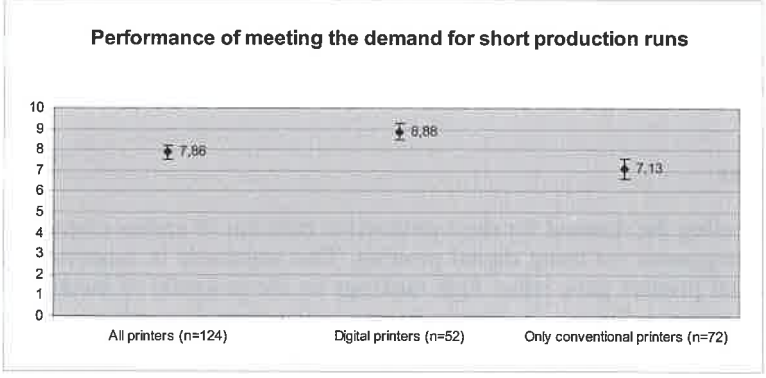

Figure 4: Mean values of performance of offering short production runs (95% confidence intervals)

Variable data printing

There was a significant difference (p-value = .000) between conventional printers and digital printers with respect to importance of providing variable data printing (figure 5). Hence, it seems like digital printers to a greater extent have realised the value of providing this service. However, regarding the performance of meeting the demand for variable data printing (among the digital printers, who offered this service) the ranking was not a top value (7.5) compared to the corresponding value for short production runs (8.88). This could be explained by having a lower value on the importance of offering variable data printing than on offering short production runs. However, it seems like there is some room for improving variable data printing services, which is considered the way of fully using the potential of digital printing.

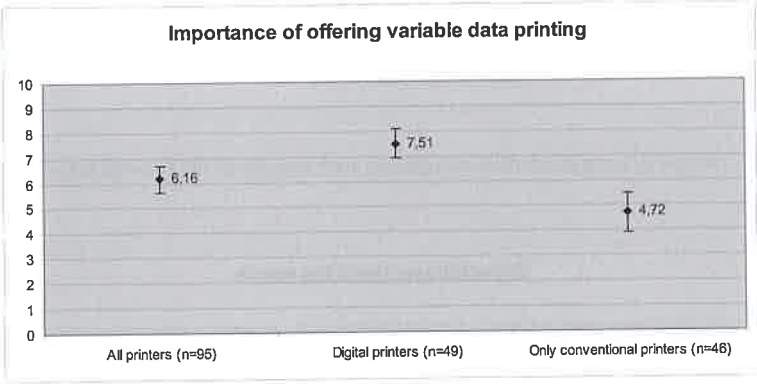

Figure 5: Mean values of the importance of offering variable data printing (95% confidence intervals)

Web interfaces

Digital printers are giving significantly higher rankings (p-value = .000) on the importance of offering printed matter through web interfaces compared to conventional printers (Figure 6). Furthermore, the share of companies that offer web interfaces are significantly higher (p-value = .001) among digital printers (Figure 7). Thus it seems like digital printers to a higher extent need web interfaces in their business.

Expectations about the future

The commercial printing industry is in agreement that production run lengths will decrease (Figure 8). Furthermore, digital printers that today offer variable data printing believe that this business will increase. However, when analysing the first two factors in Figure 8, it is indicated that the margin for variable data printing is anticipated to decrease, since the volume is expected to increase more than the revenues. Moreover, the companies that are using web interfaces (digital printers and conventional printers) believe that the usage of web interfaces will increase.

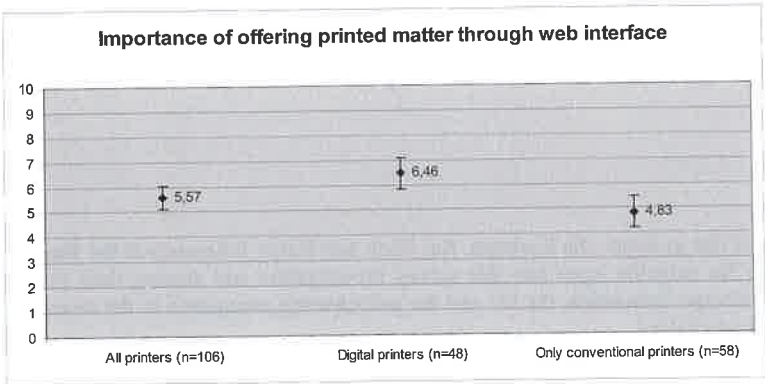

Figure 6: Importance of offering printed matters through web interfaces (95% confidence intervals)

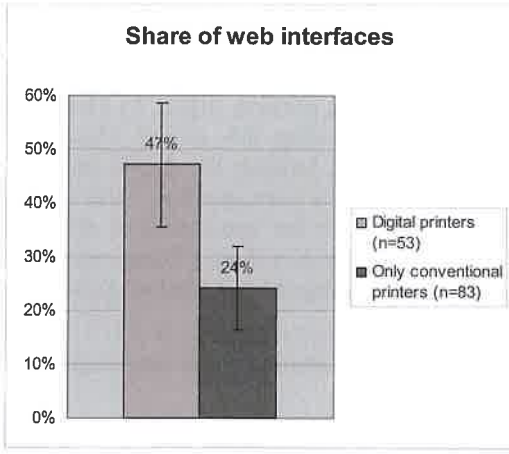

Figure 7: Share of companies that are offering web interfaces (95% confidence intervals)

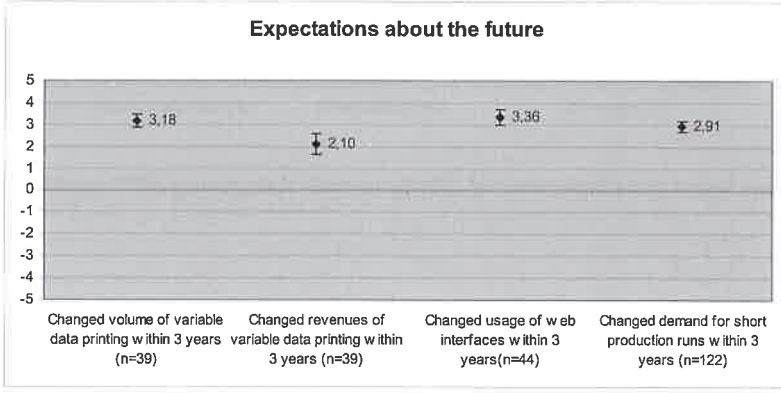

Figure 8: Expectations on future trends (95% confidence intervals)

4. Conclusions

Digital printers find it more and more important to provide variable data printing, short production runs and web interfaces compared to conventional printers. Furthermore, digital printers believe they fulfil the need for short production runs better than conventional printers. Hence, the market conditions seem to differ between digital and conventional printers. As a result, digital printers experience a somewhat lower level of competition. Furthermore, it seems like digital printers to a greater extent need web interfaces in their business.

Moreover, short production runs, variable data printing and the usage of web interfaces is expected to increase. Therefore, it seems like the commercial printing industry will experience even more challenges in the near future, a development that to a greater extent will demand the features that digital printers can more easily provide.

Acknowledgement

The authors would like to thank Ola Karlsson, Kaj Flick and Hasse Johansson at the Swedish Graphic Companies' Federation (GFF) for valuable input into this survey investigation and sharing their members list. The financial support from the Kempe foundation, the EU and the participating companies in the research program DigiPrint are also gratefully acknowledged.

References

[1] Andersson, D. R., Sweeney, D. J., & Williams, T. A., (2002), *Statistics for Business and Economics, 8th edition, South-Western*

[2] Birkenshaw, J., (2004, Apr.), The future of print on paper, Prepress and print Technology, Pira International, Retrieved January 26, 2005, from http://pira.atalink.co.uk/pulp-and-paper/163.html

[3] Mejtoft, T., (2006), *Perceived Satisfaction by Customers in the Digital Printing Value System, TAGA 2006 Proceedings, pp. 486 - 511*

[4] Keller, G., (2005), *Statistics for Management and Economics, Seventh Edition, Thomson Brooks/Cole*

[5] Podi, (2006), *Best Practices in Digital Print, Sixth Edition, Caslon & Company*

[6] Saunders, M., Lewis, P., & Thornhill, A., (2003), *Research Methods for Business Students, Third Edition, Prentice Hall*

[7] Smyth, S., (2006), *The Future of European Printing to 2011, Pira International*

Consumer expectations as drivers of media change

Cecilia Teljas, Alex Jonsson, Nils Enlund

KTH Royal Institute of Technology
Department of Media Technology and Graphic Arts, School of Computer Science and Communication
SE-10044 Stockholm, Sweden
E-mail: teljas@kth.se, alexj@kth.se, nilse@kth.se

Abstract

Media development is not only driven by new technological innovations, but to a great extent by changes in consumer habits, attitudes, and expectations on what media should offer and in what ways. This report identifies a key set of trends that define and characterize the consumers' conceptions of media today and their expectations on the media of the future. Among the main drivers of change in this respect are consumer generated content, a prevalent view of media as social amplifiers, content aggregation and search as a substitute for editorial packaging, the ubiquity and mobility of media, the trend toward context aware media, an increasing commoditization of media, a reduced willingness to pay for content,the effects of globalization, an increasing focus on environmental sustainability, and the intertwined forces of convergence and divergence in different aspects of the media landscape. Media companies should closely follow the changing trends and attitudes in society when developing strategies for expansion and survival.

Keywords

Consumer behaviour, media development, social media, strategy development, trend analysis

1. Introduction

The ways consumers are relating to media are changing. The world where mass media spoke with authorative voice through a small number of established media channels - the press, near-monopoly radio and television, high-circulation general interest magazines - is rapidly disappearing. The media landscape is widening and becoming increasingly fragmented [Fidler 1997]. Advertisers, information providers, and media companies have a widening choice of available channels for reaching out with their message. And each individual consumer can at every instant choose among a plethora of media services and products to satisfy her/his need for media information and entertainment.

This paper discusses the changes taking place within the established and emerging media communication systems. To a large degree, the changes are initiated by technological innovations - new production technology, new information delivery and interaction systems, new consumer devices - but they are also governed by social and economic factors and especially by general changes in the consumers' use of media and their expectations of what media should be and provide. A general model, based on Weibull (1985), of non-technical factors influencing media use is shown in figure 1.

The overall governing force is the *societal structures* in the area or country under consideration. A major factor is the population structure. An aging society will have different patterns of media usage and a different rate of change than a youthful society. Gender equality and multi-culturality in society also has an impact. Economic factors such as taxation, government media support, and general national economic situation have a powerful effect, as has legislation and government policies. The effects on media use are indirect, as they will primarily determine the social situation of the consumers and the media situation.

The *social situation* of the individual consumer has many aspects. Among them, a main one is the private economy of each individual, which naturally influences media choice. Other central factors are the division between work and leisure, age, family, mobility, commuting, and living conditions. For instance, the fact that in many metropolitan areas the relative number of single person households is increasing, has an immediate effect on media consumption patterns.

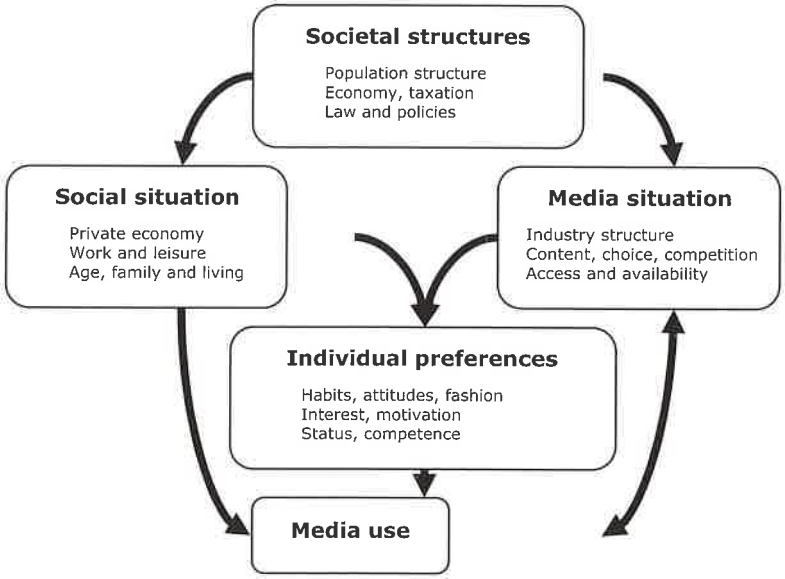

Figure 1: Non-technological factors influencing media use among consumers

The *media situation* in a country or region denotes the conditions of the media industry - the competitive situation, profitability and market situation, the relationships between public service and commercial enterprises, etc. From the consumer's point of view, it describes also the breadth and depth of available content and choice of distribution channels and platforms as well as access to and availability of technology and infrastructure, e.g., the penetration and cost of broadband connections.

In addition to influencing media use directly, these factor clusters determine, to a considerable extent, the *individual preferences* of each consumer. Here we enter an area where causes and effects are extremely difficult to distinguish - often there seem to be no logical predictors at all. Preferences are related to and dependent on such ephemeral and intangible elements as fashion trends and habits. Unexpected trendsetters may appear from nowhere and rapidly change the media consumption preferences of certain groups, subcultures, and individuals. On the other hand, long repeated consumption habits may become petrified and almost impossible to change. Media preferences are also dependent on individual interests, educational background, peer group identity, social status, attitudes, ideologies and motivations.

All these factors influence the consumers' media usage and choice of media channels in a complex manner, making predictions extremely difficult. In addition, media also change as a result of changing conceptions among consumers and enterprises. The way we see, conceive and structure our world determines how we as individuals and groups of individuals act, how we define our needs, and how we envision our future. An example: An entire generation of innovators, developers, entrepreneurs, and consumers that grew up during the 70's was influenced by the vision of the future that was perpetrated by the extremely popular television series Star Trek. To a surprisingly great extent, this vision was internalized and became a driver of technical design development during the 80's and 90's. Today's mobile telephones are conspicuously similar to the Star Trek communicators.

What are then the visions, conceptions, and attitudes regarding media that are prevalent in society today? These - in addition to social, technological, and economic factors - will have an influence on and contribute to the development of media services, media use, media channels. The visions and ideas planted in the minds of the younger generation of today will guide the development of media. From this point of departure, we will here attempt to identify and point out a key set of concepts and mental models that define and characterize the consumers' conceptions of media today and their expectations on the media of the future.

This study is based on current literature, interviews with industry representatives, and focus group discussions with young consumers. The study was performed during fall 2006 and spring 2007. In our world of continuous development in the media field, the media landscape will rapidly change and the facts reported could soon become outdated. The major trends, however, will probably prevail for a longer period.

2. It's a consumer's world!

2.1 Consumers as producers

An obvious and powerful trend in the current development of media channels and media usage is the explosion in consumer generated media content. Blogs, wikis, YouTube, Flickr, etc. are only the beginning of a paradigm shift in media communication. Technology, in the form of laptop and handheld computers, mobile phones, digital cameras, ubiquitous wireless broadband etc., has made it obvious that the media communication process is bidirectional and that each consumer can be a creator of media information. And a considerable share of media consumers actually yearn for becoming content suppliers.

We have seen an exceptionally rapid growth of consumer generated content in the form of blogs and wiki entries. The volume of consumer generated images on photo and video sites is enormous. Although most of the consumer generated material can be considered as lightweight and more of an entertainment than information value, an amazing volume of expertise is made available for free in this manner. Expert advice on anything from plumbing to programming, from drug manufacturing to international economy can be easily obtained. Serious wiki services also have a tight quality control of the material presented and several views are presented on contested matters. Consumer content is generated and made available without any monetary compensation for the creators. The satisfaction of being published, visible, and having a grateful and possibly also active audience seems to be reward enough. Altruism and enthusiasm is a hard combination to beat for competing, commercial media.

Established media have embraced consumer generated content by starting their own and hosting consumer blogs. But, increasingly, media companies are soliciting consumer generated content for their own services and products. Newspapers ask for camera phone images of topical events, TV stations appreciate video clips. The consumer generated material is very inexpensive content, indeed - sometimes the originator receives a small fee, often nothing more than a byline. Korean daily online news publisher OhMyNews relies solely on citizen journalists who write full-length articles, take photos and do background research only for fame and a fee of a few euros. In only a few years, OhMyNews has become one of the most influential public voices in Asian daily media.

Consumer generated content will likely continue to grow in importance. It will provide both a complement to established edited media and a new type of media backchannel connecting and bonding the consumers with the publisher. Among the expected consequences of this development are:

- ◊ An increasing spectrum of consumer generated niched information on the web.
- ◊ A shift of credibility and trust from publishers and their brands to individual creators.
- ◊ A blurring of the boundaries between professional journalism and lay knowledge.
- ◊ An increased need for consumers to evaluate the trustworthiness of information sources.
- ◊ An intensified democratic debate with a multitude of voices, often challenging the establishment.
- ◊ The emergence of new media genres based on consumer generated content.

2.2 Media as social amplifiers

Media do not only serve as information carriers but also as social markers, signalling status and group belonging. Their growing importance as vehicles for the establishment, the maintaining, and extending of social contexts - both traditional ones in our physical world as well as other types of structures where previously disparate groups sharing mutual interests meet and interact often regardless of geographical, political or religious boundaries will in fact create a new breed of social media. This trend toward an increased focus on media functioning as amplifying vehicles for social interaction and networking instead of as mainly sources of information has a number of implications for media companies and media users.

The media has an opportunity to create community in virtual multi-user environments by taking offline experiences and bringing them online in a powerful way. In the process they can attract new readers and viewers. For example, a TV network can have an island in Second Life where they host viewing parties. Here residents would be able to view live broadcasts, including the ads. This would replicate the kind of social interaction that currently takes place in our living rooms.

Newspapers and magazines may have an even bigger opportunity. They can, for instance, recreate the familiar and enjoyable tangible newsstand browsing experience by building a virtual one. Residents would be able to

browse and purchase electronic single copies as well as real-world subscriptions. There are many physical and web based publications that explicitly cater to the Second Life community. There is also an opportunity for amateurs and entrepreneurs to establish focused services, possibly mimicking traditional media, in a virtual environment.

In addition to establishing media services in virtual environments, media providers can use their current, established products and services to construct meeting places for communities of various kinds. Many media companies try to attract new groups of users to their brands by starting niched discussion forums, blogs, multi-user games, and communities of interest in conjunction with their current offerings. The success rate has so far not been overwhelming. Most web communities arise more or less spontaneously and are promoted through viral marketing and word-by-mouth. Established media companies' attempts to promote well-organized branded community sites are often met by distrust from the intended target group.

However, there is definitely an early mover advantage - being the first to gather a specific community of interest can lead to a dominating position and a strong cohesion and fidelity among the members. Some advertisers have succeeded in creating strong communities connected to their products by offering useful information and a social interaction environment both to customers and non-customers.

For the media consumers, an increased focus on the social amplification role of media will lead to a stronger sense of loyalty toward the media that serve the specific interests, peer groups, and private dreams of the individuals. Each person feels kinship with a multitude of different social communities at the same time. With the persons owning the same car make, with those living in the same area, with users of the same computer, with those who enjoy the same kind of music, with those of the same political views, etc. All types of communities can be reached and supported by media - something that magazine publishers have long benefited from. Internet and digital media, however, make it possible to maintain a broader selection of niched communities with very local or totally global membership.

It should be pointed out that well-known brands as such, and definitely also established media brands, can serve as amplifiers of social interaction. Carrying a copy of a specific newspaper or magazine title, or referring in a discussion to a specific television channel or program, signals identity, status and group affiliation. This can initiate meetings between individuals, establish trust, and create feelings of belonging to a group of peers.

The growing focus on the social aspects of media services and products can be expected to have the following implications.

- ◊ A growth in the number and variety of social media - communities, virtual environments, multi-user games, etc.
- ◊ Vigorous entrepreneurial activity leading to an explosive growth in niched social media.
- ◊ A growing presence of traditional media and information providers in popular, niched social media.
- ◊ A virtual media economy within the social media with currencies convertible to real life money.
- ◊ A strong focus on community building and maintenance in established, traditional media.
- ◊ A migration of media services established within digital social media to the world of physical media - e.g., virtual magazines publishing printed versions.

2.3 Willingness to pay

The easy and seemingly unpaid for access to a broad supply of quality information on the Internet has planted an attitude among consumers that information is a free resource. This is in line with the original altruistic Internet culture where the motto has been "information wants to be free" [Brand 1988].

The failure of newspaper companies and magazine publishers to develop and exploit business models for Internet content delivery that would be reasonable and acceptable to consumers has further amplified the dilemma. Giving away online content for free while charging for the same content when printed on paper has undermined the consumers' willingness to pay. The proliferation of free newspapers has also strongly influenced consumer attitudes toward paying for news.

The prevailing attitudes make it increasingly difficult to charge consumers for news and other non-special information. This leads to an increasing media dependence on advertising revenue - an area with growing competition and diminishing income due to the fragmentation of the expanding media landscape.

New commercial media channels must base their business models on advertising revenue and/or innovative charging mechanisms, at least when it comes to general information available from other sources. It will still be possible to charge consumers for specialized, premium content or services. But here looms the spectre of digital content piracy.

3. Media as commodity

3.1 Commoditization

Commodities are largely interchangeable products or services, traded solely on the basis of price. As media companies' offerings become increasingly alike, while devices for consuming media contents are more and more interchangeable, media move closer to anonymity. As a consequence, consumer loyalty to a specific media company or brand is already decreasing in the digital domain. On the World Wide Web, big players and small ones look very similar. This fact makes it difficult for the consumer to differentiate between corporations with 100+ employed journalists and a sleek organization with only a handful. This can be an advantage for the smaller media market players. At the same time it transfers the responsibility of checking and evaluating the factuality and correctness of the information to the consumer, since it is difficult to identify the background and the motives of the information provider. To make matters worse, a multitude of third-party content aggregators are only too eager to take news items out of their context, presenting them in their own service.

Without responsive action, short news flashes and stories from different sources will become increasingly indistinguishable due to their similarities both in form and content. Possible counteractions on the part of an established news provider could include - apart from investing more in journalistic efforts - value adding material or enhanced functionality to further differentiate the service from other brands.

As a counter-measure to this development, many technology-centric media companies are hiring information architects, designers, anthropologists, artists and others with "softer" skill sets. User-centric and user participatory design methods are becoming increasingly popular. Also, as markets move at a quicker pace than research laboratories can manage, the markets actually become the test beds for new applications and services. Short series are manufactured, and if they sell it is regarded as good test result and larger production series can be rolled out. Rather than creating walled gardens, an increasing number of media actors are slowly abiding to standards, although often with proprietary differentiating extensions in functionality, thereby conforming to common media formats, delivery mechanisms and means of media control and presentation. Through industry working groups and RFC documentation, de facto standards develop relatively quickly outside of the official standardization efforts. Still, the advances in neutral transport and display formats for media allow for an increased level data of interchange, searchability and conversion between previously disparate data sources.

For the consumer, it is the dawning of a era of always having access to just about any type of information, using just about any channel. With news as commodities, it is a buyers market. But there will always be information worth paying for, exclusively for those who can afford it. An important question for the next decade will be whether the gap between the have's and have not's will increase, and whether decisions made on the basis of freely available information will be good enough in a democratic society.

What impact will commoditization have on the media?

- ◊ Media content sources become at risk of being fully interchangeable.
- ◊ Fewer people will be loyal to a single brand for longer periods.
- ◊ Media equipment becomes increasingly available as electronics components are constantly cheaper - more people get access.
- ◊ Devices have less buttons but more functions than ever before. The easier to use for the consumer, the more functionality is required under the hood.
- ◊ Media companies need to increase their visibility, offering services differentiating them from others.

3.2 Aggregation and search

Editorial departments of media companies have always been media aggregators, collecting information from various sources, assessing the value, validity and relevance of the information, and editing and reformatting it

for the intended delivery channel and target audience. The aggregation of information is an established business practice.

The precondition to aggregation is access to information sources. The proliferation of accessible information sources on the web paves the way for a continued growth in aggregating media services, both services with automated collection and presentation of information and services that are edited. These services can be collections of links or they can contain the full content. Aggregated news sites on the web are, to a certain extent, cannibalizing on the editorial work of the original news sources. But on the other hand, through linking they are generating traffic to the original sites, thereby attracting advertising revenue.

An interesting emerging form of media aggregation is the so-called "mashup". A mashup is a website or application that combines content from more than one source into an integrated experience. Chicago-crime.org, e.g., combines two services - a Chicago Police Department crime web site and Google Maps - and lets the user type in a street address to see recent crimes in the neighbourhood. The site attracted 1.2 million page views within the first two weeks after it started in May 2005 [Hof 2005, Tirri 2006]. The possibilities of combining information in novel and often surprising ways are almost limitless. The metadata associated with photo housing sites such as Flickr makes it possible to mash photos with other information that can be associated with the metadata. RSS feed mashups can aggregate a user's news feeds and present them in form of a personalized digital newspaper that caters to the reader's particular interests. An example is Doggdot.us, which combines feeds from technology oriented news sources such as Digg.com, Slashdot.org, and Del.icio.us. The growth of metadata information on the Internet, in Web 2.0 and the Semantic Web, will radically increase the opportunities for creating innovative mashup services. Combining media content and media services with other types of information - geographical, demographical, commercial, etc. - will generate a multitude of new services and business opportunities.

While media aggregators generate services for a target group of users, search engines work in the opposite direction - users generate specific requests that result in a set of web pages with a corresponding content, ranked according to degree of similarity to the request. Search engines can be seen as on-demand content aggregators. In today's online world, search engines have all but replaced encyclopaedias and other traditional information resources - archives, databases, catalogues, etc. - as the primary choice of fact-finding consumers.

The use of search engines by media is twofold. Established media can utilise popular search engines to attract users and traffic by advertising, i.e. paying to obtain a special link on the results page of a search service, or by utilising the ranking algorithms of the search engine to position its link high up on the hit list. In a situation where consumers look for media information using a search engine, it becomes important for a content provider to have a prominent position. Media companies can incorporate a search engine on their own web pages, instructing the search algorithm to first list results from their own site.

Using search engines in mashups with other types of information on the Internet will probably be the most spectacular development in the emerging, metadata-rich semantic web. Consumer initiated searches can then produce results that aggregate facts, maps, numerical information, in-depth background and history, etc. from a multitude of information sources. This can create instantaneous news and fact services that surpass everything that a traditional editorial department can accomplish within reasonable time and expense limits. The drawback, as with all automatic aggregators, is that the evaluation of the gathered information with respect to reliability and objectivity is left to the consumer. The opportunities for manipulation of information and for exposing unwanted combinations of personal information are also considerable.

The trend toward an increased use of content aggregators and search engines may have the following implications.

◊ Increased competition to traditional media services from content aggregators and search engines.
◊ The emergence of niched, targeted mashups and aggregator services that attract advertising revenue.
◊ A change in consumer attitudes to information sources - aggregators seize the top-of-mind position.

3.3 Convergence and divergence

Convergence implies that different areas in the media market are developing towards each other. This brings about new competitors, from other media channels and other markets. Players previously in different corners will suddenly find themselves competing in the same arena [Appelgren 2004].

Even though there will be an increase in the number and type of media devices, they will have much the same functionality. Nevertheless, there will be a wide variety of devices and standards. Distribution requires proper adaptation of the content to the receiving device. Device divergence leads to adapted presentation, as consumers will not accept receiving content that is not correctly presented. Furthermore, with new business opportunities new players on the distribution side should be expected.

A divergence of media channels has emerged with the growing range of devices, but also since many companies attempt to reach the consumers using several channels. There is a clear trend toward having "all information on all channels", something that the consumers have willingly embraced. On the Internet, the threshold for starting a publishing activity has become significantly lower. This has led to a wider supply of content with more players wishing to have their share of the cake. Divergence is also a result of services offering different kinds of niched and even personalized content. Personalized news aggregation can be based on an individual consumer's preferences. Digital use of digital footprints and stored information about consumers as well as about their consumption habits is increasing.

Media consumers will have a broadening choice of content and media channels. On the Internet, niche content and mass media are both easily available. This also means a mix of high and low quality. In the hyper-democratic anarchy of Internet, consumers are forced to take greater responsibility and to have a critical mindset. Reliable sources may be more of an exception than a general rule. The consumers have to ask themselves questions such as; who are the senders, what are their interests, can this description be a false impression of what actually happened? In this matter trust and credibility are crucial issues for all players, especially when providing news. While the number of devices is ever growing, changes always require time and many media channels will stay around in parallel. Historically, we have maintained our "old media" even though "new media" have emerged.

Media consumer behaviour is often portrayed in a 24-hour period of media usage. Different media channels are also being used depending on what time of the day it is - a phenomenon known as day-parting. If a media brand gives the same information in its different channels with only a few updates, the customers will recognize the stories. If too much of the content is identical the consumers will turn to a competitor at some time during the day to get different news, or at least news from a different angle.

The different convergence and divergence processes will influence the media scene in many ways, e.g.:

- ◊ Competition will increase, as there will be more competitors.
- ◊ Organizational convergence will lead to powerful media conglomerates that can utilize cross promotion, content sharing, etc.
- ◊ Customer relations will be increasingly important since media contacts may be casual and the number of opportunities is growing.
- ◊ There will be more parallel channels which means that content needs to be adapted to an increasing amount of outlets.
- ◊ This broadening spectrum of content and brands puts greater responsibility on the consumer. Branding and reputation are therefore important issues for media companies.

4. Toward a new media landscape

4.1 Ubiquity and mobility

The increase of media mobility and ubiquity seems to be an inevitable development. In only a few years there will be media and communications access and availability everywhere and all the time. This development is being supported by strong forces. Common interests between the telecommunications industry and mobile phone manufacturers drive the development forward. The number of mobile services will grow rapidly during the next years. Many advanced functions are already in use in Asia. In Japan for instance, mobile payments have been reality for years.

Location identification in mobile devices will be useful in many different application fields. RFID and GPS are two technologies that will have an increasing importance and affect media devices, services and content. RFID (Radio Frequency Identification) tags in mobile devices have already been tried out. This inexpensive technology offers many new opportunities. In mobile devices, RFID can be used for transport payments, as passport identifications, or as car keys. GPS (Global Positioning System) receivers in a mobile device can

determine the location, speed and direction of the device and its user. GPS functionality is being introduced into mobile phones and other devices and offers many interesting possibilities such as high precision location-based services. A mobile media device user may be tracked and identified when requesting news or other information and the content sent back to the user may be customized according to these parameters.

Mobile devices have been around for only a relatively short period of time and their impact on the media industry will still grow as both devices and users mature. New devices enter the market with new and enhanced functions and the users will embrace the possibilities. We expect that:

- ◊ New technology will affect mobile media devices and in the extension this will also impact media as new innovative services are developed to compete for the time and money of media consumers.
- ◊ Today's restrictions to mobility in form of battery life, screen size, connectivity, input tools etc., will be removed or reduced one by one. We will see mobile devices with larger, rollable e-paper screens, long battery life, and ubiquitous connectivity. Still, there will always be restrictions.
- ◊ Media use on mobile devices will increase, and the consumers will expect to find customized information on each device.
- ◊ Media services will seamlessly move from device to device and from location to location according to the user's behaviour and contextual needs.

4.2 Context aware services

In order to be as useful and valuable as possible to the user, media should adapt themselves to the consumer's location and situation. Ideally, media should provide the information needed or wanted in each situation, in a way that is adjusted to the existing conditions. One way of making a media system perform better and be easier to use, is to make it aware of a user's intentions and situation.

Context awareness deals with the possibilities for providing systems with input derived from interpreted human intention and situation. The context when consuming media is made up of factors such as the user's current interests, the composition of the community she is currently part of, her role in the media system (reader, journalist, editor, etc.), the geographical and physical surroundings with their properties and limitations, the intentions and motives for acting, etc. Contextual awareness in the systems we use can enhance and thereby simplify our ability to control our environment, in this case specifically in interaction with media services and products.

So, rather than giving everything to everyone, media companies are investigating means for extracting information for the purpose of targeting various offerings, both editorial and commercial, in accordance with the user's preferences, location, interests, etc. There will be much more of this, with finer granularity, in the years to come. Any targeted eyeball is a premium eyeball, especially as the cost for shotgun marketing without demographics is getting increasingly expensive.

A crude form of context awareness already takes place today in both digital and physical distribution channels when editorial contents and advertisement is zoned according to geographical location on a regional level. Knowing where your audience is at as well as their interests and attitudes could in be the difference between do or die for, e.g., a small town newspaper.

We can expect that

- ◊ Media services will make increased use of information about their customers, in attempts to target them with personalized information
- ◊ Services that scale well from one mode to another will be regarded as less intrusive
- ◊ Consumer mobile phones equipped with on-board GPS and digital compasses open up for a full range of new innovative services
- ◊ Information about the individual will be more important than ever, as will the protection of privacy.

4.3 Globalization

The increasing global connectivity, integration and interdependence in the economic, social, technological, cultural, and political spheres will affect media in various ways. One aspect here is the expanding market for media products and services. Online services are already global. Internet and web content is available

everywhere and, due to the international strength of the English language, used and consumed almost all over the globe. This opens up huge markets for new media innovations but also the opportunity of transforming existing brands and products for a global market. On the other hand, media is to a large extent language and culture dependent. A global market may therefore require translations and adaptations for a large number of areas, thereby further increasing media divergence and fragmentation. This will also increase costs for exporting media services, products and brands to new markets.

One probable result of the general globalization processes may be an increased focus on local and regional media products and services. Local content is already a strong marketing advantage, since global media seldom can address topical issues in local communities - and these are matters that are important to consumers in their daily life. It should be kept in mind, however, that communities are far from always geographically localized and that global communities of interest may be more valuable to consumers than the geographical neighbourhood.

The world of media and media usage is far from homogeneous. Despite the rapid, global spreading of information and communication technology, not all have equal access to media, old or new. When it comes to digital media, there is a gap between those with regular, effective access to digital technologies and Internet access and those without. There are also differences in, e.g., economic possibilities, education, skills, and physical abilities between different groups of consumers. The deepest chasm in the digital divide is due to economic inequalities. These become visible as immense and, in some cases, growing inequalities in access and skills between industrialized and developing countries as well as between social groups within all countries.

4.4 Sustainability and environmental aspects

A major theme in the current political and social debate is the development of society in an environmentally, economically, and socially sustainable manner. The ongoing ecological changes will strengthen the citizens' awareness of environmental matters, also with respect to media. The consumers' media choice will increasingly be determined by their conceptions of the sustainability of the media channel. The attitudes toward, e.g., media based on high energy consumption may become negative enough to radically affect the market.

Media, both traditional and new, must carefully measure and assess the sustainability factors concerning their products and services, over their entire life cycles. The facts must be communicated to the consumers and explicit and visible actions must be taken to improve sustainability and reduce environmental load. There is a clear and growing demand for environmentally responsible and sustainable media.

5. Conclusions

Relating to Porter's (1985) model of five competitive forces, an aid in formulating the competitive strategy for a firm by analyzing its environment, we can describe a media market that is emerging, global, and fragmented at the same time.

In the inner market of existing media companies, competitive rivalry is fierce, resulting in many companies running up red figures for long periods in order to fight off the competition. Secondly, the threat of new market entrants might be greater than ever, as very small investments can take two guys in a garage all the way to fame and fortune for the rental fee of a rack mounted serverat a cost of about € 300 per month. The third Porter force, the bargaining power of consumers, is fueled by the increasing commoditization of media. In the fourth corner, we find the suppliers, who's influence on the media market is diminishing rapidly in many market segments. In the music industry, for instance, several of the large record companies are either in transition to go to all-digital delivery, or are subjects to mergers or acquisitions, or in denial in preparation to go belly-up. And yes, the threat of substitute products is enormous, and we have only seen the beginning.

The drivers of change in the media market are not primarily technological although they, to a great extent, are initiated by technical innovations. New technical advances will give rise to new trends and changing attitudes. So will changing economical and political circumstances as well as fashion trends. Changing consumer expectations on what media should offer - and how this should be done - will greatly affect media development. The media landscape of the future will be unpredictable but certainly exciting.

Acknowledgements

This paper is based on work commissioned by Ifra, Darmstadt, Germany, as part of the Where News? research project. Special thanks to Manfred Werfel and Jochen Dieckow of Ifra.

References

[1] Appelgren, E.: (2004), "Convergence and divergence in media - different perspectives", *Proc. ICCC 8th International Conference on Electronic Publishing*, Brasilia

[2] Brand, S. (1988), *The Media Lab: Inventing the future at MIT*, Harmondsworth, Penguin

[3] Fidler, R. (1997), *Mediamorphosis. Understanding New Media.* Thousand Oaks, Pine Forge Press

[4] Hof, R. D. (2005), "Mix, Match And Mutate", *Business Week*, July 25. Available at http://www.businessweek.com/magazine/content/05_30/b3944108_mz063.htm

[5] Porter, M. (1985), *Competitive Advantage,* New York, Free Press

[6] Tirri, H. (2006), "Ubiquitous Media", Nokia Research (seminar presentation). Available at: http://akseli.tekes.fi/opencms/opencms/OhjelmaPortaali/ohjelmat/Ubicom/fi/Dokumenttiarkisto/Viestinta_ja_aktivointi/Seminaarit/Yhteisseminaari_030506/Tirri.pdf

[7] Weibull, L. (1985), "Structural factors in gratification research" in Rosengren, K.-E. et al (eds.), *Media gratification research.* Current perspectives, London, Sage Publications

Tabloid versus broadsheet: is format change the magic bullet for newspapers? The results of a comparative eye-tracking study of a German daily

Hans-Jürgen Bucher

University of Trier, Department of Media Studies
D-54286 Trier, Universitätsring, Germany
E-mail: bucher@uni-trier.de

Abstract

This article presents an empirical study on how readers deal with newspapers in different formats: the tabloid or compact format and the broadsheet format. This comparative audience research was conducted with a multi-method design combining eye tracking, thinking aloud procedure, interviews, questionnaires and structural content analysis. The objects of the study are two German national newspapers: the broadsheet paper *DIE WELT* and the compact paper "*WELT kompakt*. Both are produced by the same newsroom team and show differences in content selection, design and visual presentation. The intention of this study is to contribute to the worldwide debate, if format change is a means to stop the decline of the circulation of newspaper and can improve its attractiveness to its readers. The findings shed some light on the reader-paper-interaction, reader` evaluations of the format and their journalistic differences. The central result is, that it is not inherent in the format of a newspaper how it is used by its readers. Rather it is the interaction between individual habits of newspaper reading on the one hand and the design and the content of a newspaper on the other hand which determine the process of reception. But in general, reading in depth is more typical of the broadsheet whereas reading cursory and superficially is more typical of the tabloid format.

Keywords

Audience research, broadsheet format, eye tracking research, newspaper design, tabloid format

1. Introduction: The global debate on tabloid versus broadsheet

There is a world wide debate if downsizing of the newspaper format could help stopping the decrease of circulation and audience reach of newspapers. One of the most prominent newspaper designers is already convinced that "tabloidization of newspapers is a global phenomenon" and predicts, that "one by one, the largest and best known newspaper titles around the world will make the transition to smaller formats" [Garcia 2005, 13]. The President of the international organisation "Society of News Design" shares a similar belief: "It occurs to me that while larger newspapers struggle for significance in our current media blitz, small newspapers can rest assure that they have a place in our society" [McNeal 2007, 2]. There is some evidence that changing the format from broadsheet into compact format indeed can position the newspaper more in the middle of a society and make it more attractive to its readers. Broadsheets across Europe which have converted themselves into tabloids, like the *Independent*, the *London Times* and the *Guardian* in Great Britain, or the *Dagens Nyheter*, *Göteborgs-Posten*, *Sydsvenska Dagbladet* in Sweden and the *Berlingske Tidende* in Denmark could rise their circulation by an average six to eight percent in the year following the conversion. The *Independent* which has been the first of the quality papers in the United Kingdom to change to compact format has even increased its circulation by 18 percent within six months after the format change [Bughin/Poppe 2005]. The vast majority of European new papers that have entered the market within the last decades have either tabloid or the slightly bigger Berliner format. All commuter papers - explicitly aiming at young and mobile readers - are without exception published in a compact format [Blackhurst 2005; Haas 2004]. Trying to imitate this strategy of success two German national dailies publish tabloids, *DIE WELT added a tabloid to its portfolio in 2004*, and the *Frankfurter Rundschau* switched to a compact format in 2007, hoping that they can participate in circulation growth especially among younger and mobile readers.

Throwing a glance at newspaper history one can learn that small formats are not an invention of our times. It is just the other way round: Newspaper history in the 17th century started with small book-like formats, because transferring the technique of printing books was the cheapest means of printing newspapers. Thus the broadsheet format mirrors the emancipation of the newspaper from book tradition: The broader amount of space and the progress in design have enabled the journalists to "map the world for its readers", as Barnhurst

and Nerone characterize the function of modern newspapers [Barnhurst/Nerone 2001, 22]. Tabloids in the sense of a compact format returned in the early 19th century when special newspapers were printed for readers in London's and New York's crowded underground, were smaller newspapers are much more convenient to read [Arnold 1981, 222].

The presented research project is dealing with these questions of format transition from a reader's perspective. Their attitude towards formats of newspapers and the respective design and concepts of journalism should be the touchstone of every measure of form, design or content. With a multi-method-design the research project compares audience' reception of a broadsheet version and a compact version of the same German daily: *DIE WELT* and *WELT kompakt*. Object of the study was the edition of the two newspapers of Friday 15th September 2006. This kind of comparison allows studying audience reactions on the same content in different forms. The main *research questions* have been:

- ◊ How important is the newspaper format to the reader and how do they evaluate the broadsheet and the tabloid version of the same newspaper?
- ◊ How does the format influence the scanning and reading processes of newspaper editions and newspaper pages? Are there different reading paths regarding the two formats?
- ◊ How does the format influence the scanning, navigating and reading processes of a whole edition of a newspaper? Are there different patterns of news selection or different reading patterns as regards the different formats?
- ◊ Are there differences in the reception of newspaper design features like pictures, teasers, briefs, ads, texts or headlines?

2. Design and methods of qualitative audience research

Newspapers are, in contrast to television and radio so called non-linear media. Readers have the freedom to decide *when* to read *what* in *which order* with *which intensity* and *how often*. It can be said that readers are, as it is the case in online media, their own director of program. Without their activities of selecting, navigating, scanning, reading in depth or reading superficially, interrupting reading and starting again there would not be a news program of the newspaper at all. The design and layout of the newspaper, the form of news, are a means to help readers to manage their reading process. For researchers this process is of rather high complexity because there are three different dimensions influencing it: *the dimension of the readers* themselves, their interests, their time budget, their previous knowledge or their media literacy; *the horizontal dimension of the reading process* itself which comprises different reader activities like scanning, reading and watching, navigating and selecting; and *the dimensions of the newspaper* as the object of reception with different layers of design decisions: the layer of the edition, the layer of the page, the layer of the double page, the layer of the cluster of articles and visuals, the layer of article elements (headlines, teaser, Subtitles etc.). Because of this complex process of newspapers reception the presented research project applies a multi-method qualitative approach to get data as rich and as thick as possible. The project combines eye tracking research, the thinking aloud procedure, interviews, questionnaires and content analysis. Processes of reception cannot be observed directly. But the combination of these methods generates quite a lot of different data, which help to reconstruct the process of newspaper reception not by post-hoc data but via direct data from the reading process itself. Besides the information from the readers in the interviews and the questionnaires or their spontaneous comments by thinking aloud especially during the eye tracking provides us with a lot of non-intentional indicators of reading behaviour:

The *exposure time* indicates the degree of interest and the amount of attention readers are spending for a special element of the newspaper.

The *quality of the eye-movement* indicates whether the subject is reading in depth or superficially or just scanning the page, the picture or the article.

The *order of the fixations* indicates the reading path or the scanning path.

The *news selection* of the reader shows what he is interested in and what does not draw his interest at all.

As we are interested in the results of the reception of a whole edition as well as in the results of single pages the study consists of two modules:
Module 1: The subjects read *Die WELT* and Die *WELT kompakt*. With an eye tracking device the eye movements are recorded while the subjects are simultaneously "thinking aloud" (= commenting) during / about their newspaper reading (n = 17, among the subjects were subscribers and non-subscribers).

Module 2: The subjects read selected pages of both newspapers, while recording their eye movements. Afterwards in an interview the subjects are asked to compare their reading experiences of the two formats (n = 25, subscribers as well as non-subscribers).

At the end of each test session all the 42 subjects are questioned in a guided interview about their evaluation of the two formats. To avoid serial effects the two newspapers are presented to each subject in an alternating, different order. Each of the two newspapers was delivered to each of the subjects` homes for one week respectively, to give them them possibility to become acquainted with it. The average age of the test persons is 31, 26 of them were younger than 30, 13 of them between 30 and 50 and two of the subjects were older than 50. 27 of the subjects are reading a daily newspaper regularly, more than half of all subjects are subscribers of a non-daily newspaper or a journal. Although on average newspaper readers in Germany are older than 31, the media use of the subjects and their habits of reading newspapers are rather ordinary.

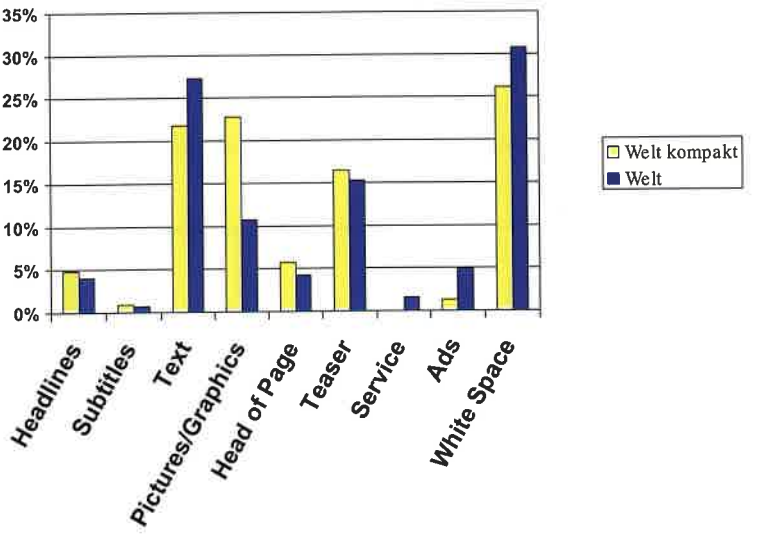

Figure 1: Percentages of spatial distribution for different elements on the front page

3. Results 1: How readers evaluate the two newspaper formats

Broadsheet and Tabloid are not only two different formats of newspapers but they also represent different concepts of journalism. A comparative content analysis of the *WELT* and the *WELT kompakt* indicates that the latter is more appropriate for the scanning and superficial reader because it contains significantly more pictures, graphics, short articles, teaser and promo boxes. On the other hand the *WELT* is more addressing the in depth reader because it contains more long articles (see Figure 1). Readers perceive the two editions of the same daily in different formats as two clearly distinct types of newspapers with different journalistic conceptions. The subjects are asked two different questions: firstly how they evaluate the content of the two newspapers and secondly how they evaluate the different formats. Regarding the content the tabloid format is associated with the attributes "short", "quick", "coloured", "shallow" and "lurid". The broadsheet edition stands for "reliable", "accurate" and "detailed information". The preferences concerning the format were univocal: 30 of the 42 participants prefer the compact format because of its manageability, usability and its transparency in the design of the content, 4 subjects prefer the broadsheet format and 8 subjects remain undecided. Half of the subjects as well prefer the content and journalistic style of the compact format because this type of newspaper gives them the feeling, not to be overstrained by an information overload. Interestingly 9 of the subjects propose to combine the journalistic style of the broadsheet with the format of the compact edition. One can conclude that the subjects by the majority would prefer the compact format.

4. Results 2: Reading patterns for the whole newspaper edition

Most of the audience research on newspapers is dealing with single pages or even smaller units like articles. This survey contains a mapping of the reading process during a whole edition of a newspaper. Figure 2 shows how much time readers spend on each single page of the editions of the two newspapers. In both formats the

title page gets the highest attention: 2:15 minutes in case of the broadsheet and 1:45 minutes in case of the compact edition. Relative to the page size of the different formats the degree of attention spent with the title page is higher in case of the compact format than in case of the broadsheet format. The time spent with other pages is highly dependent on topics, subject or sections. In both formats readers show less interest in the economy section whereas politics, foreign news and the science section get high attention. The media and entertainment section gets high attention in the broadsheet format, sports and culture are the sections with the longest exposure time in the compact format. One can also find some correlations between gender or age and the interest in special pages. For example men show significantly higher interest in page 22 of the compact version, which contains an article on the German rapper Kool Savas or in page 25 with an article on infidelity of wives. On the other hand women pay more attention to page 23 in the compact format which contains an article concerning Lady Diana and one about the French writer Michel Houellebecq.

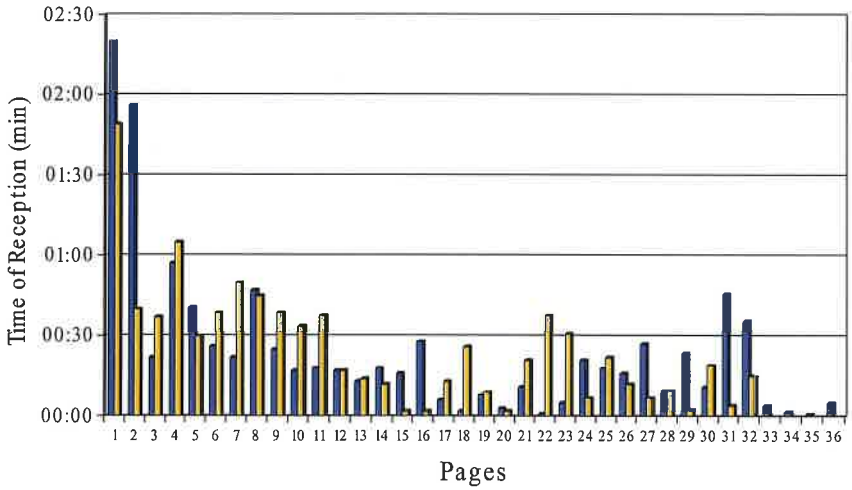

Figure 2: Exposure time for each page of Die Welt (blue, 36 pages) and Welt kompakt (yellow, 32 pages)

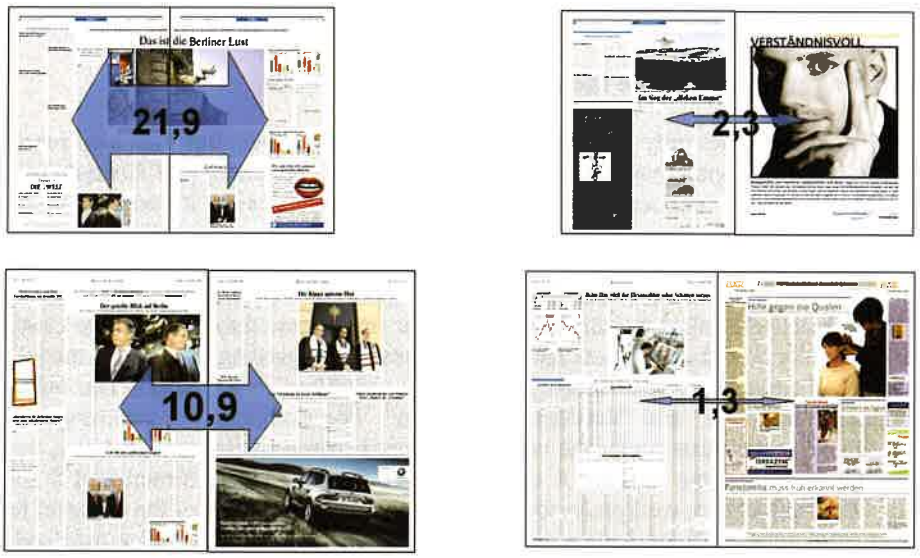

Figure 3: Jumps of eye movements between opposite pages: upper row: WELT compact with a double page-story on the left. Below: the WELT with two different opposite pages, each designed separately

The reading process of the compact format shows a pattern which one cannot find in the broadsheet format: on all the section openers the exposure time issignificantly higher than on the pages within the sections. One can conclude from this finding, that in the eyes of the readers the edition of the compact format is well structured despite the fact, that compact newspaper mostly cannot be sectionalized.

Normally newspapers are designed page by page. The eye movements show, that this is not appropriate in any case because readers also tend to perceive two facing pages as a single unit. An indication of this pattern of reception is the amount of jumps of the eye between the two pages: the more often the eye movement switches between the two pages the more readers perceive them as a coherent visual unit. Our data show, that it is the design of the double page which strongly influences this pattern of perception. Double pages which are designed as a topical unit have ten times more eye-jumps than separately designed pages (see Figure 3). An adequate strategy therefore is to design opposite pages as a double-page unit to invite readers to see them in one general visual sweep.

The results of how readers navigate the canvas of two pages show, that one can compensate for the smaller size of compact newspapers by designing stories on two opposite pages as a coherent unit. In Figure 3 both of the left examples contain the same story on two elections in Germany with partially the same pictures, texts and information graphics. The story in the compact format is read much more intensively by the test persons than the same story designed on a single page in the broadsheet version of the paper. Figure 3 also indicates very clearly that pages with advertisement or pages with stock exchange prices tend to be perceived in isolation and for a rather short time, as data of exposure time show. In general the average of eye jumps between opposite pages is higher in the compact format (9,2 jumps) than in the broadsheet format (8,0 jumps), which indicates that the compact format is perceived more as a double page newspaper.

In both formats of newspapers on all pages visuals like photographs, info-graphics, and short text formats like text boxes or short news get high attention rates. From verbal comments we learn that the latter have a dual function: Firstly, they determine a reader's decision whether to read or not to read the longer texts of that story. Secondly, they have an overview function for readers who want a quick reading. Despite these similarities there are some distinct differences in the reading pattern of pages in the two formats: Especially on the title pages the compact format stimulates a scanning pattern whereas the broadsheet favours more in-depth reading. More on that in the following section.

5. Results 3: Reading a single page: points of entry, intensity of reading and reading paths

Reading a newspaper is a highly selective process. Only a small part of the whole newspaper content is noticed by the reader and an even smaller part is read. What are the principles which manage these processes of selection? What is neglected and what is selected by the reader, in what order and how intensively is it perceived? Does this selection process differ between the compact and the tabloid format? Here are some results which can she some lighton this interaction between the newspaper and its readers. As the Eyes-on-the-News-Study of the Poynter Institute had already documented in 1991 [see Garcia/Stark 1991], there is no fixed pattern about how a newspaper page is perceived, as for example along an inverted S-Curve. Instead of that the reading and scanning process and the order in which elements of a page are seen is governed strongly by the dominant visual elements on that page. This salience effect could be observed in both types of newspapers, but with some differences: In general on the front page of the broadsheet format the headlines and the pictures attract more attention in the first part of the page exploration whereas in the compact format readers begin to read the texts much earlier. But on average on the front pages more time is spent on reading in the broadsheet: 81 percent of the total exposure time and only 68 percent in the tabloid. Again we have evidence that compact newspapers seem to be more suitable for superficial readers than for in depth readers. But this can change depending on the page design. A comparison of two double pages in the two formats shows just the opposite, namely that in the compact format the percentage of reading time is higher (77 percent) than in the broadsheet format (75 percent).

For both formats data indicate a well known effect of placement: elements on the upper parts of a page are perceived much earlier than elements on the bottom of a page. But this does not influence the intensity of perception: in some cases articles at the bottom of the page are read much longer than other articles. Figure 4 shows how attention is distributed on the different elements of the front pages. In case of the front page of the *WELT* the editorial article in the right column, a daily column in the lower right corner, the lead story and the promo boxes at the head of the page gain the highest percentage of exposure time, whereas for example the greatest part of the left column with briefs remain nearly unnoticed. By contrast the briefs placed in the left column of the *WELT* compact get a lot of reader's attention. This seems to indicate that the difference in perception is caused by a difference in design: whereas the column with briefs in the *WELT* is design and labelled as a table of contents the briefs in the *WELT kompakt* are designed as complete short articles and labelled as "News". One can conclude that complete articles are more attractive to readers than items of an index. Also of significantly high interest in the compact version are the lead story and the short article to the right of the main picture ("Attack on Apple"). A common

feature of both formats is the significantly short time of exposure in case of the pictures: obviously pictures can be perceived very quickly so that normally less time must be spent with them.

Newspaper frontpages function as a showcase for the whole edition. Despite that there is one result they have in common with other pages: short articles attract high attention independent of their position on a page. Figure 4 indicates this for the short articles at the bottom of the two front pages. The same result we get for some inside pages. One can explain this by a principle of effectiveness the readers are following and which has been formulated explicitly by some of them in the interviews: For deciding if an article is read or not readers evaluate the relation between investment (time, effort) and revenue (information, pleasure etc.). This calculation seems to be of less risk in case of short articles than in case of longer ones.

Figure 4: Distribution of attention on the front pages of the two newspapers formats (percentage of exposure time)

Going one step further one can ask, what the readers are doing while watching the different elements of a newspaper page. To measure the intensity of newspaper usage one can differentiate between the two activities reading and scanning and between the lines which are read and the ones which are not read. Figure 5 shows these results for a double page in each format

The double page in the *WELT kompakt* and the five inner columns on the left page in the *WELT* (Figure 5) contain the same package on the topic of two German state elections comprising texts, info graphics and pictures. A comparison between these two packages shows that in the the tabloid version much more text is read by many more readers than in the broadsheet. Much more text in the broadsheet page is read by many more readers in the two left columns of the left page where we find two shorter articles.

And even on the right hand page there is more reading activity than in the lead story of the two facing pages on the two German elections. These topical packages seem to be ignored almost completely. All in all the percentage of text which is read is rather small in both formats. Obviously readers practice a strong selection on what they are willing to spend their time and effort with . The presented results teach us another interesting lesson: it is not the format which decides on the amount of attention and the intensity of reading, it is the content and the design of each newspaper page.

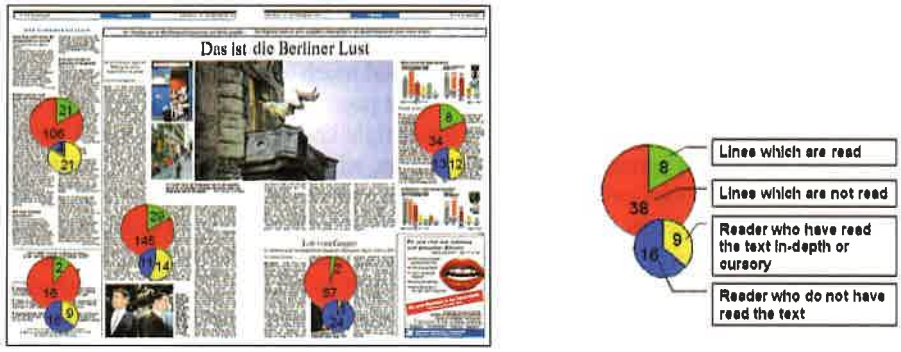

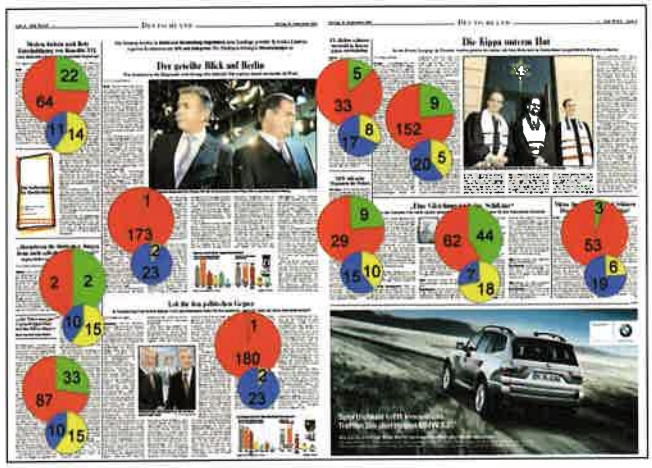

Figure 5: Reading rate and readers rate on page 2-3 in the WELT kompakt (top) and the WELT page 4-5

6. Results 4: Patterns in newspaper reading

A widely discussed problem in every type of audience research is the question if there are overall patterns of media reception. Or to put it in another way: Are there patterns of interaction between the reader and the media. In our study we have divided this question on patterns into two parts: firstly, are there different types of reading a newspaper and secondly: are there special paths readers choose when perceiving a newspaper page. I will start with the second question. There are already some interesting theories on that problem which result from some earlier eye tracking research. For example a research group from Sweden [Holsanova et al 2006; Holmqvist et al. 2005] as well the already mentioned Poynter-Institute [Garcia/Stark 1991] apprehend the reconnaissance of a newspaper page as a process which is governed by the salient visual elements on that page: "The dominant elements of design determine the reader's route, and these elements can be affected by story content, placement, size, and colour"[Garcia 1993, 132].This theory has the advantage that design can be no longer judged as an ornamental feature of newspapers but can be made responsible for the journalistic quality of it.

However this salience theory of newspaper reading results from a restricted methodological approach: all the mentioned studies are fucusing on single elements of design and ignoring to look for longer sequences of the reader`s (Singular oder Plural? Readers` = plural) eye movements. In this study we are analysing complete sequences of the perception of a page and reconstructing the clusters within these sequences. The result of this cluster analysis is that readers do not jump from one salient element to the next but that they navigate within separable zones of a page. The page is navigated zone by zone, whereas readers can repeatedly return to a specific zone. But there is a clear sequence of fixations within each zone before leaving to another one.

Moving from one zone to the next is guided by a neighbourhood principle: readers move to that zone which is situated next, they do not jump to a distant zone. Therefore reading a newspaper is much more similar to pattern recognition than to paper chase from one salient element to the next. This holistic aspect of reading a newspaper page remains out of sight for traditional eye tracking research because it is focused on single visual elements of the page. The modular layout is the complement to this theory of zone-based newspaper reading. Figure 6 shows how this zone based principle works on the two front pages of the *WELT* and the *WELT kompakt*. In both cases the readers separate the whole page into clearly distinctive zones, start with their exploration in the middle of the page and move from there to the adjacent zones. Sometimes the zones which are identified by the reader are not identical with the modules created by layout. This indicates that the perception of a page is not only determined by its design but results from an interaction between layout and reader.

The principle of zones and the principle of neighbourhood explains the distribution of attention and the process of selection. The other question of pattern concerns the intensity of reading a newspaper: is it possible to distinguish special types of reading based on the degree of reader's involvement? An indicator of the degree of involvement is the percentage of time readers are spending for reading - in contrast to the time he or she is just scanning over the page. According to that criterion and on the basis of a factor analysis one can classify readers into three different groups: In-depth readers, who spend more that 50 percent of their reception time with reading, the cursory superficial readers, whose reading time is between 20 and 50 percent, and the scanners, whose reading time is less than 20 percent.

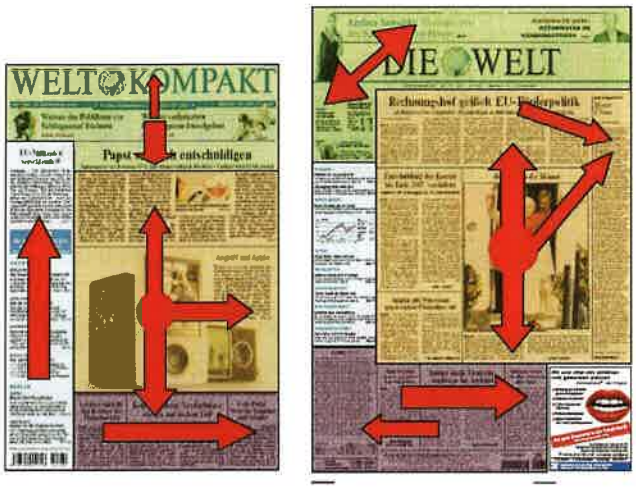

Figure 6: Zonebased reception of the frontpages of the WELT and WELT KOMPAKT

Table I: Reader types

Types of readers	Front page *WELT*	Frontpage *WELT kompakt*	Inside page *WELT*	Inside page *WELT kompakt*
In-depth-Reader	15	8	21	18
Superficial reader	8	7	0	3
Scanner	0	6	2	2
N	23	21	23	23

Table I shows that the front pages have the most distinct distribution of the tree reader types. On the front page of the *WELT* the biggest group are the in-depth-readers, and there are no scanners. On the front page of the *WELT kompakt* the three types are nearly balanced. Obviously the front page of the *WELT kompakt* stimulates a scanning pattern whereas the broadsheet favours more in-depth reading. This difference nearly disappears on inside pages which are designed as topically coherent double pages in case of the compact format. But in general for most pages of the two formats the in-depth reader is typical of the broadsheet whereas the cursory readers or the scanners are more typical of the tabloid format.

7. Conclusions

The results of our comparative research on the two types of newspaper formats show that from an audience perspective they both represent different styles of news coverage and different styles of news design. The data from different types of pages show as well, that it is not inherent in the format of a newspaper how it is used by its readers. Rather it is the interaction between individual habits of newspaper reading on the one hand and the design and the content of a newspaper on the other hand which determines the process of reception. Of course different formats prefer different forms of news. This is why the study shows some typical patterns of audience behaviour for each format. For most pages of the two formats the in-depth reader is more typical for the broadsheet whereas the cursory readers or the scanners are more typical of the tabloid format. For this reason format change in itself is not the magic bullet to stop the declining readership even if the compact format has been evaluated significantly superior to the broadsheet. A clear majority of the subjects in this study prefer the compact format because of its convenience, usability and its transparency in the design of the content. Especially the results from the reception of the double pages in the compact format show, that small format does not inhibit great journalism and in-depth-reading. The task for the future is to create reader-oriented and reader-adequate newspapers in which the format and the form of news are corresponding with each other. Newspapers in a compact format are not only miniaturizations of broadsheet newspapers. They are newspapers of their own type for which journalists have to learn a new style of news presentation including new formats of news. Of course the results of this study are influenced by the type of the two newspapers which have been investigated. There are many more types of newspapers, especially with a compact format.

Besides the reputable and more quality-oriented type of the *WELT kompakt* there are free dailies in the compact format, tabloid papers with tabloid journalism or just supplements of broadsheet newspapers in a smaller format. Further studies in audience research are necessary to get a more complete picture on how format can influence the reader-newspaper interaction.

References

[1] Arnold, E. C. (1981): Designing the Total Newspaper. New York [u.a.]

[2] Barnhurst, K. G. und Nerone, J. (2001): The form of news: a history. New York [u.a.]

[3] Blackhurst, R. (2005): The freeloading generation. In: British Journalism Review, 16. Jg., 3, S. 53 - 59

[4] Bughin, J. and Poppe, H. (2005): Dwindling readership: Are tabloids the answer? http://www.mckinseyquarterly.com/article_page.aspx?ar=1576&L2=17&L3=65 (Registration) [Downlaod 28.10.2005]

[5] Bucher, H.-J., Büffel, S., Wollscheid, J., 2005: Digital newspaper as E-paper. A hybrid medium between print an online newspaper. Darmstadt: IFRA

[6] Garcia, M. (2005): The impact of the compact. An in-depth investigation of the renaissance of the tabloid format (Version 1.0). http://www.garcia-media.com/files/GM_whitepaper050505.pdf

[7] Garcia, M. R. (1993): Contemporary newspaper design: a structural approach. Englewood Cliffs, N.J. [u.a.], 3rd Ed

[8] Garcia, M., Stark, P. 1991: Eyes on the News. Petersburg

[9] Haas, M. (2004): Kostenlose Pendlerzeitungen - ein Update. In: Ifra (Hg.): Special Reports, 6.25.2. [Free Commuter Dailies - An Update]

[10] Holmqvist, K. and Wartenberg, C. (2005): The role of local design factors for newspaper reading behaviour - an eye-tracking perspective. http://www.lucs.lu.se/ftp/pub/LUCS_Studies/LUCS127.pdf [Aufruf am 28.11.2005]

[11] Holsanova, J., Rahm, H., Hol omparing a semiotic analysis with eye-tracking measurements. In: Visual Communication, 5(1), 65 - 93

[12] McNeal, C. (2007): Editorial. In: Design, 1, S. 2

Designing community-based print products

Katri Grenman[1], Minna Forsell[1], Marjoriikka Ylisiurua[1], Hanne Roschier[1], Mikael Malanin[2]

[1] Oy Keskuslaboratorio - Centrallaboratorium Ab (KCL)
P.O. Box 70, FI-02151, Espoo, Finland
E-mail: katri.grenman@kcl.fi, minna.forsell@kcl.fi, marjoriikka.ylisiurua@kcl.fi, hanne.roschier@kcl.fi

[2] Laboratory of Media Technology, TKK
P.O. Box 5500, 02015 HUT, Finland
E-mail: mikael.malanin@tkk.fi

Abstract

The main objective of the research was to develop new print media product concepts by combining the strengths of web and print. User- and community-centered design procedures had an important role in the study, as the product concepts were developed in close collaboration with the chosen community. The design procedure was tested with a case study involving a popular online community for young people. New hybrid media product concepts were formulated and the media experience of prototype products will be tested with the community that was involved in creating the product concepts. We believe that augmenting online services with physical dimensions can be used as a way to improve the quality of the user experience and to provide possibilities for new business revenue.

Keywords

Community-centered design, hybrid media, online community, social media, user-centered design

1. Introduction

1.1 Background for the study

Print media is facing difficult challenges from other media, and the goal of this research project was to find ways to develop new and interesting print products in order to keep print media competitive and also to reach new print media users. One approach that has been used is the development of *hybrid media*, defined as combinations of print and digital media. Usually, hybrid media development has focused on ways to incorporate a digital dimension to print products (such as printed codes, which can be read using mobile phone cameras). In the current project, the target was on developing print products associated with digital media.

Users have become active participants rather than just passive receivers of media content. The phenomenon is usually called social media. Often a community effort is used to create, share and discuss the content. Services like Flickr, Wikipedia and YouTube are prime examples: they show that users are ready and willing to be educated and entertained by their peers. Our research tried to utilize this creativity and group spirit to encourage users to create and express themselves also in print. The resulting products could reach new user groups and serve a wider variety of interests and needs than what is currently achieved. The key challenge was in developing a design procedure which could be used to tie online and print media together.

1.2 User experience of hybrid media products

One of the most demanding aspects in product development is to make sure that the product is what users really want and need [Faulkner 2000]. Users' attitudes towards a certain product can be studied with the notion of user experience which combines both task and non-task oriented aspects of product use.

Katz et al. presented already in 1973 that the pleasure connected to the use of any media depends on the content, exposure to media per se and the social context of the media use. Factors affecting the quality of an online service are for example the content, structure and navigation, visual design, functionality and interactivity [Sinha et. al. 2001].

Preece (2000) mentions usability and sociability as important quality factors for online communities. Sociability refers to those social policies and technical structures that support the community's shared purpose and social interactions among members.

Developing hybrid media products requires consideration that goes beyond the user experience of one medium. In contrast to plain online services, user experience of hybrid media services consists of both the virtual and physical domains. In the case of a community we can also recognize a social domain. Care must be taken to consider the transitions and contact points between different domains. According to Dena (2006) transitions should not be *"just transitions"* but part of the entertainment experience.

Connections between the physical and virtual have previously been studied e.g. by Magerkurth et al. (2004) who present a model for the connections between the different domains. They studied computer games and saw the addition of physical and social elements as a way to enrich the user experience.

1.3 The studied online community

A large Finnish online community, IRC-Galleria (IRC Gallery), was chosen for the case study, and the preferences and needs of its users were studied. Ghoshal and Holme (2005) define Internet communities as *"... a set of HTML-pages facilitating some type of directed messages (i.e., not all messages are broadcasted to the whole community), and where each member is associated with a home page"*. Online communities are also defined to contain four main building blocks: people who interact socially, a shared purpose, policies and computer systems [Preece 2000]. IRC-Galleria meets these criteria. It is a photo gallery website with over 430,000 registered users and about 750.000 - 800.000 unique visitors each week [TNS Metrix 2007]. Over 60% of Finnish teenagers use the site, and the average age of users is 19.6 years. [Dynamoid Oy 2007] The site has evolved from a photo community into a communication medium, with people conveying information and socializing by commenting each others' pictures. The site operates on a *freemium* business model [term coined by Wilson 2006], where the basic use of the service is free and ad-supported, but users can choose to purchase a premium VIP package with additional features. Users have a long tradition in development and participation, and often suggest new features to administrators.

Although photo-sharing is usually a straightforward task, there are differences between popular photo-sharing websites. Van House (2007) has written about Flickr, stating that it is *"mostly about images, not images as adjuncts to text"* and that users said Flickr wasn't where you had discussions. In contrast, IRC-Galleria is maybe more text than picture oriented, and its themed communities are text-only discussion groups. The essence of Flickr seems to be in images and tagging, for IRC-Galleria it's more about people and communities. IRC-Galleria photographs typically have people in them, and the default picture (that can't be hidden from anybody) must be a photo of the user. In both Flickr and IRC-Galleria, most of the interaction seems to be with people users also know offline. In these cases, the photographs in both services seem to serve a similar purpose: they tell your circle of acquaintances what is happening in your life. [Van House 2007, Lehtinen 2007].

1.4 Community-centered design, participation and online communities

Access to computers and the Internet have made usability and participatory design research more popular [Jones et al. 2006]. Preece (2000) describes community-centered development as a process where the community itself is developed: the community is at the center of the design process, and the members build the community together with its developers. In IRC-Galleria, users are involved in innovating and developing the service, either by suggesting features or using the site in new, creative ways which the service grows to accommodate. VIP users can modify their profile pages with style sheets. The service has also been developed through user observation. The current state of the service is a good indication of its evolution: it has come a long way from being a gallery with just Internet Relay Chat (IRC) users' portraits.

Creating online communities is not difficult, but the challenge is in keeping members interested and having them participate actively. Peer photos can satisfy users' innate interest in other people and lead to participation in the community. [Kapoor et al. 2005] User profile pages are an essential part of online communities and social networking sites. They often include a lot of content contributed by users (in the IRC-Gallery case, for example pictures, modifications and comments), and they also help create a sense of

presence. Users often become fluent in reading and interpreting textual cues online, although the lack of social cues might be difficult at first. [Lampe et al. 2007]

Füller et al. (2004) studied involving online community members in new product development. They report that community members were capable and willing to participate in the virtual co-design process. Of the ideas and suggestions proposed by community members in their study, 3 - 15% were completely new to the marketing and R&D personnel of the company involved. The ideas were also judged to be attractive, which would suggest that communities can give valuable input in the product development process.

Although users have often been involved in product development, it's less common to use online communities to innovate on physical products. In fact, Füller et al. (2007), who studied innovation in online basketball communities, state that they found no empirical studies on the subject. Füller et al. noticed that there are online communities for almost every product type, hobby and life situation, and that these groups have a lot of consumption experience and knowledge on products. Using the knowledge of the online community is sometimes difficult, though, since manufacturing or distributing physical products in the virtual world is impossible. In their study, the researchers also noted that innovation creation was driven more by excitement than pure need.

Participation is a key factor in building thriving online communities, and people have different motivations for contributing [Bishop 2007]. In IRC-Galleria, participation can take on many forms, e.g. adding pictures, commenting, participating in community discussions, competitions and polls. Even just looking at pictures leaves a mark, since users can enable an automatic guest list feature that allows them to see who has viewed their pictures. Users also have counters that show how many times their pictures have been viewed. Participating in polls and surveys posted on the website can be attractive also to less active members, since it provides an anonymous and invisible way to make a contribution.

The IRC-Galleria site is all about interaction. The introduction to the service usually comes from real-life friends or siblings [Lehtinen 2007]. Getting attention from other members of the community, in this case comments on your pictures, is an important motivator in keeping up the interest and future participation [Lampe & Johnston, 2005]. According to Bryant et al. (2005), participation can be viewed as membership in a community, and one of the most important aspects in a community is the identity which can be both established within the community and derived from it. Although IRC-Galleria is not a major part of young people's identities as such, the communities they belong to reveal a lot about their lives and values.

2. Methods and progress of the study

2.1 User study

The starting phase of the study was getting to know the users. This was done both by observing the users-with researchers using the service themselves-and by interviewing 13 IRC-Galleria users aged 12 - 25. Users were asked about their communication and interaction, their use of the service, and their media use in general. Participants were also asked to draw two sociograms, graphic representations of the social links they have, based on their connections in the physical world and in the online service [Lehtinen 2007].

Based on the results from the interviews and observations, a workshop session for active IRC-Galleria users was organized. The seven participants were from some of the most active age groups (13 - 16 years old). In the workshop, the participants were divided into two groups. These groups had three different tasks to complete: metaphor elicitation [Zaltman & Coulter, 1995] based on the Gallery service and communication, evaluation of existing web-to-print products, and discussion on different communication methods and their benefits. The participants also filled out a questionnaire asking their opinions about the best communication media for specific use scenarios and the future of communication.

The users were not asked to develop new ideas themselves, but the workshop yielded information on what users felt was important to them and what media they used to communicate with other people. We found that the youngest participants, aged 13, didn't feel the importance of having any physical products (such as photo books) to preserve their memories. The older participants, aged 15 - 16, were already more interested in storing their memories and having something concrete instead of just files on their hard drive-which they were afraid might get destroyed if something happened to their computer.

Although parents bought the equipment and usually paid for all expenses, they were not allowed to see everything their children were doing online. Most of the participants hadn't shown all of their photographs to their parents, although parents were usually aware that their children were using photo gallery sites. Friends were very important, and the IRC-Galleria website enabled young people to share what was going on in their lives. MSN Messenger was also an important communication tool, since it enabled real-time conversations better than the website.

The importance of friends was also emphasized when it came to preserving memories. Users said that they were reluctant to remove certain photographs because of the "legendary" comments that were related to them. They even expressed interest in doing for instance a yearbook of their school class.

2.2 Developer workshop

The results gained from user studies were first analyzed with a small group of developers using affinity diagramming [Brassard 1996]. The resulting material was used in the actual developer workshop as innovation material alongside the results of user studies. Twelve developers, including researchers and IRC-Galleria staff, participated in the session.

Based on the presentations of user research data, participants wrote down their ideas and key words. The developers were divided into three groups consisting of three members each (one IRC-Galleria employee and two researchers). The groups were given a task of organizing their notes into as many groups as they wanted according to a theme of their own choosing. After this, they formulated one product concept based on each of these groups. The concept required a short description of the idea and its potential, including the financing and necessary partners.

The developer workshop yielded 25 concepts, some of which were quite alike. The concepts were entered into a worksheet and given for developers, both workshop participants and some outsiders, to evaluate. The popularity of the ideas was determined by evaluating them on a three point scale: A for excellent ideas, B for mediocre ideas and C for poor ideas. There didn't seem to be much difference between the ratings of people who had participated in the workshop and people who hadn't. The people were free to choose the basis of their evaluation themselves, and people had indeed approached the task from different directions. Most had focused on the user viewpoint, some on business potential, practicality and technical feasibility.

The five most popular ideas were chosen for a further user study. Of the 25 ideas from the workshop, 9 didn't have any print media connection. Ideas involving print media were more popular in the evaluation, which might have been due to the fact that ideas involving new IRC-Galleria features or services were more foreign to most of the evaluators. The researchers participating in the project were also more interested in product concepts combining print and web.

The chosen ideas were also quite different from each other. They are presented in Table I in order of popularity according to the developer ranking.

Table I: Best-rated product and service ideas

Position	Idea	Description
1.	Art picture exhibition	Photographs and drawings submitted by users to a vote, best pictures chosen for a real life gallery exhibition
2.	Printed information package for parents	A package telling about IRC-Galleria and its use delivered to the homes and parents of IRC-Galleria users
3. (tied)	Gallery in print	Possibility to order items with Gallery pictures on them: printed photographs, postcards, mouse pads, posters, T-shirts etc.
3. (tied)	IRC-Galleria visiting cards	Cards with the user's nickname, photo and possibly other information from the profile. Cards could also have 2D codes linking directly to the user's profile.
5.	Extension to VIP features	More features to be included the existing VIP package, e.g. more extensive user profiles, more communities, advanced guest list, TOP 10 pictures, network diagram, gossip newsletter etc.

A questionnaire was formulated to ask user preferences concerning the ideas in general. Opinions on certain features and options were asked on a 6-point Likert scale, thus making it a forced choice between the positive or negative aspects.

3. Results from the user questionnaire

The questionnaire was posted for 22.000 users on the IRC-Galleria website and received 443 replies. The amount of replies to individual questions was slightly smaller, since not all users answered every question.

Of the respondents, 27% were male and 73% female and most (68%) were between the ages of 15 and 21. This group could be labeled as "young adults". In the user workshop study, the 15-year-olds had different preferences than the users who were only a couple of years younger. This age group is interesting, because they often have an active social life and potentially face many changes in their lives during those years: finishing school, going to the army, spending a year abroad as an exchange student, starting their studies, and moving out of their parents' home. Many of these situations could encourage users to document their lives and want something concrete to preserve those memories.

Users were asked to rank the ideas in their order of preference from 1st to 5th. Figure 1 shows the rankings of the whole user group. In comparison to the whole group, the under 18-year-olds' replies accentuated the extremes; the youngest participants gave higher percentages for the highest scoring options and lower for the lowest ranking ones.

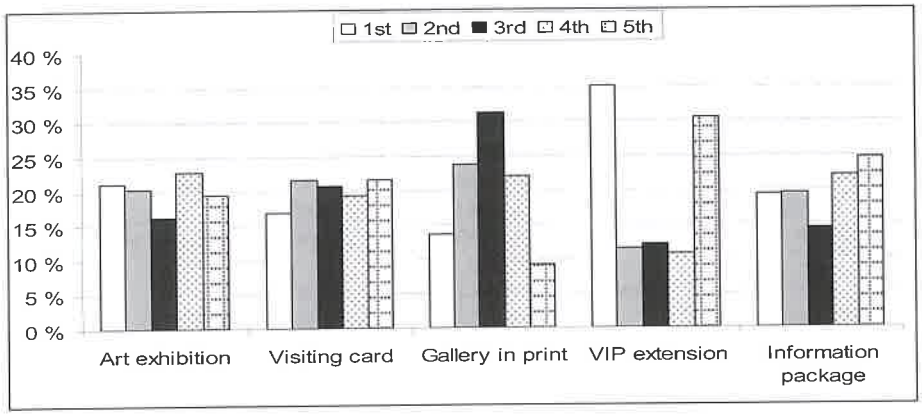

Figure 1: Idea ratings by the whole user group

The most popular concept was the VIP extension, but it also received the biggest amount of 5th place ratings. The "Gallery in print" idea had a very different popularity curve, peaking in the middle. With the under 18-year-olds, the VIP extension feature got over 39% of the 1st place rankings.

Some comments from users concerning the ideas are given in Table II. This illustrates the attitudes and preferences of users who answered the questionnaire.

There were several main themes emerging through the comments. The VIP features caused concern because of their price, which is an issue for many users. Currently the standard VIP feature package costs 10 € for a year or 3 € for two months, and these prices are already too high for some. If additional features cost more, they would be even more out of reach. On the other hand, adding new features only for the paying customers might also be seen as unfair. The attitudes towards "merchandising" or IRC-Galleria taking a step towards the physical world from the virtual world were divided. Some users want the service to stay as it is and have no link to the outside world; others want to extend the experience to the physical world. Traditionalists wished the service had stayed as it was when it started: a Web site for Internet Relay Chat users' photographs so that people could see who they were chatting with online.

Interestingly, many users saw an additional need for parental guidance by noting that the age limit for the information package for parents should be 18 and not 15 as was proposed in the questionnaire. Especially

older users were concerned that young people didn't fully understand how the pictures they posted online might become a problem.

Table II: A selection of comments on product and service ideas

Idea	Comments
Art picture exhibition	"Artwork by others CANNOT be downloaded from the Internet" "I would go to the museum, but it's probably only going to be in Helsinki" "Keep the Galleria as it is" "Spectators would be given an opportunity to be part of the exhibition through comments and voting." "You couldn't order other people's photos if the person whose photo you're ordering wouldn't allow it." "An exhibition would be great; it would encourage young and a little older people to continue drawing/painting/photographing. There are never too many creative people." "The Galleria has nowadays probably too much extra stuff and the whole system has drifted very far from its original purpose"
Printed information package for parents	"People under 15 years of age would require permission from parents/guardian in order to register in the Galleria." "Let's hike the age limit really up to 18, OK?" "I wouldn't want the package to tell my parents that I have registered in IRC-Galleria." "The package should definitely be sent to the parents of everybody under 18, it would limit greatly those "i'm 12 and i have boobs, look!" pictures put in the Galleria."
Gallery in print	"Pretty unnecessary… this kind of… merchandising" "Of course there has to be a fee for example for photographs ordered as prints. No ads, but postcards for instance could be modifiable by adding text or something else." "I wouldn't want any stranger to have prints ordered of my photographs! But I might like to order prints from my own or my friends' photographs in IRC-Galleria." "Every time that somebody would like to use my photographs I should get a message asking me whether the person in question can use my photographs."
IRC-Galleria visiting cards	"If this is made possible, nicknames need to be permanent. Name changing should be disabled." "No cell phone numbers displayed. The Galleria is a gallery, an anonymous place. Email is for exchanging contact information; you can get the cell phone number there by asking." "Sounds nice! That would be handy, like when you meet a nice person for example in a concert you can simply exchange Galleria-cards and you can then keep in touch! Great!"
Extension to VIP features	"No public friend lists under any circumstances! Otherwise you couldn't keep people you stalk on your friend list." "Possibility to win a VIP package. Some people simply can't afford it." "Every feature separately with their own price and the possibility to modify the contents of packages." "Some VIP features would become free for everyone, e.g. adding attention boxes in photographs" "Map of how users are connected... should be seen somehow as your own network, not so that anybody can see how you are linked to others, because with such services the Galleria is becoming more and more risky, a revealing place."

Concern over the copyright of pictures was apparent, but that was not the only reason people wanted to limit how their pictures would be used in print. Having total strangers order their pictures in printed format was undesirable, even if the same pictures could be viewed online at any time by the same strangers. Somehow involving print seemed to make the pictures more real.

The fear of being left out affected the outcome for the VIP features, but the same effect was visible also with the art exhibition. There were dejected comments about the exhibition from users who were almost certain that the exhibition wouldn't be held near their place of residence, but rather only in Helsinki. One of the challenges of designing physical products for a virtual community is ensuring equal opportunities for users around the country or even the globe. Online, geography doesn't matter, but in the real world it can sometimes become a hindrance.

Price was an issue in many cases. Not surprisingly, most users would prefer products that are ad-free but still do not cost anything to the users. Products that are free for users but contain ads are much less popular. Of course, this doesn't necessarily mean that they wouldn't be used if they were offered. Good quality and look are also important. According to the users, the look of the products doesn't have to bear any resemblance to the IRC-Galleria service.

Based on the questionnaire and developer opinions, as well as the novelty factor and easy implementation, two ideas were chosen for prototyping. The chosen ideas were the visiting cards and the art exhibition, even

though they didn't emerge as clear favorites in the user survey. They were chosen, because the ideas could be implemented or at least tested quite easily, thus gaining further insights about their viability and success among the target group.

There weren't big differences between the average scores for different ideas in the questionnaire. Since the project was about developing print or hybrid media products, it was noted that new VIP features were desirable but couldn't be implemented in this project. The Gallery in print idea was interesting, but quite vague. In addition, all of the products associated with the idea were already available through existing online services. The fact that IRC-Galleria photographs are resized to minimize the storage space needed further complicated the issue, because the service would have to develop a new procedure for obtaining photographs with the necessary resolution. The information package was an interesting idea, but testing it would have proved difficult since it wasn't really a service for the users of IRC-Galleria themselves rather than their parents.

4. Developing and further testing with users

Based on previous research on media, community services and connections between the physical and virtual [especially Katz et al. 1973, Preece 2000 and Magerkurth et al. 2004] and existing results from the case with IRC-Galleria a combined model for the relationships between different domains of experience was created (Figure 2).

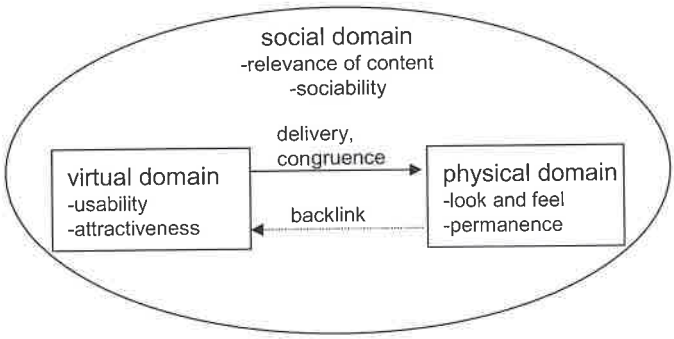

Figure 2: Relationships between the social, virtual and physical domain

For a community product, it is important that the content is relevant so that it serves the purposes of the community and its members and is sociable in nature. As in the case of IRC-Galleria, new products should support interaction between members and the chance of getting attention. For the virtual domain it is important that a usable and attractive interface that leads to the physical domain is provided. For the physical domain the most important features are the "look and feel" and permanence which cannot be fully experienced virtually. IRC-Galleria members felt that putting things on paper makes them more permanent and real both in a good (preserving memories) and bad sense (losing privacy).

Between the virtual and physical there are also the questions of the suitable level of congruence that should exist between the virtual and physical product, and how the physical product should be delivered to the user. Some IRC-Galleria users felt that the service is good as it is and no extensions should be made. The matter of delivery was paid attention to e.g. in the case of the art picture exhibition, when some users felt being left out. There is also the possibility for a back link from the physical to the virtual which can be accomplished for example with printable codes. Some IRC-Galleria users found it a great idea that they could have visiting cards with links to their profiles.

Working prototypes of the chosen concepts will be created with some variation in their functionality and appearance. After the prototype products are finished, the media experience relating to them will be tested with community members. Methods applicable for studying the overall experience of hybrid media products are determined, considering both the traditional usability and also beauty, and the hedonic, affective and experiential aspects of media use. The prototypes will be presented to test users who have the possibility to familiarize with them and make comments. In addition they are asked to perform tasks and are interviewed with semi-structured questions. The model presented in Figure 2 will be used as a basis for forming questions concerning different aspects of the user experience.

In addition, the issue of specifying how the proposed hybrid media product concepts could be produced in real-life conditions will be considered as well as the potential business model for hybrid media concepts. The business model study will involve first of all a specification of the technical platform which would facilitate cross-channel web and print content production and publishing. Furthermore, the aim is to evaluate the value that such products would create for the different actors in the publishing process and discover some critical factors for success. These tests will be finalized later this year. The eventual publication or realization of the ideas will be ultimately decided by IRC-Galleria, who will also be reviewing all the concepts from the designer workshop for their own development purposes.

5. Discussion

The design work in the process was mostly done by developers, i.e. researchers and IRC-Galleria employees. The users were involved at three stages: getting to know the community and interviews, the user workshop and the questionnaire. Users will be consulted further when testing the prototype products. The design process worked well even though the users involved were part of an online community. Recruiting individual users was sometimes hard, and much more success was met with the questionnaire which could be filled in the natural habitat of the community, i.e. online. Involving teenagers was also easier online than in person, since researchers were not present and there was thus no extra pressure.

As the research was done with a Web-based community, it was hardly surprising that users, especially the younger ones, focused on virtual extensions to current virtual services. Many users seemed reluctant to extend the online service into their physical world. Although most of the users of the service are young, there are always conservatives who would like to preserve everything as it once was, including keeping niche or sub-culture phenomena outside the reach of the masses. *"Why fix it when it isn't broken"*, commented one user. For some young users, it's also important to keep that part of their lives out of their parents' eyes, although some (especially older) members of the community were worried about what was happening and would like to see parents being informed of their children's online presence. Only a small group of respondents didn't want their parents to know they were using the service at all, but a much bigger group didn't want the information package to be sent to their parents. The under 18-year-olds were less likely to want the package for their parents, although this might be due to the fact that the over 18-year-olds didn't even expect one to be sent for their parents.

IRC-Galleria is often viewed as a tool, not something that is part of your identity. Because of this, real-life products bearing the brand might not be quite as successful as the online service: the users have no need to show the entire world that they are members of the community-which, in fact, is not a community in itself but a collection of them. Being a user of IRC-Galleria is not a way of life, although it may be one of the most important means of communication among groups of friends. The line between virtuality and physicality is very fine, and young people navigate easily between the two worlds. Eventual products must evidently give users something extra, some additional value, either by making tasks that are already possible even easier (such as ordering paper photographs through the service) or providing a completely new service that is desirable.

Distribution is always a problem in the physical world. It's difficult to achieve the same kind of geographical equality and immediacy that is possible online. The strengths of paper could turn into weaknesses in some environments; if print is for instance seen as a luxury medium, its image might be too classy for some purposes. Certain types of content fit certain platforms better than others, and print is a natural choice for services like the information package for parents. Another problem is in researching completely new things in an online environment. The ideas that are tested usually have to be based on existing things, as it is very difficult to convey the image of completely new things in an online questionnaire. Even if you did manage to do it somehow, the users could interpret the message differently and the results might not be conclusive.

6. Conclusions

The purpose of the project was to test user-centric development methods with communities in order to develop new print or hybrid media products. The project yielded new ideas that could be viable. Users were involved at several stages in the process and they participated actively. Although the users were recruited from a popular online community, the process didn't really use the power of the whole community. The formulated concepts were also more individual-based rather than ideas that could be enjoyed by the whole

community at the same time. However, the art exhibition could be an example of a unifying community experience. A hindrance for the acceptance of these innovations is that a part of the users of the online community want to preserve the status quo and not have their virtual life extended towards the physical world. Physical copies seemed to make things more real, as was witnessed with the negative and worried response to having unknown people order prints of pictures that are publicly available on the Web.

Acknowledgements

The authors would like to thank Dynamoid Oy for their cooperation.

References

[1] Bishop, J. (2007). *Increasing participation in online communities: A framework for human-computer interaction. Computers in Human Behavior 23, p. 1881 - 1893*

[2] Brassard M. (1996). *The Memory Jogger Plus +. Methuen, MA: GAOL/QPC*

[3] Bryant, S. L., Forte, A., Bruckman, A. (2005). *Becoming Wikipedian: Transformation of Participation in a Collaborative Online Encyclopedia. Proceedings of the 2005 international ACM SIGGROUP conference on Supporting group work, November 6-9, 2005, Sanibel Island, Florida, USA, p. 1 - 10*

[4] Dena, C. (2007) *Patterns in Cross-Media Interaction Design: It's much more than a URL (Part 1). Proceedings of the 1st International Conference on Crossmedia Interaction Design, March 22-25, 2007, Hemavan, Sweden, p. 4 - 10*

[5] Dynamoid Oy, *IRC-Galleria* [online]. Available from: http://irc-galleria.net/[Accessed 2 July 2007]

[6] Faulkner, X. (2000) *Usability engineering. Basingstone, Palgrave. 244 p*

[7] Füller, J. et al. (2004). *Community Based Innovation. A Method to Utilize the Innovative Potential of Online Communities. Proceedings of the 37th Hawaii International Conference on System Sciences, January 5 - 8, Hawaii, USA*

[8] Füller, J., Jawecki, G., Mühlbacher, H. (2007). *Innovation creation by online basketball communities. Journal of Business Research 60, p. 60 - 71*

[9] Ghoshal, G., Holme, P. (2006). *Attractiveness and activity in Internet communities. Physica A 364, p. 603 - 609*

[10] Jones, M. C., Rathi, D., Twidale, M. B. (2006). *Wikifying your Interface: Facilitating Community-Based Interface Translation. Proceedings of the 6th ACM conference on Designing Interactive systems, June 26 - 28, 2006, University Park, Pennsylvania, USA, p. 321 - 330*

[11] Kapoor, N., Konstan, J. A., Terveen, L. T. (2005). *How Peer Photos Influence Member Participation in Online Communities. Proceedings of the Conference on Human Factors in Computing Systems, April 2 - 7, 2005, Portland, Oregon, USA, p. 1525 - 1528*

[12] Katz, E., Blumler, J. G., & Gurevitch, M. (1973). *Uses and gratifications research. Public Opinion Quarterly, 37(4), p. 509 - 523*

[13] Lampe, C., Johnston, E. (2005). *Follow the (Slash) dot: Effects of Feedback on New Members in an Online Community. Proceedings of the 2005 international ACM SIGGROUP conference on Supporting group work, November 6 - 9, 2005, Sanibel Island, Florida, USA, p. 11 - 20*

[14] Lampe, C., Ellison, N., Steinfield, C. (2007). *A Familiar (Face)book: Profile Elements as Signals in an Onlien Social Network. Proceedings of the SIGCHI conference on Human factors in Computing Systems, April 28 - May 3, 2007, San Jose, California, USA, p. 435 - 444*

[15] Lehtinen, V. (2007), *Maintaining and Extending Social Networks in IRC-galleria. Master's Thesis. University of Helsinki, Department of Social Psychology. 97 p*

[16] Magerkurth, C., Engelke, T. and Memisoglu, M. (2004) *Augmenting the virtual domain with physical and social elements. ACM Transactions on Computers in Enterteinment, Vol 2, No 4, October 2004, 20 p*

[17] Preece, J. (2000). *Online Communities. Designing Usability, Supporting Sociability. New York, NY: Wiley*

[18] TNS Gallup, *Suomen web-sivustojen viikkoluvut* [online]. Available from: http://www.gallupweb.com/tnsmetrix/site.aspx [Accessed 13 June 2007]

[19] Sinha, R., Hearst, M., Ivory, M. (2001) *Content or graphics? an empirical analysis of criteria for award-winning websites. Proceedings of the 7th Conference on Human Factors & the Web, June 2001, Madison, WI, USA*

[20] Van House, N. A. (2007). *Flickr and Public Image-Sharing: Distant Closeness and Photo Exhibition. Proceedings of the SIGCHI conference on Human factors in Computing Systems, April 28 - May 3, 2007, San Jose, California, USA, p. 2717 - 2722*

[21] Wilson, F. *The Freemium Business Model* [online]. Available from: http://avc.blogs.com/a_vc/2006/03/the_freemium_bu.html [Accessed 15 June 2007]

[22] Zaltman, G., Coulter, R. H. (1995). *Seeing the voice of the customer: metaphor-based advertising research. Journal of Advertising Research (July/August), p. 35 - 51*

User centric approach for designing cross media applications in personal photography

Sami Vihavainen[1], *Risto Sarvas*[1], *Jaana Näsänen*[1], *Katri Grenman*[2]

[1] Helsinki Institute for Information Technology HIIT
P.O Box 9800, FI-02015 TKK, Finland
E-mail: sami.vihavainen@hiit.fi; risto.sarvas@hiit.fi; jaana.nasanen@hiit.fi

[2] Oy Keskuslaboratorio - Centrallaboratorium Ab (KCL)
P.O. Box 70, FI-02151, Espoo, Finland
E-mail: katri.grenman@kcl.fi

Abstract

The main aim of the study was to understand how people use multimedia technologies and to use that understanding in designing new cross media services.

The study looked at the future of personal photography. The research included a qualitative intervention study of ten persons' photography practices, a quantitative web-based questionnaire of photography habits and perceptions, a concept design phase with a group of ordinary people and industry and academic experts, and finally, designing, implementation and evaluation of an actual photo book service.

Based on the results we argue that designing new services in today's world of personal media, where ordinary people are more active media produces, the design should not be limited only to digital environment or print environment but to be extended to combine the best of the both platforms.

Keywords

Cross media, photography, photo book, user centered design, user generated content

1. Introduction

Digitalization and the internet have made a significant impact on media technology and the ways it is used by consumers and professionals. *Self-created media* (*i.e.*, media created by consumers, such as photographs and videos) and *professional media* (*i.e.*, broadcast and public media created by commercial media producers) have converged in a new way. As Jenkins (2006) defines it, convergence is an ongoing process or a series of intersections between different media systems in technological, industrial, cultural, and social environments. One example of this, is the flow of media content across multiple platforms. For example, the same text and image content can be published or shared in a newspaper, a mobile handset, a personal computer, and a paper printout.

In this paper we present our design process and end product for paper and digital cross media: a photo book service that combines the benefits of digital and paper as media platforms. First we discuss the benefits of both digital and paper media from the perspective of the end user, especially the personal photographer (*i.e.*, the snapshot photographer). Then we go through our methods for understanding personal photography in the 21st century and the role of paper-based products in it. We also discuss our process for designing, implementing, and evaluating the final photo book service. In the results section, we discuss the system and the lessons learned in building a cross media service. In the end, we conclude the paper and discuss the implications of our work to print and media technology in general.

1.1 The benefits of digital media

Digitalized media is often referred as *the new media.* Taking the characteristics of new media [see, *e.g.*, Manovich 2001] and putting them into the context of everyday life demonstrates the advantages digitalization brings to personal media. Due to the numerical representation of digital media there is practically no relation

between material costs and magnitude of media created. For example, one can take hundreds of photos to one memory card and also re-use the same memory card thousands of times. Requirements for storage space are minimal compared analog media, especially print media. The process of editing digital media is easier and more flexible than editing analog media. Editing can also be automated to a certain degree. For example, when a photo is taken with a digital camera, the camera immediately runs algorithms on the photo to enhance its quality or to encode it to a specific format. Also variability of digital media has made possible that nowadays media is transferred and re-used in multiple ways without degrading the quality at all. Variability also enables that, for example, the same photograph can easily be viewed on different screen-based devices such as PC, TV or mobile phone. Internet on the other hand has enabled new distribution channels. According to the Internet World Stats (2007) 16,6% of the world's population uses internet. Although he penetration is largest in Europe, North America and Australia, the biggest growth percentages in resents years have been in Africa, Middle East, Latin America and Asia.

These principles of new, digitalized media have made it possible for the ordinary people to produce and distribute self created media, in a format and scale that a few years ago was possible only for professional media houses.

1.2 The benefits of paper media

Digital media is not perfect. Paper as a media platform, has many advantages compared to digital media. The majority of the benefits come from the fact that paper is a *physical artifact* such as a photographic print or album, and not a digital object like for example a digital picture. Paper is *not a device*. To consume paper artifacts there is no need for external energy. Respectively, to consume digital media there always has to be an energy requiring device that transforms the digital information into analog. Due to the physical nature of paper it is *easily portable, handled,* and *clipped* by anyone. For example, if one sends a paper artifact to his or hers friends, he or she can also be sure that the recipients are able to see and use what they had been sent. Because of multiple formats, viewing devices, and standards, that is not always the case with digital objects. On the contrary, using a digital object may sometimes require significant familiarity with the latest technology. Paper itself has a *direct relationship to real space*, and can be, for example, posted on a wall. To post a digital picture on a wall, a specific device, or a printer, is needed to make it physical. Although paper can be easily destroyed, the history has shown that in practice paper is relatively *long lasting*. For example, books of hundred years old can still be well readable, whereas digital media is in theory everlasting, but in practice there is uncertainty on how to store them for the following generations. Paper media has *less IPR (intellectual property rights) issues* than digital media. One key reason is that it is not possible to make infinite copies of paper media. In practice this means that it becomes quickly too expensive to make several copies of media in paper format. Inexpensive copying of digital media is of course one of the key problems professional media companies are currently dealing with. To put it briefly, the intellectual property laws have a long history in adapting to paper media and the business around it - which is the opposite when it comes to digital media. In addition to functional advantages paper has also some non-functional advantages, such as *tangibility,* and *tradition and culture*. Because of tangibility, paper artifacts are individual. It is easy to develop such emotional attachments to tangible artifacts that are not possible in digital world. In traditions and cultures on the other hand, paper as a platform for media has a history of several centuries. For example, giving photographs as a gift is a well accepted tradition in many cultures.

To put it in a nutshell, paper media and digital media have different strong and weak points, and most of the advantages and disadvantages complement each other. This is the starting point in our design of cross media products and services: to view paper and digital as complementary media platforms.

1.3 Personal photography

To study the area of self created media (also called self-made media or user-generated content) we concentrate on *personal photography*. Taking non-professional photos is over one hundred year old hobby and has a long history in people's everyday lives [Ulkuniemi 2005]. It is one of the oldest forms of visual self created media. Given the long tradition personal photography has in people's everyday media environment it is possible to study it from a historical perspective - especially how the media creation technology and its uses have interacted. Chalfen (1987) is one of the first ones to truly study personal photography, *i.e.*, how people take and use photographs in their everyday life. Chalfen introduced the term "Kodak Culture" to describe

people who typically take photos in traditional events such as Christmas and birthdays and share the photos with people in the photos or people who knew the subjects of the photos. This kind of communication Chalfen called the home mode communication. An important part of Kodak Culture is also the ability to engage with the pictures. By engaging Chalfen meant that the image itself in an album is not enough tell the story around photography event but photographers tell oral stories around the photos for people who they share them with. After Chalfen, for example, Frohlich et al (2002) have got similar results about photo sharing and emphasized the role of face to face storytelling around the personal photos.

However, personal photography has not been a static phenomena in the last century but has been in constant change before Chalfens "Kodak culture" and after that. The change has happened over the years due to interaction between the technological innovations and the end-user needs [Sarvas 2006]. In recent years, digitalization has changed photography and also the whole media world dramatically. Digital cameras, camera phones, PCs and web based photo sharing communities, have largely changed the ways people take, annotate, and distribute their photographs. The fact, that costs in photography are basically the same whether one takes one or one hundred photos, and that in large amounts, digital photos are easier to handle and process than traditional film photos, has contributed that the quantity of photographs taken has increased enormously from the age of film cameras. Resent research on personal photography has been emphasized on uses of digital cameras and camera phones, and how have that new technology changed people's personal photography habits compared to film camera era. Koskinen et al. (2002) studied people's photographing and photo sharing with a combination of a digital camera and a mobile phone. They found their early camera phone type of combination to be appropriate to support storytelling. In a study of Van House et al (2005), where the focus was on the uses of camera phones in events where people wanted to share experiences with people who were not present, it was learned that storytelling done with camera phones can also be very much storytelling with images and not about images, like it is in Chalfen's home mode communication.

Internet has made it possible to show and view photographs regardless of location. It is possible to take a photo with a camera phone and immediately transfer the photo from the phone to the internet for everyone to view. Many web-based communities related to *photo sharing*, such as Flickr, the Finnish service Kuvaboxi and MySpace have emerged. Previous examples are digital image storing and management websites where social interaction between the users (e.g. commenting on each others photos) is a large part of the user experience. For example, Flickr emphasizes public sharing so that anyone can view and comment ones photos, whereas in Kuvaboxi emphasizes private sharing so that user and audience have often a pre-existing relationship (to share photos to specific audience, the user has to know the mobile phone numbers of his/hers audience). Although in both services it is possible to share photos publicly or privately, their emphases are different. In MySpace photo sharing is strongly related to social networking. There users use photos to form their personal electronic profiles about whom they really are and communicate with each other actively.

All the previous examples demonstrate how the world of personal photography has changed from the traditional photography Chalfen described. These kinds of technologies have made it possible to take thousands of photos practically for free, and share them without temporal or spatial limitations even with total strangers. These changes have actually engendered some new types of photographers. One example of this is what Miller et al (2007) call as Snaprs. For snaprs it is typical to share generally everything and they are expecting their photos would be fully viewable also to strangers.

Because of recent huge fuzz and concentration on these new technologies and services one might think that the traditional personal photography is quickly vanishing and dying away. However, like Miller et al (2007) point out, there is still a very strong genre of Kodak Culture, and for people in that genre privacy is a primary concern. They want to share their photos only with their existing social communities of friends and relatives.

What kind of a role does paper have in this digitalized personal photography environment? As discussed earlier, paper has many strong and weak points in creation and use of personal media. In photography especially, paper has some clear benefits. Paper photos are tangible and have individuality. People like to develop sentimental attachments to objects: the same paper photo in grandmother's photo album is the same photo she put there - perhaps there are her fingerprints on it. In a digital world, that kind of sentimental attachment is not possible. Printed on a right kind of paper, paper photos are also long lasting and can last through generations without a fear that it could be impossible to view them because of incompatibilities between old photo formats and new photo viewing devices. Nowadays, when digitalization is dominating the development of new photo media technologies we wanted take a slightly different perspective and start studying what kind of combinations of digital and print platforms would be useful in people's personal photography habits.

2. Methods

2.1 User - centric design

In User centric design (UCD), the principle idea is that users and their needs should be kept in the central focus during the whole design process [Preece et al. 2002]. In the definition of Vredenburg *et al.* (2002) UCD considers the practice of three principles: the active involvement of user for a clear understanding of user and task requirements, iterative design and evaluation, and a multi-disciplinary approach.

The history of "user-centric design" comes from the computer science in late 1980's from attempts to find, validate, and integrate in holistic design processes methods that would facilitate designing good interactive applications for various kinds of end-user groups. Initially the focus was on evaluation: researchers, and later also practitioners, established "usability laboratories" for studying the response of users to interactive applications intended to be used for specific tasks in specific contexts. Later the emphasis shifted to methods for eliciting and representing user requirements and needs, and methods for driving the design work on the basis of this. The ISO 9241-11 standard codified the results of this in a widely accepted and applied form [Sarvas et al. 2007].

However, as pointed earlier, from that time there have been new technological developments that have been shaking the foundations of people's use of technology in their everyday lives. First, in 1990's, the internet was introduced to the general public, and almost simultaneously the mobile telephone. During the 2000's, these technologies have converged, creating for the first time a global communications network that covers nearly the whole planet and its population. The field of communication has become more complex. Creation of useful, usable, and pleasing applications for such a wide domain challenges the present understanding and methods of user-centric design. It is no longer really feasible to elicit user needs using the methods originally developed for studying office employees working on relatively limited tasks; nor is it possible to evaluate the systems in laboratories. Instead, researchers and practitioners have started to use and adapt approaches and methods from those sciences that always have studied the behavior of people, groups, and communities in everyday life contexts: psychology, cognitive science, sociology and social psychology, microeconomics, media studies, etc. It has also been realized that design and field experimentation must be blended in a new interactive fashion in order to develop applications intended for varying real-life conditions. This latest shift in user-centricity is still being studied in the research and practitioner community. Some success has already been gained from using methods such as ethnography, end-user innovation, extensive field studies combined with analysis, but the domain is still rapidly developing. One of the fields that is screaming for better design methodology is media business, which is going through fundamental changes [Sarvas et al. 2007].

By following the principles of UCD we collected information, gained an understanding of current personal photography practices and designed and constructed a cross media application. We used five different studies The studies were part of a large research project on personal photography and paper media. The studies made were a qualitative user study on photography practices, a quantitative survey of general attitudes and practices around photography, a concept design process involving regular users and experts, a construction and an evaluation study of photo book prototypes, and a final construction and evaluation of the application itself. The studies supported each other so that each separate study gave information and building blocks for the following studies.

2.2 The qualitative user study on photography

The qualitative user study was conducted by interviewing ten people from different backgrounds regarding their photos and photography related practices in southern Finland in 2005 - 2006. The goal was to get understanding of people's use of photography related technologies, digital and print, in their everyday lives. The ten users' age, gender and occupation were as follows: 13M schoolboy, 15F schoolgirl, 23M student, 23F student, 43M entrepreneur, 43F teacher and farmer, 45M unemployed, 50F employment agent, 59F university lecturer, 61F retired. The users were not very technology savvy but new technologies such as internet, and digital cameras were not unfamiliar to them either. All of them used a computer at their homes or at least at the office. All of them, except 50F had a digital camera in use. None of them were a professional photographer. 15F and 43F had some interests in taking artistic photos. For example 15F was very keen in publishing photos in photo related web communities. 43F and 59F took photos they could use in their teaching. Otherwise participants' photography was pretty casual. They took photos to document their

everyday lives, for example photos in family events, parties and photos of grand children. Three of the participants (13M, 23F, 43M) had a camera phone of their own, but the quality of their cameras were very basic compared to camera phones they were given.

The approach of our qualitative study was ethnographic. We interviewed each test person about their photography, use of information technology, and social networks. We also looked at their photos (both digital and paper) at the same time the person telling freely about them. After the initial interview we made an intervention to each user's personal photography infrastructure by giving them a Nokia N70 camera phone, a Canon iP5200 photo printer, and access to a photo sharing web-service Kuvaboxi.fi to use for 6 - 8 weeks. We helped them to install the new devices and configured them to work with their computers and transferred their contact information from their old phone to the new one.

We also gave them basic guidance in using the new technology. However, we emphasized that they were not obliged to use any of the introduced devices or the service. After the 6 - 8 week test period we went through the captured and printed pictures with each user. We also interviewed the users about their use of the devices and the technology in general. Each of the interviews was analyzed by first making notes based on audio recording and then, by using the notes as preliminary information, analyzing the interview in a group session where a group of researcher watched the video recording, discussed about it and made notes. Based on the notes of the group sessions a user profile was reconstructed of each participants. These user profiles included the user's social network, hobbies, photography experience, and use of photography technologies (e.g. photo sharing, editing, archiving, and organizing). These analyses results were used as background information in the later phases of the study.

2.3 The quantitative survey study on photography

Even if digital photography has become an important part of to today's information society where people regularly use computers, internet and other digital equipments and services, there is no reason why new digital technology would unquestionably had supplanted the traditional photography media of physical paper photos and film cameras. To get some light for the current state personal photography in Finland, based on the preliminary results of the qualitative study, a web based questionnaire was constructed and implemented. There was a need to get information on how much do people currently use different photography related devices and services. What is "hot" and what is not? Does a digital divide exist? Do young generations use this area of information technology differently from the older generations? Do females have considerably different photographing habits than men? In print related questions, respondents were asked about the proportion of digital photos they print or get otherwise printed, and about the ways they get the prints. In both questions age and gender effect was studied.

Questionnaire was distributed through three Finnish websites: IRC-galleria (a photography related web community by Dynamoid, where majority of the users are teenagers), Kuvaboxi (a photo sharing website by Futurice), and luukku.com (an email service of the media company MTV3). The survey reached 80.770 first-time visitors (based on web browser information) and 13.564 submitted answers were recorded in our database giving a response rate of 16,8%. After pre-treatment 1.029 of the responses were eliminated and 12.532 respondents were left for the actual analysis. In the pre-treatment duplicate rows, empty rows and clear outlier answers were deleted (e.g., 9.999 shots reported to be taken per month and age being 99).

2.4 The concept design

Our third approach was the concept design phase. Based on our findings in the qualitative study, we arranged a group of experts to design concepts for personal media use. All the experts were familiar with the user profiles and other results achieved in the earlier phases. The role of paper was noted but to keep the thinking as much "out of the box" as possible it was not a requirement for the concepts. Another group, which consisted of four of the ten test persons in the qualitative study (15F, 23M, 43M, 61F), gave feedback to the concepts sketched by the experts. The purpose of this second group was to get feedback from non-experts or non-professionals early in the development phase.

The group of experts consisted of seven researchers and two industry experts. The experts had four half-day meetings: the first two meetings introduced the findings of the qualitative study, the third meeting was

designing concepts in three sub-groups, and the last meeting was the rating of the concepts and selecting the best ones In the middle of the meetings, the group of non-experts met twice and gave their idea and feedback.

2.5 The photo book prototyping

Based on the concept design phase five physical photo book prototypes were designed and tested with a group of users. The aim of the group testing was to present the prototype books to a potential group of customers. Based on the results of the quantitative and qualitative studies the focus group participants were gathered from approximately 30-year-old mothers. Fifteen users were tested in total. All of the test subjects were female and all but one of them were over 30 years old. Only two of the test subjects didn't have children. Testing was conducted in two separate arrangements. The first group consisted of twelve participants, who all had background in either printing or paper research. As a comparison the second group consisted of three participants with no background or education in paper or printing field.

The aim of the study was to discover which photo book attributes users find attractive, which features they would prefer and what could be done to improve the books. The users were also asked what they would be ready to pay for each of the books. Based on the information gathered, choosing an attractive photo album format and setting and acceptable price on it would be easier. Although the respondents had different preferences, we were able to find one album that was quite popular with all the users. In addition to this, we gathered information about the attributes and features that affect the choices users make.

2.6 The construction and evaluation of the final service

Based on all the previously gained knowledge, we started building a web browser based system for designing and ordering photo books. The context of the service was the Kuvaboxi photo sharing website, but the application was built as a separate component. The work was done in close co-operation with the designing of the prototype photo books. Also to gain knowledge about the usability of the service a small three participant user study was implemented. In that the participants designed a photo book with the constructed application and couple of weeks later received an actual photo book they each had designed. A more detailed account of the design and implementation of the system can be read in Vihonen (2007).

3. Results

Following chapters present the results of the each study phase and how did the results affected to the design and construction of the final photo book service.

3.1 The results of the qualitative study

The main result the qualitative study was the complexity of today's consumer photography technology. The digitalization of photo technology has made the use of the technology rather complicated to an "average" person. The fact that media is numerically representative, automated, and residing in abstract spaces can make digital media very abstract and difficult to understand and to control. Digital technology has made bridges, but also created barriers. That is especially if the technology has not been built to be intuitive and easy enough to use.

Through digitalization, photography has been concretely plugged into the information and communication infrastructure. An example result of this is the camera phone, which combines a camera with a phone and the Internet and mobile phone billing. To leverage the basic functionalities of digital photography, such as storage on a hard disc, sharing photos over the Internet, printing photos with the home printer, or viewing them on the computer screen, requires an interaction with a computer infrastructure. The implications of this are that photography is more technical and complex than before (if the available new technology is used), and that new personal media technology has to be designed into the existing infrastructure. For example, in designing a photo book service, the designers have to consider the web browsing technology used, the types of old photo albums and books people are familiar with, and what do people photograph and want to order as a book. In other words, designers need to understand not only the technical environment at home, but also the cultural domestic environment of conventions, practices, and traditions related to photography. For example the 61F

who had owned a digital camera already for a several years just recently learned how to transfer pictures from her camera to her computer. Previously her son-in-law did it for her so for a long time she had been dependent on outside help to do a task that is supposed to be a very basic function in today's photography. Another example of the barriers was our 59F, university teacher, who during the user tests looked at her camera phone photos almost entirely from the phone's screen because she could not figure out how to transfer the photos to her computer. She would have wanted to print some of her camera phone photos but did not understand the relationships of the camera phone, the pc, and the printer so that she could have the photos printed.

One result of the changing technology is changes in people's conventions in printing pictures. Today people have to have a reason for printing or ordering pictures in paper format, they do not need to get paper copies just to view the photos. There are several reasons not to print the photos: it costs money, prints take space, and are hard to organize. Our qualitative studies showed that the pictures printed were selected and had some value in the form of memories or stories. Also paper photos were given as gifts. Digital photos did not have any value as a gift compared to printed ones. There was also some practical reasons related to viewing photos. The family of 13M printed some of their photos so they could be given to grandparents, who did not have a computer to view digital photos. Our qualitative study also showed that photography and images have found new areas of use in people's activities. Photographs are no longer only family photos of children, travels, and events. People take pictures of mundane things, pictures for practical purposes, or use them in their work. Although we do not believe that the traditional uses of photos will disappear, there are new genres of photos that did not exist as such in the era of film photography. What is the role of paper and hybrid products in the new uses is a harder question to answer. Therefore, there is an opportunity for novel hybrid media technologies to become a fundamental part of personal media creation, and the main advantage hybrid products have over solely digital technology is paper - the culture, conventions, practices, and traditions associated with paper, and the characteristics of paper itself.

3.2 The results of the quantitative study

The qualitative study showed that paper definitely still has a role in personal photography. However, we wanted to gain more knowledge of the current magnitude of this role. The results of the quantitative study confirmed the results found in the qualitative study: People clearly place value to paper photos in certain situations. There were, however, indicators these perceptions were dependent on the age and gender of the respondents. Table I shows the effect of age on proportion of print versions got from digital photos. Based on the data it was clear that ratio of printed photos got from digital photos is bigger among older people. However, in all age groups there was a group of people how did not print photos at all. The largest set of the respondents (38,4% of all the respondents) said they get 1 - 5% of their digital photos printed.

Table I: The effect of age on proportion of print versions of digital photos

How big proportion of your digital photos do you print or otherwise get printed? * Age (Banded) Crosstabulation

			Age (Banded)					
			7 - 19	20 - 29	30 - 44	45 - 59	60+	Total
How big proportion of your digital photos do you print or otherwise get printed?	I don't get paper photos	Count	957	546	314	170	39	2026
		% within Age (Banded)	20,9%	17,0%	13,6%	14,5%	12,4%	17,5%
	1-5%	Count	1865	1299	808	386	87	4445
		% within Age (Banded)	40,7%	40,5%	35,1%	33,0%	27,7%	38,4%
	5-25%	Count	985	664	532	305	88	2574
		% within Age (Banded)	21,5%	20,7%	23,1%	26,1%	28,0%	22,3%
	25-50%	Count	463	314	263	139	40	1219
		% within Age (Banded)	10,1%	9,8%	11,4%	11,9%	12,7%	10,5%
	50-75%	Count	207	216	200	66	27	716
		% within Age (Banded)	4,5%	6,7%	8,7%	5,6%	8,6%	6,2%
	75-100%	Count	102	165	184	103	33	587
		% within Age (Banded)	2,2%	5,1%	8,0%	8,8%	10,5%	5,1%
Total		Count	4579	3204	2301	1169	314	11567
		% within Age (Banded)	100,0%	100,0%	100,0%	100,0%	100,0%	100,0%

When gender was studied it was found that it is involved in the proportion of paper photos printed (Table II). Male respondents got less printed photos than female respondents: 22% of males said they do not get prints at all, whereas 16% of female said the same. Similarly 3% of males said they get 75 - 100% of photos printed, whereas among females the number was 6%. The findings indicate that especially some younger men, do not get paper photos as much as others, whereas older women get their photos printed more often than others.

Table II: The effect of gender on proportion of print versions of digital photos

Gender * How big proportion of your digital photos do you print or otherwise get printed? Crosstabulation

			How big proportion of your digital photos do you print or otherwise get printed?						
			I don't get paper photos	1-5%	5-25%	25-50%	50-75%	75-100%	Total
Gender	male	Count	824	1623	767	283	151	127	3775
		% within Gender	21,8%	43,0%	20,3%	7,5%	4,0%	3,4%	100,0%
	female	Count	1210	2825	1818	937	566	470	7826
		% within Gender	15,5%	36,1%	23,2%	12,0%	7,2%	6,0%	100,0%
Total		Count	2034	4448	2585	1220	717	597	11601
		% within Gender	17,5%	38,3%	22,3%	10,5%	6,2%	5,1%	100,0%

When respondents were asked how they get their photos printed, the most popular way appeared to be printing them at home with a home printer (Table III). However, ordering prints via internet was also very popular. It was interesting to find out that taking a memory card to a photo shop is at third place only. That is because that procedure to get photos printed is exactly the same that what people have used to do with film cameras. The analysis of age and gender effect showed that children and teens, and people over 45 use home printing more than others. Thus it seems that photo printers have found their way in families, whereas young adults and middle aged people preferred more often to order photos via internet. It was also notable among senior people (60+) taking the memory card to a photo shop was more popular than among other age groups. That indicates they are have adapted the traditional ways of doing things. Many older people also might not have an internet access to order photos or technical skills to print photos themselves, but prefer to use professional services.

Table III: The effect of age on way to get print versions of digital photos

Age (Banded) * What is the main way you get printed versions of your digital photos? Crosstabulation

			What is the main way you get printed versions of your digital photos?							
			I don't get paper versions from digital photos	I print at home	I print at work/school	I order prints via Internet	I take my memorycard to a photo shop	I use a photo printing booth	other, what?	Total
Age (Banded)	7 - 19	Count	909	1555	295	812	761	101	101	4534
		% within Age	20,0%	34,3%	6,5%	17,9%	16,8%	2,2%	2,2%	100,0%
	20 - 29	Count	509	695	212	1040	536	63	98	3153
		% within Age	16,1%	22,0%	6,7%	33,0%	17,0%	2,0%	3,1%	100,0%
	30 - 44	Count	279	548	167	756	336	67	76	2229
		% within Age	12,5%	24,6%	7,5%	33,9%	15,1%	3,0%	3,4%	100,0%
	45 - 59	Count	171	353	87	234	198	40	56	1139
		% within Age	15,0%	31,0%	7,6%	20,5%	17,4%	3,5%	4,9%	100,0%
	60+	Count	41	107	14	52	65	11	15	305
		% within Age	13,4%	35,1%	4,6%	17,0%	21,3%	3,6%	4,9%	100,0%
Total		Count	1909	3258	775	2894	1896	282	346	11360
		% within Age	16,8%	28,7%	6,8%	25,5%	16,7%	2,5%	3,0%	100,0%

3.3 The results of the concept design phase

In the concept design phase the focus was in creating new product and service concepts based on people's everyday practices and needs related to media use and creation. Altogether 51 concepts were produced and assessed. Although the concepts were quite heterogeneous, many of the ones that got high ranks in the assessment involved a physical book. They were clustered in three groups according to the ratings they got and whether the experts agreed on the ratings (a concept would score lower if the deviation of ratings was high). Table IV shows 10 highest ranked concepts.

From the concepts one can see that the combination of digital technology, especially networking and media services, and paper technology have potential to form interesting new consumer products - new innovations. It is good to bear in mind, that these concepts were grounded on people's real uses and practices, and previous studies on family and snapshot photography. In other words, the concepts were designed for people, not to demonstrate the latest technology. Therefore, paper was included only when it made sense in the concept. Based on concept design phase a photo book application was decided to be constructed. The construction was a two-pronged task: Prototyping of physical photo books and constructing the actual photo book application.

Table IV: Names of the 10 highest ranked concepts

A cardboard book of familiar faces for babies
A digital service for creating a book of baby photos
Photos printed on any paper product
Do-it-yourself recipe book
Images and photos to paper cups
Collecting your student exchange year as a service
Ability to included relevant information on the backside of photos
A photo game for children with user's own photos
A wall calendar with last year's photos for each day
A photo book service for making any kinds of photo books

3.4 The results of the photo book protos

Five photo book prototypes were designed, made and tested. The books varied in shape, size and binding method. Their page layouts were quite different as well. The books were: pocket, A5L hard cover, A4 soft cover, A4L hard cover and A4 hard cover. The albums differed so significantly that users really had to make trade-offs when choosing their preferred album for a certain situation. Users arranged the albums in their order of preference in two different photo situations they could choose themselves (for example 'party' and 'holiday'). These situations were classified in three groups: parties, travel-holiday, and everyday-children. In addition inside the three groups, each album was given points for its ranking. The album that was ranked first by a user got 4 points, the second 3 and the last 0 points. These points were then summed. Thus, each album had a point score in each of the three categories. The albums were classified in a popularity ranking order according to their point scores. This provided us with a simple popularity comparison (Table V). The downside of this approach is that it easily hides differing opinions. If one user likes an album but all the other users hate it, the album gets a very low score even though it is the preferred option for one user. From the ranking test A5L hard cover book got the highest scores. It was ranked as a best option on all three groups (party photos, travel-holiday photos, everyday-children photos).

Table V: Results of the category preference ranking comparison

	parties		**travel-holiday**		**everyday-children**	
album	**points**	**rank**	**points**	**rank**	**points**	**rank**
pocket	19	3.	23	2.	23	2.
A5L hard cover	26	1.	36	1.	28	1.
A4 soft cover	22	2.	21	3.	18	3.
A4L hard cover	17	4.	19	4.	14	4.
A4 hard cover	12	5.	11	5.	7	5.

Following notes were also made. Users differed very much in needs and wants when it comes to photo album books. Some users wanted a book that resembled their old albums and looks self-made. Other users, however, wanted additional value from a made-to-order photo album, and specifically required that it didn't look handmade. However all in all three features of the actual book seemed to be most important: looks, price, and the actual photos.

3.5 The results of the photo book service

Based on all the information gathered by using the previously mentioned methods, a web-browser based photo book application for personal photo media was designed, implemented and evaluated.

Again the user tests were made for women (two mothers in their 30's and one grandmother in her 50's) Based on the user tests of the application, we noted that if a person wants to make a photo book, s/he is likely to spend time making it right. The book making process is not about putting photos to pages, but also about figuring out a story to tell with the photos. Also, a photo book is probably a product that people wouldn't try to make at home with a printer - a book was perceived as something that comes from printing press and time is spent making it.

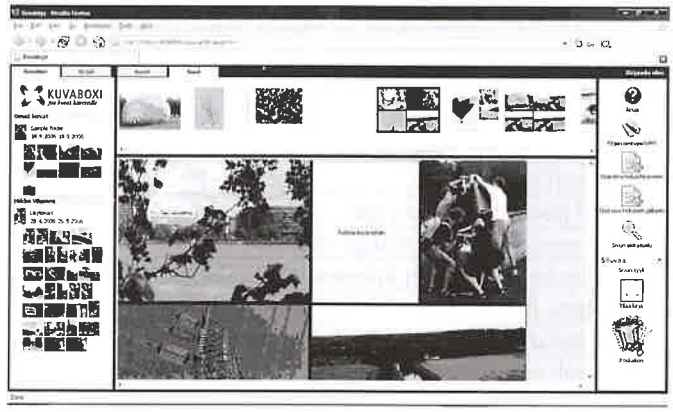

Figure 1: The web browser user interface of the photo book system

4. Conclusion

In this paper we presented our relatively broad and in-depth method in designing a cross media photo book service. Our objective was, firstly, to identify the best of both worlds: the advantages that paper and digital media have. Secondly, our goal was to design a cross media service/product that is well-grounded on user-centric design principles. The results was a photo book service. The concept of making photo books through a web interface is not a novel idea as such, nevertheless, our main contribution is in analyzing the service from the point of view of user-centric cross media.

A key point of our study is that once the advantages of different types of technologies are identified alongside with an understanding the uses of those technologies, the end result is not necessarily a high technology product. In our example photo book service, the web technology was relatively advanced but the paper and printing technology was very basic - the overall result was, nevertheless, understandable and valuable to the end-users.

In the evolving environment of self created media technology and media business (paper and digital) there are opportunities for novel products and services. The photo book is a good example (see also, *e.g.*, JPG and EON magazines or Lulu publishing service). However, to come up with successful innovations in cross media, the strong points and limitations of each technology should be understood. In our view, the current situation is such that the limitations of digital technology are often forgotten and the strong points of paper technology are overlooked.

Our future work with the photo book service is to take it outside the traditional personal photography into community services where people create visual and text media themselves (*e.g.*, gardening hobbyists). Another future step is to study the use of more advanced paper platforms (*e.g.*, paper with RFIDs or two dimensional barcodes) based on the extensive user study results we have generated.

References

[1] Frohlich, Kuchinsky, Pering C., Abbe D. & Ariss S. (2002): Requirements for Photoware. *Proc. of the Conf. on Computer-Supported CooperativeWork.* pp. 166 - 175

[2] *Internet World Stats*, Miniwatts Marketing Group, 2007. http://www.internetworldstats.com/stats.htm [referred 28. 2. 2007]

[3] Jenkins, H. 2006. *Convergence Culture,* New York University Press

[4] Koskinen, I., Kurvinen, E., Lehtonen, T.-K. *Mobile Image.* IT Press, Helsinki, 2002

[5] Manovich, L. 2001. *The Language of New Media*, The MIT Press

[6] Miller, A. D. and Edwards, W. K. 2007. Give and take: a study of consumer photo-sharing culture and practice. In *Proceedings of the SIGCHI Conference on Human Factors in Computing Systems* (San Jose, California, USA, April 28 - May 03, 2007). CHI '07. ACM Press, New York, NY, 347 - 356

[7] Preece J., Rogers Y. and Sharp H. (2002) Interaction Design. Beyond Human-Computer Interaction. John Wiley & Sons Inc

[8] Sarvas, R. (2006) *Designing User-Centric Metadata for Digital Snapshot Photography*. Doctoral Dissertation, Department of Computer Science and Engineering, Helsinki University of Technology

[9] Sarvas, R., Mäntylä, M., Turpeinen, M. (2007) *Human-Centric Design of Future Print Media*, In the Proceedings of PulPaper 2007, Helsinki, Finland

[10] TNS- gallup, http://www.gallupweb.com/tnsmetrix/, Referred 20. 03. 2006

[11] Ulkuniemi, S. 2005. *Valotetut elämät, Perhevalokuvan lajityyppiä pohtivat tilateokset dialogissa katsojien kanssa.* Doctoral dissertation, University of Lapland

[12] Van House, N., Davis, M., Ames, M., Finn, M., Viswatnathan. V. The uses of personal networks digital imaging: an empirical study of cameraphone photos and sharing, *CHI '05 Ext. Abstracts.* 2005, ACM Press (2005), 1853 - 1856

[13] Vihonen, M. Conceptualizing and Developing a Photo Book Service, Master's Thesis, Helsinki University of Technology TKK, 2007

[14] Vredenburg K, Mao J-Y, Smiwth PW and Carey T (2002) A Survey of User-Centered Design Practice. CHI Letter 4(1): 471 - 478

Potential applications for hybrid media, the benefits and the roles in the operations model

Elina Rusko, Liisa Hakola

VTT
Biologinkuja 7, Espoo
P. O. Box 1000, FI-02044 VTT, Finland
E-mail: firstname.surname@vtt.fi

Abstract

Hybrid media is defined as integration of different media, contents and functionalities - especially convergence between printed and digital media. In Japan hybrid media applications have been very popular for several years now. Hybrid media applications are seen to have potential to create many benefits. For consumers it is about getting supplementary services and easier access to existing services - saving time and effort at its best. Furthermore the benefits of hybrid media are in adding value of printed products and mobile phones, interactive communication with consumers, improving integration of printed and digital media as well as creating new ways to use the mobile phone and getting competitive advantage and means of differentiating from other service providers.

This paper studies the applications, benefits and roles in the operations model of hybrid media. Information was gathered by performing a questioning directed to related industry and research representatives, and interviewing advertising agents. This paper concentrates mainly on the results from the questioning. The hybrid media situation is different in many ways in Japan. Knowing this, it was felt important to study the opinions and expectations on hybrid media among European people, in this case in Finland, in order to help wider implementation of hybrid media and establishment of new business. The objective of the study was to study opinions on different hybrid media applications, eligible benefits, roles of different parties in the operations model and furthermore needed actions for wider implementation of hybrid media applications. The study was conducted by VTT Technical Research Centre of Finland as a part of a larger project on hybrid media.

Keywords

Hybrid media, mobile phone, operations model, two-dimensional bar codes

1. Introduction

1.1 Background

Hybrid media is defined as integration of different media, contents and functionalities - especially convergence between printed and digital media. One example of hybrid media applications is use of printed two-dimensional bar codes as a link to digital media [Hakola et al., 2005 and 2006]. A code printed on a publication or a package can be imaged with a camera phone that has a software for decoding the information in the code. The decoded information can contain a link to a website where the user can access with the network connection in his mobile phone.

In Japan these kinds of applications have been very popular since their introduction in 2003. According to a research made in February 2006 approximately 27 per cent of all mobile phone owners in Japan use hybrid media applications (NPD Group) (Figure 1). According to NTT DoCoMo - the biggest teleoperator in Japan - already in 2005 half of its 25 million clients had a phone with a barcode reader software and the majority of them used hybrid media services at least once a month. There are, however, heavy-users that use the services even four times a day.

In Japan one can not buy a mobile phone without committing to use the services of a particular teleoperator. The longer the commitment is, the cheaper the device will become. This operations model has made it possible for the teleoperator to install extra software into the mobile phone before selling it to a consumer such as software for reading two-dimensional bar codes. Companies can then make their own two-

dimensional bar codes containing a website address and add them to printed products for giving additional information or a link to a company website, or for allowing consumers to order products etc. The motives for the teleoperator to give consumers a bar code reader include adding value of the mobile phone, getting more web page visitors, improving integration of printed and digital media as well as creating new ways to use the mobile phone. The company who uses two-dimensional bar codes gets more attention and visitors to its website as well as differentiates itself from competitors. The consumer gets supplementary services and the use of the existing services gets easier. This operations model seems to work well in Japan. One Japanese mail-order company, for example, has doubled its sales after introducing a possibility to order products or read extra information by reading a two-dimensional bar code printed on the catalogue.

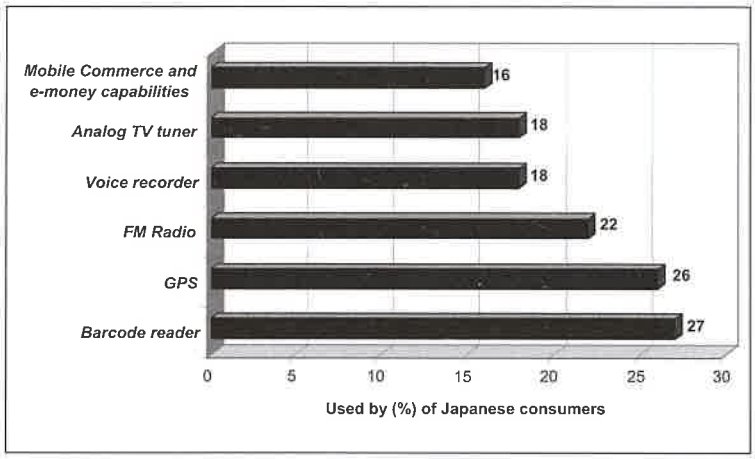

Figure 1: New features in Japanese mobile phones and how popular they are among consumers [NPD Group]

There are some factors that can be identified as the main reasons why hybrid media applications have become so popular in Japan. First of all there were no SMS messages when the mobile phones started to become common in Japan. The consumers were forced to use Internet e-mail with their mobile phones and consumers got very used to using Internet services with their mobile phones. When SMS messages were introduced in late 1990's they did not offer any real benefit to consumers and they never became very popular like in Europe or USA. Since two-dimensional bar codes often offer the same services as SMS messages in Europe or USA, they can be considered as a replacement for SMS messages in Japan. Hybrid media services usually contain a website that is browsed with the mobile phone. European consumers are not very accustomed to using Internet with their mobile phones which might prevent them from using hybrid media services. In Japan consumers have been using Internet with their mobile phones since the introduction of mobile phones so two-dimensional bar codes offer them a simple link to the website. For Japanese companies it has also been easy to introduce hybrid media services since they already have web pages tailored for mobile phone browsing available. Since the starting point has been quite different in Japan than in Europe or USA the popular Japanese hybrid media applications can not be directly transferred to Europe or USA. Instead studying new kinds of hybrid media services and business models becomes important.

1.2 Objective and scope of the study

The objective of this research was to find out if hybrid media business area could become as popular also outside Japan. The Japanese culture and hybrid media situation is very different from European ones and for that reason it was assumed in this study that Europe and USA can not directly copy the Japanese models that have proven to be successful there, because of difference in the success of SMS messages among other things. This is the main reason why this research was done in order to investigate the situation only in Europe, not in Japan. The objective was also to find out how the operations model could work in Europe and how much interest there is for hybrid media applications among industrial companies. Furthermore the objective was to roadmap what kind of hybrid media applications could be the most potential ones. The work was done by interviewing a total of 23 persons from different Finnish companies. In Finland there have been several hybrid media pilots since 2005 and companies have shown interest in this area for several years. This is why Finland was considered very suitable for carrying out this study. Consumer attitudes towards hybrid media were studied elsewhere in the same research project [Louho, 2006] and they are kept outside the scope of this paper.

2. Methods

The study consisted of two parts: a questioning directed to related industry and research representatives, and interviewing advertising agents. Priority in this paper is given to the results from the questioning.

The questioning was performed in form of a questionnaire which included evaluation of possible applications, roles in the operations model, eligible benefits, and needed actions. The questionnaire was first tested with two industry representatives before the final version. 18 people answered to the questionnaire in September 2006. Before answering the questionnaire they were briefly introduced to the subjects of the questionnaire although all the respondents had also earlier knowledge on hybrid media. The parties of the respondents are listed in Table I.

Table I: Group of representatives answering the questionnaire

Party	Number of respondents
Paper manufacturer	3
Mobile phone manufacturer	1
Teleoperator	1
Printing house	2
Digital service provider	3
Media organisation	2
Research	6

In addition, the study included interviewing five people working in advertising agencies. The interviews were performed in Finland during the autumn 2006. All the interviewees knew the principle of hybrid media beforehand and had a very positive and interested prejudice on hybrid media applications and technology. The interviews included an introduction to the subject, questions about the applications of hybrid media, and the actions needed for wider implementation.

3. Results

3.1 Evaluation of applications

In the first section of the questionnaire four potential hybrid media applications were rated by "degree of interest", "potential in 2006" and "potential in 2010". The applications were rated on a scale from one (1) to five (5), one being the lowest rate and five being the highest. The average values given to the applications in the rating are shown in Table II. Saving the information of a business card was found as the most interesting and a package related application to have the most potential.

Table II: The average values given to the applications in the rating

Application	Average value		
	Degree of Interest	Potential 2006	Potential 2010
Reading real-time TV-program information	3.44	2.22	3.00
Saving the information of a business card into mobile phone	**4.44**	2.44	3.11
Finding out the origin of a food product	4.22	2.39	**3.78**
Getting extra information of a product in an advertisement	4.17	**2.61**	3.61

In the advertising agency interviews the interviewees evaluated twelve applications based on "degree of interest" and "probability to be offered to a customer". The business card application was also rated high among the advertising agents as it was in the questionnaire. However, most of the applications introduced to the interviewees were felt interesting and most of them received an average value over four in the rating, thus the interest towards different applications was quite even among the advertising agency representatives. Four applications with the best rating among advertising agency representatives were: saving housing notice information into mobile phone, getting extra information of a product in an advertisement, receiving a special offer, and saving the information of a business card into mobile phone.

3.2 Evaluation of benefits

In the second section of the questionnaire the benefits of hybrid media were rated from given alternatives. The respondents had to choose five most important benefits of given thirteen alternatives and mark them 1 = most important benefit, 2 = second important benefit, 3 = third important benefit, and so forth. The results were rated in a way that the one marked as number one was given five points, second was given four points, third was given three points, and so forth.

According to the results from the questionnaires, added value for printed product was considered as the most important benefit of hybrid media applications. Other highly rated benefits were providing means to customer surveys, establishment of totally new business and companies, competitive advantage from other service providers, commitment for long-term co-operation, and facilitation of electronic services. The complete rating of the eligible benefits is shown in Table III. Increase in profits was included in the questionnaire although it is actually indirectly pursued through all the listed benefits.

Table III: Rating of the benefits of hybrid media applications in the questioning

Benefit	Score
Added value for printed product	62,5
Provides means to customer surveys	34
Establishment of new business and companies	33
Competitive advantage & means of differentiating from other service providers	23,5
Get customers to commit for long-term co-operation	21
Facilitate the use of electronic services	20
Increase in profits	19
Added value for mobile phone	17
More customers for printed product	10,5
Added value for electronic services	10
More customers for electronic service	8
More web page visitors	5

Interaction with end-users, activation of users, creating a service channel, and possibility for dialog were the potentials that the interviewees from advertising agencies saw that hybrid media applications bring to printed media. The applications were seen to widen the possibilities of advertising. Overall, the interviewees were most interested in applications that make every day life situations easier. The attitudes were generally very positive but on the other hand careful and realistic. Advertising agents have already spoken about the possibility of hybrid media applications to advertisers but especially the camera phone penetration seems to be seen as a problem. The advertisers do not want applications that are only available for a limited group of people.

3.3 Evaluation of Roles

In the third section of the questionnaire the most important roles in the operations model were evaluated by rating the given alternatives with the same method as the benefits were. The respondents had to choose three most important parties of the given twelve alternatives and mark them 1 = most important role, 2 = second important role, and 3 = third important role. The results were rated in a way that the one marked as number one was given three points, second was given two points and third was given one point. The results of the evaluation of the importance of roles of different parties in the hybrid media operations model are presented in Figure 2.

According to the rating publishers and packaging industry as well as advertisers, consumers, mobile phone manufacturers, and digital service providers have the most important roles in the operations model.

3.4 Needed actions

In addition to the evaluation of applications, benefits of hybrid media and the roles in the operations model, the questionnaire included a section where the respondents evaluated what actions would be needed in order

to achieve wider implementation of hybrid media applications in Finland. The actions were evaluated by rating given alternatives from an extensive list with the same method as the benefits and the roles were this time by marking seven most important actions. The rating of the importance of actions needed for wider implementation of hybrid media is listed in Table IV.

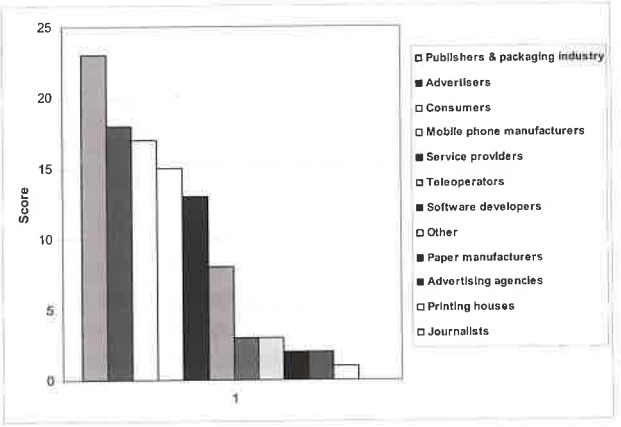

Figure 2: The importance of roles in the operations model

Table IV: Rating of the importance of actions needed for wider implementation of hybrid media

Action	Score
Marketing, making advertisers and electronic service providers familiar with the applications	86
Code reading software pre-installed in the mobile phone	74
Marketing, making consumers familiar with the applications	63
Marketing, making advertising agencies familiar with the applications	54
New applications (current ones not interesting enough)	43
Applications must provide easiest access to the service (easier than sms message)	33
Only one system in use	33
Development of mobile phones, especially camera properties	22
Development of web pages tailored for mobile phones	19
More wide spread use of 3G phones (fast data transfer)	13
Other action	13
Possibility to use different 2D bar code symbologies	12
Installation of code reading software by sms message	11
Use of hidden codes instead of 2D codes	10
Directing applications towards B2B communication	6
Changing the operational principle of current reading software	6
Directing applications towards games	5
Mobile phone & subscriber connection purchase as a package	5
Use of electronic codes instead of 2D codes	0
More than one system in use	0

Marketing and making advertisers, electronic service providers, consumers and advertising agencies familiar with the applications are among the most important actions needed for wider implementation of hybrid media according to the questioning. Furthermore, it was seen important that the code reading software is pre-installed in the mobile phone.

Among advertising agents it was seen that it would help the implementation for the consumers if the location and shape of the printed code was always the same. Hidden codes were not felt suitable for consumer applications. Because mobile phone is always carried along it was seen to provide a good user interface. However, it was pondered whether price and privacy issues would limit the use of mobile phones.

4. Discussion

As discussed already in the introduction part of this paper hybrid media situation is different in many ways in Japan - the success of SMS messages in Europe for one thing but also for other numerous reasons. The technology needed for hybrid media is also somewhat different in Japan than in Europe or USA. In Japan the teleoperator installs bar code reader software before the consumers purchases the mobile phone. So far, in Europe or USA the consumers have had to download the software themselves. However, Nokia might be starting to install bar code reader software to the newest models. At least some mobile phone models introduced in late 2006 - early 2007, have a software for reading two-dimensional bar codes. In Japan the mobile phone cameras are much better than in Europe. Japanese phones have had a possibility for taking close-up images and auto-focus lenses for a long time. These important features for hybrid media are just starting to hit European and USA markets.

Since the situation in Japan is so different from Europe and USA, it is important to recognise that in Europe and USA hybrid media may have to find applications and business models that differ significantly from those in Japan. Looking with that perspective this study gives a good start for creating the European hybrid media business model, helping wider implementation of hybrid media and establishment of new business. However, the study was focused on a limited number of issues and does not encompass all areas of hybrid media business. Especially the evaluation of different applications only represents opinions on a very limited amount of applications. On the other hand, it was neither possible nor necessary to include every hybrid media application type in the questionnaire.

The respondents in this study were a good representative group of hybrid media related industry and research representatives in Finland and the quality of the findings gives no reason for mistrust. Therefore it is assumed that the findings can be supported by new studies. However, it is known that those who are involved in technology development can not always analyse the situation objectively. In addition, it must be remembered that the information received through questionnaires and interviews is in the form of personal opinions of individual persons.

5. Conclusions

According to the survey the most important parties in hybrid media are publishers and packaging industry, advertisers, consumers, mobile phone manufacturers, and digital service providers. The role of advertising agencies was seen differently by different companies. In the future the role of the paper manufacturer will most likely be emphasized when a need to use physically even smaller codes, electronic codes and hidden codes increases.

The kind of applications that increase interaction between the consumer and the advertiser as well as applications that make everyday life easier were considered the most potential ones. Also applications related to packages were slightly emphasized. However, to reach the business stage, a lot of marketing of the hybrid media concept and applications is needed. Another necessity is to have the code reading software already installed in the mobile phone when it is purchased.

Hybrid media applications are seen to have potential to create many benefits. The benefits are especially in adding the value of printed products, interactive communication with consumers, improving integration of printed and digital media as well as creating new ways to use the mobile phone and getting competitive advantage and means of differentiating from other service providers. These benefits are the drivers for the parties involved in the hybrid media operations model to pursue towards wider implementation of hybrid media by following through the needed actions.

Acknowledgements

The authors would like to thank both the ones who answered the questionnaire and the ones interviewed for participating in this study and sharing their opinions. The authors would like to thank Finnish Funding Agency for Technology and Innovation (Tekes) for funding the research. Furthermore, the authors would like to thank Research Scientists Timo Kaljunen and Sari Vainikainen and Senior Research Scientist Pertti Moilanen for their contribution during this study.

References

[1] Hakola, L.; Linna, H., *Detection of printed codes with a camera phone. Proceedings of the 32nd IARIGAI research conference, Porvoo, Finland, 2005, p. 355 - 361*

[2] Hakola, L.; Lindqvist, U.; Linna, H.; Siivonen, T.; Södergård, C. *Roadmap on printed functionality and hybrid media. Proceedings of the 33rd IARIGAI research conference, Leipzig, Germany, 2006, 8 p*

[3] Louho, R. *Factors Affecting to the Usage of Hybrid Media Applications (in Finnish), M. Sc. Thesis, Helsinki University of Technology, 2006, 81 p*

[4] NPD Group. *Will the US Mobile Market Turn Japanese? wirelessinnovator.com, 2006*

New business models for printed functionality

Ulf Lindqvist, Liisa Hakola, Hannu Linna, Pertti Moilanen, Timo Siivonen

VTT, Espoo, Finland
Vuorimiehentie 3, P.O. Box 1000, FI-02044 VTT, Finland
E-mail: firstname.surname@vtt.fi

Abstract

Printed functionality means adding new functionalities into flexible substrate, typically paper and plastic, in addition to regular graphical properties by using printing methods. Functionality can be on the surface of the substrate or within it, or both. Printed functionality can be codes containing links to additional information. Such codes include one- and two-dimensional bar codes as well as invisible, reactive and electronic codes. Furthermore, printed functionality can be visual effects and images, multi-layer structures, printed electronics, optics and displays as well as printed sensors and indicators. Hybrid media is closely related to printed functionality. Hybrid media is defined as the integration of different media, contents and functionalities - especially convergence between fiber-based printed products and digital media.

In this study new applications of printed functionality have been innovated and tested. Finally, new business models have been developed for these applications.

Keywords

Business models, hybrid media, printed functionality, value chain

1. Introduction

So far most activities around printed functionality have dealt with technical development of new solutions and applications to substitute existing products. A full utilisation of the potentials requires a market driven approach aiming at innovative new services. A prerequisit is to understand the entire value chain from the service providers to the end users, and the role of the printing plant in this chain. This may also require completely new business models.

It has been the scope of this study to define some innovative applications of printed functionality, and to create business models for these applications. In the first step the printed functionality production has been classified and typical innovations have been defined within each cathegory. After this, the production processes for the new applications were analysed and the sufficiency of traditional printing plants to meet the technical requirements was estimated. Finally, general business models were developed for the most important types of applications.

The final aim has been to define the new role of the printing plants in the value chain of printed functionality. Special attention was paid to the performance of traditional printing plants, which types of new services are within their ability and what kind of material and immaterial investments are needed.

2. Methods

Potential innovations come to fruition when the market pull meets the technology push at the right time and in an appropriate environment. One advantageous method to search for potential innovations is to study an inventory and analyse lot of weak signals about its impact. The future can be reviewed in alternative scenarios, which are built in a so called future table. A good checklist to create the future table is the so called PESTE (Politics, Economy, Society, Technology, Environment) procedure. The innovation work itself is an intensive team work utilizing all the gathered background information. The most creative teams consist of professionals and experts with backgrounds. The spirit in the team must be open minded and eager on new ideas.

Printing can be one way to add functionality to a substrate or it can replace traditional manufacturing technologies for e.g. electrical circuits. Here we have focused on the former. The three main categories of printed functionality

are printed sensors and indicators, printed electronics and hybrid media. In the first step the technologies used in these categories were covered in a literature study. Based on this study new applications were then innovated together with representatives from the industry. The possibilities to realize these applications in industrial printing were finally evaluated by comparing the requirements of the applications to the technical potentials of the printing plants. Based on the literature study the technologies for printed functionality are presented in Table I. These technologies were used as a basis for innovating new applications and services.

Table I: Technologies for printed functionality

Categories	Technologies	Potential for integrating with printed products (packages, publications etc.)
1.1 Printed electronics	Conductor	Yes
	Capacitor	Yes
	Resistor	Yes
	Inductor	Yes
	Mask	No, meant for electronic circuits
	Via hole	No, meant for electronic circuits
	Interconnection	No, meant for electronic circuits
Printed optics	Micro lenses	No, optical fibers etc.
	Light guides	Yes
	Holograms	Yes
	Kinegrams	Yes
	Optical effects	Yes
Displays	Transistors	Element for displays
	OLED displays	In the long run
	Thermochromic displays	In the long run
	LCD displays	In the long run
Optical codes	Linear / 1D bar codes	Yes, identification
	2D bar codes	Yes, hybrid media
	3D bar codes	Yes, hybrid media
	OCR (Optical Character Recognition)	Yes, hybrid media
	Micro text	Security printing
	Digital watermarks	Yes, hybrid media
	Reactive codes	Yes, hybrid media
Electronic codes	RFID	Yes
	Electronic bar code	Yes
Other codes	Magnetic codes	Yes
1.2 Sensors *(instrumental reading)*	Temperature sensor	Yes
	Humidity sensor	Yes
1.3 Indicators *(reading with human senses)*	Freshness indicator	Yes
	Bio sensor	Yes
	Humidity indicator	Yes
	Temperature indicator	Yes
1.4 Others	Power sources	In the long run
	Solar cells	In the long run
	Bioactive applications	Yes
	Decoration	Yes

The basic value chain of printed functionality includes suppliers of raw materials, a printing company, a service provider, a technology provider, a logistic delivery chain and an end user (Figure 1). The publisher and the advertisers may be the service provider, and should always provide content to the printed product. The easiest way to include functionality is to convert data to a machine readable form. An example of this is the 2D bar code, which can be read with a camera phone equipped with suitable software. In this case the printing is made at normal speed and no special materials are needed.

Another example is a hidden code in a cereal box. The code is unique for each box offering the possibility for one-time use only. In practice the code is produced with inkjet. By reading the code the end user gets access to the services provided by the advertiser. The access is either via cellphone or web browser. The service can then be whatever in electronic form: games, music, product information etc. It should be noted that every time electronic data is transferred through a network the teleoperator is a part of the business chain.

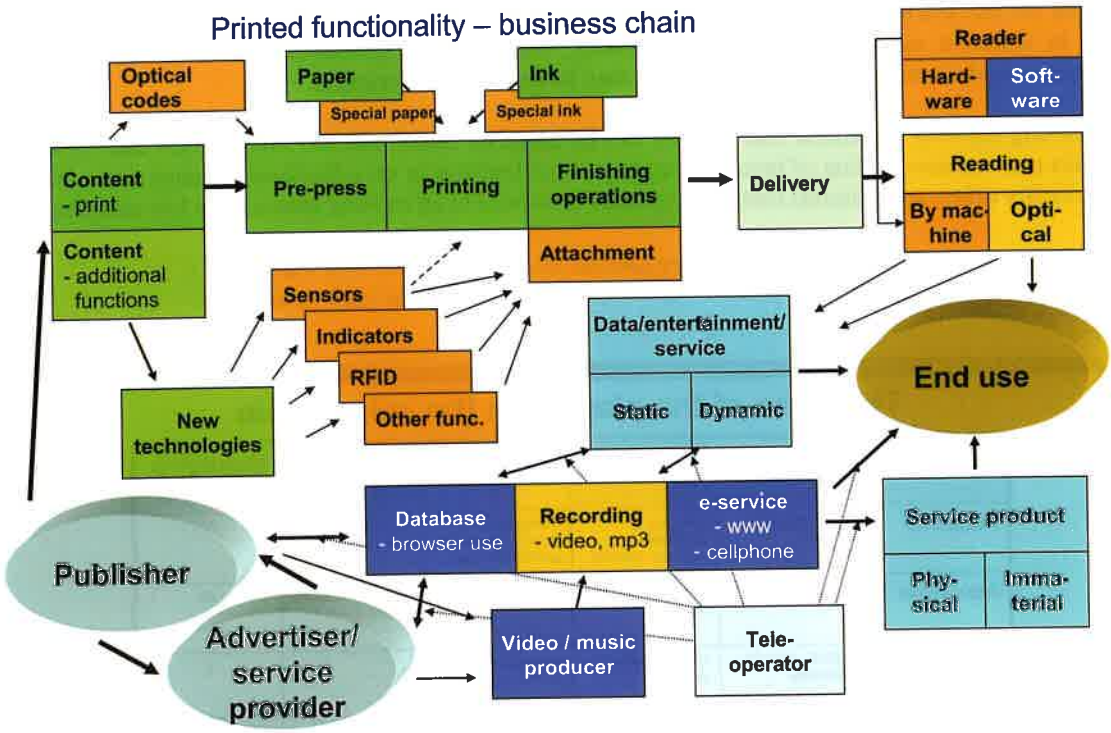

Figure 1: The value chain of printed functionality involves many new players compared to ordinary printing

When more complicated functionality is applied to the printed product, higher demands are raised on the production process. When special components are added to the printing ink the printing speed may be reduced, and an extra ink may require an additional printing unit. Sensors and indicators are examples of such applications. A beforehand printed functional component may also be added to the main product in the finishing stage. In any case it is important that all the players of the value chain of a product form a network. In the beginning everyone has the traditional role of his own in the network. However, with the future development of the value chain the most crucial question becomes: Who will rule this network?

3. Results

The starting point was to list all the players of the value chain of printed functionality and to estimate their logic possibilities to earn incomes as a part of the network. The publisher has a strong role since he has the responsibility of the content of the main product. Therefore, the publisher should be active to improve the interest for the product. The advertiser may also be active and may for instance create links from the advertisement to product information pages or access to entertainment materials. The basic role of the printing company is, of course, to offer printing capacity. But an active printing company may get additional benefit by investing in new sophisticated technology and achieve a more central position in the network. New customers mainly contact the player who controls the network. The owner of the information data file and the creator of the audiovisual content have varying roles in the network, but not necessarily a leading role. The material supplier may have a profitable business as a part of the network, but scarcely an essential role.

Innovations in printed functionality can be found by searching technical solutions or new market applications. What is new to one company is not necessarily an internationally new application. We can distinguish between known technologies, technologies new to us and technologies new to everyone. Correspondingly we may offer the applications to known markets, markets that are new to us and markets that are new to everyone. This gives in total nine possible combinations. The most critical application is, of course, to introduce completely new technology to new markets.

In the case of printed functionality, applying printed electronics, sensors and indicators to textiles would be an example of introducing new technology to totally new market applications. Also the development of 3D-codes to different applications is a new approach, whereas the application of sensors and 2D-codes to packages already is an existing technology, but may be new to many printers.

The earning capacity of printed functionality can be based on direct sell, AD sales, access and subscription, royalties and licences, selling of brands, management of logistics or on e-Business. In most cases the printed functionality offers an additional (interactive) value or service to an existing product to a low additional cost.

Table II: The players have the possibility to extend their roles in printed functionality and one of them may control the whole value chain

VTT TECHNICAL RESEARCH CENTRE OF FINLAND

The roles of the players in the value chain

	Primary role	Function	Benefit	Additional roles	Managing the chain
Publisher	Sells newspapers and ads	Pakaging (prepress), additional services	Additional services for end user; Media position stronger	Data base provider, Content creation	XXX
Advertiser	Promoting sale	Offering additional services	Increased sale	Data base provider, Content creation	XX
Technology provider	Business from new technology	Produce, sells or licens	Incomes from sales or IPR		0
Printer	**Prints and attaches**	**Printing and attaching technology**	**Additional incomes, Networking**	New technologies, Data base provider, Content creation	**X**
Materials supplier	Sells materials	Supplying of materials	Additional profit from materials, Networking	New technologies	X
Data base provider	Offering service	Data base building and updating, Interactivity	Part of the network	Content creation	X
Content provider	Content creation	Allocated visualisation	Part of the network	Data base provider	0
End user	Read the newspaper and see the ads	Interest and ability to use the additional services	New services and additional value		

VTT

An indicator of the size 5 cm^2 can easily be printed with a special ink in a newspaper, on a package or on an event ticket. Even if the special ink may be rather expensive, 1 kg of it would be enough for more than one million samples with an ordinary consumption of 2 g/m^2. The additional value of such an indicator and the new services it involves may be several times that of the original product.

In this study innovations were made by experts from the industry and scientists in brain storming meetings. Of the documented ideas 16 dealt with sensors and indicators, 21 with optical and electronic barcodes, and 9 with printed electronics. All the ideas were analysed technically and economically and the following ideas have been realised in pilots:

◊ Weather sensors produced with special inks in newspapers (Thermosensors, Humiditysensors);
◊ UV fluorescent security elements;
◊ Chromatic inks;
◊ UV indicators for sun tan cream tins;
◊ Conductive codes;
◊ Disposable event pass.

These ideas were chosen since it was analyzed that they can be realized during the project and the technology could be transferred to participating printhouses. The principal idea of the printed thermometer is presented in Figure 3.

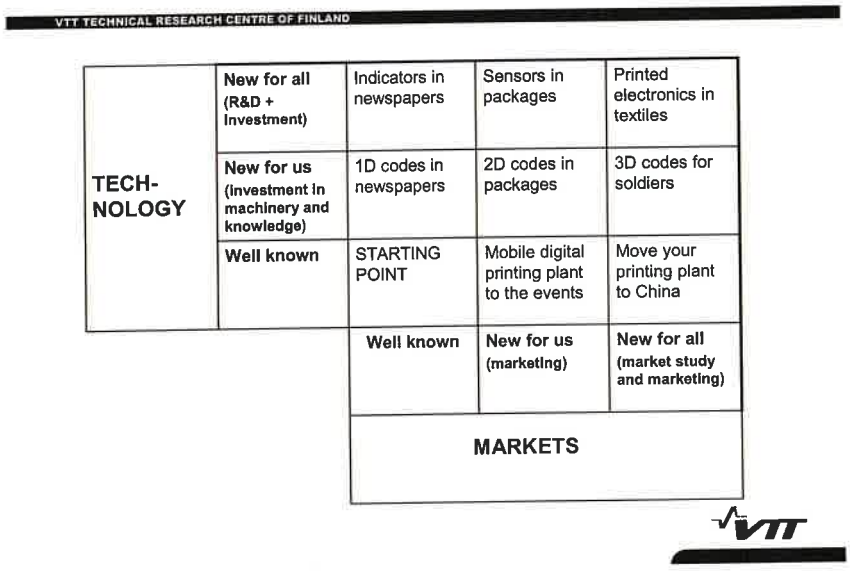

Figure 2: Printed functionality offers the possibility to beyond the well known markets with new products

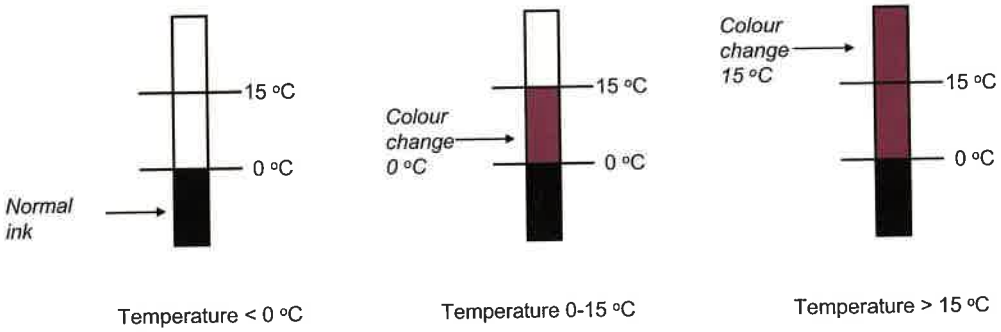

Figure 3: One example of innovations in printed functionality was to print thermometry in a newspaper with thermochromic inks

4. Conclusions

In a broad sense printed functionality includes all forms of interactivity, intelligence or additional effects transferred to a substrate using printing technology. Traditional printing plants can easily produce less complicated forms of printed functionality, such as 2D bar codes and visual effects practically without additional investments. More complicated products, like sensors, indicators, printed electronics and optics require special inks and application techniques which may be far beyond traditional printing know-how and may interfer with demands on runnability and printability.

The possibilities to find new innovative applications of printed functionality are practically unlimited, and a printer entering this business should integrate continuous innovative product development in his process. Methods for identification of innovative solutions exist, such as future tables, weak signal analysis and PESTE checklists. In addition, the new intelligent elements are usually rather small in size, so the additional material costs are marginal even if new advanced materials are needed.

On the other hand, the value network of printed functionality is very complicated and include many new players, such as the advertiser, suppliers of new technology, material manufacturers, data base providers, publishers and end users. Most of these players can have more than one role in the value chain, and theoretically anyone of them could take over and manage the entire chain. However, the publishers and content providers have better possibilities for this than e.g. material suppliers. The position of the printer would be stronger, if he also manage

the new technologies to be added, their application to the print and the data bases. Also the strategy of earning becomes more diversified than in traditional printing. It can be based on both direct sale, ads, access and subscription, royalties and licences, brands, logistics or e-Business.

According to earlier roadmappings the additional global market for functional printing will expand to fifty million euros in the next five years. A part of this growth could be directed to the printing industry, but not without an active innovation policy.

Acknowledgements

The authors are greatly indepted to the Finnish Funding Agency for Technology and Innovation TEKES for their support to the project, and to the following participating companies for the permission to publish the results: Hansaprint Oy, Ikistoori Oy, Joutsenpaino Oy, Lomakevaihtoehto Oy, M-real Oyj, Sanomapaino Oy. We also want to thank the following American companies for their valuable information during our study tour: E Ink Corporation, Fujifilm Dimatix, Litrex Corporation, MIT Auto-ID Laboratory, Mobot^{R}, NanoDynamics and Printed Electronics Consultant Bruce E. Kahn.

References

[1] Hakola, L., Lindqvist, U., Linna, H., Siivonen, T., Södergård, C., (2006), Roadmap on printed functionality and hybrid media. Proceedingd of the 33rd IARIGAI Conference, Leipzig, Germany

[2] Hakola, L., Linna, H., (2005), Detection of printed codes with a camera phone. Proceedings of the 32nd IARIGAI Conference, Porvoo, Finland, p. 355 - 361

Energy efficiency improvement for graphic/media SME´s - How it can be managed?

Anastasios Politis[1], *Michael Dattner*[2]

[1] Athens Technological Educational Institute, Greece
[2] Bergische Universität Wuppertal, Germany
E-mail: dattner@uni-wuppertal.de

Abstract

Since the graphic media industry in Europe mainly consist of SMEs, this sector has to become a knowledge industry and develop new management, production, communication and service concepts in order to survive. This objective can only be fulfilled by creating surplus value for their customers and present themselves as a full service partner for all graphic media services. Among others, the subjects on environmental protection and optimized energy efficiency become increasingly significant, nowadays.

The purpose of this paper is to draw attention to and investigate the current situation on environmental issues and in particular the energy efficiency of the European graphic arts industry. The study originates from a European Union research project.

More specifically, a principal objective of our study is to investigate the degree of awareness (owners/employers and employees) among the SMEs of the graphic media industry in the EU member states concerning the reduction of energy consumption.

This issue needs to be addressed not only as a process towards the protection of the environment by for example reducing greenhouse gas emissions, but also as a matter for management. Thus this can be considered an innovative approach, combining the visualisation of the often hidden use of energy and the provision of the technical know-how to reduce it with the necessary management structures.

Furthermore, our intention is to propose methods to visualise the SMEs awareness, to develop benchmark tools for the industry with an overview over key figures (financial, technical, management) and to provide an energy-management standard as a suggestion on how energy can become a part of management.

The study has been based on an extended survey among graphic arts SMEs in 5 European countries. Within the survey, various matters related with environmental protection, energy consumption and its reduction and the management procedures on energy efficiency have been initially investigated. The data collected will be used in future study for tailoring tools fitted exactly to the graphic arts sector.

Keywords

Energy efficiency, energy management, environmental protection, graphic arts SMEs

1. Introduction

Large, internationally operating companies that started out in the traditional graphic media business are taking advantage of the complementary media strategies and are themselves developing cross-media strategies. Against this background, the European printing market is, afflicted with a strong trend towards concentration. New "global players" from Asia, Australia and the United States are making inroads into the European market, and are thus aggravating these developments and intensifying the competition.

Largely out of touch with the innovation strategies of the large media corporations are the small and medium-sized enterprises (SMEs) of the European graphic arts industry. It can be observed that these companies are only able to participate in innovative developments in new media markets to a limited degree.

Since the graphic media industry in Europe mainly consist of SMEs, this sector has to become a knowledge industry and develop new management, production, communication and service concepts in order to survive. This objective can only be fulfilled by creating surplus value for their customers and present themselves as a full service partner for all graphic media services. Among others, the subjects on environmental protection and optimized energy efficiency become increasingly significant, nowadays.

The purpose of this paper is to draw attention to and investigate the current situation on environmental issues and in particular the energy efficiency of the European graphic arts industry. The study originates from a European Union research project [EEEI, 2007]. More specifically a principal objective of our study is to investigate the degree of awareness (owners/employers and employees) among the SMEs of the graphic media industry in the EU member states concerning the reduction of energy consumption. The study has been based on an extended survey among graphic arts SMEs in 5 European countries.

Our approach to achieve this data is via running the above mentioned case study research in Czech Republic, Greece, Germany, Hungary and The Netherlands. With the aid of the case study, our intention is to examine an as-is analysis of these countries that includes a collection of energy relevant data from the countries and the industry sectors and in particular from graphic arts companies. This data will be used for tailoring tools fitted exactly to the graphic arts sector.

Thus we intend to generate transparent key data and indicators, which are so detailed that in apparently different circumstances comparable components can be described. This is a very important precondition for establishing changes required in current managements to apply an energy efficient management in the graphic arts sector in Europe.

2. Research questions and objectives

Changes in the graphic arts and media sector cause new requirements for the companies. Particularly, middle and upper management and ownership of graphic arts SMEs face new tasks that are added in daily concerns of the companies. To name some we nowadays deal with workflow management, digital asset management, colour management, etc., etc.

The continuous increase of management tasks create the need to set the framework for a modern and efficient management of old and new tasks. Considering, however that, the protection of the environment is gaining in importance due to the dramatic changes of the climate that we all experience, we have considered of high importance the issues of energy consumption and its efficient management towards the direction of reducing energy resources by the graphic arts industry.

The question posed is to investigate whether the environmental protection and specifically the energy issue is a matter of importance for the graphic arts sector. Therefore, the purpose of this paper is to draw attention to and investigate the current situation on environmental issues and in particular the energy efficiency of the European graphic arts industry. More specifically a principal objective of our study is to investigate the degree of awareness (owners/employers and employees) among the SMEs of the graphic media industry in the EU member states concerning the reduction of energy consumption.

3. Research methodology

3.1 Literature study

Literature study was based principally on some surveys indicating the environmental issues in general and those concerning the graphic arts and media industry. In addition this part of the survey has been directed towards generic approaches on print media production developments.

3.2 Case study research

In order to extract data regarding the awareness of the graphic arts sector on environmental and energy consumption issues, an extended survey among print media companies has been developed and implemented. The survey took place in 5 European countries and included interviews and answers to a questionnaire. The questionnaire has been directed towards the investigation of graphic arts companies concerning the energy situation, policies and actions in energy efficiency. In order to obtain more accurate data, we have spread these companies over different printing methods and technologies used by the companies.

The list presented in Table I gives an idea, how many companies of each method of printing technology are taken into account in our investigation. The list is itemised by printing process type as the main criterion for

each country. We have decided to distinguish the companies between sheet-fed offset printing (including packaging printing), web-fed offset printing (heat-set, cold-set, newspapers and commercial printing), flexography printing (including narrow-web), gravure printing, silk-screen printing, digital printing and book-binding into account for our study.

Table I: Categorization of companies to be interviewed regarding energy issues

Process type	**Details / technical or other differences / keywords** (remark: this list has no logical structure)	**Try to contact per group**	**alternatively try to contact**
Sheet-fed offset printing	- Oxidative drying - UV drying	2 - 5	5 - 8
Web-fed offset printing	- Newspaper printing - Heatset offset	2 - 3	
Flexography Printing	- Solvent based inks - Water based inks - UV inks	2	5 - 6
Book-binding		1	
Gravure	- Solvent based inks - Water based inks - UV inks - Package printing	2	
Screen printing	- Fabric/textile printing - All other substrates	2 - 3	4 - 5
Digital printing	- Copy shop - book on demand - large format printing	2	
Contact over all:		**15 - 20 companies per country**	

The survey has been directed to small and medium sized enterprises according to the European rule of a maximum of 250 workers (although some companies that have responded to the survey extend this limit).

The survey started in the beginning of April 2007 within the graphic arts industry in the five countries participating at the EEEI project: Czech Republic, Hungary, Germany, Greece and the Netherlands and ended in the beginning of July 2007. All interviews have been done in the corresponding national language so five questionnaires were made on the basis of the following English version. In order to generate comparable answers we decided to work preferably with questions that can be answered with "yes", "no" or "intended".

The structure of the questionnaire includes an introduction wherewith, we want to point out our intention to sensitise our branch to the increasingly significance of environment protection and optimised energy efficiency as it is shown in Picture 1.

Furthermore, to get well-defined relations the second page starts with a field for the country name, where the interviewed company comes from. This is followed by the name and the address field completed by name and position of the contact person within the company as it is presented in Picture 2. Finally, in Picture 3 the actual 22 questions concerning energy efficiency and environmental matters are presented.
* *See Appendix*

The questionnaire has been distributed to 96 companies in the 5 countries. Data have been obtained by 67 companies. The outcomes and results from the survey are presented in the chapter "Results" of this paper.

4. The graphic arts sector, the environment and the issue of energy

As it stressed out in an Intergraf study [Comprint, 2002], the printing industry, which has occasionally been forgotten amid the media euphoria of the past decade, is returning to the centre of the discussion about ways to efficiently distribute information: "Print is back!" But this is not primarily because of the backlash and economic correction that followed the initially spectacular successes and skyrocketing stock market prices of the New

Economy boom. Rather, it is because a phase of media experimentation has more clearly revealed the respective advantages of individual classical and new media for conveying different types of information. Print is once again occupying a place in the complex interplay of different media, fulfilling definite roles in connection with providing information, communication, acquisition of knowledge, and entertainment [Comprint, 2002].

4.1 Structural developments in the graphic arts sector

At the threshold to the 21st century, the requirements faced by companies and workers in the printing and media industries have turned out to be far more extensive and complex than had been predicted by various studies and at numerous expert hearings and workshops in recent years. A steady stream of technical innovations and new market trends are raining down upon the printing and media industries. At steadily decreasing intervals, companies are adjusting their business plans to accommodate new phenomena such as multimedia, the Internet, cross-media, eBusiness etc. It can already be observed that the most innovative companies are abandoning the "traditional" organizational patterns typical of industrial production and trying out new models involving distributed production (i.e., with processes that are uncoupled from one another in both time and space) that provide a glimpse of how work will be done in the knowledge and information society of the 21st century. Such approaches concern production, administration and management structures as well [Comprint, 2002].

4.2 Impacts on management and organisation

The general direction in management concepts of the future for the graphic arts companies is *shifting from material flow to information flow*. Part of the result of this is a new demand for the development of complex information organizations which support efficient new business processes but which also need to open up unstructured spaces in management terms in order to carry out production processes which are directed to projects, services and customers in the context of a new management flexibility. Workflow management systems can in this connection make up the software technology platform for new structuring concepts [Comprint, 2002].

4.3 The sector and the environment

Based on data provided by various studies, environmental protection seems to be an issue of importance for the graphic arts industry. Again, according to an EU study for the forest industry published by Intergraf, the international association for the graphic industry, the European Graphic Industry is an industrial branch which has only a marginal impact on the environment. The industry is devoting increased resources to meeting the stricter environmental requirements.

For example, it has invested large amounts of money to limit emissions to the air (VOCs), caused by web-fed offset and gravure printing, to improve waste water management and to encourage the recycling of waste. In some EU-countries the graphic industries federations collaborate closely with government departments to agree on the best measures for environmental protection. Furthermore, at international level is co-operating with the EU-Commission to define appropriate directives in this area [Intergraf, 2004].

According to ERA (the European Rotogravure Association), in the last 2-3 years, the use of toluene has gone through in-depth investigations as a result of a Risk Assessment procedure. Because of the vital importance of toluene to this sector of the printing industry, the European Rotogravure Association has endeavoured to ensure that all reliable "scientific evidence" is appropriately taken into account during the procedures of making new regulations concerning toluene [www.era.eu.org].

Furthermore, the substitution of solvent-based products by water-based products is an interesting development, which is being successfully introduced in flexography printing techniques used for packaging printing, and in water-based adhesives [Galland et al, 2004].

4.4 The energy issue for the graphic arts sector

Based on data provided by the country reports on energy efficiency within the EEEI project, it can be concluded that many processes today are much more environmentally friendly than even 30 years ago, within

the printing industry. For the production of the same printing product fewer chemicals are needed, and environmentally and health friendly inks, additives as well as cleaning agents are available. Printing plants were among the first to introduce ecological management systems. Thus it seems an obvious step to make the lowering of energy consumption, due to the rising costs for the energy suppliers and global warming, a central topic within the industry [EEEI, 2007].

Next to the protection of finite resources the lowering of energy consumption and the change over to renewable energy sources will contribute to the protection of the environment on the whole. In this context the following environmental goals for energy use in printing plants shall serve as examples:

- ◊ Energy management for lowering energy-peak consumption;
- ◊ Efficiency increase in facility climatisation (e.g. through the pre-warming or pre- cooling of air through the soil, heat exchange in air education, use of heat generation from the machines to heat the facilities in winter);
- ◊ Efficiency increase in the generation of compressed air (tailored to suit the needs and centrally generated, monitoring leakage);
- ◊ Avoiding stand-by energy consumption in production and administration;
- ◊ Energy optimisation in the purification of waste gases;
- ◊ Using of renewable energy sources (e.g. solar energy for the generation of hot water, electricity, supply of completely or partially renewable electricity).

According to EEEI project, "The use of energy is often hidden and is not considered as a serious subject of the policy of SMEs". This appears to be the main barrier for SMEs in the Graphic-Media Industry for reducing their use of energy. However, as it is stated in the introductory text of the project, there are also regional differences within the graphic-media industry occur regarding energy that does not allow for a common approach, as it regards energy consumption and management. These are physical climate, culture and costs. According to the project objectives "The project wants to make SMEs aware of the opportunities, remove barriers and improve energy efficiency within the industry" [EEEI, 2007].

5. Results

5.1 Results - general data

The survey in the 5 countries Czech Republic, Hungary, Germany, Greece and the Netherlands, resulted in 67 questionnaires from a total of 96 companies registered to participate to the survey, a quite satisfactory response rate of 70% of the companies. In Table II, the data from the 67 companies are illustrated regarding the number of companies per country, the total number of employees and the average number of employees per country.

Table II: General data from the 67 companies that responded to the survey - Number of companies per country, t total number of employees and the average number of employees per country

Country	Number of companies that responded to the survey	Total number of employees	Employees on average per country
CZ	8	378	47
DE	19	1201*	75
GR	14	566	40
HU	8	1180	147**
NL	18	1208	67
Total	67	-	-

* *Only 16 companies provided data on the number of employees*
** *Two out of the 8 companies from Hungary employ 500 people*

Furthermore, the survey resulted in the following distribution of printing technologies used by the companies, as it is presented in Table III.

As it can be derived from the figures in Table III, many companies use more than one printing technology. Sheet-fed offset printing is dominating, followed by digital printing installations and book-binding. The most common combinations between the technologies are:

◊ Sheet-fed offset printing + production book-binding (more combinations)
◊ Sheet-fed offset printing + digital printing + production book-binding
◊ Sheet-fed offset printing + digital printing
◊ Flexography and rotogravure printing
◊ Sheet-fed offset printing + web-fed offset printing (less combinations)

Table III: Distribution of printing technologies used by the companies

Printing technology used (plus book-binding)	CZ	DE	GR	HU	NL	Total
Sheet-fed offset printing	6	17	9	6	13	51
Web-fed offset printing	4	6	0	1	2	13
Flexography printing	1	2	3	2	1	9
Rotogravure printing	0	0	3	2	1	6
Silk-screen printing	0	2	2	0	2	6
Digital printing	5	11	6	3	8	33
Production book-binding	7	6	10	2	5	30

It is worth to state that only 3 companies are pure book-binding companies. In addition, 3 out of 6 flexography and rotogravure installations are combined in packaging printing companies for printing of flexible packaging substrates - all of them in Greece.

5.2 Results - Tables with the responses from the companies in the 22 questions on energy subjects

In the following part of the paper the answers per question and per country regarding the awareness of the companies to energy issues, policies, actions and expectations are illustrated. These results are discussed in the Discussion chapter of the paper. In some cases there were no answers provided, however, this does not affect the overall structure of the outcomes from the survey. It must be also noted that, in some cases and in particular in the case of Greece, the majority of the companies has combined the answer "no" with the answer "intended" in certain questions. This has been taken into account as it regards the analysis of the outcomes.

1. Do you have any idea about your energy efficiency possibilities?

	CZ	DE	GR	HU	NL	Total 5 countries
Yes	2	8	4	3	17	34
No	6	11	10	5	1	33

2. Is there a staff member on energy matters in your company?

	CZ	DE	GR	HU	NL	Total 5 countries
Yes	2	1	2	4	15	24
No	6	15	3	4	3	31
Intended	0	3	9	0	0	12

3. Do you give energy saving information to your employees?

	CZ	DE	GR	HU	NL	Total 5 countries
Yes	1	4	2	6	10	23
No	6	13	4	1	5	29
Intended	0	2	8	0	3	13

4. Do you develop energy saving measures in your company?

	CZ	DE	GR	HU	NL	Total 5 countries
Yes	4	2	7	6	12	31
No	3	15	2	2	2	24
Intended	1	2	5	0	4	12

5. Is energy efficiency an issue when you buy new machinery?

	CZ	DE	GR	HU	NL	Total 5 countries
Yes	6	13	7	6	15	47
No	2	2	1	2	2	9
Intended	1	2	6	4	1	14

6. Do you spend a part of your yearly budget on energy saving?

	CZ	DE	GR	HU	NL	Total 5 countries
Yes	1	3	3	3	7	17
No	5	10	5	3	7	30
Intended	0	6	6	1	4	17

7. Are your customers interested in ecological products?

	CZ	DE	GR	HU	NL	Total 5 countries
Yes	3	4	1	2	11	21
No	3	12	0	2	3	20
Intended	2	12	13	4	4	35

8. Are you interested in ecological products?

	CZ	DE	GR	HU	NL	Total 5 countries
Yes	6	17	14	7	18	62
No	2	2	0	0	0	5

9. Do you have an environmental management system?

	CZ	DE	GR	HU	NL	Total 5 countries
Yes	1	4	6	3	13	27
No	7	13	2	5	2	29
Intended	0	2	6	0	3	11

10. Do you have an eco-management and audit scheme certification (EMAS)?

	CZ	DE	GR	HU	NL	Total 5 countries
Yes	0	3	1	1	0	5
No	8	16	7	7	18	56
Intended	0	0	6	0	0	6

11. Do you have an ISO-14001 certification?

	CZ	DE	GR	HU	NL	Total 5 countries
Yes	0	1	4	3	8	16
No	7	17	6	5	6	41
Intended	1	1	4	0	4	10

12. What is your yearly energy consumption in MWh?

	CZ	DE	GR	HU	NL	Total 5 countries
Data provided	3	9	5	3	18	38
Data not available	5	10	9	5	0	29

13. What are your yearly energy costs in Euros?

	CZ	DE	GR	HU	NL	Total 5 countries
Data provided	4	12	7	5	18	46
Data not available	4	7	7	3	0	21

14. How do you measure your production output?

	CZ	DE	GR	HU	NL	Total 5 countries
Data provided	1	9	13	3	18	44
No answer	7	10	1	5	0	23

15. What is your total energy consumption per amount of printed paper in Wh?

	CZ	DE	GR	HU	NL	Total 5 countries
Data provided	1	1	1	2	2	7
Data not available	7	18	13	6	16	60

16. Are you interested in further and more detailed key data?

	CZ	DE	GR	HU	NL	Total 5 countries
Yes	1	16	7	8	16	48
No	3	1	3	0	1	8
Intended	4	2	4	0	1	11

17. Are you well informed about a heat and energy recovery within your company?

	CZ	DE	GR	HU	NL	Total 5 countries
Yes	2	1	3	3	9	18
No	5	18	7	3	6	39
Intended	1	0	4	2	3	10

18. Are you able to look for some specific consumption values concerning energy?

	CZ	DE	GR	HU	NL	Total 5 countries
Yes	4	10	5	6	15	40
No	4	8	6	1	2	21
Intended	0	1	3	1	1	6

19. If you deliver data, is it necessary to make it anonymous for further research?

	CZ	DE	GR	HU	NL	Total 5 countries
Yes	7	5	3	4	5	24
No	1	14	11	4	13	43

20. Do you have any support concerning energy aspects?

	CZ	DE	GR	HU	NL	Total 5 countries
Yes	1	4	3	3	12	23
No	6	13	6	5	5	35
Intended	1	2	5	0	1	9

21. How are your expectations concerning a European exchange of energy efficiency data?

	CZ	DE	GR	HU	NL	Total 5 countries
Positive	5	15	13	3	15	51
Negative	3	4	1	1*	3	11

*Four companies from Hungary did not answered this question

22. Are you interested in more information about Energy efficiency via the EEEI project?

	CZ	DE	GR	HU	NL	Total 5 countries
Yes	5	19	14	8	18	64
No	3	0	0	0	0	3

6. Discussion and conclusions

The figures from the 67 responses to the section of energy matters generally do not show a difference in organisation structure and the availability of data among the North and the South of Europe (namely between Germany and Netherlands from the one side and Greece from the other side). There were more differences among the Germany, Greece and the Netherlands from the one side and Czech Republic and Hungary from the other side. This exists for questions regarding energy consumption and costs, for example.

Furthermore, the analysis neither included detailed comparisons among the countries for each question nor analysis between the types of the companies as it regards the use of printing technologies, except some general outcomes.

6.1 A synoptical analysis on figures provided to the 22nd questions regarding energy matters

As it regards the degree of awareness of the companies for energy efficiency (questions 1 to 6), companies are divided in the middle (50%) regarding the energy efficiency possibilities. Furthermore, they seem to be slightly nor aware or not to act towards certain measures, as it regards the employment of a staff member on energy matters in the company (question 2) with a percentage of negative answers of 46% (36% positive answers), the availability of energy saving information to the employees (question 3), with a percentage of negative answers of 45% (34% positive answers) and the action of spending a part of the yearly budget on energy saving (negative responses at 45%, positive and intended equally at 25%, question 6).

From the other side, they develop energy saving measures in your company at a percentage of 46% (negative responses at 35%, question 4) and, not surprisingly, energy efficiency is an issue when it comes to investments in new machinery and equipment (positive responses at a percentage of 70%, question 5).

Going further in questions regarding the awareness on ecological products for the customers and the companies themselves, (questions 7 regarding customers interested in ecological products and 8 regarding companies' interest in ecological products) the majority of the companies stated that customers show increasing interest for ecological - environmentally friendly print-media products (at a percentage of 53%), and with a percentage of 82% the companies stated that they are interested in ecological products (responses to questions 7 and 8 respectively).

In addition, as it regards the application of environmental, management system (question 9), and the possession of an eco-management and audit scheme certification (EMAS) and an ISO-14001 certification (questions 10 and 11 respectively), a slight majority was positive regarding the application of an environmental management system (43%), whereas there were negative responses in possessing an EMAS (84% no), and an ISO-14001 certification (negative responses at 61%).

However, it must be noted at this point that the negative responses regarding EMAS is justified because none of the companies in the Netherlands has an EMAS certification, because it is not known within the companies of the sector in this country.

Furthermore, going to the issues of availability of data regarding energy consumption in MWh (question 12), yearly energy costs (question 13) and the ways to measure production output, 9question 14), the majority of the companies responded positively and they provided data in this group of questions. However, in the following question 15 concerning the total energy consumption per amount of printed paper (or other production measurement unit) in Wh, the vast majority of the companies did not have this information (no 90%).

Furthermore, going in the degree of interest of the companies in further and more detailed key data (question 16), the vast majority of the companies are interested in further and more detailed key data (yes 72%). Their expectations are that they will give information about energy efficiency of comparable companies within the branch or insight in possible energy efficiency. Hence the majority of the companies is not well informed about a heat and energy recovery within the company (question 17, negative responses at 58%).

Regarding the next question (18) whether companies are able to look for some specific consumption values concerning energy, the majority of the companies responded positively (yes 60%). Furthermore, in question 19, companies do not think that it is necessary to make their delivered data anonymous for further research. This means that they are willing to deliver company data for processing regarding future studies in the issue of energy efficiency (64% negative to make data anonymous). This is the case in Germany, Greece and the Netherlands, whereas the majority of companies in Czech Republic want to keep the data anonymous and the companies in Hungary are divided by 50% to this question.

From the other side, a slight majority of the companies do not have any support concerning energy aspects (no 52%). Here there are differences among the countries - for example 67% of the companies in the Netherlands do have support concerning energy aspects, whereas this is not the case in Germany (68% of the companies do not have support concerning energy aspects).

Finally, as it regards the last two questions 21 about the expectations of the companies concerning an European exchange of energy efficiency data and 22 whether they interested in more information about Energy efficiency via the EEEI project, the vast majority of the companies is positive and they are interested in receiving more information about energy efficiency (77% and 96% respectively).

7. Conclusions

From the data collected via the questionnaires and the interviews made with the graphic arts companies in the 5 countries it can be concluded that there are some differences both as it regards the countries and the use of a different printing technology.

Generally speaking, it can also be concluded that energy is indeed an issue for the companies, however, when it comes to specific actions, companies are not ready to consider energy as an issue. Furthermore, energy seems to be a matter of interest in cases where energy affects the current operation of the company (such as the investment on new machinery). From the other side it is not considered a matter of when it comes to the matter of cost of each printed product-unit.

It is worthwhile to mention that there is more concern about energy consumption and management in companies with installations on web-fed offset and flexible packaging printing (employing rotogravure and flexography printing machines) and less concern (always in comparison) in companies employing sheet-fed and digital printing machines.

A general conclusion can be that it is evident that energy is an issue for the graphic arts companies but not a major one. Actions should be undertaken towards the rise of awareness of the companies regarding energy maters and in particular concrete actions and possibly tools for use in production and management.

Although there are information available regarding energy consumption and the specification of energy costs within the operation of a company, and the management or ownership of the companies follow general recommendations and the legal framework as it regards emission of VOCs and waste disposal, however, they do not follow concrete procedures and steps towards energy saving.

As a final conclusion at this point, the survey revealed that several steps need to be done towards the rise of awareness among the owners /managers of graphic arts companies in the graphic arts sector in Europe. Concrete tools for production and management should be developed towards the energy saving, the reduction of energy consumption and the protection of the environment via the application of energy efficiency management.

8. Further research

Additional survey is required in order to draw attention on the issues of environmental protection, energy consumption and its reduction and the management procedures on energy efficiency. This issue needs to be addressed not only as a process towards the protection of the environment by for example reducing greenhouse gas emissions, but also as a matter for management. Thus this can be considered an innovative approach, combining the visualisation of the often hidden use of energy and the provision of the technical know-how to reduce it with the necessary management structures.

Furthermore, our intention is to propose methods to visualise the SMEs awareness, to develop benchmark tools for the industry with an overview over key figures (financial, technical, management) and to provide an energy-management standard as a suggestion on how energy can become a part of management.

References

[1] (Comprint, 2002) "The horizon of print and publishing-opportunities in the Media economy", Comprint International report, IBI, Duesseldorf in cooperation with the University of Wuppertal, Intergraf, Comprint international 2002, IBI, Ltd., Belgium, 2002

[2] (EEEI, 2007) European energy efficiency improvement project, Introductory document, www.eeei.info, Amstelveen, The Netherlands, January 2007

[3] (Galland et al, 2004) Galland G., Carré B., Vernac Y.: DOC CTP 1852 Article, Centre Technique du Papier, Grenoble - http://www.webctp.com/

[4] (Intergraf, 2004) "Printing and the Environment", publication, Intergraf and UNI-Europa Graphical in collaboration with DG Employment and Social Affairs of the EU, Brussels 2004

Appendix

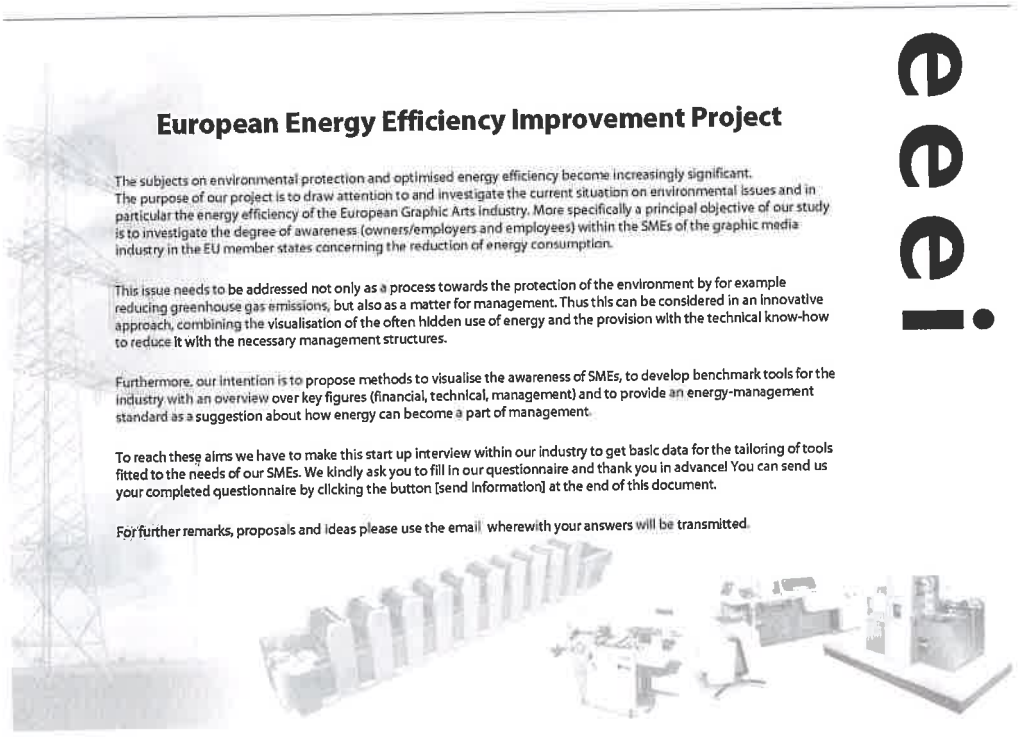

European Energy Efficiency Improvement Project

eei.

The subjects on environmental protection and optimised energy efficiency become increasingly significant. The purpose of our project is to draw attention to and investigate the current situation on environmental issues and in particular the energy efficiency of the European Graphic Arts industry. More specifically a principal objective of our study is to investigate the degree of awareness (owners/employers and employees) within the SMEs of the graphic media industry in the EU member states concerning the reduction of energy consumption.

This issue needs to be addressed not only as a process towards the protection of the environment by for example reducing greenhouse gas emissions, but also as a matter for management. Thus this can be considered in an innovative approach, combining the visualisation of the often hidden use of energy and the provision with the technical know-how to reduce it with the necessary management structures.

Furthermore, our intention is to propose methods to visualise the awareness of SMEs, to develop benchmark tools for the industry with an overview over key figures (financial, technical, management) and to provide an energy-management standard as a suggestion about how energy can become a part of management.

To reach these aims we have to make this start up interview within our industry to get basic data for the tailoring of tools fitted to the needs of our SMEs. We kindly ask you to fill in our questionnaire and thank you in advance! You can send us your completed questionnaire by clicking the button [send information] at the end of this document.

For further remarks, proposals and ideas please use the email wherewith your answers will be transmitted.

Picture 1: Introduction to the EEEI questionnaire

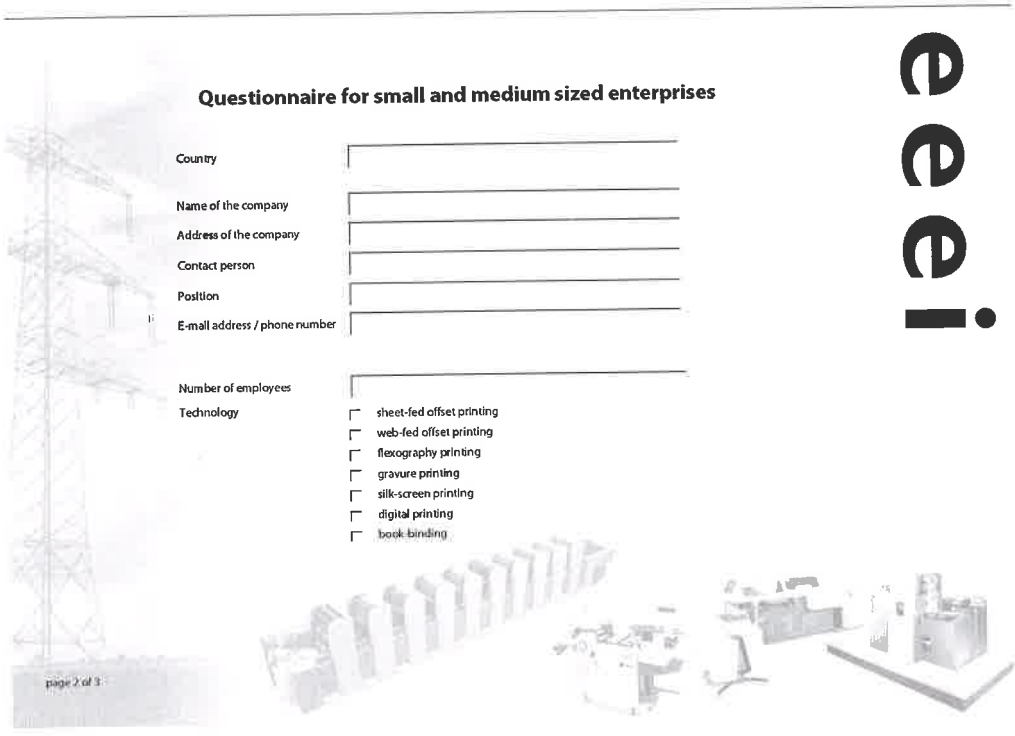

Questionnaire for small and medium sized enterprises

eei.

Country

Name of the company

Address of the company

Contact person

Position

E-mail address / phone number

Number of employees

Technology

- ☐ sheet-fed offset printing
- ☐ web-fed offset printing
- ☐ flexography printing
- ☐ gravure printing
- ☐ silk-screen printing
- ☐ digital printing
- ☐ book-binding

page 2 of 3

Picture 2: Company's data

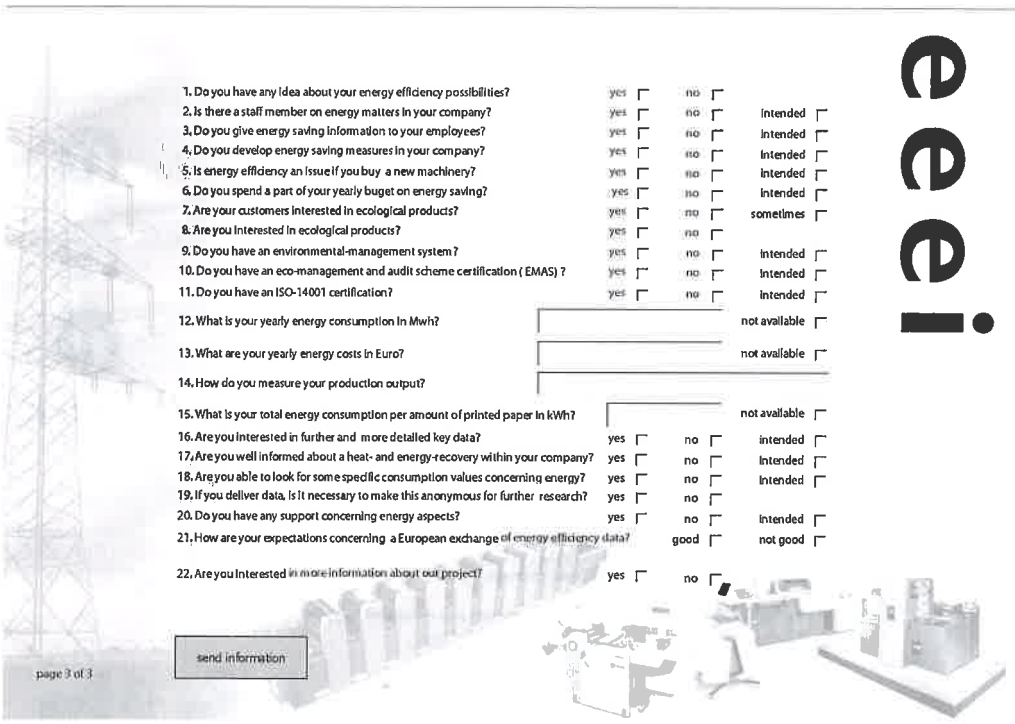

Picture 3: Actual questions on energy efficiency

Customer oriented and sustainable printed paper

Helena Wessman, Anna Leinonen, Eero Hiltunen, Minna Forsell, Catharina Hohenthal-Joutsimo

Oy Keskuslaboratorio - Centrallaboratorium Ab (KCL)
P.O. Box 70, FI-02151, Espoo, Finland
E-mail: Helena.Wessman@kcl.fi

Abstract

The future of sustainable print media offers challenging but interesting alternatives for the European printing industry. The focus cannot be only on environmentally friendly processes - it is obvious that also the product development has to be in line with the principles of sustainability. KCL's procedure for environmentally oriented product development shows how product development decisions affect the environmental load. The procedure is an applicable and transparent way of finding the interactions between customer requirements and environmental burden when designing a fiber based product. The end-user perspective is part of sustainability principles and brings out the societal point of view.

Keywords

Methodology, printed media, product development, sustainability, value chain

1. Background and introduction

Sustainability and sustainable products have become increasingly important in the printing world. The question of climate change has brought out needs to reduce energy consumption, to find out alternative energy sources and to promote material efficiency and recycling. The development is seen in business-to-business relationships and in the growing interests in this topic by consumers, who are willing to know more about product's eco-balance or carbon footprint.

There are several media brands that have committed to sustainable development and 'green products' through their value chain. It can be said that sustainability has become a tool to improve industry's competitiveness. Sustainability and life-cycle thinking are also the basic elements in the on-coming EU directives.

Sustainability should not be focused only on reduced emissions or improved recycling. It should give a holistic view on environmental, social and economic issues through the entire value chain. Sustainability should also be taken into account in all technology levels: in process and product development and in business concepts.

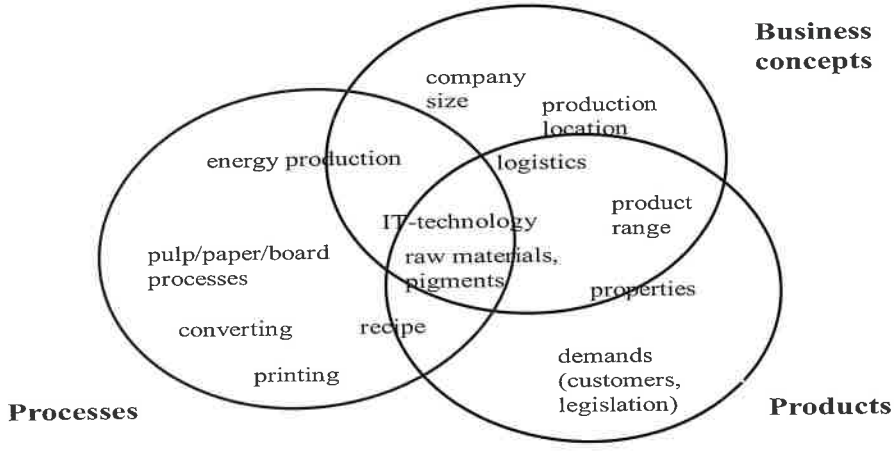

Figure 1: An extended technology level should be taken into account in sustainability assessment

Figure 1 gives an example of some technological factors, where changes affect to the whole value chain and therefore have an impact on sustainability. There are certain factors like IT-technology, raw materials and pigments which belong to all of the three technology levels.

2. Environmentally oriented product development

KCL has developed a new procedure for environmentally oriented product development that is based on the needs of the customer, the consumer and the environment. This procedure takes into account paper's life-cycle from forest to the customer and shows how the product development decisions based on customer's preferences affect the emissions. It is an example of how to combine environmental development and customer's needs already at the early stages of product planning. It gives also an example of a product-based approach in widened technology thinking.

Our target was to create a transparent link between consumer needs and environmental load. In practice, qualitative customer information was transformed into concrete numerical values that can be used to support decision-making related to product development. A case study for pharmaceutical packaging was created but the procedure can be applied to any type of printed paper or board product that is near the end-user.

The procedure consists of:

◊ Definition of the customer requirements;
◊ Specification of product properties that respond to the customer needs;
◊ Definition of the technology needed to change the product properties;
◊ Estimation of the main environmental burden caused by the new technology;
◊ Determination the environmental burden through the value chain by an eco-balance calculation.

Customer's qualitative voice was transformed into a quantitative form by the use of the QFD (*Quality Function Deployment*) method. In the QFD, the product properties that respond to the customers' needs are defined and the unit operations of the production process affecting the critical product properties are specified. The development actions were defined based on the results from the QFD matrix. The next stage of the product development procedure was to determine the environmental burden caused by the planned development actions. The method in this stage was Life Cycle Inventory (eco-balance) calculation using KCL-ECO calculation software and data from literature and forest industry specific KCL EcoData database.

3. The product development case "Pharmaceutical packaging"

The product developed in the case study was a carton box made of folding boxboard. One of the customer requirements was that the print quality needed improvement. As the reference board was assumed to be uncoated, the product development action was to replace the uncoated board with a coated one. The coating increase the grammage of the board from the original level. Coating increase also the energy consumption during the production process because additional drying phases are needed. To sum up, the first step in the calculation was to define how the planned product development action affects energy consumption and raw material demand.

The final step of the procedure was to determine the environmental burden caused by the changes in energy consumption and raw material demand. This was fulfilled by life-cycle inventory calculation including the following life cycle stages (see Figure 2):

◊ harvesting operations,
◊ transports of wood and pulp,
◊ kraft pulping process,
◊ pigment manufacturing process and the transport of pigments,
◊ folding boxboard production,
◊ energy production (including mill energy production and external electricity from the grid).

The harvesting operations included birch harvesting for the kraft pulp and spruce harvesting for the mechanical pulp. Unlike the mechanical pulping process the kraft pulping process was not integrated in the folding boxboard process. The transport distances and vehicle types were set to certain default values. For the

external electricity the average Finnish fuel mix in energy production was used. All data used for the calculation was from the KCL EcoData database.

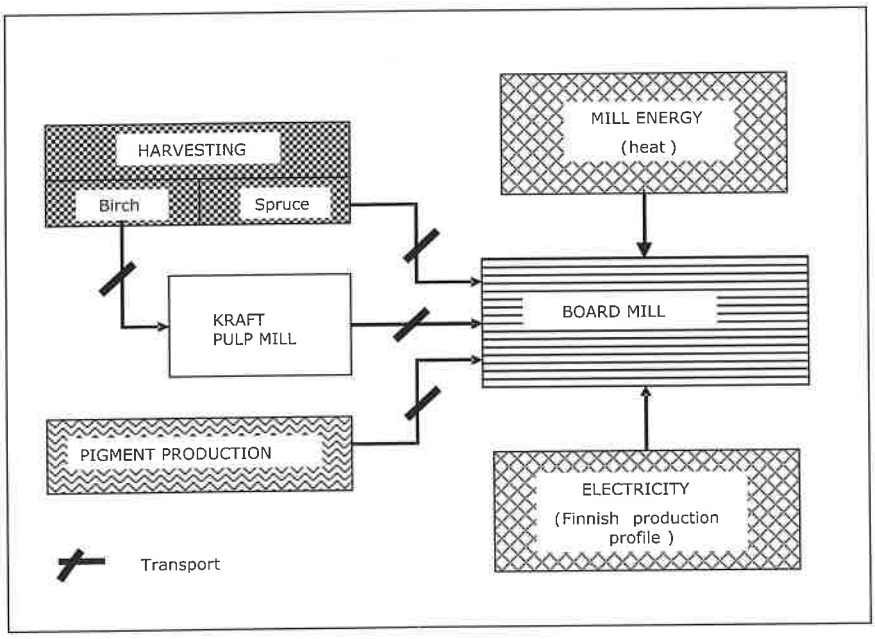

Figure 2: Flowsheet in the LCI calculation

The results in Figures 3 - 5 show that energy production is the most significant life cycle stage causing air emissions like CO_2, NO_x and SO_2. The effect of energy production on the air emissions is more than half of the total emissions in every emission type. Especially in CO_2 emissions the proportional share of energy production is remarkable. The kraft pulp mill is another significant emission source causing NO_x and SO_2.

The Figures 3 - 5 illustrate also the effect of the functional unit on the calculation results. Our aim was to show the difference between the reference product and the improved product but also the difference between two functional units. There are two optional approaches that are possible to calculate the emissions: They can be calculated either per ton (reference case and the improved product) or per constant number of packages (the improved product). Calculation per ton is the traditional approach in the paper and board mills and in LCA applications. However, from the end user's perspective, the number of packages is usually more relevant. A certain amount of packages is the primary need; the amount of material in tons needed for the manufacture is secondary. A similar situation can be found for paper products like copy papers and magazines.

The comparison per number of packages requires us to take into consideration the fact that the area of ton uncoated board is bigger than the area of the same amount of coated board. Therefore, the emissions appear to increase more when the comparison is made per number of packages [Leinonen et al., 2006].

4. Conclusions and discussion

The procedure for environmentally oriented product development shows how product development decisions affect the environmental load. The procedure is an applicable and transparent way of finding the interactions between customer requirements and environmental load in designing a fiber based product. It can be used already in the early stages of the product development process and utilized concretely in the decision-making when choosing printing or special converting processes. One of the key principles was to direct the emissions to the final product, which means that special attention should be paid to the functional unit. The case study showed that comparison per package produced higher differences in emissions. This is important to know when selecting the right functional unit for the comparisons in order to find the most beneficial product development alternatives.

Implementing a life-cycle approach is today's environmental policy. Reporting company's process emissions or energy use is not enough anymore. A responsible brand owner is expected to be aware of the sustainability

of the whole value chain, including the suppliers. Our procedure showed how eco-balance calculations can be utilized in product development. Eco-balance has been in use for many years in process benchmarking in the paper industry. Eco-balance studies have been successfully used also in future business scenarios, for instance comparing alternative concepts in logistics or raw material production.

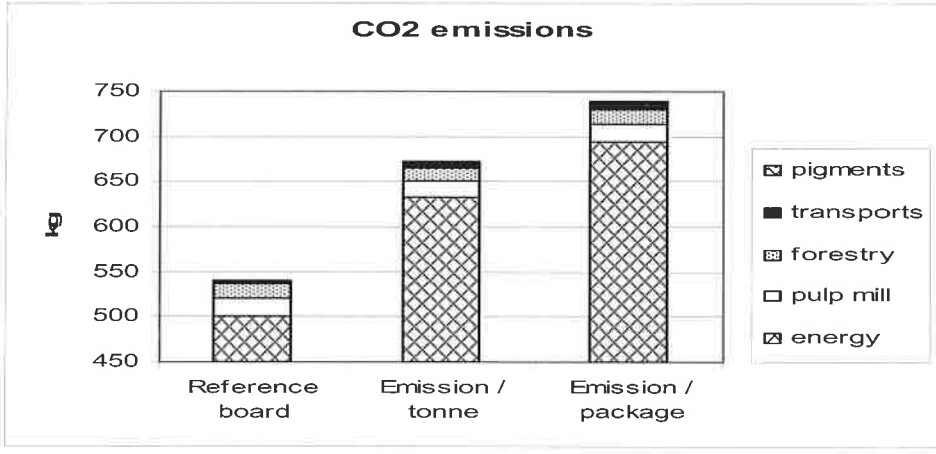

Figure 3: The change in CO_2 emissions

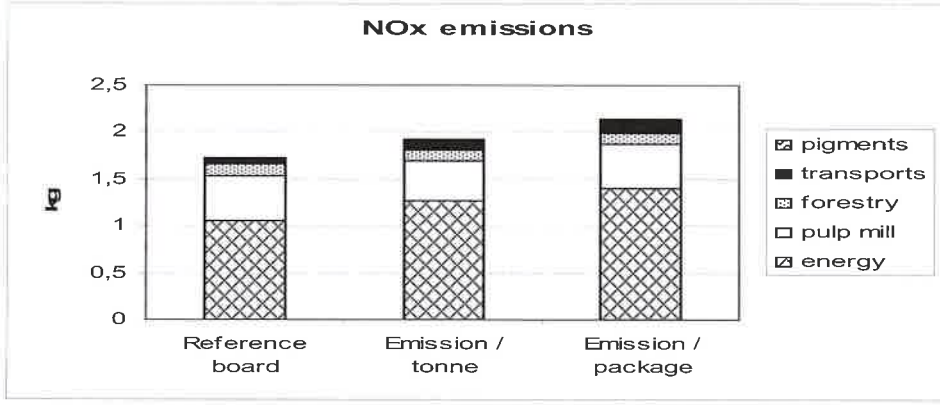

Figure 4: The change in NO_x emissions

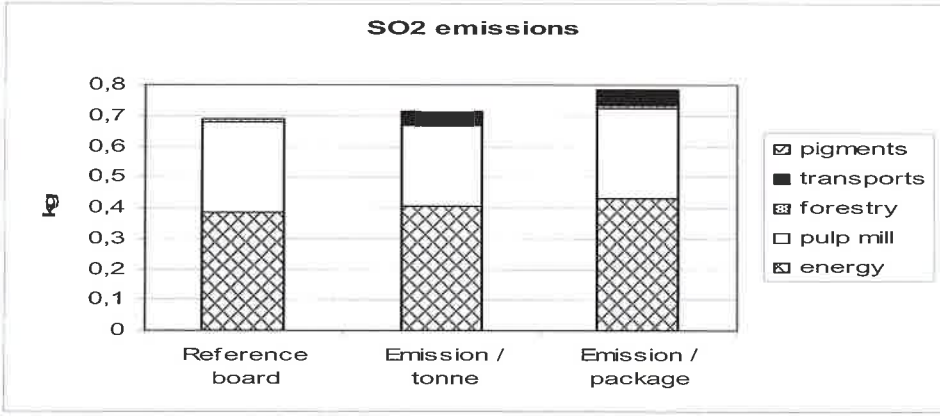

Figure 5: The change in SO_2 emissions

A strong end-user focus is the key issue in business. If we think about the end-users' attitudes, it is obvious that 'being sustainable' improves company's image among the customers and consumers. Companies or

brands that are proactive can obtain benefits, which can lead to improved material and energy balance, reduced environmental costs and better status in society. As the environmental product development case showed, data gathering should be based on the end-user's requirements, which guarantees that the product development activities could be focused on the right product properties. The end-user perspective is part of sustainability principles and brings out the societal point of view.

For the printing industry, the future of sustainable European print media offers interesting alternatives. The focus cannot be only on environmentally friendly processes - instead the product development has to be in line with the principles of sustainability. We are starting a national co-operation project in Finland, where the sustainability of the printed product's value chain will be studied together with the role of raw materials, material and energy efficiency, location of the production site and new technologies. It will be a challenge for the industry to develop suitable tools to manage the future changes proactively.

References

[1] Enroth, M., (2006) *Developing tools for sustainability management in the graphic arts industry. Doctoral Thesis, Royal Institute of Technology in Stockholm (KTH), Sweden*

[2] ReVelle J., Moran J. and Cox C., (1998) *The QFD Handbook, John Wiley & Sons, Inc. New York. 403 p*

[3] Leinonen, A., Forsell, M., Hiltunen, E., Hohenthal-Joutsimo, C., Wessman, H., (2006) *New approach to environmentally oriented product development in pulp and paper industry. Proceedings from EMAN Conference April 2006, Graz, Austria*

Referenced software and database

[1] KCL *KCL-Eco 4.0 LCA Software,* http://www.kcl.fi/page.php?page_id=166

[2] KCL *KCL EcoData database*, http://www.kcl.fi/page.php?page_id=309

Screening environmental life cycle assessment of printed, internet-based and tablet e-paper newspaper

Åsa Moberg[1,2,4], *Martin Johansson*[1], *Göran Finnveden*[2,4], *Alex Jonsson*[3,4]

[1] STFI-Packforsk, PO Box 5604, SE-114 86 Stockholm, Sweden
E-mail: asa.moberg@stfi.se; martin.johansson@stfi.se

[2] KTH, Royal Institute of Technology
Division of Environmental Strategies Research, Department of Urban Planning and Environment
School of Architecture and the Built Environment, SE-100 44 Stockholm, Sweden
E-mail: asa.moberg@infra.kth.se; goran.finnveden@infra.kth.se

[3] KTH, Royal Institute of Technology
Department of Media Technology and Graphic Arts, School of Computer Science and Communication
SE-100 44 Stockholm, Sweden
E-mail: alexj@nada.kth.se

[4] KTH, Royal Institute of Technology
Centre for Sustainable Communications
SE-100 44 Stockholm, Sweden

Abstract

Viable alternatives to conventional newspapers, such as electronic papers, e-papers or e-readers, are intended to have many of the qualities of paper, such as reading using reflective light, high resolution, 180° viewing angle. It has been suggested that the environmental impact of e-paper can be lower than for printed and internet-based newspapers. However, a life cycle perspective covering raw material acquisition, production, use and disposal should preferably be used to study the environmental performance of the different products. In this way any shift of environmental impact from one part of the life cycle to another can be avoided. In the present study a screening life cycle assessment was performed to describe the potential environmental impacts of three product systems; printed, internet-based and tablet e-paper newspapers. Results from the study show that the significant phases of the life cycle differed for the three product systems and that printed and internet-based newspapers with a longer reading time (i.e. 30 minutes/day) had a higher impact than tablet e-papers and internet-based newspapers with a shorter reading time (i.e. 10 minutes/day). Key aspects that may affect the resulting environmental performance of newspaper product systems were identified. These include number of readers per copy of printed and tablet e-paper newspapers; reading time for internet-based newspapers; lifetime of electronic devices and multi-use of electronic devices. It was concluded that tablet e-paper has the potential to decrease the environmental impact of newspaper consumption.

Keywords

E-paper, environment, electronic paper, life cycle assessment, newspaper

1. Introduction

Viable alternatives to conventional newspapers have been available for roughly three years and are often referred to as electronic papers, e-papers or e-readers. These products are intended to have many of the qualities of paper, such as reading using reflective light, high resolution, 180° viewing angle and high contrast. These properties, along with notably low power consumption, distinguish the e-paper displays from devices relying on more traditional display technology, such as LCD, CRT or plasma screen components. Apart from the display itself, the e-paper device consists mostly of standard components, such as plastic housing, low-power one-chip microprocessor, rechargeable battery, controller boards and implements for navigation, such as buttons, jog wheels or stylus for browsing through household electronic newspaper editions. Some of the devices also carry an on-board wireless radio transceiver to automatically download the latest edition on demand, which makes them similar in usage to a cellular phone but with approximately ten times larger screen.

When a tablet e-paper is used instead of a printed newspaper, the paper material, physical distribution of the printed paper, etc. are avoided. The e-paper device has substantially lower energy use during downloading and reading compared with using a computer for reading newspapers on the internet. Thus, it has been suggested that the environmental impact can be lower than for printed and internet-based newspapers. A life cycle perspective should be used to study the environmental performance of the products. In this way any shift of environmental impact from one part of the life cycle to another can be avoided.

A comparison between the three product systems using a life cycle perspective has been performed in a previous study by IZT [Kamburow, 2004] focusing on the cumulative energy use. Several studies have been made of the environmental impact of printed media and paper [e.g. Axelsson and Dalhielm, 1997; Axel Springer Verlag AG, Stora & Canfor, 1998; Johansson, 2002; Larsen et al., 2004]. Internet-based newspaper reading has been compared with reading of printed newspapers in previous studies [Hischier and Reichart, 2001; Yagita et al., 2003]. In addition, other kinds of information in printed or electronic form have been compared from an environmental perspective. Gard and Keoleian (2003) studied digital and printed journal articles. Many of the studies comparing electronic reading with reading printed matter have focused on energy or climate change [e.g. Yagita et al., 2003; Gard and Keoleian, 2003; Kamburow, 2004]. The results indicate that the reading time for internet-based newspapers is crucial [Hischier and Reichart, 2001; Yagita et al., 2003]. The number of unique readers has been shown to influence the environmental performance [Gard and Keoleian, 2003]. So far, to our knowledge, no comprehensive environmental life cycle assessment (LCA) comparing e-paper, printed and internet-based newspapers has been made.

1.1 Scope of the study

The aim of the study presented in this paper was to describe the potential environmental impacts of the three product systems printed newspaper, internet-based (web based) newspaper and tablet e-paper newspaper. Sundsvalls Tidning (ST) was used as a model newspaper, as this Swedish newspaper has been produced and distributed as a printed newspaper, an internet-based newspaper and a tablet e-paper newspaper. ST has performed a full-scale test with an iRex Iliad e-paper device, and was thus able to provide important input. A major part of the newspaper data defining the three product systems studied was obtained from ST, for example edition, number of pages and number of readers. The scope of the study was firstly to study a newspaper from a European perspective, with European electricity mix and waste flows, etc. In addition, a Swedish scenario was tested. In this paper, which is an elaboration of a larger technical report [Moberg et al., 2007], the emphasis is on the European scenario.

2. Methods

Life Cycle Assessment (LCA) is a method to assess the potential environmental impacts and resources used throughout a product's life from raw material acquisition through production, use and disposal. The term 'product' can also include services. An ISO standard has been developed for LCA, providing a framework, terminology and some methodological choices [ISO, 2006]. An LCA is divided into four phases: Goal and Scope Definition, Inventory Analysis (which is a compilation of the inputs and the outputs of the system [Rebitzer et al., 2004], Life Cycle Impact Assessment (LCIA), and Interpretation. The results from the Inventory analysis are a compilation of the inputs (resources) and the outputs (emissions) from the product over its life cycle in relation to the functional unit. The latter is a description of the functions that the product (or service) provides. All results in an LCA are related to this functional unit. In comparative studies, the definition of the functional unit is essential so that the alternatives are compared on a fair basis.

The LCIA phase is divided into several elements, some of which are regarded as optional [ISO, 2006]. The first elements of the LCIA (Classification and Characterisation) are based on more or less traditional natural science and aim to describe the contribution from the studied system to a number of environmental impact categories such as resource depletion, human health impacts and ecological consequences. One of the optional elements of LCIA is called weighting and includes a valuation of different impact categories against each other. This may include different types of monetisation methods or multi-criteria decision analysis techniques [Pennington et al., 2004]. In this step different types of values are required and natural science alone is thus not enough.

A full LCA can be time-consuming and resource-intensive. Instead of starting with a full LCA, an alternative approach can be to perform a screening LCA with the aim of identifying the most important aspects of the

studied system. If necessary, more detailed studies can then be directed to these important aspects [Lindfors et al., 1995]. A screening LCA is usually performed using easily accessible data. Since the aim is to identify the most important processes, data quality is of less importance than in a full LCA. However, it is important to include all processes and materials that can be of major importance, but if some processes or materials are known to be of minor importance, they can be excluded.

2.1. Functional unit

The functional unit of the study was 'the consumption of newspaper during one year by one unique reader'. The three product systems were studied separately and no combinations were made within the scope of this study (e.g. reading of an internet-based newspaper combined with a printed version).

2.2 Environmental impact categories

Several different environmental impact categories were assessed; resources used (non-renewable, renewable and total), acidification, climate change, eutrophication, photochemical oxidant (photo-oxidant) formation, ozone depletion and toxicity based on Guinée (2002) and Finnveden and Östlund (1997). In addition to the results for each impact category, two different kinds of weighting methods were used; Ecotax 02 [Finnveden et al., 2006] and Ecoindicator 99 [Goedkoop and Spriensmaa, 2000]. Ecotax is a monetary method where the weighting is based on environmental taxes and fees in Sweden. The Ecotax method has two alternative weighting factors, minimum (min) and maximum (max), representing the span of taxes and fees on various substances within the same impact category. Ecoindicator 99 is a panel method where the members of the panel are asked to rank and weight three damage categories: ecosystem quality, human health and resources.

2.3 Studied systems

In the screening LCA performed, the studied systems included activities from the cradle to the grave. For the printed newspaper this meant that forestry, pulp and paper production, editorial work, prepress, printing and distribution of the newspaper were covered, including the production of supply material. The user phase (reading) and waste management of the waste newspaper were also considered. For the internet-based newspaper the production of PC and screen, editorial work, distribution, user phase (reading on screen) and waste management of the waste PC and screen were covered. Similarly, for the tablet e-paper newspaper the production of the tablet e-paper device, work, distribution, user phase (reading on screen) and waste management of waste tablet e-paper device were considered. Transportation in different stages of the life cycles was also included.

Most of the data used were from Ecoinvent 1.2 and the GaBi 4.112 database. Some of the inventory data for printing were derived from earlier studies at STFI-Packforsk [e.g. Axelsson and Dalhielm, 1997; Strömberg, 1998]. The PC, screen and tablet e-paper device were modelled by LBP at Stuttgart University, mainly based on data from the GaBi 4.112 database. For a full list of references, see Moberg et al. (2007). Easily available data could not be found for all the activities of the respective systems. In general, all supply materials were not followed from the cradle. Some major data gaps included the journalists' fieldwork (i.e. travel); production of tablet e-paper e-ink screen; e-infrastructure for the distribution of the internet-based and tablet e-paper newspapers and recycling of electronic waste.

The results presented in this paper are mainly for a European scenario. This means that the newspaper company and the reader were assumed to be European and European energy mixes and waste management practices were used. The electronic equipment (PC, screen and e-paper device) was assumed to be produced in China. Content production was distributed equally between each unique reader, independent of the product used. The editorial work was inventoried as energy use (electricity and heat). The total number of unique readers was assumed to be 86.000 per day (see Table I). The energy data used for editorial work were taken from another, smaller newspaper (15.000 copies and 28 pages compared with 32.000 copies and 40 pages in the studied case). The data included both electricity and heat: 6480 MJ/edition [Lindblad, 2001].

2.4 Printed newspaper

The printed newspaper studied is described in Table I. Data were mainly based on information from Sundsvalls Tidning. The amount of copies and readers were estimated from the current edition and the

assumption that 2 000 readers will change to tablet e-paper [S. Boström, personal communication 2006]. The paper used was assumed to be European average 45 g/m^2 DIP (de-inked pulp)-containing newsprint. Data from an internal STFI-Packforsk database [Mint, 2005] gave an estimated fuel consumption for urban distribution of 0.0043 litre fuel/newspaper. The reading time, 30 minutes, was based on information from the Swedish Newspaper Publishers' Association [TU, 2006].

2.5 Internet-based newspaper

The internet-based newspaper studied is described in Table I. The data on readers per day and size of the electronic newspaper were taken from Sundsvalls Tidning [S. Boström, personal communication 2006]. The reading time of 10 minutes per day was based on Holsanova and Holmqvist (2004). Data on down-loading and power of electronic equipment were assumptions made based on information on average equipment. It was assumed that a home computer (PC and screen) was used and that this computer was used in total for 4 hours per day on average. This assumption was based on a compilation of studies of computer use patterns by Jönbrink and Amen (2006) where the range of active use time for a home computer was reported to be 2 - 6 hours per day.

Table I: Description of the newspaper product systems studied

Parameter	Printed newspaper	Internet-based newspaper	Tablet e-paper newspaper
Edition	32.000 copies/day, 6 days/week	7 days/week	7 days/week
Size	40 pages, tabloid (40x28 cm^2)	2.5 MB/day	5 MB/day (2.5 MB two times per day)
Number of readers	76.000 unique readers/day (2.4	8.000 unique readers/day	2.000 unique readers /day
Paper	45g/m^2 DIP-containing newsprint		
Server power			900 W
Up-loading speed (server)			3 MB/s (24Mbits/s), (0.0025 MB/day & reader)
E-paper power (down-loading)			0.75W
Down-loading speed		0.25 MB/s (2 Mbits/s)	0.25 MB/s (2 Mbits/s)
Power (reading)		Computer 160W Screen 120 W	Tablet e-paper 0.001W
Reading time	30 minutes/day	10 minutes/day (4% of total use)	30 minutes/day (50% of total use)
Use for other purposes		3 hours 50 minutes	30 minutes/day
Life time of electronic product		5 years	1 year

The lifetime of the computer was assumed to be 5 years [H. Wendschlag, personal communication 2007]. In this study 70% recycling and 30% incineration of electronic equipment were assumed. This may be an overestimation of recycling and an underestimation of landfill [Moberg et al., 2007].

In the comparison two versions of the internet-based newspaper product system were included. The average reading time, which was 10 minutes for the internet newspaper, was complemented with a product system with 30 minutes of reading. In the 30 minutes case, the downloading was estimated to be 5.5 MB/day, compared with 2.5 MB/day for the 10 minutes reading case.

2.6 Tablet e-paper newspaper

The tablet e-paper newspaper product system is still under development. Data for this product system were therefore relatively hard to access within the scope of this study and estimations were made.

The tablet e-paper newspaper studied is described in Table I. The data on readers per day was is an approximation of a probable scenario in 5 years time [S. Boström, personal communication 2006]. The reason

for not studying the situation as it is today was that this scenario would not be feasible, i.e. a tablet e-paper newspaper system including only the approximately 10 readers that were part of the ST trial. The e-paper newspaper was sent to the readers twice a day in this case.

Technical data regarding the e-paper device (e.g. power) relate to the iRex Iliad tablet e-paper device used by Sundsvalls Tidning [P. Leurs, personal communication 2006]. Data on the server power and uploading speed were based on estimations. The reading time, 30 minutes per day, was an assumption based on the reading time for printed newspaper [TU, 2006]. Use of the e-paper device other than for reading newspapers includes reading e-books, e-documents, e-journals, etc. and a rough estimation of the time for other use was 30 minutes per day. The time for other use is uncertain, since the tablet e-paper is not yet frequently used and information on user behaviour was not readily available. The assumption of a lifetime of 1 year was based on an assumption of rapid development of this new product, resulting in an actual lifetime that is shorter than the technical lifetime. It can be assumed that the actual lifetime will increase as the e-paper device matures. The waste management of the tablet e-paper device was based on the same assumptions as for the waste management of the PC and screen.

2.7 Comparison between printed, internet-based and tablet e-paper newspapers

A comparison was made between the three product systems in which two versions of the internet-based newspaper product system were included. The average reading time, which was 10 minutes for the internet newspaper, was complemented with a product system with 30 minutes of reading. It can be questioned whether the same reading time would be used irrelevant of the medium (printed, internet-based or tablet e-paper) if only one of these news sources were to be used. If this were the case, then the comparison of the same reading times would be more relevant. However, it can be argued that the internet-based newspaper fulfils a different function [Holmqvist et al., 2003; Holsanova and Holmqvist, 2004], which involves a shorter reading time. Then the comparison is delimited by the difference in function (benefit).

3. Results

The results presented here are a selection of the results presented in Moberg et al (2007). It should be noted that the uncertainties were large for the toxicological impact categories. There were knowledge gaps that made it difficult to characterise toxicological impacts, and there were many data gaps concerning toxicological emissions in the data inventories. It is still important to include toxicological impacts, but to be aware of the uncertainties. In addition, the data used for the production of the tablet e-paper were uncertain due to lack of specific data.

3.1 Printed newspaper

The paper caused the main environmental impact of the printed newspaper. This is in line with previous studies, e.g. Enroth (2006) states that the use of paper (forestry, pulp and paper production) generally gives rise to 30 - 70% of the total environmental impact of printed paper products. Generally, printing gave rise to the second largest impact, but several other activities gave rise to comparable impacts in several impact categories. Paper caused 55 - 70% of the total weighted impact according to the weighting methods used. Using the Ecotax 02 method min version, printing was the second most important activity and thereafter landfill, editorial work, paper transport and prepress gave rise to similar levels of total impact. When the Ecotax 02, max version was used, printing and editorial work came second to paper, followed by prepress with a slightly lower total weighted value. Distribution was not significant when Ecotax 02 was used, partly due to toxic emissions being missing to a large extent for the distribution inventory data. With the weighting method Ecoindicator 99, printing was second to paper again, followed by paper transport, editorial work, distribution and prepress. It can be noted that in the Swedish scenario, where rural distribution was assumed to have higher fuel consumption per newspaper, distribution had the second highest weighted impact using the Ecoindicator 99 (paper generally caused the main impact of the printed newspaper life cycle also in the Swedish scenario).

3.2 Internet-based newspaper

The energy use for reading was the main contributor in all impact categories: acidification, eutrophication, photo-oxidant formation, ozone depletion and global warming. Editorial work, screen production and PC

production were the other main contributors. Regarding toxicological impacts the incineration of waste electronics (plastic parts) made up a considerable part of the total potential impact. The results for the internet-based newspaper reflected the shorter reading time of 10 minutes.

The weighted results showed similar trends. The energy for reading gave rise to the main total impact, roughly 50%. Using the Ecotax 02 minimum version, the editorial work and incineration of waste electronics were second in impact, while PC and screen production did not contribute significantly. However, when the maximum version of the Ecotax 02 was used, editorial work and screen production were second in impact, followed by PC production, while incineration was not significant. With the Ecoindicator 99 weighting, editorial work came second to energy for reading, followed by PC and screen production with similar values. Generally, it can be noted that in the Swedish scenario the impact of the internet-based newspaper product system was generally lower and the energy for reading had a lower share of total impact. This was due to differences in electricity mix, UCTE in the European case and Nordel in the Swedish case, where the latter consists of 60% hydropower.

3.3 Tablet e-paper newspaper

The production of the tablet e-paper device made up the largest part of the impact categories in general for the tablet e-paper newspaper life cycle. The editorial work also made a significant contribution. In the toxicological impact categories, the incineration of waste electronics (plastic parts) was important. The weighted results were the same for Ecotax 02 (max) and Ecoindicator 99: e-paper production made up the major part of the total weighted results (about 75%) and the rest was the editorial work. However, when the Ecotax 02 (min) weighting method was used editorial work, e-paper production and incineration all made up one third of the total weighted results.

3.4 Weighted results

Weighted results are inherently uncertain. Using different weighting methods within the same study illustrates this uncertainty and emphasises the need to interpret the results and consider underlying assumptions and data. The total weighted results of the three product systems consisted mainly of toxicological impacts when Ecotax 02 was used, but when Ecoindicator 99 was used the main impact category was resources (fossil fuels) and human health (respiratory). Different categories of toxicological impacts were significant with the different versions of Ecotax 02 (minimum and maximum) and the total weighted values differed considerably. This shows both the uncertainty of weighting and the uncertainty regarding toxicological impacts.

3.5 Comparisons

Regarding the comparisons made between the product systems, it can be questioned whether it is relevant to compare 10 minutes reading on the internet with 30 minutes reading a tablet e-paper. The function and benefit may be too different, even when comparing 30 minutes of reading on the internet with 30 minutes of reading a tablet e-paper or a printed newspaper, and the benefit or function provided may not be the same [e.g. Holmqvist et al., 2003; Holsanova and Holmqvist, 2004]. It was not possible to cover this issue in this study, but it should be kept in mind.

The total energy in resources used for one year's consumption of a newspaper by a unique reader varied from 860 down to 280 MJ in the European scenario (Figure 1). The highest value of 860 MJ was the same for the printed newspaper and the internet-based newspaper with a reading time of 30 minutes. There was a difference of 70 MJ/year and unique reader between the internet-based (10 min) and tablet e-paper newspapers where the tablet e-paper had the lower value. The pattern was the same for the other resource use impact categories studied (abiotic depletion potential and exergy).

The energy in resources used for the tablet e-paper was mainly from the e-paper production. Since the reading of the tablet e-paper newspaper was assumed to make up half the total use time of the tablet e-paper, half the resources used in production of the device were allocated to this product system. In the case of the internet-based newspaper, only 4% of the total use of the home computer and screen was assumed to be dedicated to reading the newspaper (10 minutes out of 4 hours). The lifetime of the tablet e-paper was also assumed to be

shorter than that of the home computer and screen, 1 year and 5 years respectively. Thus there is the potential to increase resource efficiency for the tablet e-paper newspaper.

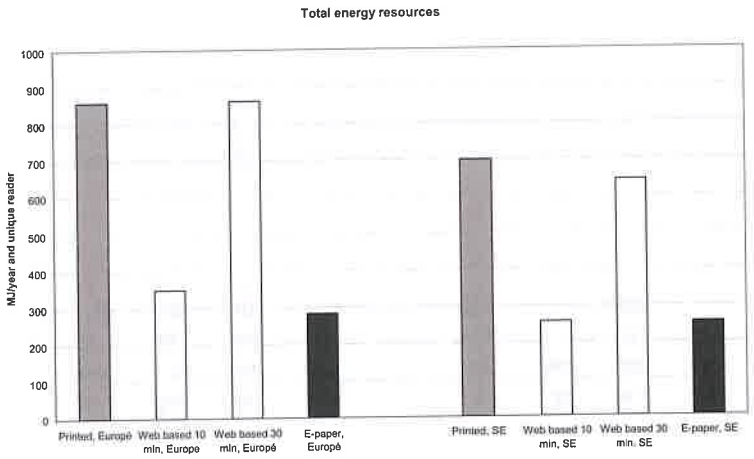

Figure 1: Total energy in resources used (MJ/year and unique reader) for newspaper product systems in a European scenario and a Swedish (SE) scenario

For eutrophication, ozone depletion and photo-oxidant formation, the printed newspaper had the largest potential impact. Regarding acidification, the internet-based newspaper (30 min) was the major contributor, followed by the printed paper. On a lower level, the tablet e-paper and the internet-based newspaper (10 min) had similar values in the impact categories acidification, eutrophication and photo-oxidant formation. For ozone depletion, the potential impact was in the same range for the tablet e-paper, the internet-based newspaper (30 min) and the printed newspaper product system.

Regarding the global warming impact category, the internet-based newspaper (30 min) had the largest contribution; 35 kg CO_2/year and unique reader, followed by the printed newspaper with 28 kg CO_2/year and unique reader. The internet-based (10 min) and tablet e-paper newspapers had a global warming potential of 14 and 13 kg CO_2/year and unique reader, respectively. This can be compared with a 200 km trip by private car, which gives rise to roughly 30 kg CO_2 (assuming 0.15kg CO_2/km).

The internet-based (30 min) and printed newspapers had similar impact values in the toxicological impact categories. The internet-based (10 min) and tablet e-paper newspapers also had similar values but lower than for the other two product systems.

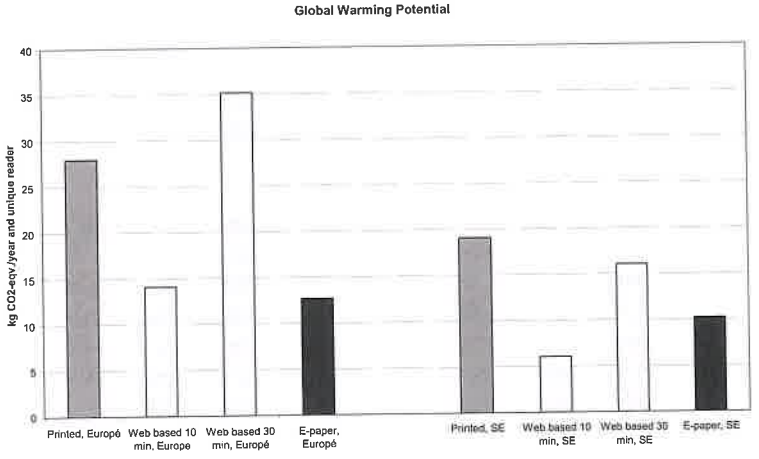

Figure 2: Global warming potential (kg CO_2-eqv/year and unique reader) for newspaper product systems in a European scenario and a Swedish (SE) scenario

The total weighted results of the product systems Ecotax 02 (min version) and Ecoindicator 99 showed similar patterns, where the printed newspaper product system gave rise to the highest values followed by the internet-based newspaper with 30 minutes of reading. The tablet e-paper newspaper and the internet-based newspaper with 10 minutes reading had lower total weighted values. The tablet e-paper newspaper had higher total weighted values than the internet-based version in the Swedish scenario due to lower impact from the energy use for reading, as the Nordel electricity mix was used. Using the Ecotax 02 max version, the internet-based newspaper with 30 minutes reading per day was ranked highest, followed by the printed, internet-based (10 minutes reading) and tablet e-paper newspapers. However, in the Swedish scenario the tablet e-paper newspaper was second to the internet-based (30 minutes reading), closely followed by the printed newspaper.

4. Discussion

The newspaper product systems studied differed concerning the medium in which they are displayed/ distributed. The production of the substrate/device was shown to be of major importance from an environmental perspective: paper production for the printed newspaper, PC and screen production for the internet-based newspaper and e-paper device production for the tablet e-paper newspaper. The influence of these production activities on the total life cycle impact of the systems depended on the total use of the respective substrate/device. In this study, the environmental performance of the printed newspaper was related to each unique reader. This means that the environmental impact of a single copy of the printed newspaper was split between 2.4 unique readers. It was assumed that the internet-based newspaper was read for 10 minutes/day or 30 minutes/day and that the computer was used for a total time of 4 hours per day. If the total use time were for example 2 hours per day instead, the impact caused by production (and waste management) of the PC and screen allocated to the internet-based newspaper life cycle would be roughly doubled. The impact from the tablet e-paper device was in accordance with the PC and screen, highly sensitive to the assumed lifetime and the total use time per day of the equipment. In the study it was assumed that the tablet e-paper newspaper was read for 30 minutes/day and that the device was used for a total time of 1 hour per day. The lifetime of the tablet e-paper device was assumed to be one year. The environmental impact of the tablet e-paper newspaper would decrease with a longer lifetime, which is probable as the product matures.

In the comparison between the different newspaper product systems, the results showed that the ranking from an environmental point of view was in general that tablet e-paper and the internet-based newspaper with a shorter reading time (10 minutes per day) gave rise to a lower environmental impact than the printed version. However, with a reading time of 30 minutes per day the environmental impact of the internet-based newspaper was often in the same range as that of the printed newspaper, sometimes higher and sometimes lower. Similar results were presented by Hischier and Reichart (2001) in their comparison between printed newspaper, television and internet. These authors showed that using the internet for around 25 minutes or watching television for roughly 1.5 hours gave an environmental impact of similar magnitude to that of a printed newspaper. Their results were presented as weighted values, using Ecoindicator 99.

As illustrated by the two scenarios, European and Swedish, the electricity data used can also influence the results as the impacts vary between the sources of electricity. In our study this also illustrated the different relative importance of life cycle phases of the product systems. The tablet e-paper product system generally had its main impact where the tablet e-paper was produced (China) and this was not altered in the scenarios, whereas the internet-based newspaper user phase was significant and the conditions for the user phase changed between the scenarios.

Yagita et al. (2003) compared printed and internet-based newspapers regarding CO_2 emissions, excluding waste treatment. They concluded that the resulting emissions were dependent on whether a desktop or a notebook PC was used, as the notebook uses less energy. With their assumptions the internet-based newspaper gave rise to lower CO_2 emissions than the printed version as long as the PC was not used for more than 1.4 hours and 1.1 hours per day for notebook and desktop respectively. The emissions from the life cycle of the printed newspaper were calculated to be 0.32 kg CO_2/copy of newspaper [Yagita et al., 2003]. This can be compared with the results of the present study, recalculate as 0.22 kg CO_2/copy of newspaper. Yagita et al. (2003) compared the printed newspaper copy with the internet-based newspaper and did not consider the possibility of more than one reader per copy.

The results of the present study indicated that in many impact categories, the differences were small between the internet-based newspaper with 10 minutes reading time and the tablet e-paper newspaper. In the

comparison by Kamburow (2004), the e-paper newspaper resulted in a larger cumulative energy use compared with printed and internet-based newspapers. The energy figure was roughly 5 and 25 times higher for the e-paper newspaper when the electronic news was distributed via the internet and UMTS respectively. In a sensitivity analysis DAB distribution was shown to give substantially lower energy use and the e-paper newspaper resulted in total energy figures in the same range as the printed and internet-based newspapers. As we were not able to cover e-infrastructure in our study, this could be an interesting topic for future studies.

4.1 Missing data

In our study, screening data were used in some cases and some data were missing. The main inventory data lacking for the internet-based and tablet e-paper systems included electronic distribution infrastructure and material recycling of parts of the waste electronic devices. For the tablet e-paper, data for the e-ink screen were also missing and the component mix of the PWBs (printed wiring boards) was taken from the electronic component configuration of a personal computer motherboard. For the printed newspaper, data on the production of certain supply chemicals, etc. were missing. These missing data may have resulted in underestimation of the potential environmental impact. For material recycling the effect of the missing data is difficult to predict and depends on the processes (energy use, use of chemicals, emissions, etc.) for recycling and for the virgin production avoided. Regarding the assumption on electronic components for the tablet e-paper, the effect on the results is hard to anticipate.

Not all impact categories were equally well covered. In general, LCA covers energy-related resources and emissions better than process-specific and material-specific impacts. In particular, emissions of toxicological concern are often overlooked in LCAs [Finnveden, 2000]. This means that the results for the toxicological impact categories should be interpreted with special care. It may be particularly important for producers and users of the tablet e-paper to check the chemicals used in the product in order to avoid backlashes.

4.2 Future potential

All systems studied have the potential for improvement. For the tablet e-paper it can be assumed that the potential is rather large, since this is a new product system that is undergoing development. The relative environmental impacts may be lowered through extending the lifetime, more use for other purposes/ combinations of several functions in one product, considering the waste management, etc. In the development of the product, it should be considered that the product should not end up as hazardous waste after fulfilling its purpose since this will lead not only to environmental impact, but also to more costly waste management.

5. Conclusions

Some overall conclusions are:

- ◊ Tablet e-paper has the potential to decrease the environmental impact of newspaper consumption.
- ◊ Key aspects for the environmental performance of newspaper product systems include:
  - ◊ Number of readers per copy of printed and tablet e-paper newspapers
  - ◊ Reading time for internet-based newspaper
  - ◊ Lifetime of electronic devices
  - ◊ Multi-use of electronic devices
- ◊ The production and waste management/disposal of the electronic devices become significant activities as the energy use during the use phase is decreased, i.e. the tablet e-paper.
- ◊ The energy use for editorial work becomes significant as the energy use during the user phase is decreased, i.e. for the tablet e-paper and even in the other product systems the editorial work is notable.

Acknowledgements

This work was performed as a co-operation between STFI-Packforsk and the Royal Institute of Technology (KTH), Division of Environmental Strategies Research and Department of Media Technology and Graphic Art. In addition, the study was a forerunner in the recently established Centre for Sustainable Communications, a Vinnova Centre of Excellence at KTH. STFI-Packforsk and the Swedish Newspaper Publishers' Association (TU) financed this study. The

authors would like to thank the reference group including Birgit Backlund, STFI-Packforsk; Svenåke Boström, Sundsvalls Tidning; and Alex Jonsson Media Technology and Graphic Arts at the Royal Institute of Technology. iRex Technologies, through Philip Leurs, are acknowledged for helpfully providing information about the Illiad e-paper device.

References

[1] Springer A. Verlag AG, Stora and canfor, (1998), *LCA Graphic Paper and Print Products, INFRAS, Zürich*

[2] Axelsson U. and Dalhielm R., (1997), *Miljöprofilering - livscykelanalys av grafiska produkter del 2, (In Swedish), IMT, Teknikrapport 3/97, Stockholm*

[3] Enroth M., (2006), *Developing tools for sustainability management in the graphic arts industry, Doctoral thesis in Media Technology and Graphic Arts, Royal Institute of Technology, Stockholm*

[4] Finnveden, G., (2000), *On the Limitations of Life Cycle Assessment and Environmental Systems Analysis Tools in General. Int. J. LCA, No 5, pp. 229 - 238*

[5] Finnveden, G., Eldh, P. and Johansson, J., (2006), *Weighting in LCA Based on Ecotaxes – Development of a mid-point method and experiences from case studies, Int J LCA, No 11, Special issue, pp. 81 - 88*

[6] Finnveden, G. and Östlund, P., (1997), *Exergies of Natural Resources in Life Cycle Assessment and Other Applications, Energy, No 22, pp. 923 - 931*

[7] Gard D. L. and Keoleian G. A., (2003), *Digital versus Print. Energy performance in the selection and use of scholarly journals. Journal of Industrial Ecology, Vol 6, No 2, pp 115 - 132*

[8] Goedkoop, M. and Spriensma, R., (2000), *The Eco-indicator 99. A damage oriented method for Life Cycle Impact Assessment. Methodology Report, third edition, Amsterfort: PRé Consultants B.V.*

[9] Guinée, J. B. (Ed.), (2002), *Handbook on Life Cycle Assessment, Operational Guide to the ISO Standards, Kluwer Academic Publishers, Dordrecht*

[10] Hischier R. and Reichart I., (2001), *Environmental impact: A comparison between print and electronic media Proceedings of the 3rd Ecopapertech Conference, pp 397 - 406*

[11] Holsanova J. and Holmqvist, K., (2004), *Med blick på nätnyheter. Ögonrörelsestudier av läsning i nätbaserade tidningar, (Looking at net news. Eye tracking study of net paper reading) (In Swedish), In: Holmberg C-G. and Svensson J. (eds.), Mediekulturer, Hybrider och Förvandlingar. Carlsson förlag*

[12] Holmqvist K., Holsanova J., Barthelson M. and Lundqvist D., (2003), *Reading or Scanning? a study of newspaper and net paper reading. In: Hyönä J., Radach R. and Duebel H. (eds.) The Mind's Eye: Cognitive and Applied Aspects of Eye Movements Research, Elsevier*

[13] ISO, (2006), *Environmental management - Life cycle assessment - Requirements and guidelines, International Organisation for Standardisation, International Standard ISO 14044*

[14] Johansson M., (2002), *Livscykelanalys av arkoffsettryckning. Jämförande analys av vattenfri och konventionell offsettryckning samt computer-to-plate och konventionell prepress, (In Swedish), Framkom Rapport 2002:9*

[15] Jönbrink A. K. and Amen R., (2006), *Intermediate step report for EuP study Lot 3, Task 3, Consumer behaviour and local infrastructure, EuP preparatory study, TREN/D1/40-2005, Lot 3, Task 3, Draft report, 22 December 2006. Available on: http://extra.ivf.se/ecocomputer/default.asp*

[16] Kamburow C., (2004), *E-paper – Erste Abschätzung der Umweltsauswirkungen. Eine ökobilanzielle Betrachtung am Beispiel des Nachrichtenmediums Zeitung, (In German) IZT WerkstattBericht Nr 67, Berlin*

[17] Larsen H. F., Hansen M. S. and Hauschild M., (2004), *Ecolabelling of printed matter Part II – Life cycle assessment of model sheet fed offset printed matter, Final draft, Ministry iof Environment and Energy, Denmark, Danish Environmental Protection Agency*

[18] Lindblad S., (2001), *Life-cycle Assessment of distribution of daily newspapers in sparsely populated areas, Framkom report 2001:4, Stockholm*

[19] Lindfors, L.-G., Christiansen, K., Hoffman, L., Virtanen, Y., Juntilla, V., Hanssen, O. J., Rönning, A., Ekvall, T. and Finnveden, G.(1995), *Nordic Guidelines on Life-Cycle Assessment, Nord 1995:20, Nordic Council of Ministers, Copenhagen, Denmark*

[20] Mint, (2005), *Miljönyckeltal och miljönätverk för tidningsföretag, (In Swedish) (Environmental indicators and network for newspaper companies), Internal database STFI-Packforsk*

[21] Moberg, Å., Johansson, M., Finnveden, G. and Jonsson A., (2007), *Screening environmental life cycle assessment of printed, web based and tablet e-paper newspaper, Report from the KTH Centre for Sustainable Communications, ISSN: 1654-479X, TRITA-SUS Report 2007:1, Stockholm*

[22] Pennington, D. W., Potting, J., Finnveden, G., Lindeijer, E. W., Jolliet, O. Rydberg, T. and Rebitzer, G., (2004), *Life Cycle Assessment (Part 2): Current Impact Assessment Practise, Environment International, No 30, pp. 721 - 739*

[23] Rebitzer, G., Ekvall, T., Frischknecht, R., Hunkeler, D., Norris, G., Rydberg, T., Schmidt, W.-P., Suh, S., Weidema, B. P. and Pennington, D., (2004), *Life cycle assessment: Part 1: Framework, goal and scope definition, inventory analysis, and applications, Environment International, No 30, pp. 701 - 720*

[24] Strömberg A., (1998), *Jämförande livscykelanalys - vegetabiliska och mineralbaserade svarta tidningstryckfärger, Uppdragsrapport,(In Swedish), IMT, Stockholm*

[25] TU, (2006), Svensk dagspress 2006. *Fakta om marknad och medier, (In Swedish), Swedish Newspaper Publishers' Association*

[26] Yagita H., Tahara K., Genchi Y., Sagisaka M., Inaba A. and Matsuno Y., (2003), *The evaluation of the amount of CO2 emission concerned with information delivery - Case studies for net-delivered type news paper, Paper presented at the SETAC LCA Case study Symposium, December 2003*

Index of authors

Agić, Darko 141
Antoine, Christine 49
Arnold, Manfred 31

Bablyuk, Evgeny 243
Bakanov, Vadim 243
Belgacem, Naceur 307
Blayo, Anne 123, 307
Bloch, Jean-Francis 23, 123, 221
Bould, David 69
Bucher, Hans-Juergen 355
Burri, Peter 31

Casey, Paul 205
Cheng, Hui-wen 313
Cherry, John 69
Chung, Robert 131, 197
Claypole, Tim C. 69, 77, 163, 205
Curtil, Denis 285

Daneault, Claude 23
Dattner Michael 401
de Gracia, Vicente 109
Deganello, D. 77
Drolet, François 23
Držková, Markéta 267
Dubé, Martin 23, 221
Dufresne, Alain 5
Dörsam, Edgar 257
Đorđević, Dejana 251

Enlund, Nils 3, 345

Farenbrukh, Konstantin 243
Finnveden, Göran 419
Forsell, Minna 365, 413

Gane, Patrick A. C. 31, 115
Gerhardt, Jérémie 147
Gerstner, Philip 115
Gethin, D. T. 77
Golob, Gorazd 251
Gregor Svetec, Diana 251
Grenman, Katri 365, 375
Grolichová, Klára 267

Hakola, Liisa 387, 395
Hamblyn, Simon 69
Hardeberg, Jon Y. 147
Hejduk, Jiří 267
Herzau-Gerhardt, Ulrike 293
Hiltunen, Eero 413
Hohenthal-Joutsimo, C. 413
Hsieh, Yung-Cheng 313
Hsu, Fred 131
Hupp, Heike 257
Hübner, Gunter 297

Jašúrek, Bohumil 101
Jean-Francis, Bloch 123
Jewell, Eifion H. 163, 205
Johansson, Martin 419
Jonsson, Alex 345, 419

Kagerer, Karl-Heinz 31
Kaplanová, Marie 101
Kitazawa, Susumu 181
Koehly, Rodolphe 285
Kolseth, Petter 59
Kraushaar, Andreas 189
Kruse, Björn 171

Laine, Janne 153
Lamminmäki, Taina 231
Leinonen, Anna 413
Lestelius, Magnus 85
Lie, Christer 59
Lindqvist, Ulf 395
Linna, Hannu 395
Liu, Wuhui 131

Madden, Barry 31
Malanin, Mikael 365
Mandić, Lidija 141
Mangin, Patrice J. 23, 221
Mattila, Ulla 15
Medlege, Franck 307
Mejtoft, Thomas 327, 337
Mercier, Christophe 221
Moberg, Åsa 419
Moilanen, Pertti 395

Nagel, Henning 293
Nonaka, Michitaka 181
Novotny, Erzsébet 213
Nyström, Daniel 171
Näsänen, Jaana 375

Olsson, Robert 85
Otero, Susana 109

Palmer, Barry 163
Paltakari, Jouni 115
Pap, Klaudio 277
Passoja, Soile 15
Peralba, Magalie 221
Pieruccini, Stephanie 93
Pineaux, Bernard 123
Politis, Anastasios 401
Purontaus, Jarkko 31
Puukko, Pasi 231

Remenárová, Katarína 101
Ridgway, Cathy J. 31
Ristolainen, Matti 31
Roschier, Hanne 365
Rouault, Hélène 307
Rusko, Elina 387

Sánchez-Alandí, Amparo 109
Sarvas, Risto 375
Siivonen, Timo 395
Sneck, Asko 15
Strgar Kurečić, Maja 141

Teljas, Cecilia 345
Till, Werner 297

Urban, Philipp 189

Vališ, Jan 101
van de Ven, Theodorus G. M. 285
van Stam, Jan 85
Vernhes, Pierre 123
Viström, Magnus 327, 337
Vihavainen, Sami 375

Wanderley, Marcelo M. 285
Wells, Nigel 205
Wessman, Helena 413
Williams, Scott 93

Yang, Li 85, 171
Ylisiurua, Marjoriikka 365

Žiljak Vujić, Jana 277
Žiljak, Ivana 277
Žorž, Boštjan 251